

Elements  
of  
Electrical  
Machine  
Design



Still  
and  
Siskind

THIRD  
EDITION

McGraw-Hill



ELEMENTS OF  
ELECTRICAL MACHINE DESIGN



# ELEMENTS OF ELECTRICAL MACHINE DESIGN

ALFRED STILL

Professor Emeritus of Electrical Engineering  
Purdue University

CHARLES S. SISKIND

Associate Professor of Electrical Engineering  
Purdue University

THIRD EDITION

McGRAW-HILL BOOK COMPANY, INC.

*New York    Toronto    London*

1954



## ELEMENTS OF ELECTRICAL MACHINE DESIGN

Copyright, 1924, 1932, 1954, by the McGraw-Hill Book Company, Inc. Printed in the United States of America. All rights reserved. This book, or parts thereof, may not be reproduced in any form without permission of the publishers.

III

## PREFACE TO THE THIRD EDITION

When the second revision of "Elements of Electrical Design" was undertaken, it was felt that, in view of the many curriculum changes in colleges and universities since the last edition, the present volume should be concerned primarily with the principles and practices of electrical *machine* design. It was decided, therefore, to delete all material not directly related to rotating electrical machinery and transformers, and to transfer and rearrange discussions of basic design principles of electric, magnetic, and electrostatic circuits, originally included in the first six chapters. It is believed that such arrangement of subject matter will serve to unify the treatment of machine design as well as to coordinate fundamentals and design procedures.

The plan of first presenting general discussions relating to materials of construction and the arrangements and proportions of such materials, following with the derivation of useful design formulas, and concluding with the solution of illustrative design examples has been retained. This procedure has proved extremely effective in emphasizing the close relationship between physical constructions and operating characteristics of electrical equipment; it does not attempt to indicate how the industrial designer, through empirical short cuts, proceeds in the design of a particular piece of apparatus to fulfill given specifications.

To conform with recent practice, certain design constants, involving the use of improved electrical sheet steels and insulations, have been modified. These modifications indicate a tendency toward smaller machines as well as toward better operating performance. This is particularly significant in the additions of a completely new (now operating) direct-current generator design in Chap. 3, and a ribbon-core, cruciform-section transformer of modern design in Chap. 12. Other significant additions involve the design of a wound-rotor induction motor with the commonly employed wave winding, the analysis of induction-motor performance by the equivalent-circuit method, basic discussions concerned with stator-rotor slot combinations and rotor-bar skew in induction motors, and alternating-current and direct-current armature windings. A number of new drawings have been included where these were found necessary to supplement text discussions and illustrate physical dimensions and proportions of worked-out designs.



It will be noted that the title of this (the third) edition has been changed to "Elements of Electrical Machine Design"; this is appropriate in view of the contents of the revised text.

The author of this revision, a former student and colleague of Professor Alfred Still, wishes to express his sincere appreciation to Professor Still, a distinguished engineer and eminent teacher, for his inspiration and guidance.

CHARLES S. SISKIND

---

## PREFACE TO THE FIRST EDITION

This book is an attempt to provide the student following courses in electrical engineering with a text in which the problems of the designing engineer are used to illustrate the applications of fundamental laws in the design of practical machines and apparatus. It is the result of ten years of experience in teaching electrical design at Purdue University, a period during which the writer has become more and more convinced of the advantage to be gained from striving always to obtain a concrete mental conception of the hidden actions which produce visible or measurable results. Thus, in the design of electromagnets and high-voltage insulators, the reader is urged to picture the imaginary flux lines and the equipotential surfaces which are everywhere normal to the direction of these lines. In studying the action of electric generators and motors, the electromotive forces developed in the armature windings are consistently represented as being due to the cutting by the conductors of imaginary magnetic lines of flux.

Although the greater part of the material here presented is new, the writer has not hesitated to borrow from his "Principles of Electrical Design" when the inclusion of this previously published material did not seem contrary to the plan of the book. Through the courtesy of Messrs. John Wiley and Sons it has been possible to include in the chapter on Transformers some data and other material which have already been published in the writer's "Principles of Transformer Design."

In the selection of material, its arrangement, and the manner of presenting it, much help has been derived from the advice and suggestions received from a large number of teachers interested in Electrical Design for college students following courses in Electrical Engineering.

Further remarks on the purpose and scheme of the book, together with a few suggestions as to how it may be used to the best advantage as a college text, will be found in the introductory chapter.

ALFRED STILL



## CONTENTS

PREFACE TO THIRD EDITION . . . . .	v
PREFACE TO FIRST EDITION . . . . .	vii
LIST OF SYMBOLS . . . . .	xv
CHAPTER 1. INTRODUCTORY . . . . .	1
CHAPTER 2. DYNAMO ELECTRIC MACHINERY—GENERAL DESIGN PRINCIPLES. . . . .	7
1. Electromotive Force Generated in Conductors Moving through a Magnetic Field . . . . .	7
2. The Output Formula . . . . .	8
3. Number of Poles—Pole Pitch—Frequency . . . . .	13
4. Length of Air Gap and Pole-shoe Design. . . . .	16
5. Illustrative Example . . . . .	18
Test Problems . . . . .	19
CHAPTER 3. ARMATURE WINDINGS AND ARMATURE DESIGN PRINCIPLES . . . . .	20
6. Types of Armature Winding . . . . .	20
7. Coil Constructions . . . . .	20
8. Coil and Commutator Pitches . . . . .	21
9. Armatures with Segments-to-Slots Ratio Greater than One . . . . .	24
10. Equalizing Connections for Lap-wound Armatures . . . . .	27
11. Frog-leg Windings . . . . .	29
12. Number of Slots . . . . .	31
13. Insulation of Dynamo Windings—Materials. . . . .	32
14. Number of Commutator Segments—Diameter of Commutator . . . . .	35
15. Current Density in Armature Conductors . . . . .	36
16. Armature-winding Resistance and Core Length . . . . .	37
17. Armature Core and Teeth—Usual Flux Densities . . . . .	40
18. Illustrative Example. Design of D-C Generator Armature . . . . .	41
19. Other Problems Connected with the Design of Direct-current Dynamos. . . . .	53
Test Problems . . . . .	56
CHAPTER 4. COMMUTATION AND DESIGN OF COMMUTATING POLES . . . . .	59
20. Theory of Commutation . . . . .	59
21. Magnetic Flux Due to Armature Currents . . . . .	62
22. Formulas for Calculating Armature Flux and End Flux in the Zone of Commutation . . . . .	63
23. Effect of Slot Flux . . . . .	67
24. Formulas for Calculating Slot Flux . . . . .	69
25. Formula for Calculating the Total Flux in Zone of Commutation . . . . .	70
26. Effect of Several Coil Sides in One Slot—Full-pitch Windings . . . . .	71
27. Effect of Short-pitch Winding on Slot-leakage Flux. . . . .	71



28. Illustrative Example. Calculation of Short-circuit EMF . . . . .	71
29. Commutating Poles . . . . .	72
30. Illustrative Example. Design of Commutating Poles for D-C Generator	75
31. Commutating Field Obtained by Brush Shift . . . . .	80
32. Brush-contact Resistance as an Aid to Commutation . . . . .	81
33. Compensating or Pole-face Windings . . . . .	85
34. Sundry Details Affecting Commutation . . . . .	87
Test Problems . . . . .	89
 CHAPTER 5. TOOTH RELUCTANCE AND ARMATURE REACTION—DESIGN OF FIELD MAGNETS AND WINDINGS . . . . .	91
35. Effect of Armature Slots on Permeance of Air Gap . . . . .	91
36. Calculation of Tooth Density in Terms of Air-gap Density . . . . .	94
37. Correction for Taper of Teeth . . . . .	96
38. Illustrative Example. Relation between Air-gap Density and Ampere- turns for Air Gap and Teeth . . . . .	97
39. Armature Reaction—Demagnetizing Ampere-turns Due to Armature Currents . . . . .	101
40. Internal Resistance Drop and Overcompounding . . . . .	105
41. Leakage Flux from Field Poles of Dynamo . . . . .	105
42. Illustrative Example. Leakage Flux between Dynamo Field Poles . . .	108
43. Distribution of Flux Density over Armature Surface . . . . .	112
44. Practical Method of Plotting Flux-distribution Curves. . . . .	114
45. Effect of Armature Current in Modifying Air-gap Flux Distribution. .	115
46. Leakage Factor in Multipolar Dynamos . . . . .	116
47. Design of Field Magnets and Windings . . . . .	117
48. Illustrative Example. Design of Field-magnet Coil for Dynamo. . .	123
49. Open-circuit Saturation Curve of Dynamo . . . . .	125
50. Illustrative Example. Design of Dynamo Field Magnets and Windings	126
Test Problems . . . . .	135
 CHAPTER 6. LOSSES, VENTILATION, AND TEMPERATURE RISE . . . . .	137
51. Introductory . . . . .	137
52. Losses in Laminated Iron Cores . . . . .	137
53. Illustrative Example. Calculation of Armature-core Losses . . . . .	141
54. Friction Losses at Commutator Surface . . . . .	142
55. Illustrative Example. Calculation of Commutator Losses. . . . .	143
56. Temperature Rise of Commutators . . . . .	144
57. Illustrative Example. Temperature Rise of Commutator. . . . .	145
58. Temperature Rise of Armatures . . . . .	146
59. Calculation of Temperature Rise of Self-ventilated Armatures with Radial Ducts . . . . .	148
60. Illustrative Example. Temperature Rise of Dynamo Armature . . . . .	151
61. Efficiency. . . . .	152
62. Design of Continuous-current Motors. . . . .	154
63. Illustrative Example. Efficiency of Generator . . . . .	154
64. Intermittent Heating and Thermal Capacity . . . . .	155
65. Illustrative Example. Relation between Time and Temperature Rise .	159
66. Internal Temperature—Thermal Conductivity . . . . .	160
67. Illustrative Example. Temperature Rise in Armature Conductors . .	165
Test Problems . . . . .	166

CHAPTER 7. ALTERNATING-CURRENT MACHINERY—SYNCHRONOUS GENER- ATORS . . . . .	168
68. Introductory . . . . .	168
69. Electromotive Force Developed in Windings . . . . .	170
70. Power Output of Three-phase Generator. . . . .	175
71. Pole Proportions and Specific Loading . . . . .	176
72. Flux Density in Air Gap—Length of Air Gap . . . . .	178
73. Armature Windings . . . . .	181
74. Current Density in Armature Conductors . . . . .	187
75. Tooth and Slot Proportions . . . . .	187
76. Length and Resistance of Armature Winding . . . . .	187
77. Full-load Developed Voltage . . . . .	188
78. Reactive Voltage Drop in A-C Armature Windings. . . . .	189
79. Total Losses to Be Radiated from Armature Core. . . . .	193
80. Cooling and Temperature Rise of Stators . . . . .	195
81. Illustrative Example. Forced Ventilation of Turbo-generator . . .	196
82. Illustrative Example. Design of Armature (Stator) of A-C Generator .	197
Test Problems . . . . .	207
 CHAPTER 8. SYNCHRONOUS GENERATORS ( <i>Continued</i> ). . . . .	209
83. The Magnetic Circuit . . . . .	209
84. Shape of Pole Face—Distributed Field Windings . . . . .	210
85. Magnetomotive Force and Flux Distribution with Cylindrical Field Magnet . . . . .	212
86. Armature MMF in A-C Generators . . . . .	214
87. Armature MMF of Single-phase Alternator. . . . .	218
88. Slot-leakage Flux . . . . .	220
89. Calculation of Equivalent Slot Flux . . . . .	226
90. Method of Determining Position of Maximum Armature MMF . . . .	229
91. Illustrative Example. Design of Field Magnet (Rotor) of Turbo- generator . . . . .	231
 CHAPTER 9. SYNCHRONOUS GENERATORS ( <i>Concluded</i> ). . . . .	248
92. Voltage Regulation. . . . .	248
93. Regulation on Zero Power Factor . . . . .	250
94. Regulation on Any Power Factor . . . . .	252
95. Short-circuit Current . . . . .	253
96. Efficiency . . . . .	258
97. Illustrative Example. Regulation and Short-circuit Current of Turbo- alternator. . . . .	259
Test Problems . . . . .	263
 CHAPTER 10. POLYPHASE INDUCTION MOTORS—DESIGN OF THREE-PHASE MOTOR . . . . .	265
98. Introductory . . . . .	265
99. Design of Induction Motors . . . . .	266
100. Usual Values of Flux Density and Specific Loading . . . . .	267
101. Usual Values of Slot Pitch . . . . .	273
102. The Output Equation . . . . .	273
103. Peripheral Velocity—Ventilating Ducts. . . . .	275
104. Losses in Stator Core and Teeth . . . . .	276



105. Stator Windings—Current Density . . . . .	276
106. Rotor Windings—Current Density . . . . .	278
107. End-ring Current in Squirrel-cage Rotors . . . . .	281
108. Relation between Slip and Rotor Resistance . . . . .	282
109. Illustrative Example. Design of Squirrel-cage Induction Motor . . . . .	284
110. Illustrative Example. Design of Stator for Wound-rotor Induction Motor . . . . .	294
Test Problems . . . . .	305
CHAPTER 11. POLYPHASE INDUCTION MOTORS ( <i>Continued</i> ) . . . . .	306
111. The Circle Diagram . . . . .	306
112. Magnetizing Current of Induction Motor . . . . .	309
113. Total No-load Current in Stator Windings . . . . .	311
114. Leakage Flux in Induction Motors . . . . .	312
115. Calculation of Leakage Flux in Slots and Air Gap. . . . .	313
116. Reactive Voltage Drop in Induction Motor. . . . .	317
117. Equivalent Resistance of Windings . . . . .	318
118. Construction of Circle Diagram from Design Data . . . . .	318
119. Use of Circle Diagram in Calculating Torque . . . . .	320
120. Illustrative Example. Characteristics of Induction Motor Determined from Design Data and Circle Diagram . . . . .	322
121. Circle-diagram Limitations . . . . .	329
122. The Equivalent Circuit . . . . .	329
123. Illustrative Example. Characteristics of Induction Motor Determined from Design Data and Equivalent-circuit Diagram . . . . .	331
124. Heating of Induction Motors. . . . .	336
125. Illustrative Example. Temperature Rise of Induction Motor . . . . .	337
CHAPTER 12. ALTERNATING-CURRENT TRANSFORMERS . . . . .	339
126. Introductory . . . . .	339
127. Theory of the Transformer . . . . .	339
128. Classification and Types of Transformers . . . . .	341
129. The Output Equation—Volts per Turn of Winding . . . . .	343
130. Usual Limits of Flux Density and Current Density . . . . .	344
131. Insulation . . . . .	346
132. Space Factors . . . . .	348
133. Usual Proportions of Built-up Cores. . . . .	348
134. Arrangement of Coils—Leakage Reactance. . . . .	351
135. Calculation of Exciting Current . . . . .	352
136. Magnetic Leakage in Transformers—Voltage Regulation. . . . .	353
137. Calculation of Reactive Voltage Drop . . . . .	355
138. Transformer Vector Diagram Showing Effects of Leakage Flux . . . . .	360
139. Formulas for Voltage Regulation. . . . .	361
140. Efficiency . . . . .	362
141. Temperature Rise of Oil-immersed Transformers . . . . .	364
142. Effect of Corrugations in Vertical Sides of Containing Tank. . . . .	366
143. Cooling Oil in Transformer Tanks by Water Circulation . . . . .	368
144. Hottest-spot Temperature of Transformer Coil . . . . .	369
145. Illustrative Example. Design of Distribution Transformer . . . . .	370
146. Transformers with Ribbon Cores. . . . .	381
147. Illustrative Example. Design of Distribution Transformer . . . . .	383

148. Design of High-voltage Power Transformers . . . . .	392
149. Design of Instrument Current Transformers . . . . .	393
150. Calculation of Phase Angle and Current Ratio. . . . .	394
151. Illustrative Example. Design of Current Transformer for Watthour Meter . . . . .	396
Test Problems . . . . .	403
CHAPTER 13. MECHANICAL DESIGN OF ELECTRICAL MACHINERY . . . . .	406
152. Relation between Mechanical and Electrical Machine Design . . . . .	406
153. Mechanical Forces on Current-carrying Conductors in a Magnetic Field . . . . .	406
154. Unbalanced Magnetic Pull . . . . .	409
155. Design of Stator Frames . . . . .	412
156. Pole Cores and Pole Shoes . . . . .	414
157. Shafts and Bearings . . . . .	415
158. High-speed Rotors—Centrifugal Force . . . . .	416
159. Mechanical Design of Commutators. . . . .	421
160. Sundry Details of Mechanical Design . . . . .	427
APPENDIX I . . . . .	431
APPENDIX II. . . . .	436
INDEX. . . . .	439



## LIST OF SYMBOLS

- $A$  = area of cross section  
 $A$  = area of contact of brushes on commutator, sq in.  
 $a$  = temperature coefficient of resistance at 0°C  
 $a$  = ratio of copper thickness to total thickness in layer of coil winding  
  
 $B$  = magnetic flux density, gauss or lines per sq cm  
 $B$ , and  $B''$  = magnetic flux density, lines per sq in.  
 $B_a$  = density of "interpolar" armature flux  
 $B_e$  = flux density of magnetic field cut by end connections during commutation  
 $B_g$  =  $\begin{cases} \text{in d-c machines, average flux density in air gap under pole face} \\ \text{in a-c machines, average flux density in air gap over pole pitch} \end{cases}$   
 $B_g$  = average air-gap density over tooth pitch  
 $B_{gc}$  = air-gap density under center of pole (d-c machines on open circuit)  
 $B_p$  = flux density in air gap under commutating pole  
 $B_s$  = flux density in slot and parallel spaces occupied by air or insulation  
 $B_t$  = flux density in iron of armature teeth  
 $B \ \& \ S$  = Brown and Sharpe, or "American" wire gage  
 $b$  = ratio of copper thickness to total thickness measured across layers of coil winding  
 $b$  = number of brush sets on commutator  
 $b_s$  = ratio of brush shift to brush pitch in d-c machine  
  
 $C$  = number of commutator segments on d-c armature  
 $C_s$  = number of armature (or stator) conductors per slot  
 $c$  = coefficient of friction  
 $c$  = cooling coefficient—the constant in "emissivity" formulas, watts per sq in. per °C rise of temperature  
 $c$  = empirical coefficient used in transformer design (refer to p. 344)  
 $c_d$  = cooling coefficient for radial vent ducts  
  
 $D$  = outside diameter of armature core or inside diameter of stator core, in.  
 $D_c$  = diameter of commutator  
 $d$  = diameter of wire, mils  
 $d$  = diameter of shaft in bearing, in.  
 $d$  = inside diameter of armature core, in.  
 $d$  = depth of armature or stator slot, usually inches—also length of tooth  
 $d$  = winding factor (a-c generators); takes account of coil pitch and width of phase belt  
 $d_e$  = "equivalent" length of tooth  
  
 $E$  = electromotive force (emf); potential difference, volts  
 $E$  = volts across terminals of magnet coil  
 $E$  = Young's modulus of elasticity



- $E_c$  = volts per conductor  
 $E_m$  = mean value of emf  
 $E_p$  = primary impressed volts (transformer)  
 $E_r$  = generated voltage in rotor of induction motor at slip frequency  
 $E_s$  = secondary terminal volts (transformer)  
 $E_s$  = reactive voltage drop per phase due to slot inductance  
 $E_t$  = terminal voltage  
 $E_1$  = the product of secondary volts ( $E_s$ ) by the transformation ratio (transformers)  
 $e$  = instantaneous value of emf, volts  
 emf = electromotive force, volts  
  
 $F$  = force  
 $F$  = magnetomotive force (mmf), gilberts  
 $f$  = frequency (number of cycles per second)  
  
 $g$  = separation between primary and secondary transformer coils  
 $g$  = length of air gap  
  
 $H$  = magnetizing force (oersted), gilberts per cm  
 $h$  = radial depth of commutator segment  
 hp = horsepower  
  
 $I$  = current, amp  
 $I$  = moment of inertia of section  
 $I_c$  = amp per armature (or stator) conductor  
 $I_e$  = current in end rings of squirrel-cage rotors  
 $I_e$  = total exciting current (transformers and induction motors)  
 $I_e$  = rms value of magnetizing current component (transformer and induction motor)  
 $I_p$  = primary current (transformer)  
 $I_r$  = current in rotor winding (induction motor)  
 $I_s$  = secondary current (transformer)  
 $I_w$  = rms value of in-phase component of exciting current (transformers and induction motors)  
 $I_1$  = transformer primary current less the exciting current  
 $i$  = instantaneous value of current, amp  
  
 $K$  = a numerical constant  
 $k$  = a numerical constant  
 $k$  = distribution factor of a-c winding  
 $k$  = resistance of conductor material in ohms per circular mil per in.  
 $k$  = the ratio  $\frac{\text{pole arc}}{\text{length of armature core}}$   
 $k$  = thermal conductivity, watts per cu in. per °C  
 $k$  = the multiplier for "equivalent" tank surface in formula (149)  
 $k'$  = pitch factor of a-c winding  
 kv = kilovolts  
 kva = kilovolt-amperes  
 kw = kilowatts  
  
 $L_c$  = length of cylindrical surface of commutator, in.  
 $l$  = a length expressed in units defined in text

- $l$  = length of path in direction of flux  
 $l$  = a dimension in air permeance formulas, cm  
 $l$  = length of magnet coil (units, see text)  
 $l$  = mean length per turn of winding (transformer reactance formulas)  
 $l_a$  = gross length of armature core, also stator core of induction motor, usually in.  
 $l_c$  = length of brush-contact surface measured parallel to shaft, in.  
 $l_s$  = total length (both ends) of armature coil outside of slots  
 $l_n$  = net length of iron in armature core and stator of induction motor  
 $l_p$  = length of commutating pole face measured parallel to shaft  
 $l_v$  = total (axial) width of all radial vent ducts in armature core  
 $l'$  = projection of armature coils outside of slot, cm  
 $lf$  = leakage factor  
  
 $M$  = thickness of insulating mica in commutator  
 $M$  = bending moment, in.-lb  
 $(M)$  = circular mils per amp  
 $M_a = (TI)_a$   
 $m$  = a multiplier  
 $m$  = degree of multiplicity of d-c armature winding  
 $m$  = mean length per turn of wire, in.  
 $(m)$  = circular mils  
 mmf = magnetomotive force, gilberts  
  
 $N$  = number of revolutions per minute  
 $n$  = number of armature slots per pole (d-c machines)  
 $n$  = number of high-low groups of transformer windings  
 $n$  = number of radial air ducts in armature core  
 $n$  = number of phases  
 $n_r$  = total number of rotor slots (induction motor)  
 $n_s$  = number of slots per pole per phase  
 $n_1$  = total number of stator slots (induction motor)  
  
 $P$  = permeance (magnetic circuit)  
 $P$  = pull per pole, lb  
 $P$  = pressure, lb per sq in.  
 $p$  = number of poles  
 $p$  = thickness of primary winding in one high-low transformer section  
 $p_1$  = number of electrical paths in parallel in armature winding  
  
 $q$  = specific loading—ampere-conductors per in. of armature periphery  
  
 $R$  = resistance, ohms  
 $R$  = magnetic reluctance  
 $R$  = the "equivalent" resistance of both windings in transformers (p. 361), and induction motors (p. 318)  
 $R$  = a radius  
 $R_c$  = brush-contact resistance per sq in. of surface  
 $R_d$  = radial depth of armature stampings below slots  
 $R_e$  = end-ring resistance in squirrel-cage rotors  
 $R_A$  = thermal resistance  
 $R_s$  = resistance at 0°C, ohms



- $R_r$  = resistance of rotor windings; also "equivalent" resistance of rotor windings, ohms  
 $R_t$  = resistance at  $t^\circ\text{C}$ , ohms  
 $R_t$  = resistance measured between terminals of induction motor stator winding  
 $R''$  = resistance between opposite faces of a cu in. of conductor material, ohms  
 $r$  = a radius  
 $r$  = the ratio  $l/w$  of coil cross section  
 $r$  = the ratio  $\frac{\text{pole arc}}{\text{pole pitch}}$   
 $r$  = the ratio  $\frac{\text{number of stator slots}}{\text{number of rotor slots}}$
- $S$  = number of slots in d-c armature  
 $S$  = surface; area of cooling surface, sq in.  
 $S$  = stress, lb per sq in.  
 $s$  = slot width  
 $s$  = slip of induction motor rotor  
 $s$  = thickness of secondary winding of one high-low transformer section  
 $sf$  = winding space factor
- $T$  = number of turns in a coil or winding  
 $T$  = one-half of the number of conductors per slot in a d-c dynamo  
 $T_p$  = number of turns in transformer primary  
 $T_s$  = number of turns in transformer secondary  
 $T_1$  and  $T_2$  = number of turns in one high-low group of transformer windings (primary and secondary respectively)
- $\left. \begin{matrix} TI \\ (TI) \end{matrix} \right\}$  = ampere-turns  
 $(TI)_a$  = armature ampere-turns per pole  
 $(TI)_g$  = ampere-turns required for air gap  
 $t$  = temperature; temperature rise,  $^\circ\text{C}$   
 $t$  = time, sec  
 $t$  = width of tooth in slotted armature, usually in.  
 $t$  = radial thickness of insulation (units, see text)  
 $t_c$  = time of commutation, sec  
 $t_d$  = difference between internal and surface temperatures,  $^\circ\text{C}$
- $V$  = volume of copper in coil, cu in.  
 $V_c$  = surface velocity of commutator, cm per sec  
 $V_t$  = volts per turn (transformer windings)  
 $v$  = peripheral velocity, feet per minute (fpm)  
 $v_c$  = peripheral velocity of commutator, fpm  
 $v_d$  = average velocity of air in radial vent ducts, fpm
- $W$  = power, watts  
 $W$  = width of brush (circumferential)  
 $W$  = weight of revolving body, lb  
 $W_a$  = brush width (arc) referred to armature periphery  
 $w$  = depth (or thickness) of winding in magnet coil, usually in.  
 $w$  = width of stator slot opening (induction motor)

- $w$  = total losses (iron + copper) in transformers, watts  
 $w_r$  = width of rotor slot opening (induction motor)
- $X$  = reactance, ohms  
 $X_e$  = end-connection reactance per phase in synchronous generators
- $Y_c$  = commutator pitch of d-c armature winding, in segments  
 $Y_s$  = coil pitch of d-c armature winding, in slots
- $Z$  = total number of face conductors (d-c armature)  
 $Z$  = number of inductors in series *per phase winding* (a-c generator and induction motor)  
 $Z_p$  = number of inductors per pole in a-c generators  
 $Z'$  = total number of inductors (all phases) on armature of a-c generator and stator of induction motor

## GREEK LETTERS

- $\alpha$  = angle denoting slope of coil side in end connections of armature winding  
 $\alpha$  = phase angle (current transformers)  
 $\beta$  = angle of lag of current behind phase of open-circuit emf  
 $\beta$  = electrical degrees between adjacent slots in a-c machine  
 $\gamma$  = coil span in a-c armature winding, in electrical degrees  
 $\Delta$  = current density; amp per sq in.  
 $\delta$  = length of air gap—tooth top to pole face  
 $\delta$  = clearance between armature-winding coils  
 $\delta$  = deflection of axis of shaft  
 $\delta_e$  = "equivalent" air gap  
 $e$  = base of natural or hyperbolic logs = 2.7183  
 $\eta$  = efficiency  
 $\theta$  = an angle expressed in degrees or radians (see text)  
 $\theta$  = power-factor angle; angle of lag of current behind voltage ( $\cos \theta$  = power factor)  
 $\lambda$  = slot pitch, usually in.  
 $\lambda$  = pitch of corrugations on transformer tanks  
 $\lambda_e$  = "equivalent" pitch of corrugations on transformer tanks  
 $\lambda_r$  = rotor-slot pitch  
 $\mu$  = permeability =  $B/H$   
 $\pi$  = 3.1416 (approx)  
 $\rho$  = resistivity or specific resistance, ohms or megohms per cm cube or per cu in.  
 $\tau$  = pole pitch measured on armature surface, usually in.  
 $\tau_c$  = coil pitch (d-c armatures)  
 $\Phi$  = magnetic flux, maxwells  
 $\Phi$  = flux entering armature from one pole  
 $\Phi_a$  = "interpolar" armature flux  
 $\Phi_c$  = flux entering armature from interpole  
 $\Phi_d$  = flux entering armature core through roots of teeth (commutation)  
 $\Phi_e$  = total flux cut by one end of armature coil during commutation  
 $\Phi_s$  = total flux per pole cut by end connections (both ends) of polyphase winding  
 $\Phi_{sL}$  = equivalent slot flux in armature length  $l_s$



## LIST OF SYMBOLS

- $\Phi_{es}$  = "equivalent" slot-leakage flux (magnetic circuit closed through roots of teeth)  
 $\Phi'_{es}$  = "equivalent" slot-leakage flux (magnetic circuit closed through tops of teeth)  
 $\Phi'_{es}$  = equivalent slot flux per cm of armature length  
 $\Phi_l$  = leakage flux, maxwells  
 $\Phi_p$  = flux linking with primary windings of transformer  
 $\Phi_s$  = flux linking with secondary windings  
 $\Phi_{ss}$  = slot leakage flux (two slots)  
 $\Phi_t$  = total flux in zone of commutation, combining  $\Phi_a$ ,  $\Phi_s$ , and  $\Phi_{ss}$   
 $\phi$  = power-factor angle, primary side of transformer  
 $\psi$  = "internal" power-factor angle  
 $\omega = 2\pi f$

## CHAPTER 1

## INTRODUCTORY

**The Purpose of the Book.** The art of designing electrical machines cannot be acquired by the reading of books, and it may be said at the outset that the purpose of this text is not to train designing engineers, but to aid all students of electrical engineering in understanding the fundamental principles of electrical machines through their application to concrete designs.

No attempt has been made to present practical methods of design as followed by the professional designer, partly because no two designers follow exactly the same procedure, but mainly because the adoption of design sheets similar to those used by the commercial designer, and the introduction of time-saving approximations, would tend to defeat the end which the authors have in view.

In explaining procedure in design an attempt has been made to base all arguments on scientific facts, and to build up a design in a logical manner from known fundamental principles. This is admittedly different from the method followed by the practical designer, who uses empirical formulas and "short cuts," justified only by experience and practical knowledge. It must not, however, be supposed that a commercial machine can be designed without the aid of some rules and formulas which have not been developed from first principles, for the simple reason that the factors involved are either so numerous or so abstruse that they cannot all be taken into account when deriving the final formula or equation. In any case, the constants used in all formulas, even when developed on strictly scientific lines, are invariably the result of observations made on actual tests; and many of them, such as the coefficients of friction, magnetic reluctance, and eddy-current loss, are subject to variation under conditions which it is difficult to determine. The formulas used in design are, therefore, frequently empirical, and they yield results that are often approximations only; but an effort will be made to explain, whenever possible, the scientific basis underlying the formulas used in this book.

It is generally recognized that fundamentals—or the primary laws on which theories are based—cannot properly be taught without showing their practical application. That is the chief function of laboratory courses in the curriculum of engineering colleges. The student obtains



data from machines and apparatus, and he then analyzes these data with a view to ascertaining whether or not the observed results are in agreement with certain fundamental laws which are supposed to be universally applicable. Another way of teaching fundamentals is to apply the theory in the design of some machine or engineering device, the nature and required performance of which are specified. This is entirely different from the work in the laboratory. The designer does not dissect—he creates. The difference between a laboratory course and a course in machine design is the difference between analysis and synthesis. Both are necessary for the complete understanding of the basic laws usually referred to as fundamentals.

The engineer is rarely able to solve a problem by the simple process of substituting numerical values for symbols in one or more formulas. He is generally confronted with a number of simultaneous problems for which there is not one solution, but many solutions. It is his business to effect a compromise between several conflicting requirements and find a solution which will fulfill the desired purpose in an economical manner.

Although engineering judgment is not easily acquired in college, the practice of machine design calls for the exercise of individual judgment to a greater extent than almost any other course of study. All the conditions and governing factors are rarely known accurately at the outset, and the designer must frequently make a number of assumptions and estimates before he can determine some particular proportion or dimension; but, having done this, he will apply tests based upon established scientific principles as a check on his judgment, so that in the end he may satisfy himself that his machine will conform with the specified requirements.

**What the Student Is Expected to Know.** The knowledge required of the student includes elementary mathematics, the use of vectors for representing a-c quantities, the principles of electricity and magnetism, and some familiarity with electrical apparatus and machinery, such as may be acquired in the laboratories of teaching institutions equipped for the training of electrical engineers, or in the handling and operation of electrical plants in manufacturing works and power stations. He should be generally familiar with the cgs system of units (centimeter, gram, second) as used by the physicist and its relation to the engineer's system of units (inch, pound, minute). The tendency in this text is to use the engineer's units, the dimensions of completed designs being expressed in feet and inches; but there must necessarily be a certain amount of conversion from centimeter to inch units, and vice versa. This may, at first sight, appear objectionable; but, in the opinion of the authors, there is something to be gained by having to transform results from one system of units to another. The process helps to counteract the tendency of mathematically trained minds to lay hold of symbols and formulas and

treat them as realities, instead of striving always to visualize the physical (or natural) reality which these symbols stand for.

Conversion factors will be used throughout the book to convert inches into centimeters (1 in. = 2.54 cm); square inches into square centimeters (1 sq in. = 6.45 sq cm); flux density of  $B''$  lines per square inch into flux density of  $B$  gauss or lines per square centimeter ( $B'' = 6.45B$ ), and magnetomotive force of  $TI$  ampere-turns into  $Hl$  gilberts ( $TI = Hl \div 0.4\pi$ ). The student is expected to be thoroughly familiar with these conversion factors so that he will recognize them in the text.

**Range and Limitation—Scheme of This Book.** This book treats of the elements of electrical machine design. It is not a compilation of design constants and other information of value to the experienced designer; it does not discuss in detail the latest improvements in electrical machinery, neither does it provide the student with drawings and tables of figures giving the over-all dimensions, weights, and construction details of modern machines. Nevertheless, it is believed that the method of design here presented is one which will yield satisfactory results when developing new types of machines, or when it is not necessary to take account of existing patterns and tools.

When designing an electric generator, *the practical designer is usually compelled to use stock frames and armature punchings and adapt these to the requirements of the specification.* He must effect some sort of compromise between the ideal design and a design which will comply with manufacturing conditions. In the method here followed, the assumption is made that the designer is given a free hand to produce a machine that will, in all respects, be suitable for the work it has to perform, and of which the cost and efficiency will be generally in accordance with present-day requirements. The various steps in the design will be followed in logical sequence, and, if the work appears unnecessarily detailed and drawn out, it must be remembered that the method has an educational, apart from a practical, value; it illustrates the application of theoretical principles to a concrete case and shows how the practice of engineering is largely a matter of scientific guesswork. The experienced designer will be able to skip many of the intermediate steps here purposely included, because he will be able to rely on the engineering judgment he has acquired during years of practice in similar work.

Engineering is the economical application of science to material ends, and, if the items of cost and durability are omitted from a problem, the results obtained—however important from other points of view—have no engineering value. The cost of all finished work, including that of the raw materials used in construction, is the cost of labor. Provided the work is carefully done, the element of time becomes, therefore, of the greatest importance. A student in a technical school may be able to



produce a neat and correct drawing, but the salary he could earn as a draftsman in an engineering business might be very small, because his rate of working will be slow. The designer must always have in mind the question of cost, not only material cost—which is fairly easy to estimate—but also labor cost, which depends on the size and complication of parts, accessibility of screws and bolts, and similar factors. These things are rarely learned thoroughly except by actual practice in engineering works, but the student should try to realize their importance and bear them in mind.

Although this book contains no chapter treating exclusively of economic problems, the question of cost—or of economy, involving the efficiency of machines—has not been overlooked, and the student's attention is frequently called to this important feature of all design problems.

Because of the close connection between mechanical and electrical engineering, especially in the work of the designing engineer, it has seemed desirable to include one chapter dealing with the mechanical features of electrical machine design. This is Chap. 13 at the end of the book.

A feature of this text which calls for a few words of explanation is the inclusion of test problems at the conclusion of the chapters. These are short problems to which the answers are given, and they are of an entirely different nature from the design problems in the body of the text, which are examples in design worked out in detail. The test problems are not necessarily design problems, but if the reader is able to solve these *without reference to the text*, this will be an indication that he has a fair knowledge of the subject dealt with in the chapter to which these problems refer.

**How to Use the Text.** If anything of value is to be learned from the study of machine design, the time devoted to actual design work (*i.e.*, in the working out of practical design problems) should greatly exceed the time spent in studying the text. In order to familiarize himself with the elements of electrical engineering and obtain a thorough understanding of the application of fundamental laws and relations to the design of practical machines, it is necessary for the student to shoulder responsibilities and rely upon himself rather than turn to the book or the instructor to overcome all his difficulties. In this way only will confidence and self-reliance be developed. The enterprising student who has studied the text with a view to understanding the fundamental principles upon which the numerical examples are based may work out problems in design by following his own methods, regardless of the particular practice advocated by a book or teacher. He is usually in a position to check his results and satisfy himself that they are substantially correct. This will give him far more encouragement and satisfaction than the blind application of proved rules and formulas. By making mistakes—which are frequently

due to oversights or omissions—and by having to go over the same ground a second or a third time in order to rectify them, an important lesson is learned, namely, that one must resist the tendency to jump at conclusions, and that unsystematic or slipshod work is always uneconomical and ineffective.

Thus, in using the text, the numerical examples and problems in design should be considered mainly as illustrating the application of fundamental principles that have been presented and discussed in preceding articles. If the student has studied the text and followed step by step the problem illustrating the procedure in carrying out an actual design, he should be in a position to work out a similar design problem himself; but if he has not mastered the elements upon which the design is based, he will gain nothing and waste a considerable amount of time by following item by item one of the numerical problems, merely substituting for the figures in the text the values obtained from the data of his own particular problem.

The close relation between mechanical and electrical engineering will be evident to anyone who attempts to design any part of an electrical machine in all its details, and some training in mechanical engineering is, therefore, necessary for the designer of electrical machinery; but actual experience in the shops is particularly helpful to the designer, because it gives him a knowledge of the qualities of engineering materials and the best shapes and proportions of machine parts.

Although the work done in the drafting room is not necessarily designing, it does not follow that the designer need know nothing about engineering drawing. The art of making neat sketches or clear and accurate drawings of the various parts of a machine is learned only by practice; yet every engineer, whatever line of work he may follow, should be able not only to understand and read engineering drawings but to produce them himself at need. It is particularly important that he should be able to make neat dimensioned sketches of machine parts, because, in addition to the practical value of this accomplishment, it is an indication that he has a clear conception of the actual or imagined thing and can make his ideas intelligible to others; moreover, in practice the designer finds the use of neat sketches extremely helpful when discussing problems with his associates.

It is suggested that clear dimensioned sketches (not necessarily to scale) be made of the various parts of a design as the work proceeds, and that in every case an outline drawing *to scale* be made of the completed design. This need not be an elaborate drawing including all mechanical details, but such details as are shown should be correctly represented and the drawing should give the over-all dimensions of the assembled parts. The illustrations of Chap. 13 and a few others throughout the book should



be helpful in making such outline drawings; but no attempt has been made in this text to deal adequately with the mechanical design of electrical machinery.

For the proper administration of a course in electrical design, the authors are of the opinion that no class period—apart from lecture or recitation periods—should be of shorter duration than three consecutive hours, and that the best results are not to be expected from classes consisting of a large number of students. Conferences between the instructor and individual student, in which the special problems of a particular design are discussed, are generally of very great value, and these are possible only in comparatively small classes. There is no doubt that the mass of apparently unrelated material in all but the very simplest design problems tends to confusion, and this is where the instructor's help is of particular value. There are conflicts and compromises in almost every piece of engineering work, and the manner in which these are met and dealt with may be learned in carrying through successfully a series of problems in design.

## CHAPTER 2

### DYNAMO ELECTRIC MACHINERY—GENERAL DESIGN PRINCIPLES

**1. Electromotive Force Generated in Conductors Moving through a Magnetic Field.** A generator is a machine in which a system of electric conductors moves relatively to a magnetic field and so develops an emf which will cause a current to flow when the circuit is closed. It will subsequently be shown how the amount of magnetic field produced by an electric current may be calculated, but the immediate problem will be concerned with how the desired terminal voltage may be obtained by causing the armature conductors to cut the magnetic flux which crosses the air gap from pole face to armature core.

The d-c motor is merely a dynamo of which the action has been reversed; that is to say, instead of providing mechanical energy to drive the armature conductors through the magnetic field, an electric current from an outside source is sent through the armature winding which, by revolving in the magnetic field, converts electrical energy into mechanical energy. In the design of a d-c motor, the procedure is exactly the same as for a d-c generator, and in the following pages the dynamo will be thought of mainly as a generator.

The average value of the emf developed in a circuit of  $T$  turns when  $\Phi$  maxwells are added to or removed from the circuit in the time  $t$  seconds is

$$E_m = \frac{\Phi \times T}{t \times 10^8} \quad \text{volts} \quad (1)$$

For the condition  $T = \text{unity}$ , this formula is clearly seen to express the well-known relation between rate of change of flux and resulting emf, namely, that 100,000,000 *maxwells cut per second generate 1 volt*. This is the fundamental law upon which all quantitative work in dynamo design is based.

At any particular moment it is the rate of change of the flux in the circuit that determines the instantaneous value of the voltage, or, in symbols,

$$\text{Instantaneous volts in circuit of one turn} = - \frac{d\Phi}{dt} \times 10^{-8}$$



where the negative sign is introduced because the developed emf always tends to set up a current the magnetizing effect of which *opposes* the change of flux.

Consider a dynamo with any even number of poles  $p$ . Figure 1 shows a four-pole machine with one armature conductor driven mechanically at a speed of  $N$  rpm through the flux produced by the field poles. If  $\Phi$  stands for the amount of flux entering or leaving the armature surface *per pole*, we may write

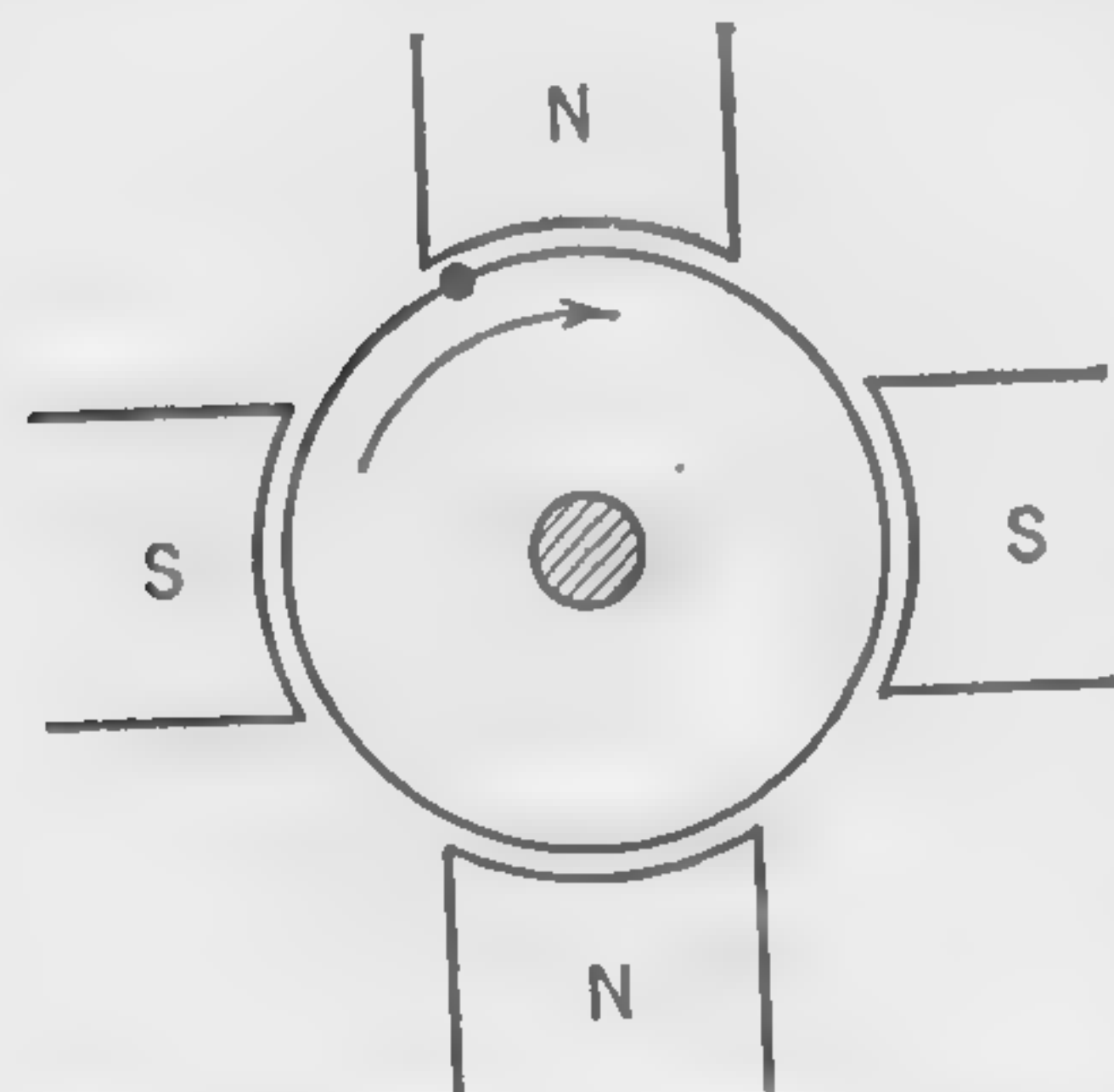


FIG. 1. Single armature conductor cutting flux of four-pole dynamo.

$$\text{Volts generated per conductor} = \frac{\Phi p N}{10^8 \times 60}$$

It is not at present necessary to discuss the different methods of winding armatures, but let there be a total of  $Z$  "active" conductors on the armature. Then, if the connections of the individual coils are so made that there are  $p_1$  electrical circuits in parallel in the armature, the generated volts will be

$$E = \frac{\Phi p N Z}{60 \times p_1 \times 10^8} \quad (2)$$

This is the fundamental voltage equation for the dynamo; it gives the average value of the emf developed in the armature conductors, and, since the virtual and average values are the same in the case of continuous currents, the formula gives the actual potential difference as measured by a voltmeter across the terminals when no current is taken out of the armature. Under loaded conditions, the emf as calculated by formula (2) is the terminal voltage plus the internal  $IR$  pressure drop.

The expression "face conductors" may be used to define the conductors the number of which is represented by  $Z$  in the voltage formula. It is evident that this number includes not only the top conductors, but also those that may be buried in the armature slots. The word "inductor" is sometimes used in the place of "face conductor," and where either word is used in the following pages it must be understood to refer to the so-called "active" conductor lying parallel to the axis of rotation.

**2. The Output Formula.** The part of the dynamo to be designed first is the armature. After the preliminary dimensions of the armature have been determined, it is a comparatively simple matter to design a field system to furnish the necessary magnetic flux. The designer is usually given the following data:

Kilowatt output  
Terminal voltage  
Speed—revolutions per minute

Sometimes the proper speed has to be determined by the designer, as in getting out a line of stock sizes of some particular type of machine; in that case he will be guided by the practice of manufacturers and the safe limits of peripheral speed. Other conditions, such as temperature rise, degree of compounding, sparkless commutation of current, may be imposed by specifications, but, if the designer can evolve a formula which will give him an approximate idea of the weight or volume of the armature, this will be of great assistance to him in determining the leading dimensions for a preliminary design. Modifications or corrections can easily be made later, after all the influencing factors have been studied in detail. Many forms of the output formula are used by designers. The formula is based on certain broad assumptions and is used for obtaining approximate dimensions only. Attempts to develop exact output formulas of universal application should not be encouraged because it is not possible to include all the influencing factors. The art of designing will always demand individual skill and judgment, which cannot be embodied in mathematical formulas.

Let  $\Phi$  = maxwells per pole (full load)

$p$  = number of poles

$N$  = revolutions per minute

$Z$  = total number of "active" conductors

$E_c$  = volts per conductor

$I_c$  = amperes per conductor

The output of the armature, expressed in watts, will be

$$W = Z E_c I_c \quad (3)$$

The voltage per conductor is

$$E_c = \frac{\Phi p N}{60 \times 10^8} \quad (4)^*$$

where the unknown quantity  $\Phi$  may be expressed in terms of flux density and armature dimensions. Thus

$$\Phi p = 6.45 B_a l_a \pi D r \quad (5)$$

where  $B_a$  = average flux density in the air gap under the pole face, gauss

$l_a$  = gross length of armature core, inches

$D$  = diameter of armature core, inches

$r$  = the ratio  $\frac{\text{pole arc}}{\text{pole pitch}}$

\* Since  $\Phi$  is the flux actually cut by the armature conductors, the voltage  $E_c$  is that which is generated or developed in the conductor. The output, as given by formula (3), should, strictly speaking, be thought of as including the  $I^2 R$  losses in the machine; but for the purpose of this sort need not be considered in developing an output formula, the purpose of which is to obtain approximate figures for the dimensions of the armature.



It will be seen that the quantity  $l_a \times \pi Dr$  is the area in square inches of the armature surface covered by the pole shoes, while  $6.45B_g$  is the flux in the air gap per square inch of polar surface.

The pole pitch is usually thought of as the distance from center to center of pole measured on the armature surface; and the ratio  $r$  is, therefore, a factor by which the total cylindrical surface of the armature must be multiplied to obtain the area covered by the pole shoes—the effect of “fringing” at the pole tips being neglected.

Substituting for  $\Phi p$  in Eq. (4) its value as given by Eq. (5), and putting this value of  $E_c$  in Eq. (3), we have

$$W = \frac{6.45B_g l_a \pi Dr N Z I_c}{60 \times 10^8} \quad (6)$$

from which it is necessary to eliminate  $Z$  and  $I_c$ , if the formula is to have any practical value.

A quantity that varies somewhat with the specifications of a machine, *i.e.*, kilowatt output, speed, and voltage, and whose value may be reasonably estimated by the experienced designer, is the *specific loading*, defined as the ampere-conductors per inch of armature periphery and represented by the symbol  $q$ . Thus

$$q = \frac{Z I_c}{\pi D}$$

whence

$$Z I_c = q \pi D$$

Substituting in Eq. (6) we have

$$\begin{aligned} l_a D^2 &= \frac{W}{N} \left( \frac{10^8}{1.064 B_g q r} \right) \\ &= \frac{W}{N} \left( \frac{6.06 \times 10^8}{B_g'' q r} \right) \end{aligned} \quad (7)$$

This is not an empirical formula, since it is based on fundamental scientific principles, and it is capable of giving valuable information regarding the size of the armature core, provided the quantities  $B_g$ ,  $q$ , and  $r$  can be correctly determined.

The quantity  $B_g$  will depend upon the flux density in the armature teeth, which, in turn, depends upon the proportions of the teeth and slots. If the flux density in the teeth is very high, this may lead to (a) an excessive number of ampere-turns on the field poles to overcome tooth reluctance, and (b) excessive power loss in the teeth through hysteresis and eddy currents.

As a guide in selecting a suitable gap density for the preliminary calculations, the accompanying table may be used. The column headed  $B_g''$

is the apparent air-gap density expressed approximately in lines per square inch.

APPROXIMATE VALUES OF APPARENT AIR-GAP DENSITY

Output, kw	$B_g''$	Output, kw	$B_g''$
5	37,000	750	61,000
10	42,000	1,000	62,000
20	45,000	1,500	62,500
30	47,000	2,000	63,000
40	48,500	2,500	63,500
50	50,000	3,000	64,000
100	53,000	4,000	65,000
200	56,500	5,000	65,500
300	57,500	7,500	66,500
400	58,500	10,000	67,000
500	59,000	Larger	67,500

The expression “apparent gap density” means that the flux is supposed to be distributed uniformly over the face of the pole and the effect of fringing is neglected. Thus

$$B_g'' = \frac{\text{total flux per pole}}{\text{area of pole face}}$$

It is customary to think of this as the average density over the armature surface covered by the pole face, in which case

$$B_g'' = \frac{\Phi}{l_a \times \tau \times r}$$

where  $\Phi$ ,  $l_a$ , and  $r$  have the same meaning as in formula (5), and  $\tau$  is the pole pitch or length of arc from center to center of pole measured on the armature periphery. The lower values of  $B_g''$ , corresponding to the smaller outputs, are required mainly because the increased taper of the teeth with the smaller armature diameters would lead to abnormally high densities at the root of the teeth if the air-gap density were not reduced.

The quantity  $q$  in formula (7) is determined, in the first place, by the heating limits, but armature reaction and sparkless commutation have some bearing upon its value; it is further affected by such practical considerations as cost of manufacture and operating efficiency. The larger values of specific loading are, as a rule, preferable in the design of machines having given specifications; they may be increased (1) by reducing the armature diameter, or (2) by increasing the number of armature conductors. However, a reduction in  $D$  must be accompanied by an increase in armature-core length  $l_a$  because reasonable flux densities must



not be exceeded; moreover, an increase in  $Z$  means that the reactance voltage will be raised, an objectionable tendency. Practical values of specific loading range between 350 and 650 for noninterpole machines and about 400 to 1,300 for those with commutating poles; the larger quantities apply, in general, to dynamos having the higher output ratings. The accompanying table lists suitable values for use in formula (7).

APPROXIMATE VALUES OF  $q$  FOR INTERPOLE DYNAMOS  
(Ampere Conductors per Inch of Armature Periphery)

Output, kw	$q$	Output, kw	$q$
5	400	750	950
10	450	1,000	1,000
20	500	1,500	1,050
30	550	2,000	1,100
40	600	2,500	1,150
50	625	3,000	1,200
100	700	4,000	1,225
200	800	5,000	1,250
300	850	7,500	1,275
400	875	10,000	1,300
500	900	Larger	1,300

The quantity  $r$  in formula (7) usually has a value between 0.6 and 0.8, a common value being 0.7. When the machine is provided with commutating interpoles, the ratio  $\frac{\text{pole arc}}{\text{pole pitch}}$  must be small in order to make room for the interpole. In this case a figure between 0.6 and 0.64 would be selected as a suitable value for  $r$ .

If the speed of rotation  $N$  is not specified, it is necessary to make some assumptions regarding the *peripheral velocity* of the armature. This velocity lies between 3,000 and 10,000 fpm; the lower values corresponding to machines of which the speed of rotation is low, while the higher values would be applicable to belt-driven dynamos, or to direct-coupled sets, of which the prime mover is a high-speed engine or high-head water-wheel. When the generator is coupled to a steam turbine, the speed is always exceptionally high, and the surface velocity of the armature may then attain 3 or 4 miles per min. The discussion of steam-turbine-driven generators, in so far as the electrical problems differ from those of the lower-speed machines, will be taken up in connection with alternator design.

The peripheral velocity in feet per minute is

$$v = \frac{\pi D N}{12}$$

whence

$$N = \frac{12v}{\pi D}$$

*Relation of  $l_a$  to  $D$ .* The output equation (7) shows that there is a definite relation between the *volume* of the armature and the output, provided the quantities represented by the symbols  $B_g''$ ,  $q$ , and  $r$  can be estimated. In order to determine the relation between the length  $l_a$  and the diameter  $D$ , certain further assumptions must be made. Thus

$$l_a = \frac{\pi D r}{p k} \quad (8)$$

where  $p$  = the number of poles, and  $k$  is the ratio  $\frac{\text{pole arc}}{\text{armature length}}$ .

A square cross section of the pole core under the windings will lead to economy of copper in the field winding, but, owing to the large proportion of the end-connection copper compared with the "active" copper on the armature, a fairly large axial length of armature core is not uneconomical. A value for  $k$  as low as 0.667, i.e.,  $l_a = 1.5 r r$ , will usually not be objectionable. If the pole face is square—a design that is sometimes employed— $k = 1$  and, for interpole machines,

$$\frac{D}{l_a} = \frac{p}{\pi r} = 0.5p \text{ (approx); i.e., } D = \frac{p}{2} l_a \text{ (approx)}$$

It is not always possible or desirable to provide a square pole face, and, indeed, it is necessary to check the dimensions of the armature core by calculating the peripheral velocity. If a suitable value for the peripheral velocity can be assumed, the diameter is readily calculated because

$$D = \frac{12v}{\pi N}$$

**3. Number of Poles—Pole Pitch—Frequency.** For calculating the relation between the length and diameter of armature core by formula (8), the number of poles  $p$  must be known. The selection of a suitable number of poles will be influenced by considerations of frequency and pole pitch.

*Frequency of D-C Machines.* The frequency of currents in the armature conductors and of flux reversals in the armature core generally lies between 30 and 60 cycles per second in continuous-current generators. The frequency is  $f = (p/2) \times (N/60)$  whence

$$p = \frac{120f}{N} \quad (9)$$



This relation is useful for determining the probable number of poles when the diameter and, therefore, the peripheral velocity are not known.

**Pole Pitch.** The distance between pole centers is limited by armature reaction. It will readily be understood that the armature ampere-turns per pole will be proportional to the pole pitch, except for variations in the specific loading  $q$ . With a large number of ampere-turns per pole on the armature, it is necessary to provide a correspondingly strong exciting field in order that the armature shall not overpower the field and produce excessive distortion of the air-gap flux, resulting in poor regulation and sparking at the brushes with changes of load. Reasonable practical values for ampere-conductors per pole (*i.e.*, in the space of one pole pitch) are given in the accompanying table.

#### APPROXIMATE VALUES OF AMPERE-CONDUCTORS PER POLE

Output, kw	$ZI_c/p$
Up to 100	10,000 or less
100 to 500	10,000 to 15,000
500 to 1,500	15,000 to 20,000
Over 1,500	Up to 25,000

**Ampere-turns on Armature.** Exactly what is meant by the expression "ampere-turns per pole," when applied to the armature winding, should be clearly understood. In a two-pole machine, the total number of

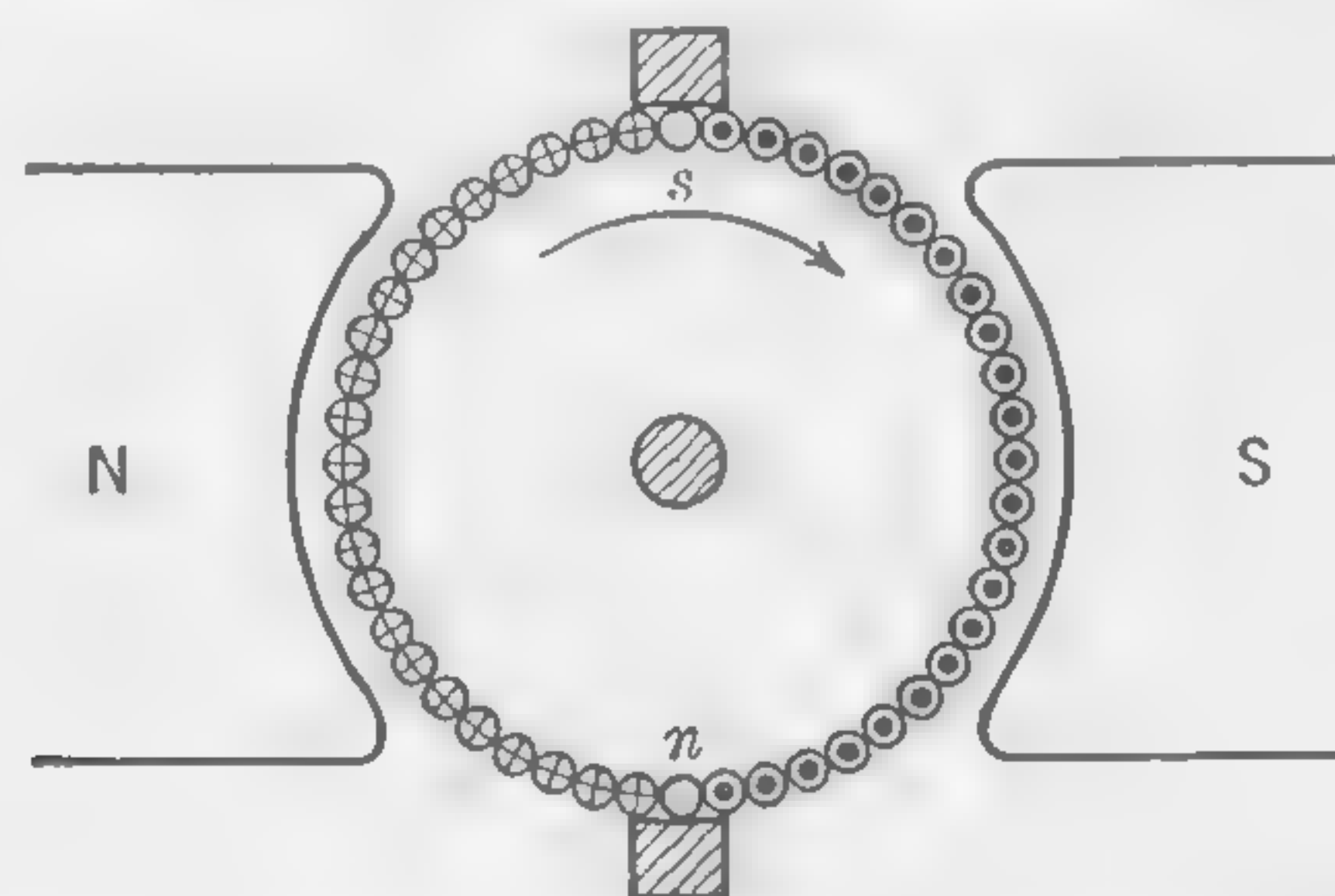


FIG. 2. Current distribution in windings of bipolar armature.

ampere-turns on the armature is  $TI = (Z/2) \times I_c$ , because the current  $I_c$  in  $Z/2$  conductors on one-half of the armature surface is balanced by an equal but opposite current in  $Z/2$  conductors on the other half of the armature surface, as indicated in Fig. 2. Now, since there are two poles, we may say that the ampere-turns per pole are

$$(TI)_a = \frac{1}{2} \frac{ZI_c}{2}$$

or just half the number of ampere-conductors in a pole pitch. This rule applies also to the multipolar machines. Thus, in Fig. 3, the horizontal datum line may be thought of as the developed surface of a four-pole

dynamo armature. The brushes are so placed on the commutator that they short-circuit the coils when the coil sides are approximately halfway between the poles. It is, therefore, permissible to show the brushes in this diagram as if they were actually in contact with the conductors on the "geometric neutral" line. The armature mmf will always be a maximum at the point where the brushes are placed, *because the direction of the current in the conductors changes at this point*, producing between the brushes belts of ampere-conductors of opposite magnetizing effect, as indicated in

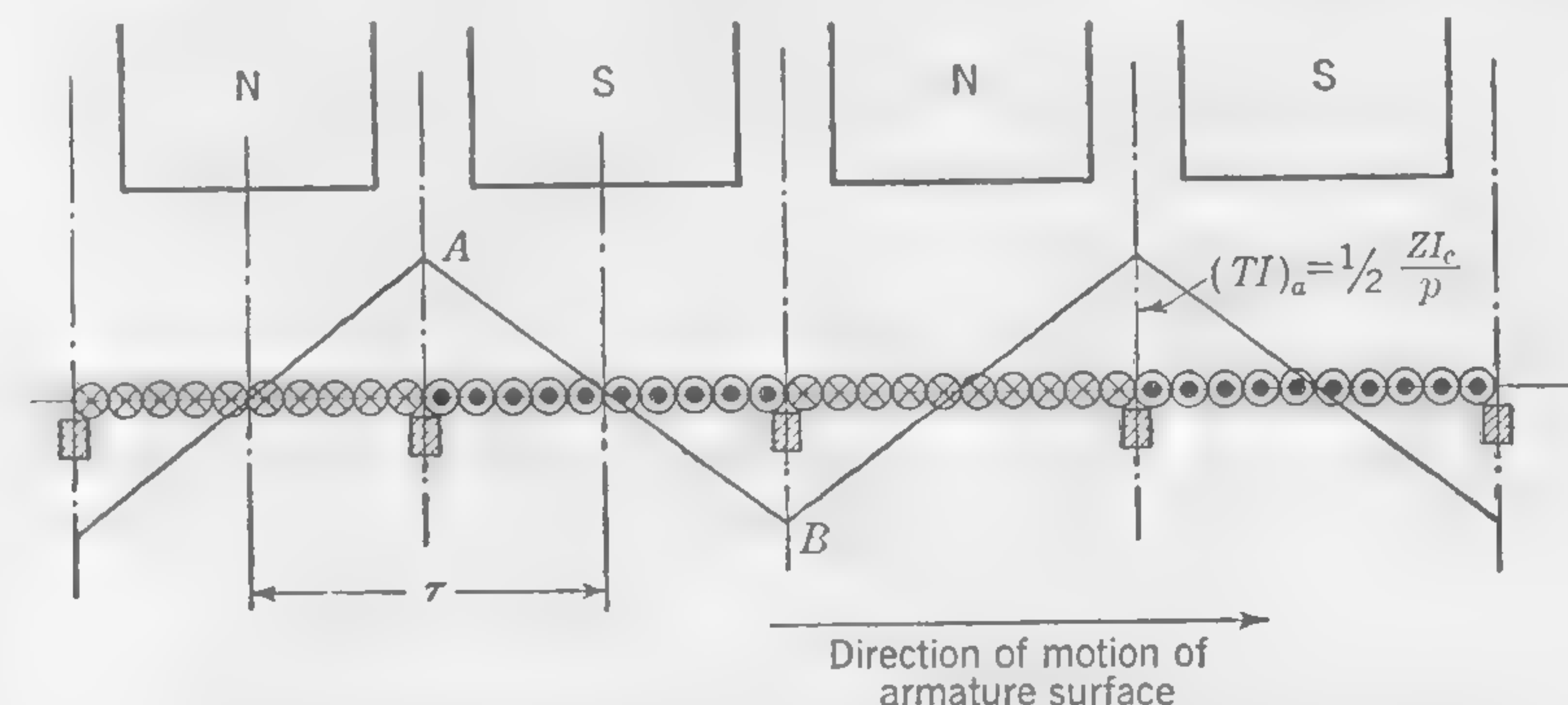


FIG. 3. Magnetic effect of armature currents in multipolar dynamo.

Fig. 3. The broken straight line indicates the distribution of the armature mmf over the surface. Its maximum positive value occurs at A and its maximum negative value at B. These maximum ordinates are of the same height and equal to one-half the ampere-conductors per pole pitch, as will be readily understood by inspecting the diagram. Thus, whether the machine is bipolar or multipolar, the armature ampere-turns per pole are

$$\begin{aligned} (TI)_a &= \frac{1}{2} (\text{amp-conductors per pole pitch}) \\ &= \frac{ZI_c}{2p} \end{aligned} \quad (10)$$

In practice, a safe upper limit for the pole pitch is  $\tau = 26,000/q$ . If  $q = 1,300$ , the maximum allowable pole pitch is  $\tau = 20$  in., which dimension is rarely exceeded in ordinary types of dynamos.

**Number of Poles.** A large number of poles reduces the amount of the flux per pole and shortens the length of the magnetic circuit. This leads to a reduction in weight and cost of material, but a very large number of poles, especially in machines of small output, involves a large number of parts and an increase in cost of labor. The best number of poles for a machine of given speed and output is controlled partly by these considerations and partly by the amount of the current to be collected by each



brush arm. It is well to avoid the collection of more than about 500 amp per brush arm. Values as high as 1,000 amp per brush arm are used in connection with low-voltage machines; but, on machines wound for 250 to 500 volts, the current collected per brush arm usually lies between the limits of 600 and 300 amp.

As a guide in selecting a suitable number of poles for a preliminary design, the accompanying table may be of use. It is based on the usual practice of manufacturers.

NUMBER OF POLES AND USUAL SPEED LIMITS OF DYNAMOS

Output, kw	No. of poles	Speed, rpm
2 or less	2	Over 1,250
2 to 75	4	900 to 1,750
75 to 200	6	Up to 1,200
200 to 500	6 or 8	Up to 1,200
500 to 1,500	8 to 12	Up to 900
1,500 to 2,500	12 or 14	Up to 500
2,500 to 5,000	14 to 24	Up to 375

After selecting what seems to be a reasonable number of poles from this table, and working out preliminary dimensions, a check should be made on the amperes per brush arm, the frequency, the pole pitch, the ampere-conductors per pole, and the peripheral velocity of the armature *before definitely deciding upon the number of poles.*

If the machine is driven by a high-head water turbine or by an a-c motor—as in motor-generator sets—the speed would be somewhat higher, and the number of poles fewer, than the average figures as given in the preceding table.

When using this or any other table or data intended to assist the designer with approximate values, it is necessary to exercise judgment, or at least be guided by common sense. For instance, it may be necessary to depart from the values given in the table in the case of machines direct-coupled to slow-running engines.

**4. Length of Air Gap and Pole-shoe Design.** The controlling factor in determining the air gap is the armature strength or ampere-turns per pole of the armature. If the mmf due to the armature greatly exceeds the excitation on the field poles, there will be trouble due to field distortion under load, which will lead to poor regulation and commutation difficulties. In machines without commutating poles, which rely upon brush shift to prevent sparking (a type of machine rarely met with nowadays), a safe rule is to provide an air gap such that the open-circuit ampere-turns required for the air gap alone—assuming a smooth core and no added reluctance due to slots—would be equal to the ampere-turns

on the armature at full load. Thus if  $(TI)_g$  are the ampere-turns per field pole required to overcome the reluctance of an air gap of length  $\delta$ , we may write  $(TI)_g = (TI)_a$ , where  $(TI)_a$  stands for the armature ampere-turns as calculated by formula (10). This gives for  $\delta$  the value:

$$\delta = \frac{(TI)_a \times 0.4\pi}{2.54B_g} \quad \text{in.}$$

or, approximately,

$$\delta = \frac{1}{2} \frac{(TI)_a}{B_g} \quad \text{in.} \quad (11)$$

where  $B_g$  is in gauss and may be taken as the apparent flux density in the air gap under the pole face on the assumption that there is no fringing.

When machines are provided with commutating poles, there is no brush shift with increase of load and therefore no directly demagnetizing effect due to the ampere-turns on the armature. The air gap as calculated by formula (11) may then be reduced from 30 to 50 per cent. This leads to the following convenient approximate formula in which the air-gap density  $B_g''$  is expressed in maxwells per square inch of the area under the pole face. Thus:

$$\delta = \frac{1}{2} \frac{(TI)_a}{B_g} \times 0.62 = \frac{1}{2} \times \frac{ZI_c/2p}{B_g''/6.45} \times 0.62 = \frac{ZI_c}{pB_g''} \quad \text{in.} \quad (12)$$

In this formula  $Z$  = total number of conductors in the armature slots;  $I_c$  = amperes per conductor, and  $p$  = number of poles.

The air gap in modern dynamos and motors of standard design with commutating poles is very closely approximated by the formula:

$$\delta = 0.04 \sqrt{D + 3} \quad \text{in.} \quad (13)$$

where  $D$  = diameter of armature core in inches. Formula (13) may be used as a check on the gap length calculated by formula (12), but it does not apply to machines with armatures smaller than 15 in. diameter. When pole-face windings (see Art. 33) are used, a further reduction may be made, the controlling factors then being mechanical clearance and possible decentralization of armature due to wear of bearings, ventilation difficulties, and eddy currents caused by "tufting" of flux lines at tooth tips.

The length of the air gap determined by formulas (12) and (13) must not be uniform under the entire pole face but must be shaped to give a gradually increasing distance toward both pole tips. The air gap at the tips (just before the usual rounding off at the extreme ends) is generally  $1\frac{1}{2}$  to 2 times the air gap under the center of the pole. This practice permits the flux-density distribution to taper off from a maximum under the pole center to zero near the neutral zone, and results in improved commutation and a tendency to reduce magnetic noises in toothed armatures.



Figure 4 illustrates the general shape of a pole shoe and indicates the useful flux as it passes from the pole shoe to the cylindrical armature core.

**5. Illustrative Example.** Make preliminary calculations to determine the major dimensions for an interpole generator that will have an output of 200 kw at 250 volts when operating at a speed of 1,200 rpm.

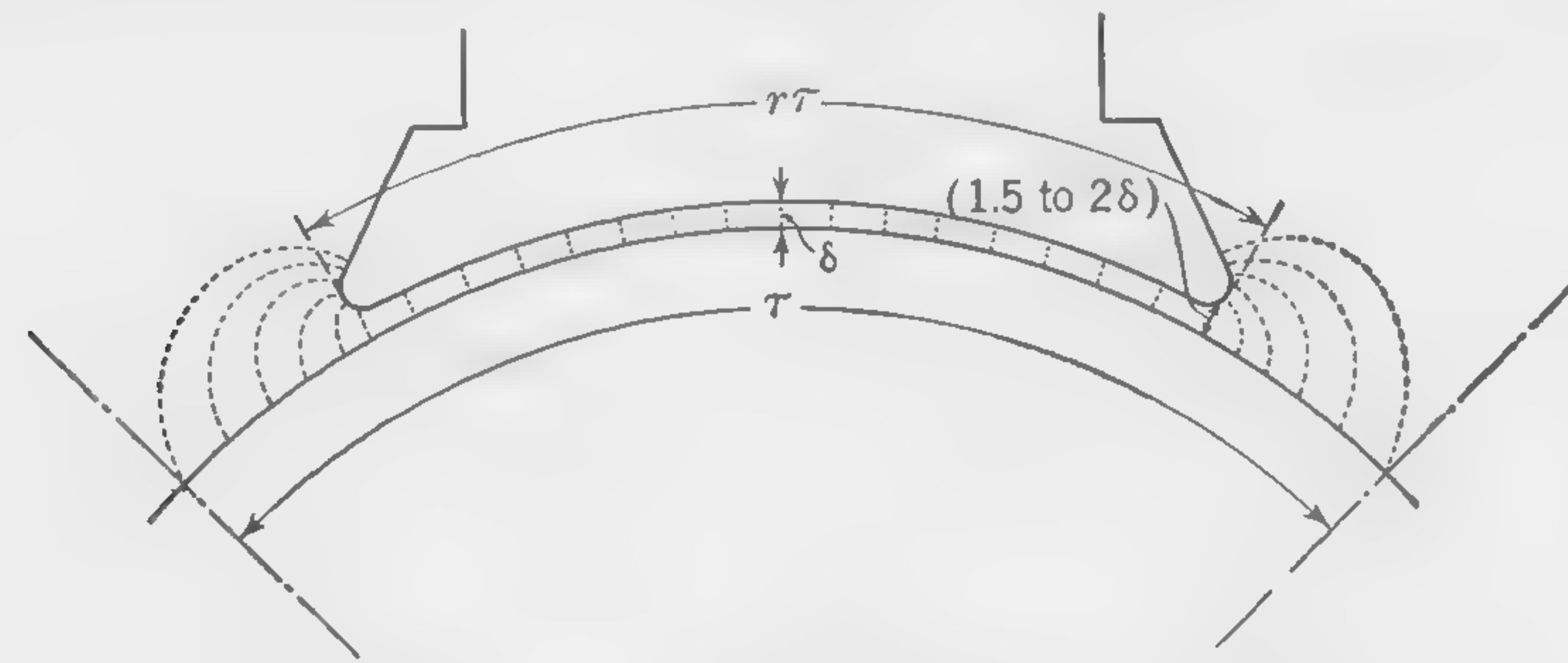


FIG. 4. General shape of pole shoe and flux distribution.

Starting with output formula (7), it is seen that the values of  $B_g''$ ,  $q$ , and  $r$  must be selected from data previously given. Taking  $B_g'' = 56,500$ ,  $q = 800$ , and using  $r = 0.63$ ,

$$l_a D^2 = \frac{200,000}{1,200} \left( \frac{6.06 \times 10^8}{56,500 \times 800 \times 0.63} \right) = 3,550$$

For a 200-kw 1,200-rpm machine, 6 poles will be satisfactory, so that

$$f = \frac{6 \times 1,200}{120} = 60 \text{ cps}$$

Using a rectangular pole face, where  $l_a = 1.25r\tau$ ,

$$l_a = \left( 1.25\pi \times \frac{0.63}{6} \right) D = 0.413D$$

thus

$$0.413D^3 = 3,550$$

from which

$$D = \sqrt[3]{8,600} = 20.5 \text{ in.}$$

and

$$l_a = \frac{3,550}{20.5^2} = 8.5 \text{ in.}$$

The peripheral velocity will be

$$v = \frac{\pi \times 20.5 \times 1,200}{120} = 6,430 \text{ fpm}$$

A tentative air gap of  $\delta = \sqrt{20.5 + 3}/25 = 0.19 \text{ in.}$  will be chosen, and this will be increased to 0.3 in. at the pole tips.

The pole arc  $r\tau = 0.63\pi \times 20.5/6 = 6.75 \text{ in.}$

### TEST PROBLEMS

*One volt is generated in a conductor when flux is cut at the rate of 100,000,000 maxwells per sec.*

1. A circular coil containing 100 turns of wire has a mean diameter of 14 cm. Calculate the mean value of the voltage generated in the winding when the plane of the coil is moved from a position normal to a uniform magnetic field of 10,000 gauss into a position parallel to the field in  $\frac{1}{60}$  sec. *Ans. 92.5 volts.*

2. A coil consisting of 23 turns of insulated wire is wound around one tooth of a slotted armature core. When the speed of the armature is such that the coil travels the distance of one pole pitch in 0.018 sec the average value of the emf induced in the winding is 2 volts. Calculate the maximum amount of the flux which passes through the coil at the instant when it is under the center of any one of the pole faces. *Ans. 78,300 maxwells.*

3. The "active" conductor in the slot of a d-c armature is 16 in. long. The average flux density under the poles is 60,000 maxwells per sq in., and the poles cover 75 per cent of the armature surface. Calculate the number of armature conductors which must be connected in series to develop 280 volts when the peripheral velocity of the armature is 60 ft per sec. *Ans. 54.*

4. Given a d-c machine: number of poles = 10; frequency = 20; peripheral velocity = 3,000 fpm. Calculate diameter of armature in inches. *Ans. 47.8.*

5. What is the number of poles in a d-c generator with a 36-in. diameter armature of which the peripheral speed is 3,000 fpm when the frequency is 21.2 cps? *Ans. 8.*

6. In a six-pole dynamo with an armature 18 in. in diameter, the pole faces cover 61 per cent of the armature surface, and the flux per pole is 2,000,000 maxwells. Calculate the axial length of the armature core corresponding to an average air-gap density of 6,500 gauss under the pole faces. *Ans. 7.9 in.*

7. What is the current per armature conductor in a four-pole d-c generator with a total of 288 armature conductors when the load is such as to produce 2,160 amp-turns per pole on the armature? *Ans. 60 amp.*

8. Given the following particulars relating to a d-c generator: number of poles = 12; armature diameter = 60 in.; gross length of armature core = 12 in.; ratio of pole arc to pole pitch = 0.65; flux per pole in air gap = 6,000,000 maxwells; armature ampere-turns per pole = 6,000. Calculate (a) the average flux density in air gap under pole face; (b) the specific loading (ampere-conductors per inch of armature periphery). *Ans. (a) 49,000 maxwells per sq in.; (b)  $q = 763$ .*

9. A 30-kw 125-volt d-c generator has an armature whose diameter is 12 in. If one-half of the total current passes through each conductor, calculate the total number of armature conductors for a specific loading  $q$  of 630. *Ans. 198.*

10. Calculate the average flux density in the air gap of a d-c generator, given the following particulars: armature diameter = 19 in.; number of poles = 6; ratio of pole arc to pole pitch = 0.65; speed of armature in rpm = 870; volts generated in each armature conductor = 2.92. *Ans. 52,000 lines per sq in.*



## CHAPTER 3

## ARMATURE WINDINGS AND ARMATURE DESIGN PRINCIPLES

**6. Types of Armature Winding.** Modern d-c machines employ two general types of armature winding; these are designated *lap* and *wave*. They are distinguished from each other in two general ways: (1) from the standpoint of construction they differ only by the manner in which the coil ends are connected to the commutator segments; (2) from the standpoint of an electrical circuit they differ in the number of parallel paths between positive and negative brushes. The simplest armature windings are called *simplex*, i.e., *simplex-lap* and *simplex-wave*; they are, by far, the most widely used arrangements in present-day practice. Other modifications of lap and wave types are called *multiplex*, i.e., *multiplex-lap* and *multiplex-wave*; these differ from those of simplex construction by having more parallel paths between plus and minus brushes. Multiplex-lap windings are seldom employed, and only occasionally on very low-voltage dynamos; also, designers rarely find a need for an independent multiplex-wave winding, its use being limited, for the most part, to the combination lap-wave winding, the so-called *frog-leg* winding.

Simplex-lap windings have as many parallel paths as main poles; simplex-wave windings have two parallel paths regardless of the number of poles. Since wave-wound armatures operate more satisfactorily than do those with *lap windings without equalizers* they are nearly always used on dynamos when the current per circuit does not exceed 250 to 300 amp. The degree of multiplicity of a multiplex winding indicates the relative number of parallel paths with respect to the number in a simplex winding. Hence, designating the multiplicity of a winding by the term "plex," (1) the number of parallel paths in a lap winding is  $p \times \text{plex}$ , and (2) the number of parallel paths in a wave winding is  $2 \times \text{plex}$ .

**7. Coil Constructions.** The individual coils of all d-c armature windings are so constructed that when placed in the core slots they build up two layers of coil sides, one on top of the other; for this reason they are often referred to as *double-layer* windings. The practice is to employ diamond-shaped coils made in special forming machines. The rear and front bends are constructed so that one coil side is on a circumferentially higher level

than the other; this construction makes it possible to place the higher side in the top of a slot and the lower side in the bottom of a slot. Figure 5 illustrates how this is done for one coil of a lap or wave winding.

Coils for lap and wave windings are identically formed. The only construction difference between them, however, is the manner in which the coil ends are brought out. In lap windings, the ends usually emerge midway between the sides so that connections may be made to segments that are close together; in wave coils, the ends are brought out at the sides so

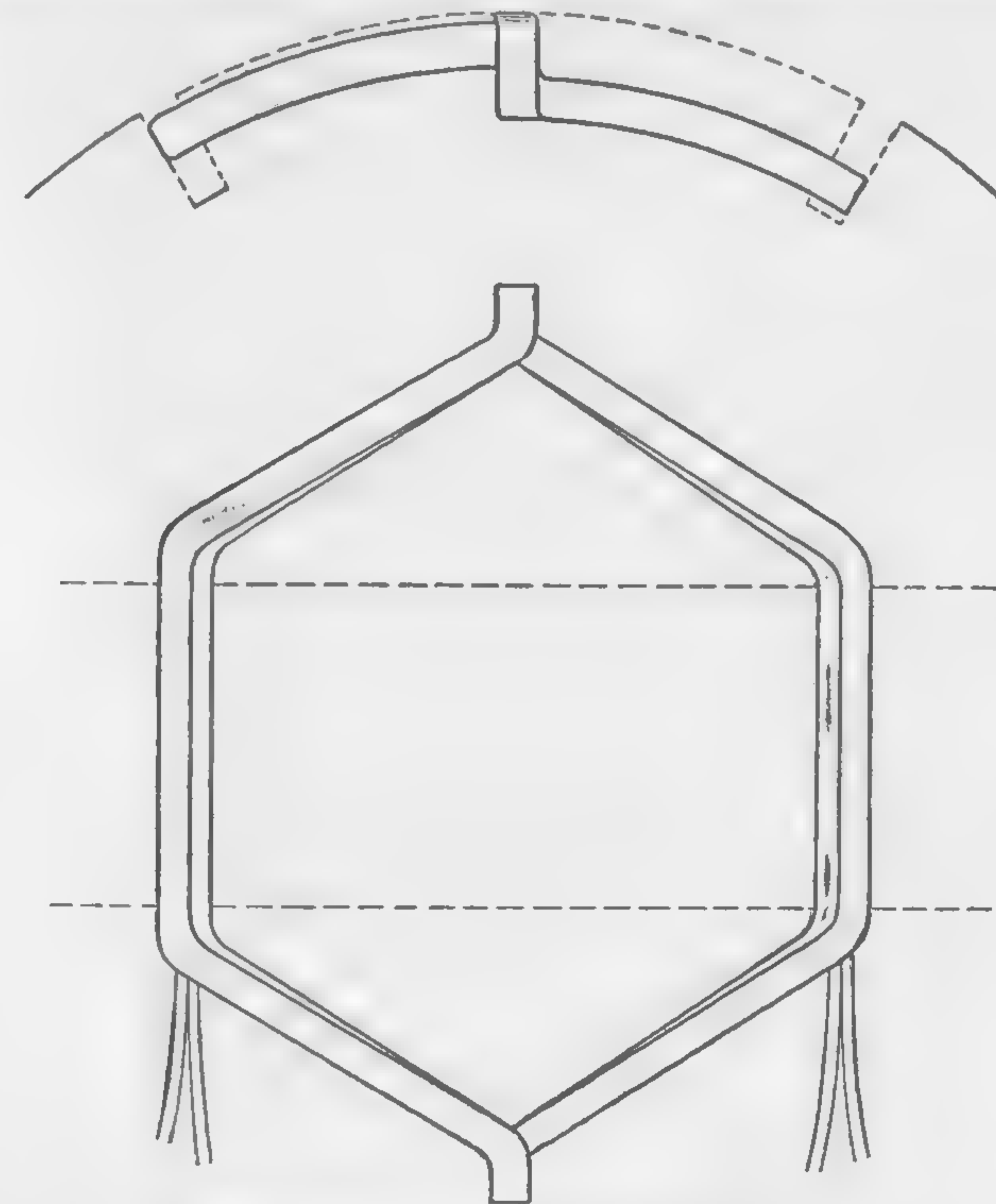


FIG. 5. Form-wound armature coil.

that they may easily be bent outward for connection to segments about 360 electrical degrees apart, i.e.,  $2\pi D_c/p$  approximately, where  $D_c$  is the commutator diameter. Figure 6 indicates how two-turn lap and wave coils are connected to the commutator.

**8. Coil and Commutator Pitches.** The two most important aspects of coils for d-c armature windings are (1) its *coil pitch*, and (2) its *commutator pitch*. The first of these refers to the distance between the two sides of the individual coils. Measured in terms of slots, it is determined in exactly the same way for all windings, whether lap or wave, simplex or multiplex. The fundamental rule that fixes the coil pitch in any given



machine is: the distance between the two sides of a coil must be equal (or very nearly so) to the number of slots in one pole pitch. The reason for this is that: (1) in a generator, the voltages generated in the two sides of a coil can be additive only when they occupy similar positions under poles of opposite polarity at the same instant, (2) in a motor, the forces developed

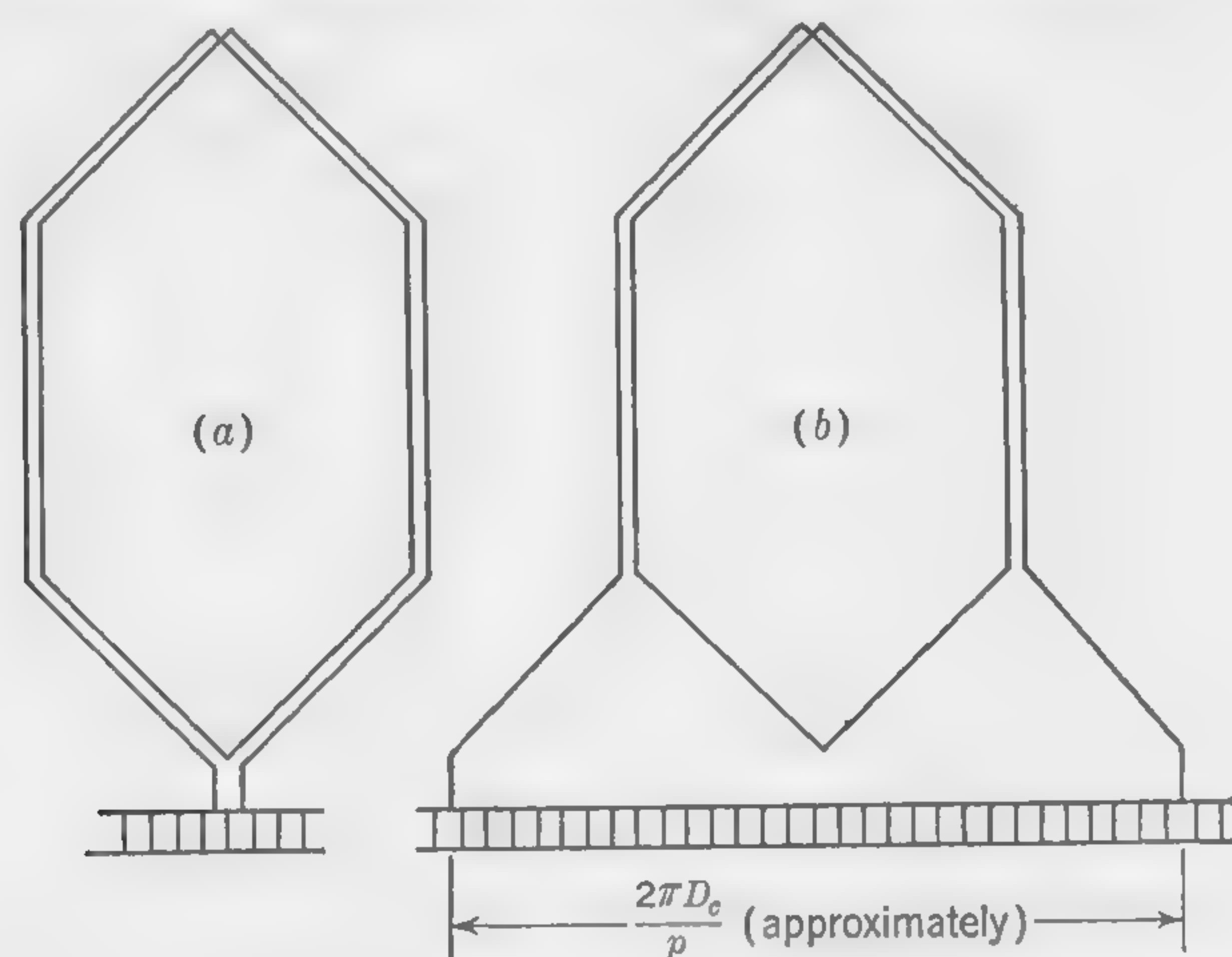


FIG. 6. Coil connections to the commutator for: (a) simplex-lap winding; (b) wave winding.

in the two sides of a coil can be in the same direction, clockwise or counter-clockwise, only when they occupy similar positions under poles of opposite polarity at the same instant. The foregoing rule may be expressed by the formula

$$Y_s = \frac{S}{p} - k \quad (14)$$

where  $Y_s$  = coil pitch, in slots

$S$  = number of slots

$k$  = any part of  $S/p$  that must be subtracted to make  $Y_s$  an integer

When the coil span is exactly 180 electrical degrees, *i.e.*, when  $k = 0$ , the winding will be *full pitch*; under all other conditions, *i.e.*, when  $k \neq 0$ , the winding is *fractional pitch* and is said to be *chorded*. Chording has the effect (1) of slightly reducing the generated voltage in a generator, (2) of slightly reducing the developed torque in a motor, and (3) of widening the commutating zone. Since the latter effect is particularly objectionable it is customary to limit the degree of chording to less than one slot pitch in noninterpole machines, and one-half of one slot pitch in interpole machines.

The commutator pitch, symbolized by  $Y_c$ , refers to the distance on the commutator between the two ends of a coil element. Measured in terms of commutator segments its value, for a *lap* winding, is equal merely to its multiplicity; thus,  $Y_c$  equals 1, 2, 3, 4, etc., for simplex-, duplex-, triplex-, quadruplex-, etc., lap windings, respectively, these numbers indicating that the coil ends are joined to segments 1 and 2, 1 and 3, 1 and 4, 1 and 5, etc., for values of  $Y_c$  that are equal to 1, 2, 3, 4, etc., respectively.

Although a lap winding may be placed on an armature having *any* number of segments, this is not possible when the wave type is employed. To understand why this is so it must be pointed out that d-c windings are *closed-circuit* windings, and in this respect are *singly reentrant* when they are simplex; *i.e.*, proceeding from any segment, the entire winding must be completely traced before reentering the starting point. This means that a simplex-wave winding will have one degree of reentrancy only if the number of segments is properly selected with respect to the number of pairs of poles. The calculated value of  $Y_c$  must, in fact, be such that, after tracing the winding *once* around the commutator the last-coil element must arrive one segment behind, or one segment ahead, of the starting segment; therefore, repeated tracings around the commutator cause the arrival segment to continue to drop back or fall forward one segment at a time *until the complete winding closes on the starting segment*. Moreover, when the winding is duplex-, triplex-, quadruplex-, etc. wave the arrival segment, after one round of tracing, is 2, 3, 4, etc., segments, respectively, behind or ahead of the starting segment. This simple analysis makes it possible to write the following empirical formula for the commutator pitch of a wave winding:

$$Y_c = \frac{C \pm m}{p/2} \quad (15)$$

where  $Y_c$  must be an integer

$C$  = number of commutator segments

$m$  = degree of multiplicity

Two examples should make this clear. The commutator pitch  $Y_c$  of a simplex-wave winding, placed on a 227-segment 6-pole armature, is  $(227 + 1)/3 = 76$ ; therefore, each armature-coil element will be connected to segments 1 and 77. This means that, starting at segment 1, the winding is traced to segments 77, 153, and 229, *i.e.*, segment 2, after one round; note that segment 2 is one ahead of segment 1, which is correct for simplex-wave. Again, the commutator pitch  $Y_c$  of a triplex-wave winding, placed on a 240-segment 6-pole armature, is  $(240 - 3)/3 = 79$ ; each armature-coil element will, therefore, be connected to segments 1 and 80. Thus, starting at segment 1, the winding is traced once around the com-



mutator to segments 80, 159, and 238; note that segment 238 is three behind segment 1, which is correct for triplex-wave.

Observe particularly that whether the plus or minus sign in formula (15) is used depends upon which of the two symbols yields an integer for  $Y_c$ ; in some cases, as in 4-pole simplex-wave windings, *either* one will be satisfactory.

Figure 7 represents a diagram of a 4-pole simplex-lap winding for an armature with 16 slots and 16 segments; note that each of the single-turn coils is connected to adjacent segments. Figure 8 shows a similar type of

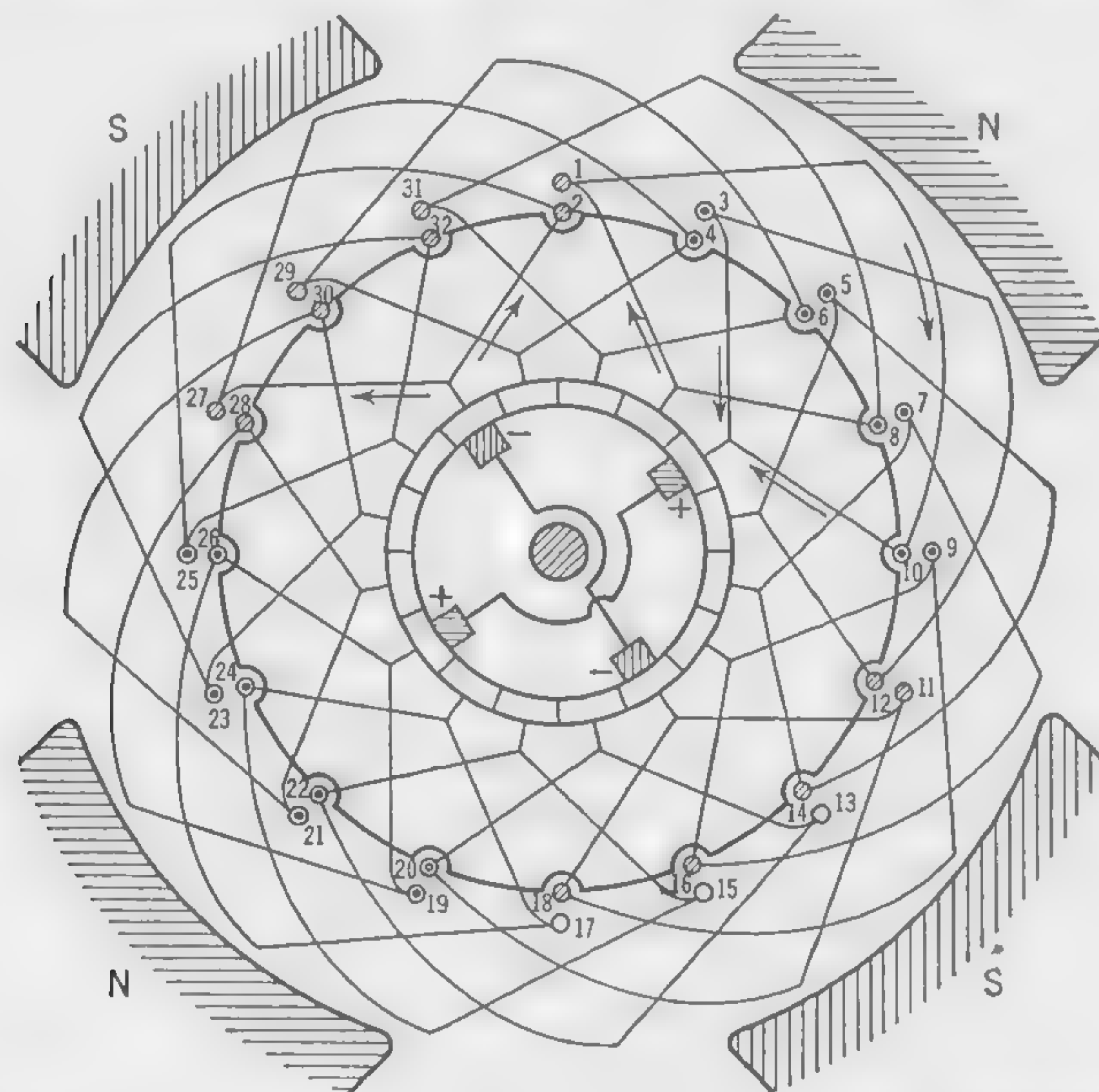


FIG. 7. Diagram of a simplex-lap winding for a 4-pole 16-slot 16-segment armature.

diagram of a 4-pole simplex-wave winding for a 17-segment 17-slot armature; in this case  $Y_c = (17 - 1)/2 = 8$ , which means that each single-turn coil is connected to segments 1 and 9. [Note that the minus sign was used in formula (15), although the plus sign is equally satisfactory.]

**9. Armatures with Segments-to-Slots Ratio Greater than One.** Modern armatures are frequently designed with more commutator segments than slots for the following reasons: (1) For a given terminal emf the voltage between adjacent segments decreases as the number of commutator bars is increased. This reduces the reactance voltage per short-circuited coil and thereby tends to improve commutation. (2) As the number of core slots is reduced the teeth become mechanically stronger, and this results in less damage to laminations and coils in manufacture. (3) For a comparatively large number of segments, the choice of an arma-

ture core with one-half, one-third, one-fourth, etc., as many slots means that fewer coils—multielement coils to be sure—will be necessary; this reduces the manufacturing cost.

Each completely formed coil will contain as many elements as the ratio of segments to slots. (An element is that part of an armature winding that is connected to two commutator segments.) Thus, if the ratio is 2, 3, 4, etc., the individual coils will have 2, 3, 4, etc., elements, respectively. This is illustrated by Fig. 9 for two-element, three-element, and four-element simplex-lap coils. (Similar types of coils would be used for wave

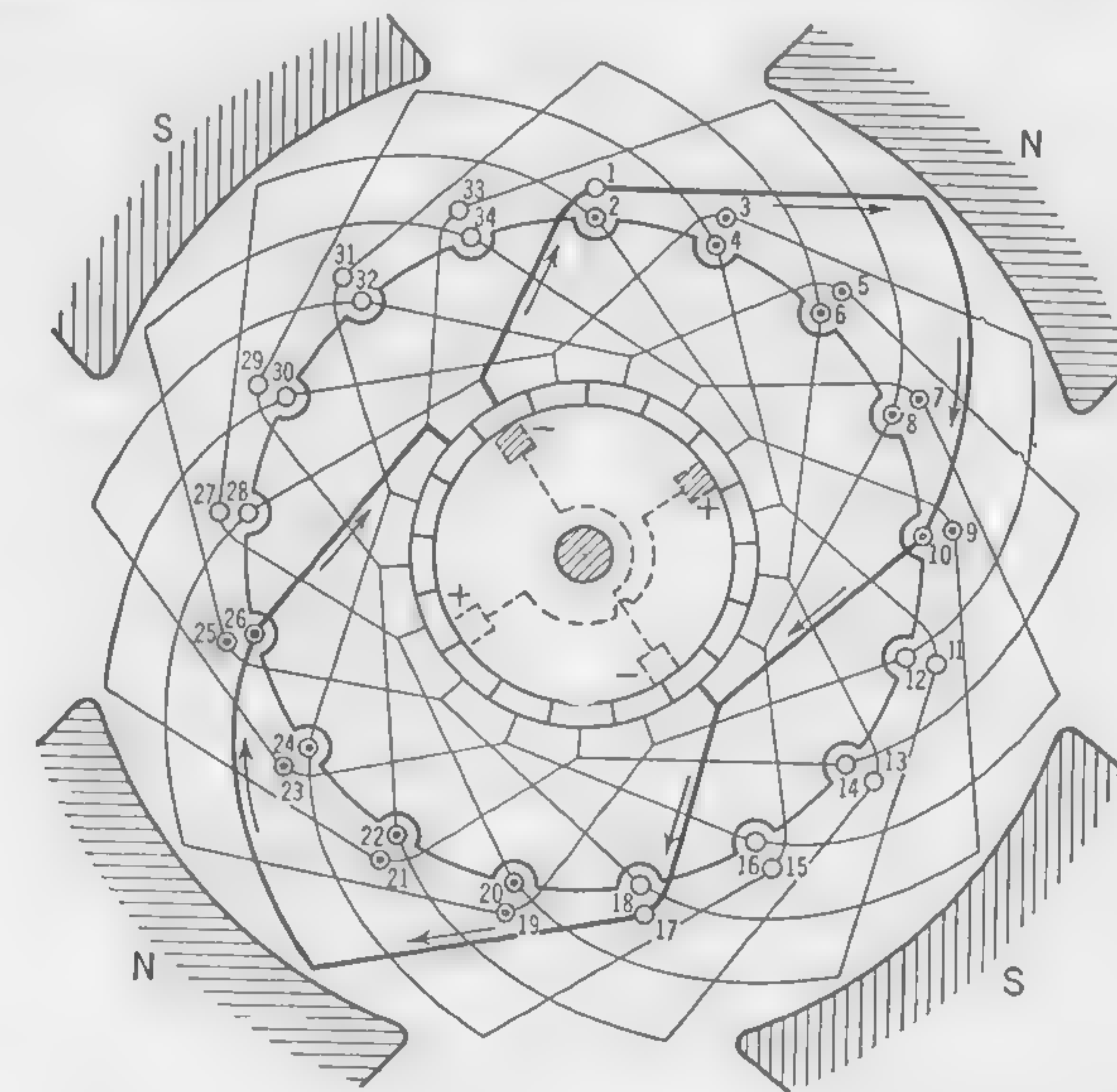


FIG. 8. Diagram of a simplex-wave winding for a 4-pole 17-slot 17-segment armature.

windings, although the commutator connections would follow the principles previously given.) To further emphasize the importance of armature windings having multielement coils, as well as the systematic arrangement of the coils and their commutator connections, a complete diagram of a simplex-wave winding is given in Fig. 10; this is for a 13-slot 39-segment 4-pole armature in which  $Y_s = 13\frac{3}{4} - \frac{1}{4} = 3$  and  $Y_c = (39 - 1)/2 = 19$ .

Four-pole machines with ratings up to about 75 kw for generators and 100 hp for motors are manufactured in considerable numbers. These are generally simplex-wave wound when the voltage is high enough to limit the current to about 250 amp per armature-winding path. Furthermore, the design of many armatures in the ranges indicated makes it desirable to employ a segment-to-slot ratio of 2. Now then, since four-pole simplex-wave-wound armatures *must* have an odd number of segments—



formula (15)—the number of slots cannot be *exactly* half that many, because an odd number divided by two always yields an integer plus one-half. In such cases, the designer, having selected the proper *odd* number of segments for a four-pole simplex-wave winding, must use one-half slot more than required, with the result that the completed winding, with its

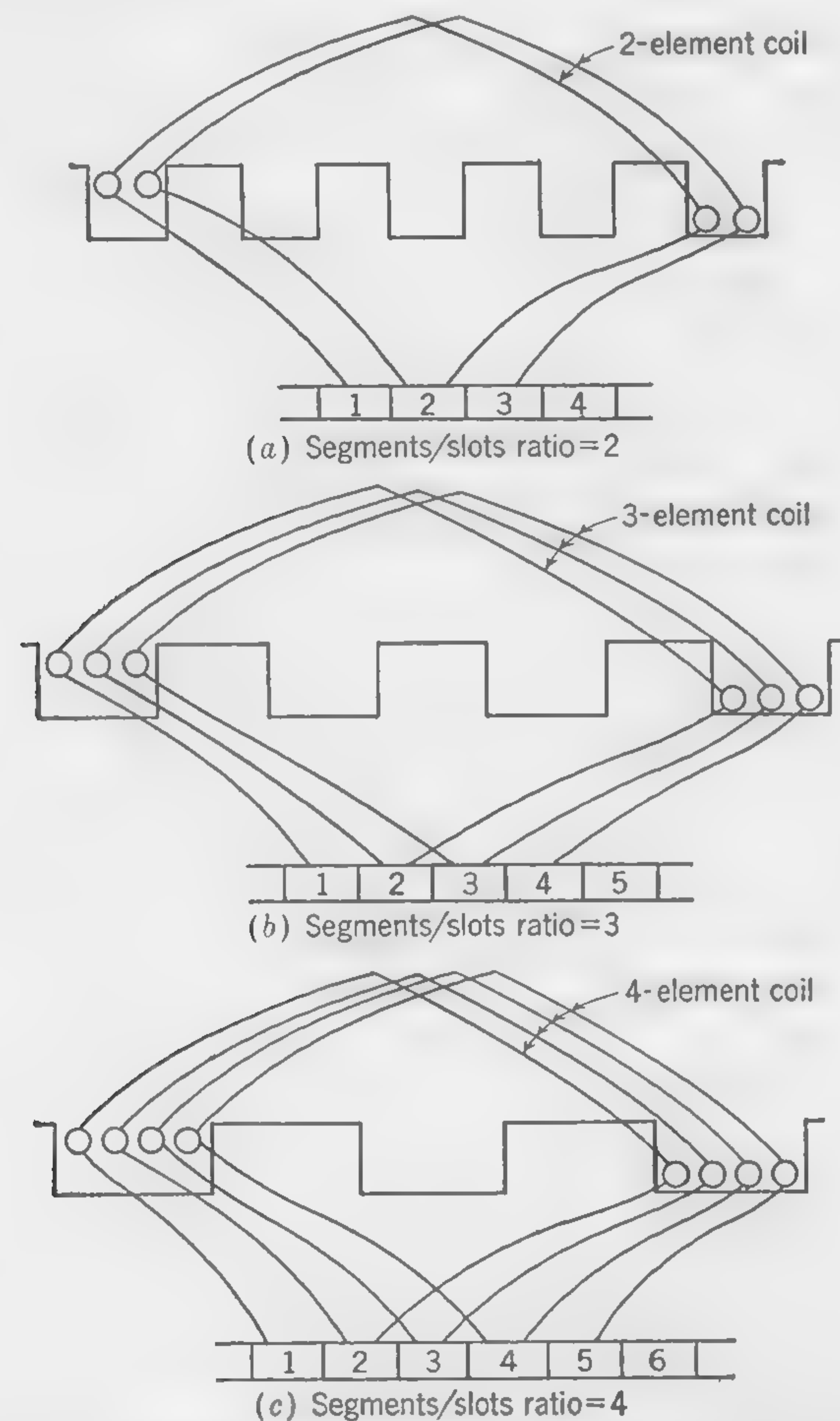


FIG. 9. Sketches illustrating multielement simplex-lap coils.

two-element coils, has an excess of one element (one-half of a coil) that cannot be connected to the commutator. This extra element is left in the armature for mechanical balance and, being open-circuited, serves no electrical function; it is called a "dummy" or "dead" element.

Armatures with three or more times as many segments as slots (approximately) are also used for four-pole simplex-wave armatures. Practical examples of segment-slot combinations requiring dummy elements are:

39 segments, 20 slots; 73 segments, 37 slots; 89 segments, 45 slots; 93 segments, 47 slots; 95 segments, 32 slots; 119 segments, 40 slots; 227 segments, 76 slots. In general, dummy elements must be employed in all windings that are placed on armatures whose segments-to-slots ratios are not integers. Figure 11 illustrates a complete winding diagram in which a dummy element is used.

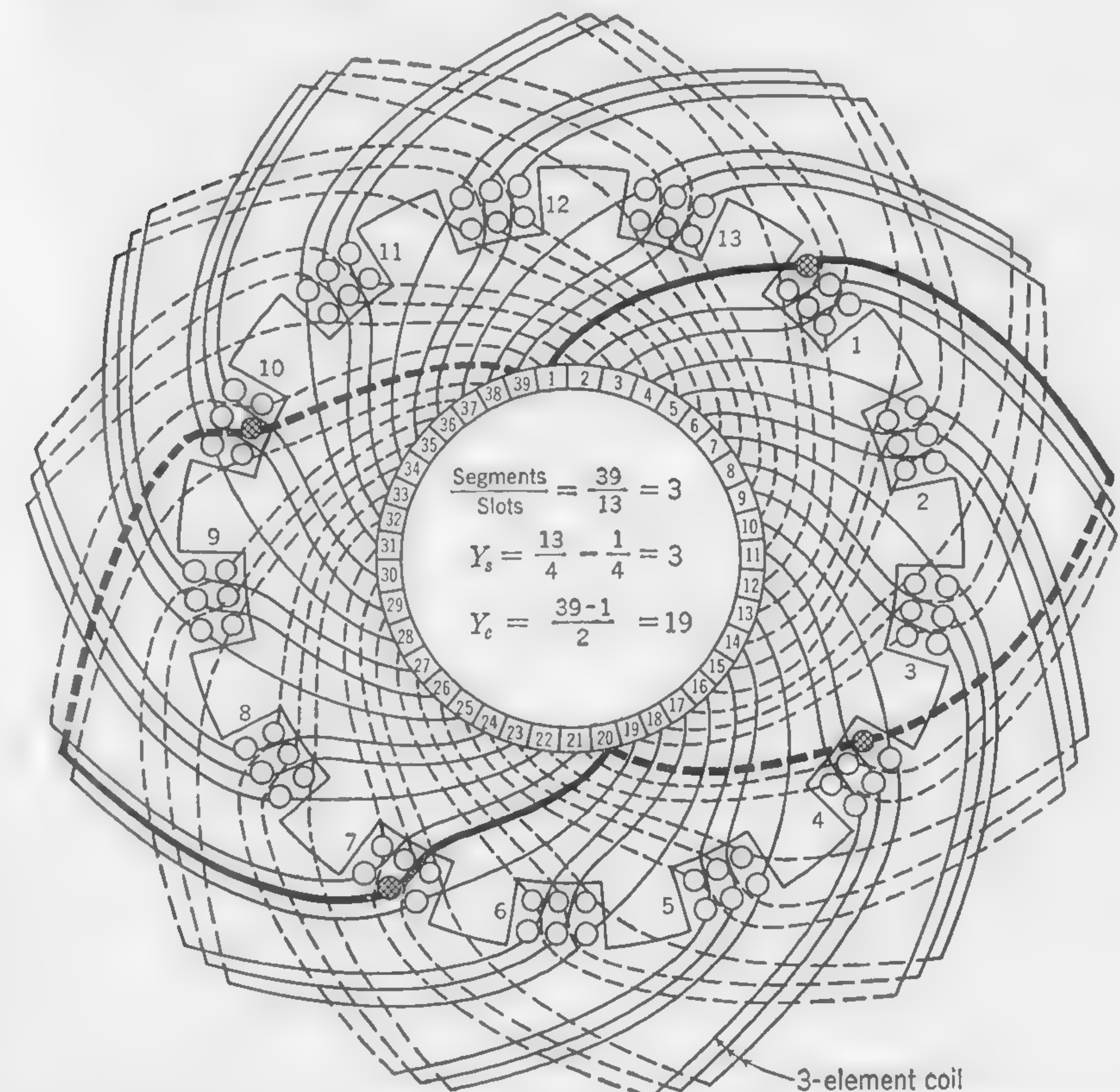


FIG. 10. Diagram of four-pole simplex-wave winding for armature with three times as many segments as slots.

**10. Equalizing Connections for Lap-wound Armatures.** If the magnetic circuits of the various parallel paths in a lap-wound dynamo are not of equal reluctance, there will be an unbalancing of the generated emfs, producing circulating currents through the brushes. The inequality of the magnetic permeances is usually due to eccentricity of the armature relative to the bore of the poles, and, even when the unbalancing effect is small in a new machine, it is likely to increase, because of wear of the bearings.



By providing easy paths for the out-of-balance current components, it is possible to equalize the differences of pressure before the current reaches the brushes.

In large machines with armature cores built up of sheet steel sectors all punched from the same die, the number of coils in the armature winding will be a multiple of the number of pairs of poles. It is, therefore, easy to select points on the winding which should always be exactly at the same

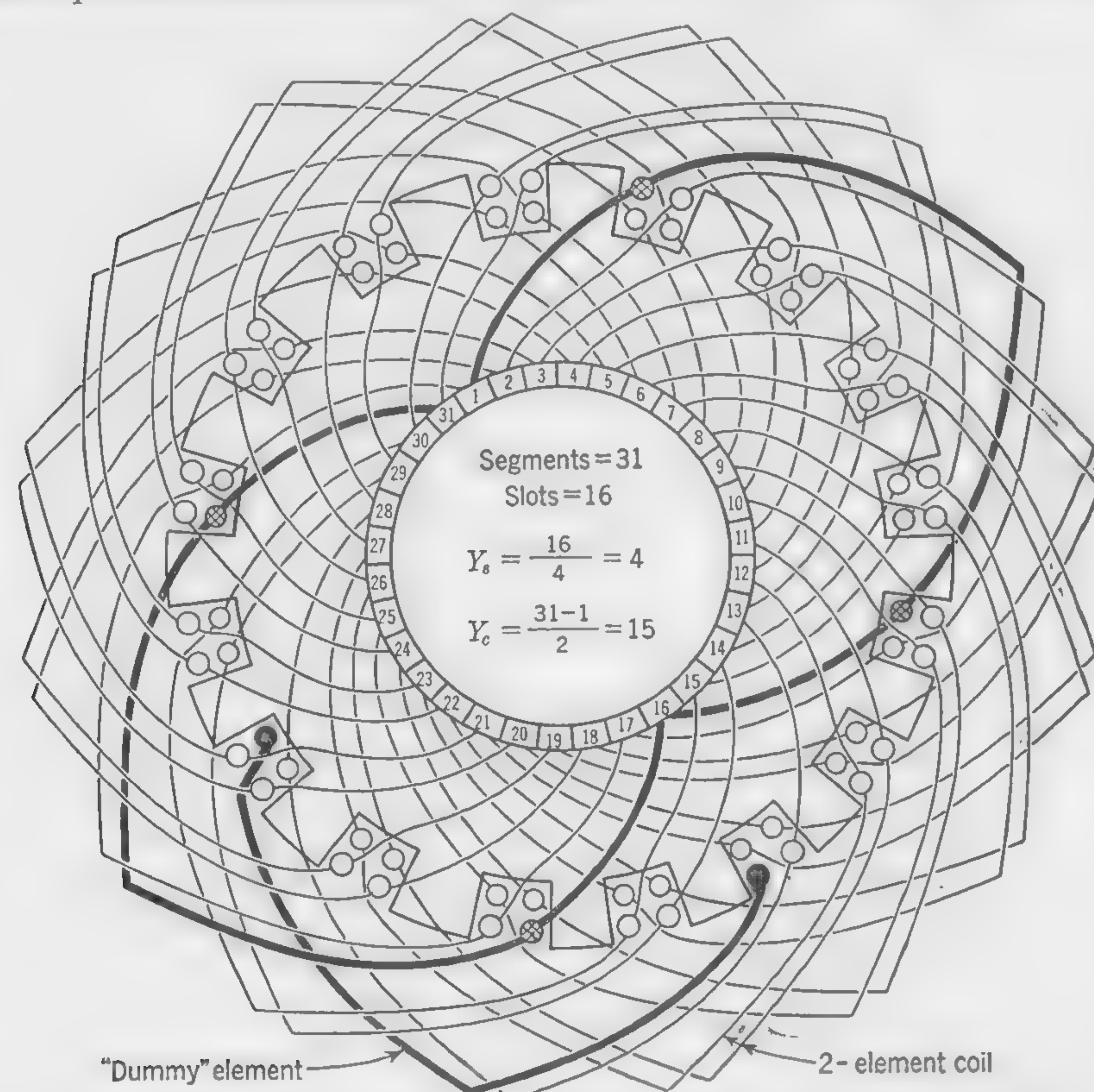


FIG. 11. Diagram of four-pole wave winding showing a "dummy" element.

potential. Thus, in an eight-pole machine, commutator bars spaced exactly 90 mechanical degrees (360 electrical degrees) apart can be permanently joined by equalizing connections at the back of the commutator. If all the bars are so connected the best possible equalizing effect is obtained; but it is not unusual to provide only one-third or one-fourth of the total number of bars with equalizing connections, the cross section of which is about one-half to three-quarters of the armature conductor section.

In some designs a number of insulated copper rings are provided at the

back of the armature and connected to points on the winding which would be at the same potential if the amount and distribution of the magnetic flux were exactly the same under all the poles.

The equalizing connections of lap-wound armatures do not entirely prevent the unbalancing of currents in the armature windings; but by providing a short circuit to the paths through brushes and connecting leads of the same sign, they tend to maintain the equality of currents through the various brush sets. In the simplex-wave winding, with only two armature paths in parallel, equalizing connections are not necessary because each of the two parallel paths is made up of conductors that are distributed more or less uniformly under all the poles.

To illustrate how equalizers are connected at the commutator end of a lap winding, assume a 6-pole 54-slot 162-segment armature. Since 360 electrical degrees is represented by a distance that is equivalent to  $162/3 = 54$  segments, each of the 54 equalizers, for 100 per cent equalization, will be joined to three points on the commutator 54 bars apart. The following table lists the connections to be made.

1-55-109	10-64-118	19-73-127	28-82-136	37-91-145	46-100-154
2-56-110	11-65-119	20-74-128	29-83-137	38-92-146	47-101-155
3-57-111	12-66-120	21-75-129	30-84-138	39-93-147	48-102-156
4-58-112	13-67-121	22-76-130	31-85-139	40-94-148	49-103-157
5-59-113	14-68-122	23-77-131	32-86-140	41-95-149	50-104-158
6-60-114	15-69-123	24-78-132	33-87-141	42-96-150	51-105-159
7-61-115	16-70-124	25-79-133	34-88-142	43-97-151	52-106-160
8-62-116	17-71-125	26-80-134	35-89-143	44-98-152	53-107-161
9-63-117	18-72-126	27-81-135	36-90-144	45-99-153	54-108-162

**11. Frog-leg Windings.** Wave windings are, in general, less complicated than equalized-lap windings, easier to install and service, and less expensive. However, since a simplex-wave winding has only two parallel paths, each of which is practically restricted to a maximum of about 250 amp, the upper limit for machines using this type of winding is approximately 500 amp; for 250 volts, this means a maximum rating of 125 kw. For higher-current values equalized-lap windings are usually employed, although multiplex-wave windings having  $2m$  paths are sometimes attempted.

A construction that combines the advantages of both the lap and wave types is the so-called *frog-leg* winding, developed by the Allis-Chalmers Manufacturing Company. Actually a combination of a simplex-lap and a multiplex-wave winding, the latter section has a plex that provides it with the same number of parallel paths as are in the lap section; thus, every frog-leg winding has  $2p$  parallel paths. Moreover, since every series combination of a lap element and a wave element, which is connected to two segments exactly 360 electrical degrees apart, develops zero



net voltage, each of these lap-wave combinations acts like an equalizer; all frog-leg windings are, therefore, 100 per cent equalized.

The unique design feature of the frog-leg winding is that each complete coil is made up of a lap and wave portion; the lap portion has its ends *brought in* for connection to adjacent segments, while the wave portion has its ends *bent outward* for connection to segments about 360 electrical degrees apart. In selecting the number of commutator bars for a particular frog-leg winding, two important conditions must be fulfilled, namely, (1) a multiplex-wave winding having a plex equal to  $p/2$  must be possible—see formula (15), and (2) segments  $\div p/2$  must be an integer. One example is a 216-segment commutator for a six-pole frog-leg winding.

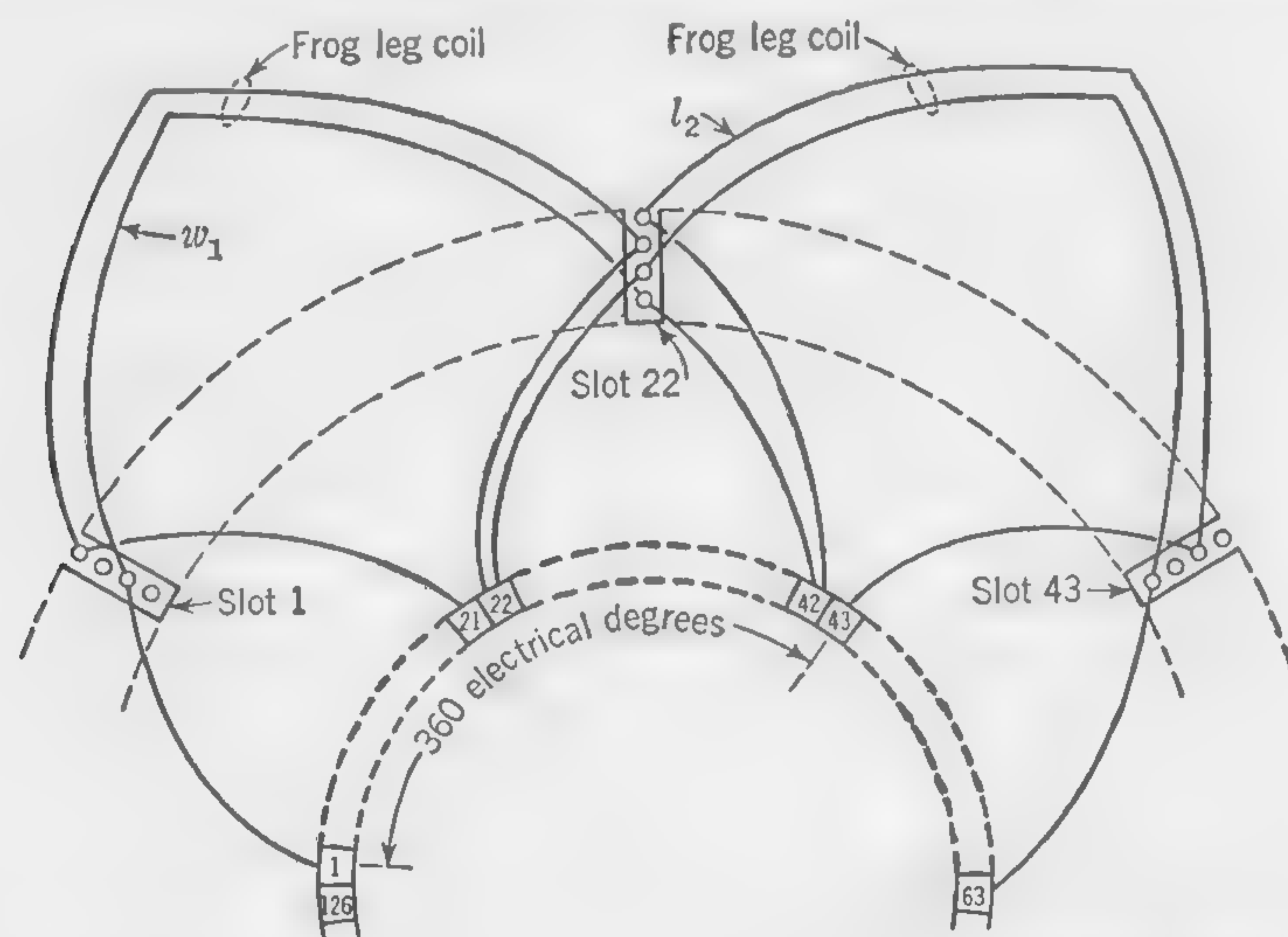


FIG. 12. Diagram showing two frog-leg coils for a six-pole winding in an armature having 126 slots and segments.

This requires a triplex-wave portion having a commutator pitch  $Y_c = (216 + 3)/3 = 73$ ; note also that  $216/3 = 72$ , an integer. Another example is a 120-segment commutator for an eight-pole frog-leg winding. The wave portion will be quadruplex so that  $Y_c = (120 - 4)/4 = 29$ ; also,  $120/4 = 30$ , an integer.

Figure 12 illustrates two frog-leg coils, properly shown in slots and connected to the commutator, for a 6-pole 126-slot and 126-segment armature. The coil pitch  $Y_s = 126/6 = 21$ , and the commutator pitch for the triplex-wave section is  $Y_c = (126 - 3)/3 = 41$ . Note particularly that wave element  $w_1$  and lap element  $l_2$  are in series between segments 1 and 43, exactly 360 electrical degrees apart; in this respect they act as an equalizer as well as voltage-generating elements. The winding will have 12 parallel paths, and each slot will contain four layers of conductors.

**12. Number of Slots.** Although the calculation of flux densities in the teeth will be dealt with later, it may be stated that it is usual to design the slot with parallel sides and make the slot width from 0.3 to 0.5 of the slot pitch. It is very common to make slot and tooth width the same (*i.e.*, one-half the pitch) on the armature surface, but in order to obtain the proper flux density in the teeth, the ratio  $\frac{\text{tooth width}}{\text{slot width}}$  should be about 1.1 to 1.5.

What has been referred to as the slot pitch may be defined as the quotient: armature surface periphery divided by the total number of slots. The slot pitch will usually be between  $\frac{1}{2}$  in. in small machines and  $1\frac{1}{4}$  in. in large machines with a large air gap and pole pitch. A very common value for the slot pitch is 1 in., or thereabouts. With a slot pitch of  $1\frac{1}{4}$  in. the slot will usually be  $\frac{1}{2}$  in. or even less. The slot depth is determined to a large extent by the diameter of the armature, because with a small diameter and slots with parallel sides the flux density is likely to be excessive near the root of the tooth if the slot is deep. A depth of  $1\frac{1}{4}$  in. is not frequently exceeded in armatures 10 in. in diameter, but an armature 48 in. in diameter may have slots 2 in. deep, or more. The ratio of slot depth to slot width usually lies between the limits 3 and 5 in modern dynamos. It is obvious that a small number of teeth would lead to a reduction of space taken up by insulation and, generally speaking, would lead also to a saving in the cost of manufacture. Other considerations, however, show that there are many points in favor of a large number of teeth. Unless the air gap is large in relation to the slot pitch, there will be appreciable eddy-current loss in the pole pieces on account of the tufting of the flux lines at the tooth top. Again, pulsations of flux in the magnetic circuit are more likely to be of appreciable magnitude with few than with many teeth, and, when the tooth pitch is wide in relation to the space between pole tips, commutation becomes difficult because of the variation of air-gap reluctance in the zone of the commutating field.

Consideration in the selection of the number of slots must also be given to the manner in which the air-gap reluctance between the pole faces and the irregularly shaped armature-core surface is affected by the rotating armature. To avoid *flux pulsations*, *i.e.*, changes in air-gap flux, a condition that gives rise to pole-shoe iron losses and magnetic noise, the air-gap reluctance per pair of poles should be practically constant; the latter is generally attained if the number of slots per pair of poles is an odd integer, or, to put it another way, if the slots per pole is an integer plus  $\frac{1}{2}$ . Moreover, if the flux is to be prevented from *oscillating* forward and backward across the pole faces, the air-gap reluctance under the pole faces must be kept reasonably constant for all relative positions of pole shoes and armature core; this condition is approximated by (1) properly cham-



fering (beveling) the tips of the pole shoes; (2) making the slots narrow in proportion to the width of the teeth; and (3) making the number of slots that are exposed to each pole shoe equal to an integer plus  $\frac{1}{2}$ . Figure 13 illustrates the foregoing discussion and indicates how flux pulsations and oscillations are minimized. Note particularly that, in the two extreme armature-core positions of Figs. 13a and b, with  $6\frac{1}{2}$  slots per pole, the air-gap reluctance per pair of poles remains constant; also, with  $4\frac{1}{2}$  slots per chamfered pole face the air-gap reluctance between pole face and core is essentially unchanged.

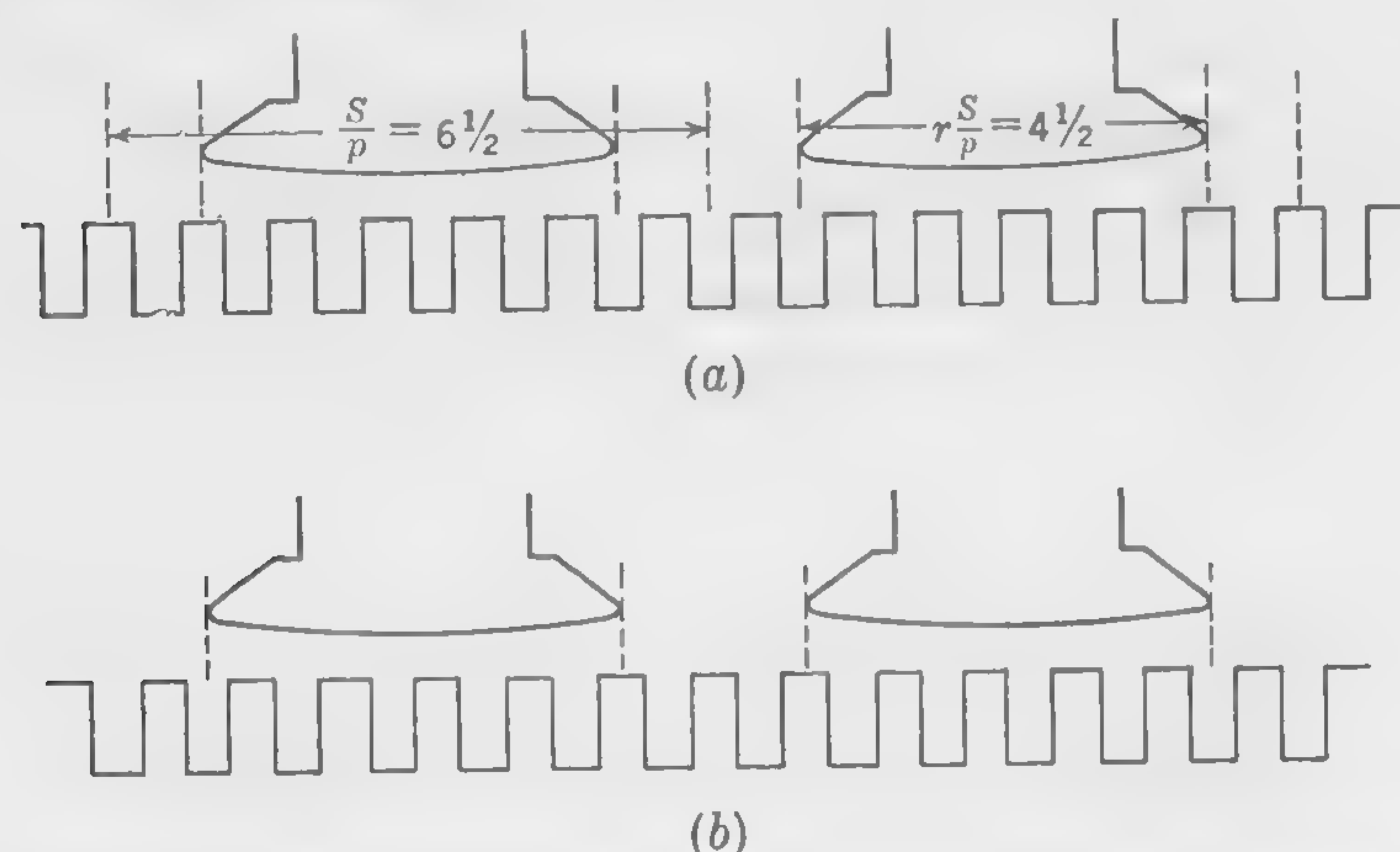


FIG. 13. Sketches illustrating that the air-gap reluctance per pair of poles, and under the pole faces, is practically constant when  $S/p$  and  $rS/p$  are integers plus  $\frac{1}{2}$ .

In actual designs it is frequently neither possible nor desirable to fulfill both of the conditions indicated; in such cases the number of slots per pole arc should be an integer, with the slots per pole equal to an integer plus  $\frac{1}{2}$ .

**13. Insulation of Dynamo Windings—Materials.** The average voltage between the terminals of an armature coil for a d-c dynamo rarely exceeds 25 volts, and it follows that the potential difference between the conductors in one coil cannot be very high. The copper conductors are usually insulated with cotton spun upon the wire in two layers. Cotton braiding is sometimes used on large conductors of rectangular section, and a silk covering is used on very small wires where a saving of space may be effected and an economical design obtained notwithstanding the high price of the silk covering. A triple cotton covering is occasionally used when the potential difference between turns exceeds 20 volts. Conductors of large cross section may be insulated by a covering of cotton tape put on when the coil is being wound.

In addition to the comparatively small amount of insulation on the

wires, a substantial thickness of insulation must be provided between the armature core and the winding as a whole. The materials used for slot lining are:

1. Vulcanized fiber, leatheroid or fish paper, red-rope paper, press-board, presspahn, horn fiber, etc., all of which, being tough and strong, are used mainly as a mechanical protection, because they are more or less hygroscopic and cannot be relied upon as high-voltage insulators, especially when moisture is present. These materials, when dry, withstand about 300 volts maximum per mil, in thin sheets, before breakdown.

2. Mica, micanite, mica paper or cloth. These materials are good insulators, and the pure mica or the micanite sheet will withstand high temperatures. Sheet micanite is built up of small pieces of mica split thin and cemented together by varnish. The finished sheet is subjected to great pressure at high temperatures in order to expel the superfluous varnish. Mica is hard and affords good protection against mechanical injury; but it is not suitable for insulating corners or surfaces of irregular shape. It will withstand about 1,000 volts maximum per mil before breakdown. The disruptive strength of micanite paper or cloth is about 600 volts maximum value.

3. Treated fabrics, such as varnished cambric; linen treated with boiled linseed oil (empire cloth), etc. These provide a means of applying a good insulating protection to coils of irregular shape. Linseed oil is commonly used in the preparation of these insulating cloths and tapes because it has good insulating properties and remains flexible for a very long time. These materials withstand about 600 volts per mil before breakdown; but the disruptive strength decreases rapidly with increase of temperature.

Since thermal aging greatly affects important chemical properties of insulation it is most significant in determining the life of a winding. It is for this reason that the maximum permissible temperature of a machine will depend upon the kinds of insulating materials that are employed in the construction of dynamos. *Class A* insulations, most generally employed for generators and general-purpose motors, consist of *organic* substances; the armatures and unexposed fields must not have a temperature rise of more than  $40^{\circ}\text{C}$  above the ambient temperature. *Class B* insulations consist of *inorganic* materials in built-up form with organic binding substances; machines employing such materials are permitted to have a temperature rise of  $75^{\circ}\text{C}$ . When dynamos must operate under extremely high-temperature conditions *Class H* materials are used; these consist of such substances as mica, asbestos, Fiberglas, and silicone materials and binders, and permit operation at temperatures that are  $70^{\circ}\text{C}$  above class B insulations.

It is common practice to impregnate the finished armature coil with an insulating compound and press it into shape at a fairly high temperature.



When this is done, ordinary untreated cotton tape is used in place of the varnished insulation.

Figure 14 shows a typical slot lining for a 600-volt winding. This can, however, be modified in many respects. It is obvious that the insulation should be so arranged as to leave the greatest possible amount of space for the copper conductors. Part of the insulation is usually wrapped around the coils before these are assembled in the slots. The balance of the required insulation is then in the form of a slot lining which projects a short distance beyond the ends of the slot. It is essential to have a sufficient thickness of insulation between the cotton-covered wires and the

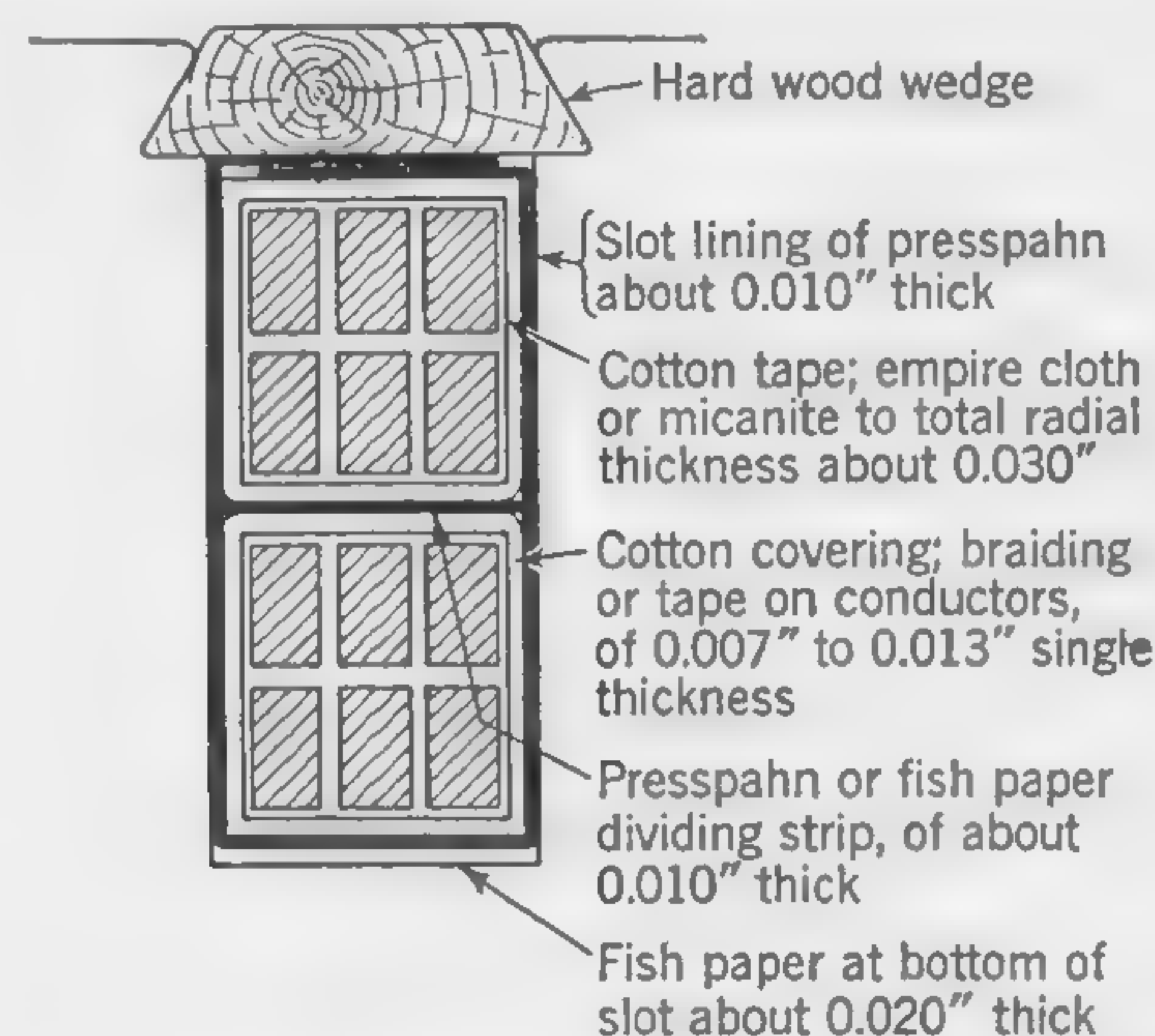


FIG. 14. Insulation of conductors in armature slot.

sides of the slot which are at ground potential. The following formula may be used for determining a suitable thickness in mils on *one side* of the slot in d-c machines for voltages between 220 and 1,500. This includes a small allowance (from 5 to 6 mils) for clearance to permit the completed coil to be forced into the slot.

$$\text{Insulation thickness in mils} = 27 + \frac{E}{30} \quad (16)$$

where  $E$  is the voltage of the dynamo or motor. This thickness of insulation must also be provided between the upper and lower coil sides in the slot.

It is important to recognize the fact that the insulating materials between the armature winding and the core, *i.e.*, the ground, must not only provide sufficient resistance to protect the machine against electrical surges as well as in normal operation, but must also act to cushion a winding that is continually subjected to mechanical vibrations and stresses. The ground-insulation thickness is, therefore, somewhat heavier than is required under static conditions. The AIEE standardization rules take

these matters into account by requiring a ground test at a 60-cycle effective emf of 1,000 plus twice the voltage rating of the machine for 1 min, the test being applied after the windings have risen to the normal operating temperature.

**14. Number of Commutator Segments—Diameter of Commutator.** Machines may be built with a number of commutator bars equal to the number of slots in the armature core. In this case there will be one coil per slot (*i.e.*, two coil sides in each slot). There is, however, no reason why the number of coil elements\* should not be greater than the number of slots. The usual number of commutator segments per slot is from one to three in low-voltage machines, with a maximum of four or five in low-speed dynamos for high voltages. A large number of bars improves commutation but increases the cost of the machine; a large diameter of commutator is necessary in order that the individual sector shall not be too thin. The copper bars are insulated from each other by mica, usually about 0.03 in. thick, increasing to  $\frac{1}{20}$  in. for machines of 1,000 volts and upward. It follows that a commutator with a very large number of segments is less easily assembled and less satisfactory from the mechanical standpoint than one with fewer segments.

The best way to determine the proper number of commutator bars for a particular design of dynamo is to consider the voltage between neighboring bars. This voltage is variable and depends upon the distribution of the magnetic flux over the armature surface, and upon the position of the armature coil under consideration. The maximum potential difference between adjacent commutator bars rarely exceeds 40 volts, and the average voltage should be considerably lower than this. The average voltage between bars may be defined as the potential difference between + and - brush sets divided by the number of commutator segments counted between the brushes of opposite sign. As a rough guide, it may be stated that the value of 15 volts (average) between segments should not be exceeded in machines without interpoles. About double this value is permissible as an upper limit on machines with commutating interpoles, especially if they are provided with compensating pole-face windings which prevent the distortion of flux distribution under load. In practice the allowable average voltage between commutator bars is based upon the machine voltage and, to some extent, upon the kilowatt output, although few designers appear to pay much attention to the influence of the current in determining the number of commutator segments. As an aid to design, the following values may be used for the purpose of deciding upon a suitable number of coils and commutator bars in machines provided with commutating poles.

\* The expression *coil element* as here used denotes that unit of an armature winding of which the ends are connected to two commutator bars.



Machine voltage	Volts between commutator segments
110 to 125	3 to 9
220 to 250	4 to 12
500 to 600	6 to 18
1,000 to 1,200	8 to 21

As the effects of any irregularities on the commutator surface are accentuated by high speeds, it is usual to limit the surface velocity of the commutator to about 4,800 fpm when possible; values as high as 6,500 fpm are sometimes permissible in high-speed, high-capacity machines when the commutators are properly designed for the upper ranges of peripheral velocities. The diameter of the commutator in large machines is generally about 60 per cent of the armature diameter, while in small machines this ratio may be as high as 0.80. The surface width of commutator bar may be from 0.17 to 0.8 in., a not uncommon width in modern interpole generators being 0.5 in. on machines for 300- to 600-kw output.

**15. Current Density in Armature Conductors.** The permissible current density in the armature windings is limited by temperature rise. The hottest accessible part of the armature, after a full-load run of sufficient duration to attain very nearly the maximum temperature, should not be more than 40 or 45°C above the room temperature. No definite rules can be laid down in the matter of armature-conductor section, because the ventilation will be better in some designs than in others, and a large amount of the heat to be dissipated from the armature core is caused by the iron loss which, in turn, depends upon the flux density in teeth and core.

The current density in the armature windings generally lies between the limits of 1,700 and 3,500 amp per sq in., although values as high as 5,000 are sometimes permissible in machines of low rating that are exceptionally well ventilated. If the armature were at rest, the permissible current density would be approximately inversely proportional to the specific loading  $q$  (*i.e.*, to the ampere-conductors per inch of armature periphery). When the armature is rotating, the additional cooling effect due to the movement through the air will be some function of the peripheral velocity, and, for speeds up to about a mile a minute—or (say) 6,000 fpm—the permissible increase of current density will be approximately proportional to the increase in speed. The constants for use in an empirical formula expressing these relations are determined from tests on actual machines, and the following formula is proposed for use in deciding upon a suitable current density in the armature winding:

$$\Delta = \frac{k}{q} + \frac{v}{4} \quad (17)$$

where  $\Delta$  and  $v$  stand for amperes per square inch and peripheral velocity in feet per minute respectively, and  $k$  is a constant between 400,000 and 700,000, an average value being 500,000. (The higher values of  $k$  should be used in machines that are especially well ventilated.)

**16. Armature-winding Resistance and Core Length.** Before the resistance drop and the  $I^2R$  losses in the armature can be calculated, it is necessary to estimate the length of wire in a coil. This length may be considered as made up of two parts: (1) the “active” part, being the straight portion in the slots, and (2) the end connections.

The appearance of the end connection is generally as shown in Fig. 15, and, since the pitch of the coil is measured on the circumference of the

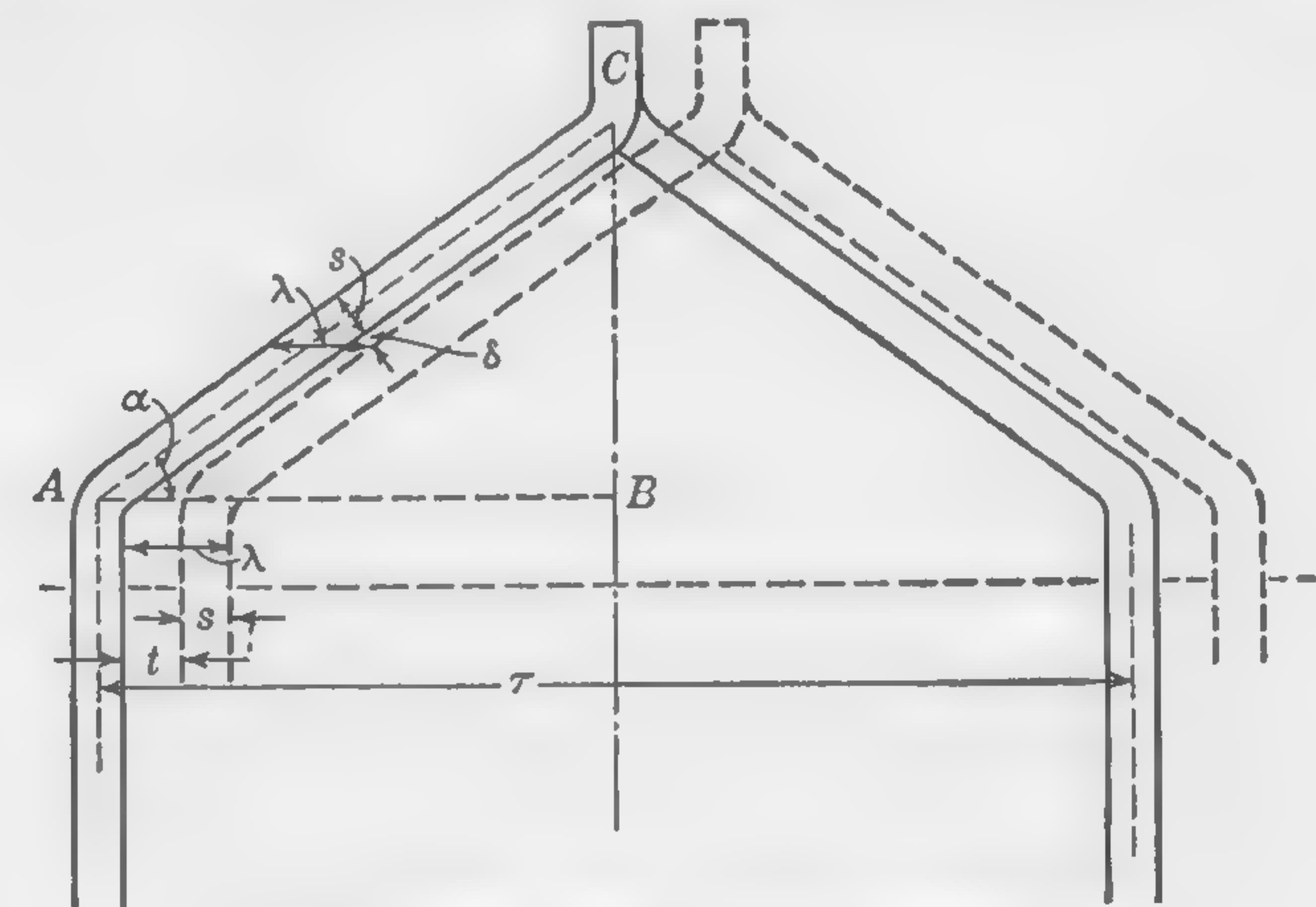


FIG. 15. End connections of armature coil.

armature core, the sketch actually represents the coils laid out flat, before springing into the slots.

The angle  $\alpha$  which the straight portion of the end connections makes with the edge of the armature core is  $\sin^{-1} [(s + \delta)/\lambda]$  where  $\lambda$  is the slot pitch,  $s$  the slot width, and  $\delta$  any necessary clearance between the coils. This clearance, about 10 to 15 mils, is generally provided to improve ventilation. For approximate calculations on machines up to 600 volts, the angle  $\alpha$  may be calculated from the relation  $\sin \alpha = 1.15s/\lambda$ .

In practice, the angle  $\alpha$  usually lies between 30 and 40°. The length of the straight part  $AC$  (Fig. 15) is  $BA/\cos \alpha$  where  $BA$  is half the coil pitch, or  $\tau/2$  in the case of a full-pitch winding. The portion of the end connections between the end of the slot and the beginning of the straight portion  $AC$  is about  $\frac{3}{4}$  in. in low-voltage machines, increasing to 1 in. in machines for pressures between 500 and 1,500 volts. The allowance for the loop where the coil is bent over to provide for the lower half



of the coil clearing the upper layer of conductors will depend upon the depth of the coil side, and, therefore, upon the depth of the slot. If  $d$  is the total depth, in inches, an allowance equal to  $2d$  will be sufficient for this loop. The *total length* of coil outside the slots of a low-voltage armature will, therefore, be

$$l_e = \left( \frac{2\tau}{\cos \alpha} + 4d + 3 \right) \text{ in.} \quad (18)$$

where  $\tau$  must be taken to represent the coil pitch instead of the pole pitch if the winding is of the chorded or short-pitch type. For preliminary or approximate calculations, formula (18) may be simplified by making certain assumptions. For voltages between 220 and 600, an approximate formula for the total length of coil outside slots in inches is

$$l_e = \frac{9D}{p} + 5 \quad (19)$$

where  $D$  = core diameter in inches, and  $p$  = number of poles.

The average length per turn of one coil will be  $2l_a + l_e$ , where  $l_a$  is the gross length of the armature core. A small addition should be made for the connections to the commutator, especially if the coil has few turns. The resistance of each coil, and therefore, of each electrical path through the armature, may now be readily calculated. In arriving at the resistance of the armature as a whole—and this is calculated for a temperature of  $75^\circ\text{C}$ —it is important to note carefully the number of coils in series in each armature path, and the number of paths in parallel between the terminals of the machine. As a check on the calculated figures, the  $IR$  drop, or the  $I^2R$  loss, in the armature of commercial machines, expressed as a percentage of the terminal voltage or of the rated output, as the case may be, is usually as stated below:

	Per cent
In 10-kw dynamo.....	4.0 to 5.3
In 30-kw dynamo.....	2.8 to 3.8
In 50-kw dynamo.....	2.4 to 3.2
In 100-kw dynamo.....	1.8 to 2.5
In 200-kw dynamo.....	1.4 to 2.0
In 300-kw dynamo.....	1.0 to 1.6
In 500-kw dynamo.....	0.8 to 1.3
In 1,000-kw dynamo.....	0.6 to 1.2

In order to calculate the weight of iron and the flux density in an armature core, it is necessary to determine the total thickness of iron in the armature stampings, or the net axial length of the armature core.

This is simply the gross length of the armature core *less* the space taken up by ventilating ducts and insulation between armature stampings. Even when a suitable allowance has been made for the spaces between the assembled sections of the armature core, a further correction must be made to allow for the varnish between the stampings. The space taken up by this insulation will vary between 7 and 10 per cent of the total space. Thus, if  $l_a$  is the gross length of the armature core, and  $l_v$  the total width of all vent ducts, the net length of the armature core will be

$$l_n = 0.92(l_a - l_v) \quad (20)$$

if the space occupied by the insulation between laminations is 8 per cent. The ventilating spaces in self-cooling machines consist of radial ducts provided by inserting special ventilating plates at intervals of 2 to 4 in.,

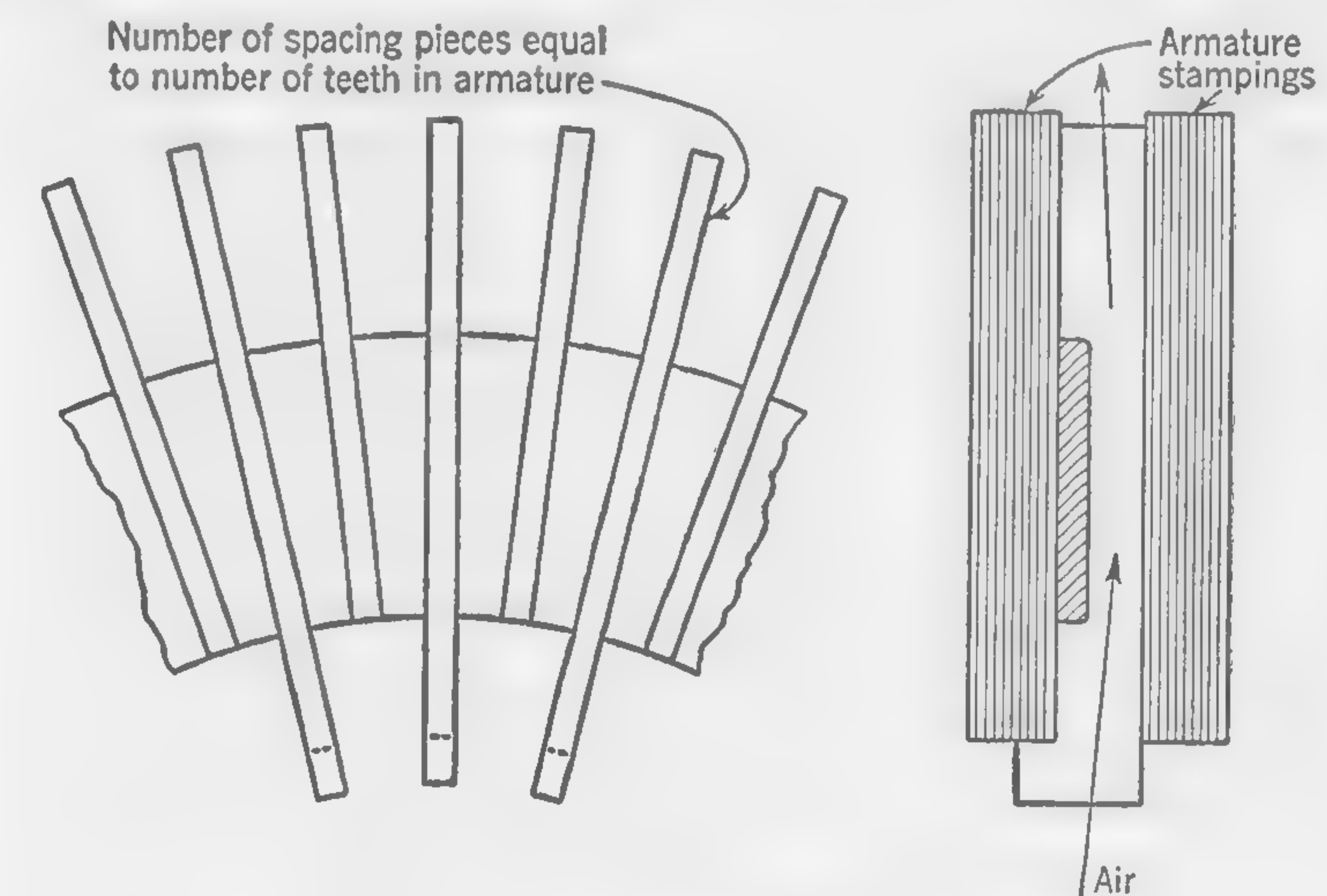


FIG. 16. Cast brass ventilating plate.

and so dividing the armature core into sections around which the air can circulate. The width of these ventilating spaces (measured in a direction parallel to the axis of rotation) is rarely less than  $\frac{3}{8}$  or more than  $\frac{1}{2}$  in. in machines without forced ventilation. A narrower opening is likely to become choked up with dust or dirt, while the gain due to a wider opening is very small and does not compensate for the necessary increase in gross length of armature. The ventilating plates usually consist of iron stampings similar in shape to the armature stampings, but thicker. Radial spacers of no great width, but of sufficient strength to resist crushing or bending, are riveted or spot-welded to the flat plates; they are so spaced as to coincide with the center of each tooth and allow



the air to pass outward by providing a number of small openings on the cylindrical surface of the armature. Brass castings are also used to separate the sections of armature stampings (see Fig. 16).

Openings must also be provided between the shaft and the inside bore of the armature, through which the cool air may be drawn to the radial ventilating ducts. The radial spacers on the ventilating plates assist the passage of the air through the ducts, their function being similar to that of the vanes in a centrifugal fan.

**17. Armature Core and Teeth—Usual Flux Densities.** The flux density in the core below the teeth will be determined by considerations of both heating and efficiency. The same thing may be said of the tooth density, but in this case the total weight of iron is relatively small, and higher densities are permissible. It is desirable to have a high flux density in the teeth because this leads to a "stiffer" field and reduces the distortion of air-gap flux distribution caused by the armature current. Better voltage regulation is thus obtained, and also improved commutation. If the density in the teeth is forced to very high values, the losses will be excessive, especially if the frequency is also high; another disadvantage is the large magnetizing force necessary to overcome the reluctance of the teeth.

The accompanying table gives the flux densities in teeth and core that are rarely exceeded in ordinary designs of continuous-current machines.

UPPER LIMITS OF FLUX DENSITY IN DYNAMO ARMATURES  
(Maxwells per Sq In.)

Frequency, $f$	Density in teeth (at center)	Density in core
10	150,000	95,000
20	142,000	90,000
30	135,000	85,000
40	130,000	80,000
50	126,000	76,000
60	123,500	73,000

For preliminary calculations and the proportioning of tooth and slot widths it is sufficient to determine the "apparent" tooth density which is always somewhat greater than the actual density. The whole of the flux from each pole is supposed to enter the armature through the teeth under the pole (the effect of fringing at pole tips being neglected); and, if the teeth are not of uniform section throughout their length, the average section will be used for calculating the "apparent" flux density.

Thus, let

$\Phi$  = the total flux per pole

$\tau$  = pole pitch

$\lambda$  = tooth pitch

$t$  = width of tooth at center

$l_n$  = net length of iron in armature

$r$  = ratio  $\frac{\text{pole arc}}{\text{pole pitch}}$

then the number of teeth under each pole is  $r(\tau/\lambda)$  and the flux per tooth is  $\Phi\lambda/r\tau$ . The flux density in the tooth, on the assumptions previously made, would, therefore, be  $\Phi\lambda/r\tau l_n$  gauss, if the dimensions are expressed in centimeters.\*

**18. Illustrative Example. Design of D-C Generator Armature.** Design an armature suitable for a d-c generator provided with commutating poles, to run at 1,200 rpm and develop 230 volts on open circuit and 250 volts at full-load output of 300 kw. The particulars contained in the design sheet (see p. 42) are more than sufficient for the needs of the practical designer; but they serve a useful purpose as a guide in making the calculations. The items are numbered for easy reference, and it will be found convenient to calculate the required dimensions and quantities generally in the order given, although the particular arrangement here adopted need not be adhered to rigidly. Two columns are provided for the numerical values, and they are supposed to be filled in as the work proceeds. The first of these columns is to be used for assumed values or preliminary estimates, while the last column is reserved for the corrected final values.

The actual calculations follow the design sheet, and they are shown in sufficient detail to be self-explanatory. The calculation of items of which the numerical values are obviously derived from previously obtained quantities will not always be shown in detail. The design sheet should be followed item by item, and, where the method of calculation is not clear, the succeeding pages should be consulted for explanations and references to the text.

All numerical calculations have been worked out on the slide rule, and a high degree of accuracy in the results is not claimed.

\*The tooth density depends upon the *maximum* value of the air-gap density, which is here supposed to be given by the expression  $\Phi/r\tau l_a$ , where  $l_a$  is the gross length of the armature core. Actually, the maximum value of the air-gap density would be somewhat less than this on open circuit, and somewhat more under full-load conditions because of the unequal distribution of the flux density under the pole face due to armature reaction.



## DESIGN SHEET FOR ARMATURE OF D-C GENERATOR—PART 1

Item No.	Specifications: 300 kw; 230/250 volts; 1,200 rpm	Symbol	Preliminary or assumed values	Final values
<i>Armature Core and Winding</i>				
1	Number of poles.....	$p$	6	6
	Frequency.....	$f$	.....	60
2	Ratio of pole arc to pole pitch.....	$r$	0.64	0.64
3	Specific loading.....	$q$	850	875
4	Apparent air-gap flux density (open circuit).....	$B_g''$	57,500	50,700
5	Line current (full load).....	$I$	.....	1,200
6	Type of winding.....	.....	.....	lap
7	Armature current per circuit.....	$I_c$	201.8	.....
8	Output factor ( $l_a D^2$ ).....	.....	4,850	4,970
9	Armature diameter, in.....	$D$	22	22
10	Peripheral velocity, fpm.....	$v$	6,900	6,900
11	Total number of face conductors.....	$Z$	292	300
12	Number of slots.....	$S$	.....	75
13	Number of conductors per slot.....	.....	.....	4
14	Axial length of armature core; gross, in.....	$l_a$	9.75	10.25
15	Flux per pole (open circuit).....	$\Phi$	$3.833 \times 10^6$	.....
16	Pole pitch, in.....	$\tau$	11.5	.....
17	Pole arc, in.....	$r\tau$	7.37	.....
18	Area covered by pole face ( $r\tau l_a$ ), sq in.....	.....	71.8	75.5
19	Dimensions of armature conductors, in. units.....	.....	.....	$2(0.07 \times 0.58)$
20	Slot pitch, in.....	$\lambda$	.....	0.922
21	Slot width, in.....	$s$	.....	0.4
22	Slot depth, in.....	$d$	.....	1.4
23	Tooth width, in. At top.....	$t$	.....	0.522
	At root.....	.....	.....	0.405
	Average.....	.....	.....	0.463
24	Number of radial ventilating ducts.....	$n$	.....	3
25	Width of radial ducts, in.....	.....	.....	0.375
26	Net length of armature core, in.....	$l_n$	7.94	8.40
27	Net tooth section under pole, at center, sq in.....	.....	29.4	31.2
28	Apparent density in teeth under pole, at center, sq in.....	$B_t''$	130,300	123,100
29	Length per turn of armature coil, in.....	.....	.....	56
30	Resistance of one turn, ohms at 60°C.....	.....	.....	0.000542
31	Resistance of armature, ohms.....	.....	.....	0.0023
32	$IR$ drop in armature, volts.....	.....	.....	2.74
33	$I^2R$ loss in armature winding, watts.....	.....	.....	3,320
34	Estimated full-load flux per pole.....	.....	.....	$4.27 \times 10^6$
35	Flux density in armature core below teeth.....	.....	73,000	72,600
36	Internal diameter of core stampings, in.....	.....	.....	12.2
37	Weight of iron in core (without teeth), lb.....	.....	.....	407
38	Weight of iron in teeth, lb.....	.....	.....	115
39	Total weight of armature stampings, lb.....	.....	.....	522

## DESIGN OF ARMATURE WINDING AND CORE

*Item 1: Number of Poles and Frequency.* Refer to Art. 3. Either six or eight poles might be suitable, but, since the armature speed is fairly high, six poles will probably be best for a trial design. The frequency is, therefore,

$$f = \frac{6 \times 1,200}{120} = 60$$

*Item 2: Ratio of Pole Arc to Pole Pitch.* Refer to Art. 2. Since the machine will be provided with commutating poles, a suitable value for this ratio is  $r = 0.64$ .

*Items 3 and 4: Specific Loading and Air-gap Density.* Refer to Art. 2. From the table on page 12, select  $q = 850$ , and from table on page 11, select  $B_g'' = 57,500$ . These are tentative selections and will be modified to suitable values as the design proceeds.

*Item 5: Line Current.*  $I = 300,000/250 = 1,200$  amp.

*Item 6: Type of Winding.* Refer to Art. 6. Since the current per path should not exceed 250 to 300 amp it is clear that a lap winding must be used in this case. (A wave winding with two parallel paths would make  $I_c$  about  $1,200/2 = 600$  amp.)

*Item 7: Armature Current per Circuit.* The current in each armature circuit will be one-sixth of the line current if the shunt-exciting current is neglected. A table giving usual values of shunt-field current, expressed as a percentage of the output current, will be found on page 121. Assuming a shunt excitation of 0.9 per cent, the full-load current in each armature conductor will be about  $(1,200/6)(1 + 0.009) = 201.8$  amp.

*Items 8, 9, and 10: Armature Diameter.* Refer to Art. 2. By formula (7)

$$l_a D^2 = \frac{300,000}{1,200} \times \frac{6.06 \times 10^8}{57,500 \times 0.64 \times 850} = 4,850$$

using a rectangular pole face, where  $k$  in Eq. (8) equals 0.71

$$l_a = \frac{\pi \times 0.64}{6 \times 0.71} \times D = 0.472D$$

Hence

$$D = \sqrt[3]{4,850/0.472} = \sqrt[3]{10,600} = 22 \text{ in.}$$

A rectangular pole face, with the armature length equal to about 1.4 times the pole arc, is desirable in this design because of the comparatively high speed. For the diameter calculated, the peripheral velocity



will be

$$v = \frac{\pi \times 22 \times 1,200}{12} = 6,900 \text{ fpm}$$

Before proceeding with the design, it will be well to see whether or not a number of poles different from the number selected from the trial calculation would be satisfactory. The following numerical quantities should be checked against the usual values found in commercial machines.

a. The frequency  $f = 60$  is near the upper permissible limit; if eight poles were selected the frequency would be 80 cps, an excessive value.

b. The peripheral velocity  $v = 6,900$  fpm is reasonable from the standpoint of mechanical stresses and good ventilation.

c. The ampere-conductors per pole rarely exceed 25,000 (see p. 14). A large pole pitch  $\tau$ , due to a small number of poles, calls for a greater amount of iron in the magnetic circuit and a larger air gap under the pole face to reduce the effect of armature reaction on the flux distribution in the air gap. In this design, the approximate number of armature ampere-conductors per pole

$$\frac{ZI_c}{p} = \frac{ZI_c}{p} \times \frac{\pi D}{\pi D} = \frac{q\pi D}{p} = \frac{850\pi \times 22}{6} = 9,800$$

which is well below the upper limit. The design may, therefore, proceed on the basis of six poles.

Items 11, 12, and 13: *Number of Inductors, Slots, and Conductors per Slot.* Refer to Art. 2.

$$Z = \frac{\pi Dq}{I_c} = \frac{\pi \times 22 \times 850}{201.8} = 292$$

With four conductors per slot, this would mean a preliminary number of slots of  $292\frac{1}{4} = 73$ , and a slot pitch  $\lambda$  of  $\pi \times 22/73 = 0.945$ ; see Art. 12, and note that this is reasonable. Next, calculating the number of slots per pole it is found to be  $73/6 = 12\frac{1}{6}$ . However, since it is desirable to have an odd integer of slots per pair of poles so that the slots per pole will be an integer plus  $\frac{1}{2}$ , the total number of slots will be increased to 75; thus, slots per pair of poles equal  $75/3 = 25$ , and slots per pole equals  $12\frac{1}{2}$ . Also note that the number of slots embraced by each pole arc is an integer in this design; i.e.,  $12\frac{1}{2} \times 0.64 = 8$ . With the final value of  $Z = 300$ ,  $q$  is, therefore,  $300 \times 201.8/22\pi = 875$ .

Item 14: *Axial Length of Armature Core.* This may be determined from the final value of the output factor  $l_a D^2$ ; since this is inversely proportional to  $q$ , it is equal to

$$l_a D^2 = 4,850 \times 850/875 = 4,710$$

and

$$l_a = \frac{4,710}{(22)^2} = 9.75 \text{ in.}$$

This length is, however, subject to correction if later flux density calculations indicate that this is desirable.

Item 15: *Flux per Pole (Open Circuit).* Using the value of  $Z$ , determined in item 11,

$$\Phi = \frac{230 \times 60 \times 6 \times 10^8}{6 \times 1,200 \times 300} = 3,833,000 \text{ maxwells}$$

Items 16, 17, and 18: *Pole Pitch, Pole Arc, and Pole Area.*

$$\text{Pole pitch } \tau = \frac{\pi \times 22}{6} = 11.5 \text{ in.}$$

Pole arc  $= r\tau = 0.64 \times 11.5 = 7.37$  in. Note that  $l_a/r\tau = 9.75/7.37 = 1.32$  instead of the value 1.4, originally assumed.

Pole area  $= r\tau l_a = 7.37 \times 9.75 = 71.8$  sq in.

The apparent air-gap flux density can now be computed and compared with the assumed value in item 4.

Thus,

$$B'_a = \frac{3,833,000}{71.8} = 53,400 \text{ lines per sq in.}$$

Note that this is less than the assumed value as used in formula (7) for the calculation of the output factor.

Items 19 to 22: *Dimensions of Slots and Armature Conductors.* By formula (17) on page 36, for a well-ventilated machine

$$\Delta = \frac{700,000}{875} + \frac{6,900}{4} = 2,525 \text{ amp per sq in.}$$

whence

$$\text{Area of cross section} = \frac{I_c}{\Delta} = \frac{201.8}{2,525} = 0.080 \text{ sq in.}$$

It is necessary now to find by trial the best arrangement of 300 conductors, item 11, in 75 slots, item 12.

The slot pitch (refer to Art. 12) is

$$\lambda = \frac{\pi \times 22}{75} = 0.922 \text{ in.}$$

In order to determine the actual dimensions of the armature conductors, it will first be convenient to assume a width of slot. This should be about 0.4 in., which makes the ratio of tooth width to slot



width 1.305, a reasonable value. Since a wire having an area of 0.08 in. is rather heavy and difficult to bend and shape, it will be desirable to use two conductors in parallel in the winding copper and to arrange them as shown in Fig. 17. This arrangement suggests itself because there exists the possibility of having either twice as many commutator segments as slots or the same number of segments as slots.

The width of each of the four side-by-side rectangular conductors will now be determined. The slot insulation on each side of the slot, by formula (16), is  $27 + (250/30) = 35$  mils, and the cotton covering on each conductor will add a total of about 16 mils to its thickness. The space left for each of the four copper conductors is, therefore,

$$\frac{0.4 - (3 \times 0.016) - (2 \times 0.035)}{4} = 0.07 \text{ in.}$$

Since the copper area of two conductors is 0.08 sq in. it follows that each conductor will have a depth of

$$\frac{0.08}{2 \times 0.07} = 0.572 \text{ in., or (say) } 0.58 \text{ in.}$$

Finally, the slot depth can be determined. Allowing about one-third of the slot width for the hardwood or fiber wedge, or 0.135 in., and 35 mils for each of the insulation spaces above, below, and between the coils,

$$d = 0.135 + (3 \times 0.035) + (2 \times 0.58) = 1.4 \text{ in.}$$

Thus, in Fig. 17,  $s = 0.4$  in., and  $d = 1.4$  in.

Using the dimensions thus far calculated, it will be desirable to check and see if the flux density in the teeth is not excessive (item 28).

**Item 23: Tooth Dimensions.** The width at the top of the tooth is  $t = \lambda - s = 0.922 - 0.4 = 0.522$  in.

The circumference of the circle through the bottom of the slots is  $\pi \times (22 - 2.8) = 60.3$ ; and since the slots have parallel sides, the width of tooth at the root is  $(60.3/75) - 0.4 = 0.405$  in.

The average tooth width is, therefore, 0.463 in.

**Items 24 and 25: Ventilating Ducts.** Refer to Art. 16. Not more than three ducts should be necessary in an armature 9 to 11 in. long, with each duct  $\frac{3}{8}$  in. wide.

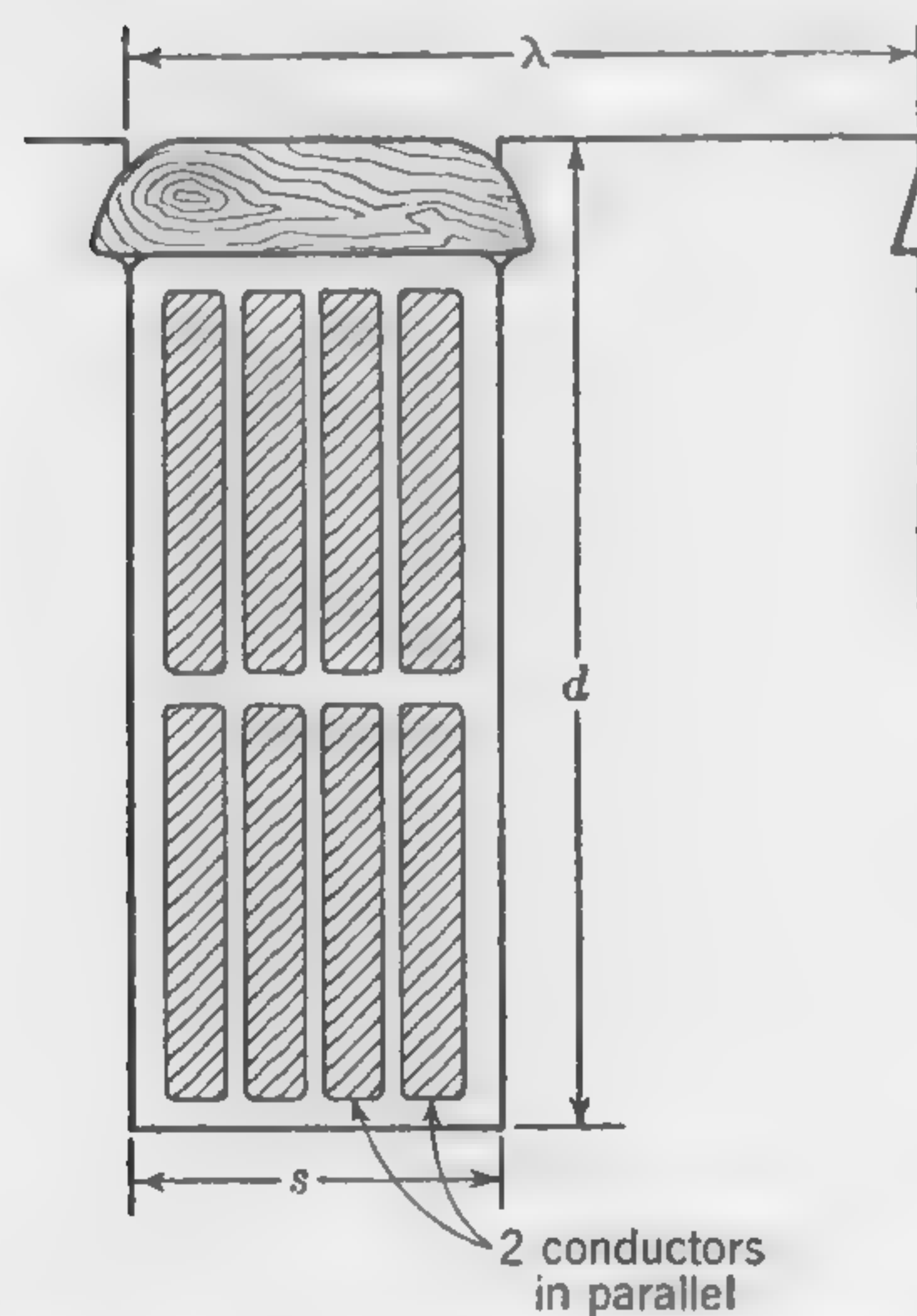


FIG. 17. Arrangement of conductors in slot.

**Item 26: Net Length of Armature.** Refer to Art. 16.

$$l_n = 0.92(9.75 - 3 \times 0.375) = 7.94$$

**Item 27: Net Cross Section of Teeth under Pole.** The cross section of iron in the teeth under one pole, at the midsection, is

$$7.94 \times 0.463 \times \frac{7}{8} \times 0.64 = 29.4 \text{ sq in.}$$

**Item 28: Flux Density in Teeth.** Refer to Art. 17. The apparent flux density at the center of the tooth, under open-circuit conditions, is,

$$\frac{3,833,000}{29.4} = 130,300 \text{ lines per sq in.}$$

Note that this value is above the upper limit given in the table on page 40 for 60 cycles. It will, therefore, be necessary to correct (increase) the length of the armature core to bring the flux density down to a reasonable figure. After some preliminary calculations an armature length  $l_a = 10.25$  in. was found to be satisfactory. Thus,

$$l_a D^2 = 10.25 \times 22^2 = 4,970$$

$$B'_o = \frac{3,833,000}{7.37 \times 10.25} = 50,700 \text{ lines per sq in.}$$

$$r\tau l_a = 7.37 \times 10.25 = 75.5 \text{ sq in.}$$

$$l_n = (10.25 - 1.125)0.92 = 8.4 \text{ in.}$$

$$B'_t = \frac{7.94}{8.4} \times 130,300 = 123,100 \text{ lines per sq in.}$$

**Item 29: Length per Turn of Armature Coil.** Referring to Art. 16,

$$\sin \alpha = \frac{1.15s}{\lambda} = \frac{1.15 \times 0.4}{0.922} = 0.5; \cos \alpha = 0.866$$

By formula (18),

$$l_s = \frac{2 \times 11.5}{0.866} + (4 \times 1.4) + 3 = 35.2 \text{ in., or (say) } 35.5 \text{ in.}$$

Therefore, the total length per turn  $= l_s + 2l_a = 35.5 + 20.5 = 56$  in.

**Items 30 to 33: Armature Resistance.** Since the resistance of a conductor of a given material at a given temperature is directly proportional to its length and inversely proportional to its cross section, a very convenient and easily remembered rule is that the resistance of copper is 1 ohm per cir-mil inch at a temperature of 60°C. Therefore, the resistance of one turn at 60°C will be

$$R = \frac{56}{2(0.07 \times 0.58) \times \frac{1}{\pi} \times 10^6} = 0.000542 \text{ ohm}$$



there being  $(4/\pi) \times 10^6$  cir mils in 1 sq in. With a total of  $300\frac{1}{2} = 150$  turns divided into six parallel paths (a six-pole lap winding), the resistance per circuit will be  $0.000542 \times (150/6) = 0.0136$  ohm, and the total armature resistance will be one-sixth of this, or 0.0023 ohm.

The  $IR$  drop in the armature winding is  $0.0136 \times 201.8 = 2.74$  volts, or 1.1 per cent of the full-load terminal voltage. This compares favorably with the approximate figures given in Art. 16.

The watts lost in the armature winding (item 33) are  $2.74 (201.8 \times 6) = 3,320$ .

*Item 34: Full-load Flux.* More flux must enter the armature at full load than at no load because the speed is assumed to be constant and the terminal emf is higher. Moreover, in addition to the specified increase in *terminal* voltage from 230 at no load to 250 at full load, it is necessary to *develop* (generate) enough voltage to overcome the internal resistances. Assuming a brush-contact drop of 2 volts, and a series-field and commutating-field drop of about one-half that in the armature winding, the total generated voltage at full load must be

$$250 + 2 + 2.74 + 1.37 = 256.1 \text{ volts}$$

The full-load flux must, therefore, be

$$3,833,000 \times \frac{256.1}{230} = 4,270,000 \text{ maxwells}$$

*Items 35 and 36: Flux Density in Armature Core. Internal Diameter.* Usual flux densities for different frequencies are given in the table in Art. 17. A density of 73,000 will be suitable. Bearing in mind that the air-gap flux divides into two equal parts below the teeth, the armature-core flux is one-half of the total flux. Therefore,

$$R_d \times l_n \times 73,000 = \frac{\Phi}{2}$$

whence the radial depth  $R_d$  of the armature core below the teeth is

$$R_d = \frac{4,270,000}{2 \times 8.4 \times 73,000} = 3.48 \text{ in., or (say) 3.5 in.}$$

The internal diameter of the core stampings is, therefore,

$$22 - (2 \times 3.5) - (2 \times 1.4) = 12.2 \text{ in.}$$

*Item 37: Weight of Iron in Core.* The weight of a cubic inch of iron is 0.28 lb, and the total weight of iron in the core below the teeth will, therefore, be

$$0.28 \times 8.4 \times \frac{\pi}{4} [(22 - 2.8)^2 - (12.2)^2] = 407 \text{ lb}$$

*Item 38: Weight of Iron in Teeth.*

$$0.28 \times 1.4 \times (0.463 \times 75) \times 8.4 = 115 \text{ lb}$$

where the figure 0.463 is the width of tooth at the center.

*Item 39: Total Weight of Armature Stampings.*

$$407 + 115 = 522 \text{ lb}$$

#### DESIGN SHEET FOR ARMATURE OF D-C GENERATOR—PART 2

Item No.	Specifications: 300 kw; 230/250 volts; 1,200 rpm	Symbol	Preliminary or assumed values	Final values
Commutator and Brushes				
40	Diameter of commutator, in.....	$D_c$	....	15
41	Average volts per turn of armature winding.	...	....	10
42	Number of turns between bars.....	...	....	1
43	Total number of commutator bars.....	...	....	150
44	Bar pitch, in.....	...	....	0.314
45	Width of copper bar (on surface), in.....	...	....	0.284
46	Radial depth of bar, in.....	...	....	2.25
47	Current density at brush-contact surface, amp per sq in.....	$\Delta_b$	40	40.4
48	Contact area per brush set, sq in.....	...	10.09	10
49	Brush arc (circumferential width), in.....	...	....	1.0
50	Axial brush length (total) per set, in.....	...	....	10
51	Number of brushes per set.....	...	....	8
52	Axial length of commutator, in.....	$L_c$	....	14.5
53	Brush-contact drop, volts.....	...	....	2.3
54	Brush-contact loss, watts.....	...	....	2,780
55	Brush-friction loss, watts.....	...	....	3,190
56	Total brush loss, watts.....	...	....	5,970
57	Drawing to scale giving leading dimensions of armature and commutator .....	...	Fig. 18	

#### DESIGN OF COMMUTATOR AND BRUSHES

The design will now proceed with the calculation of the dimensions of the commutator and brushes, and other important information concerning them. For this purpose the student will find it necessary to refer to Chap. 13 for details concerning mechanical considerations.

*Item 40: Diameter of Commutator.* Refer to Art. 14. A diameter of commutator not exceeding 80 per cent of the armature-core diameter is generally found practical, although a reasonably good rule to follow is to make  $D_c = D/2 + 4$  in. Thus,

$$D_c = 22\frac{1}{2} + 4 = 15 \text{ in.}$$



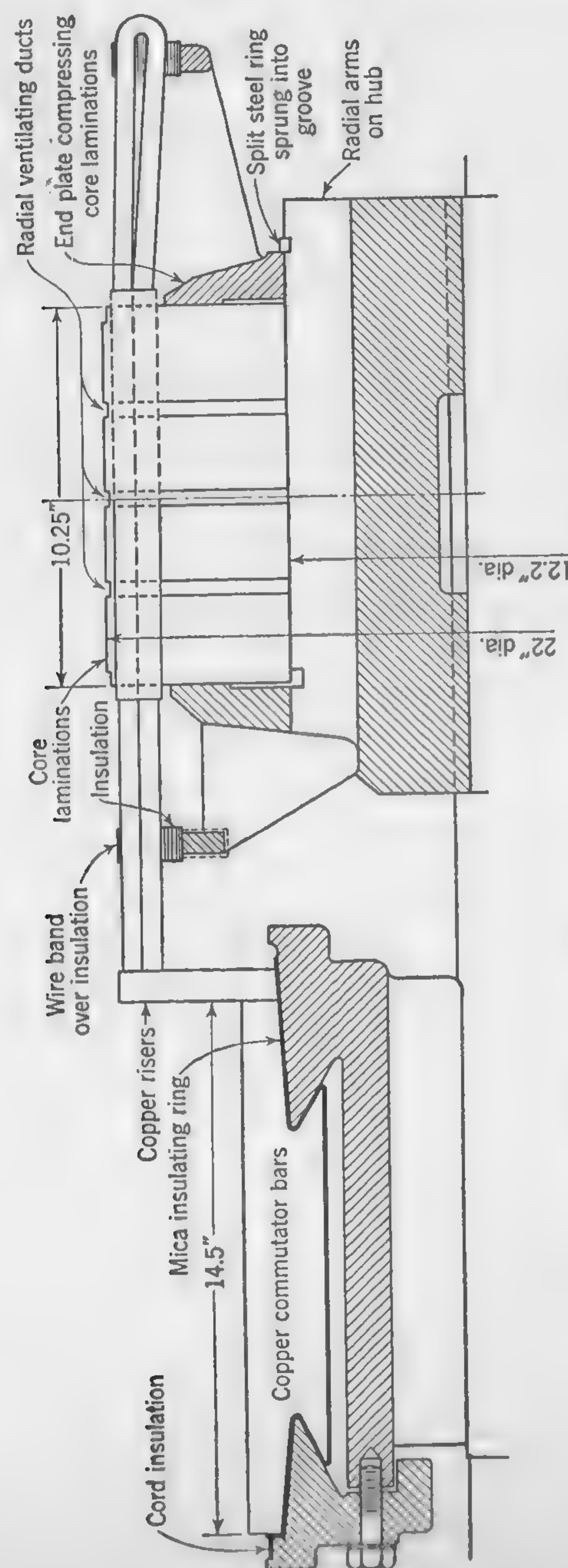


Fig. 18. Section of core and commutator for illustrative example of Art. 18.

## Art. 18 ARMATURE WINDINGS AND DESIGN PRINCIPLES 51

This is 68.2 per cent of the core diameter and makes the peripheral velocity  $0.682 \times 6,900 = 4,700$  fpm, near the upper limit. This dimension is subject to correction if the thickness of the individual bars does not work out satisfactorily.

*Items 41 to 43: Number of Commutator Bars.* The potential difference between adjacent commutator segments in a 250-volt machine might be anything between 4 and 12 volts. The average volts per turn of armature winding are

$$\frac{E}{Z/2p_1} = \frac{250}{300/12} = 10 \text{ volts}$$

If the commutator is constructed with the same number of segments as slots there will be two turns between adjacent segments; this will mean a potential difference of 20 volts between segments, because, for a lap winding and four effective conductors per slot, there will be two turns per element. The width of the commutator segment will, moreover, be excessive, as a simple calculation should indicate. It will, therefore, be desirable to use 150 commutator segments, with a resulting improvement in commutation and a more suitable, narrower, segment.

*Items 44 and 45: Width of Commutator Segments.* The bar pitch is  $\pi \times \frac{15}{150} = 0.314$  in. and, with mica 0.03 in. thick, the bar width is  $0.314 - 0.03 = 0.284$  in. at the commutator surface.

*Item 46: Radial Depth of Segment.* The proper depth of copper in the cross section of the commutator bar is usually determined by mechanical considerations (Chap. 13). It must be sufficient to prevent appreciable deflection (or bending) under the action of centrifugal force. In large machines, with commutators of considerable length, the depth of the bar should, therefore, be considered in connection with peripheral velocity and the (axial) distance between points of support. For peripheral velocities up to about 4,500 fpm the radial depth of the commutator segment should be about  $h = (D_c + 15)/15$ ; for higher peripheral speeds the depth should be increased in proportion to the square of the velocity. Thus,

$$h = \frac{15 + 15}{15} \times \frac{(4,700)^2}{(4,500)^2} = 2.19 \text{ in., or (say) 2.25 in.}$$

*Items 47 to 51: Dimensions of Brushes.* Unless a very soft quality of carbon is used, the current density over the brush-contact surface is about 30 to 50 amp per sq in., (see Fig. 38). Taking 40 as a preliminary value, to be modified later if necessary to accommodate a standard size of brush, the contact surface of one set of brushes will be  $(6 \times 201.8)/(3 \times 40) = 10.09$  sq in. A 1-in. width of brush, Art. 34, will cover a little over three bars, which is reasonable for an armature with 150 segments and simplex-lap winding. The total length of brushes per set, measured in a direction



parallel to the axis of the machine, will then be  $10.09/1.0 = 10.09$ , or (say) 10 in., which can be made up of eight brushes  $1\frac{1}{4} \times 1$  in. The current density will thus be increased slightly to  $40 \times (10.09/10) = 40.4$  amp per sq in.

*Item 52: Length of Commutator.* In addition to the 10 in. which must be provided for the eight  $1\frac{1}{4}$ -in. carbon brushes, the axial length of the commutator face must allow for the following: (a) brush holders and clearances =  $8 \times \frac{5}{16} = 2\frac{1}{2}$  in.; (b) staggering of (+) and (-) brushes =  $\frac{5}{8}$  in.; (c) end clearance for brushes = 1 in.; (d) end play =  $\frac{3}{8}$  in. The total length will, therefore, be  $L_c = 10 + 2\frac{1}{2} + \frac{5}{8} + 1 + \frac{3}{8} = 14.5$  in.

*Item 53: Brush-contact Drop.* Referring to Fig. 38, the brush-contact drop for hard carbon at about 40 amp per sq in. is 2.08. Allowing 10 per cent for roughness, chipping, and irregularities, this drop will be about 2.3 volts.

*Items 54 to 56: Brush Losses.* The brush-contact loss will be  $2.3 \times (6 \times 201.8) = 2,780$  watts.

The brush-friction loss may be calculated by using formula (48), page 143, where

$$W_f = \frac{cPAND_c\pi \times 746}{12 \times 33,000}$$

Using  $c = 0.25$  for hard carbon,  $P = 2$  lb per sq in. for a peripheral speed greater than 4,000 fpm.

$$W_f = \frac{0.25 \times 2 \times (10 \times 6) \times 1,200 \times 15 \times \pi \times 746}{12 \times 33,000} = 3,190 \text{ watts}$$

Total brush loss =  $2,780 + 3,190 = 5,970$  watts.

*Item 57.* The illustration (Fig. 18) gives the leading dimensions of armature and commutator as worked out in this design. The diameter of the shaft supporting the armature may be calculated by formula (160) in Chap. 13 treating of mechanical features of the design of electrical machinery. This is  $0.84 \sqrt[3]{\frac{300,000}{1,200}} = 5\frac{1}{4}$  in.

Another assembly of armature core and commutator, suitable for a machine of small output, is shown in Fig. 19. This construction provides openings for ventilation inside the armature core, but there is no provision for air circulation inside the commutator. The construction here shown would be suitable for small armatures with core stampings up to 16 in. in diameter.

For large machines, the design of Fig. 19 would not be suitable. Figure 20 illustrates one of many possible types of construction for machines with armatures 30 in. in diameter and larger. In this design,

the two end rings with brackets carrying the coil supports are separate from the spider, which is keyed to the shaft and drives the core stampings, as indicated in the cross section above the end view. The end rings are machined to slide inside the grooved projections on the spider arms, and, when the bolts are tightened up, the assembled armature core is held securely in position.

An alternative construction for large machines is shown in Fig. 196. This avoids the use of bolts for compressing the core stampings by substituting for them a steel ring sprung into a machined groove. The same method is used for assembling the stampings of the small armature of Fig. 19.

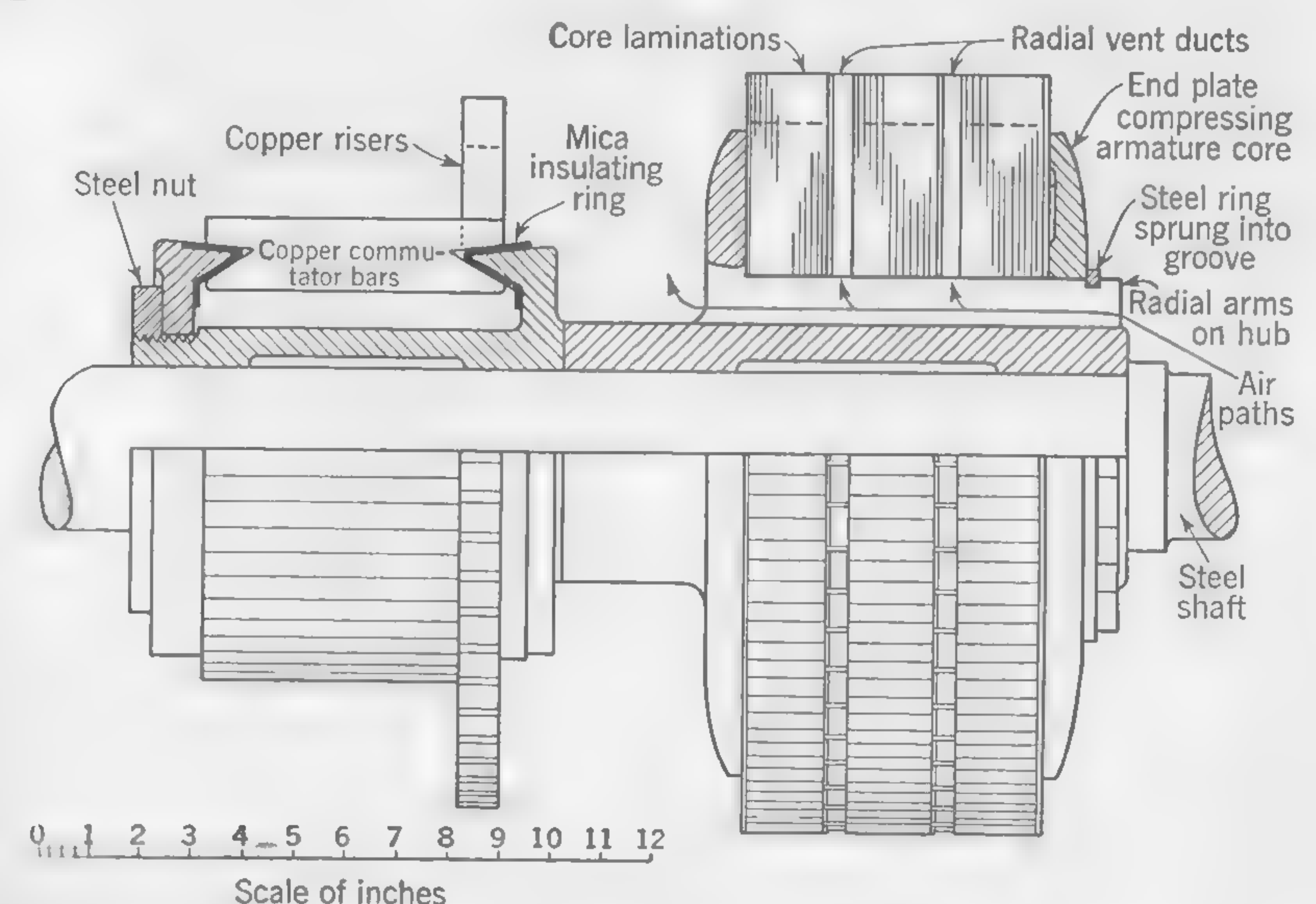


FIG. 19. Assembly of armature core and commutator for small dynamo or motor.

**19. Other Problems Connected with the Design of Direct-current Dynamos.** The manner in which the dimensions and windings of an armature for a given output, speed, and voltage may be designed has been indicated in the foregoing illustrative example, and, since the current and flux densities and the proportions generally are based on data derived from practical experience, it is probable that the design will be satisfactory. It should be noted, however, that no calculations have been made to determine the losses in the iron, or the probable temperature rise; neither is it certain that the commutator will work sparklessly at all loads. This important matter of commutation will be treated briefly in the following chapter, and the calculation of iron losses will be discussed in Chap. 6, dealing with heating and the predetermination of temperature rise.



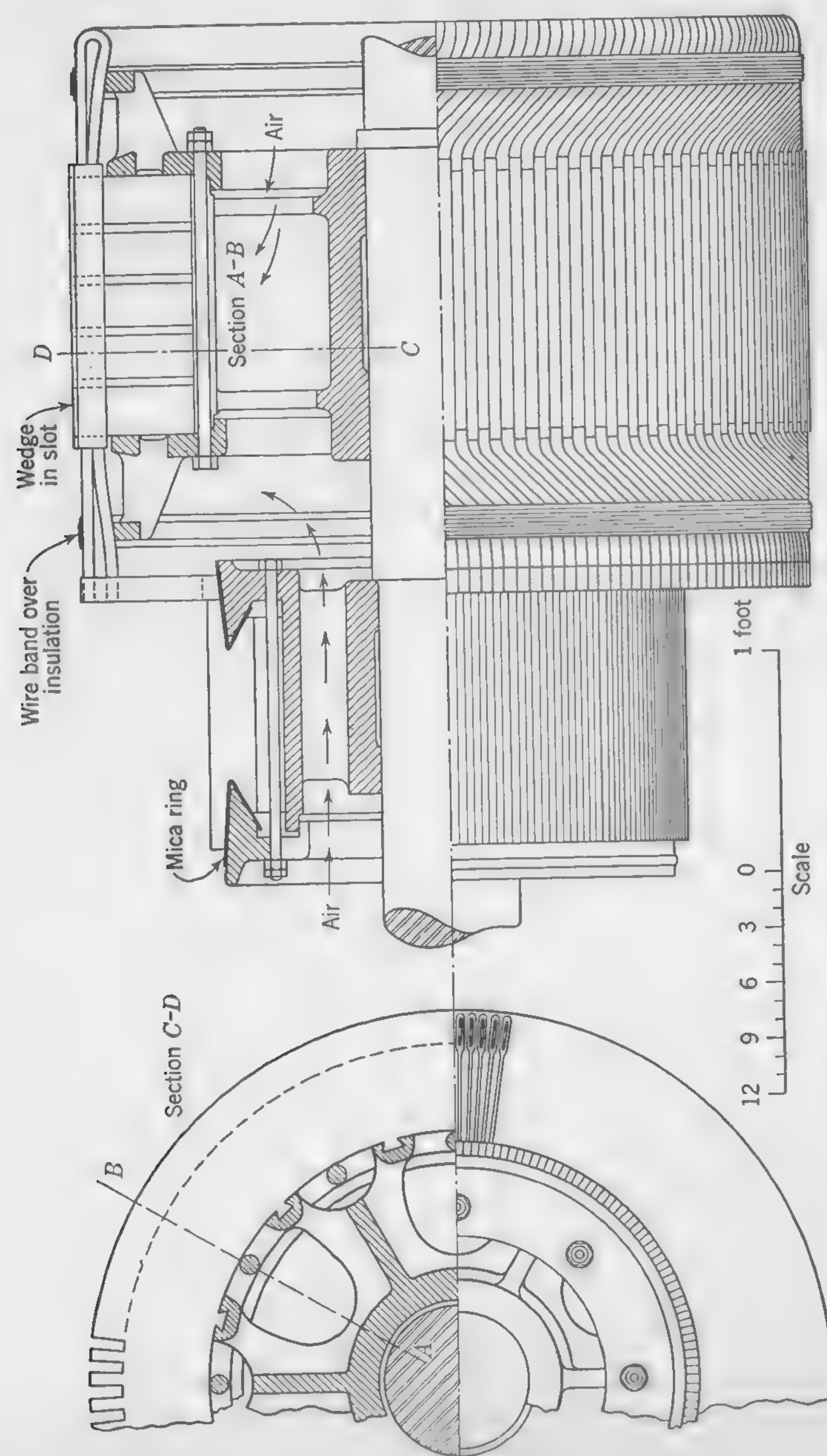


Fig. 20. Armature and commutator for d-c machine of large output.

Assuming the armature, as designed, to be satisfactory in these respects, the remainder of the problem consists in designing a field system of electromagnets capable of providing the required flux in the air gap. This problem is similar to that of designing an electromagnet for any other purpose. It might appear, therefore, that little more need be said in connection with the design of a direct-current generator, but it must be remembered that certain assumptions were made in order that the broad questions of design might not be obscured by too much detail, and in order also that the leading dimensions of the machine might be decided upon.

It was assumed that the flux in the air gap was uniformly distributed under the pole face; but is it so distributed, and, if not, how does this affect the tooth saturation and the ampere-turns required to overcome the reluctance of the teeth and gap? What is the influence of the air-gap flux distribution on armature reaction and voltage regulation, and how can we calculate the field excitation required at different loads in order that the proper terminal voltage may be obtained? These and similar questions cannot be answered without a more thorough study of the magnetic field cut by the conductors, at full load as well as on open circuit.

Again, with a nonuniform field under the poles, the flux density in the teeth may be much higher than would be indicated by calculations based on a uniform field, and this might lead to excessive heating and low efficiency.

Although this book treats of the elements of electrical machine design, the student must not overlook the fact that electric machine design is largely—in some cases, mainly—dependent upon the correct application of *mechanical* principles. Thus the strength and stiffness of shaft and bedplate, friction losses in bearings, the proper balancing of rotating parts of high-speed machines, all come within the province of the mechanical engineer.

Finally, in electrical machines and apparatus, as in every manufactured article or engineering undertaking, the chief end of the engineer is to satisfy the specified conditions *efficiently* and *economically*. Every design should perform the duty required of it and comply with the conditions of the specification in the most economical and efficient manner, and the designer should, therefore, always bear in mind:

1. First cost (material and labor)

2. Cost of losses  $\left\{ \begin{array}{l} \text{Losses in copper} \\ \text{Losses in iron} \\ \text{Mechanical losses (bearing} \\ \text{friction and windage)} \end{array} \right\} \text{Efficiency}$



3. Durability (life): mechanical strength; resistance to wear and tear (depreciation); temperature rise, which, if too high, will lead to deterioration of materials and ultimate breakdown.

A first design is rarely a final design, and the factors here mentioned may be controlled by changes in the materials, dimensions, or proportions of the machine; but they cannot be embodied in rules or formulas of general application, which, perhaps, explains why machine design is an art rather than a science, involving—in addition to a sound knowledge of fundamentals—the “engineering judgment” which comes from experience and enables the practiced designer to make a close estimate of the required proportions or dimensions. All such estimates are finally checked by applying tests based upon established scientific principles or fundamental laws.

The various matters here briefly referred to will be taken up in more or less detail as occasion arises. An effort will be made to avoid introducing any subject not necessary for the solution of the particular problem under consideration. The main purpose of the following chapters is to illustrate how the fundamental principles presented in the earlier chapters may be applied to the solution of practical design problems.

### TEST PROBLEMS

1. Given a d-c dynamo: developed volts = 100; total number of slots = 53; number of inductors per slot = 6; number of poles = 4; speed = 1,000 rpm; winding, series (or wave). Calculate the flux per pole. *Ans.* 943,000 maxwells.

2. A certain four-pole simplex-lap-wound d-c generator has 768 armature inductors and revolves at 20 rps. If the flux per pole = 715,000 maxwells, calculate the generated voltage. *Ans.* 109.8 volts.

3. The lap-wound armature of a six-pole generator has 600 active conductors. The speed is 1,000 rpm. The area of each pole face is 100 sq in., and the average air-gap flux density under the pole face is 8,000 gauss. Calculate the emf between positive and negative brushes. *Ans.* 516 volts.

4. A shunt-wound 12-pole 500-kw dynamo, with simplex-lap-wound armature, has a terminal emf of 600 volts at full load. The armature is wound with 5,000 ft of copper wire of 40,000 cir mils cross section. Assuming 2 volts drop at the brushes, and neglecting the current in the field coils, calculate the emf which must be developed in the armature at full load. (Ohms per circular mil-foot = 12.) *Ans.* 610.7 volts.

5. The average value of the emf induced in a single full-pitch armature coil in a 10-pole generator is 10 volts. Calculate the number of turns in the coil, given that the speed of the armature is 250 rpm, and that the useful flux per pole is 2,000,000 maxwells. *Ans.* 6.

6. It is desired to connect nine equalizer rings to the proper commutator bars of a 10-pole lap-wound d-c generator, and to space them uniformly. If there are 270 commutator bars on the machine, what numbered bars must be connected to ring 1 and to ring 3, given that bar 1 is connected to ring 1? *Ans.* 1, 55, 109, 163, 217, 271, 325, 379, 433, 487, 541, 595, 649, 703, 757, 811, 865, 919, 973, 1027, 1081, 1135, 1189, 1243, 1297, 1351, 1405, 1459, 1513, 1567, 1621, 1675, 1729, 1783, 1837, 1891, 1945, 1999, 2053, 2107, 2161, 2215, 2269, 2323, 2377, 2431, 2485, 2539, 2593, 2647, 2701, 2755, 2809, 2863, 2917, 2971, 3025, 3079, 3133, 3187, 3241, 3295, 3349, 3403, 3457, 3511, 3565, 3619, 3673, 3727, 3781, 3835, 3889, 3943, 3997, 4051, 4105, 4159, 4213, 4267, 4321, 4375, 4429, 4483, 4537, 4591, 4645, 4699, 4753, 4807, 4861, 4915, 4969, 5023, 5077, 5131, 5185, 5239, 5293, 5347, 5401, 5455, 5509, 5563, 5617, 5671, 5725, 5779, 5833, 5887, 5941, 5995, 6049, 6103, 6157, 6211, 6265, 6319, 6373, 6427, 6481, 6535, 6589, 6643, 6697, 6751, 6805, 6859, 6913, 6967, 7021, 7075, 7129, 7183, 7237, 7291, 7345, 7399, 7453, 7507, 7561, 7615, 7669, 7723, 7777, 7831, 7885, 7939, 7993, 8047, 8101, 8155, 8209, 8263, 8317, 8371, 8425, 8479, 8533, 8587, 8641, 8695, 8749, 8803, 8857, 8911, 8965, 9019, 9073, 9127, 9181, 9235, 9289, 9343, 9397, 9451, 9505, 9559, 9613, 9667, 9721, 9775, 9829, 9883, 9937, 9991, 10045, 10099, 10153, 10207, 10261, 10315, 10369, 10423, 10477, 10531, 10585, 10639, 10693, 10747, 10801, 10855, 10909, 10963, 11017, 11071, 11125, 11179, 11233, 11287, 11341, 11395, 11449, 11503, 11557, 11611, 11665, 11719, 11773, 11827, 11881, 11935, 11989, 12043, 12097, 12151, 12205, 12259, 12313, 12367, 12421, 12475, 12529, 12583, 12637, 12691, 12745, 12799, 12853, 12907, 12961, 13015, 13069, 13123, 13177, 13231, 13285, 13339, 13393, 13447, 13501, 13555, 13609, 13663, 13717, 13771, 13825, 13879, 13933, 13987, 14041, 14095, 14149, 14203, 14257, 14311, 14365, 14419, 14473, 14527, 14581, 14635, 14689, 14743, 14797, 14851, 14905, 14959, 15013, 15067, 15121, 15175, 15229, 15283, 15337, 15391, 15445, 15499, 15553, 15607, 15661, 15715, 15769, 15823, 15877, 15931, 15985, 16039, 16093, 16147, 16201, 16255, 16309, 16363, 16417, 16471, 16525, 16579, 16633, 16687, 16741, 16795, 16849, 16903, 16957, 17011, 17065, 17119, 17173, 17227, 17281, 17335, 17389, 17443, 17497, 17551, 17605, 17659, 17713, 17767, 17821, 17875, 17929, 17983, 18037, 18091, 18145, 18199, 18253, 18307, 18361, 18415, 18469, 18523, 18577, 18631, 18685, 18739, 18793, 18847, 18901, 18955, 19009, 19063, 19117, 19171, 19225, 19279, 19333, 19387, 19441, 19495, 19549, 19603, 19657, 19711, 19765, 19819, 19873, 19927, 19981, 20035, 20089, 20143, 20197, 20251, 20305, 20359, 20413, 20467, 20521, 20575, 20629, 20683, 20737, 20791, 20845, 20899, 20953, 21007, 21061, 21115, 21169, 21223, 21277, 21331, 21385, 21439, 21493, 21547, 21601, 21655, 21709, 21763, 21817, 21871, 21925, 21979, 22033, 22087, 22141, 22195, 22249, 22303, 22357, 22411, 22465, 22519, 22573, 22627, 22681, 22735, 22789, 22843, 22897, 22951, 23005, 23059, 23113, 23167, 23221, 23275, 23329, 23383, 23437, 23491, 23545, 23599, 23653, 23707, 23761, 23815, 23869, 23923, 23977, 24031, 24085, 24139, 24193, 24247, 24301, 24355, 24409, 24463, 24517, 24571, 24625, 24679, 24733, 24787, 24841, 24895, 24949, 25003, 25057, 25111, 25165, 25219, 25273, 25327, 25381, 25435, 25489, 25543, 25597, 25651, 25705, 25759, 25813, 25867, 25921, 25975, 26029, 26083, 26137, 26191, 26245, 26299, 26353, 26407, 26461, 26515, 26569, 26623, 26677, 26731, 26785, 26839, 26893, 26947, 27001, 27055, 27109, 27163, 27217, 27271, 27325, 27379, 27433, 27487, 27541, 27595, 27649, 27703, 27757, 27811, 27865, 27919, 27973, 28027, 28081, 28135, 28189, 28243, 28297, 28351, 28405, 28459, 28513, 28567, 28621, 28675, 28729, 28783, 28837, 28891, 28945, 29000, 29054, 29108, 29162, 29216, 29270, 29324, 29378, 29432, 29486, 29540, 29594, 29648, 29702, 29756, 29810, 29864, 29918, 29972, 30026, 30080, 30134, 30188, 30242, 30296, 30350, 30404, 30458, 30512, 30566, 30620, 30674, 30728, 30782, 30836, 30890, 30944, 30998, 31052, 31106, 31160, 31214, 31268, 31322, 31376, 31430, 31484, 31538, 31592, 31646, 31700, 31754, 31808, 31862, 31916, 31970, 32024, 32078, 32132, 32186, 32240, 32294, 32348, 32402, 32456, 32510, 32564, 32618, 32672, 32726, 32780, 32834, 32888, 32942, 32996, 33050, 33104, 33158, 33212, 33266, 33320, 33374, 33428, 33482, 33536, 33590, 33644, 33698, 33752, 33806, 33860, 33914, 33968, 34022, 34076, 34130, 34184, 34238, 34292, 34346, 34400, 34454, 34508, 34562, 34616, 34670, 34724, 34778, 34832, 34886, 34940, 34994, 35048, 35102, 35156, 35210, 35264, 35318, 35372, 35426, 35480, 35534, 35588, 35642, 35696, 35750, 35804, 35858, 35912, 35966, 36020, 36074, 36128, 36182, 36236, 36290, 36344, 36398, 36452, 36506, 36560, 36614, 36668, 36722, 36776, 36830, 36884, 36938, 36992, 37046, 37100, 37154, 37208, 37262, 37316, 37370, 37424, 37478, 37532, 37586, 37640, 37694, 37748, 37802, 37856, 37910, 37964, 38018, 38072, 38126, 38180, 38234, 38288, 38342, 38396, 38450, 38504, 38558, 38612, 38666, 38720, 38774, 38828, 38882, 38936, 38990, 39044, 39098, 39152, 39206, 39260, 39314, 39368, 39422, 39476, 39530, 39584, 39638, 39692, 39746, 39800, 39854, 39908, 39962, 40016, 40070, 40124, 40178, 40232, 40286, 40340, 40394, 40448, 40502, 40556, 40610, 40664, 40718, 40772, 40826, 40880, 40934, 40988, 41042, 41096, 41150, 41204, 41258, 41312, 41366, 41420, 41474, 41528, 41582, 41636, 41690, 41744, 41798, 41852, 41906, 41960, 42014, 42068, 42122, 42176, 42230, 42284, 42338, 42392, 42446, 42500, 42554, 42608, 42662, 42716, 42770, 42824, 42878, 42932, 42986, 43040, 43094, 43148, 43202, 43256, 43310, 43364, 43418, 43472, 43526, 43580, 43634, 43688, 43742, 43796, 43850, 43904, 43958, 44012, 44066, 44120, 44174, 44228, 44282, 44336, 44390, 44444, 44498, 44552, 44606, 44660, 44714, 44768, 44822, 44876, 44930, 44984, 45038, 45092, 45146, 45200, 45254, 45308, 45362, 45416, 45470, 45524, 45578, 45632, 45686, 45740, 45794, 45848, 45902, 45956, 46010, 46064, 46118, 46172, 46226, 46280, 46334, 46388, 46442, 46496, 46550, 46604, 46658, 46712, 46766, 46820, 46874, 46928, 46982, 47036, 47090, 47144, 47198, 47252, 47306, 47360, 47414, 47468, 47522, 47576, 47630, 47684, 47738, 47792, 47846, 47900, 47954, 48008, 48062, 48116, 48170, 48224, 48278, 48332, 48386, 48440, 48494, 48548, 48602, 48656, 48710, 48764, 48818, 48872, 48926, 48980, 49034, 49088, 49142, 49196, 49250, 49304, 49358, 49412, 49466, 49520, 49574, 49628, 49682, 49736, 49790, 49844, 49898, 49952, 50006, 50060, 50114, 50168, 50222, 50276, 50330, 50384, 50438, 50492, 50546, 50600, 50654, 50708, 50762, 50816, 50870, 50924, 50978, 51032, 51086, 51140, 51194, 51248, 51302, 51356, 51410, 51464, 51518, 51572, 51626, 51680, 51734, 51788, 51842, 51896, 51950, 52004, 52058, 52112, 52166, 52220, 52274, 52328, 52382, 52436, 52490, 52544, 52598, 52652, 52706, 52760, 52814, 52868, 52922, 52976, 53030, 53084, 53138, 53192, 53246, 53300, 53354, 53408, 53462, 53516, 53570, 53624, 53678, 53732, 53786, 53840, 53894, 53948, 54002, 54056, 54110, 54164, 54218, 54272, 54326, 54380, 54434, 54488, 54542, 54596, 54650, 54704, 54758, 54812, 54866, 54920, 54974, 55028, 55082, 55136, 55190, 55244, 55298, 55352, 55406, 55460, 55514, 55568, 55622, 55676, 55730, 55784, 55838, 55892, 55946, 56000, 56054, 56108, 56162, 56216, 56270, 56324, 56378, 56432, 56486, 56540, 56594, 56648, 56702, 56756, 56810, 56864, 56918, 56972, 57026, 57080, 57134, 57188, 57242, 57296, 57350, 57404, 57458, 57512, 57566, 57620, 57674, 57728, 57782, 57836, 57890, 57944, 57998, 58052, 58106, 58160, 58214, 58268, 58322, 58376, 58430, 58484, 58538, 58592, 58646, 58700, 58754, 58808, 58862, 58916, 58970, 59024, 59078, 59132, 59186, 59240, 59294, 59348, 59402, 59456, 59510, 59564, 59618, 59672, 59726, 59780, 59834, 59888, 59942, 60000, 60054, 60108, 60162, 60216, 60270, 60324, 60378, 60432, 60486, 60540, 60594, 60648, 60702, 60756, 60810, 60864, 60918, 60972, 61026, 61080, 61134, 61188, 61242, 61296, 61350, 61404, 61458, 61512, 61566, 61620, 61674, 61728, 61782, 61836, 61890, 61944, 62000, 62054, 62108, 62162, 62216, 62270, 62324, 62378, 62432, 62486, 62540, 62594, 62648, 62702, 62756, 62810, 62864, 62918, 62972, 63026, 63080, 63134, 63188, 63242, 63296, 63350, 63404, 63458, 63512, 63566, 63620, 63674, 63728, 63782, 63836, 63890, 63944, 64000, 64054, 64108, 64162, 64216, 64270, 64324, 64378, 64432, 64486, 64540, 64594, 64648, 64702, 64756, 64810, 64864, 64918, 64972, 65026, 65080, 65134, 65188, 65242, 65296, 65350, 65404, 65458, 65512, 65566, 65620, 65674, 65728, 65782, 65836, 65890, 65944, 66000, 66054, 66108, 66162, 66216, 66270, 66324, 66378, 66432, 66486, 66540, 66594, 66648, 66702, 66756, 66810, 66864, 66918, 66972, 67026, 67080, 67134, 67188, 67242, 67296, 67350, 67404, 67458, 67512, 67566, 67620, 67674, 67728, 67782, 67836, 67890, 67944, 68000, 68054, 68108, 68162, 68216, 68270, 68324, 68378, 68432, 68486, 68540, 68594, 68648, 68702, 68756, 68810, 68864, 68918, 68972, 69026, 69080, 69134, 69188, 69242, 69296, 69350, 69404, 69458, 69512, 69566, 69620, 69674, 69728, 69782, 69836, 69890, 69944, 70000, 70054, 70108, 70162, 70216, 70270, 70324, 70378, 70432, 70486, 70540, 70594, 70648, 70702, 70756, 70810, 70864, 70918, 70972, 71026, 71080, 71134, 71188, 71242, 71296, 71350, 71404, 71458, 71512, 71566, 71620, 71674, 71728, 71782, 71836, 71890, 71944, 72000, 72054, 72108, 72162, 72216, 72270, 72324, 72378, 72432, 72486, 72540, 72594, 72648, 72702, 72756, 72810, 72864, 72918, 72972, 73026, 73080, 73134, 73188, 73242, 73296, 73350, 73404, 73458, 73512, 73566, 73620, 73674, 73728, 73782, 73836, 73890, 73944, 74000, 74054, 74108, 74162, 74216, 74270, 74324, 74378, 74432, 74486, 74540, 74594, 74648, 74702, 74756, 74810, 74864, 74918, 74972, 75026, 75080, 75134, 75188, 75242, 75296, 75350, 75404, 75458, 75512, 75566, 75620, 75674, 75728, 75782, 75836, 75890, 75944, 76000, 76054, 76108, 76162, 76216, 76270, 76324, 76378, 76432, 76486, 76540, 76594, 76648, 76702, 76756, 76810, 76864, 76918, 76972, 77026, 77080, 77134, 77188, 77242, 77296, 77350, 77404, 77458, 77512, 77566, 77620, 77674, 77728, 77782, 77836, 77890, 77944, 78000, 78054, 78108, 78162, 78216, 78270, 78324, 78378, 78432, 78486, 78540, 78594, 78648, 78702, 78756, 78810, 78864, 78918, 78972, 79026, 79080, 79134, 79188, 79242, 79296, 79350, 79404, 79458, 79512, 79566, 79620, 79674, 79728, 79782, 79836, 79890, 79944, 80000, 80054, 80108, 80162, 80216, 80270, 80324, 80378, 80432, 80486, 80540, 80594, 80648, 80702, 80756, 80810, 80864, 80918, 80972, 81026, 81080, 81134, 81188, 81242, 81296, 81350, 81404, 81458, 81512, 81566, 81620, 81674, 81728, 81782, 81836, 81890, 81944, 82000, 82054, 82108, 82162, 82216, 82270, 82324, 82378, 82432, 82486, 82540, 82594, 82648, 82702, 82756, 82810, 82864, 82918, 82972, 83026, 83080, 83134, 83188, 83242, 83296, 83350, 83404, 83458, 83512, 83566, 83620, 83674, 83728, 83782, 83836, 83890, 83944, 84000, 84054, 84108, 84162, 84216, 84270, 84324, 84378, 84432, 84486, 84540, 84594, 84648, 84702, 84756, 84810, 84864, 84918, 84972, 85026, 85080, 85134, 85188, 85242, 85296, 85350, 85404, 85458, 85512, 85566, 85620, 85674, 85728, 85782, 85836, 85890, 85944, 86000, 86054, 86108, 86162, 86216, 86270, 86324, 86378, 86432, 86486, 86540, 86594, 86648, 86702, 86756, 86810, 86864, 86918, 86972, 87026, 87080, 87134, 87188, 87242, 87296, 87350, 87404, 87458, 87512, 87566, 87620, 87674, 87728, 87782, 87836, 87890, 87944, 88000, 88



segments. Its winding is of the simplex-wave type and the current density in each conductor is 2,400 amp per sq in. Calculate (a) the volts between adjacent commutator segments, (b) the commutator pitch, (c) the area of cross section of each conductor.

Ans. (a) 13.65 volts, (b) 88, (c) 0.104 sq in.

17. The following particulars are given in connection with the armature of a d-c generator: slots = 41, commutator segments = 82, winding = simplex-wave, poles = 6, size of armature conductor = 0.06 in.  $\times$  0.3 in., current density in the armature conductor = 3,000 amp per sq in., volts between commutator segments = 16.8. Calculate the kilowatt output of the machine. (Neglect the losses due to shunt-field current.)

Ans. 25 kw.

18. A 75-kw 125-volt generator has an armature containing 200 commutator segments and a six-pole simplex-lap winding. The armature is tested (with the brushes lifted off the commutator) by connecting two diametrically opposite commutator segments to a d-c supply with an ammeter and rheostat in series. The current is adjusted to 80 amp, and the voltage drop between two adjacent segments is then found to be 0.044 volt. (a) Calculate the actual (operating) armature resistance. (b) Calculate the armature voltage drop under full-load conditions.

Ans. (a) 0.00612 ohm, (b) 3.68 volts.

## CHAPTER 4

### COMMUTATION AND DESIGN OF COMMUTATING POLES

**20. Theory of Commutation.\*** A d-c dynamo is provided with a commutator in order that unidirectional currents may be drawn from armature windings in which the current actually alternates in direction as the conductors pass successively under poles of opposite kind. As each coil in turn passes through the zone of commutation, it is short-circuited by the brush, and during the short lapse of time between the closing and

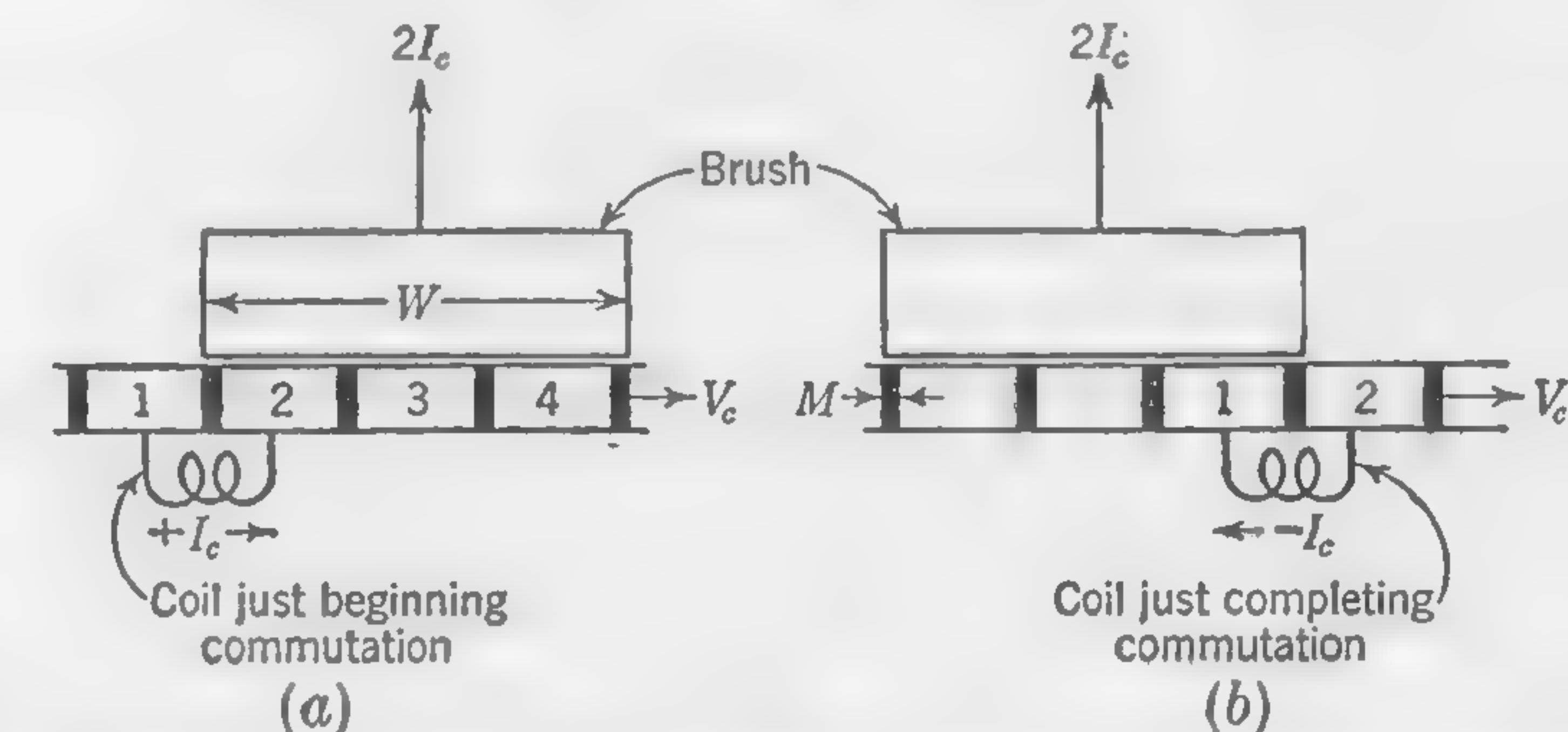


FIG. 21. Sketches illustrating two stages in the commutation process of a coil.

opening of this short circuit the current in the coil must change from a steady value of  $+I_c$  to a steady value of  $-I_c$ . Referring to Fig. 21,

Let  $W$  = surface width of brush (brush arc) in centimeters

$M$  = thickness of insulating mica in centimeters

$V_c$  = surface velocity of commutator in centimeters per second

\* This article and, indeed, the greater part of this chapter contain much that has already been published under the title *Commutation in Continuous Current Dynamos* in the *Journal of the Franklin Institute* of May, 1922, to which the student is referred for a more detailed discussion of the conditions leading to sparkless commutation. See also B. G. Lamme, *A Theory of Commutation and Its Application to Interpole Machines*, *Trans. AIEE*, vol. 30, pp. 2359-2404; the very complete treatment in C. O. Hawkins, "The Dynamo," vol. 2, Chap. XX, Sir Isaac Pitman & Sons, Ltd., 1923; and L. Dreyfus, "Commutation in Large D-C Machines," Julius Springer, 1929.



The time of commutation in seconds may then be written

$$t_c = \frac{W - M}{V_c}$$

Since  $M$  is usually small with reference to  $W$ , it is generally permissible to express the time of commutation as  $t_c = W/V_c$ ; that is to say, the time taken by any point on the commutator surface to pass under the brush is approximately the same as the duration of the short circuit. It is during this time  $t_c$  that the current in the commutated coil must pass through zero value in changing from the full armature current of  $+I_c$  to the full armature current of  $-I_c$ . If  $R$  is the resistance of the short-circuited coil, and if any possible disturbing effect of brush-contact resistance be neglected, it is evident that the emf in the coil should be  $e = I_c \times R$  at the commencement of commutation. At the instant of time when the current is changing its direction (*i.e.*, when no current is flowing in the coil), the emf is  $e = 0 \times R = 0$ . At the end of the time  $t_c$ , when the coil is just about to be thrown in series with the other coils of the armature winding carrying a current  $-I_c$  amp, the emf in the coil should be  $e = -I_c \times R$ . It is when the emf in the coil has some value other than this ideal value that sparking is likely to occur.

Consider a closed coil of wire of  $T$  turns moving in a magnetic field. At the instant of time  $t = 0$ , the total flux of induction passing through the coil is  $+\Phi_0$  maxwells, and, at the instant of time  $t = t_c$  sec, the total flux through the coil is  $+\Phi_t$  maxwells. Then, on the assumption that the flux links equally with every turn in the coil, the *average value of the emf* developed in the coil during the interval of time  $t_c$  is

$$E_m = \frac{(\Phi_t - \Phi_0)T}{t_c \times 10^8} \quad \text{volts} \quad (21)$$

If  $R$  is the ohmic resistance of the coil and  $e$  is any instantaneous value of the emf produced by the cutting of the actual magnetic field in the neighborhood of the coil, the instantaneous value of the current in the coil is  $i = e/R$ , because  $e$  is the only emf in the circuit tending to set up a current. The usual conception of a distinct flux due to the current  $i$  producing a certain flux linkage, known as the self-inductance of the circuit, is avoided; but its equivalent has not been overlooked since the mmf due to the current in the coil is a factor in the production of the flux actually linked with this current at the instant of time considered.

The wires in the coil undergoing commutation will be thought of as cutting through a total flux of induction, expressed in magnetic lines or maxwells, this flux being the resultant of the magnetizing forces of field coils and armature windings combined.

If a full-pitch armature coil is short-circuited by the brush while half-way between the  $N$  and  $S$  pole tips—that is to say, while the coil sides are in the geometric neutral zone—the magnetic fluxes due to the main poles are canceled and their effect need not be considered. It is then only the flux set up by the armature winding itself (considered separately from the field fluxes) which is effective in producing an emf in the coil undergoing commutation. The fact that the flux from the field poles which passes through the short-circuited coil is the same at the end as at the beginning of commutation—when this occurs in the “geometric” neutral

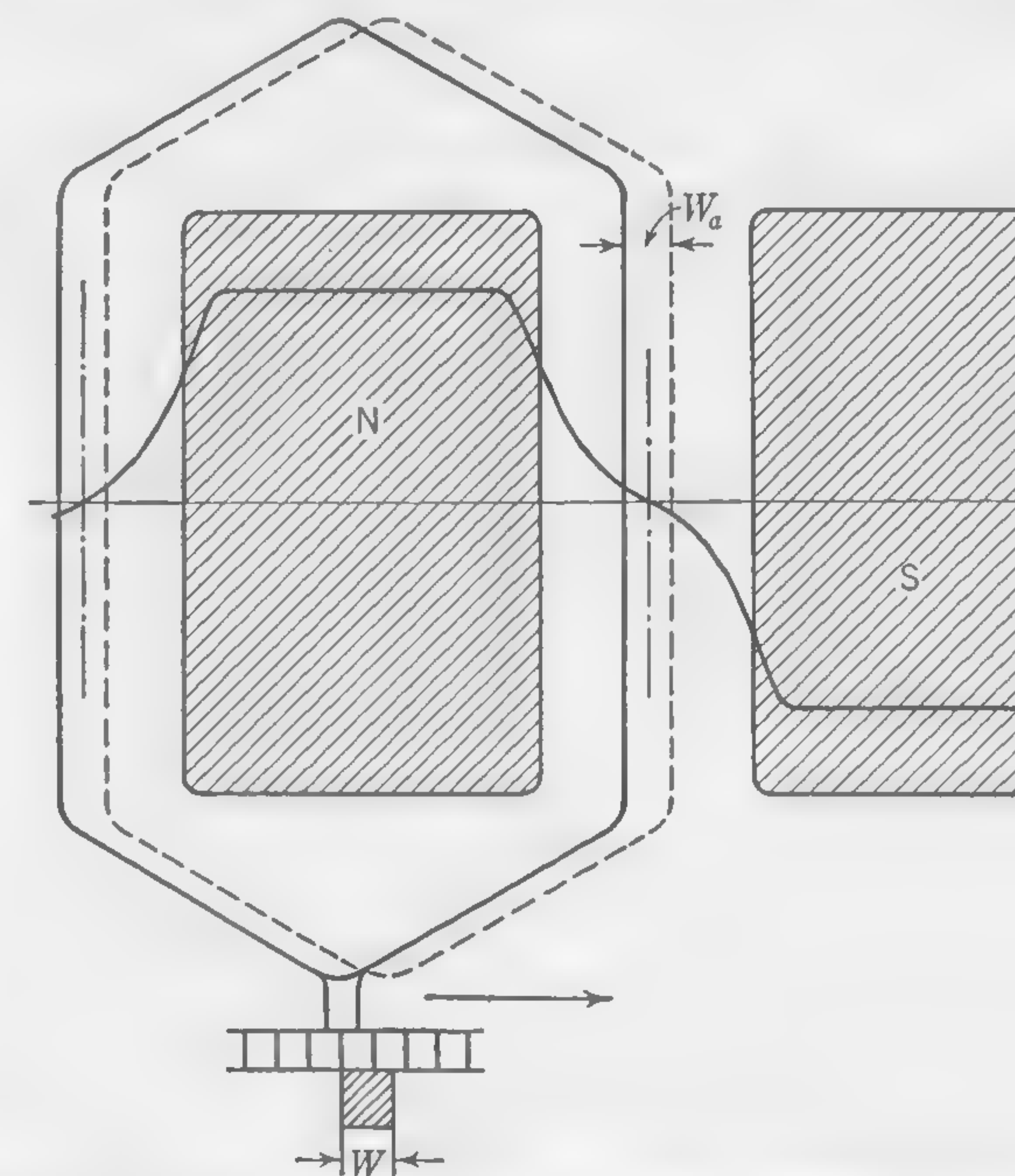


FIG. 22. Short-circuited coil with brushes in neutral position (flux due to field coils only).

zone—is clearly shown in Fig. 22. Here  $W_a$  is the distance of travel of the armature conductors during the time of short circuit; it may be defined as the brush width referred to the armature periphery. Thus  $W_a = W(D/D_c)$ , where  $W$  is the brush width (or brush arc),  $D$  is the diameter of the armature, and  $D_c$  is the diameter of the commutator. The curve shows the distribution of flux density over the armature surface, being positive, or (say) from the  $N$  pole, when measured above the datum line, and negative, or of opposite polarity, when measured below the datum line. It is obvious that with all poles of the same size and shape, excited with the same number of ampere-turns, the flux density will be zero on a line exactly halfway between the poles; and, since the



resultant flux through a coil of width equal to pole pitch is *exactly the same for both positions of the coil* shown in the figure, it follows that the mean voltage developed in the coil while moving through the distance  $W_a$  is zero.\* If this distribution of flux in the commutating zone were not disturbed by the currents in the armature conductors, commutation would offer no serious difficulties even under heavy loads.

**21. Magnetic Flux Due to Armature Currents.** The brushes are still supposed to be in such a position that the coil sides are at a point midway between poles when the mica which separates the two ends of the coil is under the center of the brush; this would be midway between

the two extreme positions of Fig. 21(a) and (b). When considering the changes in flux density brought about by the currents in the armature windings, it is permissible and convenient to think of the magnetic fluxes in the zone of commutation, which are due to the armature current, as distinct from other fluxes, and also as *fixed in space* and, therefore, *cut* by the armature conductors as they move across it. For those who may experience difficulty in conceiving of a *stationary* flux due to currents in *moving* armature conductors which are themselves cutting this same flux, it may be more convenient to revert to formula (21) and consider merely what is the difference  $(\Phi_i - \Phi_0)$  between the amount of flux which links with the coil at the

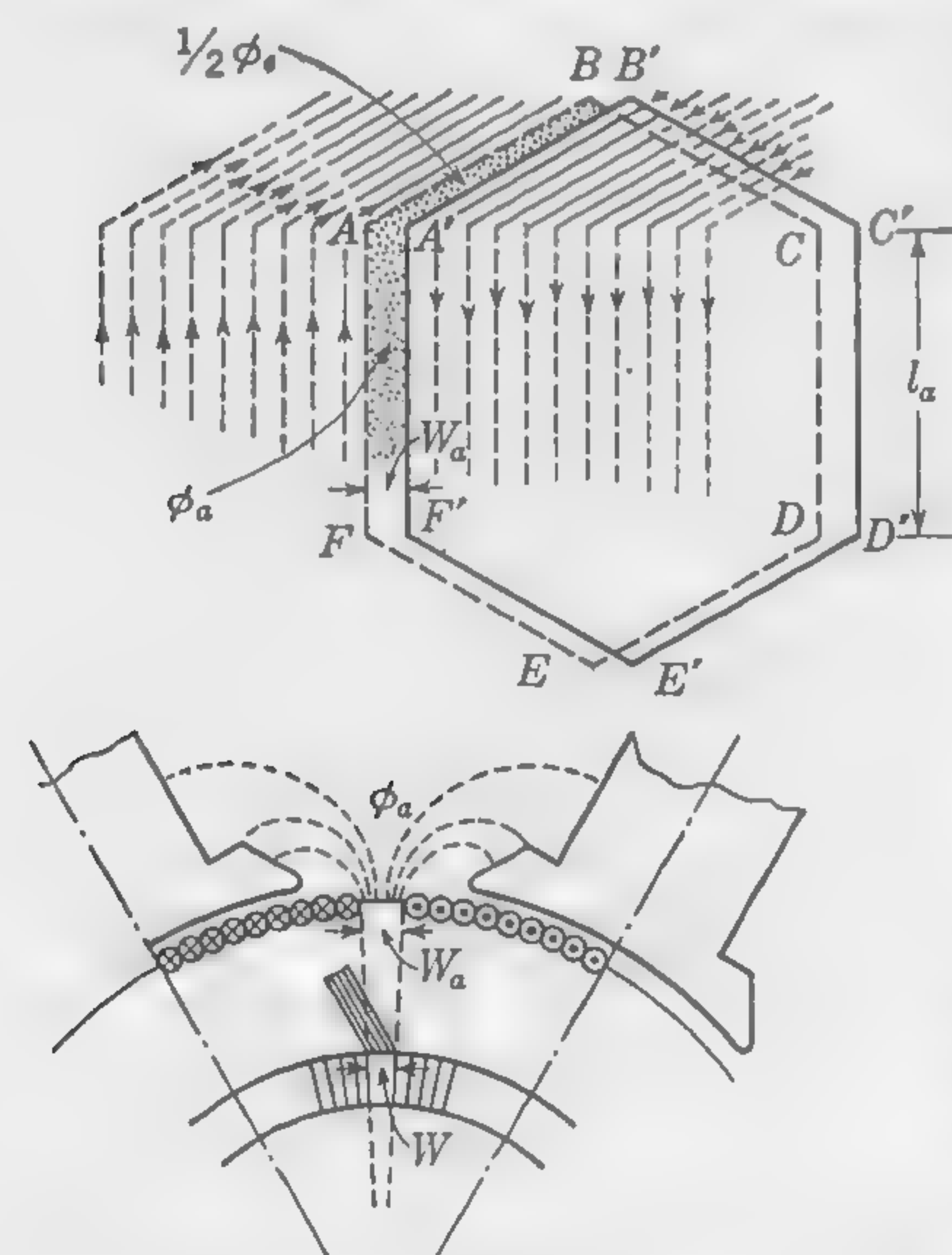


FIG. 23. Magnetic flux in zone of commutation due to currents in armature.

end of the period of short circuit and that which linked with the coil at the beginning of the period of short circuit. If this difference is zero, commutation will have taken place in a neutral field, which is the ideal condition for sparkless commutation.

In Fig. 23 the dots between the two extreme positions of the coil undergoing commutation indicate flux lines, all of the same polarity, which are due to the armature currents only. The fact that the armature

\* Although this principle is now generally recognized, there was considerable controversy on the subject of commutation between the years 1902 and 1913 when M. Marius Latour maintained in the face of considerable opposition that, if the average emf generated in the armature coil during the time of short circuit is to be zero, the total resultant flux linking with the coil at the end of commutation must be the same in amount as at the beginning of commutation.

ampere-turns will produce some flux  $\Phi_a$  in the zone of width  $W_a$  and length  $l_a$  (i.e., the gross length of the armature core) is generally understood, but that the same is true of the end connections is not always so clearly realized. It will, however, be evident from an inspection of Fig. 23 that flux of the same kind as that in the space  $FAA'F'$  will be found in the space  $ABB'A'$ , although it may be of lower density. This flux is due to the conductors running parallel to  $AB$  carrying currents which are opposite in direction on the two sides of the space considered. What has been said of the space  $ABB'A'$  applies equally to the flux cut by the portion  $FE$  of the end connections, and, if the coil side  $EFAB$  cuts through a positive flux  $(\Phi_a + \Phi_e)$ , it will readily be seen that coil side  $BCDE$  cuts through an equal amount of negative flux, so that the difference in the amount of flux enclosed by the coil at the end and beginning of commutation [the quantity  $\Phi_i - \Phi_0$  of formula (21)] is  $2[\Phi_a + (2)(\frac{1}{2})\Phi_e]$ . This difference of flux will always occur unless the brushes are shifted so as to bring the short-circuited conductors into a field from the main poles sufficient to annul it, or unless commutating poles are provided.

Whether in a generator or motor, the flux due to the armature currents is always such as to set up emfs in the short-circuited coil tending to oppose reversal of the current. It is for this reason that the important element in the problem of commutation, from whatever point of view it is approached, is the correct determination of the field in which the short-circuited coil is moving. With slotted armature cores, as used in modern machines, the current in the conductors lying in the slots will set up a difference of magnetic potential between the sides of the teeth which form the boundaries of the slot. The resulting flux component, known as the "slot flux," will also have an effect on commutation, but before considering this in some detail it will be well to explain how the armature flux  $\Phi_a$  and the end flux  $\Phi_e$  may be calculated.

**22. Formulas for Calculating Armature Flux and End Flux in the Zone of Commutation.** It is not possible to develop an accurate general formula for the amount of the "armature flux" cut by the short-circuited coils. By armature flux is meant the flux due to the ampere-turns of the armature which passes between the field poles and the tops of the armature teeth comprised in the zone of commutation (the space  $W_a$  of Figs. 22 and 23). The path taken by the flux lines is not easily predetermined, and it will depend not only upon the slope and distance apart of the pole shoes, but also upon the position of the brushes.

The flux entering the zone of commutation of width  $W_a$  exactly halfway between the two pole tips is due to the armature mmf only, because the mmfs of the two field poles neutralize at this point. When the field poles are excited, the flux path will be between the armature core and the field pole of opposite kind, generally as indicated in Fig. 24. The length of



this flux path, whether it terminates at the pole shoe or higher up on the side of the pole core, depends mainly upon the distance between the pole tips, or  $(1 - r)\tau$ , where  $\tau$  = pole pitch and  $r$  is the ratio of pole arc to pole pitch.

The following empirical formula may be used for calculating the flux entering the armature core at a point halfway between the main poles when the position of the brushes is such that commutation takes place with the coils in the geometric neutral zone:

$$\Phi_a = \left[ \frac{0.92 W_a l_a}{(1 + 2/p)(1 - r)D} \right] Z I_c \quad \text{maxwells} \quad (22)$$

where  $Z$  = the total number of armature conductors carrying a current  $I_c$ ,  $p$  = the number of poles, and  $D$  = the armature diameter in inches.

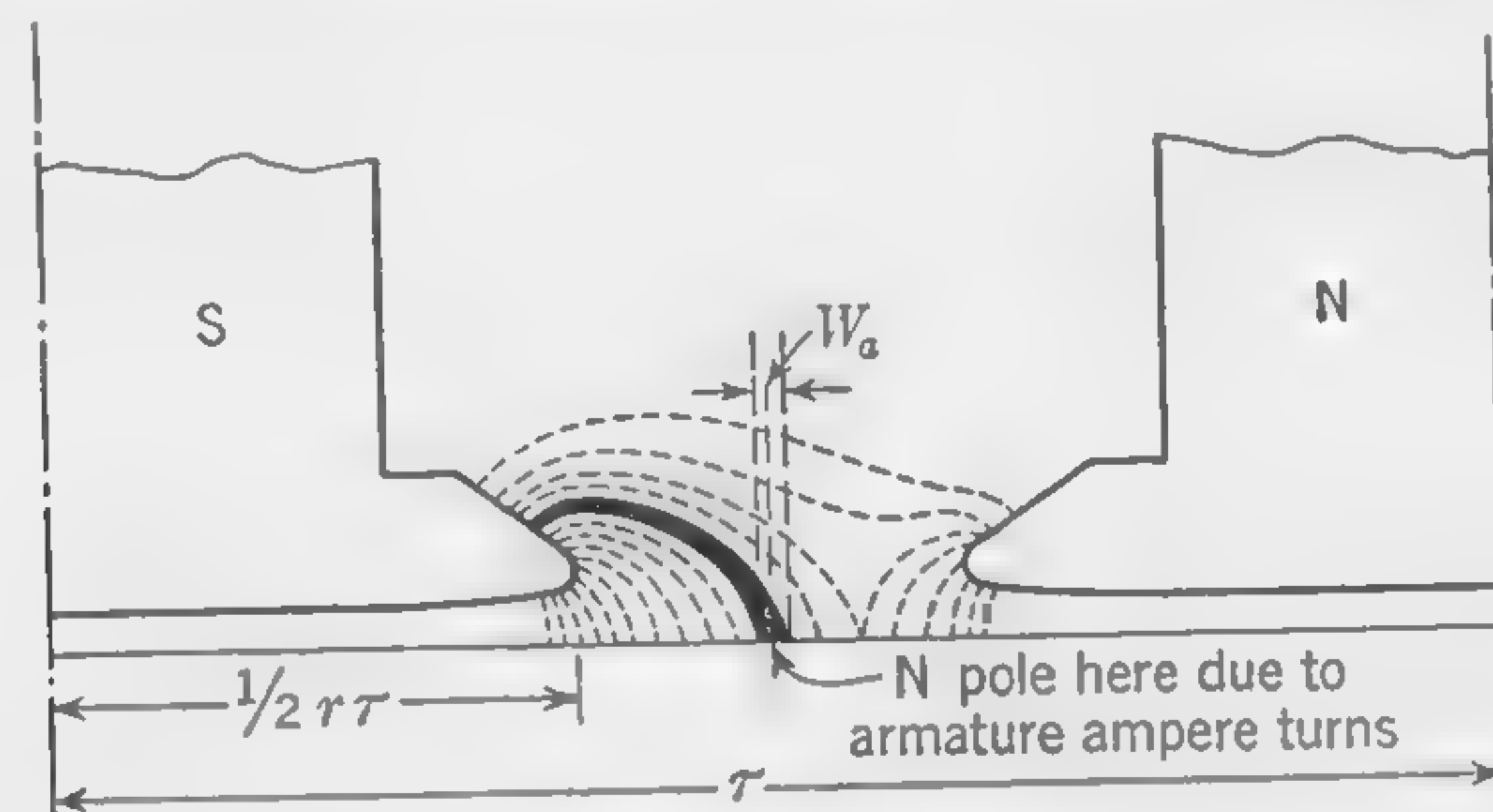


FIG. 24. Flux due to armature currents entering commutation zone of width  $W_a$ .

**Formula for "End Flux."** Formulas for calculating the flux cut by the end connections of the armature winding are not applicable to all sizes of machines and types of winding, and they should be considered as approximations only, unless they contain empirical constants which have proved to be reasonably accurate for the particular type of armature to which they apply. By making certain assumptions, A. Still developed a formula which he found to be sufficiently accurate for the purposes of the designer. The required formula should give a value for the total end flux  $\Phi_e$  or twice the amount of flux represented in Fig. 23 by the dots contained in the space  $ABB'A'$ . This will be compensated for by one commutating pole on the assumption that there are as many commutating poles as main poles.

Referring to Fig. 25, the flux which has to be calculated is that which is set up by currents in the end connections themselves in a space of area  $2W_a l'$  where  $W_a$  is as defined on page 61, and  $l'$  is the axial projection or overhang of the armature coils outside the laminated core. The dimension  $l'$  should be the equivalent overhang which may be estimated in the manner to be explained later and given by formula (25). Dimensions will be understood to be expressed in centimeter units unless otherwise

stated. The coil pitch in the diagram Fig. 25 is shown as being equal to the pole pitch  $\tau$ , but this is not important, and the amount of the end flux which is cut by a coil side in the geometric neutral zone changes very little with the pitch of the armature coils.

We shall, in the first place, neglect the effect of neighboring masses of iron in the paths of the magnetic flux and assume these paths to be circles of average diameter  $x$  (see Figs. 25 and 26). The line  $QR$  represents a circle in a plane perpendicular to the axis of the armature at a distance  $y$  cm from the plane passing through the points where the end connections change their direction to return through armature slots approximately a pole pitch away from the starting point. With  $\mu = 1$ ,  $B$  will

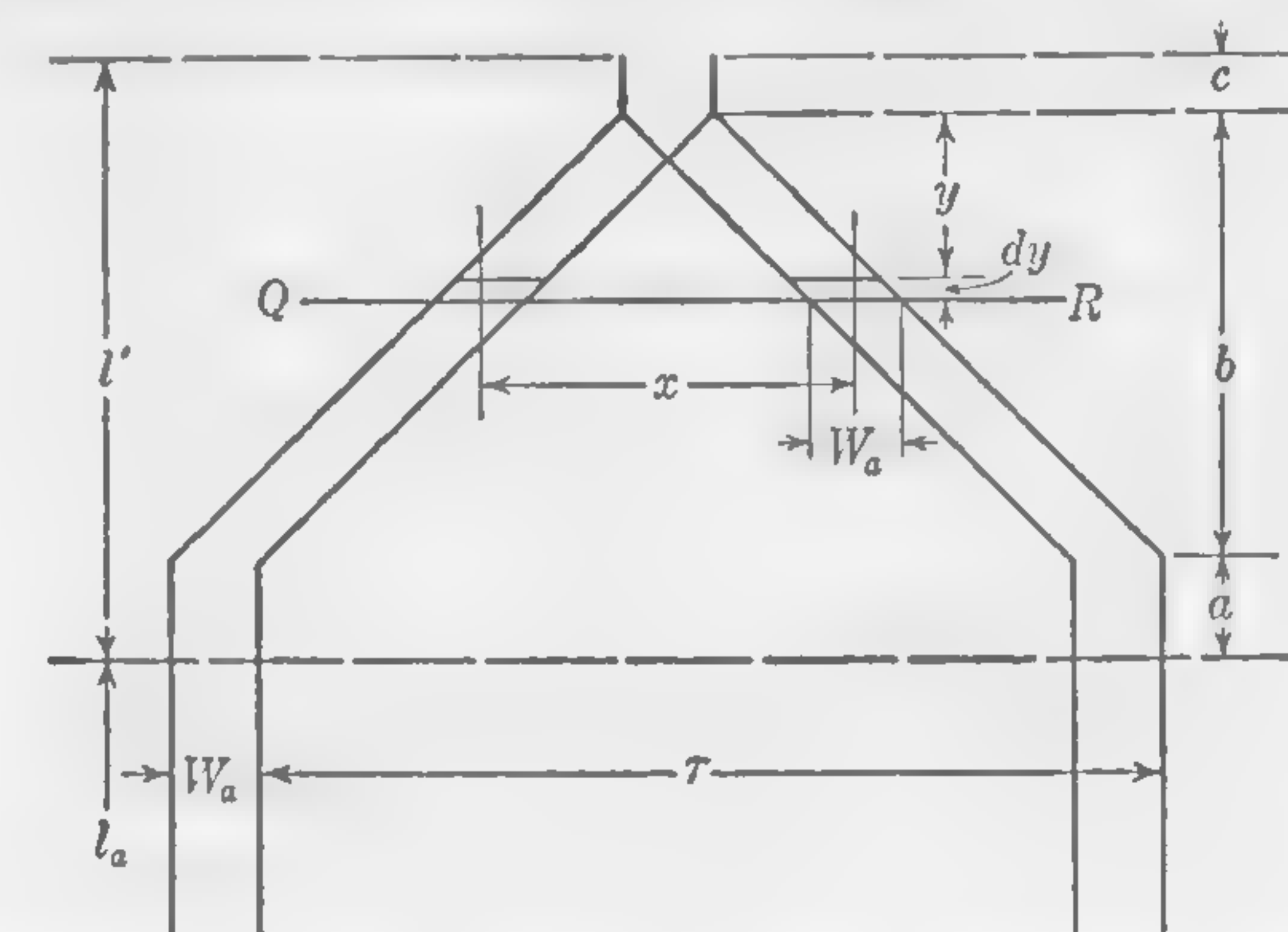


FIG. 25. Position of end connection at start and finish of commutation.

have the same numerical value as  $H$ , and the value of  $B$  in the small space of area  $W_a dy$  is simply the mmf divided by the length of path which is assumed to be  $\pi x$ .

The figures in the small squares of Fig. 26 are proportional to the ampere-turns tending to establish magnetic flux through these squares. Their value is determined by summing up the currents in the end connections which surround each individual area. It will be observed that the mmf tending to establish end flux in the zone  $AB$ , through which the end connection of the short-circuited coil is moving, falls off according to a straight-line law as the distance beyond the armature core increases.

The maximum armature ampere-turns per pair of poles [see formula (10) on page 15] are  $ZI_c/p$  and the mmf tending to set up flux in a circular path of diameter  $x$  and cross section  $W_a dy$  is  $0.4\pi(ZI_c/p)(y/b)$  gilberts. Since  $y/b = x/\tau$ , the length of the path is  $\pi x$  which may be written  $\pi\tau(y/b)$ , whence the flux density in the space considered is

$$B = H = \frac{\text{mmf}}{\text{length of path}} = 0.4 \frac{ZI_c}{p\tau}$$

Since this quantity is independent of either  $x$  or  $y$ , we may assume that,



if there were no iron in the path of the end flux, the flux density would have a constant value throughout the space  $AA'B'B$  of Fig. 23.

Introducing a coefficient  $k$  to take care of the decreased reluctance of the flux paths due to proximity of the poles, coil supports, steel binding

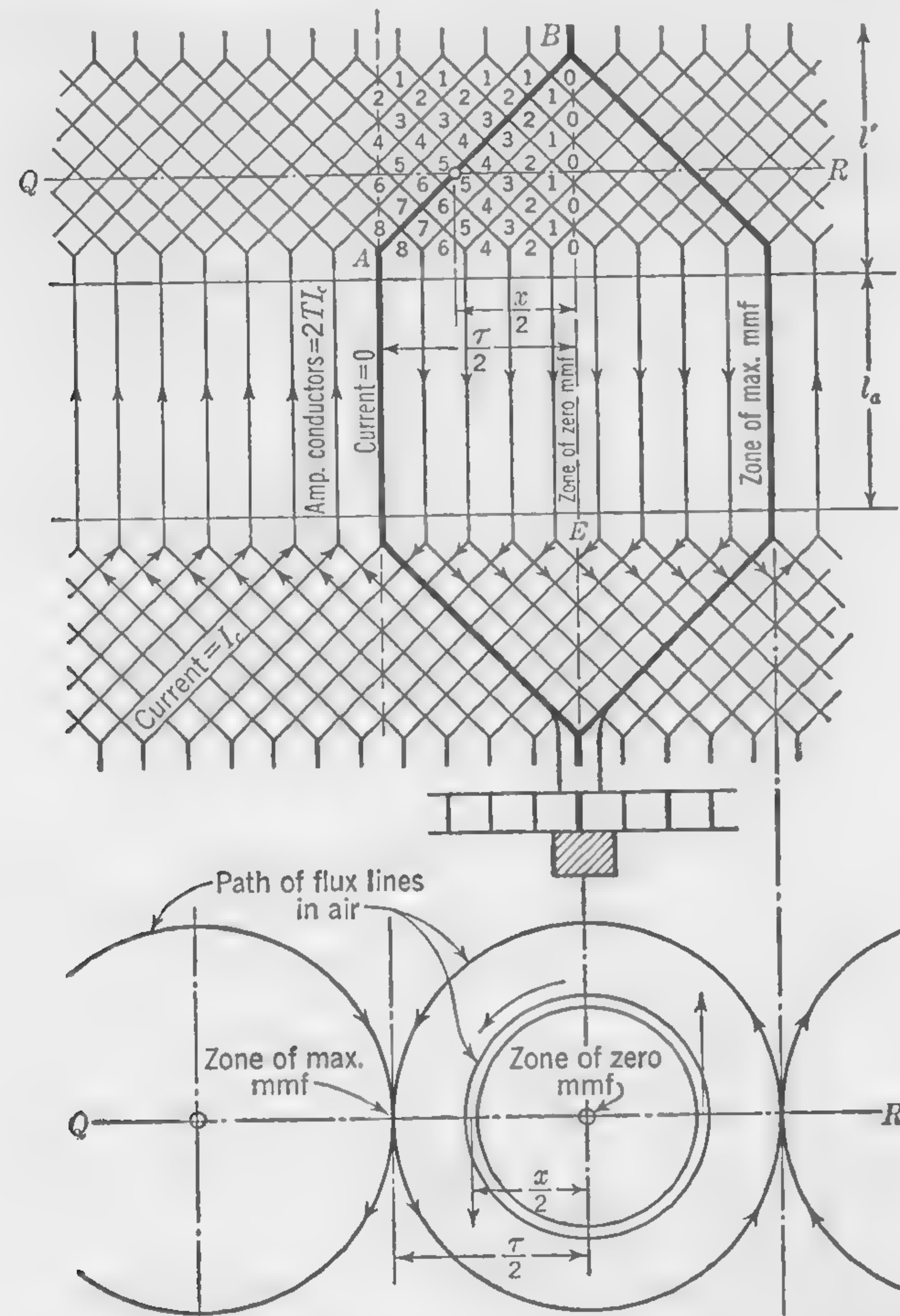


FIG. 26. Diagram illustrating calculation of end flux in zone of commutation.

wire, and other neighboring iron, the density of the end flux in the zone of commutation may be written:

$$B_e = 0.4k \frac{ZI_c}{p\tau} \quad \text{gauss} \quad (23)$$

or

$$B_e = k \frac{ZI_c}{8D} \quad \text{gauss (approx)} \quad (23a)$$

where the armature diameter  $D$  must be expressed in *centimeters*.

The value of  $k$  in modern machines will usually be between 2 and 3. A good average value to use in the formulas is  $k = 2.5$ .

The end flux  $\Phi_e$  which is cut by *one side* of the short-circuited armature coil is, therefore,

$$\Phi_e = 2.5 \frac{ZI_c}{8D} \times 2l'W_a = \left[ \frac{0.625l'W_a}{D} \right] ZI_c \quad \text{maxwells} \quad (24)$$

where  $l'$  should be the *equivalent* overhang in *centimeters* beyond the ends of the slots in order to include the flux cut by the loops where the coils bend over from the upper to the lower layer.

Referring to Fig. 27, we may write

$$l' = a + b + \frac{\pi}{2}c$$

where  $a$  is the straight part of the coil side between the end of the slot and the first bend, and  $c$  is the mean radius of the loop at the extreme end of the coil. A close approximation to the length  $b + (\pi/2)c$  is the quantity  $(\tau_c \tan \alpha + d)/2$  where  $\tau_c$  is the coil pitch which may be equal to, or less than, the pole pitch  $\tau$ , the angle  $\alpha$  is as indicated in Fig. 27, and  $d$  is the slot depth. Thus

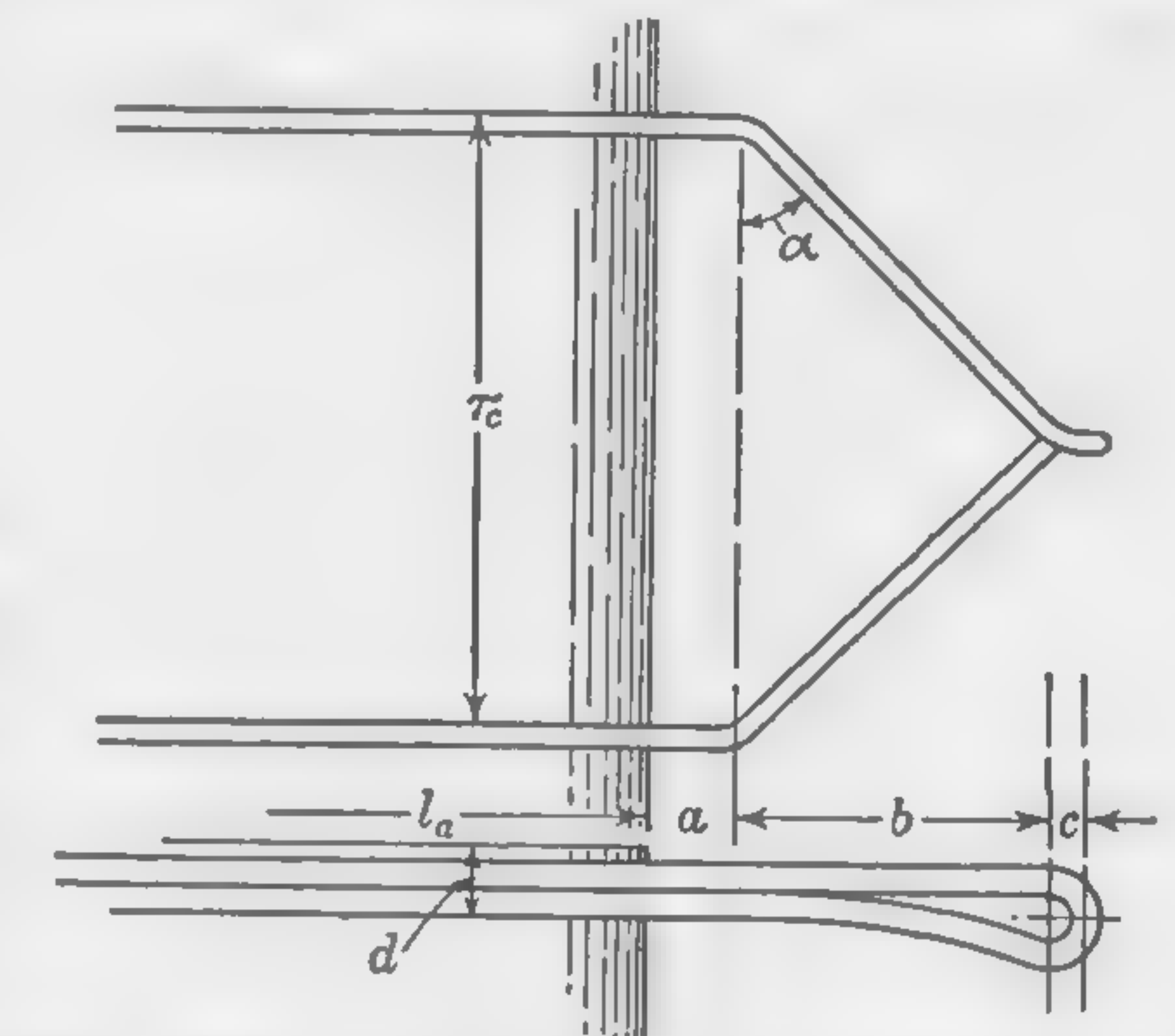


FIG. 27. Illustrating overhang of armature coils.

$$l' = a + \frac{\tau_c \tan \alpha + d}{2} \quad (25)$$

For a rough approximation, the equivalent overhang may be assumed equal to one-half the pole pitch, or

$$l' = 0.5\tau \quad (\text{approx}) \quad (25a)$$

Since  $\tau$  (in centimeters)  $= \pi D/p$ , Eq. (24) may now be rewritten in a more convenient form as follows:

$$\begin{aligned} \Phi_e &= \left[ \frac{0.625 \times 0.5\pi D/p \times 2.54W_a}{D} \right] ZI_c \\ &= \left[ \frac{2.5W_a}{p} \right] ZI_c \quad \text{maxwells} \end{aligned} \quad (24a)$$

where  $W_a$  is expressed in *inches*.

**23. Effect of Slot Flux.** Practically all modern generators and motors have slotted armatures and, since the effect of the slot leakage flux on



commutation has not yet been discussed, it will be necessary to consider it before proceeding further. In Fig. 28 an attempt has been made to represent, by the usual convention of magnetic lines, the flux due to the armature current alone, which enters or leaves the armature periphery in the interpolar space *when the field magnets are not excited*. The position chosen for the brushes is the geometric neutral (*i.e.*, the point midway between two poles) and the magnetic lines leaving the teeth will cross the air spaces between armature surface and field poles and so close the magnetic circuit. The brush is supposed to cover an angle equal to twice the slot pitch. The current in the conductor just before the short circuit occurs is  $+I_c$ , the current in the conductor occupying the slot corresponding to a position under the center of the brush is zero, and the current in

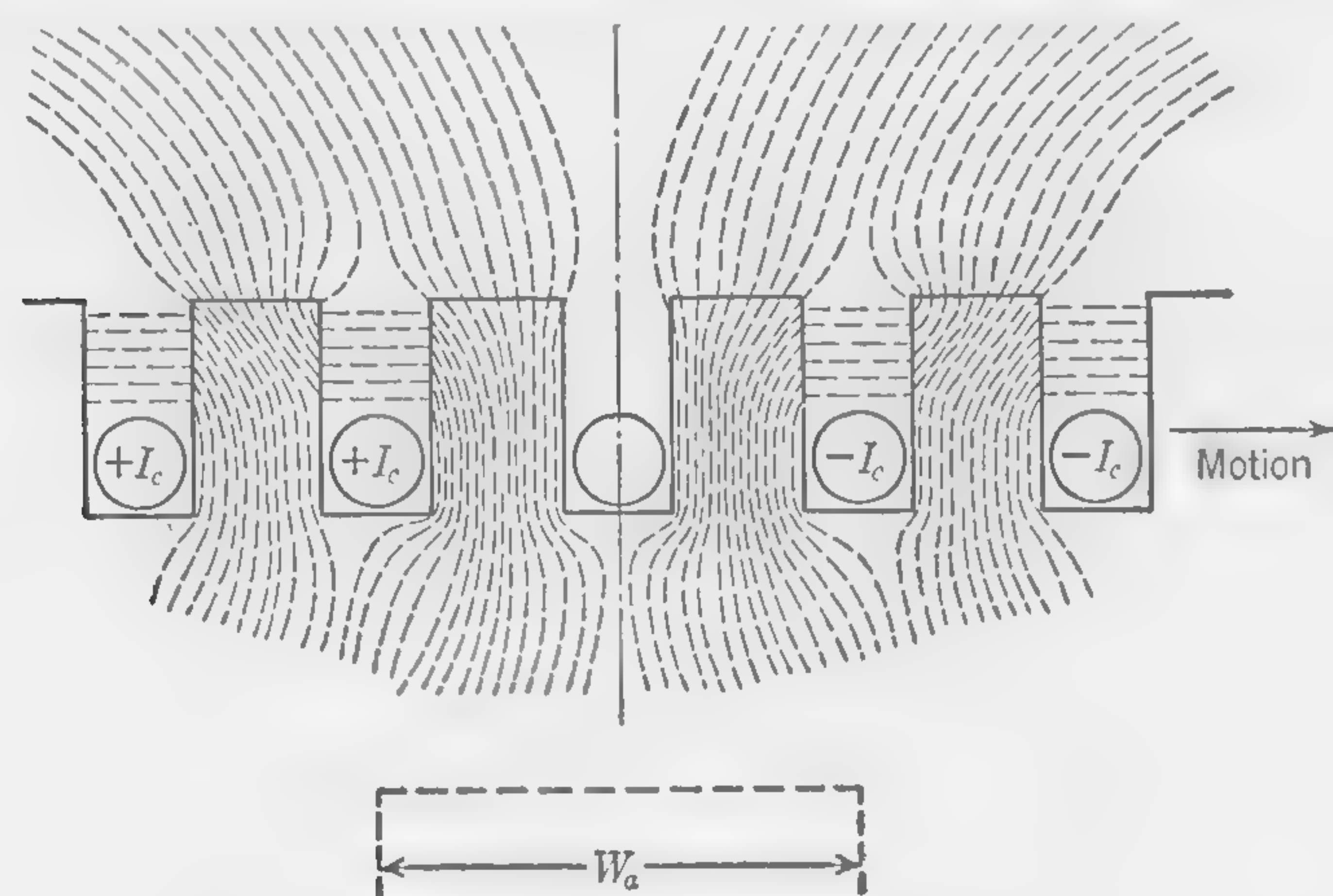


FIG. 28. Flux distribution in commutation zone.

the conductor just passing out from the short circuit is  $-I_c$ . The armature is supposed to be rotating, and it will be seen that the conductors in which the current is being commutated are cutting the flux set up by the armature as a whole. It is important to note that the flux cut by a conductor, while traveling between the two extreme positions during which the short circuit obtains, is *not* limited to the flux passing into the air gaps from the tops of the teeth included between these positions of the conductor but includes also the flux due to the currents in the short-circuited conductors, *which crosses the slot above the conductor\* and leaves the armature surface by teeth which are not included between the two extreme positions of the short-circuited coil*. This picture of the conductor cutting the field set up by the armature currents is especially useful when calculations are

\* For the sake of simplicity, a single conductor is shown at the bottom of each slot and the whole of the slot flux is supposed to link with it. The calculation of the "equivalent" slot flux will follow.

made by considering the separate component fluxes due to distinct causes, all combining to produce the actual or resultant flux. It is not difficult to see that the flux shown in Fig. 28 is never such as to generate an emf tending to reverse the current in the short-circuited conductor; rather, this flux gives rise to an emf that tends to oppose current reversal.

**24. Formulas for Calculating Slot Flux.** Instead of all the slot flux passing above the conductors to which it owes its existence, as shown in Fig. 28, much of this flux will actually pass through the copper in the slot. In order to simplify the calculations and yet obtain formulas of sufficient accuracy for the purpose of the designer, the whole of the slot—including the space usually occupied by the wedge—will be supposed occupied by the coils, the slot dimensions (in centimeters) being as indicated in Fig. 29. It will be convenient to assume the same number of commutator bars as there are slots, and each slot to be filled with  $2T$  conductors, each carrying  $I_c$  amp. (This follows from the assumption of a full-pitch winding.) Thus no account will be taken of the fact that a small space occurs between upper and lower coils, where the slot flux will not pass through the material of the conductors. The lines of the slot flux will be supposed to take the shortest path from tooth to tooth; the small amount of flux that may follow a curved path from corner to corner of tooth at the top of the slot will be neglected. Refinements of this nature may be introduced, if desired, when solving the problem for a concrete case. If the usual assumption is made that the reluctance of the iron in the path of the magnetic lines is negligible in comparison with the slot reluctance, the small portion of slot flux in the space  $dx$  (Fig. 29), considered 1 cm long axially (*i.e.*, in a direction perpendicular to the plane of the paper), is

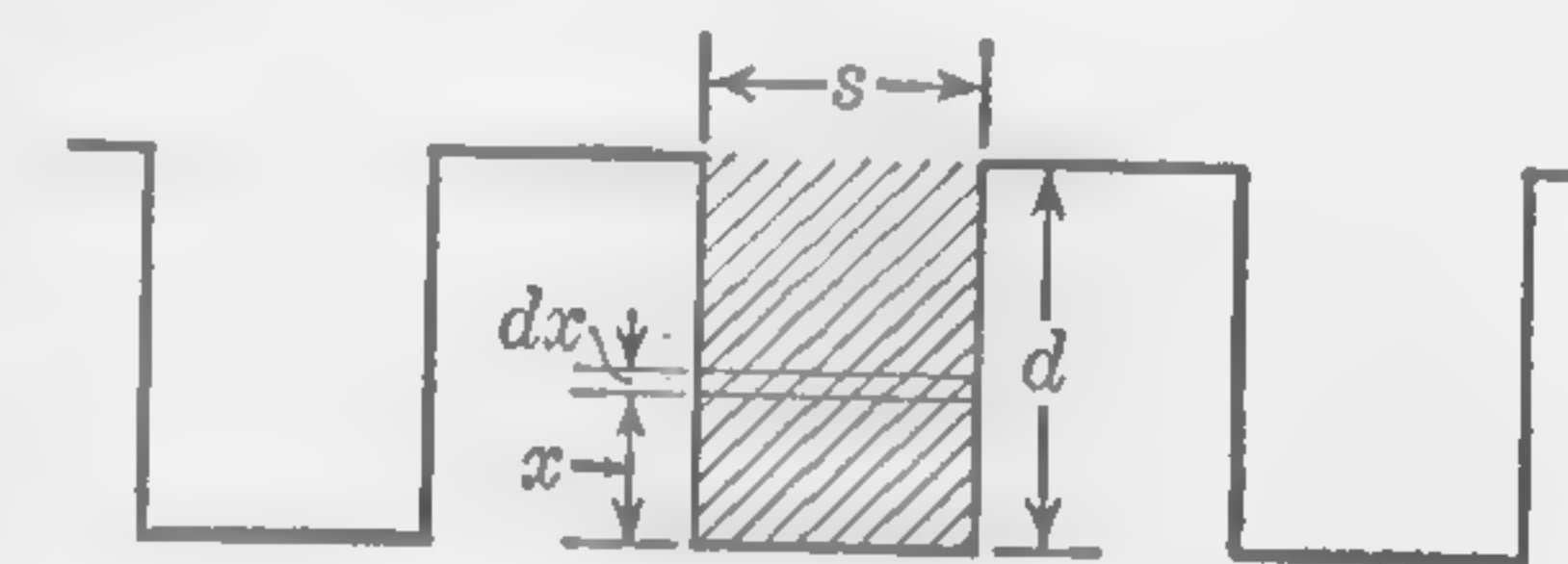


FIG. 29. Illustrating slot-flux calculations.

$$d\Phi' = F \times dP$$

where  $dP$  is the permeance of the air path. Thus

$$d\Phi' = 0.4\pi (2TI_c) \frac{x}{d} \times \frac{dx}{s}$$

and the total slot flux *per centimeter of axial length* in the zone of commutation—being *twice* the flux per slot (see Fig. 28)—is

$$\begin{aligned} \Phi_s' &= \frac{0.8\pi(2TI_c)}{ds} \int_0^d x dx \\ &= \frac{0.8\pi d T I_c}{s} \end{aligned} \quad (26)$$



Since this flux is not cut equally by all the conductors in the slot, the volts generated in the short-circuited coil by the cutting of this leakage flux will depend upon what may be termed the *equivalent* slot flux. This may be defined as the amount of flux which, if cut by all the conductors in the slot, would generate in the coil the same emf as results from the cutting of the actual slot flux. Thus, the element of flux in the space of depth  $dx$  (Fig. 29) links only with  $2T(x/d)$  conductors,\* and the equivalent amount of flux which, if cut by all the conductors in the slot, would generate the same emf is, therefore,

$$d\Phi'_{\text{equivalent}} = d\Phi \times \frac{x}{d}$$

whence

$$\begin{aligned}\Phi'_{\text{equivalent}} &= \frac{0.8\pi TI_c}{d^2s} \int_0^d x^2 dx \\ &= \frac{0.8\pi d}{3s} TI_c \quad \text{maxwells per slot}\end{aligned}$$

The total slot flux cut by each coil side during commutation, being twice the flux per slot, as previously explained, the final expression for the equivalent slot flux *per centimeter axial length* of the armature, when the path of the flux lines is up through the root of the tooth and outward across the slot through the copper of the conductors, is

$$\Phi'_{es} = \frac{1.6\pi d}{3s} TI_c \quad \text{maxwells} \quad (27)$$

Since  $T = Z/2S$ , and the armature length is  $2.54l_a$ , where  $l_a$  is in inches, the total equivalent slot flux for a length  $l_a$  in. becomes

$$\Phi_{es} = \frac{1.6\pi d}{3s} \times \frac{Z}{2S} \times I_c \times 2.54l_a = \left( \frac{2.1dl_a}{s \times S} \right) ZI_c \quad \text{maxwells} \quad (28)$$

**25. Formula for Calculating the Total Flux in Zone of Commutation.** Since the total interpolar flux in the zone of commutation is represented by the sum of the three components given by formulas (22), (24a), and (28), a convenient, single equation may be written, combining them as follows:

$$\Phi_t = \left[ \frac{0.92W_a l_a}{(1 + 2/p)(1 - r)D} + \frac{2.5W_a}{p} + \frac{2.1dl_a}{s \times S} \right] ZI_c \quad \text{maxwells} \quad (29)$$

\* These calculations are based on the assumption of a large number of turns in the armature coils. When the winding consists of only one or two conductors of large cross section in each slot, the current distribution will not be quite uniform, as here assumed.

**26. Effect of Several Coil Sides in One Slot—Full-pitch Windings.** When developing formulas (26) and (27) for the slot flux and equivalent slot flux, two assumptions were made: (1) that the number of commutator segments was the same as the number of armature slots, and (2) that the coil pitch was the same as the pole pitch. When there are several coil elements per slot, which occurs when the number of commutator segments is greater than the number of slots, the current at the beginning and end of the commutation period has not the maximum value  $+I_c$  and  $-I_c$  in all the conductors occupying the slot for which it is desired to calculate the leakage flux. The slot-leakage flux is then not correctly given by formulas (26) and (27), and, for a closer approximation to actual conditions, a modifying factor should, therefore, be introduced. In other words, a mean value for the current in the slot which sets up the leakage flux should be substituted for the maximum value  $I_c$ .

**27. Effect of Short-pitch Winding on Slot-leakage Flux.** Although chorded windings will usually slightly reduce the amount of armature flux in the zone of commutation and also the end flux, it is in the amount of the slot flux that their effect is most noticeable.

Given the ratio of number of commutator bars to number of slots, the number of commutator bars covered by the brush, and the number of slots chorded or the difference between the number of slots in the pole pitch and the number of slots spanned by the armature coil, it is possible to determine the average value of the ampere conductors in the slot at both the beginning and the end of commutation.

By assuming the ideal or "straight-line" current reversal in the short-circuited coils, the mmf which sets up the slot flux may be determined graphically without much difficulty, and the proper correction to the formulas (26) and (27) can then be applied. A. Still has proposed elsewhere\* formulas for these correction factors, and it is not proposed to reproduce them here. The formulas (26) and (27) for full-pitch windings give the maximum values for the slot flux.

**28. Illustrative Example Calculation of Short-circuit EMF.** The foregoing analysis will now be illustrated by the solution of a problem in which the approximate values of the total commutating-zone flux and the induced emf in the coil during short circuit will be calculated. For this purpose the following information, taken from an actual d-c generator design, is given:

Output rating = 500 kw

Volts = 460

Speed  $N$  = 900 rpm

Number of poles  $p$  = 6

\* Commutation in Continuous Current Dynamos, *J. Franklin Inst.*, May, 1922.



Diameter of core  $D = 28$  in.  
 Diameter of commutator  $D_c = 21$  in.  
 Length of core  $l_a = 14.5$  in.  
 Ratio of pole arc to pole pitch  $r = 0.63$   
 Number of slots  $S = 108$   
 Number of commutator segments = 216  
 Number of conductors per slot  $2T = 4$   
 Slot width  $s = 0.39$  in.  
 Slot depth  $d = 1.6$  in.  
 Type of winding = simplex-lap  
 Brush arc  $W = 1$  in.

Calculations:

$$I_c = \frac{500,000}{460 \times 6} = 181 \text{ (The shunt-field current is neglected.)}$$

$$W_a = 2\frac{8}{21} \times 1.0 = 1.34 \quad Z = 108 \times 4 = 432$$

$$\Phi_t = \left[ \frac{0.92 \times 1.34 \times 14.5}{(1 + \frac{2}{6})(1 - 0.63)28} + \frac{2.5 \times 1.34}{6} + \frac{2.1 \times 1.6 \times 14.5}{0.39 \times 108} \right] 432 \times 181$$

$$= (1.295 + 0.558 + 1.157)432 \times 181 = 235,000 \text{ maxwells}$$

Since there are four conductors per slot (twice as many commutator segments as slots), and the winding is simplex lap, each short-circuited coil will have *one turn* connected between adjacent segments.

$$\text{Time of commutation } t_c = \frac{W_a}{\text{peripheral velocity of core (in./sec)}}$$

$$= \frac{1.34}{\pi \times 28 \times \frac{900}{60}} = 0.00102 \text{ sec}$$

Average value of the emf generated in the short-circuited coil is, therefore,

$$\frac{2\Phi_t \times \text{turns per element}}{t_c \times 10^8} = \frac{2 \times 235,000 \times 1}{0.00102 \times 10^8} = 4.6 \text{ volts}$$

**29. Commutating Poles.** These are auxiliary poles situated halfway between the main poles and excited by a series winding so proportioned as to furnish the amount of flux necessary to counteract the effect of the armature mmfs in the zone of commutation. In machines furnished with commutating poles, the portion of the armature periphery covered by the main poles is usually limited to 0.65 of the total periphery.

In Fig. 30 the face of the commutating pole is supposed to cover the *full length* of the armature core and to be wound with sufficient ampere-turns to overcome the armature mmf and force a certain amount of flux into the armature teeth comprised in the zone of commutation. In this case the flux required to balance or counteract the flux cut by the end connections of the short-circuited coil has been neglected, and the flux shown entering the teeth under the commutating pole is the slot flux only. If the face of the commutating pole were shorter than the axial length of the armature core (as is usually the case), there would also be a certain amount of what has previously been referred to as the armature flux to be compensated for; but Fig. 30 has been drawn solely for the purpose of showing how the slot flux—which cannot be annulled like the armature flux—is supplied by

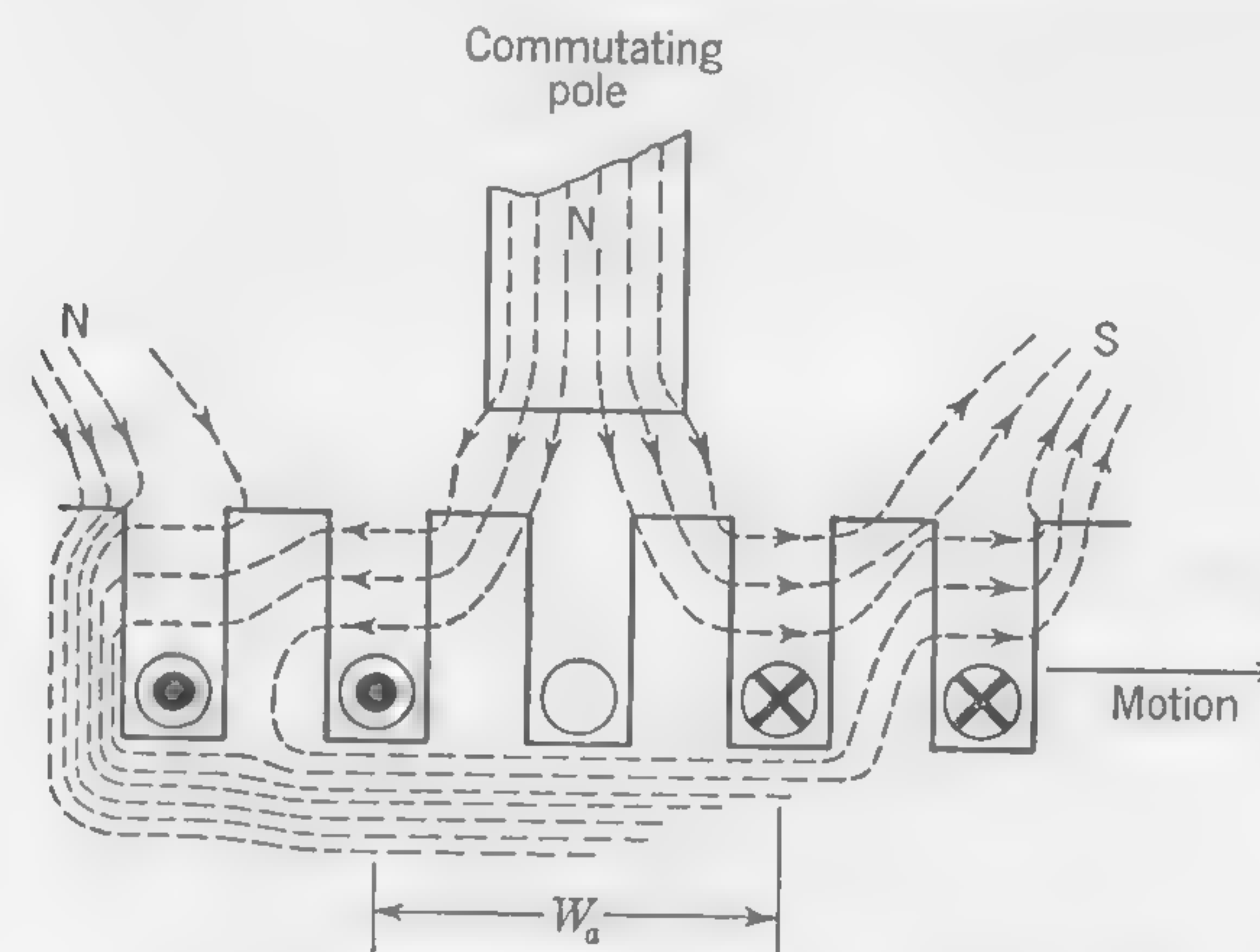


FIG. 30. Slot flux supplied by commutating pole.

the commutating pole, and, since it no longer passes outward through the roots of the teeth, as shown in Fig. 28, is not cut by the coil as it travels over the space of width  $W_a$ . When the conductors fill the slot instead of being concentrated at the bottom, as shown in Fig. 30, a portion of the slot flux is cut by a portion of the conductors in the slot. It is, therefore, necessary to consider what shall be understood by the equivalent slot flux when this flux is supplied by the commutating pole (or leading pole tip when the brushes are shifted), because this will no longer have the same value as given by the previously developed formula (27).

The element of flux  $d\Phi$  in the space  $dx$  (see Fig. 29) no longer links with  $T(r/d)$  conductors, as when the slot flux was considered as passing outward through the roots of the teeth, but with  $2T[(d-x)/d]$  conductors. The equivalent flux *per centimeter* axial length of slot, when no part of this flux passes into the armature core below the teeth is, therefore,



$$\begin{aligned}
 \Phi'_{es} &= 2 \int_0^d d\Phi \times \frac{d-x}{d} \\
 &= \frac{1.6\pi T I_c}{d^2 s} \int_0^d x(d-x)dx \\
 &= \frac{1.6\pi d}{6s} T I_c
 \end{aligned} \quad (30)$$

or just half the equivalent slot flux as given by formula (27), and one-third of the total slot flux as given by formula (26).

Assuming first that the axial length of the commutating pole is the same as the armature core, the former must be provided with sufficient ampere-turns to (1) nullify the armature ampere-turns that produce  $\Phi_a$ , and (2) inject sufficient flux into the armature so that an emf is developed that is exactly equal and opposite to that generated by the cutting of the unannulled flux  $\Phi_e$  and  $\Phi_{es}$ . When this desired condition is attained there will be no change in flux through the coil during the time of commutation  $t_c$ , and

$$\Phi_c = \Phi_e + \Phi_{es} \quad (31)$$

When, as indicated by Fig. 31, the axial length of the commutating pole  $l_p$  is shorter than the armature-core length (and this is generally the

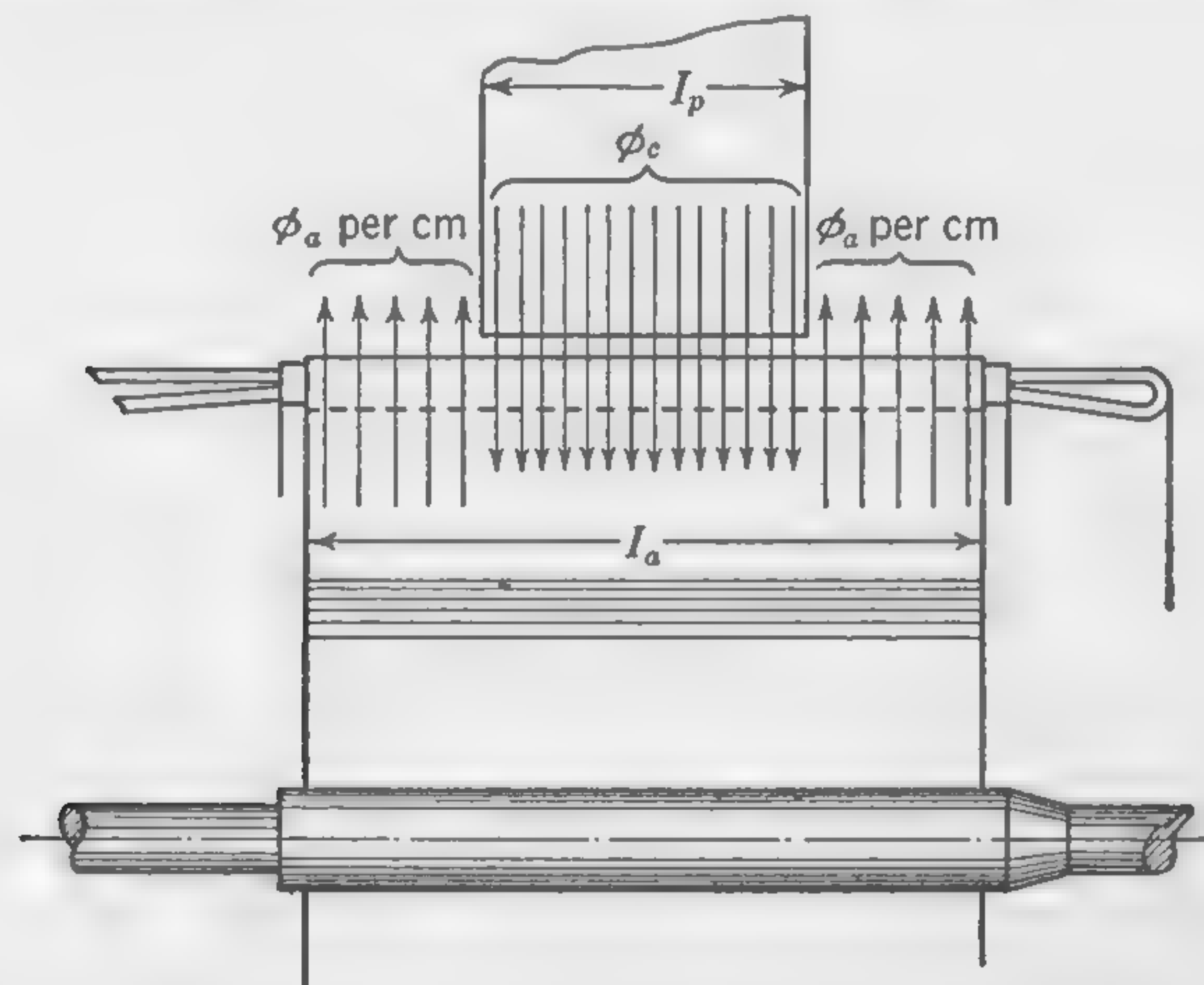


FIG. 31. Illustrating "armature flux" opposing current reversal where armature surface is not covered by commutating pole.

case in the design of modern d-c machines), an additional component of flux must be injected into the armature by the commutating pole to compensate for the unannulled portions of the armature flux  $\Phi_a$  that exist in the two ends beyond the commutating pole. This additional flux, which is equal to  $\Phi_a(l_a - l_p)/l_a$ , will then permit the armature to generate a suffi-

ciently greater, oppositely directed emf to ensure sparkless commutation. As a result, the commutating pole must be designed to inject a flux into the armature equal to

$$\Phi_c = \Phi_a \left( \frac{l_a - l_p}{l_a} \right) + \Phi_e + \Phi_{es} \quad \text{maxwells} \quad (32)$$

Substituting the values given by formulas (22), (24a), and (28) in Eq. 32, the commutating pole flux

$$\Phi_c = \left[ \frac{0.92 W_a (l_a - l_p)}{(1 + 2/p)(1 - r)D} + \frac{2.5 W_a}{p} + \frac{2.1 d l_a}{s \times S} \right] Z I_c \quad \text{maxwells} \quad (33)$$

Knowing the amount of flux to be provided by each commutating pole, its cross section can be decided upon and the necessary exciting ampere-turns calculated, bearing in mind the following requirements:

1. The average air-gap density should be low (preferably not exceeding 20,000 maxwells per sq in. with full load on the machine), to allow for increase on overloads.

2. The leakage factor should be as small as possible. This involves keeping the width and axial length of interpole small, thus conflicting with condition 1 and presenting one of the difficulties of commutating-pole design.

3. The minimum width of pole face must be such that the equivalent pole arc (which includes an allowance for fringing) shall be somewhat wider than the commutating zone of width  $W_a$ .

4. The effect of the commutating pole being to increase the flux in that portion of the yoke which lies between the interpole and the main pole of opposite polarity, it is important to see that the resulting flux density in this part of the magnetic circuit is not excessive.

5. The total line current should, if possible, pass through all the interpole windings in series; that is to say, parallel circuits should be avoided because of the possibility that the current may not be equally divided. If the total current is too great, a portion may be shunted through a diverter. The diverter should be partly inductive, the resistance being wound on an iron core in order that the time constants of the main and shunt circuits may be approximately equal. If this is not done, the winding on the commutating pole will not take its proper share of the total current when the change of load is sudden, and this may lead to momentary destructive sparking.

### 30. Illustrative Example. Design of Commutating Poles for D-C Generator.

(a) *Determining the Axial Length of Commutating Pole.* Using the given data and the calculated results of the example of Art. 28,  $l_p$  will



first be found, on the assumption that the machine will have the same number of interpoles as main poles.

Selecting a preliminary flux density in the air gap under the commutating pole,  $B_p''$ , of about 17,900 lines per sq in.

$$\Phi_c = W_a B_p'' l_p = 1.34 \times 17,900 l_p = 24,000 l_p$$

But, by formula (32),

$$\begin{aligned} \Phi_c &= (1.295 \times 432 \times 181) \left( \frac{14.5 - l_p}{14.5} \right) + (0.558 \times 432 \times 181) \\ &\quad + (1.157 \times 432 \times 181) \\ &= 101,200 - 7,000 l_p + 43,600 + 90,500 \end{aligned}$$

Equating the two values of  $\Phi_c$

$$l_p = \frac{101,200 + 43,600 + 90,500}{24,000 + 7,000} = \frac{235,300}{31,000} = 7.6 \text{ in., or (say) } 7.5 \text{ in.}$$

Solving for air-gap flux and flux density

$$\begin{aligned} \Phi_c &= 101,200 - (7,000 \times 7.5) + 43,600 + 90,500 = 182,800 \text{ maxwells} \\ B_p'' &= \frac{182,800}{1.34 \times 7.5} = 18,200 \text{ maxwells per sq in.} \end{aligned}$$

(b) *Determining the Ampere-turns on Commutating Pole.* Since this calculation depends, in part, upon the so-called *equivalent air gap* between the commutating pole and the slotted armature core, it will first be necessary to decide upon an actual air gap  $\delta$ , and then evaluate  $\delta_e$  (refer to Chap. 5, p. 92). Upon the assumption that the air gaps under the main commutating poles are equal, an average value of  $\delta$ , as calculated by formulas (12) and (13), page 17, may be used. Selecting a main-pole air-gap flux density  $B_g'' = 59,000$  (see table, p. 11),  $\delta$ , by formula (12),  $= (432 \times 181) / (6 \times 59,000) = 0.221$ . By formula (13),  $\delta = 0.04\sqrt{28 + 3} = 0.223$  in. Thus, the average value of  $\delta = 0.222$  in.

The equivalent air gap  $\delta_e$  may now be found by making use of formulas (37), (37a), and (37b) (p. 92), and taking an average, or, as in this case, applying only formula (37b). Thus:  $\lambda = 28\pi/108 = 0.815$  in., and  $t = 0.815 - 0.39 = 0.425$  in. Therefore,

$$\delta_e = \frac{0.815}{0.425/0.222 + (5 \times 0.39)/(5 \times 0.222 + 0.39)} = 0.254 \text{ in.}$$

The ampere-turns on the commutating pole must be sufficient, at full load, (1) to overcome the reluctance of the equivalent air gap between the pole face and the slotted armature when the air-gap density is 18,200 maxwells per sq in., (2) to oppose the armature mmf, and (3) to overcome the reluctance of the iron portions of the magnetic circuit. The full-load

ampere-turns required to overcome the air gap will, therefore, be

$$(NI)_g = 0.313 \times 18,200 \times 0.254 = 1,450$$

and the ampere-turns required to oppose the armature mmf, neglecting the fact that the current in the coils short-circuited by the brushes is less than in the remaining portion of the winding, will be, by formula (10) on page 15,

$$\frac{ZI_c}{2p} = \frac{432 \times 181}{2 \times 6} = 6,510$$

The small mmf to overcome the reluctance of the iron core of the commutating pole will be estimated to be 10 per cent of  $(NI)_g + ZI_c/2p$ , and the total ampere-turns on each pole must, therefore, be  $1.1(1,450 + 6,510) = 8,756$  at full load.

(c) *Determining the Dimensions of the Commutating-pole Winding.* Since the full-load current (neglecting the shunt-field current) is  $500,000/160 = 1,086$  amp, the required number of turns per pole  $= 8,756/1,086 = 8.05$ , or (say) 8 turns. A winding with a larger number of turns per pole may, however, be provided, in which case the final adjustment may be made on test by shunting a portion of the current through a diverter. An alternate procedure is to provide sufficient space to accommodate the calculated number of turns and then determine the exact number of turns by test to give sparkless commutation by applying a temporary winding to the cores and connecting this winding to a convenient d-c circuit.

Still another method, quite satisfactory, for adjusting the strength of the commutating poles is to provide packing plates or "shims" between the pole core and the yoke ring. Then, when the machine is placed on test, an adequate number of nonmagnetic shims may be used to replace the magnetic pieces until the magnetic reluctance is properly altered; it is possible in this way to adjust the magnetic circuit without changing the air gap between pole face and armature core.

If the winding consists of bare copper strip on edge, the current density may be as high as 1,500 amp per sq in. Assuming a value of about 1,450 in this design, which is probably high enough to avoid undue temperature rise, the cross section of copper required is  $1,086/1,450 = 0.75$  sq in. For a conductor as large as this it will be desirable to use two strips of wire in parallel, each one having dimensions  $1\frac{1}{2}$  by  $\frac{1}{4}$  in. The cross section of the commutating pole will then be generally as shown in Fig. 32, wherein the dimensions of the main poles have been assumed and are probably about what would be required in a machine of the specified output.

(d) *Determining the Leakage Factor for the Commutating Pole.* It will be desirable, at this point, to make calculations to determine the total flux and flux density at the outer section of the commutating pole, i.e., where the commutating pole is bolted to the yoke. Recognizing the fact



that considerable flux will *leak* between the interpoles and neighboring main poles, it should be clear that the flux density near the yoke section will be greater than in the air gap. Therefore, the *leakage factor*, which is defined as the ratio  $\frac{\text{useful flux} + \text{leakage flux}}{\text{useful flux}}$ , will be equal to

$$lf = \frac{\Phi_c + \Phi_l}{\Phi_c} \quad (34)$$

and, in the usual case, will be rather large. However, in a good design it is necessary that the maximum flux density be kept low enough so that operation will take place below the knee of the magnetization curve, even at overloads, where magnetic saturation is avoided; under this condition, the commutating-pole flux will be directly proportional to the load current.

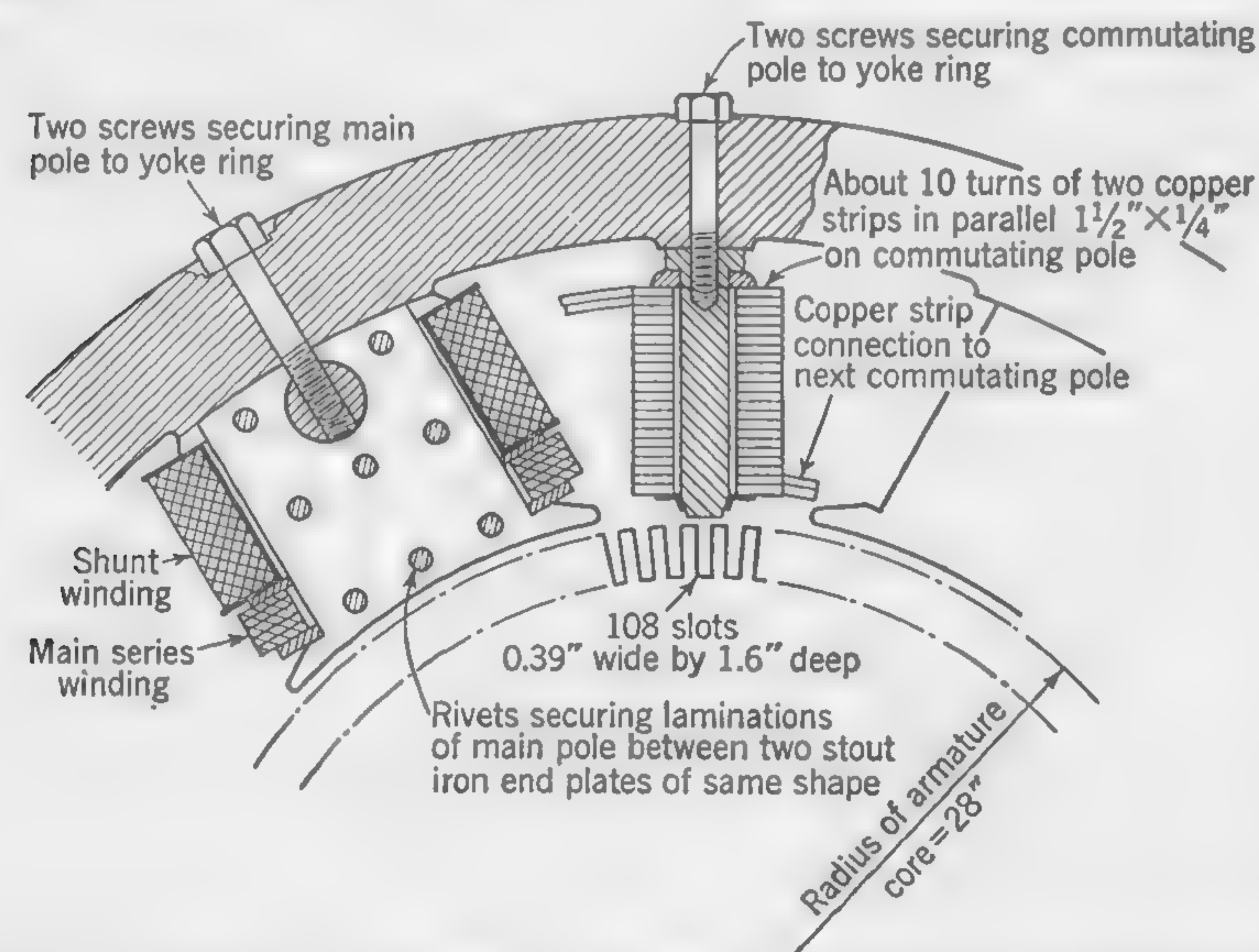


FIG. 32. Tentative field design for Illustrative Example of Arts. 28 to 30(c).

To simplify leakage flux calculations it will be desirable to assume that the main and commutating poles, between which the flux leakage takes place, are parallel to each other, although, being bolted to a cylindrical yoke, they are actually inclined to each other at some angle; the parallel face assumption will not, however, involve serious error. Furthermore, referring to the greatly simplified sketch in Fig. 33, it will be satisfactory to assign the following arbitrary values to labeled dimensions:  $h = 30$  to  $35\delta$ ;  $c = 0.6r\tau$ ;  $b = 0.5(\tau - c - w)$ ; finally, the dimension  $w$  will be made about 10 per cent larger than  $w_a$  to make sure that an adequate flux spread is provided for the commutating zone.

Since leakage flux will exist between a main and a commutating pole of opposite polarities in the spaces approximately enclosed by the broken lines in the lower sketch of Fig. 33, it will be convenient to divide the field into three parts, as indicated. Thus, the leakage permeance of the air between  $xy$  and  $x'y'$  will be  $P_1 = hl_p/b$ . The nonuniform leakage path between  $yy'$  and  $zz'$  involves a more complicated method of calculation of leakage permeance, but Finnis has developed a formula that yields a reasonably accurate determination of this quantity and one that checks rather well with calculations made by plotting flux-distribution maps (to be discussed in a later article); Finnis's leakage-permeance formula for the two end portions is

$$2P_w = 2 \times 2.54h \times \frac{2}{\pi} \log_e \left[ 1 + \frac{w}{b} + \sqrt{\left(\frac{w}{b}\right)^2 + \frac{2w}{b}} \right] \quad (35)$$

Having determined the leakage permeances, their sum, since they are in parallel, may be multiplied by *one-half* the maximum mmf between main and commutating pole, the *average* mmf, to give the leakage flux.

In the given design:

$$h \cong 30 \times 0.222 = 7 \text{ in.}; c = 0.6 \times 0.63 \times \frac{28\pi}{6} = 5.5;$$

$$w \cong 1.1 \times 1.34 = 1.5 \text{ in.}$$

$$b \cong 0.5 \left( \frac{28\pi}{6} - 5.5 - 1.5 \right) = 3.9 \text{ in.}$$

$$P_1 = \frac{(7 \times 7.5)(6.45)}{3.9 \times 2.54} = 34$$

$$P_w = 2 \times 2.54 \times 7 \times \frac{2}{\pi} \log_e \left[ 1 + \frac{1.5}{3.9} + \sqrt{\left(\frac{1.5}{3.9}\right)^2 + \frac{2 \times 1.5}{3.9}} \right] = 18.8$$

The total leakage permeance will, therefore, be

$$P_l = 34 + 18.8 = 52.8$$

Assuming that the number of ampere-turns on main and commutating

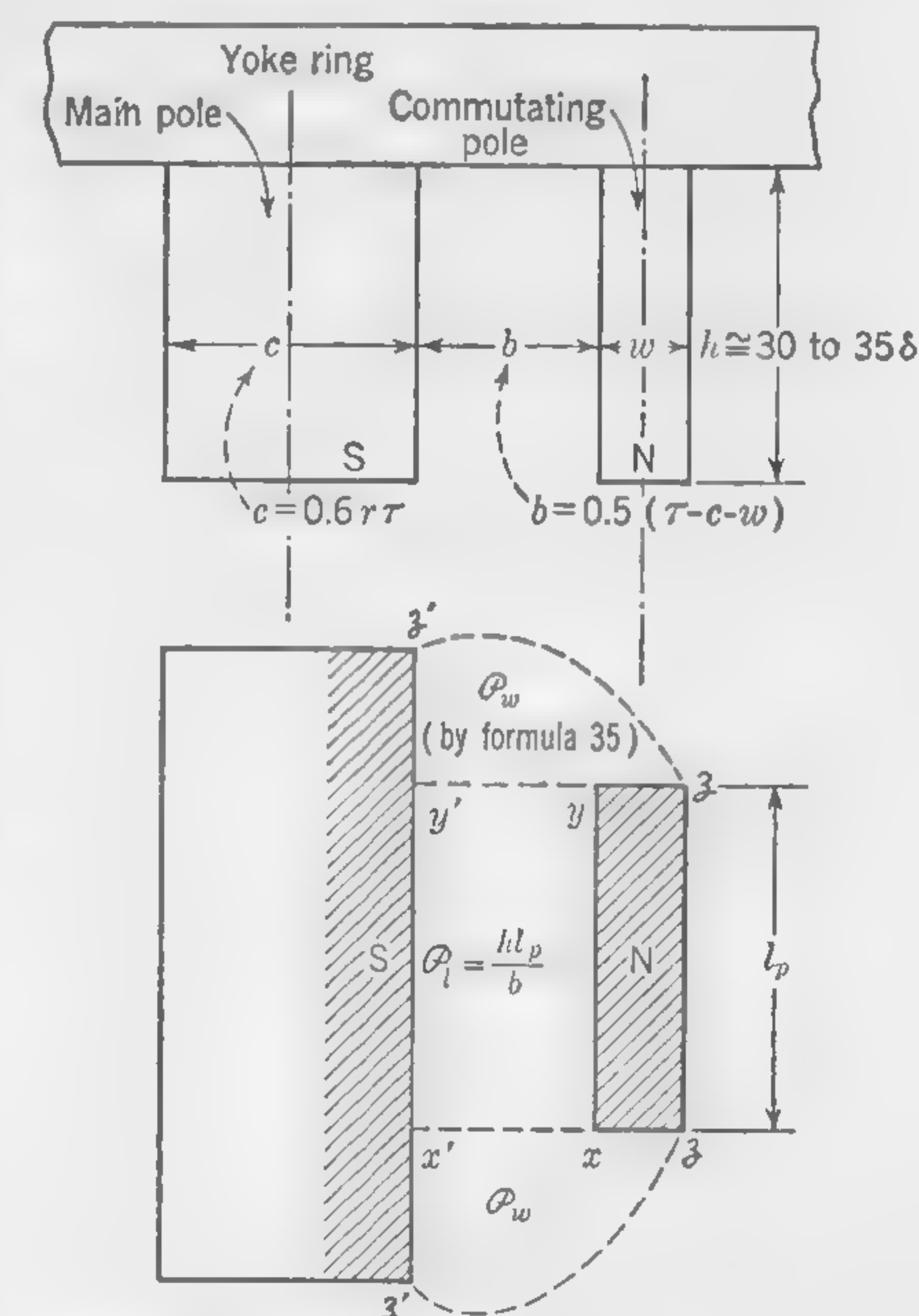


FIG. 33. Sketch illustrating method for calculating approximate pole dimensions to determine the leakage flux.



poles are to be equal, the total leakage flux from each interpole will be

$$\Phi_l = \frac{2 \times 0.4\pi \times 8,756}{2} \times 52.8 = 580,000 \text{ maxwells}$$

Since the flux entering the armature core from the commutating pole “fringes” from the corners of the pole face, the useful flux will be somewhat greater than that previously calculated; this may be as much as 50 per cent more, so that  $\Phi_c$  will probably be about  $1.5 \times 182,000 = 273,000$  maxwells. The maximum flux at the yoke section will, therefore, be

$$\Phi_{II} = 580,000 + 273,000 = 853,000$$

and the leakage factor is

$$lf = \frac{853,000}{273,000} = 3.12$$

Finally, calculating the maximum-flux density in the pole core (near the yoke ring) under full-load conditions

$$B'' = \frac{853,000}{1.5 \times 7.5} = 75,900 \text{ lines per sq in.}$$

Although the average flux density throughout the length of the pole will be considerably lower, this is somewhat high. However, by providing a tapered pole, with a width of 2 in. near the yoke, the maximum flux density may be brought down to a more reasonable figure. Thus

$$B'' \text{ (near yoke)} = \frac{853,000}{2 \times 7.5} = 56,800 \text{ lines per sq in.}$$

and

$$B'' \text{ (near air gap)} = \frac{273,000}{1.5 \times 7.5} = 24,200 \text{ lines per sq in.}$$

Figure 34 is a sketch illustrating the commutating-pole design; it clearly shows and identifies the arrangement and dimensions of the various details.

**31. Commutating Field Obtained by Brush Shift.** Very few machines are built nowadays in which sparkless commutation is obtained by moving the brushes in order to find in the fringe from the main poles a magnetic field which will bring about proper reversal of the current in the coils undergoing commutation. Graphical methods may be used to obtain a very close approximation to the true distribution of flux density in the air gap under load conditions, and the problem then resolves itself into finding the brush position which will place the short-circuited coil in a reversing field of such strength as will satisfy the condition indicated by

formula (31), which applies to an interpolate covering the full length of the armature core.

It is, however, possible to design machines that will work sparklessly without commutating poles and without brush shift. This is because of the contact resistance of carbon brushes, which is an aid to commutation, for reasons explained in the following article.

**32. Brush-contact Resistance as an Aid to Commutation.** When copper brushes are used, destructive sparking is likely to occur even when a comparatively small emf is induced in the short-circuited coil. The contact resistance of carbon brushes assists the reversal of current and

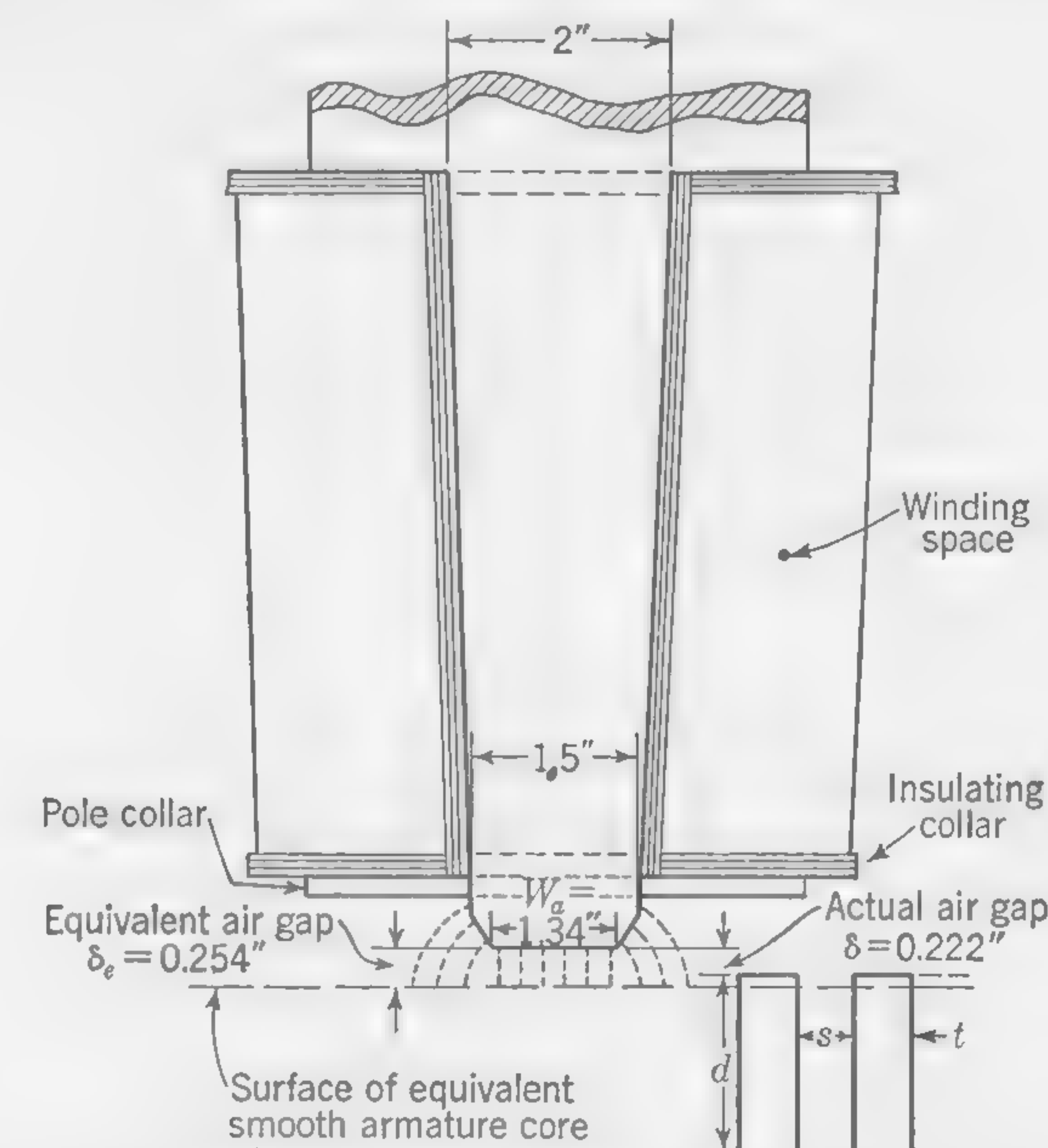


FIG. 34. Commutating pole for Illustrative Example of Art. 30(d).

thus allows of sparkless commutation, even with an appreciable departure from the ideal condition of zero value for the average short-circuit emf. At the beginning and end of the commutation period, the field in which the coil moves should be such as to produce an emf in the short-circuited coil of the value  $e = I_c R$  where  $I_c$  is the current per path of the armature circuit and  $R$  is the resistance of the short-circuited coil. On the assumption of a uniform current density over the surface of the brush, the brush-contact resistance need not be taken into account, as will be clear from the following considerations. Figure 35 shows a brush of width  $W$  covering several segments of the commutator. The total current entering the brush is  $2I_c$ , and, with density assumed constant over the surface of the contact, the current entering the brush over any surface of width



$w$  is  $2I_c(w/W)$ . To calculate the volts  $e$  that must be developed in the coil of resistance  $R$  when the distance yet to be traveled before the end of commutation is  $w$ , consider the sum of the potential differences in the local circuit  $AabB$  which is closed through the material of the brush. This leads to the equation

$$e = iR - i_a R_a + i_b R_b \quad (36)$$

where  $R_a$  and  $R_b$  are contact resistances depending upon the areas of the surfaces through which the current enters the brush. Under the con-

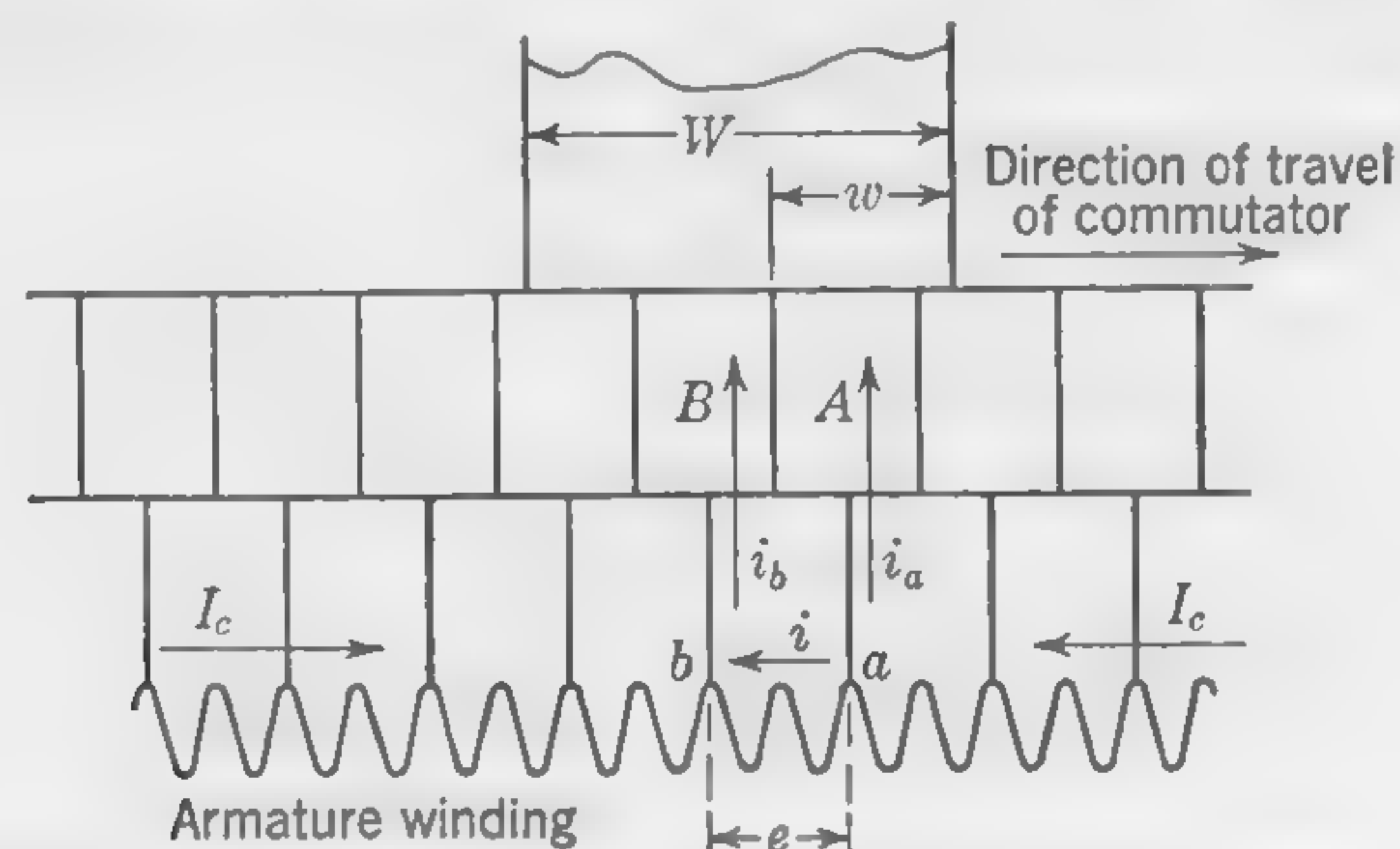


FIG. 35. Illustrating effect of brush-contact resistance (first position of short-circuited coil).

ditions shown in Fig. 35, the two contact surfaces are equal, and the currents  $i_a$  and  $i_b$  are, therefore, also equal. It follows that the voltage drops  $i_a R_a$  and  $i_b R_b$  are equal and cancel out from the Eq. (36). The same may be shown to be true when the distance  $w$  yet to be traveled by

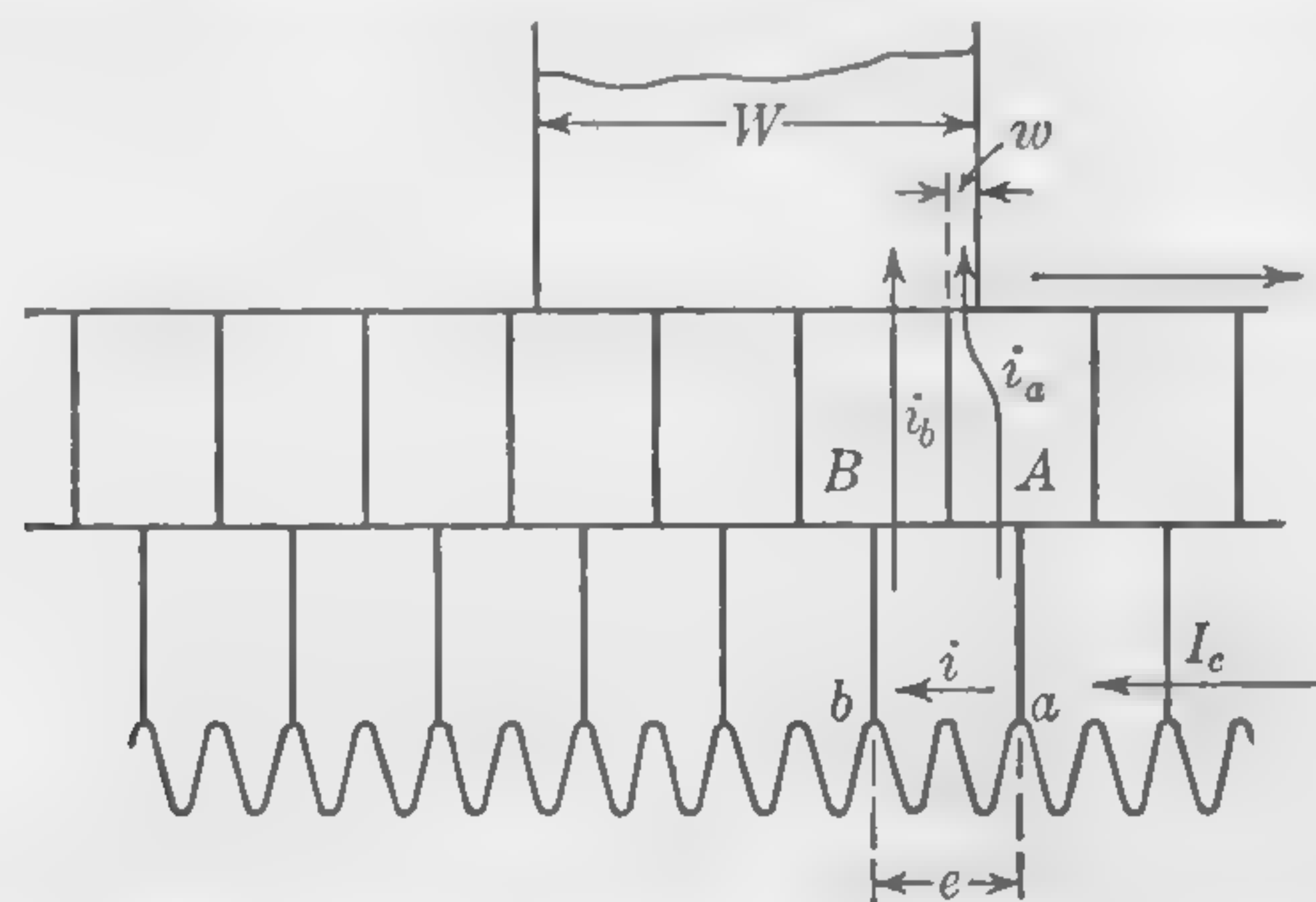


FIG. 36. Illustrating effect of brush-contact resistance (second position of short-circuited coil).

the commutator is less than the width of the brush segment, and it therefore follows that, with *straight-line commutation* and the *uniform current density over the brush-contact surface* which necessarily results from the straight-line curve of current reversal, the only emf to be developed in the short-circuited coil is  $e = iR$ .

Thus, although the *average* short-circuit emf during the time of commutation should be zero, the ideal voltage in the coil at the beginning and end of commutation is plus or minus  $I_c R$ , irrespective of the material or contact resistance of the brush.

We shall now consider how, and to what extent, a departure from the ideal conditions is permissible when carbon brushes are used. In Fig. 36 the commutator is shown as having moved forward under the brush, leaving the distance  $w$  yet to be traveled before the segment  $A$  passes from under the brush considerably smaller than in Fig. 35. If the current

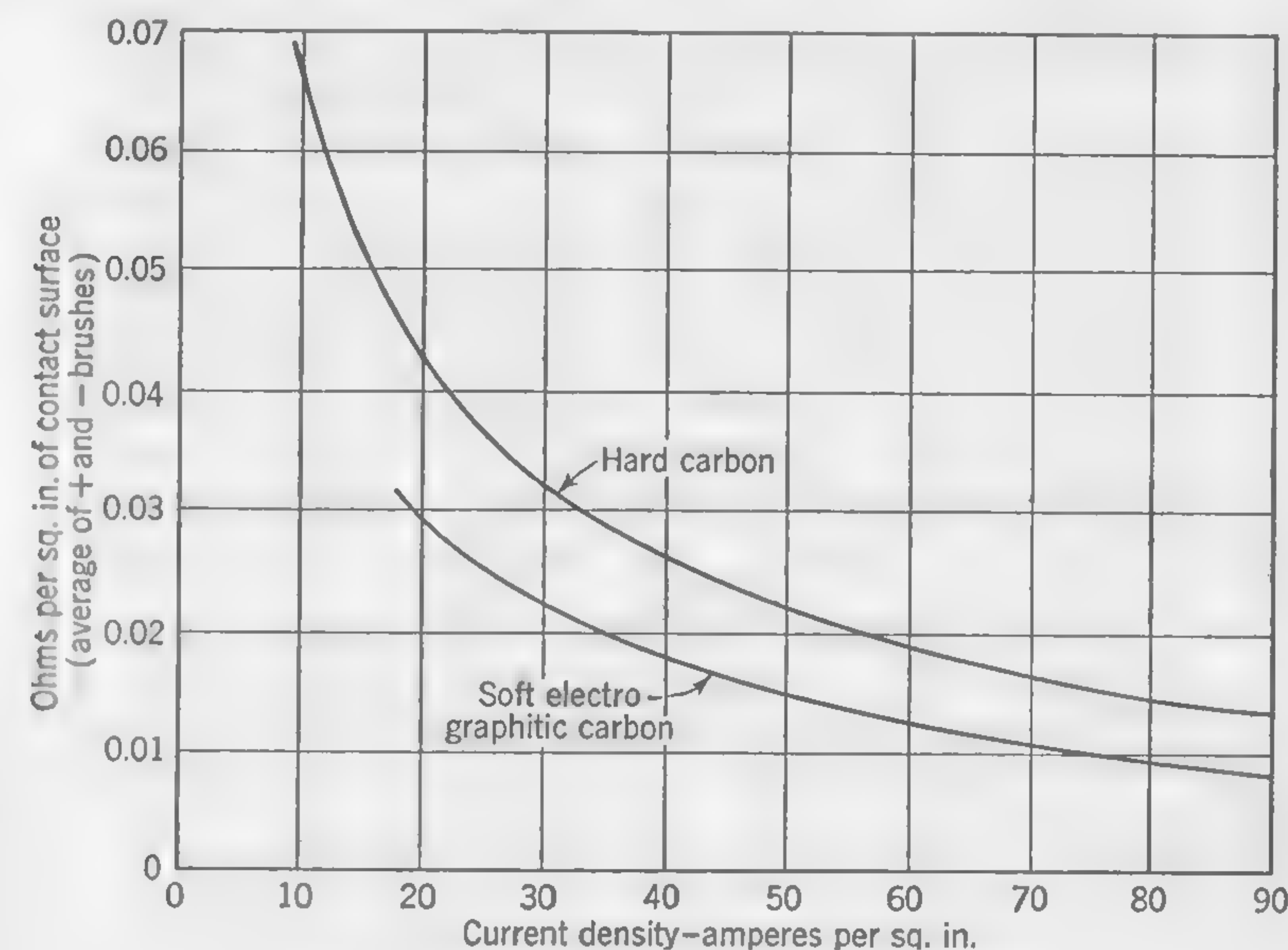


FIG. 37. Contact resistance of carbon brushes.

density under the portion  $w$  of the brush be allowed to exceed the density under the remaining portion of width  $(W - w)$ , the opposition to the passage of the current component  $i_a$  will increase and the greater potential drop at this point will assist in bringing the current  $i$  in the coil more nearly up to the value  $I_c$ , which it must reach at the instant the mica passes from under the brush. It is true that, under steady conditions, the contact resistance of carbon brushes decreases greatly with increase of current density, as indicated by the curves of Fig. 37, and it might be argued that, since the potential drop (see Fig. 38) is not very much greater with a density of 100 amp per sq in. than with a normal density of 10 amp per sq in., the corrective effect of the contact resistance of carbon brushes must be very small. However, when the current density is rapidly fluctuating, even between wide limits, it is found that the specific



contact resistance will remain approximately constant at all points under the brush.

Let  $R_c$  stand for the specific contact resistance of the carbon brush when the average current density per square inch of surface is  $\Delta$ ; and let  $\Delta_w$  be the greater current density in the space of width  $w$  (see Fig. 36)

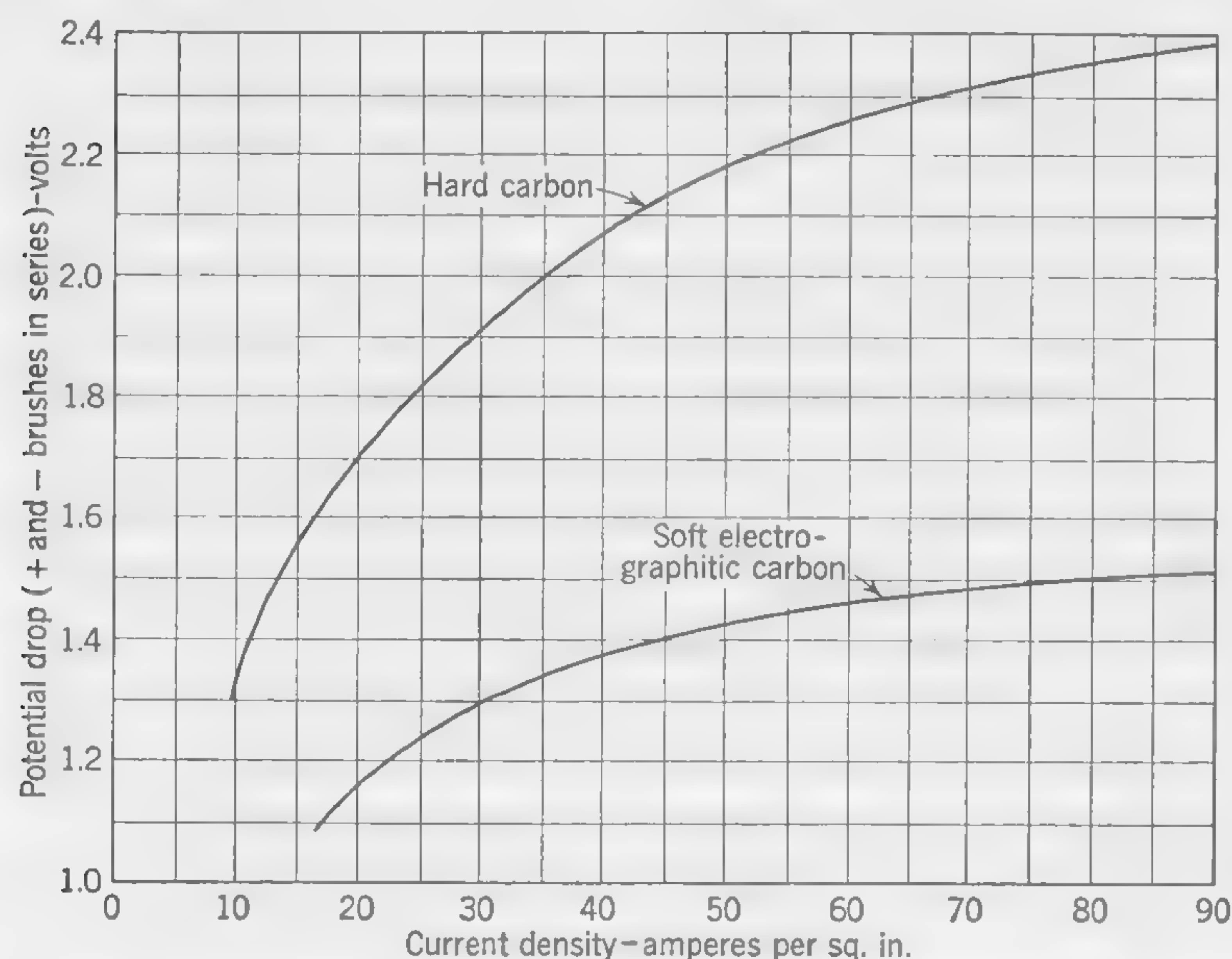


FIG. 38. Potential drop due to surface resistance of carbon brushes.

resulting from an induced voltage  $e$  in the short-circuited coil which opposes reversal of the current. Then

$$e = iR - \Delta_w R_c + \Delta R_c$$

but as the space  $w$  becomes smaller, due to the travel of commutator surface from left to right, the current  $i_a$  decreases and  $i$  becomes more and more nearly equal to  $I_c$ , so that, for the condition at the end of commutation, we may write

$$e = I_c R - R_c(\Delta_w - \Delta)$$

Let  $k$  stand for the ratio  $\Delta_w/\Delta$ , then

$$e = I_c R - R_c \Delta(k - 1)$$

As an example, assuming an upper safe limit for  $\Delta_w$  of 120 amp per sq in. and  $\Delta = 40$ , we have  $k = 3$ , and, since  $R_c \Delta$  is always about 1 volt, the permissible variation from the ideal value of  $e = I_c R$  at the end of commutation is seen to be 2 volts. If this variation from the ideal voltage

is exceeded, there is likely to be trouble due to sparking, even when carbon brushes are used. In practice the high-contact resistance of carbon brushes will not only permit slight departures from the correct average value of the reversing field provided by commutating poles (or by the main poles when sparkless commutation is obtained by moving the brushes), but it will also take care of the pulsations and fluctuations in the short-circuit emf and so prevent great irregularities in the local current passing through the coil *via* the brush-contact surface.

The permissible amount of variation from the ideal voltage in the short-circuited coil can be accurately determined only by actual test, because it will depend upon the particular grade of carbon used for the brushes and other factors which cannot very well be taken account of in the calculations. There are very few designs of dynamos in which the carbon brush alone will bring about satisfactory commutation without the aid of a reversing field to counteract the flux set up in the zone of commutation by the currents in the armature windings.

*Example. Illustrating Application of Commutation Formulas.* In the example of Art. 28 the short-circuit emf at full load in the commutated coils of a given machine was calculated by applying formulas based upon the theory discussed in earlier articles. The average value of this short-circuit emf was found to be 4.6 volts. In Art. 30 commutating poles were designed which would counteract this emf and permit the reversal of the current in the coil to take place without sparking at the commutator surface. Let us now assume that there are no commutating poles but that the carbon brushes will take care of a variation of 1.5 volts above or below the ideal value for sparkless commutation. The resistance of the one turn of armature winding which forms the short-circuited coil in the example referred to would probably not exceed 0.001 ohm, so that, with the current  $I_c = 181$  amp, the ideal value for the voltage in the coil at the end of commutation would be  $e = 181 \times 0.001 = 0.18$  volt, and the difference  $4.6 - 0.18 = 4.42$  volts could not be taken care of by the brush-contact resistance. Since a variation of 1.5 volts from the ideal value of the short-circuit emf is permissible, the machine will probably work sparklessly with carbon brushes commutating in the geometric neutral zone with a load of  $1.5/4.42$  or (say) 34 per cent of full load, if the pulsations in the local short-circuit current are negligible. With a load exceeding 34 per cent of rated full load it would, however, be necessary to resort to brush shift or provide commutating poles in order to obtain a reversing field and so counteract the effects of the various fluxes in the commutating zone which are due to the armature currents.

**33. Compensating or Pole-face Windings.** A pole-face compensating winding consists of balancing coils passing through slots in the pole face and carrying the full current of the machine; that is to say, they are con-



nected in series with the commutating pole windings and the compounding series turns (if any) on the main poles. The connections between the pole-face compensating coils are so made that the current in these will always tend to neutralize the magnetic effect of the currents in the armature coils and so prevent distortion of the flux under the pole face.

With brushes on the geometric neutral as in interpole machines, field distortion has very little to do with commutation; but, obviously, if a winding is provided in slots through the pole shoes to annul the cross-magnetizing ampere-turns of the armature winding, *the amount of winding necessary on the commutating poles will be greatly reduced.* The problem of interpole design remains nevertheless practically unchanged, because,

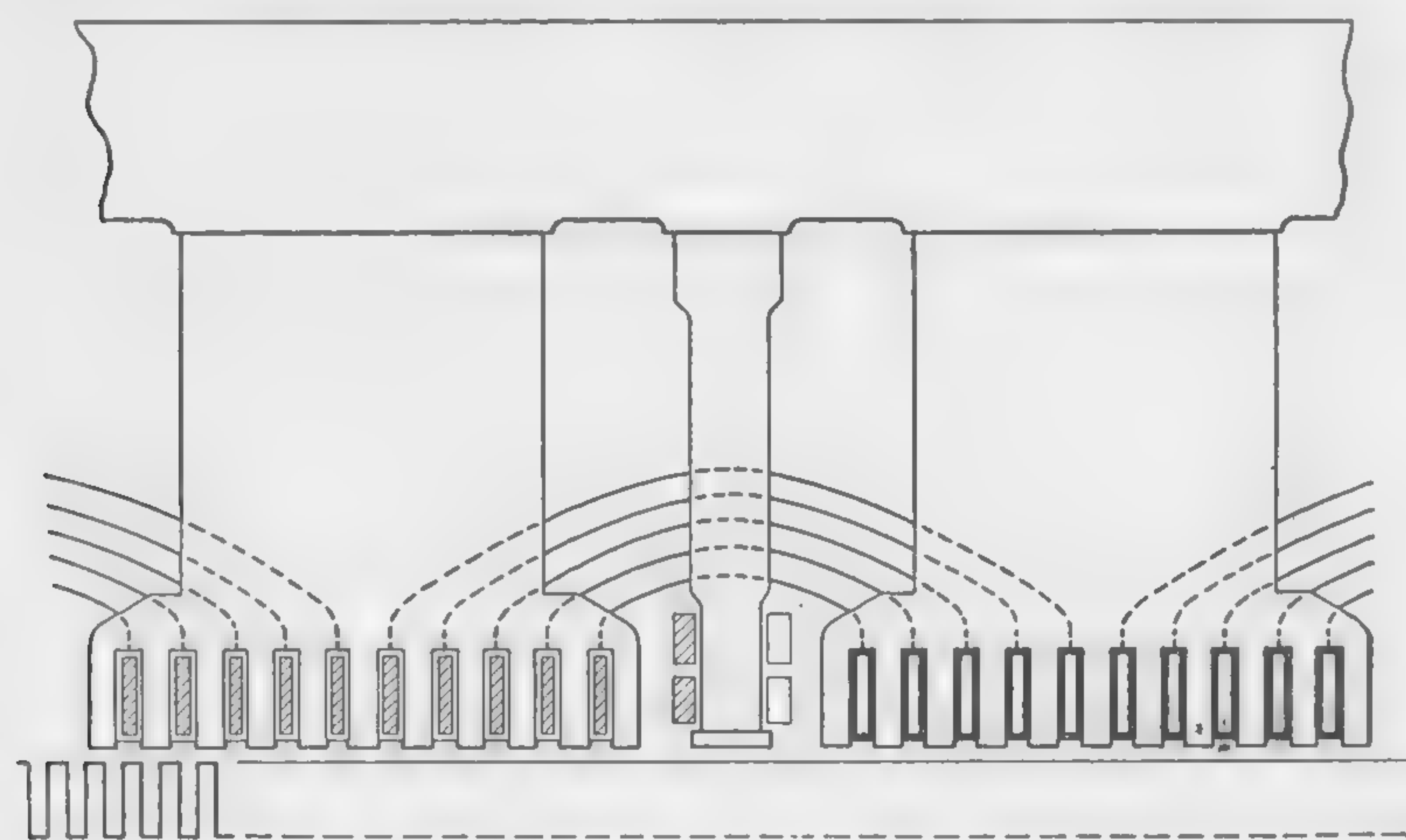


FIG. 39. Diagram of pole-face windings.

if sparkless commutation is to be obtained, the amount of flux entering the armature in the zone of commutation must be the same whether or not pole-face windings are used.

It is true that, with fewer ampere-turns on the commutating poles, there will be less leakage flux between commutating and main poles (refer to Art. 30*d*), and the pole shoes may cover a somewhat larger portion of the armature surface than in machines which are not provided with compensating windings. This is indicated in Fig. 39 which shows a pole-face winding consisting of rectangular copper bars passing through slots punched in the laminations with which the field poles are constructed. In an actual machine, the axes of the poles would, of course, not be parallel as in this diagram. The armature periphery would be a circle instead of a straight line.

One advantage of compensating or pole-face windings is the improvement of the "field form" and the avoidance of local flux concentration

in the air gap when the machine is heavily loaded. This greatly reduces the tendency to flash over at the commutator surface, a trouble which has very little connection with the reversal of current in the coil undergoing commutation.

A drawing showing the outline of the main-pole lamination for a rather large d-c generator is given in Fig. 40; note particularly the four large circular holes in the pole faces for the compensating winding. The 12-pole 460-volt compound machine for which this lamination was designed has a rating of 1,750 kw at 600 rpm.

**34. Sundry Details Affecting Commutation.** The quality of the carbon used for the brushes, together with the pressure between brush and commutator surface, will determine the heating due to friction and, therefore, to some extent, the dimensions and proportions of the commutator. The pressure between brush and commutator is usually adjusted by springs, so that it shall be from 1 to  $2\frac{1}{2}$  lb per sq in. of contact surface. In order to avoid excessive temperature rise, the current density with hard carbon brushes is generally limited to about 40 to 50 amp per sq in. of brush-contact surface. A sufficient cooling surface is thus provided from which the heat developed through friction and  $I^2R$  loss may be radiated. The number of commutator bars covered by the brush is not a matter of great importance, but it is only rarely that the width of brush (brush arc) is such as to cover more than  $3\frac{1}{2}$  bars when the armature winding is of the simplex type. The usual width of brush is something between the limits  $\frac{5}{8}$  and  $1\frac{1}{4}$  in., and, as a further check on the desirable dimensions, the width should not exceed one-tenth of the pole pitch referred to the commutator surface. The width of the brush having been determined and a suitable current density decided upon, the total axial length per brush set may be calculated, and the length of the commutator decided upon.

The individual brush rarely exceeds  $1\frac{1}{2}$  in., measured parallel to the axis of rotation, and is usually about 1 in.; when a greater length of contact surface is required, several brush holders are provided on the one spindle or brush arm. Even in small machines, the number of brushes

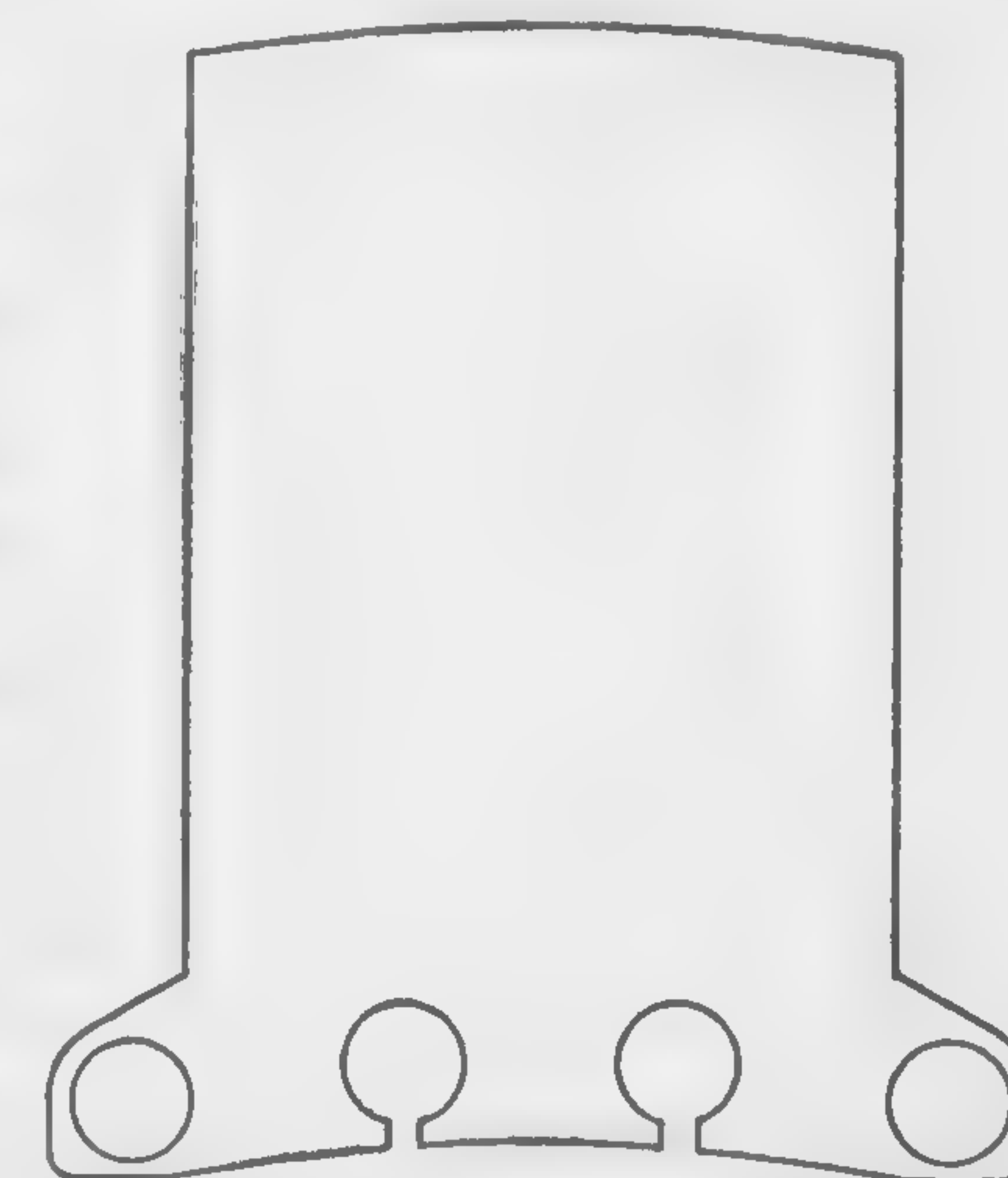


FIG. 40. Main-pole lamination, showing holes in the pole face for the compensating winding, for a large d-c generator.



per set should not be less than two, so as to allow of examination and adjustment while running. When the contact area of the individual brush is small, a higher current density is permissible than when fewer brushes of larger size are used. The final check in the matter of commutator design is the probable temperature rise, which will be considered in Chap. 6 treating of various heating problems. For low-voltage machines, economy may frequently be effected by using the graphitic brushes with current densities as high as 75 amp to the square inch of contact surface. It is an interesting, but not very clearly explained, fact that the temperature rise of the negative brushes in a generator is greater than that of the positive brushes. In other words, the watts lost are greater when the current flow—according to the popular conception—is from carbon to copper, than when it is from copper to carbon. The resistances given in Fig. 37 have been averaged for the + and - brushes.

On low-voltage dynamos, when the current to be collected is very large, copper brushes must be used. The resistance of the contact between brush and commutator is then much lower than with carbon brushes and the current density may be as high as 200 amp per sq in. of contact surface. The contact-surface resistance may be anything between 0.0007 and 0.0028 ohm per sq in., a safe figure for the purpose of calculating the brush losses being 0.002 ohm. If the current density at the contact surface is 150 amp per sq in. (a very common value), the total loss of voltage at the brushes will be  $0.004 \times 150 = 0.6$  volt, instead of about 2 volts, which is usual with carbon brushes.

A perfectly true cylindrical commutator surface is essential to sparkless running. The different sets of brushes should be "staggered" in order to cover the whole surface of the commutator and so prevent the formation of grooves. For the same reason—and also to ensure more even wear of the journals and bearings—some end play should be allowed to the shaft. In large machines it is not uncommon to provide some device, in the form of an electromagnet with automatically controlled exciting coil, to ensure that the desirable longitudinal motion of the rotating parts will be obtained.

Owing to the hardness of the mica insulation in relation to that of the copper bars, there is a tendency for the mica to project slightly above the surface of the copper. This naturally leads to sparking troubles, and it is generally the practice to groove or "undercut" the commutator between bars, cutting down the mica about  $\frac{1}{16}$  in. below the surface, leaving an air space as the insulation between the bars. This undercutting process may have to be repeated as the commutator wears down in use.

The design of brushes and holders is a matter of great importance; as a general rule, it may be said that the lighter the moving parts of

brush and holder, the better the conditions in regard to sparking when the surface of the commutator is not absolutely true.

A peripheral velocity exceeding 4,800 fpm should be avoided if possible. When this velocity exceeds 5,000 fpm, special attention must be paid to the mechanical construction and balancing of the commutator. With peripheral speeds of 7,000 to 8,000 fpm, not uncommon for commutators of high-speed dynamos, it is usual to provide nickel-steel rings shrunk on the outside of the bars over insulating bands of mica. These, and other mechanical details of high-speed machinery, must, however, be studied elsewhere as their discussion is not included in the scope of this book (Fig. 189 shows a commutator with steel rings to hold the bars in position). The pitch of the bars at the commutator surface should preferably not be less than 0.2 in., because, with the mica of the usual thickness (0.03 to 0.035 in.), the bar might be mechanically unsatisfactory if the thickness were reduced below this limit.

### TEST PROBLEMS

Since the subject of commutation cannot conveniently be studied or illustrated by short numerical problems, the few simple test problems here given will be followed by some general questions which require written answers. These are accompanied by references to the text, so that the reader may familiarize himself with the contents of this chapter and understand their application to the practice of dynamo design.

1. Given an 8-pole dynamo, simplex-lap-wound: terminal volts = 200; total number of armature conductors  $Z = 960$ ; average volts between commutator segments = 10. Calculate the number of turns in a coil connected across adjacent commutator bars.

Ans. 3.

2. In an armature provided with a full-pitch winding, there are two coil sides in each slot, and each coil side consists of four conductors carrying 65 amp. The slots in the armature core are  $\frac{1}{2}$  in. wide by 1 in. deep and 10 in. long. The space occupied by the conductors measures 0.8 in. from the bottom of slot. Calculate the slot flux in the space above the coils, assuming the sides of the slot to be parallel throughout.

Ans. 6,650 maxwells.

3. What is the approximate value of the contact resistance of a carbon brush carrying 75 amp?

Ans.  $\frac{1}{45}$  ohm.

4. Given a multiple- (lap-) wound 8-pole dynamo, 300 kw, 400 volts. Calculate the contact area of each positive brush set if the surface current density is 40 amp per sq in.

Ans. 4.7 sq in.

5. Given a six-pole simplex-lap (or multiple) winding; current in each armature circuit = 40 amp; current density at brush-contact surface = 30 amp per sq in. Calculate the area of contact of one set of positive (or negative) brushes.

Ans. 2.67 sq in.

6. A six-pole dynamo is provided with six brush studs carrying carbon brushes. There are two brushes per stud, and the contact area of each brush is  $\frac{3}{8}$  by 1 in. The total  $I^2R$  loss at brush-contact surface is 150 watts, and the resistance of 1 sq in. of contact surface is 0.0225 ohm. Calculate (a) the current density at brush-contact surface, (b) the total voltage drop due to brush-contact resistance.

Ans. (a) 38.5 amp per sq in., (b) 1.73 volts.



7. Given a machine without commutating poles and with brushes placed on the "geometric neutral" (*i.e.*, so as to short-circuit the coils when the conductors are in the space midway between poles). Name the three components of flux cut by the coil undergoing commutation which generate emfs opposing current reversal and tending to produce sparking.

*Ans.* (a) The armature interpolar flux  $\Phi_a$  (Art. 22), (b) the end flux  $\Phi_e$  (Art. 22), (c) the slot flux  $\Phi_s$  (Arts. 23 and 24).

8. How is the effect of armature flux (or interpolar flux) counteracted?

*Ans.* By opposing the armature mmf, and so annulling this flux component (brush shift). By annulling part of the flux and balancing the remaining flux (commutating poles of shorter axial width than main poles). (Refer to Arts. 29 and 30.)

9. How is the effect of end flux counteracted?

*Ans.* By injecting an equal but opposite amount of flux in the commutating zone from the interpole or fringe from main pole.

10. How is the effect of slot-leakage flux counteracted?

*Ans.* It cannot be annulled, but it is supplied by commutating pole, or fringe from main pole, its direction in the iron of the armature teeth being such that it no longer tends to oppose or retard the reversal of current in the short-circuited coil.

11. What is meant by "equivalent slot flux"? Is this greater or smaller in amount than the actual slot flux?

*Ans.* It is an imaginary component of the total flux tending to oppose reversal of current in the short-circuited coil. It may be defined as the amount of flux which, if cut by all the conductors in the slot, would generate in the coil the same emf as results from the cutting of the actual slot flux. It is *smaller* than the actual slot flux which, being distributed throughout the depth of the slot, does not all link with all the conductors in the slot.

12. Why is a low-flux density desirable in the air gap under face of commutating pole?

*Ans.* Large leakage factor due to proximity of interpole and main pole tends to saturate iron core. Low density in iron at full load is necessary to provide for reversing flux being approximately proportional to growth of armature current on overloads. When  $B$  is above "knee" of  $B$ - $H$  curve, this proportionality ceases.

13. Why are commutating poles wound with series turns?

*Ans.* All flux components tending to oppose current reversal in short-circuited coil are proportional to the armature current, therefore the compensating fluxes provided by commutating pole should be proportional to current output.

14. If a machine is provided with compensating pole-face windings, are as many ampere-turns required for excitation of the commutating poles as on a similar machine but without pole-face windings? Give reasons.

*Ans.* No. The ampere-turns required must overcome reluctance of air gap and interpole in order to establish the necessary reversing flux in the zone of commutation, but the pole-face windings will generally be sufficient to balance the armature mmf which otherwise must be counteracted by additional ampere-turns on the commutating poles. (Refer to Art. 33.)

15. Assuming that the reversing field provided by the commutating poles is not exactly what would be necessary to produce "ideal commutation," explain why carbon brushes will be more effective than copper brushes in preventing sparking.

*Ans.* The higher contact resistance of carbon assists reversal of current. (Refer to Art. 32 including example.)

## CHAPTER 5

### TOOTH RELUCTANCE AND ARMATURE REACTION —DESIGN OF FIELD MAGNETS AND WINDINGS

In order to design the field poles of a dynamo, it is necessary to calculate the total flux per pole under full-load conditions, and, in order to determine the number of ampere-turns which are required to establish this flux, it is necessary to calculate not only the reluctance of the complete magnetic circuit, but also the demagnetizing effect of the armature currents, which has to be neutralized by additional ampere-turns on the field poles when the machine is working under load.

*The portion of the magnetic circuit of which the reluctance is most difficult to calculate is the air gap and teeth in machines with slotted armatures.*

**35. Effect of Armature Slots on Permeance of Air Gap.** A correct flux plot of the magnetic lines entering the top and sides of the armature tooth is shown in Fig. 41. This takes no account of magnetic saturation of the iron, but the assumption of very

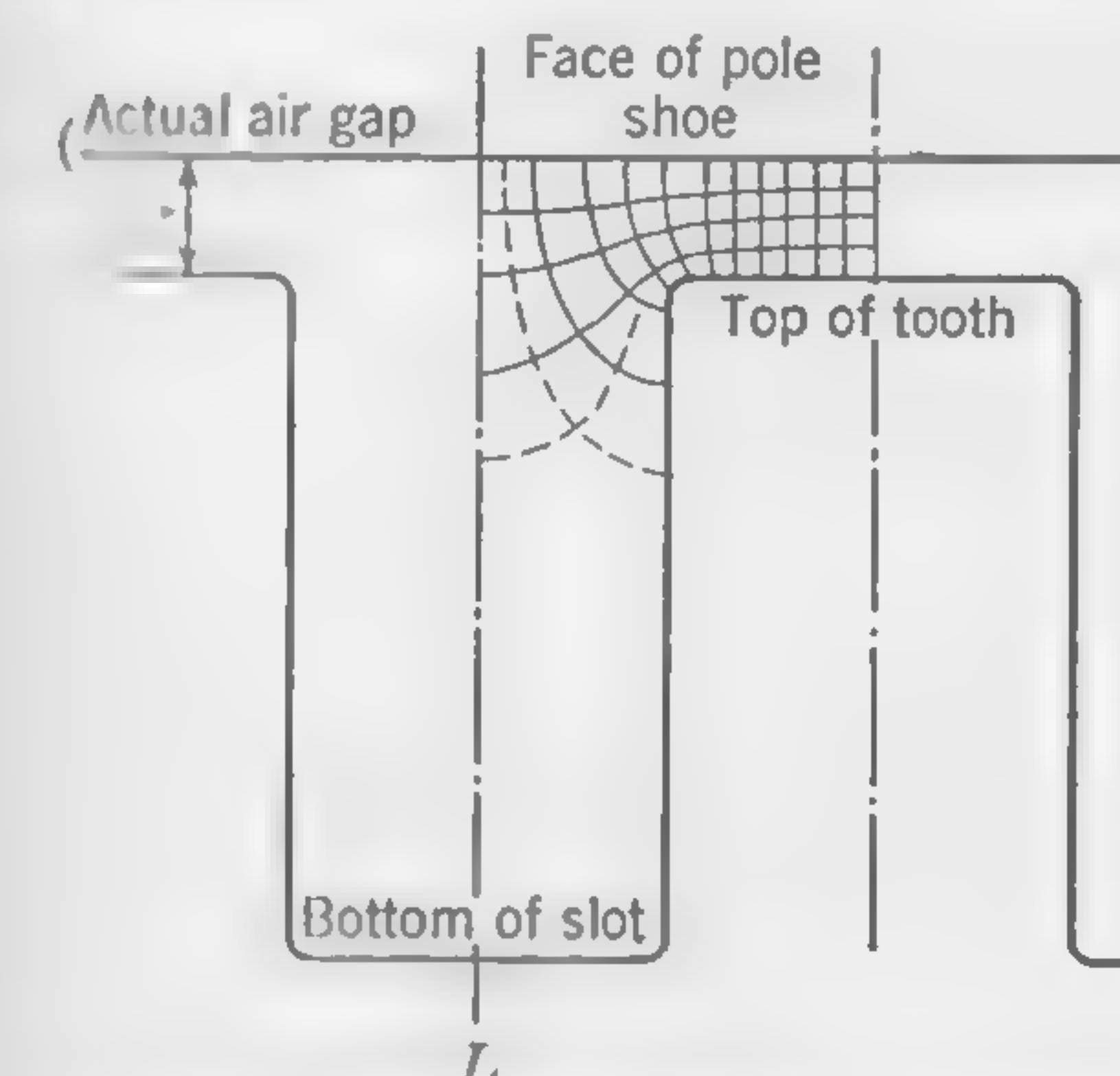


FIG. 41. Flux-plot of magnetic field between pole face and slotted armature.

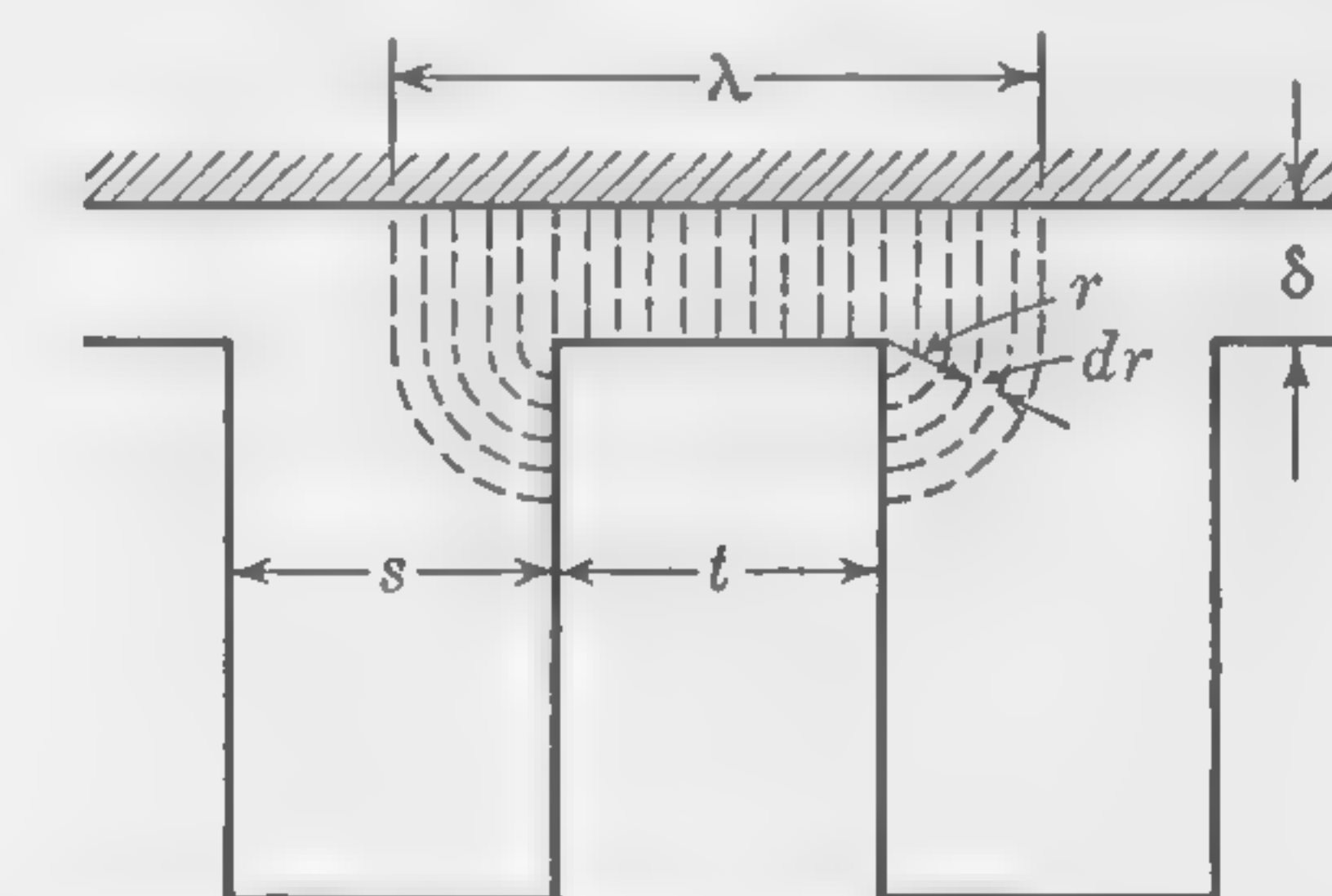


FIG. 42. Approximate shape of flux lines entering slotted armature (low flux density).

high permeability of the iron is justified since the flux density is usually comparatively low near the top of the tooth.

In order to explain how the permeance of the air paths between pole face and slotted armature may be calculated, the magnetic lines will be supposed to follow the paths indicated in Fig. 42. The tooth is drawn, for convenience, with parallel sides, and the magnetic lines entering the



sides of the tooth are supposed to follow a path consisting of a straight portion of length  $\delta$ , equal to the actual air clearance, and a circular arc of radius  $r$ , all as indicated in the figure. This is obviously an arbitrary assumption, but it is convenient for calculation and gives very good results.

Consider a portion of the air gap 1 cm long axially (*i.e.*, in a direction normal to the plane of the section shown in Fig. 42) and note that the permeance over the slot pitch of width  $\lambda$  is made up of two parts: (*a*) the permeance  $P_1$  between pole face and top of tooth, of value  $P_1 = t/\delta$ , and (*b*) the permeance  $2P_2$ , where  $P_2$  is the permeance between the pole face and *one side* of the tooth. The permeance of any small section of thickness  $dr$  and depth 1 cm measured axially, as indicated in Fig. 42, is

$$dP_2 = \frac{dr}{\delta + (\pi r/2)}$$

whence

$$\begin{aligned} P_2 &= \frac{2}{\pi} \int_0^{s/2} \frac{dr}{(2\delta/\pi) + r} \\ &= \frac{2}{\pi} \log_e \frac{\delta + (\pi s/4)}{\delta} \end{aligned}$$

The average permeance *per square centimeter* over the tooth pitch at center of pole is, therefore,

$$\begin{aligned} P_{\text{sq cm}} &= \frac{P_1 + 2P_2}{\lambda} \\ &= \frac{\frac{t}{\delta} + \frac{4}{\pi} \log_e \left( \frac{\pi s}{4\delta} + 1 \right)}{\lambda} \end{aligned}$$

where the tooth pitch  $\lambda$  is expressed in centimeters.

The reciprocal of this quantity is the reluctance  $R$  per square centimeter of air-gap cross section for an average length, or what may be called an *equivalent air-gap length*, equal to  $\delta_e$ . Since  $R = l/A = \delta_e/A$ , and  $A = 1$  sq cm it follows that

$$\delta_e = \frac{\lambda}{\frac{t}{\delta} + \frac{4}{\pi} \log_e \left( \frac{\pi s}{4\delta} + 1 \right)} \quad (37)$$

A modified formula, which takes account of the fact that the flux lines do not follow the exact paths as assumed in Fig. 42 and agrees very closely with the mathematical results obtained by F. W. Carter,\* is

\* The reader is referred to C. C. Hawkins, "The Dynamo," Sir Isaac Pitman & Sons, Ltd., 1922, vol. 1, p. 491, where Carter's coefficient has been used in preparing curves giving the ratio between the "equivalent" and actual air gap.

$$\delta_e = \frac{\lambda}{\frac{t}{\delta} + 2 \log_e \left[ \frac{1}{2} \left( \frac{s}{\delta} \right) + 1 \right]} \quad (37a)$$

This is the length of air gap that would be necessary to give the same air-gap reluctance between pole and armature if the actual toothed armature were replaced by a smooth-core armature.

A formula which is simpler to use than formula (37) is that proposed by T. C. Baillie;\* it gives values for  $\delta_e$  very closely approximating those obtained from formula (37a) and also from the use of Carter's coefficient. It checks within 2 per cent of experimental values obtained by J. F. H. Douglas.† When put in the same form as formula (37) it may be written

$$\delta_e = \frac{\lambda}{\frac{t}{\delta} + \left( \frac{5s}{5\delta + s} \right)} \quad (37b)$$

For most modern machines  $\delta_e$  is generally found to be 15 to 25 per cent larger than  $\delta$ .

If the radial ventilating ducts in the armature are closely spaced, or exceptionally wide, the gap  $\delta_e$  for the equivalent smooth-core armature, as given by the above formulas, might have to be slightly modified, but

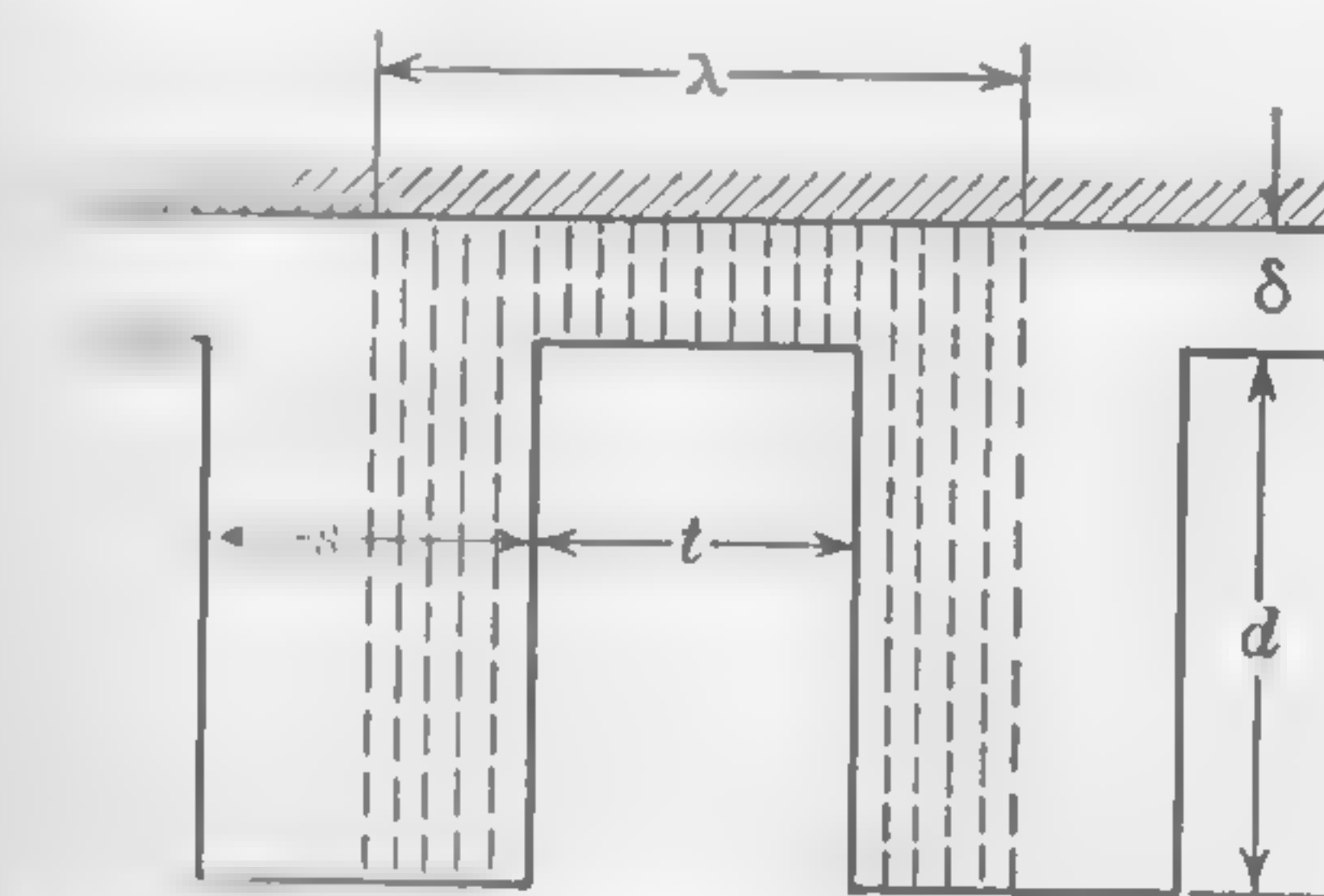


FIG. 43. Flux lines entering slotted armature (very high flux density).

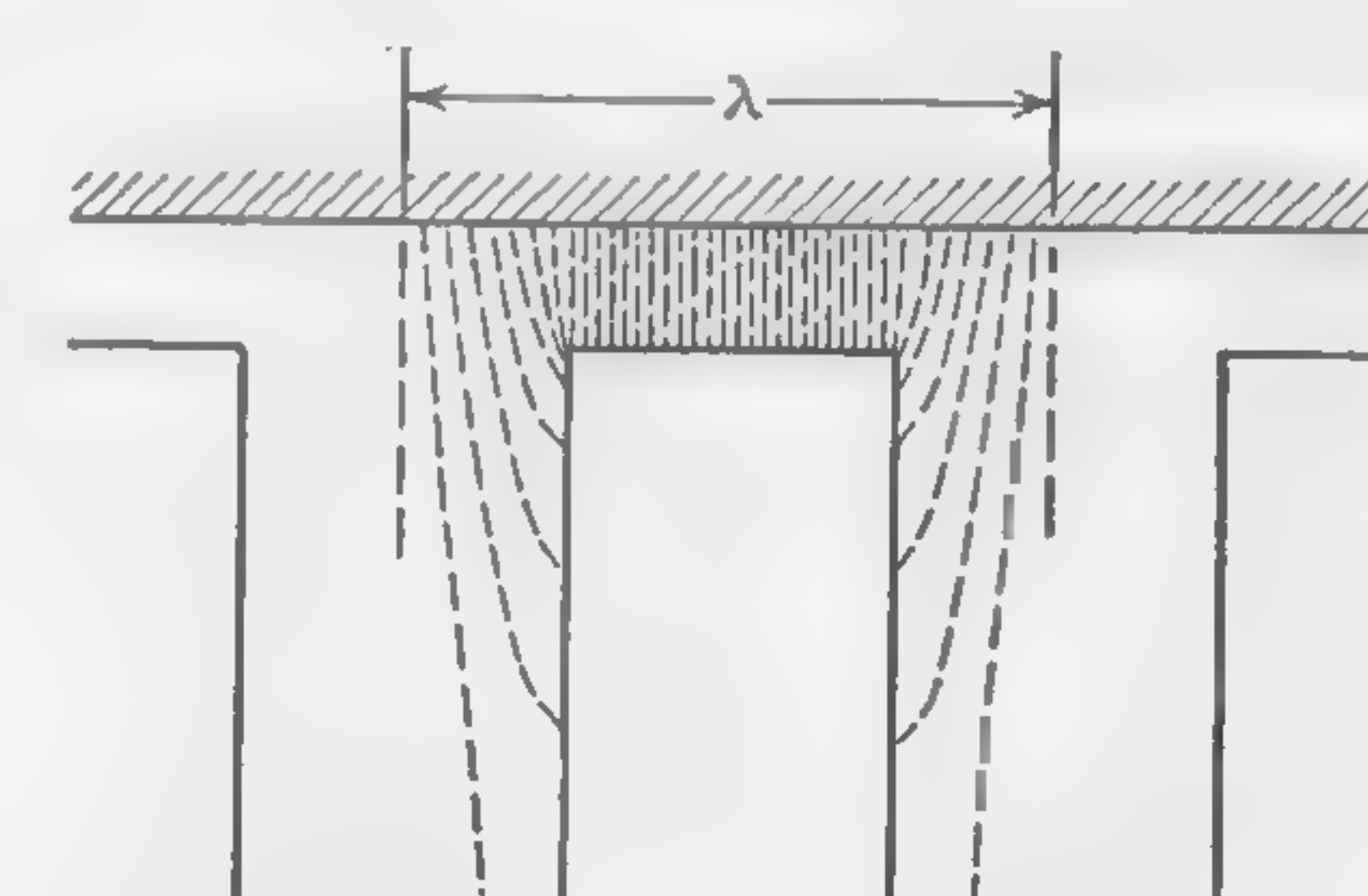


FIG. 44. Flux lines entering slotted armature (high flux density in tooth).

the calculation of fringing at the sides of vent ducts is usually an unnecessary refinement.

Consider now Fig. 43, which illustrates the extreme case of a highly saturated tooth. The lines of flux are shown parallel over the whole of the slot pitch, a condition which is approached—but never attained—when the density in the tooth is forced up to higher and higher values. It is obviously only when the permeability of the iron in the tooth becomes equal to unity—that is to say, equal to the permeability of the air paths—

\* The Electrician, p. 491, Jan. 8, 1909.

† The Reluctance of Some Irregular Magnetic Fields, Trans. AIEE, vol. 39, p. 1089, June 29, 1915.



that this parallelism of the flux lines would occur. This is an extreme, and, indeed, an impossible, condition; but, since, even at comparatively low flux densities in the iron of the teeth, there will be some flux passing directly from the pole face to the bottom of the slot in addition to the flux lines indicated in Fig. 42, a close approximation to actual conditions may be obtained by assuming a parallel field between the pole face and the iron at the bottom of the slot superimposed upon the field of Fig. 42. The resultant or actual field in the air gap and slot will then be somewhat as indicated by the flux lines in Fig. 44. With low values of tooth density, the mmf between the tooth tops and the bottom of the slots will be small, and few flux lines will pass from the pole face into the armature core without entering the teeth; but with higher tooth densities the mmf to overcome tooth reluctance becomes large, and more flux will be diverted into the parallel path and pass directly from the pole face to the bottom of the slot. The amount and distribution of the flux in air gap and slot will, therefore, change with every alteration in tooth density.

**36. Calculation of Tooth Density in Terms of Air-gap Density.** Notwithstanding the fact that the inclusion of the flux component which passes directly from pole face to bottom of slot will modify the length of the equivalent air gap and cause this to be dependent upon the flux density in the teeth, no appreciable error will be introduced by considering the reluctance of air gap, teeth, and slots as consisting of two reluctances in series: (1) The reluctance of the equivalent air gap (as calculated by the formulas (37) for the center of the pole face), and (2) the reluctance of the tooth and slot in parallel. The calculation of this latter quantity depends upon a knowledge of the actual flux density in the tooth. For low densities in the iron—up to about 14,000 gauss—the actual tooth density will be approximately equal to the apparent density; that is to say, practically all the flux entering the armature over one tooth pitch will pass into the core through the root of the tooth. For densities exceeding 14,000 gauss, and even for lower values when the depth of slot is small in relation to the air gap, the calculations should take account of that component of the total flux which goes from the pole face to the bottom of the slot without entering the teeth.

The following symbols will be used in the calculations:

$B_g$  = the average air-gap flux density at armature surface [i.e., the average density over one tooth pitch of width  $(t + s) = \lambda$  and length  $l_a$ ]

$B_t$  = the actual flux density in the tooth

$\mu$  = the permeability of the iron in the teeth

$B_s$  = the flux density in the slot and parallel spaces occupied by air or insulation

$l_a$  = the gross length of the armature core

$l_n$  = the net length of the armature core (iron only)

The other dimensions are given in the sketch of Fig. 45.

The full mmf necessary to overcome the reluctance of air gap and teeth is assumed to act between two cylindrical equipotential surfaces, one being the pole face and the other being the cylindrical surface passing through the bottom of the slots and the roots of the teeth. The further assumption is now made that this total drop of magnetic potential is the summation of two potential differences in series, the one value  $B_g \delta_e$  due to air-gap reluctance, and the other of value  $(B_t/\mu) d_e$  due to tooth reluctance. Since the flux component in the slots and parallel spaces not occupied by iron will depend upon the total difference of potential between the two equipotential surfaces previously defined, we may write the equation

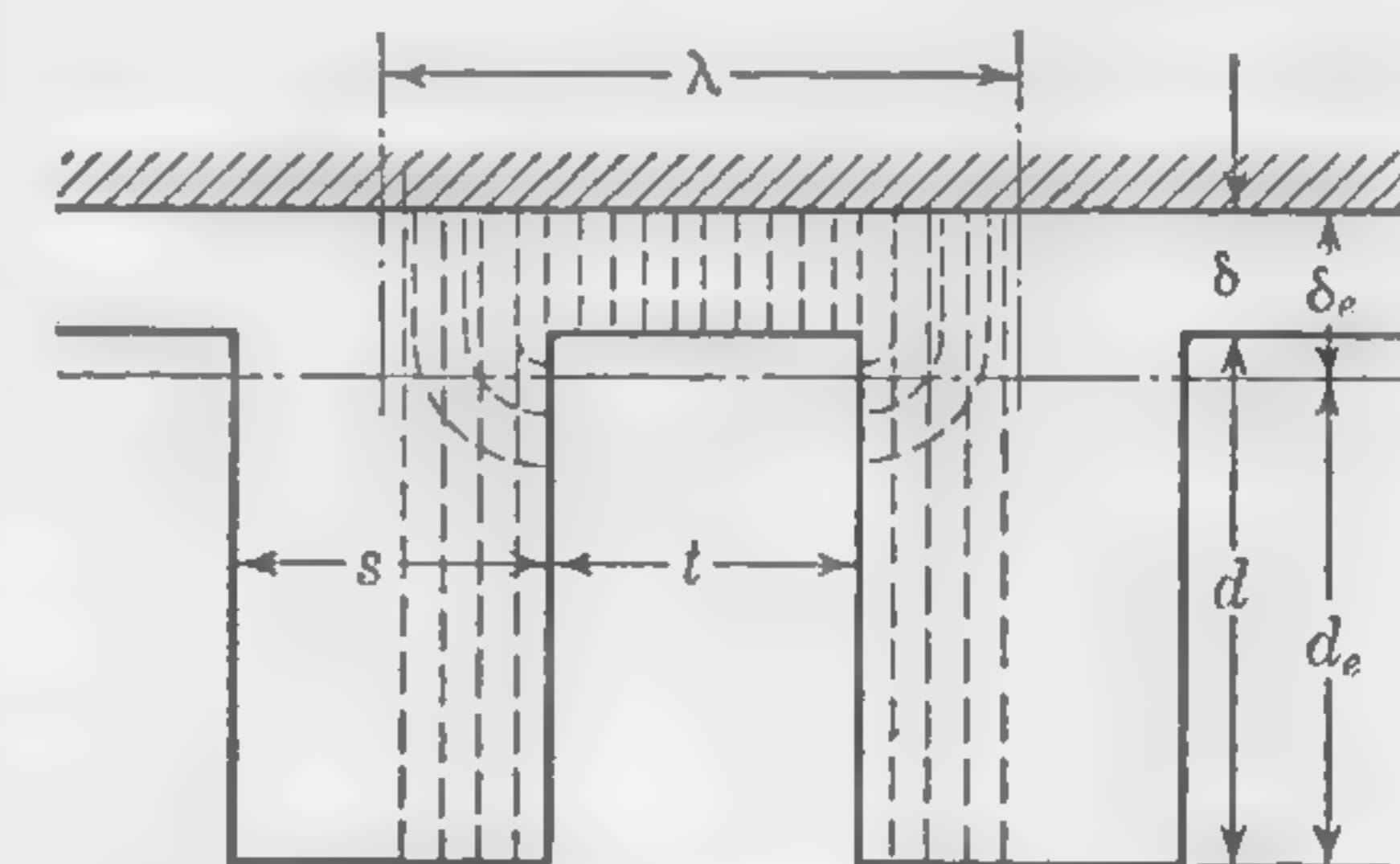


FIG. 45. Illustrating tooth-density calculations.

$$B_s(d_e + \delta_e) = \frac{B_t}{\mu} d_e + B_g \delta_e$$

whence

$$B_s = B_t \frac{d_e}{\mu(d_e + \delta_e)} + B_g \frac{\delta_e}{(d_e + \delta_e)} \quad (38)$$

The total amount of flux entering the armature over the space of one tooth pitch is

$$B_g \lambda l_a = B_t t l_n + B_s (\lambda l_a - t l_n) \quad (39)$$

By inserting for  $B_s$  in this equation the value given by (38), it is possible to express  $B_g$  in terms of  $B_t$ , the final expression being

$$B_g = B_t \left[ \frac{(d_e + \delta_e) + \frac{d_e}{\mu} \left( \frac{\lambda l_a}{t l_n} - 1 \right)}{d_e (\lambda l_a / t l_n) + \delta_e} \right] \quad (40)$$

By selecting a number of values for  $B_t$ , the corresponding values of  $\mu$  can be obtained for the particular quality of iron used in the armature. The air-gap density  $B_g$  can thus be calculated and a curve plotted giving the relation between  $B_g$  and  $B_t$  for the particular design under consideration and for any value of tooth density.

It is interesting to note the form taken by formula (40) for the limiting condition of tooth saturation. When the density is very high and the permeability  $\mu$  approaches unity



$$B_g = B_t \quad (40a)$$

which is obviously correct. When the permeability  $\mu$  is extremely high, as it is when a machine is operating normally, formula (40) becomes

$$B_g = B_t \left[ \frac{(d_e + \delta_e)}{d_e(\lambda l_a / t l_n) + \delta_e} \right] \quad (40b)$$

a formula which will be sufficiently accurate for all practical purposes when the value of  $B_t$  is less than (say) 14,000 gauss.

The formula (40b) shows that the actual tooth density is never quite equal to what is known as the apparent tooth density, which assumes that all the flux leaving the pole face goes through the teeth. On this assumption the relation would be

$$B_g = B_t \left( \frac{t l_n}{\lambda l_a} \right) \quad (41)$$

Since it is impossible for the air gap  $\delta$  and therefore the equivalent air gap  $\delta_e$  to be equal to zero, the conditions to satisfy formula (41) do not exist in practical machines.

**37. Correction for Taper of Teeth.** The assumption of parallel sides to the tooth is justified only when the diameter of the armature is large in relation to the slot pitch or when taper slots are used in order to provide a uniform cross section throughout the whole length of the tooth. The dimension  $t$  in formula (40) should preferably be the width at the *center* of the tooth. When the field system revolves, as in most alternators, the armature teeth will usually be wider at the root than at the top, and but little error will be introduced by taking for  $t$  the average width for the purpose of calculating the average tooth density and the corresponding ampere-turns required for the teeth.

The case of a tooth with considerable taper, in which the density at the root is in excess of (say) 12,000 gauss, may be dealt with by the application of Simpson's rule. Owing to the fact that a portion of the flux enters the tooth at the sides, the flux density in the top of the teeth will not be very high, and the reluctance of the tooth over the portion of its length equal to the difference  $d - d_e$  (see Fig. 46) may be neglected; the tooth will, therefore, be considered as having a total length  $d_e$  with a width  $t_e$  at the top  $t_r$  at the root, and a mean thickness of  $t_m$  halfway between these two sections. In order to simplify the calculations the assumption is now made that the total flux in the tooth remains unaltered through all other cross sections.\*

\* This is not a correct assumption when the root density is very high, because in that case flux will leak out from the sides of the tooth to the bottom of the slot, and at some distance from the bottom of the slot (the taper being as indicated in Fig. 46) the total flux in the tooth will be greater than at the root cross section.

The value of the magnetizing force  $H$  (or the ampere-turns required per unit length) can then be determined for any section of the tooth by referring to the  $B$ - $H$  curves for the iron used in the armature. It is sufficient to determine  $H$  for three sections only. If these values are

$H_r$  at the narrowest section

$H_e$  at the widest section

$H_m$  at the center section

then, on the assumption that the portion of the  $B$ - $H$  curve involved is a parabola, Simpson's approximation is

$$\text{Average } H = \frac{1}{6}H_r + \frac{2}{3}H_m + \frac{1}{6}H_e \quad (42)$$

By referring to Fig. 46, it will be seen that  $H_e$  is taken at the section which would be the top of the tooth if the air gap were increased from  $\delta$

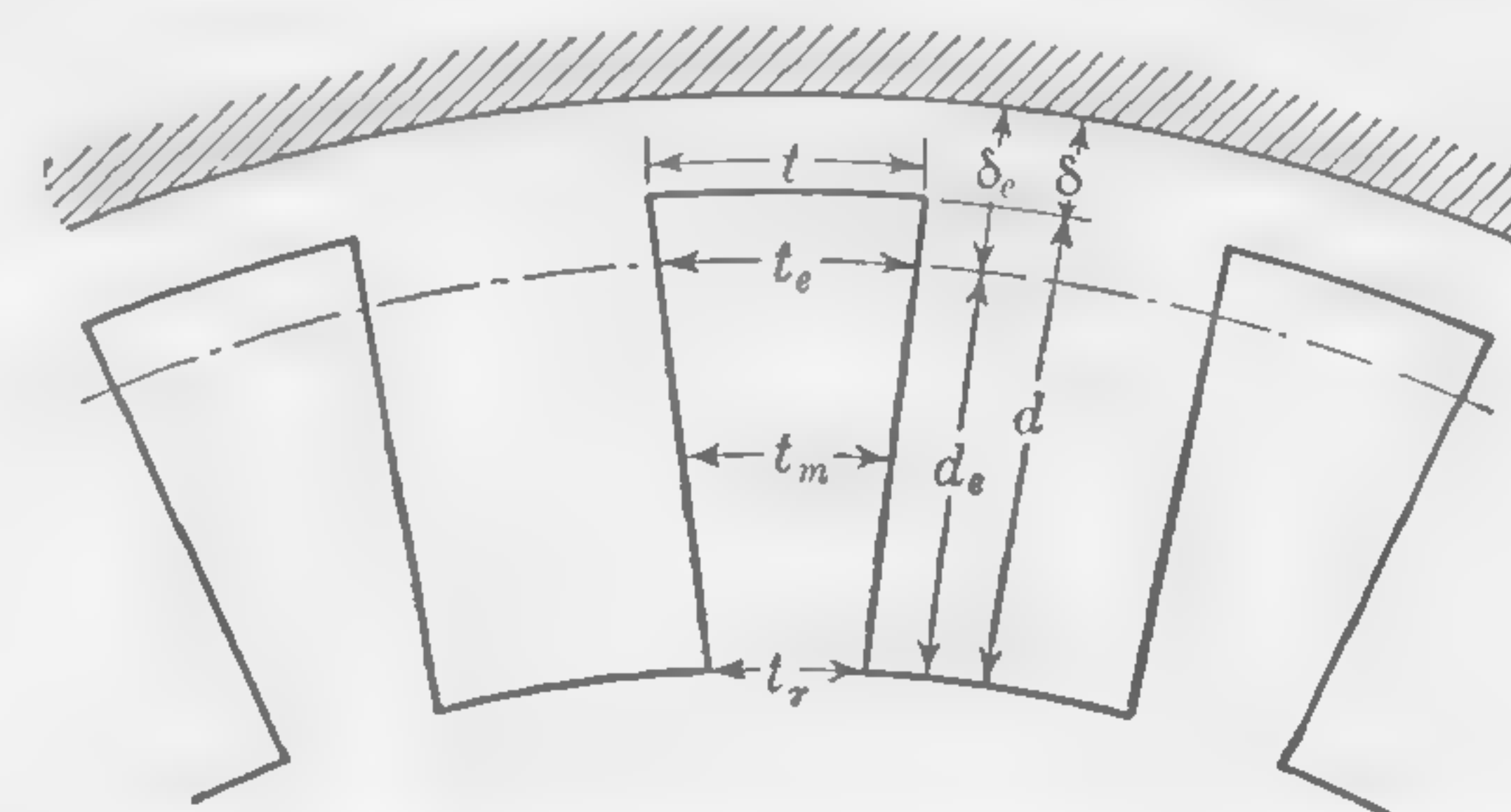


FIG. 46. Illustrating mmf calculations for taper teeth.

to the "equivalent" value  $\delta_e$ . This is recommended as a good practical compromise, and the mmf in gilberts required to overcome the reluctance of the tooth is  $H \times d_e$  where  $d_e$ , the equivalent length of tooth, must be expressed in centimeters. Obviously, formula (42) can easily be modified to give an average value for the ampere-turns per inch.

**38. Illustrative Example. Relation between Air-gap Density and Ampere-turns for Air Gap and Teeth.** Plot a curve giving the relation between the average flux density in the air gap over the tooth pitch and the ampere-turns to overcome the reluctance of the air gap, teeth, and slots.

For the purpose of this problem it will be desirable and instructive to use the design data of Art. 18. These quantities are:

Outside diameter of armature core  $D = 22$  in.

Gross length of armature core  $l_a = 10.25$  in.

Net length of armature core (iron only)  $l_n = 8.4$  in.

Depth of slot  $d = 1.4$  in.

Width of slot  $s = 0.4$  in.

Width of slot at top  $t = 0.522$  in.



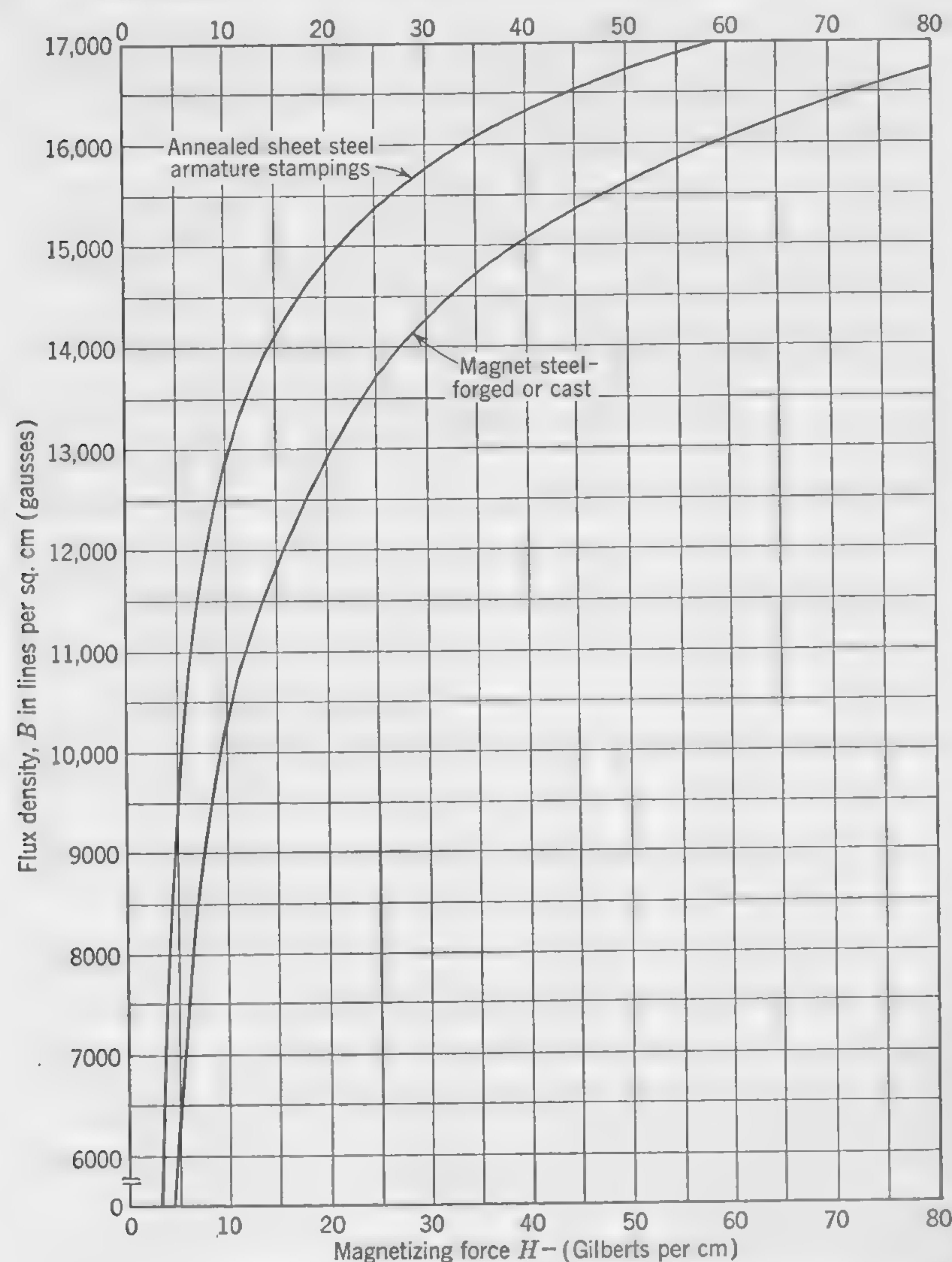


FIG. 47. Magnetization curves at comparatively low values of flux density.

Slot pitch  $\lambda = 0.922$  in.Number of face conductors  $Z = 300$ Number of poles  $p = 6$ Armature current per circuit  $I_a = 201.8$  ampAir-gap flux density  $B_g'' = 50,700$  lines per sq in.

The air gap will first be determined: By formula (12)

$$\delta = \frac{300 \times 201.8}{6 \times 50,700} = 0.199 \text{ in.}$$

by formula (13)

$$\delta = 0.04 \sqrt{22 + 3} = 0.20 \text{ in.}$$

Using a value of  $\delta = 0.20$  in. the equivalent air gap, by formula (37a), is

$$\delta_e = \frac{0.922}{0.522/0.2 + 2 \log_e [1/2(0.4/0.2) + 1]} = 0.23 \text{ in.}$$

Data for the  $B_g$  versus  $NI$  per pole curve must be obtained in two steps, the first of which requires the plotting of a  $B_t$  versus  $B_g$  curve. Calculations for the latter make use of formula (40) in connection with the

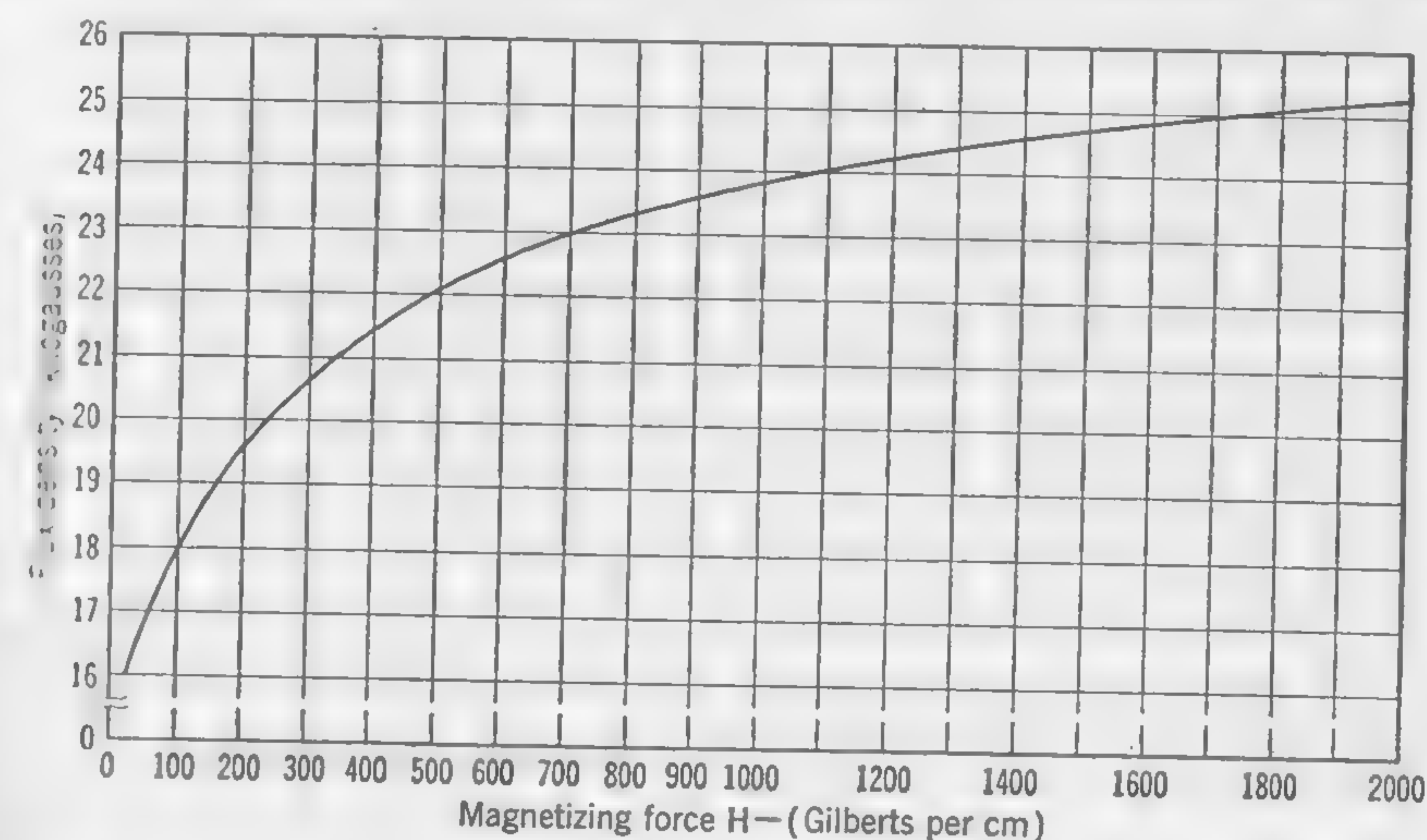


FIG. 48. Magnetization curve for sheet-steel armature stampings at high values of flux density.

graphs of Figs. 47 and 48, and the fact that  $\mu = B/H$ . The calculated values of tooth width at the four sections indicated by Fig. 46 are:  $t = 0.522$  in.;  $t_r = 0.405$  in.;  $t_m = 0.464$  in.;  $t_e = 0.520$  in.

Selecting arbitrary tooth flux densities  $B_t$  calculations are then made as indicated in the table. When the proper values are substituted in formula (40)  $B_g = B_t [0.45 + (0.55/\mu)]$ .

$B_t$ , at $t_m$ (assumed)	$H$ (from curves, Figs. 47 & 48)	$\mu = \frac{B_t}{H}$	$B_g$ (by formula 40)
12,000	8	1,500	5,400
18,000	100	180	8,150
21,000	345	61	9,650
25,000	1,800	14	12,200



The curve (Fig. 49), which has been plotted from the figures in the table, gives the relation between the flux density in the air gap and the corresponding density in the iron at the center of the tooth for any value of air-gap density.

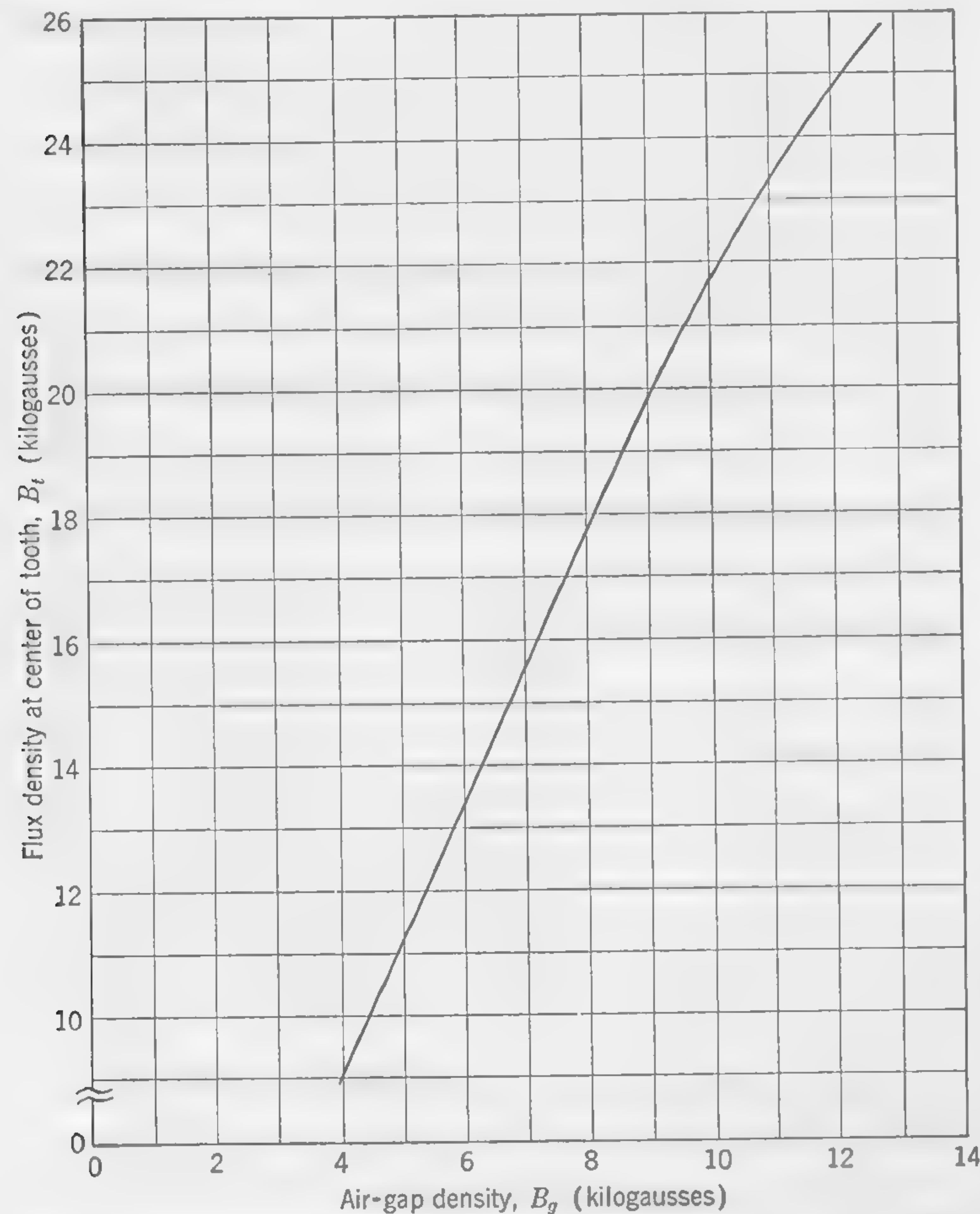


FIG. 49. Relation between tooth density and air-gap density (Art. 38).

The final step is to calculate the ampere-turns required for the air gap and teeth, and to plot a curve which will give this relation for all values of air-gap density. The results of these calculations are given in tabular form on page 101. Taking the columns in order, we have:

*First Column.* Any assumed values of air-gap density, including the highest value likely to be attained under full-load conditions.

*Second Column.* The corresponding values of flux density in the iron at the center of the tooth, read off curve of Fig. 49.

*Third Column.* The corresponding magnetizing force, read off  $B$ - $H$  curves of Figs. 47 and 48.

*Fourth Column.* The flux density at root of tooth, being values in column 2 multiplied by the ratio  $t_m/t_r = 0.464/0.405$ .

*Fifth Column.* The corresponding value of  $H$ .

*Sixth Column.* The flux density at top of tooth, being values in column 2 multiplied by the ratio  $t_m/t_e = 0.464/0.520$ .

*Seventh Column.* The corresponding value of  $H$ .

*Eighth Column.* The average magnetizing force or gilberts per centimeter for the iron in the teeth calculated by applying Simpson's rule [formula (42)].

*Ninth Column.* The ampere-turns required to overcome the reluctance of the teeth, being

$$(TI)_t = \frac{Hd_e \times 2.54}{0.4\pi}$$

where  $d_e$  in this example has the value  $(1.4 + 0.2) - 0.23 = 1.37$  in.

The final step in this method of procedure is to plot the curves of Fig. 50. Here the curve marked *teeth* is plotted from the values in the table. It gives the ampere-turns to overcome the reluctance of the teeth for any value of air-gap density  $B_g$ . The ampere-turns to overcome the reluctance of the air gap of equivalent  $\delta_e = 0.23$  in. are

$$TI_g = \frac{B_g \times 0.23 \times 2.54}{0.4\pi} = 0.465B_g$$

a relation that is represented by the broken straight line in Fig. 50. All that is now necessary is to add the ampere-turns for the tooth to those of the air gap in order to obtain the final curve giving ampere-turns required to overcome the joint reluctance of the air gap, teeth, and slots for any value of the average flux density  $B_g$  in the air gap over the space of one tooth pitch.

$B_g$	At middle		At root		At top		$H$ Formula (42)	$(TI)_t$
	$B_t$	$H_m$	$B_t$	$H_r$	$B_t$	$H_e$		
(1)	(2)	(3)	(4)	(5)	(6)	(7)	(8)	(9)
10,000	21,700	440	24,900	1,700	19,400	190	609	1,690
9,000	19,800	220	22,700	620	17,700	85	264	731
7,000	15,500	27	17,800	90	13,800	13	35	97
5,000	11,300	7	13,000	11	10,100	6	8	22

**39. Armature Reaction—Demagnetizing Ampere-turns Due to Armature Currents.** Figure 51 is generally similar to Fig. 3 of Art. 3, which is intended to show how the maximum ampere-turns per pole, due to the



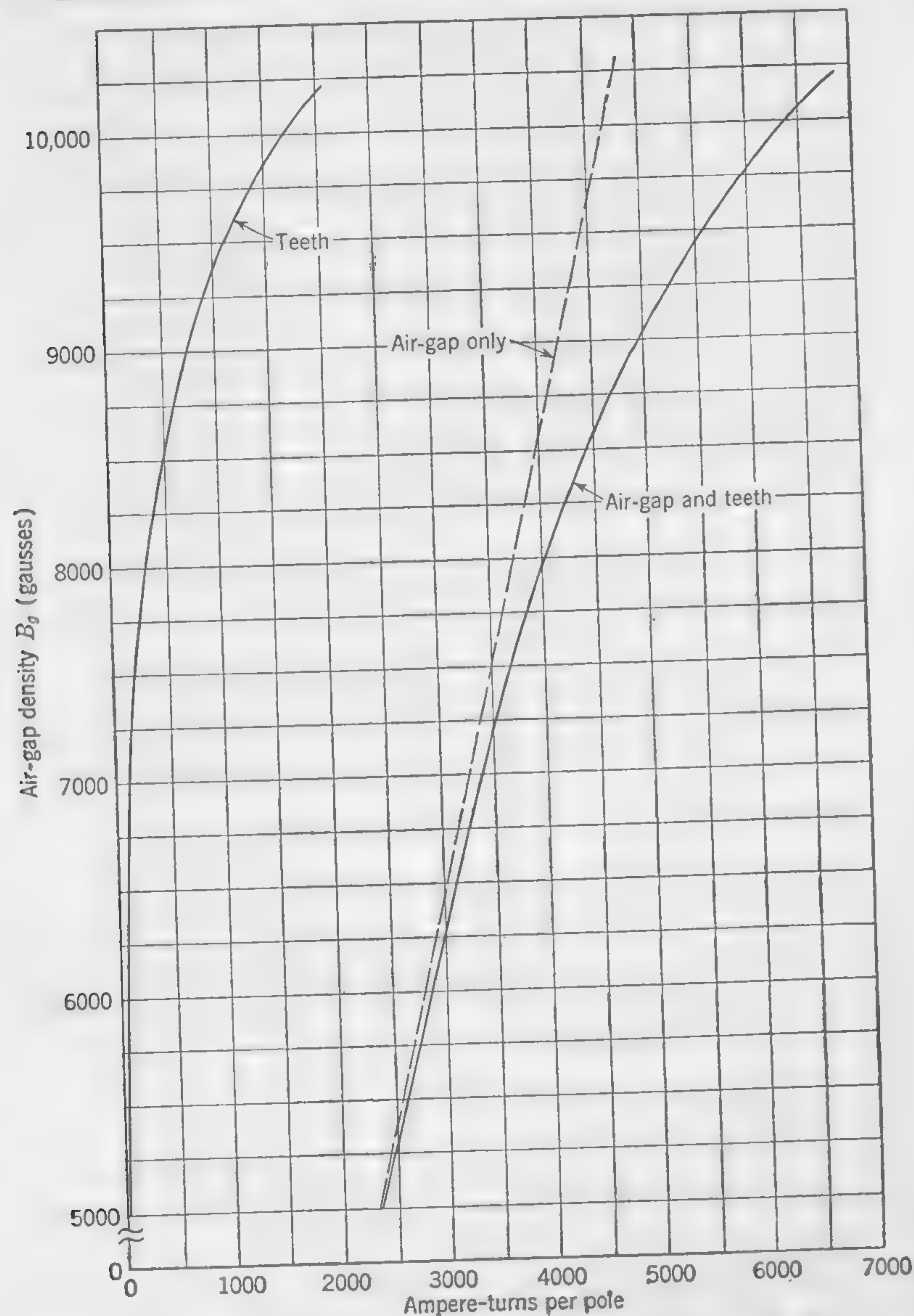


FIG. 50. Ampere-turns required for air gap and teeth (Art. 38).

armature currents of a multipolar dynamo, occur at the points where the brushes are in (electrical) contact with the armature windings. It was also shown that the maximum value of the armature ampere-turns per pole is

$$(TI)_a = \frac{ZI_a}{2p}$$

The small arrows in Fig. 51 indicate the direction of the flux lines which the mmfs of main poles and armature tend to establish. The actual distribution of mmf over the surface of the armature will be, at any point, the resultant of the mmfs at this point due to the currents in both field and armature windings. Since the sheets of armature current of width equal to the pole pitch  $\tau$  alternate in direction around the armature periphery, they tend to produce alternate north and south poles at the armature surface, as indicated by the small letters  $n$  and  $s$  in Fig. 51. The broken straight line, of which the ordinates are a measure of the armature ampere-turns, indicates the distribution of the mmf, due to armature currents only, over the periphery of the armature. If measurements taken above the datum line indicate an mmf which tends to set up flux lines entering the armature surface from outside, the lines in Fig. 51 correctly indicate the mmf distribution over the armature surface for direct

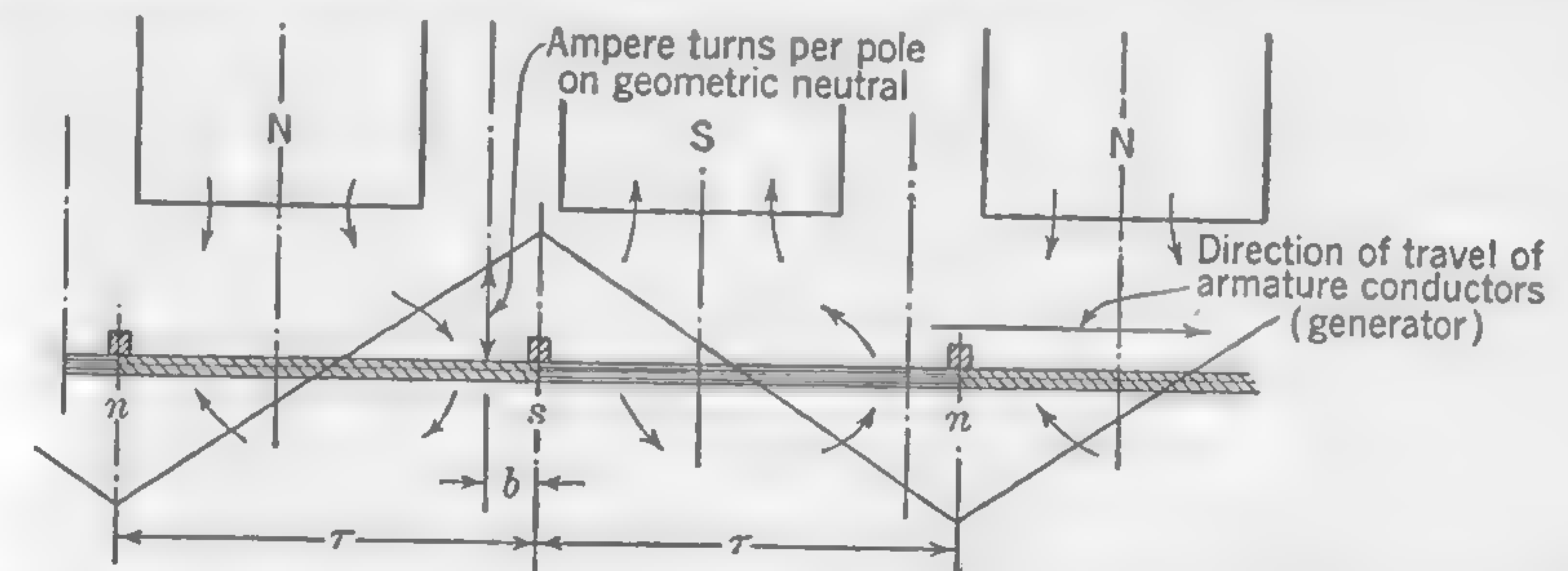


FIG. 51. Distribution of armature mmf, showing displacement with brush shift.

comparison with similar curves which may be drawn of the mmf due to the field poles. It should be clearly understood that these curves indicate only the *tendency* to establish magnetic flux leaving or entering the surface of the armature; the actual flux density in the air gap at any given point on the armature surface will, of course, depend upon the permeance between field poles and armature at the point considered.

The brushes are shown in Fig. 51 as having been moved forward from the geometric neutral position through an angle corresponding to a distance  $b$  measured on the armature periphery. Therefore, if  $b_s$  is the brush shift expressed in terms of the brush pitch, this may be written

$$b_s = \frac{\text{brush shift}}{\text{brush pitch}} = \frac{b}{\tau}$$

Figure 52 shows how the curve of armature mmf may be combined with the curve of field-pole mmf to produce a resultant mmf curve from which the flux distribution under load may be predetermined. The curve marked  $P$  indicates approximately the mmf distribution over the armature surface on open circuit when the field excitation is acting alone and



there is no appreciable current in the armature conductors. This curve falls to zero at points exactly midway between poles because of the equal but opposite magnetizing effects of adjacent poles of opposite polarity. If curve *A* indicates the armature mmf distribution at full load, the resultant mmf tending to set up flux between pole and armature core at full load is indicated by the curve *R*, which is merely the algebraic sum of corresponding ordinates of the two curves. The flux resulting from this full-load distribution of mmf (with constant field excitation) would have been approximately the same as on open circuit if the brushes had not been moved from the neutral position; but, owing to brush shift, there is a demagnetizing effect, due to the armature currents, the average

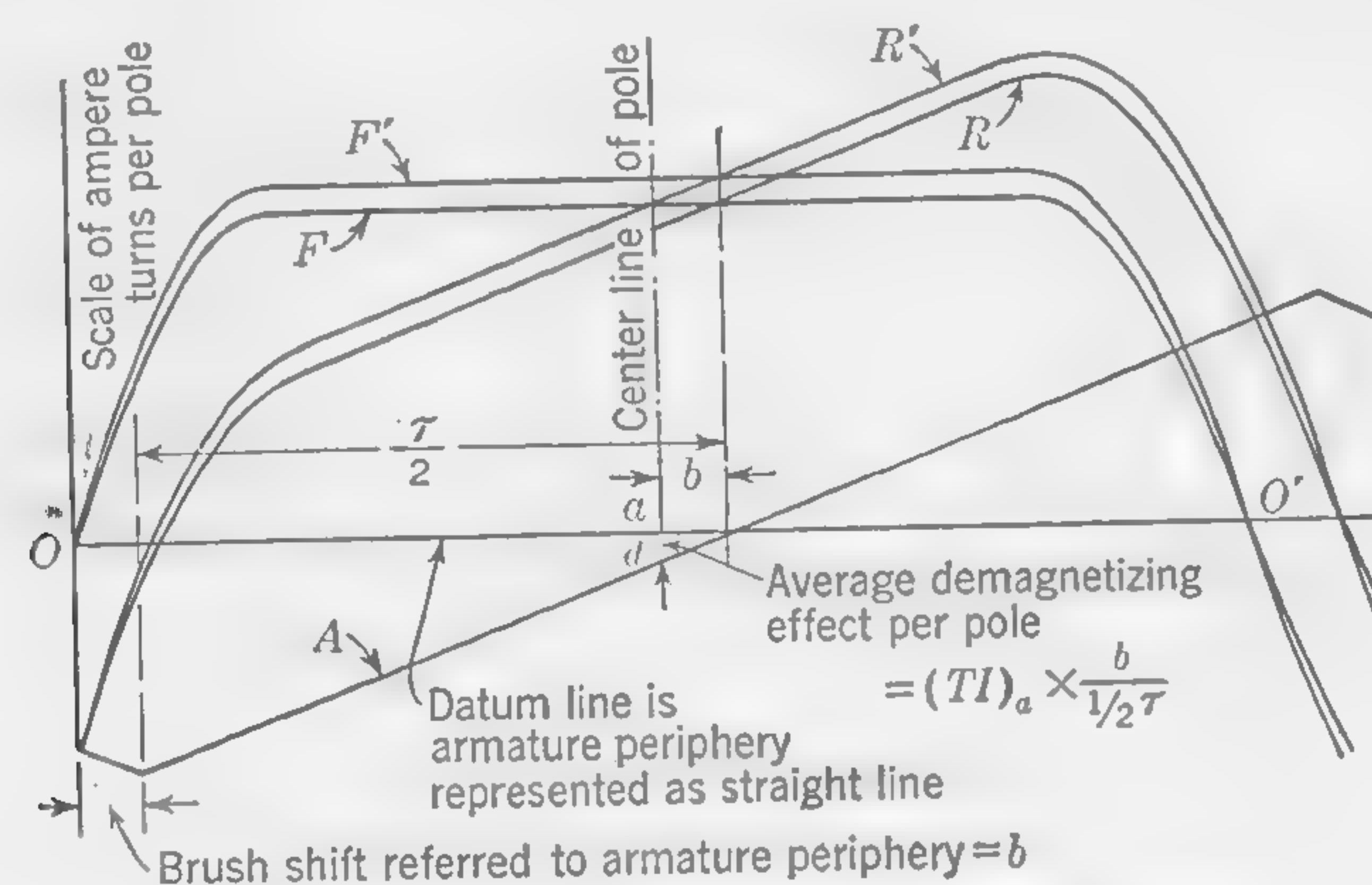


FIG. 52. Addition of field and armature mmfs.

value of which is approximately equal to the distance *ad* in Fig. 52. The value of this demagnetizing effect in terms of brush shift is seen to be  $(TI)_a \times \frac{b}{1/2\tau}$ , or

$$\text{Armature demagnetizing ampere-turns per pole due to brush shift} \begin{cases} = 2b_s(TI)_a \\ = \frac{b_s Z I_a}{p} \end{cases} \quad (43)$$

where  $b_s = \frac{\text{brush shift}}{\text{brush pitch}}$ , as previously defined.

If, now, we increase the ampere-turns on the field pole (by means of a series winding) by the amount of formula (43), we may plot the curves *F'* and *R'* in Fig. 52, and it will be seen that the latter indicates the full-load distribution of mmf over armature surface which will send into the armature approximately the same amount of flux as on open circuit. Actually, more flux is required to compensate for voltage drops in series

windings and also to produce overcompounding if required. Also the flux distortion due to the cross-magnetizing effects of the armature circuits may cause a certain loss of flux on account of magnetic saturation of the teeth where the air-gap density has a maximum value, and this may have to be compensated for by still further additions to the field ampere-turns. This, however, is a minor effect of armature reaction which will not be discussed here.

**40. Internal Resistance Drop and Overcompounding.** The amount by which the full-load flux entering the armature of a constant-speed machine must exceed the flux required on open circuit may be determined approximately by estimating the probable voltage drop in the series winding (if any) and at the brush-contact surfaces. In the case of compound-wound machines, it will be known at the outset whether the dynamo is to be flat-compounded or overcompounded. Overcompounding is resorted to when the voltage drop in the circuit fed by the machine is likely to be high. The terminal voltage may then be 5 or even 10 per cent higher at full load than on open circuit. The balance of the emf to be developed at full load consists of:

- The *IR* drop in armature winding
- The *IR* drop in series field (if any)
- The *IR* drop in interpole winding (if any)
- The *IR* drop at brush-contact surface

Item *a* can readily be calculated from the armature winding data. Item *b* may be estimated at from one-fifth to one-half the armature drop. Item *c* may be estimated at from one-fifth to one-half the armature drop. Item *d* may be estimated at 2 to 3 volts when carbon brushes are used and is practically constant for machines of widely different voltages and outputs.

By totaling these items of internal loss of pressure, and adding thereto the required terminal volts at full load, the full-load developed voltage *E'* is obtained, and the required flux per pole at full load is calculated by multiplying the known flux per pole at no load by the ratio *E'/E*, where *E* is the open-circuit terminal voltage of the machine.

**41. Leakage Flux from Field Poles of Dynamo.** If we could correctly sketch the leakage flux distribution in a multipolar dynamo not only in the plane perpendicular to the shaft, as indicated by the dotted lines in Fig. 53, but also in planes normal to this section, it would be possible to determine with considerable accuracy the total leakage flux which gets across from pole to pole without passing through the armature. We could simply have to measure the average cross section of each path of this redrawn and divide this by its length in order to obtain its permeance. The sum of the permeances of all such flux paths between the two poles would then be the total permeance of the air paths between them.



In Figs. 54 and 55 an attempt has been made to represent the actual distribution of flux lines: (1) for the condition of one pole acting alone without interference from neighboring poles, and (2) for the practical condition of neighboring poles of equal strength and opposite polarity. The machine to which these diagrams apply is a continuous-current dynamo of pole pitch 37 cm, pole arc 27 cm, and equivalent air gap of

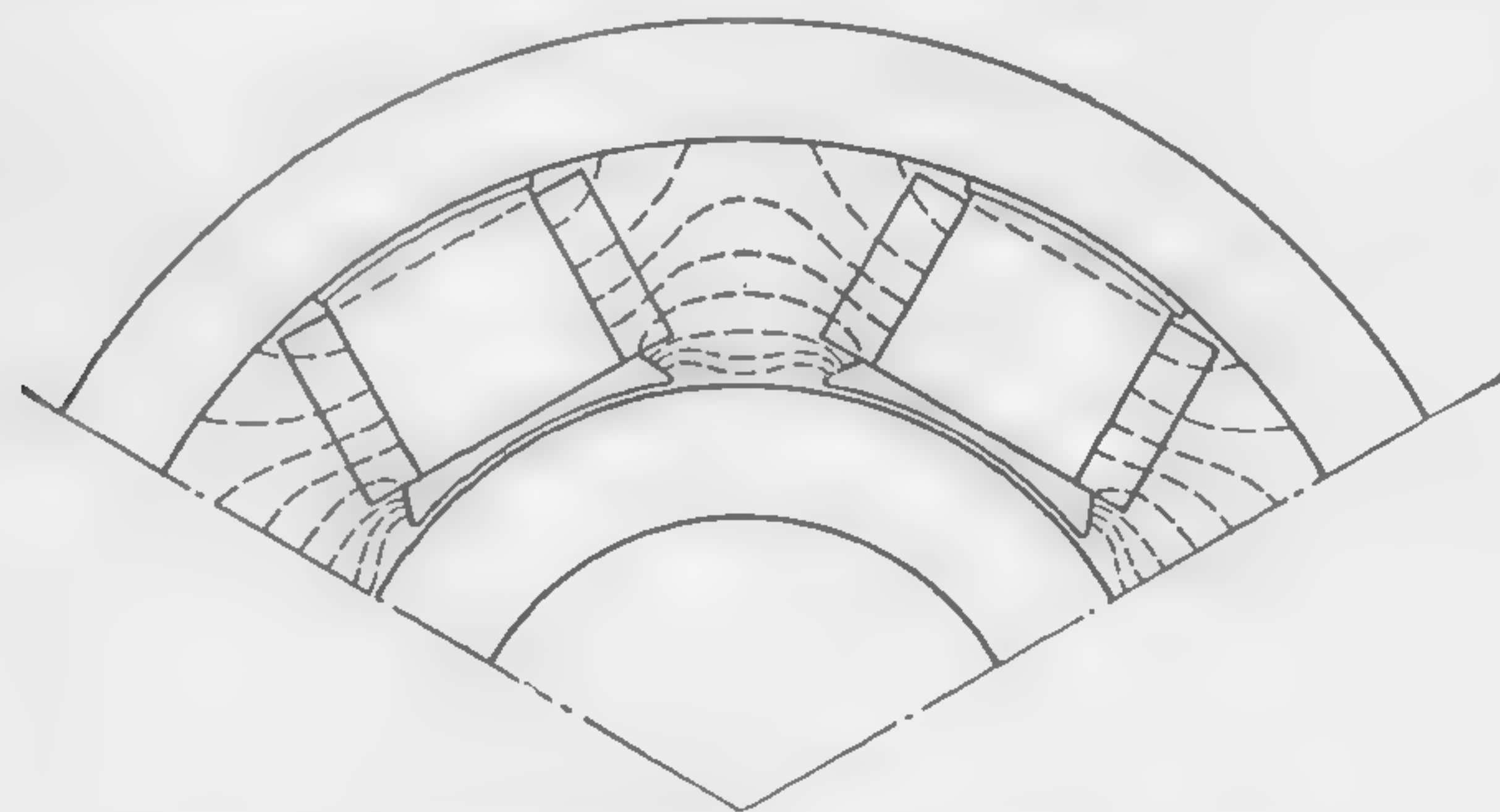


FIG. 53. Leakage flux in multipolar dynamo.

0.8 cm at center of pole face. The air gap is of uniform length except near the pole tips, where it is slightly increased, as indicated on the drawings. With a little practice and ample time in which to perform the work, diagrams of flux distribution, such as those of Figs. 54 and 55, can be drawn, and they will indicate with a fair degree of accuracy the actual arrangement of the flux lines.

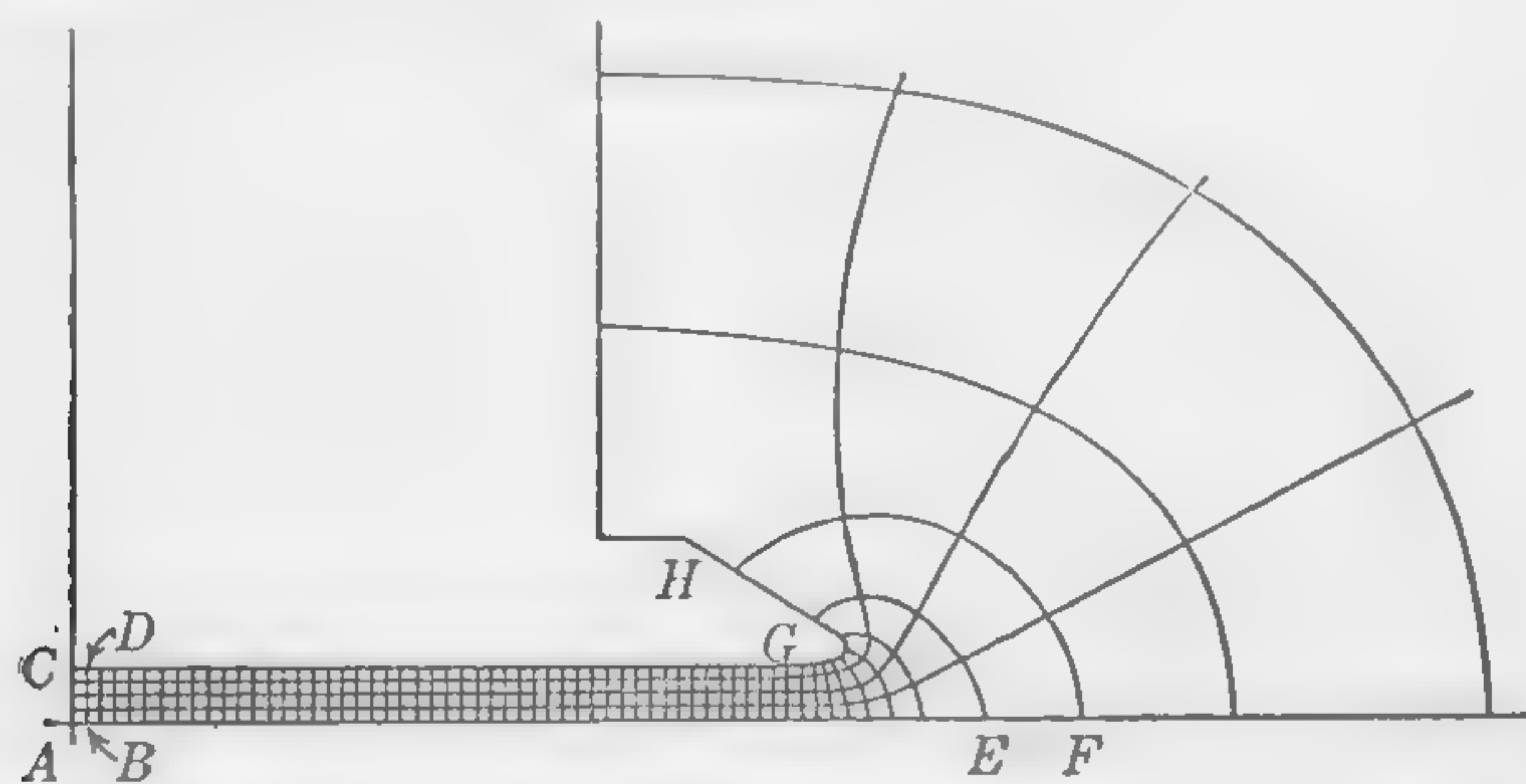


FIG. 54. Flux lines between pole and armature of dynamo (one pole acting alone).

A section perpendicular to the shaft through the pole shoe and armature is considered, and all flux lines in the gap are supposed to lie in planes parallel to this section. Equipotential lines are drawn in directions which seem reasonable to the draftsman, and tubes of flux, *all having the same permeance*, are then drawn with their boundary lines perpendicular at all points to the equipotential lines. At the first trial it will generally be found that these conditions cannot be fulfilled, but,

by altering the direction of the tentative equipotential lines, the work is repeated until the correct arrangement of lines is obtained. The tube of induction  $ABCD$  (Fig. 54) is the first to be drawn. Its permeance in the particular case considered is 0.25, because it consists of four portions in series, each one of which is exactly as wide as it is long (a thickness of 1 cm measured axially is assumed). Proceeding outward from left to right, and making each section of the individual tube of induction as wide as it is long, the permeance of every one of the component areas in the diagram is always unity, and any complete tube, such as  $EFGH$ , has the same permeance (in this example 0.25) as every other tube. The computation of the total permeance between the pole shoe and armature over any given area is thus rendered exceedingly simple. Although the armature surface is represented as a straight line in the accompanying

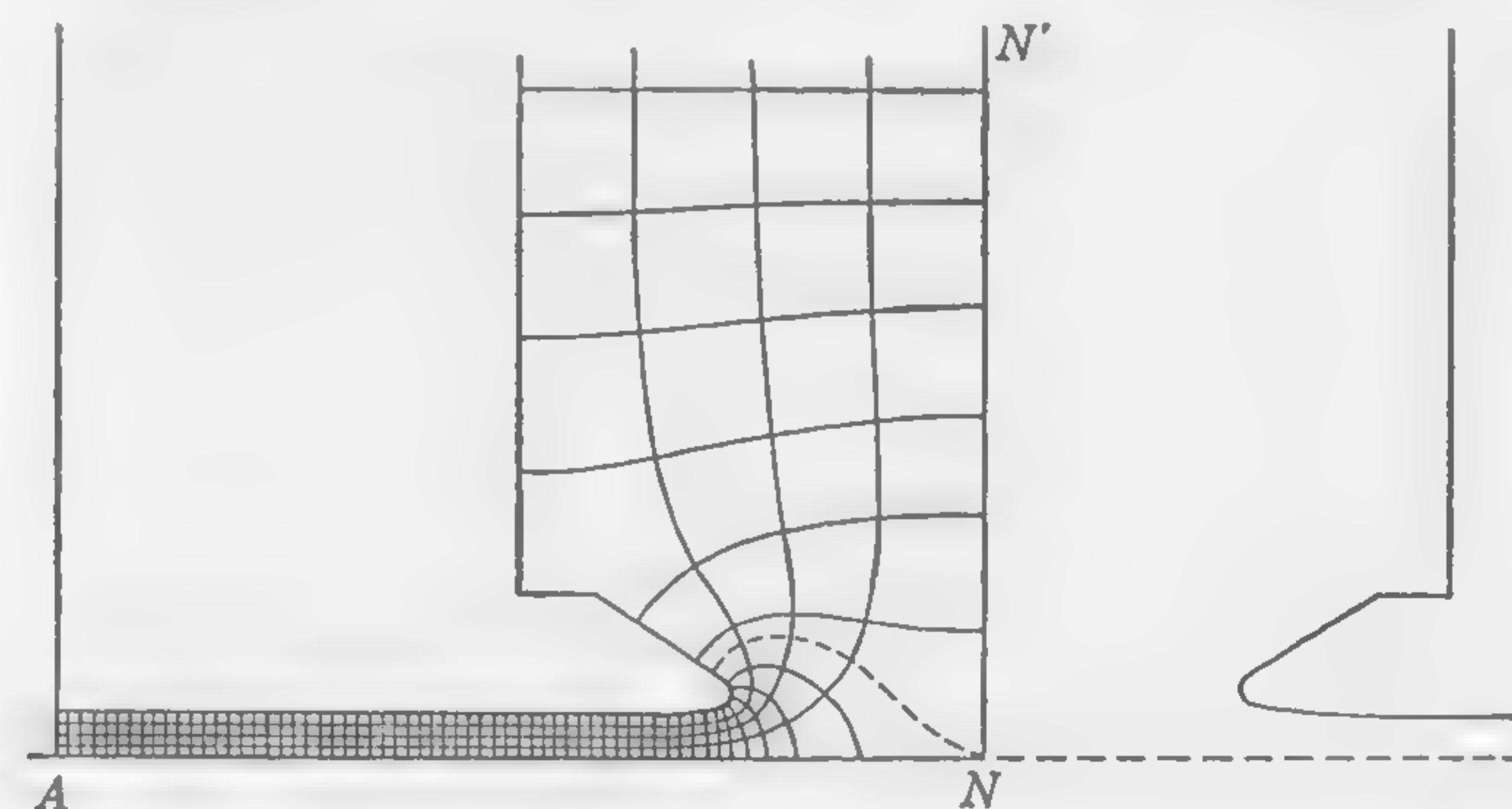


FIG. 55. Flux lines from pole of dynamo (effect of neighboring poles).

illustrations, the actual curvature of the armature may be taken into account if preferred, and indeed it is no more difficult to make the flux plot with the circumference of the armature core drawn to the proper scale than with the so-called "developed" armature surface as here shown.

In Fig. 55 the flux lines have been drawn to ascertain the effect of the neighboring pole in altering the distribution over the armature surface in the interpolar space. The perpendicular  $NN'$  has been erected at the geometric neutral point and may be considered as the surface of an iron plate forming a continuation of the armature surface  $AN$ . Thus  $ANN'$  will be an equipotential surface, between which and the polar surface the intermediate equipotential surfaces must lie.

It may be mentioned that in Figs. 54 and 55, and also in other flux-line diagrams, the pole core under the windings cannot properly be considered as being at the same magnetic potential as the pole shoe, relatively to the armature. The proper correction can be introduced in calculating



the flux in each tube of induction and this will be done in the numerical example to follow.

The flux density at all points on the armature periphery is easily calculated when the flux lines have been drawn. Thus, since each tube of induction encloses the same number of magnetic lines, exactly the same amount of flux will enter the armature in the space  $EF$  (Fig. 54) as in the space  $AB$ . If  $B_{ab}$  is the flux density in the tube  $CDAB$  at the center of the pole face, the average density over the space  $EF$  will be

$$B_{ef} = B_{ab} \times \frac{AB}{EF}$$

Similarly, in Fig. 55, which shows not only the lines from pole face to armature but also the leakage paths between adjacent poles, the reluctance of each of the spaces 4 units in length by 1 unit in width is simply  $\frac{4}{1} = 4$  for every centimeter of pole width measured parallel to the shaft (*i.e.*, perpendicular to the plane of the drawing). Since the flux lines are shown only as far as the neutral plane between the poles, the flux in any one of these spaces between a north pole and the adjacent south pole will be

$$\Phi = F \times p_w \times 1/8$$

where  $p_w$  is the width of the pole in centimeters measured in the direction parallel to the shaft, and  $F$  is the total mmf due to the windings on both poles. This mmf will not be the same for all the flux paths shown in Fig. 55 but will increase from zero value near the yoke ring to maximum value where the pole shoe is attached to the pole core.

**42. Illustrative Example. Leakage Flux between Dynamo Field Poles.** This problem will illustrate a method for calculating leakage flux which is quicker and less tedious than the somewhat more accurate method of dividing the flux plot into squares, as previously explained. It is proposed to estimate approximately the amount of the leakage flux between field poles in order that the proper cross section of iron may be provided in the pole cores and yoke ring.

The dimensions and other required particulars are as follows:

Number of poles = 6

Diameter of armature core = 29 in.

Axial length of armature core = 11 in.

Cross section of pole under windings =  $11 \times 7.5 = 82.5$  sq in.

Pole arc (*i.e.*, width of pole shoe measured on armature circumference) = 11 in.

Total flux per pole entering armature =  $6.6 \times 10^6$  maxwells

Ampere-turns on field = 7,500 per pole

The pole pitch, or distance between centers of poles measured on the

armature periphery, is

$$\tau = \frac{\pi \times 29}{6} = 15.2 \text{ in.}$$

The application of formulas for the estimation of leakage flux between poles and between pole and yoke ring in planes perpendicular to the shaft does not always yield satisfactory results, and in a new design it is preferable to sketch the flux lines as in Fig. 56 and then calculate the permeance of the air paths from measurements made on the drawing.

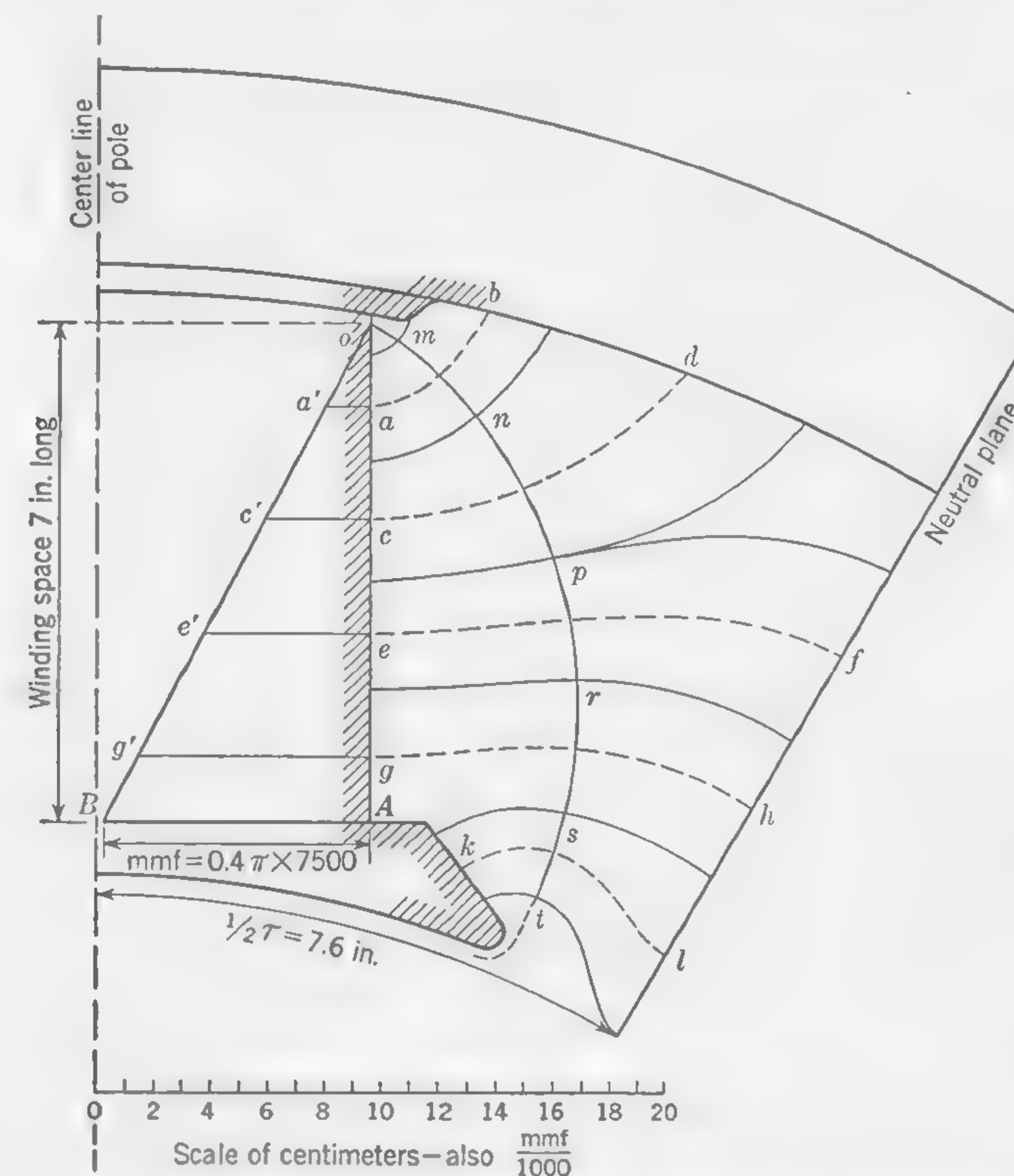


FIG. 56. Sketch for calculation of leakage flux in dynamo.

Figure 56 is constructed by first drawing one-half of the pole, including the space comprised between armature periphery and yoke ring up to the neutral plane halfway between the poles. The probable direction of the flux lines is then indicated, bearing in mind what has previously been said in connection with flux plotting. No attempt has been made in Fig. 56 to do more than indicate approximately the position of the flux lines, and very little time has been spent in drawing them. Their position is determined largely by drawing the solid line *mt* to represent an *equi-potential surface* midway (magnetically) between the pole surface and the



neutral plane\* which may be considered as continuing along the inner surface of the yoke ring. The flux lines must be drawn so as to cross the solid line *mt* approximately at right angles. Any arbitrary number of flux tubes may be drawn, and they need not all be of the same permeance. The dotted center line in each tube is a measure of its mean length, while its cross section is obtained by multiplying the axial length of the pole by the portion of the line *mt* included between the boundary lines of the flux tube. It should be noted that the mmf tending to set up flux in these air paths will depend upon the number of ampere-turns of the field winding which link with the magnetic circuit considered. This may be estimated by making the distance *AB* represent, to any convenient scale, the total mmf per pole and then joining *B* to the point *o*, where the mmf is zero.† The length of any other perpendicular, such as *cc'* on *oA*, intersecting *oB* at *c'*, will then be a measure of the mmf tending to establish flux in the path of mean width *np* and mean length *cd*. Separate calculations are made for the flux in each path as sketched, and the sum of these component fluxes will be the total number of maxwells leaving one side of the pole and pole shoe in planes perpendicular to the axis of the dynamo. Thus the flux in the path of width *np* and mean length *cd* is calculated as follows:

The mean width of the path (scaled off the drawing) is  $np = 5.7$  cm, whence the mean cross section of the path is  $5.7 \times 11 \times 2.54 = 159$  sq cm.

The mean length of the path (scaled) is  $cd = 12.5$  cm, whence the permeance is  $P_{cd} = 159/12.5 = 12.75$ . The mmf which causes the leakage flux from this portion of the pole surface is *cc'*, which scales 3,700 gilberts, whence  $\Phi_{cd} = 3,700 \times 12.75 = 47,200$  maxwells.

Similar calculations give corresponding values of leakage flux in the other air paths. These values are:

For path <i>ab</i>	29,000
For path <i>cd</i>	47,200
For path <i>ef</i>	45,500
For path <i>gh</i>	75,500
For path <i>kl</i>	100,000
Total	297,200, or (say) 300,000 maxwells

\* A check on the correct position of the equipotential line *mpt* is obtained by observing that the portion of any flux tube on the right of this line has the same reluctance as the portion of the same tube on the left. Thus if *pr* is to be used as a measure of the average cross section of the flux tube of length *ef*, the ratio of average length to average width should be the same for the two portions of this tube.

† This construction assumes the field winding to be distributed uniformly over the length of the pole core in a single layer of negligible thickness. Refer to group of papers, Graphical Determination of Magnetic Fields, *Trans. AIEE*, vol. 40, 1927, pp. 112, 136, and 141.

The other flux paths to be considered are those between the two pairs of end faces of the pole core that lie in the same planes (under the windings) and those between the end faces of the pole shoes that lie in the same planes. For calculating these components of the total leakage flux, it is generally permissible to use the formulas for permeance of air paths between similar faces of equal area lying in the same plane, and, in order to simplify these calculations, we shall assume the neighboring poles to be parallel, with a distance between centers equal to the actual pole pitch as measured on the periphery of the armature.\*

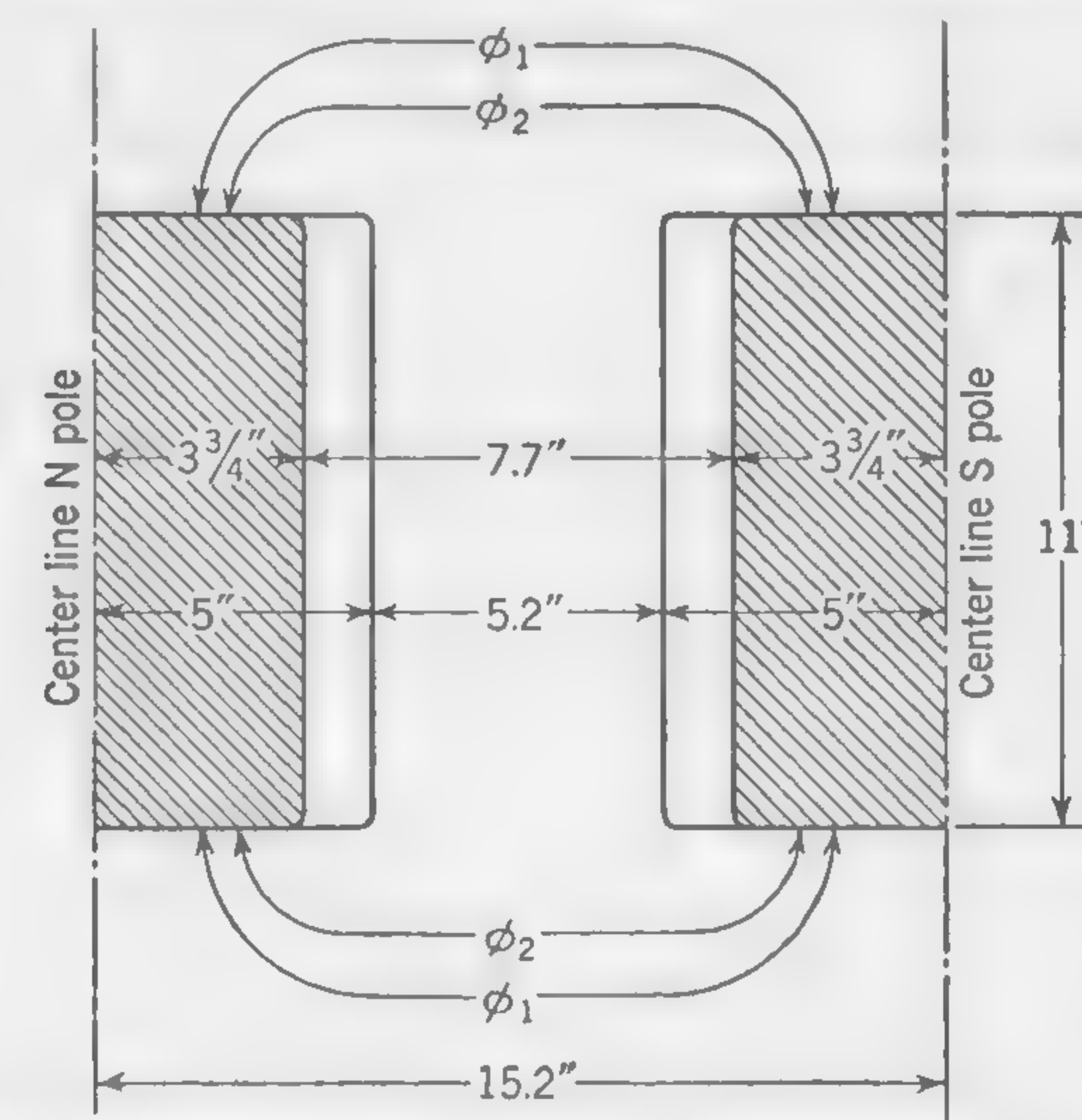


FIG. 57. Leakage-flux paths from outside surfaces of dynamo field magnets.

The leakage fluxes still to be estimated are shown in Fig. 57. They are: (a) twice the flux  $\Phi_1$  between one-half the end face of a north pole and one-half the end face of the adjacent south pole, and (b) twice the flux  $\Phi_2$  between half the pole shoe of a north pole and half the pole shoe of the adjacent south pole. The dimensions, in inches, are shown on the sketch (Fig. 57), the spacing between pole shoes being somewhat greater than the actual clearance between pole tips because, in order to simplify the calculations and make use of the formulas for rectangular surfaces, the actual shape of the outside face of the pole shoe (as shown in Fig. 56) is supposed to be replaced by an equivalent rectangle 10 in. long by 1 in.

\* It may be argued that, since the pole cores are actually farther apart at the ends where they meet the yoke ring, a somewhat wider spacing of the equivalent parallel pole arrangement would be more reasonable; but since the flux lines passing from the sides of the pole cores into the sides of the yoke ring will not be considered in the calculations, the closer spacing of the equivalent parallel poles will compensate for this omission, and the method here followed is found to give satisfactory results in practice.



wide. We are now able to use formula (35) on page 79 for the calculation of both these flux components. For the permeance of the air path between the end faces of the pole cores, we have

$$2P_1 = \frac{2 \times 7 \times 2.54}{\pi} \log_e \left[ 2 \times \frac{3.75 + \sqrt{(3.75)^2 + (7.7 \times 3.75)}}{7.7} + 1 \right] = 14.8$$

A similar calculation for the permeance of the air path between the end faces of the pole shoes gives  $2P_2 = 2.8$ .

When calculating the flux in the air paths of which the permeances are  $P_1$  and  $P_2$  respectively, it is necessary to bear in mind that the mmf causing the flux component  $\Phi_1$ , which passes out of the pole core through the exciting coils, is the average mmf between adjacent poles, or one-half the total mmf of a pair of poles. Then

$$2\Phi_1 = (0.4\pi \times 7,500) \times 14.8 = 139,000 \text{ maxwells}$$

and

$$2\Phi_2 = (2 \times 0.4\pi \times 7,500) \times 2.8 = 53,000 \text{ maxwells}$$

Summing up the several calculated components of the leakage flux, we have a total of 492,000 maxwells for one-half of the pole. This estimate of the leakage flux does not include all possible flux paths, and, as previously mentioned, it will be advisable to increase the calculated value about 25 per cent, which brings the total of the leakage lines up to 616,000 maxwells. The useful flux per pole, as given with the other numerical data, was  $6.6 \times 10^6$  maxwells, whence the total flux per pole is  $6,600,000 + (2 \times 616,000) = 7,832,000$  and the leakage factor is

$$lf = \frac{7,832,000}{6,600,000} = 1.19 \text{ (approx)}$$

The maximum value of the flux density in the pole core will be

$$\frac{7,832,000}{11 \times 7.5} = 95,000 \text{ lines per sq in.}$$

This maximum density will occur at the end of the pole core where it is attached to the yoke ring.

**43. Distribution of Flux Density over Armature Surface.** In Art. 2 the average flux density in the air gap under the pole face was defined as

$$B_g = \frac{\Phi}{l_a \times r\tau}$$

wherein the numerator is the flux per pole entering the armature, and the denominator is the gross length of the armature core multiplied by the

pole arc measured on the armature surface, or the area under the pole face through which the total flux would enter the armature if there were no spreading of the flux lines from the edges of the pole face.

The actual flux distribution over the armature surface, when the current in the armature conductors is zero, or merely such as to provide the shunt-field excitation, may be determined by making a flux plot similar to Fig. 55. If the neighboring poles were removed, the flux plot would be as in Fig. 54. It does not take long to make such a flux plot extending as far as the neutral zone or up to the pole tip of the neighboring pole. From this a curve can be plotted, the ordinates of which are a measure of the air-gap flux density which would be obtained at the armature surface for any position under or between the poles if the mmf between pole shoe and armature surface were constant in value up to and even beyond

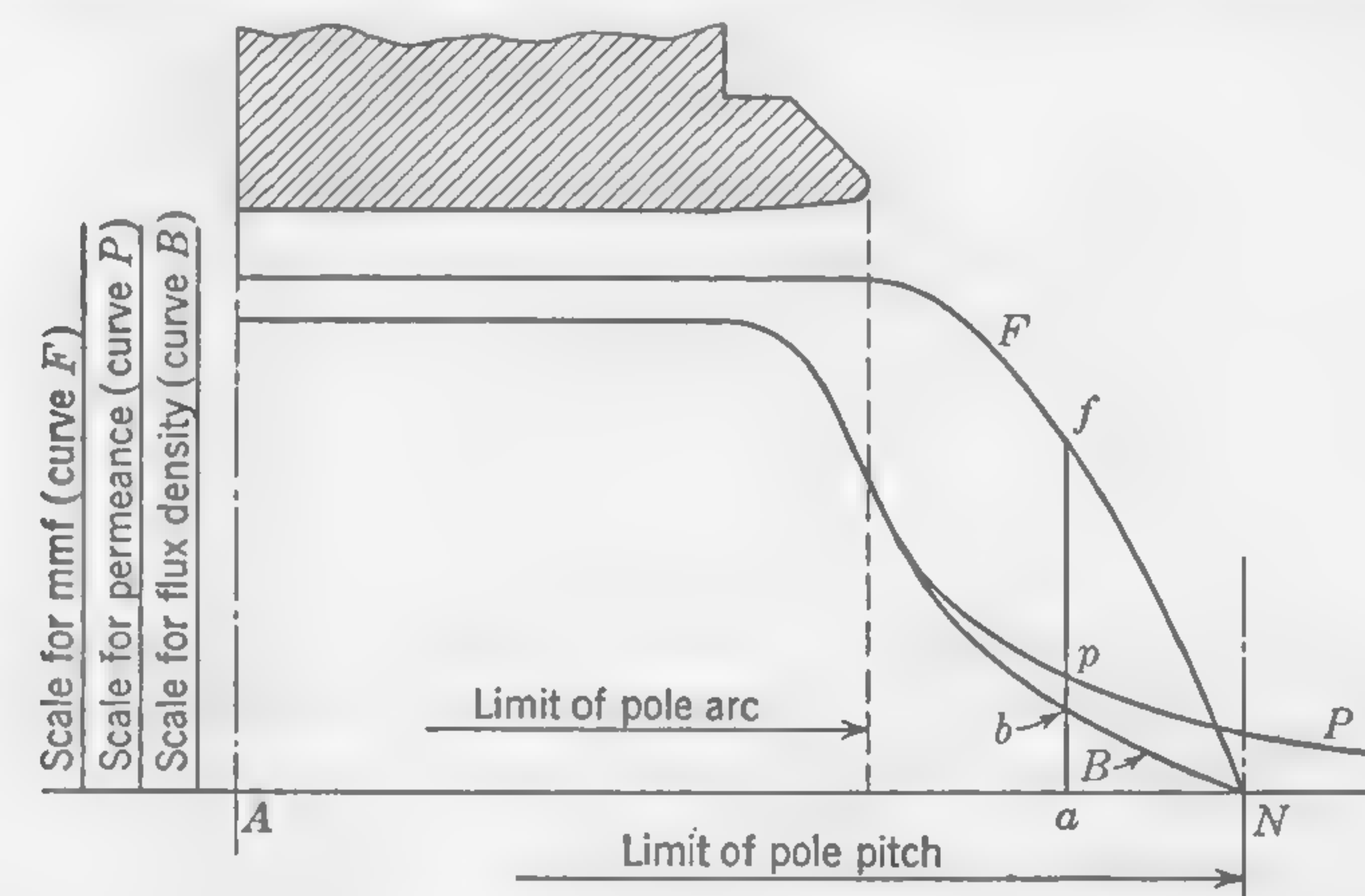


FIG. 58. Curves showing distribution of air-gap permeance, mmf, and flux density.

the position midway between the poles. For example, since the flux tube  $HGEF$  (Fig. 54) contains as many unit tubes as the flux tube  $CDAB$  under the center of the pole shoe, it follows that the average flux density in the space  $AB$  is  $EF/AB$  times the average flux density in the space  $EF$ .

Assume that the curve  $P$  (Fig. 58) has been obtained in this manner, while the curve  $B$  has been obtained from Fig. 55 which takes account of the proximity effect of the oppositely excited poles. Note that the flux curve  $P$  may also be thought of as a permeance curve, that is to say, a curve of which the ordinates are a measure of the permeance per square centimeter of armature surface between pole shoe and armature. The reason for this is that  $\text{flux} = \text{mmf} \times \text{permeance}$ , and, since the mmf between pole shoe and armature is the same for all points on the armature surface (when the proximity effect of neighboring poles is neglected), it follows that *permeance* is directly proportional to *flux*, and *permeance*



*per square centimeter* is directly proportional to *flux per square centimeter* or to the air-gap density expressed in gauss.

When the curve  $P$  (Fig. 58), which may be called the "permeance curve" and calibrated as such, has been drawn, and also the curve  $B$  (in gauss), which is the true open-circuit flux distribution curve (taking account of the effect of neighboring poles), the third curve  $F$ , which represents the resultant mmf between pole shoe and armature, may be constructed. The ordinate  $af$  of this curve at any point  $a$  on the armature periphery considered in relation to the poles is simply the ratio of the flux density in gauss to the permeance per square centimeter, *i.e.*,  $af = ab/ap$  gilberts. In this manner the shape of the mmf curves such as  $F$  and  $F'$  (Fig. 52) may be determined.

**44. Practical Method of Plotting Flux-distribution Curves.** Draw the pole shoe and armature periphery to scale (preferably full size) as will be explained later in Art. 50. Sketch the flux and equipotential

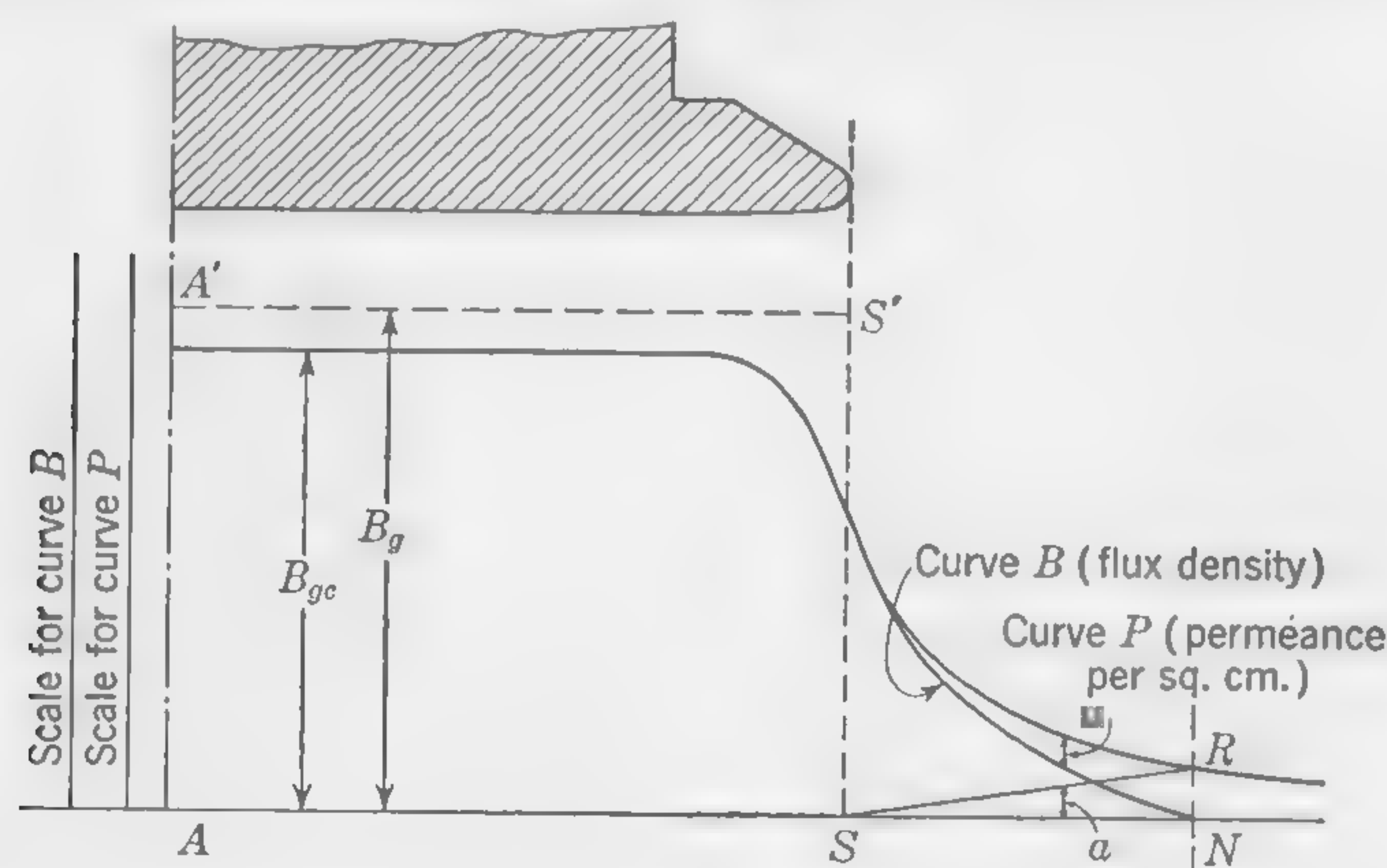


FIG. 59. Curve of open-circuit flux distribution derived from permeance curve.

lines to form approximate squares as explained in connection with Fig. 54. Note that the air-gap permeance per square centimeter of armature surface under the center of pole face is simply the reciprocal of the "equivalent" air gap  $\delta_e$  expressed in centimeters, as calculated in Art. 35, and the permeance per square centimeter at another point such as about halfway between  $E$  and  $F$  (Fig. 54) is  $(1/\delta_e) \times (AB/EF)$ . Now plot the permeance curve marked  $P$  in Fig. 59 where the distance  $AN$  is one-half the pole pitch  $\tau$ , and  $AS$  is one-half the pole arc  $r\tau$ . The flux distribution curve may be constructed without resorting to a second flux plot by drawing the straight line  $SR$  and subtracting the ordinates of this line from the curve  $P$ . This yields results quite accurate enough for practical purposes.

In order to calibrate the open-circuit flux curve  $B$  thus obtained, it is necessary to know the total flux per pole entering the armature. Let this be  $\Phi$  maxwells. Now measure the area under the curve  $B$ . This may be done with the aid of a planimeter or by averaging ordinates. Construct the rectangle  $AA'S'S$  of exactly the same area. The height of this rectangle will be a measure of the average density under the pole face on the assumption that there is no fringing or spread of flux beyond the pole tips, and this is known to be  $B_g'' = \Phi / r\tau l_a$  lines per sq in. as defined in Art. 2. In this manner a scale is provided for the flux curve  $B$  which should preferably be replotted to a convenient scale. The curve  $F$ , showing resultant mmf under open-circuit conditions, may also be derived as explained in connection with Fig. 58.

It is obvious that the maximum value of the actual air-gap density on open circuit is less than the previously used value of  $B_g$  which is the height of the dotted rectangle of Fig. 59. With the shape of pole shoe and length of air gap as found in modern machines, the center ordinate  $B_{gc}$  of the curve  $B$  (Fig. 59) will usually be about  $[r/(0.85r + 0.15)]B_g$ , where  $r$  is the ratio of pole arc to pole pitch. Expressed in terms of known dimensions, this value becomes

$$B''_{gc} = \frac{\Phi}{(0.85r + 0.15)\tau l_a} \quad \text{lines per sq in.} \quad (44)$$

where  $\Phi$  is the flux per pole on open circuit.

**45. Effect of Armature Current in Modifying Air-gap Flux Distribution.** The distribution of armature mmf was discussed in Art. 39, and Fig. 52 shows how the addition of the armature mmf to field mmf produces the resultant mmf curve  $R$  or  $R'$  when the machine is operating under load.

In order to plot the full-load flux curve such as the curve *C* (Fig. 60), we may read the corresponding values of flux density and mmf from the curve marked *air gap, teeth, and slots* (Fig. 50). This will give correct results for all points on the armature surface where the air gap has the same length  $\delta$  as under center of pole. For points nearer to and beyond the pole tips, the changing permeance of the air paths as expressed by the curve *P* (Fig. 59) must be taken into account, the flux density being always equal to  $\text{mmf} \times \text{permeance per square centimeter}$ . The effect of tooth reluctance for points beyond the pole tips is negligible, but, wherever the density is high enough to make the ampere-turns for the teeth appreciable, the correction to be made can be obtained from the curve marked *teeth* in Fig. 50.

The distortion of flux distribution caused by armature reaction in machines not provided with pole-face windings (Art. 33) may produce considerably greater iron loss in the armature teeth at full load than on



open circuit. The flux density in the teeth corresponding to the maximum air-gap density, as read off Fig. 60, is obtained from a curve similar to Fig. 49. The maximum value of air-gap density due to field distortion under load may be 20 per cent greater than the maximum value when the machine is operating on open circuit. The curves of Fig. 60 refer to a machine without commutating poles because a certain amount of brush shift has been assumed, and this leads to a direct weakening of the field excitation caused by the demagnetizing ampere-turns on the armature. The ratio of full-load developed voltage to no-load voltage, assuming the speed to remain constant, is simply the ratio of the area under the curve *C* to the area under the curve *B*, and this is a check on the correctness of the field excitation.

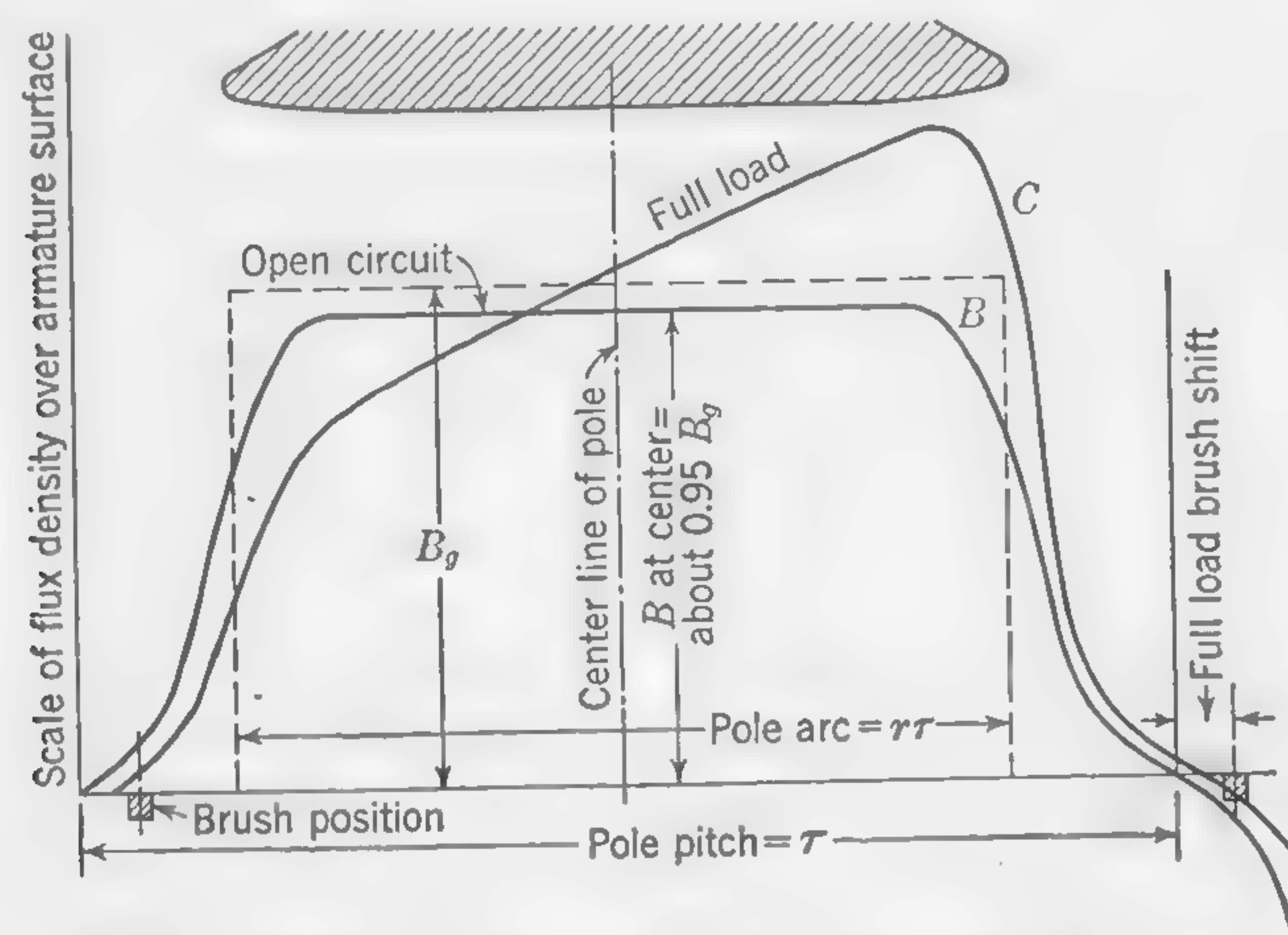


FIG. 60. Curves of flux distribution over armature surface.

**46. Leakage Factor in Multipolar Dynamos.** The design of a new machine should always include calculations for the probable amount of leakage flux and the leakage factor [formula (34), p. 78] before the cross section of the iron in the pole cores and yoke ring are decided upon; this is necessary because flux densities must be kept within reasonable limits in these portions of the magnetic circuit. Accurate information concerning these quantities will generally require the plotting of a flux map similar to that of Fig. 55, and computations that follow the procedure given in the illustrative example of Art. 42.

Most industrial designs, however, make use of available standard parts, employed not only in the interest of economy but because satisfactory performance is possible with them. Leakage factors have, as a rule, been determined for used laminations, and this generally means that it is possible to omit the plotting of a flux map and other calculations.

The accompanying table lists representative leakage coefficients whose values, when used, will yield reasonable cross sections of pole cores and frame.

Output, kw	Leakage coefficient
50	1.25 to 1.12
100	1.22 to 1.11
200	1.20 to 1.10
500	1.18 to 1.09
1,000	1.16 to 1.08
1,500	1.14 to 1.07
2,000	1.12 to 1.06

**47. Design of Field Magnets and Windings.** The problem of designing the field magnets and their associated yoke and windings generally involves the proper proportioning and arrangement of the iron and copper sections of the stationary magnetic and electric circuits. For a new machine, that is, one that does not make use of a standard lamination, this work requires the careful coordination of such matters as (1) determining the correct pole and yoke dimensions, (2) calculating the number of ampere-turns for the windings, (3) selecting the correct size or sizes of copper wire for the windings, and (4) estimating the probable temperature rise of the field under normal operating conditions. Since all phases of the design are interdependent it is necessary to check certain calculations and frequently to modify dimensions or sizes if they subsequently yield results that seem to be unreasonable.

**1. Pole and Yoke Dimensions.** Calculations for the various dimensions of pole and yoke will depend upon acceptable shapes, and permissible values of maximum flux densities. It is important to note, in this connection, that field ampere-turns and the probable temperature rise of the winding will depend, in part, upon the required mmf for the pole and yoke.

Solid poles are rarely used in present-day designs. This is especially true when the armatures have open slots. Although the eddy-current losses in solid pole shoes may be small if the air gap is large, or when semi-closed slots are used, completely laminated poles are standard practice except in very small machines. The thickness of the laminations need not be less than 25 mils (0.025 in.), and the pole-core assembly requires the riveting or welding together of a stack that has an axial length slightly less than the armature length  $l_a$ ; the pole length parallel to the shaft is usually  $l_a - 1.5\delta$ . The pole shoe is shaped to give a gradually increasing air gap at the tips (Fig. 4); the air gap at the tips (just before the usual rounding off at the extreme end) is generally  $1\frac{1}{2}$  to 2 times the air gap under the center of the pole. The illustrative example of Art. 50 emphasizes the foregoing in some detail.



2. *Shunt- and Series-field Ampere-turns.* The shunt field of a d-c dynamo must generally develop an mmf that is practically constant over the normal operating range and, acting with the series field, whose mmf depends upon the load current, the total number of ampere-turns in a compound machine must be capable of overcoming the reluctances of the various parts of the magnetic circuit when required flux densities are established in the armature. For a given air-gap flux density the magnetizing forces (ampere-turns per unit of length) can be found for the core below the teeth, the pole core and shoe, and the yoke (Fig. 61); the latter numerical quantities are then multiplied by the respective magnetic-circuit lengths, and, together with the number of ampere-turns for the air gap and teeth taken from Fig. 50, their sum will represent the necessary total.

As indicated above, the series winding on the field magnets carries the line or armature current and thus adds to the constant excitation of the shunt coils a number of ampere-turns generally in accordance with the demand for a stronger field. The series turns are frequently placed at one end of the pole (see Fig. 32), under which condition the total radial winding space available may be divided in proportion to the ampere-turns required on the shunt and series coils, respectively. In some designs the series coils are placed directly over those of the shunt winding; with this arrangement some space is usually left between them to permit the free passage of air for ventilating purposes.

When the total number of ampere-turns required per pole is known, the number of ampere-turns in the series field can easily be calculated; then with a known value of load current the number of series-field turns per pole may be computed. If it is not possible to fulfill exactly this specified condition (only full or half turns may be used) a slightly greater number of turns is provided, in which case a diverter must be used to shunt a portion of the total current; a diverter is merely a resistance connected to bypass the same per cent of total current as the per cent excess of series-field turns. Thus if the required series ampere-turns per pole is 2,000, and the current is 300 amp, the calculated number of turns per pole is  $2,000/300 = 6\frac{2}{3}$ . Since  $6\frac{1}{2}$  turns will not be sufficient, the winding may consist of  $7\frac{1}{2}$  turns, and the current required through the coils is, therefore,  $2,000/7.5 = 267$  amp. The balance of 33 amp must be shunted through a diverter whose resistance  $R_D = R_{SE}(267/33)$  ohm, where  $R_{SE}$  is the series-field resistance.

3. *Shunt- and Series-field Wire Sizes.* Where a coil of wire is connected directly across a constant, or nearly constant, source of emf, as is the case with the shunt-field winding, the developed ampere-turns are directly proportional to the cross-sectional area of the conductor used in its construction and, for all practical purposes, independent of the number of

turns. Moreover, the temperature rise will, in general, diminish as the number of turns is increased. The following analysis will show that these relationships are valid. As previously pointed out (Art. 18, Item 30), the resistance of a copper conductor at 60°C is directly proportional to its

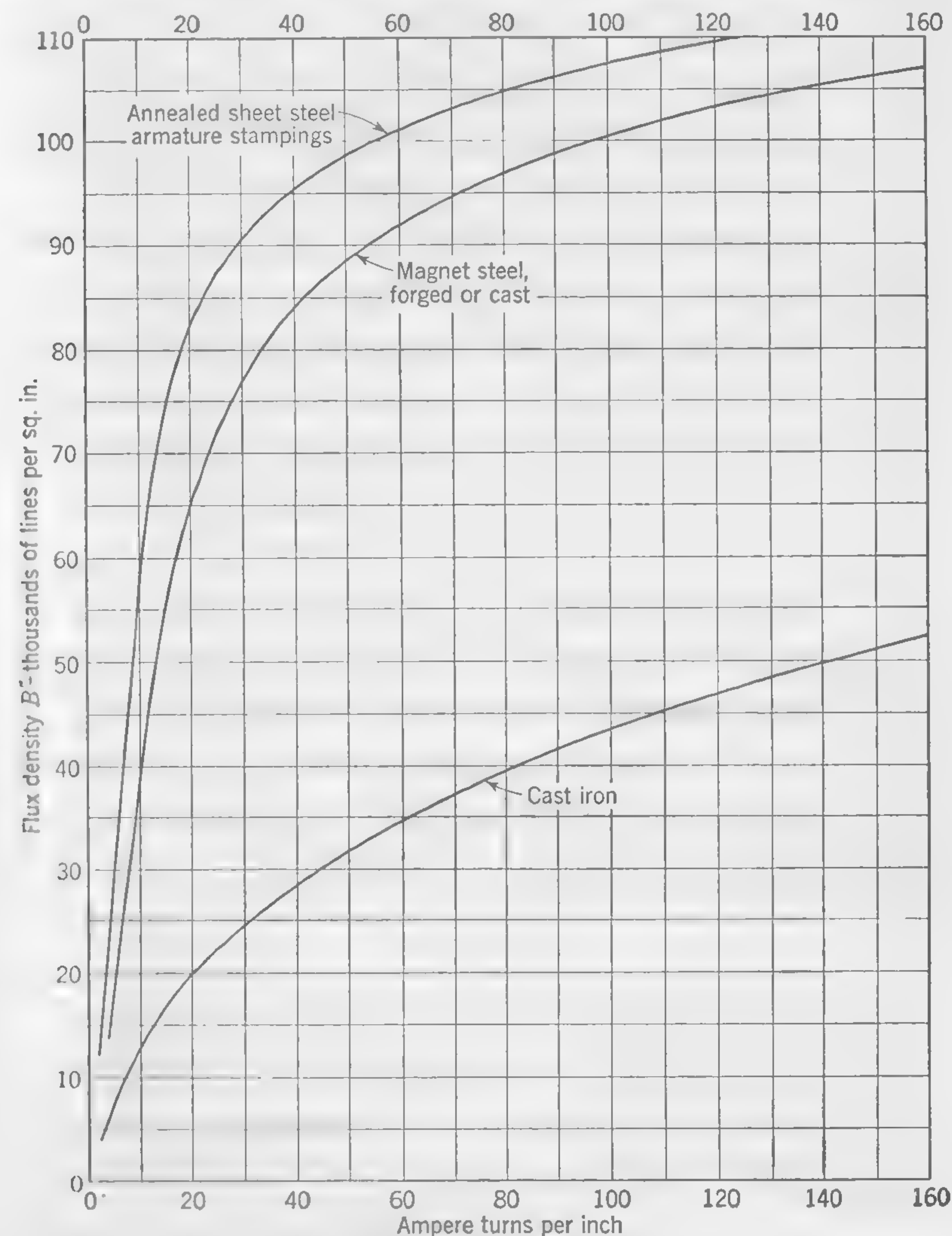


FIG. 61. Magnetization curves (inch units).

length  $l$  in inches and inversely proportional to the circular-mil area ( $m$ ); i.e.,  $R = l/(m)$  ohms. Since the length of wire in one field coil is equal to the product of the mean length per turn  $m$  and its number of turns  $T$ ,  $R_{coil} = m \times T/(m)$ . But the coil resistance is also equal to the ratio of



the coil voltage  $E/p$  ( $p$  coils in series) to the coil current  $I$ . Thus, equating the two values of  $R_{\text{coil}}$ ,

$$\frac{m \times T}{(m)} = \frac{E/p}{I}$$

from which

$$(m) = \frac{m \times (TI) \times p}{E} \quad (45)$$

For a coil of rectangular shape, Fig. 62,  $m = 2(u + v) + \pi w$  so that,

$$(m) = \frac{[2(u + v) + \pi w] \times (TI) \times p}{E} \quad (45a)$$

Formula (45a) indicates that a field coil that is wound around a form of fixed dimensions  $u$  and  $v$  and is connected to  $E/p$  volts will develop ampere-turns practically proportional to the wire size; the possible variation of the dimension  $w$  will alter this proportionality only slightly. Note

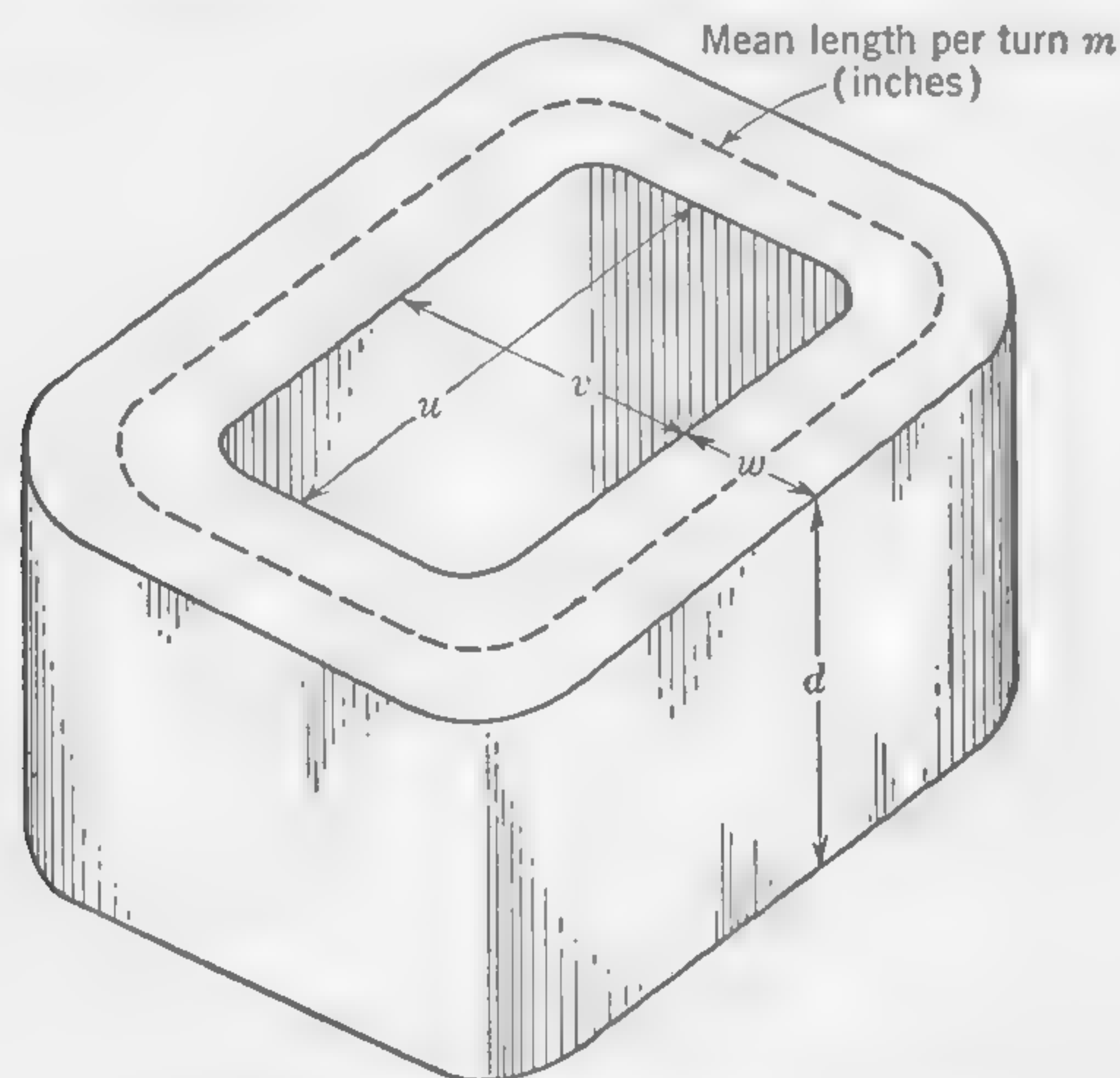


FIG. 62. Field coil of rectangular shape.

also that any increase in the number of turns by increasing  $d$  (turns per layer) or  $w$  (number of layers) will result in an equivalent change in coil resistance to lower the current. It follows, therefore, that the  $I^2R$  loss in the field, a measure of the temperature rise, will decrease with an increase in the number of turns.

In compound-wound machines it is customary to allow a voltage drop in a shunt-field rheostat of about 15 per cent of the terminal emf. The wire size for the shunt-field coils should, therefore, be calculated on the assumption that the impressed voltage  $E$ , formula (45a), is 15 per cent

less than the terminal voltage of the machine. With shunt-wound generators, the field rheostat plays a more important part; it must be designed to give the required variation in field strength between no load and full load, at constant speed, or, in the case of a motor, to provide for the required speed variation. The amount by which the excitation has to be varied—apart from the requirements to compensate for the effects of temperature changes—may be determined by reference to the saturation curve.

To find the wire size for the shunt winding, a good procedure is to assume a dimension  $w$ , not more than about 3 in. to avoid local heating inside the coil; then, with known values of  $(TI)$ ,  $w$ ,  $v$ ,  $p$ , and  $E$ , use formula (45a). The next step is to determine the number of turns that can be fitted into a space  $w \times d$  sq in., after which the resistance and current may be calculated. In well-designed machines the shunt-field currents should usually be less than the values given below, where the currents are expressed as percentages of the full-load rated currents of the machines:

Output of machine, kw	Exciting current percentage of rated current
10	3.0
25	2.5
50	1.6
100	1.2
200	0.9
300	0.7
500	0.5
1,000 and larger	0.3 to 0.4

The wire size of the series-field winding is found by dividing the known full-load current  $I_{SE}$  by an assumed current density  $\Delta$ , in amp per sq in. Thus

$$A = \frac{I_{SE}}{\Delta} \quad \text{sq in.} \quad (46)$$

The current density in field windings, both shunt and series, will usually be between 800 and 1,600 amp per sq in., the larger values applying to high-speed well-ventilated machines, and in the case where the series field is placed near the pole shoe. If the current to be carried exceeds 100 amp, the coils may be made of flat copper strip wound edgewise by means of a special machine. For small currents, cotton-covered wires of square or rectangular section are commonly used, round wires being rarely employed, unless the diameter is less than that of a No. 8 B & S gage.

1. *Temperature Rise of Field Windings.* The problem of keeping the temperature rise of field coils within safe limits (40 to 50°C) is complicated by the fact that the fanning action of the rotating armature will have an



important effect upon the machine's ability to dissipate heat. Moreover, when the spacing between coils is wide and when the presence of commutating poles is not a factor in restricting the free circulation of air, the main poles are likely to run cool. It should, therefore, be clear that the rate at which heat energy can be carried away from the surface of a coil will depend, among other things, upon the general construction of the machine, upon the nature and area of the cooling surface, and the heat-absorbing properties of the surrounding medium. These considerations lead to the conclusion that empirical coefficients, the results of experience as well as experimental investigation, must be used for predetermining the temperatures likely to be attained by machines operating under specified conditions. Thus, if

$S$  = cooling surface in square inches

$W = I^2R$  loss in watts

$t$  = temperature rise in degrees Centigrade, being the observed difference of temperature between the surface of the hot conductor within the coil and the surrounding medium

we have the following relation

$$W = c \times S \times t$$

where  $c$  is the cooling coefficient expressed in watts per square inch per degree Centigrade difference in temperature. Whence

$$t = \frac{W}{c \times S} \quad (47)$$

The graphs of Fig. 63 show typical experimental relationships between the cooling coefficient  $c$  and the peripheral speed of the armature for two typical spacing arrangements of field coils. The curve marked  $A$  applies to machines with wide spacing between poles and good ventilation, while curve  $B$  should be used when the main poles are close together, or when commutating poles interfere with the free circulation of air around the main windings. The cooling coefficient will necessarily depend upon the type and size of machine, and it should, if possible, be determined from tests made upon generators or motors generally similar to the one being designed. The modern tendency in design seems to be toward increased output by improvements in the qualities of the insulating and magnetic materials and in methods of ventilation. Field coils are now frequently built with sectionalized windings so arranged that air has free access not only between the subdivisions of the winding, but also between the inside of the coils and the pole core. The gain is not always proportionate to the total cost and space required, but decisions in such matters are frequently made on the basis of other factors; the cooling coefficients given

in Fig. 63 are not applicable to such special designs and should not be used unless properly modified.

**48. Illustrative Example. Design of Field-magnet Coil for Dynamo.** Given an 8-pole shunt-wound 220-volt d-c generator with a cross section of iron in each pole core of 4 by 10 in. Referring to Fig. 62, the winding space  $d$  for the exciting turns is 6.5 in. long and the inside dimensions of the former  $u$  and  $v$ , on which the coil is wound, are 4.25 by 10.25 in. Design a suitable winding to give approximately 8,500 amp-turns per pole when

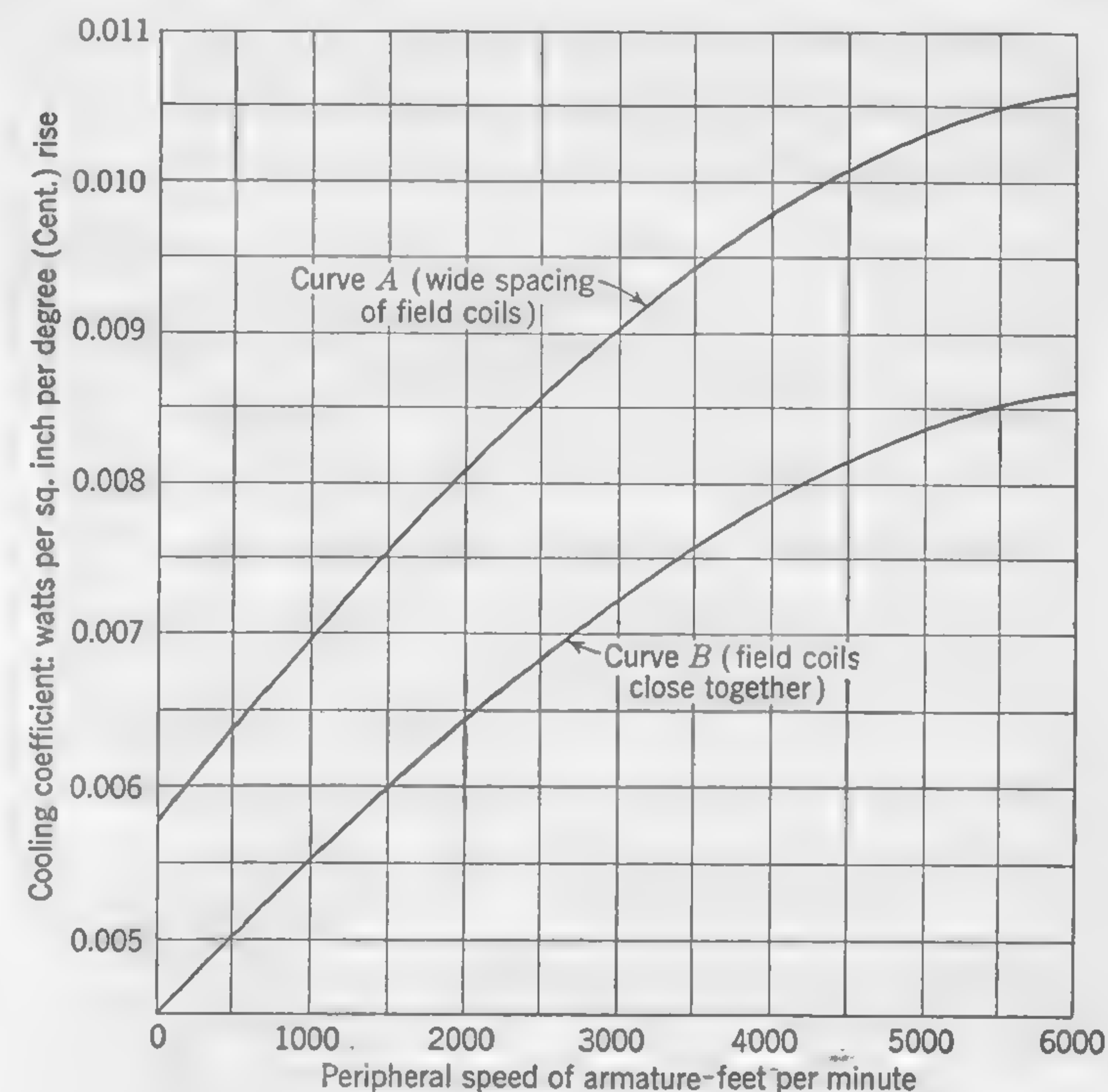


FIG. 63. Cooling coefficients for field coils of dynamos.

an external field rheostat absorbs 15 per cent of the voltage. The temperature rise at the surface of the field coils is not to exceed  $45^{\circ}\text{C}$  and is not to be less than  $35^{\circ}\text{C}$ . Assume an average coil temperature of  $60^{\circ}\text{C}$  and a cooling coefficient of 0.009 watt per sq in. per  $^{\circ}\text{C}$  rise in temperature.

Since the width of the winding  $w$  is unknown, it will be proper to assume a reasonable value for this dimension and then proceed with the required calculations. Then, if the temperature rise does not fall within the specified limits a correction can be made in  $w$ , decreasing it, for example, if the higher temperature rise is desired; it is generally a simple matter to make the necessary adjustments and calculations.



Assuming a value of  $w = 2$  in., the mean length of turn

$$m = 2(4.25 + 10.25) + (\pi \times 2) = 35.3 \text{ in.}$$

By formula (45), the circular mil area of the conductor is

$$(m) = \frac{35.3 \times 8,500 \times 8}{0.85 \times 220} = 12,850 \text{ cir mils}$$

The nearest standard size (of larger cross section), is No. 9 B & S, the particulars of which, obtained from Table I (p. 431) are:

$$\text{Circular mils} = 13,090$$

$$\text{Cross section} = 0.01028 \text{ sq in.}$$

$$\text{Resistance per 1,000 ft at } 60^\circ\text{C} = 0.921 \text{ ohm}$$

$$\text{Approx number of turns per inch of dc} = 7.88$$

Allowing about  $\frac{1}{4}$  in. at the ends for insulation it will be possible to wind  $6.25 \times 7.88$ , or (say) 49 wires in each layer. Also, with a coil width of 2 in., and allowing some space for insulating paper between layers, there will be  $7.88 \times 1.9$ , or (say) 15 layers. Therefore,

$$\text{Turns per coil} = 49 \times 15 = 735$$

Since each turn has an average length of 35.3 in.

$$\text{Length of wire per coil} = 735 \times \frac{35.3}{12} = 2,160 \text{ ft}$$

and

$$\text{Resistance per coil at } 60^\circ\text{C} = 2.16 \times 0.921 = 1.99 \text{ ohms}$$

The exciting current will be

$$I = \frac{220 \times 0.85}{8 \times 1.99} = 10.8 \text{ amp}$$

Checking the number of ampere-turns it is found to be  $735 \times 10.8 = 8,650$ , which is more than 8,500 by the factor  $13,090/12,850$  because a standard wire, having an area slightly larger than required, was used.

The surface area of the coil being equal to the product of its perimeter and the mean length of each turn,

$$S = 2(6.5 + 2) \times 35.3 = 600 \text{ sq in.}$$

The temperature rise, by formula (47), will, therefore, be

$$t = \frac{(10.8)^2 \times 1.99}{0.009 \times 600} = 40^\circ\text{C}$$

Checking on the current density in the conductor,

$$\Delta = \frac{10.8}{0.01028} = 1,050 \text{ amp per sq in.}$$

which is reasonable.

It should be pointed out that some saving in winding cost could be effected by reducing the width of the coil, dimension  $w$ , thereby cutting down on the number of turns; this would, however, increase the exciting current, though not the number of ampere-turns, and boost the temperature rise.

**49. Open-circuit Saturation Curve of Dynamo.** In Illustrative Example, Art. 38, the method of plotting the curves of Fig. 50 was explained. The curve marked *air gap and teeth* gives the ampere-turns required per pole to overcome the total reluctance between the pole face and the bottom of the armature slots for different values of the average air-gap flux density. To these ampere-turns must be added the ampere-turns necessary to overcome the reluctance of the entire magnetic circuit, including armature core, pole core, and yoke ring. Instead of plotting the relation between ampere-turns and air-gap density, it is desirable to plot a curve connecting field ampere-turns per pole, and emf generated in the armature. This is merely a matter of changing the scale of the ordinates of the curve since, in constant-speed machines, the developed voltage is obviously proportioned to the flux cut by the conductors and, therefore, to the flux density in the air gap.

In Fig. 64 the dotted curve  $OM$  gives the relation between ampere-turns and developed voltage for air gap and teeth only, while  $OFN$  is the "saturation curve" for the complete machine and takes account not only of the air-gap and tooth reluctance, but also of the reluctance of the other parts of the magnetic circuit. Any horizontal distance, such as  $MN$ , between the two curves is a measure of the ampere-turns required to overcome this additional reluctance. The ordinate  $OE_o$  is the terminal voltage on open circuit,  $OE_t$  is the terminal voltage at full load (the machine is assumed to be overcompounded), and  $OE_a$  is the necessary *developed* voltage at full load (i.e., the voltage that must be generated in the armature conductors by the cutting of the flux in order that the terminal voltage at full load shall be  $OE_t$ ).

Draw a straight line connecting the origin  $O$  of the curve and the point  $F$  corresponding to the no-load voltage, and produce this to  $G$ , where it meets the horizontal line representing full-load terminal voltage. Then, since the ampere-turns on the shunt at no load are  $OA$ , they will obviously have increased to  $OB$  at full load on account of the higher terminal voltage (the "long shunt" connection is here assumed). The ampere-turns necessary to produce the required full-load flux will be  $OC$ , but in machines not provided with commutating poles, the field excitation must be greater than this in order to balance the demagnetizing effects of the armature current. If the amount of the forward lead given to the brushes is known, the armature demagnetizing ampere-turns due to brush shift may be calculated by formula (43) of Art. 39. This is the distance  $CD$  (Fig. 64).



These ampere-turns have to be put on the field poles, not to increase the air-gap flux and thus develop a higher voltage but merely to counteract the effects of the armature current and restore the air-gap flux to its original value on open circuit. It is, therefore, correct to say that additional ampere-turns approximately equal to this amount must be added to the field windings in order that the necessary flux shall be cut by the armature conductors. It follows that  $OD$  represents the total ampere-turns required per pole at full load. Of this total amount,  $OB$  will be due to the shunt winding, and the balance  $BD$  must be provided by the series winding.

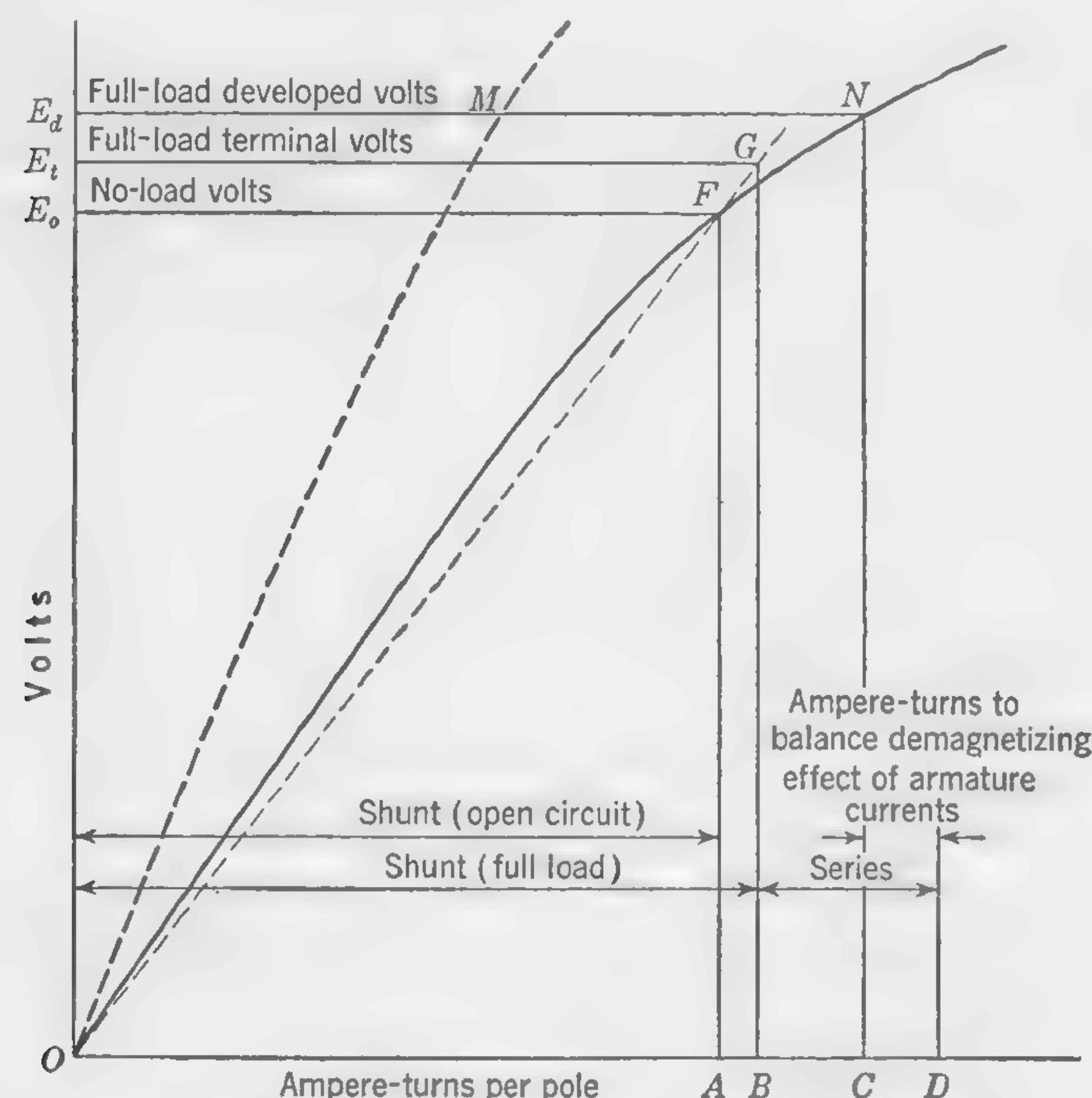


FIG. 64. Open-circuit "saturation" curve of dynamo.

**50. Illustrative Example. Design of Dynamo Field Magnets and Windings.** Design the magnetic circuit—poles, yoke ring, and field-magnet windings—of a 6-pole 300-kw generator with commutating poles, driven at a constant speed of 1,200 rpm and provided with an armature wound to give a terminal voltage of 230 volts on open circuit, increasing to 250 volts at full load. It is assumed that the armature has been designed and that the dimensions and other values as given in the Illustrative Example, Art. 18, are to be used. It is also assumed that the "equivalent air gap" and the ampere-turns for the air gap, teeth, and slots have been calculated as explained in connection with the Illustrative

Example, Art. 38. The curve of Fig. 50 is to be used as data for this problem. The various items to be calculated are listed on the accompanying design sheet, which is followed by notes explaining the calculations.

### DESIGN OF POLES, YOKE, AND WINDINGS

**Item 7: Leakage Factor.** Refer to Art. 46. This may be estimated at 1.15. This value may later be checked by drawing a flux-leakage map, like that previously explained (Art. 42), after the preliminary pole dimensions are determined.

**Items 8 and 9: Cross Section of Pole Core.** Refer to Art. 40 for calculation of the full-load flux per pole. This flux, as estimated in Art. 18, is  $4.27 \times 10^6$  maxwells. The maximum flux density in the pole core will occur in the cross section near the yoke ring, and, being determined by the total flux, *i.e.*, useful and leakage flux, may be fairly high. From the  $B$ - $H$  curve of Fig. 61, it appears that 95,000 lines per sq in. will not require an excessive number of ampere-turns. The pole-core cross section must, therefore, be

$$A_c = \frac{4.27 \times 10^6 \times 1.15}{95,000} = 51.7 \text{ sq. in.}$$

The dimension of the pole shoe measured parallel to the shaft will be about  $l_a = 1.5\delta$  (see Art. 47), the numerical values of  $l_a$  and  $\delta$  being given in items 1 and 6. Thus

$$l_{\text{core}} = 10.25 - (1.5 \times 0.20) = 9.85 \text{ in., or (say) } 9\frac{7}{8} \text{ in.}$$

The width of the pole core should, therefore, be

$$w_{\text{core}} = \frac{51.7}{9.875} = 5.25 \text{ in.}$$

**Item 10: Length of Winding Space on Pole.** Refer to Art. 47, and the Illustrative Example of Art. 48. This dimension will tentatively be made  $6\frac{1}{2}$  in. and is subject to change if later temperature-rise calculations indicate that it should be modified. It should be noted that the radial dimension of the pole must correspond approximately with that of the commutating pole, which was not designed for this machine. However, the dimensions for the main and commutating poles are not particularly critical at this stage and may be altered one way or another when the final design is completed and accurate drawings must be prepared for the manufacture of the machine.

**Items 12 and 13: Flux Density in Frame.** This should be about the same as, or somewhat less than, the maximum density in the core. Selecting 90,000 lines per sq in., and remembering that the total useful and leakage flux divides as it enters the yoke, with one-half passing in each



DESIGN SHEET FOR POLE CORES, FRAME, AND FIELD WINDINGS OF  
D-C GENERATOR

(Dimensions in inches unless otherwise stated)

Item No.	Specifications: 300 kw; 230/250 volts; 1,200 rpm, allowable temperature rise of field coils = 45°C	Symbol	Preliminary or assumed values	Final values
Given or Assumed Data				
1	Number of main poles.....	$p$	.....	6
2	Number of commutating poles.....	...	.....	6
3	Diameter of armature core.....	$D$	.....	22
4	Axial length of armature core; gross.....	$l_a$	.....	10.25
5	Ratio pole arc to pole pitch.....	$r$	.....	0.64
6	Air gap under center of pole.....	$\delta$	.....	0.20
7	Leakage factor.....	$l_f$	1.15	
(All other required data to be taken from Illustrative Examples, Arts. 18 and 38)				
Calculations				
8	Maximum flux density in pole core (full load).....	...	95,000	
9	Cross section of pole core.....	$A_c$	.....	51.7
10	Length (radial) of winding space on pole.....	...	$6\frac{1}{2}$	
11	Flux density in frame (yoke ring).....	...	90,000	
12	Cross section of yoke ring.....	...	27.3	28.0
13	Outside diameter of frame (from sketch, Fig. 65).....	...	.....	42
14	$TI$ per pole for total magnetic circuit (no load).....	...	.....	4,080
15	$TI$ per pole on shunt field (full load)....	...	.....	4,440
16	$TI$ per pole in series winding.....	...	.....	475
17	$TI$ per pole total at full load.....	...	.....	4,915
18	Length of winding space for shunt coils..	...	.....	$5\frac{1}{2}$
19	Width of winding space for shunt coils... $w$	...	.....	1.25
20	Size of shunt-field wire (B & S gage).....	...	.....	No. 14 square
21	Number of turns of wire per shunt-field coil.....	...	.....	1,168
22	Shunt-field current (full load).....	...	.....	3.82
23	Number of turns of series winding per pole.....	...	.....	$\frac{1}{2}$
24	Cross section of series winding.....	...	.....	0.75
25	Resistance (hot) of series winding (ohms)...	...	.....	$165 \times 10^{-6}$
26	$I^2R$ loss in series-field coils (watts).....	...	.....	240
27	Surface temperature rise of field coils (degrees C).....	...	.....	38.7°C

direction, the minimum cross section of the yoke ring should, therefore, be

$$A_y = \frac{4.27 \times 10^6 \times 1.15}{2 \times 90,000} = 27.3 \text{ sq in.}$$

The width and thickness to give this cross section will depend upon the design, but it will be well to proceed on the basis of a yoke overhang, measured parallel to the shaft, of about 2 in.; this construction will

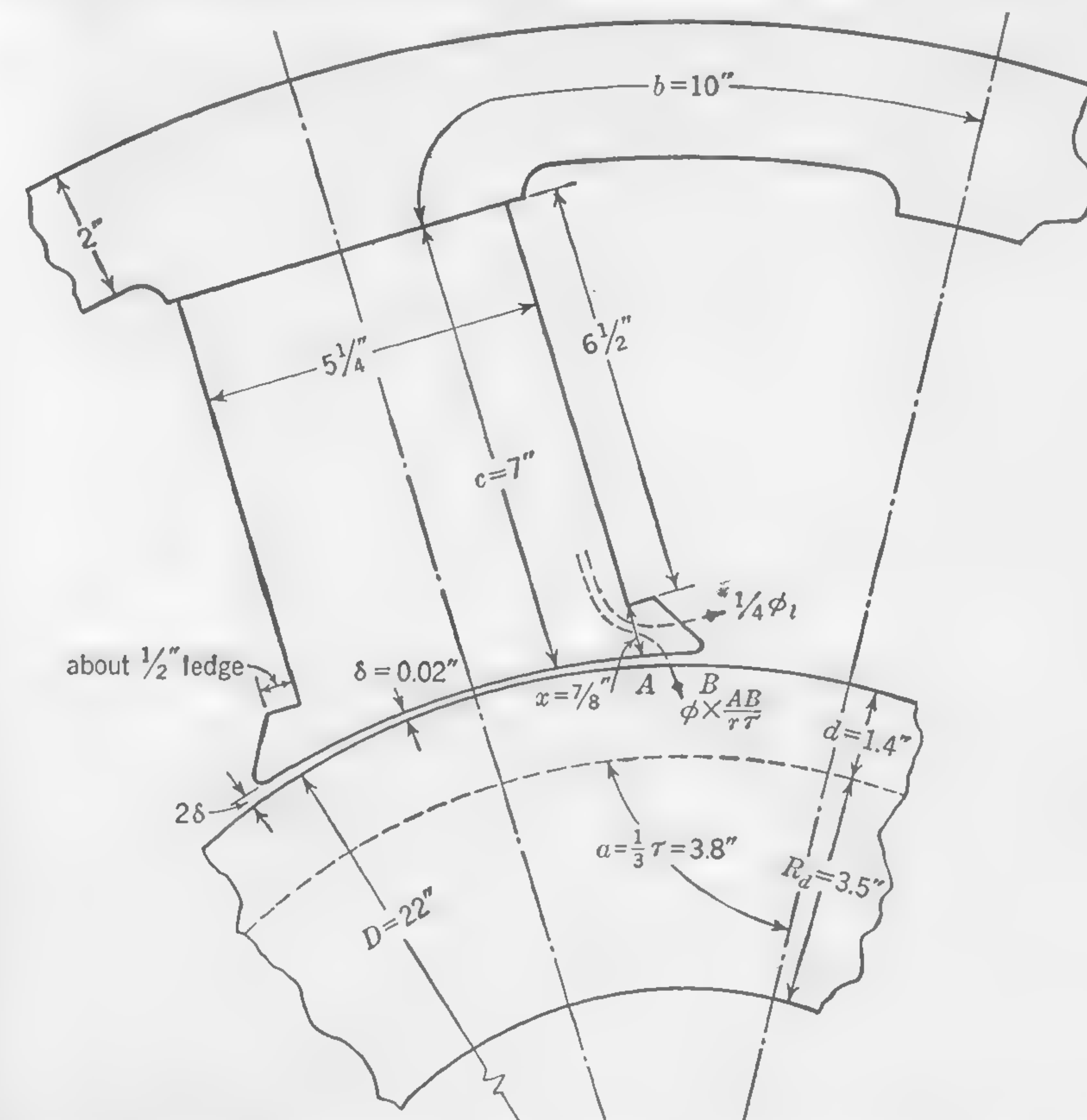


FIG. 65. Design of pole core and yoke ring for Illustrative Example of Art. 50.

provide a yoke extension that is about as wide as the field coils. Assuming a width of about 14 in. (axially) and a rectangular cross section, using a standard slab of structural steel that is formed into a cylinder and butt-welded, the yoke thickness will be

$$w_{\text{yoke}} = \frac{27.3}{1.4} = 1.95 \text{ in., or (say) 2 in.}$$

The pole shoe in Fig. 65 is drawn as explained in Art. 4 and Fig. 4, and



also in Art. 47, with the air gap at the pole tips somewhat greater than under the center of the pole. The pole tips are rounded off with a radius of about  $\frac{1}{8}$  in., and a thickness of metal  $x = \frac{7}{8}$  in. is provided between pole face and the ledge that supports the field coils. This thickness is calculated so that sufficient metal is provided at this point to avoid magnetic saturation of the pole tips. The flux passing through the section of  $9.875x$  sq in., where 9.875 is the thickness of the pole shoe measured parallel to the shaft, is assumed to consist of two components: (1) the flux leaking from the pole tip, which may be taken at about one-quarter of the total estimated leakage flux; and (2) the flux entering the armature teeth in space  $AB$ , which is approximately equal to the flux per pole multiplied by the ratio  $\frac{\text{arc } AB}{\text{pole arc}}$ . In this design, the length  $AB$  is approximately  $(7.37 - 5.25)/2 = 1.06$  in., where the number 7.37 is the pole arc  $rr$  (item 17 in Art. 18) and the number 5.25 is the pole width (Fig. 65). The two flux components are equal to

$$\Phi_x = \left( \frac{0.15 \times 4,270,000}{4} \right) + \left( \frac{1.06}{7.37} \times 4,270,000 \right) = 775,000 \text{ maxwells}$$

Assuming a flux density of 95,000 lines per sq in. as in the remainder of the pole core

$$x = \frac{775,000}{9.875 \times 95,000} = 0.825 \text{ in., or (say) } \frac{7}{8} \text{ in.}$$

Having drawn Fig. 65 to scale, a more accurate estimate of the leakage factor may now be made by plotting a flux-leakage map (Art. 42). It is not proposed to repeat these calculations in connection with the field design now under consideration, but it will be assumed that the leakage factor 1.15 as already estimated (item 7) is found to be correct, so that no change need be made in the dimensions of the magnetic circuit before proceeding with the calculations for the open-circuit saturation curve.

*Items 14 to 17: Ampere-turns per Pole for Total Magnetic Circuit. Plotting the Open-circuit Saturation Curve.* Refer to Art. 49. The calculations of the total ampere-turns on each pole of the machine, to develop on open-circuit a given voltage, are shown in the table on page 131. Suitable values of terminal voltage are selected to obtain points on the saturation curve. One of the values should be slightly higher than the developed emf under full-load conditions. It is not necessary to make the calculations for very low voltage, because the reluctance of the iron parts of the magnetic circuit is negligible. For each selected value of developed emf the ampere-turns for the complete magnetic circuit are calculated; the component parts include (1) the air gap and teeth, (2) the armature core below the teeth, (3) the yoke, and (4) the pole core. The

OPEN-CIRCUIT SATURATION CURVE DATA  
(Table for Calculating Ampere-turns for Total Magnetic Circuit)

No-load voltage.....	210	230	245	260
Flux entering armature per pole, maxwells.....	3,500,000	3,833,000	4,080,000	4,330,000
Flux density:				
Armature core ( $\Phi/2 \times 29.4$ ).....	59,500	65,200	69,500	73,700
Pole core ( $1.125\Phi/51.7$ )..	76,200	83,500	88,800	94,200
Yoke ring ( $1.15\Phi/2 \times 28$ )	71,900	78,700	83,700	89,000
Air gap ( $\Phi/81.8$ ).....	42,700	46,800	49,800	53,000
	(6,620 gauss)	(7,260 gauss)	(7,730 gauss)	(8,220 gauss)
Amp-turns per in.:				
Armature } Fig. 61.....	10	12	14	16
Pole core }	17	22	28	38
Yoke ring }	25	32	38	52
Amp-turns:				
Armature ( $l = 3.8$ in.)...	38	46	53	61
Pole core ( $l = 7$ in.)....	119	164	196	266
Yoke ring ( $l = 10$ in.)...	250	320	380	520
Air gap and teeth (Fig. 50).....	3,200	3,550	3,850	4,250
Total .....	3,607	4,080	4,479	5,097

first and second items are determined on the basis of the *useful* flux; the third item involves one-half of the total useful and leakage flux. To determine the ampere-turns for the pole core, the fourth item, the *average* flux should be used; this may be estimated as equal to

$$\Phi_{\text{avg}} = \frac{1}{3}(2\Phi_y + \Phi_p)$$

where  $\Phi_y$  is the maximum flux in the pole core at the yoke ring, and  $\Phi_p$  is the flux in the pole core at the end nearest the pole shoe. Assuming one-half of all the leakage flux to pass from the pole shoes, the flux in the core nearest the pole shoe is

$$\Phi_p = \Phi + \frac{1}{2}\Phi_l = \Phi + \frac{1}{2}\Phi(lf - 1) = \frac{\Phi}{2} + \frac{lf \times \Phi}{2}$$

By making the necessary substitutions, what has been referred to as the average flux in the pole core may be written:

$$\Phi_{\text{avg}} = \frac{1}{3} \left[ (2lf \times \Phi) + \frac{\Phi}{2} + \frac{lf \times \Phi}{2} \right] = \left( \frac{1 + 5lf}{6} \right) \Phi$$

In this design  $lf = 1.15$ , whence  $\Phi_{\text{avg}} = 1.125\Phi$ , the meaning of which is



that the pole-core flux is calculated on the assumption that the leakage factor is 1.125 instead of 1.15, as used in estimating the flux in the yoke.

After the various flux densities are calculated for given values of flux, Fig. 61 should be used to determine the ampere-turns per inch for the armature core, pole core, and yoke portions of the magnetic circuit; the latter are then multiplied by their respective lengths of path, indicated on Fig. 65, to yield the corresponding ampere-turns. (Note that the armature core length  $a$  is taken as  $\frac{1}{3}\tau$ .) The number of ampere-turns for the air gap and teeth are, of course, taken from the previously plotted graph of Fig. 50. The density in the air gap which determines the ampere-turns required is the maximum value of the average density over a tooth pitch (*i.e.*, the average air-gap density under the center of the pole face). Using formula (44) of Art. 44, the maximum value of the air-gap density is

$$B''_{ac} = \frac{\Phi}{(0.85r + 0.15)\tau l_a} = \frac{\Phi}{[(0.85 \times 0.64) + 0.15]11.5 \times 10.25} = \frac{\Phi}{81.8}$$

The curve (Fig. 66) is plotted from the results of the calculations as given in the table. It shows the connection between the open-circuit emf and the corresponding ampere-turns of excitation per pole.

Referring to Fig. 66, note the following:

1. Shunt-field ampere-turns per pole on open circuit (230 volts) = 4,080.
2. Shunt-field ampere-turns per pole at full load (250 volts) = 4,440.
3. Total ampere-turns for shunt- and series-field coils (256.1 volts) = 4,915; the required generated emf for a full-load terminal voltage of 250 volts was calculated in Art. 18.
4. Series-field ampere-turns at full load =  $4,915 - 4,440 = 475$ .

*Items 18 to 22: Shunt-field Winding.* Refer to Art. 47 and the Illustrative Example of Art. 48. Allowing about  $\frac{1}{2}$  in. for insulation at the top and bottom and for space between shunt and series coils, the total length of the winding space will be 6 in. Dividing this length in proportion to the shunt and series ampere-turns, the shunt coil will occupy  $(4,440/4,915)6 = 5\frac{1}{2}$  in., and the series coil  $\frac{1}{2}$  in. Next, allowing about  $\frac{1}{4}$  in. for insulation space between coils and pole core, the inside dimensions of the shunt and series coils will be  $5\frac{1}{2}$  by  $10\frac{1}{8}$  in. Assuming a total thickness of winding  $w = 1\frac{1}{4}$  in., the mean length per turn  $m$  will, therefore, be  $2(5\frac{1}{2} + 10\frac{1}{8}) + (1\frac{1}{4}\pi)$ , or about 36 in. It will be supposed that a shunt-field rheostat absorbs 15 per cent of the voltage on open circuit, so that, by formula (45), page 120.

$$(m) = \frac{36 \times 4,080 \times 6}{0.85 \times 230} = 4,500 \text{ cir mils}$$

Referring to the Wire Table II (see Appendix), the standard size of square

wire of cross section nearest to this calculated value is No. 14 AWG; it has an area of 4,545 cir mils and will wind 182 turns per sq in. Having a resistance of 2.78 ohms per 1,000 ft at 75°C, the resistance at 60°C will be  $2.78 \times (234.5 + 60/234.5 + 75) = 2.65$  ohms per 1,000 ft. Since

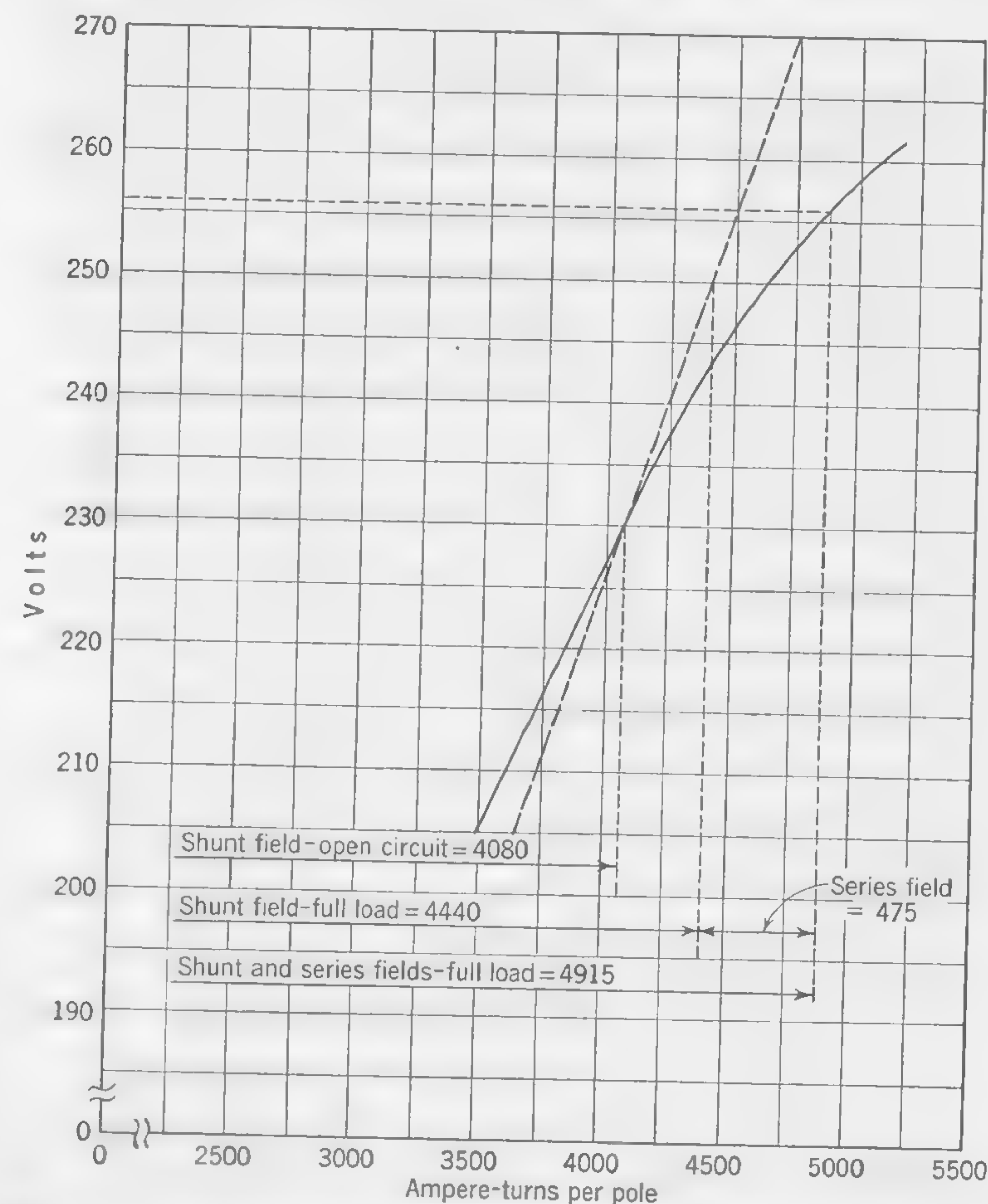


FIG. 66. Open-circuit saturation curve for Illustrative Example of Art. 50.

182 wires per sq in. means about  $13\frac{1}{2}$  wires per in., there will be  $5\frac{1}{2} \times 13\frac{1}{2} = 74$  wires per layer, and  $1\frac{1}{4} \times 13\frac{1}{2} = 17$  layers. Making allowance for manufacturing tolerances and paper insulation between layers, it will be assumed that there will be  $73 \times 16 = 1,168$  turns per coil.

The resistance per coil is

$$\frac{36 \times 1,168 \times 2.65}{12 \times 1,000} = 9.28 \text{ ohms}$$



and the current will be

$$\frac{230 \times 0.85}{6 \times 9.28} = 3.51 \text{ amp at no load, and } \frac{250}{230} \times 3.51 = 3.82 \text{ amp at full load}$$

Checking on the ampere turns, these are  $1,168 \times 3.51 = 4,100$  at no load, and  $1,168 \times 3.82 = 4,450$ , which are correct. The current density at full load will be

$$\frac{3.82}{4,545/(4/\pi \times 10^6)} = 1,070 \text{ amp per sq in.}$$

which is reasonable.

*Items 23 to 26: Series-field Coils.* Refer to Art. 47. The series turns may be placed at either end of the pole, preferably near the pole shoe (see Fig. 32), or they may be wound outside the shunt winding. As previously calculated, the space available in a radial direction is about  $\frac{1}{2}$  in. On the basis of the comparatively few series-field ampere-turns per pole required—475—and the rather large current—1203.8 amp—only  $\frac{1}{2}$  turn will be needed for each of the series-field coils. Since the copper will be completely exposed and subject to good cooling near the armature surface, a high value of current density, 1,600 amp per sq in., will be used; the cross section will, therefore, be 0.75 sq in. This winding may consist of two flat copper strips in parallel, wound on edge, each one  $\frac{1}{4} \times 1\frac{1}{2}$  in. Assuming the same mean length of turn as in the shunt winding, 36 in., and adding an estimated 50 in. for connections between successive coils, the total length of series-field copper will be  $(6 \times \frac{1}{2} \times 36) + 50 = 158$  in. The total series-field resistance will be

$$R_{\text{series}} = \frac{158}{0.75 \times 4/\pi \times 10^6} = 165 \times 10^{-6} \text{ ohm}$$

and the total copper loss in the series field will be

$$I^2 R = (1,203.8)^2 \times 165 \times 10^{-6} = 240 \text{ watts}$$

*Item 27: Temperature Rise of Field Coils.* Refer to Art. 47, and the Illustrative Example of Art. 48. The total cooling surface of the windings on each pole is  $2(6 + 1\frac{1}{4}) \times 36 = 522$  sq in. The watts lost in the shunt and series coils on one pole is

$$240/6 + (3.82)^2 \times 9.28 = 175 \text{ watts}$$

The coefficient of cooling, from curve *B* of Fig. 63, for a peripheral velocity of more than 6,000 fpm (6,900 in this design) will be 0.0087; whence, by formula (47), page 122, the temperature rise is

$$t = \frac{175}{0.0087 \times 522} = 38.7^\circ\text{C}$$

This is well below the permissible upper limit of about  $45^\circ\text{C}$  and should, therefore, provide a measure of safety in view of certain assumptions; a final check on actual temperature rise would, of course, be made when the completed machine is placed on test.

### TEST PROBLEMS

1. Given an air path  $\frac{7}{8}$  in. long, what ampere-turns are required to produce a flux density of 2,160 gauss? Ans. 3,820.
2. Calculate the ampere-turns necessary to establish a flux of 20,000 maxwells across an air gap  $\frac{1}{4}$  in. long and 4 sq in. in cross section. Ans. 391.
3. What is the drop of magnetic potential in a piece of iron 3 in. long when the flux density is 12,000 gauss, given that the permeability is 600? Ans. 152 gilberts.
4. In a certain iron flux path of uniform cross section, the permeance is 22 and the potential drop is 1,300 gilberts. The length of the path is 12 in. and its area of cross section is 0.3 sq in. Calculate:
  - (a) The total flux Ans. 28,600 maxwells.
  - (b) The flux density Ans. 14,800 gauss.
  - (c) The magnetizing force Ans.  $H = 42.6$  oersteds.
  - (d) The permeability of the iron Ans.  $\mu = 347$ .
5. In a portion of an iron magnetic circuit of 3 sq cm cross section, the total magnetic flux is 30,000 maxwells. Calculate the permeability of the iron, given that the drop of magnetic potential over a length of 5 cm is 25 gilberts. Ans. 2,000.
6. A magnetic circuit contains two air gaps in series: the first is 0.1 in. long with a cross section of 8 sq in.; the second is 0.2 in. long with a cross section of 10 sq in. The magnetizing force in the first gap is 1,500 oersteds. Calculate the ampere-turns required to overcome the reluctance of the two gaps in series. Ans. 787.
7. A magnetic circuit includes two air gaps in parallel. Gap 1 is 0.25 in. long and 4 sq in. in cross section; gap 2 is 0.15 in. long and 3 sq in. in cross section. Calculate (a) the reluctance of the two gaps in parallel, (b) the ampere-turns required to establish a total flux of 50,000 maxwells across the gaps. Ans. (a) 0.0141, (b) 560.
8. Given: tooth pitch = 1.4 in.; slot width = 0.65 in.; ratio net to gross length of armature core = 0.85. Calculate the average air-gap density over one tooth pitch when the apparent tooth density is 130,000 lines per sq in. (Assume that the cross section of the tooth is uniform throughout its length.) Ans. 59,200 lines per sq in.
9. Given: permeance of air gap over one tooth pitch = 300; ampere-turns for air gap = 2,200; tooth pitch = 1.6 in.; dimension of air gap measured parallel to shaft = 11 in. Calculate the average air-gap flux density over tooth pitch in maxwells per square inch. Ans. 47,200.
10. Given the following information: gross axial length of armature = 12 in.; radial dimension of air gap = 0.25 in.; radial dimension of equivalent air gap = 20 per cent greater than the actual air gap; tooth pitch = 1.25 in. Calculate the air-gap permeance over one tooth pitch. Ans. 127.
11. Given a flat-compound-wound d-c generator: total armature resistance = 0.02 ohm; kilowatt output = 15; terminal volts = 110; total brush drop = 2 volts; drop in series-field windings = 1.2 volts. Calculate the voltage developed in the armature at full load. Ans. 115.93 volts.
12. An overcompounded dynamo gives 108 volts at terminals on open circuit when driven at 800 rpm, and 112 volts under full-load conditions when the speed has dropped to 750 rpm. The full-load flux in the armature core is then 12 per cent greater than



on open circuit at the higher speed. Calculate the total series  $IR$  drop in the machine, including armature, brushes, and series-field windings. *Ans. 6 volts.*

13. Given a flat-compounded d-c generator: total armature resistance = 0.04 ohm; output = 20 kw; terminal volts = 222; total brush drop = 2 volts; series-field drop = 2 volts. Calculate the flux per pole entering armature at full load, given that the flux pole on open circuit is 800,000 maxwells and that the speed at full load is 5 per cent lower than on open circuit. *Ans. 870,000 maxwells.*

14. In a multipolar machine with simplex series (or wave) winding, a flux density of 6,000 gauss in the air gap produces 100 volts at terminals on open circuit. The resistance of all + (or all -) brush contacts is 0.005 ohm. The resistance of the series-field coils is 0.005 ohm. The resistance of each path through armature winding is 0.02 ohm. What increase in air-gap density is required to produce flat compounding, given that the line current is 200 amp? *Ans. 300 gauss.*

15. Given: length of the pole core = 10 in.; cross section of pole core = 80 sq in.; flux in pole core = 8,200,000 maxwells; permeability of the iron = 800. Calculate the ampere-turns necessary to overcome the reluctance of the pole core. *Ans. 402.*

16. Given: d-c generator; flux per pole in air gap = 755,000 maxwells; diameter of pole core = 3.5 in.; length of pole core =  $3\frac{1}{8}$  in.; leakage factor = 1.2; permeability = 486. Calculate (a) the density (in gauss) in pole core, (b) the ampere-turns needed to overcome the reluctance of the pole core. *Ans. (a) 14,580, (b) 189.2.*

17. Given: length per pole of flux path in frame (yoke ring) = 8 in.; cross section of frame =  $7\frac{1}{2}$  sq in.; permeability of iron in frame = 90; mmf drop, per pole, in frame = 2,000 amp-turns; leakage factor = 1.15. Calculate the flux per pole in air gap. *Ans. 936,000 maxwells.*

18. Given: flux density in armature core below slots = 80,000 lines per sq in.; net axial length of armature core = 10 in.; radial depth of core below slots = 3 in.; leakage factor = 1.25; cross section of yoke ring = 40 sq in. Calculate the flux density in yoke ring. *Ans. 75,000 lines per sq in.*

19. Given: shunt winding with 3,000 amp turns per pole; length of mean turn = 24 in.; terminal volts = 110; number of poles = 6; pressure drop across shunt rheostat = 18.2 per cent. Calculate the size of shunt wire in circular mils (temperature of winding assumed to be 60°C). *Ans. 4,800.*

20. Given: a 50-kw flat-compounded 220-volt 6-pole simplex-lap-wound generator in which the copper loss in the shunt-field winding is  $2\frac{1}{2}$  per cent of the output. Calculate (a) the line current at full load, (b) the current in the armature conductors. *Ans. (a) 227.2 amp, (b) 38.8 amp.*

21. A d-c generator is designed to give a terminal voltage of 220 at no load and 230 at full load. The total field ampere-turns per pole are 6,000 at no load and 8,200 at full load. Calculate the number of ampere-turns per pole in the series winding assuming the long shunt connection and the same armature speed at full load as at no load. *Ans. 1,925.*

22. Given: overcompounded d-c generator; open-circuit volts = 100; full-load volts = 110; full-load line current = 400 amp; shunt-field ampere-turns per pole on open circuit = 4,000; total field ampere-turns per pole at full load = 4,900; number of poles = 12; number of series-field turns per pole =  $1\frac{1}{2}$ ; resistance per turn of series winding = 0.0002 ohm. Calculate (a) the ampere-turns provided by the series winding at full load, (b) the resistance of the necessary diverter. *Ans. (a) 500, (b) 0.018 ohm.*

## CHAPTER 6

### LOSSES, VENTILATION, AND TEMPERATURE RISE

**51. Introductory.** The designer of electrical machinery aims to produce a machine which will be (1) efficient (have small losses in relation to output); (2) durable (capable of resisting wear and tear and deterioration of materials); and (3) cheap (able to compete in price with other designs which satisfy the needs of the user). The questions of heating and temperature rise have to be considered mainly in relation to item (1) because, although high temperatures will frequently lead to greater losses and decreased efficiency, it is principally their effect upon the insulation which has to be considered.

Power losses in rotating electrical machines may be divided into two general classifications, namely (1) those which are caused by the *rotation of the armature*, and (2) those which result from a *current flow* in the various parts of the dynamo. The former, consisting of bearing, wind, and brush friction, hysteresis and eddy currents, are designated *rotational losses*; the latter, consisting of the armature, the several fields, and the brush contact drop, are termed *copper losses*. An additional loss, generally indeterminate in nature, is caused by flux distortion and commutation. The table on page 138 lists these losses and indicates how they are affected and determined.

A great deal of attention has been given of recent years to obtaining increased output for a given weight of materials by improvements in ventilation and the heat-resisting qualities of insulating materials. An exhaustive discussion of heating problems is impossible in these pages, but in this chapter it is proposed to consider briefly: (1) how to calculate the losses in the iron; (2) how, by proper ventilation, to get rid of the heat due to both iron and copper losses and estimate the surface temperature rise; (3) how to predetermine approximately the "hottest spot" temperature when the surface temperature is known.

**52. Losses in Laminated Iron Cores.** The loss due to hysteresis in iron subjected to periodical reversals of flux may be expressed by the formula

$$\text{Watts per pound} = K_h B^{1.6} f$$

where  $K_h$  is the hysteresis constant which depends upon the magnetic



## DYNAMO LOSSES

Losses			Affected by	How determined
Rotational or stray power	Friction	Bearing	Speed changes	By test or calculation
		Windage		
		Brush		
	Armature core	Hysteresis	Speed and flux changes	
		Eddy current		
Copper		Armature winding	Load	$I_A^2 \times R_A$
		Series field		$I_A^2 \times R_{SE}$
		Interpole field		$I_A^2 \times R_I$
		Compensating field		$I_A^2 \times R_C$
		Shunt field		$I_f^2 \times R_f$
		Brush contact		$E_B \times I_A$
		Stray load		

qualities of the iron. The symbols  $B$  and  $f$  stand as before for the flux density and the frequency.

An approximate expression for the loss due to eddy currents in laminated iron is

$$\text{Watts per pound} = K_e(Bft)^2$$

where  $t$  is the thickness of the laminations, and  $K_e$  is a constant which is proportional to the electrical conductivity of the iron.

With the aid of such formulas, the hysteresis and eddy-current losses can be calculated separately and then added together to give the total watts lost per pound. This method will give good results in the case of transformers; but when the reversals of flux are due to a rotating magnetic field, as in dynamo-electric machinery, the losses do not follow the same laws as when the flux is simply alternating; and, moreover, there are many causes leading to losses in built-up armature cores which cannot easily be calculated. These additional losses include eddy currents due to burrs on the edges of stampings causing metallic contact between adjacent plates. There are also eddy currents produced in the armature stampings, due to the fact that the flux cannot everywhere be confined to a direction parallel to the plane of the laminations. Some flux enters the armature at the two ends and also the sides of the teeth through the spaces provided for ventilation. Since this flux enters the iron in a direction normal to the plane of the laminations, it is sometimes accountable

for quite appreciable losses. For these reasons, calculations of core losses should be based on the results of tests conducted with built-up armatures rotated in fields of known strength.

Figure 67 refers to a good quality of stampings and is to be used only in connection with the design of rotating machinery. The values read off Fig. 67 must be multiplied by the frequency in cycles per second to obtain the watts per pound. There are great variations of quality in armature stampings, and values obtained from Fig. 67 would not be

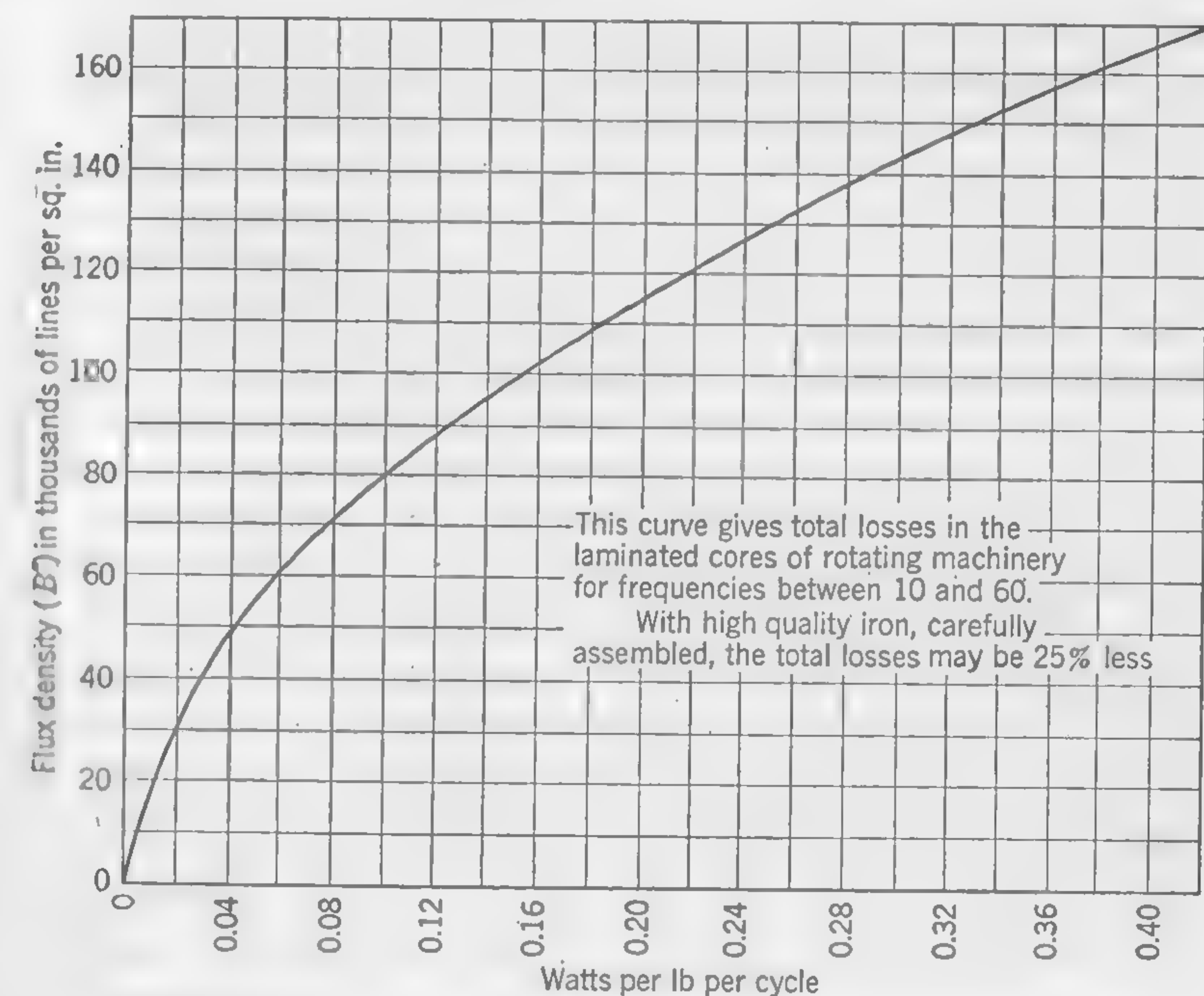


FIG. 67. Curve for calculating iron losses in dynamos and motors.

sufficiently reliable for the use of the commercial designer of any but small machines. By taking pains in assembling the stampings to avoid burrs and short circuits between adjacent plates, the total iron loss may be considerably reduced.

When calculating the watts lost in the armature core, it is necessary to consider the teeth independently of the section below the teeth. This is because the flux density in the teeth is not the same as that in the body of the armature.

The calculation of the watts lost in the core below the teeth is a simple matter, provided the assumption can be made that the flux density has the same value at all points of the section midway between poles. Although incorrect, this assumption is very commonly made; and, for the purpose of estimating the rise in temperature, the flux density may be



calculated by dividing half the total flux per pole by the net cross section of the armature core below the teeth.

In order to calculate the losses in the armature teeth, it is necessary to know exactly what is the flux density at all sections of the tooth. This is not readily calculated, because some of the flux from the pole pieces enters the armature through the sides of the teeth and the bottom of the slots. Again, in the case of armatures of small diameter having teeth of which the taper may be considerable, the change of section alters the flux density and the degree of saturation, so that it is almost impossible to determine accurately the average value of the tooth density for use in calculating the watts lost. A method of calculation which yields good results in practice is to estimate as nearly as possible the flux density in taper teeth at a distance from the narrow end equal to *one-third of the tooth length*, and then read the value of the watts per pound corresponding to this density off the iron-loss curve (Fig. 67). This is considered as a mean value of the watts per pound and is multiplied by the weight of iron in the teeth to obtain the total loss in the teeth. The tooth density required for the calculation of power losses is obviously the density which will occur when the tooth is in the zone of maximum air-gap density, and, owing to flux distortion caused by armature mmf, this is not definitely known for full-load conditions unless air-gap flux distribution curves similar to curve *C* of Fig. 60 are plotted. If the complete flux-distribution curves are not plotted, the probable maximum value of air-gap density must be estimated and the density in the teeth calculated therefrom.

A high tooth density is an advantage from the point of view of field distortion. It can easily be understood that a high density, by saturating the teeth, will have a tendency to resist the changes in the air-gap flux distribution brought about by the cross-magnetizing effects of the armature currents; but the losses in the teeth may become a considerable percentage of the total losses and their correct determination a matter of importance.

As a guide to the permissible losses in the armature punchings of d-c machines, the following figures will be useful. They are based on modern practice and should not be greatly exceeded if the efficiency and temperature rise are to be kept within reasonable limits.

Output of machine, kw	Core loss, expressed as percentage of output
10	2.8 to 3.2
20	2.5 to 3.0
50	2.0 to 2.4
100	1.5 to 1.8
500	1.3 to 1.5
1,000	1.2 to 1.4

**53. Illustrative Example. Calculation of Armature-core Losses.** Calculate the full-load iron loss in the armature designed in the Illustrative Example of Art. 18. The following information taken from the design sheet will be needed:

- Item 1. Frequency = 60 cps.
  - Item 10. Peripheral velocity of core = 6,900 fpm.
  - Item 14. Axial length of armature core (gross) = 10.25 in.
  - Item 26. Axial length of armature core (net) = 8.4 in.
  - Item 17. Pole arc = 7.37 in.
  - Item 22. Slot depth = 1.4 in.
  - Item 23. Tooth width: top = 0.522 in., root = 0.405 in., average = 0.463 in.
  - Item 34. Full-load flux per pole =  $4.27 \times 10^6$  maxwells.
  - Item 36. Internal diameter of core = 12.2 in.
  - Item 37. Weight of iron in core (without teeth) = 407 lb.
  - Item 38. Weight of iron in teeth = 115 lb.
- Losses in Core below Teeth. The flux density is

$$\frac{4,270,000}{2(8.4 \times 3.5)} = 72,700 \text{ lines per sq in.}$$

From Fig. 67, the watts per pound per cycle at this density is 0.085. The total loss in the core (excluding teeth) is, therefore,

$$0.085 \times 60 \times 407 = 2,075 \text{ watts}$$

*Losses in Teeth.* The width of tooth at a section one-third up from the bottom of the slot is  $0.405 + \frac{1}{3}(0.522 - 0.405) = 0.444$  in. The average air-gap flux density at full load under the pole face is

$$B_g'' = \frac{4,270,000}{10.25 \times 7.37} = 56,600 \text{ lines per sq in.}$$

Owing to armature distortion (see Fig. 60) the *maximum* air-gap flux density at full load in a machine without compensating windings is higher than the average value. This maximum density may be predetermined with a fair degree of accuracy by considering the combined effect of the field and armature mmf (curve *R'* of Fig. 52) across a path of which the permeance is that of the air gap and tooth combined, in the neighborhood of the pole tip; this, however, involves a considerable amount of calculation, not particularly justified. An assumption that yields reasonably good accuracy is that the maximum air-gap density at a point near the pole tip is 20 per cent greater than the average under the pole face. This,  $B_{g(\max)}'' = 56,600 \times 1.2 = 67,900$  lines per sq in., or  $67,900/6.45 = 10,500$  gauss. The corresponding tooth density read from Fig. 49 is  $B_t = 22,500$  gauss. This is the density where the tooth



thickness is  $t_m = 0.463$  in. (Fig. 68). For the cross section of tooth one-third of the distance from the bottom of the slot

$$B_t = 22,500 \times \frac{0.463}{0.444} = 23,400 \text{ gauss, or } 151,000 \text{ lines per sq in. (approx)}$$

Referring again to Fig. 67, the loss per pound per cycle at this density is

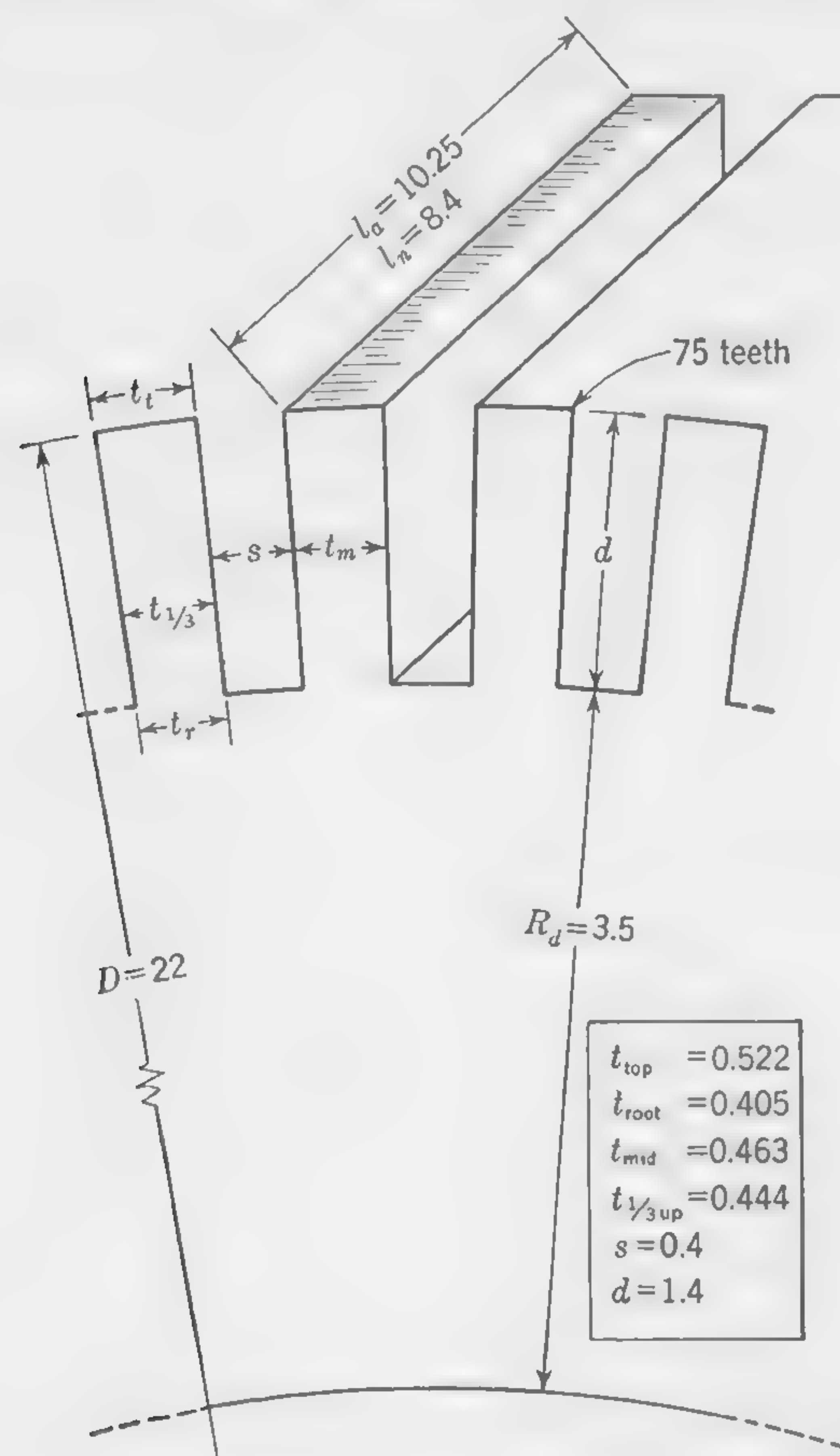


FIG. 68. Tooth and core dimensions for Illustrative Example, Art. 53:

0.33 watt. The total loss in the teeth is, therefore,

$$0.33 \times 60 \times 115 = 2,280 \text{ watts}$$

Combining the core and teeth losses, the total loss in the armature stampings is  $2,075 + 2,280 = 4,355$  watts.

**54. Friction Losses at Commutator Surface.** While considering the losses which have to be dissipated in the form of heat, it may be well to discuss the manner in which the commutator losses may be computed.

The  $I^2R$  loss due to brush-surface resistance is calculated like any other electrical resistance loss, but, in order to determine the losses due to the mechanical friction of brushes on commutator, the coefficient of friction must be known. This coefficient will depend not only upon the quality of the carbon brush but also on the condition of the commutator surface.

Let  $P$  = the pressure of the brush on the commutator, pounds per square inch of contact surface (usually from  $1\frac{1}{2}$  to 2 lb but as high as 3 to 5 lb in small machines such as automobile generators)

$c$  = the coefficient of friction

$A$  = the total area of brush-contact surface, square inches

$v_c$  = the peripheral velocity of the commutator, feet per minute

then the friction loss is  $cPAv_c$  ft-lb per min.

If  $D_c$  is the diameter of the commutator in inches, and  $N$  is the number of revolutions per minute,

$$v_c = \frac{\pi D_c N}{12}$$

The friction loss, expressed in watts, is

$$W_f = \frac{cPAND_c\pi \times 746}{12 \times 33,000} \quad (48)$$

The coefficient of friction with carbon brushes may be as low as 0.1 and as high as 0.45. The value of  $c$  for a good quality of carbon brush of medium hardness might lie between 0.18 and 0.28 but this coefficient is not reliable, as it depends upon many factors which cannot easily be accounted for.

The peripheral speed of commutator surface has a decided influence upon the coefficient of friction, which is higher for low speeds and lower for high speeds. Average values for  $c$  are given below.

**Hard Carbon and Electrolytic Graphite.** These materials are used with surface current densities from 35 to 50 amp per sq in. Use  $c = 0.23$  for surface speeds between 1,000 and 3,000 fpm.

**Soft Graphitic Carbon.** Used with current densities of 40 to 65 amp per sq in. Use  $c = 0.18$  for surface speeds of 2,000 to 5,000 fpm.

**Copper-graphite.** Used on low-voltage machines when the current is not so large as to necessitate copper brushes. The current density may be as high as 90 to 95 amp per sq in. Use  $c = 0.16$  for surface speeds of 1,000 to 3,000 fpm.

**55. Illustrative Example. Calculation of Commutator Losses.** Calculate the total losses at the surface of the commutator designed in the Illustrative Example of Art. 18. The following data, taken mainly from the design sheet, will be needed:

Speed  $N = 1,200$  rpm.



Full-load current (neglecting shunt-field current) = 1,200 amp.

Item 40. Diameter of commutator = 15 in.

Item 47. Current density at brush-contact surface = 40.4 amp per sq in.

Item 48. Contact area per brush set = 10 sq in.

Brush pressure (assumed) = 1.5 lb per sq in.

**Brush-resistance Losses.** Referring to Fig. 38, the potential drop across the plus (+) and minus (−) brushes, at about 40 amp per sq in., using soft graphitic carbon, is approximately 1.38 volts. To this figure it will be advisable to add about 10 per cent because the uneven distribution of current density over the brush-contact surface always increases the losses. Assuming a 1.5-volt drop, the brush-contact  $I^2R$  loss is  $1.5 \times 1,200 = 1,800$  watts.

**Brush-friction Losses.** The peripheral velocity of the commutator surface is  $v_c = (\pi \times 15 \times 1,200)/12 = 4,710$  fpm. Using soft graphitic carbon and assuming a coefficient of friction  $c = 0.18$ , the friction loss, by formula (48), page 143, is

$$W_c = \frac{0.18 \times 1.5 \times (6 \times 10) \times 4,710 \times 746}{33,000} = 1,730 \text{ watts}$$

Combining the contact-drop and friction losses, the total commutator losses are  $1,800 + 1,730 = 3,530$  watts.

**56. Temperature Rise of Commutators.** The effect of rotation on the temperature rise of armatures and commutators is not quite the same as on rotating coils. The calculations of armature heating are complicated by the effects of the cooling ducts, and the heat emissivity from the polished surface of a commutator is not the same as from coils of insulated wire or the broken surface of a slotted armature.

The watts that can be dissipated per square inch of commutator surface will depend on many factors which cannot be embodied in a formula. The peripheral velocity of the commutator surface will undoubtedly have an effect upon the cooling coefficient; but the influence of high speeds on the cooling of revolving cylindrical surfaces is not so great as might be expected. The design of the risers (*i.e.*, the copper connections between the commutator bars and the armature windings) has much to do with the effective cooling of small commutators; but this factor is of less importance when the axial length of the commutator is considerable.

Some designers consider only the outside cylindrical surface of the commutator when calculating temperature rise; but this leads to unsatisfactory results in the case of short commutators. In the formula here proposed, it is assumed that the risers add to the effective cooling surface up to a limiting radial distance of 2 in.; that is to say, if the risers are longer than 2 in., the area beyond this distance will be considered ineffective in

the matter of dissipating heat losses occurring at the commutator surface. The external surface of the carbon brush holders is helpful in keeping down the temperature and it will be taken into account by assuming that the cooling surface of the commutator is increased by an amount equal to  $2l_c b$  sq in.; where  $l_c$  is the total width of one set of brushes, measured parallel with the axis of the commutator, and  $b$  is the total number of brush sets.

The cooling area, as indicated in Fig. 69, will, therefore, consist of the cylindrical surface  $\pi D_c L_c$ ; the surface of the risers  $(\pi/4)(D_r^2 - D_c^2)$ ; the surface of the exposed ends (if any) of the copper bars, of value  $(\pi/4)(D_c^2 - D_e^2)$ ; and the allowance of  $2l_c b$  for the brush holders.

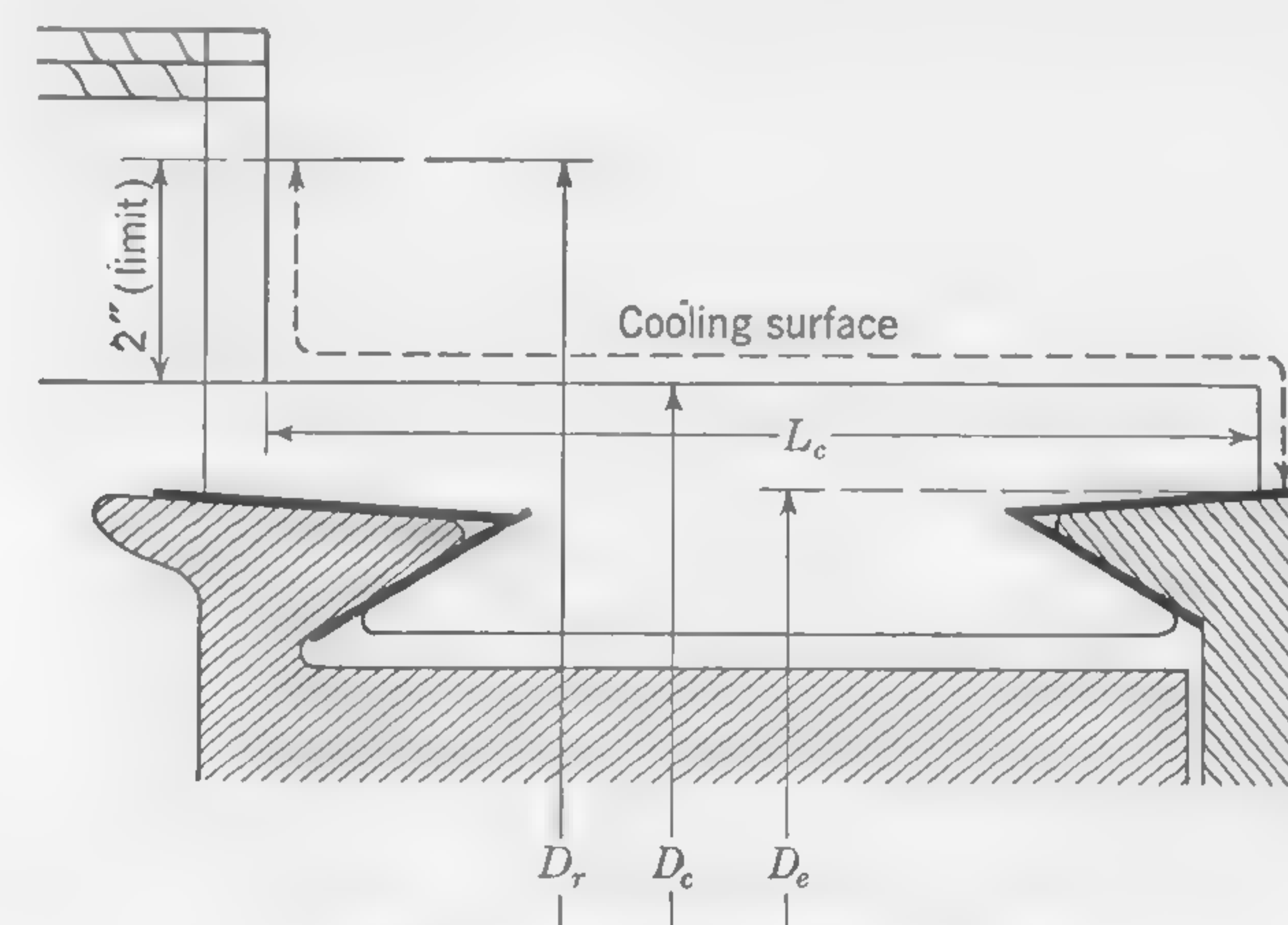


FIG. 69. Cooling surface of commutator.

The cooling coefficient proposed for calculating the temperature rise of the commutator is

$$c = \frac{W}{tS} = \left( 0.025 + \frac{v_c}{100,000} \right) \quad (49)$$

where  $W$  = the total watts to be dissipated

$S$  = the cooling area computed as above in square inches

$v_c$  = the peripheral velocity of the cylindrical surface of the commutator in feet per minute

$t$  = the temperature rise in degrees Centigrade

The allowable temperature rise, *i.e.*, the limiting value of  $t$  in formula (49), is usually from 55 to 65°C.

**57. Illustrative Example. Temperature Rise of Commutator.** Calculate the temperature rise of the commutator designed in the Illustrative Example of Art. 18. The following data, taken from the design sheet, together with estimated values as indicated, will be needed:



Item 40. Diameter of commutator = 15 in.

Item 52. Axial length of commutator = 14.5 in.

Total width of 8 brush holders per set, each one  $1\frac{1}{2}$  in. wide (measured parallel to shaft) = 12 in.

Number of brush sets = 6.

Radial depth of exposed ends of copper bars (assumed to be about  $\frac{2}{3}$  of radial depth of bar, item 46) = 1.5 in.

$D_e$  (see Fig. 69) =  $15 - 3 = 12$  in.

$D_r$  (see Fig. 69) =  $15 + 4 = 19$  in. In the formula given above it is assumed that the risers add up to a limiting distance of 2 in. (In this design the actual over-all riser diameter is about 22 in., the core diameter.)

Velocity of commutator =  $\pi \times 15 \times 1,200/12 = 4,710$  fpm.

Combining the three portions of the commutator surface, and the brush-holder surface, the total cooling surface is

$$S = \left[ (\pi \times 15 \times 14.5) + \frac{\pi}{4} (19)^2 - (15)^2 \right] + \frac{\pi}{4} [(15)^2 - (12)^2] + (2 \times 12 \times 6)$$

$$= 997 \text{ sq in., or (say) } 1,000 \text{ sq in.}$$

The cooling coefficient, by formula (49), is

$$c = \left( 0.025 + \frac{4,710}{100,000} \right)$$

$$= 0.0721 \text{ watt per sq in. per degree centigrade rise in temperature}$$

The total watts dissipated, as calculated in Illustrative Example of Art. 55, are 3,530 watts. Whence

$$t = \frac{3,530}{0.0721 \times 1000} = 49^\circ\text{C}$$

It should be pointed out that soft graphitic carbon was used in this design in order to keep the brush-contact and friction losses down to acceptable values; with hard carbon these losses would be extremely high and would cause the temperature rise to exceed the allowable  $65^\circ\text{C}$ .

**58. Temperature Rise of Armatures.\*** The rotation of the armature of an electric generator will produce a draft of air which may be sufficient to carry away the heat due to  $I^2R$  and hysteresis losses without the aid of a blower or fan. Self-ventilating machines are less common at the present time than they were a few years ago; but, by providing a sufficient number

\* For a broad but clear statement of the attitude towards the cooling of electrical machines together with much other valuable data, the reader is referred to D. B. Hoesason, *The Cooling of Electrical Machines*, *J. Inst. Elec. Engrs. (London)*, January, 1931. See also the Discussion on this paper in *J. Inst. Elec. Engrs. (London)*, June, 1931. Also: *ASA Bulletin C50*, 1943; *AIEE Standards* 1, June, 1947; *Trans. AIEE*, vol. 68, pp. 206-212, 1949.

of suitably proportioned air ducts in the body of the armature, machines of moderate size may still be built economically without forced ventilation. The manner in which radial air ducts are constructed in self-ventilating armature cores was described in Art. 16.

When forced ventilation is adopted, a fan or centrifugal blower may be provided at one end of the armature. This may assist the action of radial ventilating ducts, or it may draw air through axial ducts. When axial air ducts are provided, the radial ventilating spaces may be entirely omitted, and the gross length of the armature may, therefore, be reduced. The ventilation is through holes punched in the armature plates which, when assembled, will provide a number of longitudinal openings running parallel with the armature conductors. These openings may be circular in section and should preferably not be less than 1 in. in diameter, especially when the axial length of the armature is great, because they will otherwise offer too much resistance to the passage of the air and will also be likely to become stopped up with dirt.

One advantage of axial ducts—which, however, can only be used with forced ventilation—is that the heat from the body of the armature can travel more easily to the surface from which the heat is carried away than in the case of radial ducts. When the cooling is by radial ducts, the heat due to the hysteresis and eddy-current losses in the core must travel not only through the iron, which is a good heat conductor, but also through the insulating varnish between laminations, which is a poor conductor of heat. The thermal conductivity of the assembled armature stampings is from forty to fifty times greater in the direction parallel to the plane of the laminations than in a direction perpendicular to this plane. For this reason, radial vent ducts, to be effectual, must be provided at frequent intervals. The thickness of any one block of stampings between radial vent ducts rarely exceeds 3 in.

The coefficients for use in calculating temperature rise are based on data obtained from actual machines, and, owing to variations in design and proportions, they are, at the best, unreliable. When forced ventilation is adopted—whether with radial or axial vent ducts—it is possible to design the fans or blowers to pass a given number of cubic feet of air per second, and the quantity can readily be checked by tests on the finished machine.

A good practical rule for estimating the quantity of air necessary to carry away the heat when forced ventilation is used is based on the fact that a flow of 1 cu ft of air per minute will carry heat away at the rate of 0.55*t* watts,\* where *t* is the number of degrees Centigrade by which the

\* This is an approximate average value for this quantity which is not constant because the weight of a cubic foot of air depends upon temperature and barometric



temperature of the air has been increased while passing over the heated surfaces. Thus, if the difference in temperature between the outgoing and incoming air is not to exceed  $18^{\circ}\text{C}$ , it will be necessary to provide at least *100 cu ft of air per minute for each kilowatt lost in the machine.*

If the difference of temperature between the outgoing and ingoing air does not exceed  $20^{\circ}\text{C}$ , the temperature rise of the hot surfaces in contact with this air is not likely to exceed  $60^{\circ}\text{C}$ .

The power required to drive the ventilating fan is not very easily estimated, as it depends upon the velocity of the air through the passages. The velocity of the air through the ducts and over the cooling surfaces is usually from 3,000 to 5,000 fpm and should preferably not exceed 6,000 fpm; with higher velocities the friction loss might be excessive.

As a very rough guide to the power required to drive the ventilating fans, the following figures may be useful:

For 50-kw dynamo, 300 watts  
For 400-kw dynamo, 1,500 watts  
For 1,000-kw dynamo, 3,000 watts

In designing machines with forced ventilation, the size and configuration of the various air passages must be carefully studied with a view to preventing very high air velocities and consequent increase of loss by friction.

**59. Calculation of Temperature Rise of Self-ventilated Armatures with Radial Ducts.** Specifications for electrical machinery usually state that the temperature rise of any accessible part shall not exceed a given amount after a full-load run of about 6-hr duration. The permissible rise of temperature over that of the surrounding air will depend upon the room temperature. It usually lies between  $45$  and  $50^{\circ}\text{C}$ . The surface temperature is actually of little importance and is no indication of the efficiency of a machine, but, by keeping the surface temperature below a specified limit, the internal temperatures are not likely to be excessive, and the durability of the insulation—upon which the life of the machine is largely dependent—will thereby be ensured. The designer must, however, see that ventilating ducts or surfaces are provided at sufficiently frequent intervals to allow the heat to be carried away without requiring very great differences of temperature between the internal portions of the material where the losses occur and the surfaces in contact with the air.

Assuming that ventilating ducts are provided at sufficiently frequent intervals to ensure that the internal temperatures will not be greatly in excess of the surface temperatures, it is merely necessary to see that the cooling surface is sufficient to dissipate the watts lost in the iron and copper of the armature.

In calculating the losses and the cooling surfaces of the armature, we

shall assume that the current density in the conductors has been so chosen that the end connections will not be appreciably hotter than the armature as a whole. If this density does not exceed the value as calculated by formula (17) on page 36, it may be assumed that the temperature rise of the end connections will not exceed  $45^{\circ}\text{C}$ , and the watts to be dissipated by the cooling surfaces of the armature core will consist of:

1. The hysteresis and eddy-current losses in the teeth
2. The hysteresis and eddy-current losses in the core below the teeth
3. The  $I^2R$  losses in the "active" portion of the armature winding (*i.e.*, the portion which lies within the slots)

All these losses can be calculated in the manner previously explained. The copper loss to be taken into account is not the total  $I^2R$  loss in the armature winding but is this total loss multiplied by the ratio  $2l_a/(2l_a + l_e)$ , where  $l_a$  is the gross length of the armature core, and  $l_e$  is the length of the end connections of one coil, as calculated by formula (18) of Art. 16.

The various cooling surfaces may be considered separately, and the watts carried away from each surface computed independently. The total cooling surface may conveniently be divided into:

1. The outside cylindrical surface of the (rotating) armature
2. The inside cylindrical surface over which the air passes before entering the radial cooling ducts
3. The entire surface of the radial ventilating ducts, and the two ends of the armature core

The cooling effect of the external surface at the two ends of the armature core is generally similar to that of the radial ventilating spaces, and it is convenient to think of the two end rings as being equivalent to an extra duct. Thus, in Fig. 70, the number of ducts is shown as five, and the cooling surface of each duct (both sides) is  $(\pi/2)(D^2 - d^2)$ . The calculations would be made on the assumption that there are six ducts. If the number of radial vent ducts provided is  $n$ , the total cooling surface

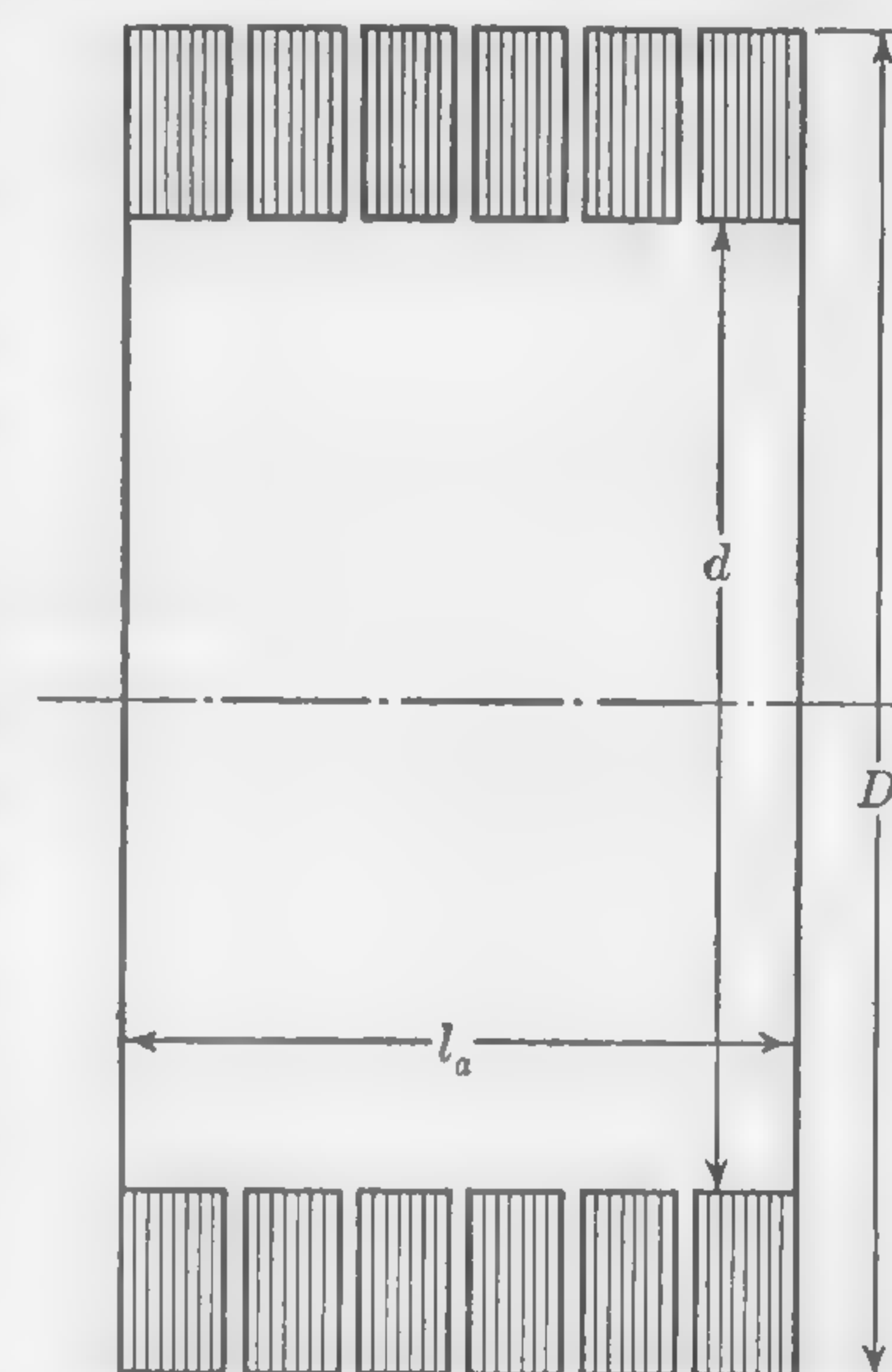


FIG. 70. Section through armature core.



of the ducts and the two ends of the armature will be

$$\frac{\pi}{2} (D^2 - d^2)(n + 1)$$

The outside cylindrical surface of the armature will be taken as  $\pi D l_a$ , where  $l_a$  is the gross length, no deduction being made for the space taken up by the vent ducts. The cooling surface of the end connections beyond the core is not taken into account.

The area of the inside cylindrical surface is  $\pi d l_a$ .

The watts dissipated by the cylindrical cooling surfaces may be calculated by the formula

$$W = tS \left( \frac{1,500 + v}{100,000} \right)$$

where  $W$  = the watts dissipated

$t$  = the surface temperature rise in degrees Centigrade

$S$  = the cooling area in square inches

$v$  = the peripheral velocity in feet per minute

This formula is generally similar to one originally proposed by Dr. Gisbert Kapp.

If  $c$  is a cooling coefficient, representing the watts that can be dissipated per square inch of surface for  $1^\circ\text{C}$  difference of temperature, we have

$$c = \frac{1,500 + v}{100,000} \quad (50)$$

and the temperature rise will be

$$t = \frac{W}{cS}$$

where  $W$  stands for the watts that have to be dissipated through the cooling surface  $S$ .

The watts dissipated by the air ducts and end surfaces may be calculated by the formula

$$W = tS \frac{v_d}{100,000}$$

where  $W$ ,  $t$ , and  $S$  have the same meaning as before, but  $v_d$  stands for the average velocity of the air through the ducts in feet per minute. This velocity is very difficult to estimate in the case of self-ventilating machines, but the constant in the formula has been selected to give good average results if  $v_d$  is taken as one-third of the peripheral velocity of the armature.

If  $c_d$  is a cooling coefficient representing the watts that can be dissipated per square inch of duct surface for each degree Centigrade rise of temperature, we have

$$c_d = \frac{v_d}{100,000} \quad (51)$$

and the temperature rise of the vent duct surfaces will be

$$t = \frac{W}{c_d S}$$

where  $W$  stands for the watts that have to be dissipated through the surface of area  $S$ .

**60. Illustrative Example. Temperature Rise of Dynamo Armature.** Calculate the surface temperature rise of the armature designed in the Illustrative Example of Art. 18. The following data, taken from previously calculated results, will be needed:

Item 9. Armature diameter = 22 in.

Item 10. Peripheral velocity of armature = 6,900 fpm.

Item 14. Armature length = 10.25 in.

Item 24. Number of ventilating ducts = 3.

Item 29. Length per turn of armature coil = 56 in.

Item 33.  $I^2R$  loss in armature winding = 3,320 watts.

Item 36. Internal diameter of core stampings = 12.2 in.

Total iron losses, as calculated in Illustrative Example of Art. 53, 4,355 watts.

*Losses to Be Dissipated.* These losses, as previously explained, consist of the total iron losses in the core and teeth, together with that portion of the copper loss which occurs in the conductors embedded in the slots. The latter are

$$\frac{2 \times 10.25}{56} \times 3,320 = 1,200 \text{ watts}$$

The total loss to be dissipated will, therefore, be

$$4,355 + 1,220 = 5,575 \text{ watts}$$

*Cooling Surfaces.* The outside cylindrical surface is

$$S_o = \pi \times 22 \times 10.25 = 708 \text{ sq in.}$$

The inside cylindrical surface is

$$S_i = \pi \times 12.2 \times 10.25 = 392 \text{ sq in.}$$

The area of both sides of three ventilating ducts and of the two ends of the armature is, approximately,

$$S_d = \frac{\pi}{4} [(22)^2 - (12.2)^2] \times 8 = 2,100 \text{ sq in.}$$

*Temperature Rise.* Since the peripheral velocity of the outside surface of the armature is 6,900 fpm, the inside surface of 12.2 in. in diameter is

$$v_i = \frac{12.2}{22} \times 6,900 = 3,830 \text{ fpm}$$



The cooling coefficients for the cylindrical surfaces are, therefore, by formula (50)

$$c_o = \frac{1,500 + 6,900}{100,000} = 0.084$$

and

$$c_i = \frac{1,500 + 3,830}{100,000} = 0.0533$$

The cooling coefficient for the ducts and ends will be, by formula (51)

$$c_d = \frac{6,900/3}{100,000} = 0.023$$

The watts that can be dissipated per degree rise in temperature are:

For the outside cylindrical surface	=	0.084 × 708	=	59.5
For the inside cylindrical surface	=	0.0533 × 392	=	20.9
For the ducts and end surfaces	=	0.023 × 2,100	=	48.3
Total			=	128.7

The calculated temperature rise is, therefore,

$$t = \frac{5,575}{128.7} = 43.3^{\circ}\text{C}$$

**61. Efficiency.** Although there is no direct connection between efficiency and temperature rise, the losses as calculated for determining temperature rise enter also in the efficiency calculations. The efficiency of an electric generator is the ratio of power output to power input, or

$$\text{Efficiency} = \frac{\text{output}}{\text{output} + \text{losses}} = 1 - \frac{\text{losses}}{\text{output} + \text{losses}}$$

In computing the total losses, an estimate has to be made of the power lost through windage and bearing friction. It is almost impossible to predetermine these quantities accurately. The loss due to air friction will depend upon the design of the armature and arrangement of poles and frame, apart from the actual surface velocity, while the bearing friction will depend upon the number and size of the bearings, the method of lubrication, the weight of the rotating parts, and the method of coupling to the prime mover. The factors to be taken into account are so numerous and so difficult to determine, that, in the case of new designs or departures from standard types, it is usual to group these losses together and make a reasonable allowance for them in the calculations of efficiency. The friction losses will increase with both the surface velocity and the volume; and, since the volume is measured by the output factor  $l_a D^2$  [refer to Art. 2 and formula (7)], tests upon machines of varying outputs and speeds indicate that the values given in the following table may be used with reasonable accuracy when these losses are to be estimated.

TABLE OF APPROXIMATE BEARING FRICTION AND WINDAGE LOSSES

Peripheral velocity, fpm	$l_a D^2$						
	300	500	750	1,300	2,500	4,500	7,000
2,000	100	125	150	200	250	300	400
3,000	150	200	250	350	450	600	750
4,000	250	300	450	550	750	1,000	1,300
5,000	350	400	650	900	1,350	1,700	2,100
6,000	450	500	850	1,300	1,900	2,500	3,100
7,000	550	600	1,100	1,750	2,800	3,500	4,400

In predetermining the efficiency, it is important that all the power losses in the machine be taken into account. These losses should include the losses in rheostats and diverters, which may be considered as part of the machine.

As a check on calculations, the efficiencies in the following table may be referred to. They represent fair averages of what may be expected in machines of modern design.

TABLE OF EFFICIENCIES OF MODERN DYNAMOS

Kw	Rpm	Efficiency, per cent			
		Full load	$\frac{3}{4}$ load	$\frac{1}{2}$ load	$\frac{1}{4}$ load
5	1,750	82.3	81.8	79.4	69.8
5	1,150	81.8	80.2	78.5	69.5
10	1,750	85.0	84.0	81.5	71.0
10	1,150	83.5	83.4	81.3	72.0
20	1,150	87.1	86.8	84.8	77.2
20	900	86.5	86.3	84.7	76.8
20	750	85.2	84.8	83.4	76.5
25	1,150	86.9	86.7	84.8	81.0
25	900	86.6	86.3	84.6	79.7
25	750	86.2	86.0	84.6	79.7
50	1,150	89.0	88.7	87.3	81.8
50	750	88.3	87.5	84.8	78.0
75	1,150	90.3	90.0	88.3	83.2
75	750	89.8	89.4	88.2	83.1
100	1,150	90.8	90.4	88.8	84.8
100	750	90.3	90.1	88.5	84.3
200	1,150	93.1	92.8	91.3	85.0
200	750	91.7	91.0	89.2	84.3
300	1,150	93.9	93.2	91.2	86.2
300	750	91 to 93			
500 and larger	750	93 to 95			



**62. Design of Continuous-current Motors.** The dynamo, being a reversible machine, may be used as a generator to convert mechanical into electrical energy or as a motor to convert electrical into mechanical energy. If the machine is to be used as a motor, the efficiency should first be estimated by referring to the figures in the preceding article. This efficiency, in the case of a motor, is the ratio output/input, whence

$$\text{Kilowatt input} = \frac{\text{horsepower} \times 746}{\text{efficiency} \times 1,000}$$

and the design may proceed exactly as if the machine were to be used as a generator to give this particular kilowatt output at the specified speed.

On account of the conditions under which they have to operate, dynamo machines when used as motors are more often totally enclosed than when used as generators. In the case of the larger units, forced ventilation would then be resorted to, but the smaller sizes may be self-cooling. The temperature rise is then largely equalized throughout the machine, and somewhat higher surface temperatures are allowable than in the case of open-type machines. A temperature rise of 55 to 60°C, by thermometer, is usually allowable inside the machine, but this means that the temperature rise of the enclosing case must be considerably less, say 30 or 35°C.

In the absence of data on the particular type of enclosed motor under consideration, a cooling coefficient *c* of 0.007 to 0.009 may be used. This figure denotes the number of watts that can be radiated per degree Centigrade rise of temperature from every square inch of the entire external surface of the enclosed motor.

**63. Illustrative Example. Efficiency of Generator.** Calculate the efficiencies of the 300-kw 230/250-volt 1,200-rpm generator designed in Art. 18 and Art. 50, for outputs ranging from 25 to 150 per cent of rated load. The following data, taken from previously calculated results, will be needed:

- Item 33, Art. 18.*  $I^2R$  loss in armature winding at full load = 3.32 kw.
- Item 22, Art. 50.* Shunt-field current at full load = 3.82 amp.
- Item 26, Art. 50.*  $I^2R$  loss in series-field winding at full load = 0.24 kw.
- From Art. 53.* Core losses = 4.355 kw.
- From Art. 55.* Brush  $I^2R$  loss at full load = 1.8 kw.
- From Art. 55.* Brush-friction losses = 1.73 kw.

In preparing the accompanying table, listing the various quantities required for these calculations, several assumptions were made. These are: (1) the machine is connected "long-shunt," which means that the armature, series field, and interpole field carry the total armature current; (2) the terminal emf rises linearly from 230 at no load to 250 at full load,

then rises to 252.5 and 255 at overloads of 125 and 150 per cent, respectively; (3) the commutating-field loss is estimated as 1.75 times the series-field loss at full load, because this field was not designed for the specifications given (in the actual machine design this loss would, of course, be known); (4) the iron loss is constant at all loads, although flux-density changes with load changes would affect this quantity somewhat; (5) the

EFFICIENCY CALCULATION TABLE FOR ILLUSTRATIVE EXAMPLE

	Per cent of rated kw output					
	25	50	75	100	125	150
Output, kw.....	75	150	225	300	375	450
Terminal voltage....	235	240	245	250	252.5	255
Amperes:						
Line (load).....	300	600	900	1,200	1,500	1,800
Shunt field.....	3.59	3.67	3.74	3.82	3.86	3.90
Armature.....	303.6	603.7	903.7	1203.8	1503.9	1803.9
Losses, kw:						
Armature $I^2R$ ....	0.211	0.832	1.805	3.220	5.180	7.470
Series field.....	0.015	0.060	0.135	0.240	0.375	0.540
Commutating field	0.026	0.105	0.236	0.420	0.657	0.946
Shunt field.....	0.843	0.880	0.917	0.950	0.975	0.995
Brush $I^2R$ .....	0.330	0.790	1.310	1.800	2.350	2.900
Brush friction....	1.730	1.730	1.730	1.730	1.730	1.730
Core.....	4.355	4.355	4.355	4.355	4.355	4.355
Friction and wind-						
age.....	3.700	3.700	3.700	3.700	3.700	3.700
Stray.....	0.750	1.500	2.250	3.000	3.750	4.500
Total losses....	11.960	13.952	16.438	19.415	23.072	27.136
Input, kw.....	86.960	163.952	241.438	319.415	398.072	282.136
Efficiency.....	0.8622	0.9148	0.9317	0.9392	0.9422	0.904

brush  $I^2R$  loss is determined by using Fig. 38 for the various current densities at the brushes, and adding about 10 per cent, as explained in Art. 55; (6) the stray-load loss was computed as 1 per cent of the various output values, as indicated in the table on page 138; (7) referring to the table on page 153, the bearing friction and windage losses were estimated as 3.7 kw, for a peripheral velocity of 6,900 fpm and an  $l_a D^2$  of 4,970 (see table, Art. 18).

**64. Intermittent Heating and Thermal Capacity.** So far, consideration has been given only to the surface temperature rise after a condition



of equilibrium has been established, that is to say, after a balance has been obtained between watts dissipated, area of cooling surface, and temperature rise, as expressed by formula (47) of Art. 47. The time required to bring a given machine or part of a machine to its final temperature will depend upon the mass of the material to be heated and its specific thermal capacity, and not merely upon the rate at which energy will have to be dissipated from the cooling surfaces after the final temperature has been attained. When a machine has been loaded only a short time, and before the final temperature has been reached, the total energy loss consists of (1) the energy stored in the material due to its increase in temperature, and (2) the energy which is dissipated from the cooling surfaces by radiation and ventilation. Space does not permit of an exhaustive discussion of the heating effects of intermittent service, more common in the operation of motors than generators, and, indeed, the designer is usually concerned with the problem of keeping the maximum possible temperature within safe limits when service is continuous, but the following heating problems will be briefly discussed:

*a.* The temperature rise of a coil which is alternately carrying full current and carrying no current during *short* periods of time extending over many hours, so that the cooling surface is the chief factor

*b.* The relation between time and temperature rise when apparatus is in use at only rare intervals of time, with long periods allowed for cooling, so that the factor of importance is the capacity for heat

*c.* The combined effect of thermal capacity and surface radiation on temperature rise

*Case a.* During a period of 1 min, the current is passing through the coil for a known short interval of time and is then switched off for another known period, so that, out of a total of 60 sec, the current flows through the coil during  $h$  sec only; the temperature rise can then be calculated by making the assumption that the watts to be dissipated are not  $W = I^2R$ , but  $W_h = (I^2R \times h)/60$ .

This method cannot be safely used if the "on" and "off" periods are long, but no general rule can be formulated in this connection because the size of the coil is an important factor.

*Example.* Assume a field that is designed to have a final temperature rise of  $38.3^\circ\text{C}$ , with an  $I^2R$  loss of 54 watts. Suppose this coil to be used so that it repeats the following cycle continuously for a considerable length of time:

Coil energized during 4 sec  
Coil off during 3 sec  
Coil energized during 6 sec  
Coil off during 3 sec

This is equivalent to dissipating continuously  $54 \times \frac{4+6}{4+3+6+3} = 33.7$  watts, and the approximate temperature rise would be  $38.3 \times (33.7/54) = 23.9^\circ\text{C}$ .

*Case b.* If used only at rare intervals of time, with long periods allowed for cooling down, a coil can be worked at very high current densities. The temperature rise is then determined solely by the specific heat of the copper and its total weight or volume.

The specific heat of a substance is the number of calories required to raise the temperature of 1 gram  $1^\circ\text{C}$ . The specific heat of water at ordinary temperatures being taken as unity, that of copper is about 0.093. One calorie will raise 1 g of water  $1^\circ\text{C}$ ; and, since 1 cal is equivalent to  $42 \times 10^6$  ergs (or dyne-centimeters), it follows that to raise 1 g of copper  $1^\circ\text{C}$  in 1 sec work must be done at the rate of  $0.093 \times 42 \times 10^6$  ergs per second. But 1 watt is the rate of doing work equal to  $10^7$  ergs per sec; and 1 lb = 453.6 g; this leads to the conclusion that the power to be expended to raise 1 lb of copper  $1^\circ\text{C}$  in 1 sec is

$$\frac{0.093 \times 42 \times 10^6 \times 453.6}{10^7} = 177 \text{ watts}$$

A cubic inch of copper weighs 0.32 lb, and  $177 \times 0.32$ , or (say) 57 watts, will, therefore, raise the temperature of 1 cu in. of copper  $1^\circ\text{C}$  in 1 sec—assuming no heat to be radiated or conducted away from the surface of the coil.

In this manner it is possible to calculate how long a coil for occasional use can be left in circuit without damage to insulation. A temperature rise of 50 to  $55^\circ\text{C}$  is generally permissible in making calculations on the heat-capacity basis.

Let  $V$  = cubic inches of copper in the coil

$W = I^2R$  loss in watts

$t$  = permissible temperature rise, degrees Centigrade

then, on the assumption that no heat is lost by radiation or surface cooling, we have:

$$\left. \begin{array}{l} \text{Time, in seconds, required to} \\ \text{raise coil temperature } t^\circ\text{C} \end{array} \right\} = \frac{57 \times V \times t}{W} \quad (52)$$

*Example.* A coil consisting of 70 lb of copper wire carries  $4\frac{1}{2}$  amp with 50 volts across terminals continuously without overheating. How long could this coil be safely left in circuit with 110 volts across terminals?

Assuming a limiting temperature rise of  $55^\circ\text{C}$ , the remaining quantities for use in formula (52) are  $V = 70/0.32 = 219$  cu in., or (say) 230 cu in.



to allow for heat absorption by the insulation, and  $W = 110 \times 4.5 \times 110/50 = 1,090$  watts; whence, by formula (52),

$$\text{Time} = \frac{57 \times 230 \times 55}{1,090} = 662 \text{ sec, or } 11 \text{ min } 2 \text{ sec}$$

*Case c.* Formula (52) may be used as the basis of a graphical construction illustrating how the quantity of material in a coil carrying an electric current influences the rate at which the temperature increases. In Fig. 71, measurements on the horizontal axis represent lapse of time, and

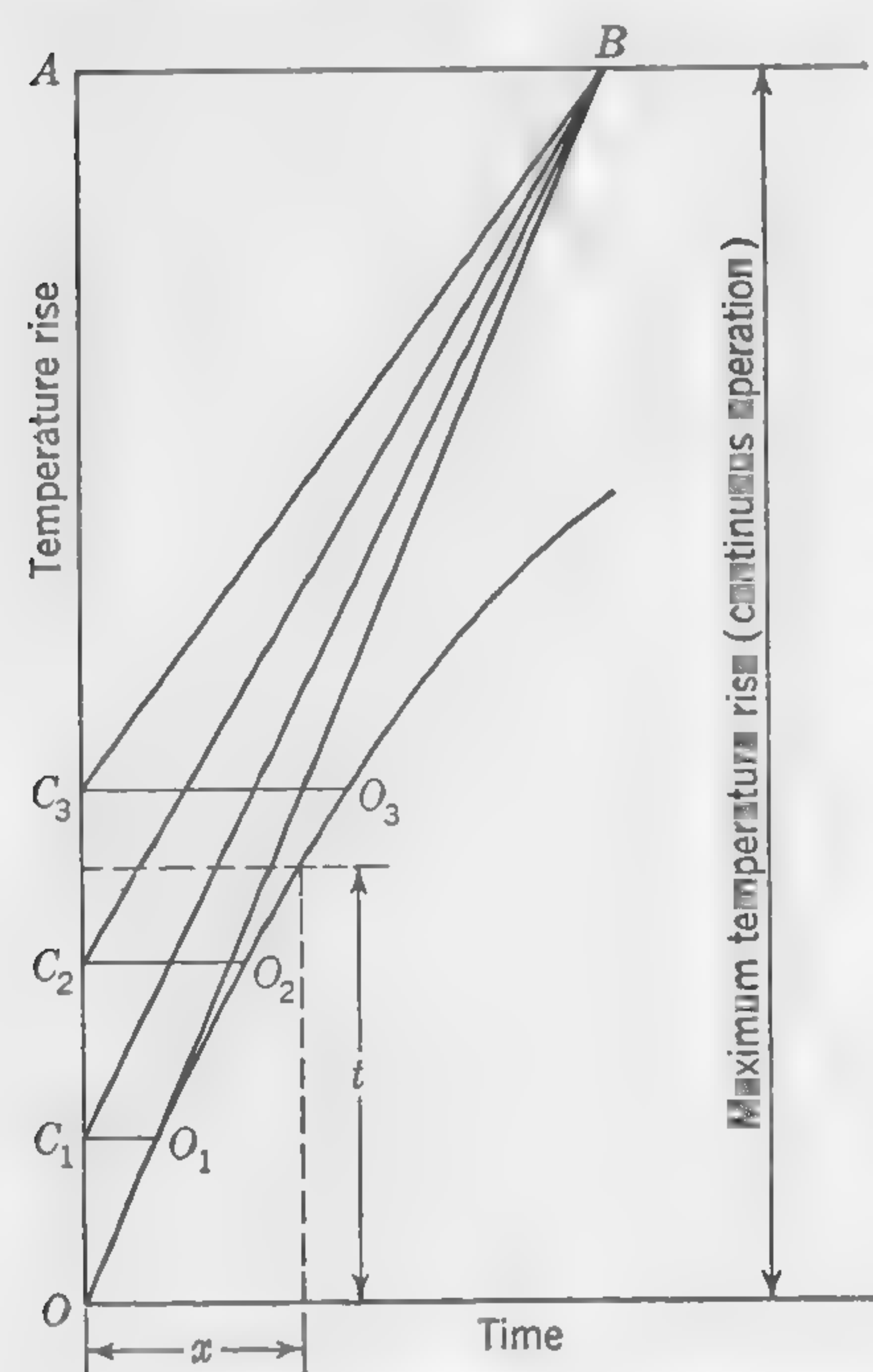


FIG. 71. Graphical illustration of relation between time and temperature rise.

rate of increase at *zero time* when there is no difference of temperature between coil surface and surrounding air to cause heat radiation. After a short interval of time, represented by the distance  $C_1O_1$ , the temperature rise of the coil is  $OC_1$  and, on the assumption of a constant cooling coefficient, the watts radiated will be  $W \times (OC_1/OA)$ , leaving  $W \times (C_1A/OA)$  to increase the temperature of the coil. The new rate of temperature increase will, therefore, be  $C_1A/AB$ , so that the "slope" of the time-temperature curve after the lapse of time  $C_1O_1$  is  $O_1O_2$  drawn parallel to  $C_1B$ . Similarly, after another short lapse of time, when the temperature rise is  $OC_2$ , the slope of the time-temperature curve has changed to  $O_2O_3$  drawn

measurements on the vertical axis represent temperature rise. Let the distance  $OA$  represent the ultimate temperature rise after a considerable lapse of time with constant  $I^2R$  losses ( $W$ ) in the coil. This is the temperature rise which will cause the total energy loss to be carried away by ventilation of the surfaces, none being available to produce a further increase of the coil temperature. Now calculate by formula (52) the *time* required to raise the temperature of the coil  $OA$  degrees, *assuming no radiation from the cooling surfaces*. Set this time off as  $AB$  on a line parallel to the time axis, and join  $OB$ . Obviously, the "slope" of  $OB$ , or the ratio  $\frac{OA}{AB}$ , being  $\frac{\text{temperature rise}}{\text{time}}$ , is the rate

of temperature increase, assuming no radiation. It is, therefore, the

Art. 65 LOSSES, VENTILATION, TEMPERATURE RISE 159

parallel to  $C_2B$ . And so on until, if the steps are small enough, the envelope of the well-known logarithmic time-temperature curve has been drawn.\* A convenient practical construction is explained in connection with the following problem.

**65. Illustrative Example. Relation between Time and Temperature Rise.** A coil is wound with 97 lb of copper wire. The voltage across the terminals is such that the  $I^2R$  loss is maintained at 500 watts, and the total area of the cooling surfaces is 520 sq in. Calculate the approximate time required to raise the temperature of the coil  $50^\circ\text{C}$  above that of the surrounding air.

Assuming a cooling coefficient  $c = 0.0056$  watt per sq in. per degree centigrade rise of temperature, the final temperature rise, by formula (47), would be

$$t = \frac{500}{0.0056 \times 520} = 172^{\circ}\text{C}$$

Although the weight of copper in the coil is given as 97 lb, this should be increased about 5 per cent to allow for the heat capacity of the cotton insulation. (For an impregnated coil this allowance should be considerably greater.) Then, by formula (52), the time required to raise the temperature of the coil 172°C, assuming no surface radiation, is

$$\frac{57 \times 172}{500} \times \frac{102}{0.32} = 6,250 \text{ sec, or (say) 1 hr 44 min}$$

The graphical solution of this problem is indicated in Fig. 72. Set off  $OA$  on the temperature scale equal to the final temperature rise of  $172^{\circ}$ , and  $AB$  (parallel to the time axis) of length representing 104 min. Join  $OB$ . To the right of  $B$ , on the prolongation of the line  $AB$ , set off equal divisions corresponding to the divisions on the horizontal axis (in this instance each division is equal to 10 min of time). From the point where the ordinate 1 (the 10-min ordinate) meets the line  $OB$ , draw the line 1-2

\* The equation to the time-temperature curve, of which the line  $OO_1O_2O_3$  (Fig. 71)

is an approximation, is  $t = OA (1 - e^{-\frac{x}{AB}})$ , where  $t$  = temperature rise,  $e = 2.7183$ , and  $x$  = the lapse of time, or distance from  $O$  on the time axis, expressed in the same units as the distance  $AB$ . It is easy to calculate  $t/OA$  in terms of  $x/AB$  and so determine points on the time-temperature curve as an alternative method to the graphical construction of Fig. 71. A few values are given in the following table:

$\frac{x}{AB}$	$\left(\frac{t}{OA}\right) \times 100$
0.5	39.3
1.0	63.2
2.0	86.5
3.0	95.0
4.0	98.2



which, if produced, would meet  $AB$  at 1. This gives the point 2 on the required curve. From the point 2 draw the line 2-3 which, if produced, would meet the line  $AB$  at 2; and so on. (This construction is indicated by the dotted lines 6-6 and 9-9.) If this diagram is compared with Fig. 71, it will be seen that, although there is a difference in the methods of construction, the resulting curves are identical. Reading from Fig. 72 it is found that about 35 min will be required to raise the temperature of the coil  $50^\circ\text{C}$ . This coil must, therefore, not be left in circuit longer than

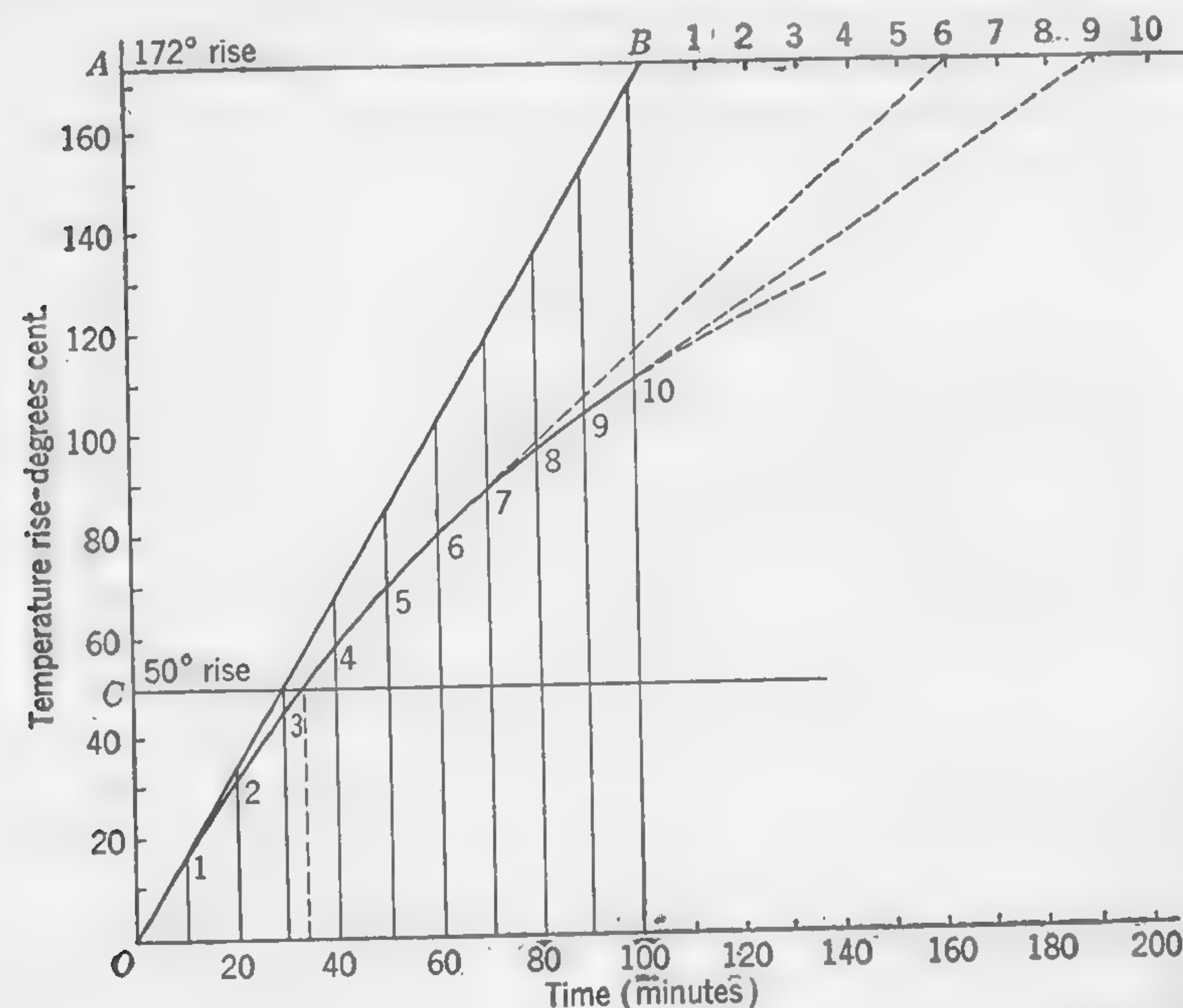


FIG. 72. Graphical solution of problem in Illustrative Example, Art. 65.

35 min continuously. It must then be allowed to cool off before it can be again excited for another period of 35 min.

**66. Internal Temperature—Thermal Conductivity.** If the cross section of a magnet coil is very large, or if the insulation around a conductor is very thick, there is a danger of exceptionally high internal temperatures, even when the temperature of the external surface is considerably below what might cause injury to the insulating material. Materials such as cotton, silk, and paper should preferably never be subjected to temperatures exceeding  $95^\circ\text{C}$ ; but when they are specially treated or impregnated with a view to increasing their heat-resisting qualities, or when they are immersed in oil (as in transformers), they will withstand without deterioration temperatures up to, but not exceeding,  $130^\circ\text{C}$ .

The problem about to be considered is how to determine the approxi-

mate difference of temperature between the outside surface of a coil, from which the heat is being carried away, and the *hottest spot* inside the windings, from which the heat must travel *through* the copper and insulation before it can be dissipated from the surface. The thing we are concerned with here is, therefore, the rate at which heat will be conducted through the body of the material, while in previous temperature calculations the important factor was the rate at which heat could be radiated or dissipated from the heated surface.

Figure 73 is supposed to represent a section through a very large flat plate, of thickness  $l$ , consisting of any homogeneous material. Assuming

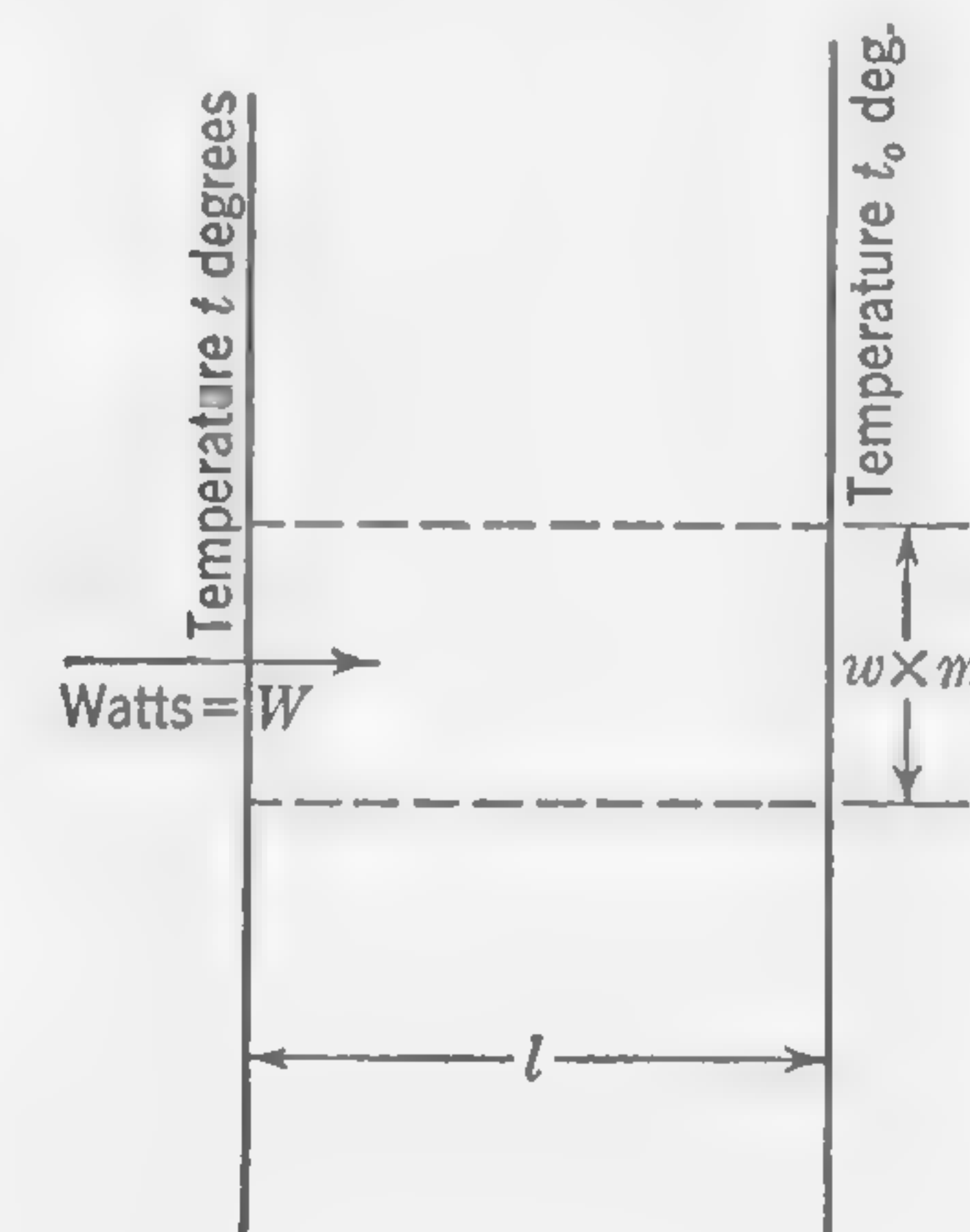


FIG. 73.

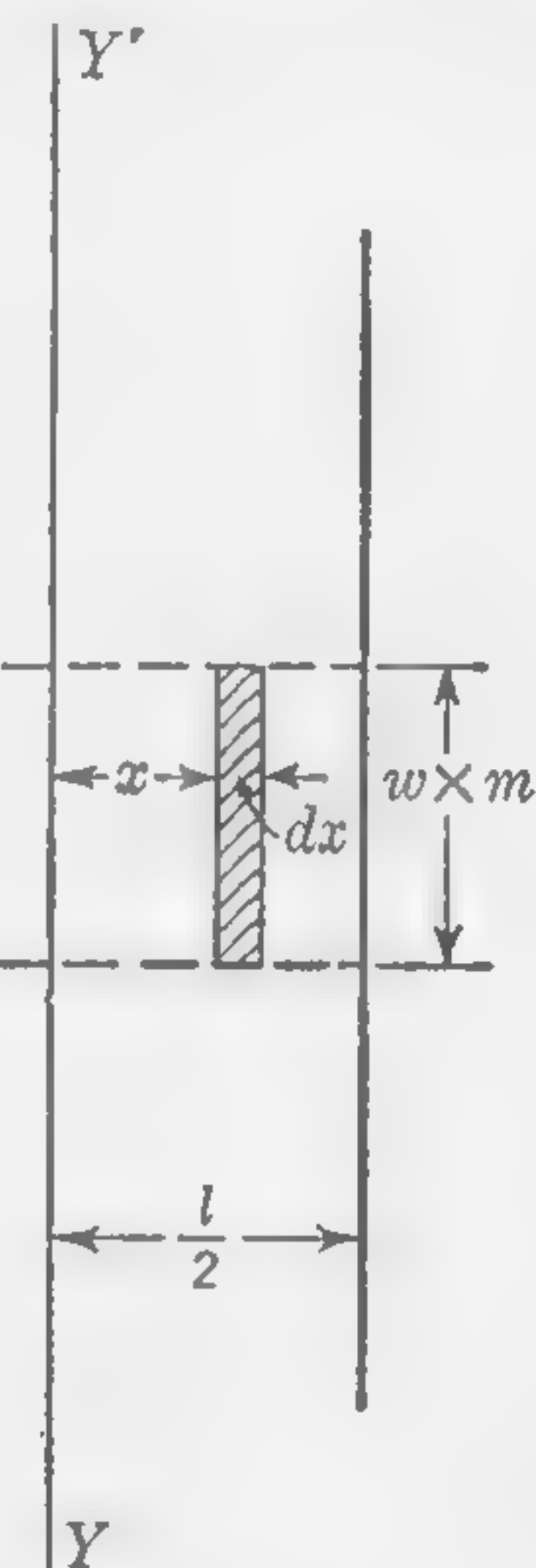


FIG. 74.

FIGS. 73 and 74. Illustrating thermal conductivity of plates.

that a temperature difference  $t_d = t - t_0$   $^\circ\text{C}$  is maintained between the two sides of the plate, the heat flow, expressed in watts, through a portion of the plate of area  $w \times m$  can be calculated as follows: the resistance offered by the material of the plate to the passage of heat may be expressed in *thermal ohms*, the thermal ohm being defined as the thermal resistance which causes a drop of  $1^\circ\text{C}$  per watt of heat flow. Thus, if  $R_h$  is the thermal resistance of the heat path under consideration,

$$R_h = \frac{t_d}{W} \quad (53)$$

which permits heat conduction problems to be solved by methods of calculation similar to those used in connection with the electric circuit.

Let  $k$  be the thermal conductivity of the material, expressed in watts per inch cube per degree centigrade difference of temperature between



opposite sides of the cube; then the thermal resistance of a heat path of length  $l$  in. and cross section  $A$  sq in. is  $R_h = (1/k)(l/A)$ . Substituting in formula (53) we get

$$t_d = W \frac{l}{kA} \quad (54)$$

The watts of heat flow crossing the area  $(w \times m)$ , indicated in Fig. 73, is

$$W = \left( \frac{w \times m}{l} k \right) t_d \quad (55)$$

A similar case is illustrated in Fig. 74, but the heat is now supposed to be generated in the mass of the material itself. The plate is still considered to be very large relative to its thickness, so that the heat flow from the center outward will be in the direction of the horizontal dotted lines. A uniformly distributed electric current of density  $\Delta$  amp per sq in. is supposed to be flowing to or from the observer, and the highest temperature will be on the plane  $YY'$  passing through the center of the plate. Assuming this plate to be of copper with a resistivity of  $0.84 \times 10^{-6}$  ohm per cu in. at a temperature of about  $80^\circ\text{C}$ , the watts lost in a section of area  $x \times w$  sq in. and length  $m$  in. will be

$$\begin{aligned} W_x &= (\Delta x w)^2 \times 0.84 \times 10^{-6} \times \frac{m}{xw} \\ &= 0.84 \times 10^{-6} \Delta^2 w m x \end{aligned} \quad (56)$$

By adapting formula (55) to this particular case, the difference of temperature between the two sides of the section of thickness  $dx$  (Fig. 74) is seen to be

$$dt_d = W_x \times \frac{dx}{wm \times k}$$

whence

$$\begin{aligned} t_d &= \frac{0.84 \times \Delta^2}{10^6 k} \int_0^{\frac{l}{2}} x dx \\ &= \frac{0.84 \Delta^2 l^2}{8 \times 10^6 k} \quad ^\circ\text{C} \end{aligned} \quad (57)$$

The value of  $k$  for copper is about 10 watts per cu in. per  $^\circ\text{C}$ .

The problem of applying these principles to practical calculations is complicated by the fact that the heat does not travel along parallel paths as in the preceding examples, and, further, that the thermal conductivity of the built-up coil depends upon the relative thickness of copper and insulating materials, a relation which is usually different across the layers of winding from what it is in a direction parallel to the layers.

Figure 75 represents the cross section of a coil with the layers of wire lying in the direction of the axis  $AA$ , the number of layers being such as to produce a total depth of winding equal to  $w$  measured in the direction of the axis  $BB$ . The whole of the outside surface of this coil is supposed to be maintained at a constant temperature by the surrounding oil or air. In other words, it is assumed that there is a constant difference of temperature of  $t_d$  degrees between the hottest spot (supposed to be at the center  $O$ ) and any point on the surface of the coil.

The heat generated in the mass of the material is thought of as traveling outward through the walls of successive imaginary spaces of rectangular section and length  $m$  (measured perpendicularly to the plane of the section

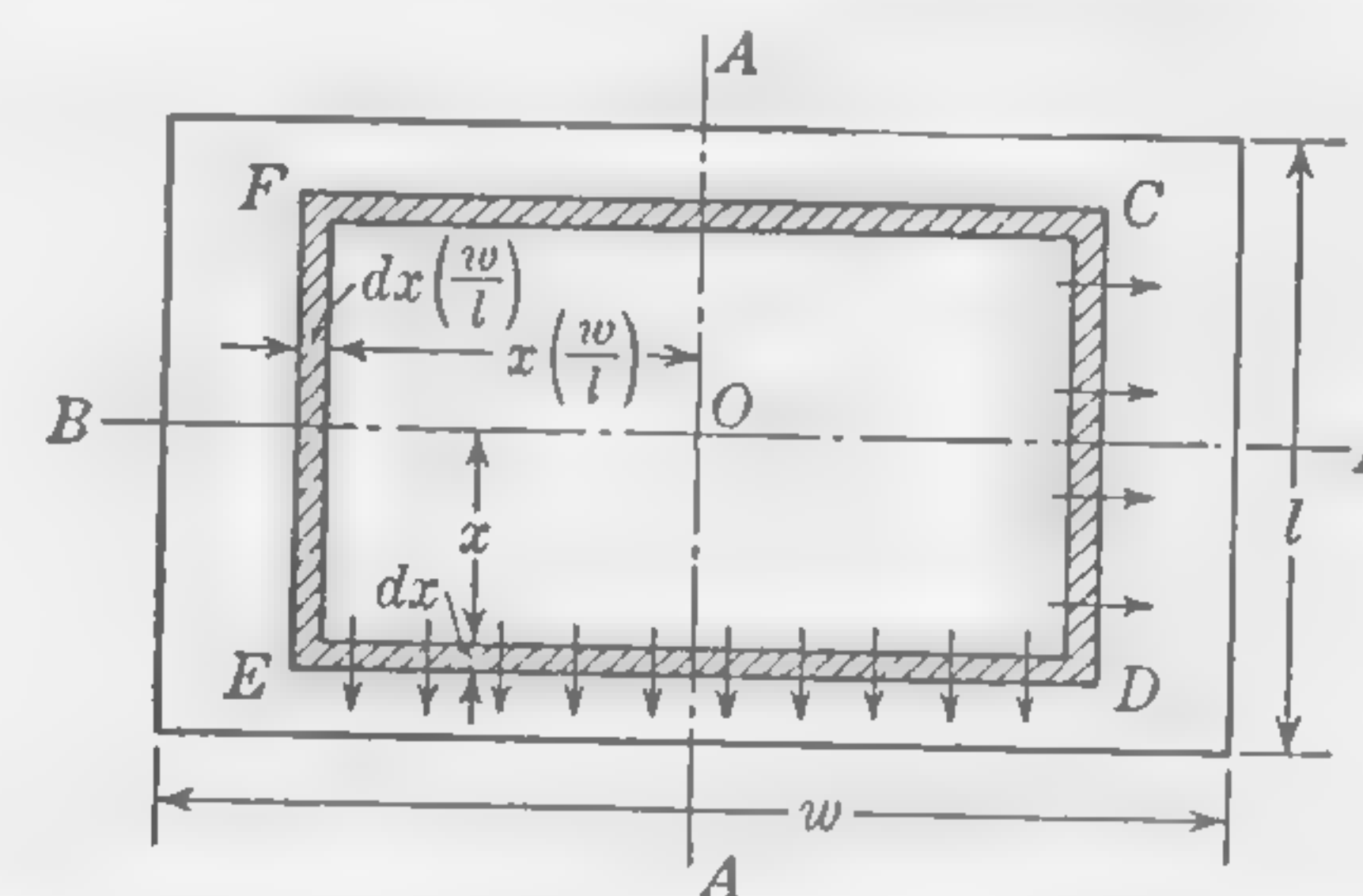


FIG. 75. Illustrating heat travel from center to outside of coil section.

shown in Fig. 75), as indicated in the figure, where  $CDEF$  is the boundary of one of these imaginary spaces, the walls of which have a thickness  $dx$  in the direction  $AA$ , and a thickness  $dx(w/l)$  in the direction  $BB$ .

According to the relation expressed by formula (53), we may say that the difference of temperature between the inner and outer boundaries of this imaginary wall is  $dt_d$  = the heat loss in watts, occurring within the space  $CDEF \times$  the thermal resistance of the boundary walls. Consider the heat flow through the boundary surface of which the area is  $CDEF \times m$ . Let  $k_a$  and  $k_b$  stand for the average thermal conductivities of the coil along the layers and across the layers of winding respectively (*i.e.*, in the directions of the axes  $AA$  and  $BB$ , respectively); then the thermal resistance of the imaginary boundary wall is

$$\frac{1}{k_a} \left[ \frac{dx}{(DE + FC)m} \right] + \frac{1}{k_b} \left[ \frac{dx(w/l)}{(CD + EF)m} \right]$$

and if  $W_x$  stands for the watts passing through this area, we may write

$$dt_d = W_x \times \frac{1}{\frac{(DE + FC)mk_a}{dx} + \frac{(CD + EF)mk_b}{dx(w/l)}}$$



which simplifies into

$$dt_d = W_x \frac{dx(w/l)}{4mx[k_a(w/l)^2 + k_b]} \quad (58)$$

If  $W$  = the total  $I^2R$  loss in the coil, we may write

$$W_x = W \left( \frac{2x}{l} \right)^2$$

Inserting this value in formula (58) and integrating between the limits  $x = 0$  and  $x = l/2$ , the final result is

$$t_d = \frac{W}{8m[k_a(w/l) + k_b(l/w)]} \quad ^\circ\text{C} \quad (59)$$

wherein  $m$  is the dimension perpendicular to the cross section  $w \times l$  (*i.e.*, the mean length per turn of a coil winding) expressed in *inches*.

**Thermal Conductivity of Insulation.** The coefficients  $k_a$  and  $k_b$  are the heat conductivities along the layers and across the layers of winding respectively. Their value depends not only upon the thermal conductivities of the copper and insulating material, but also upon the relative thickness of each along the paths of heat travel.

Let  $a$  = thickness of copper per inch total measured along the layers of the winding (*i.e.*, in the direction of the axis  $AA$  of Fig. 75), and let  $b$  = the thickness of copper per inch total measured across the layers of winding (*i.e.*, in the direction of the axis  $BB$ ); then if  $k_c$  and  $k_i$ , respec-

#### APPROXIMATE THERMAL CONDUCTIVITY OF MATERIALS

(Watts per in. cube per  $^\circ\text{C}$ )

Micanite.....	0.0045
Press board (varnished).....	0.005
Cotton insulation (untreated).....	0.002
Cotton insulation (impregnated or varnished).....	0.006
Assembled iron cores (along laminations).....	1.2
Assembled iron cores (across laminations).....	0.025

tively, stand for the thermal conductivity of copper and insulation (as shown in table above) it follows that

$$k_a = \frac{1}{(a/k_c) + [(1-a)/k_i]} \quad (60)$$

Usually it is permissible to omit the term  $a/k_c$ , which is very small compared with  $(1-a)/k_i$ ; then

$$\left. \begin{aligned} k_a &= \frac{k_i}{1-a} \text{ (approx)} \\ k_b &= \frac{k_i}{1-b} \text{ (approx)} \end{aligned} \right\} \quad (61)$$

If there is no extra insulation between the layers of wire, the heat conductivity is about the same in both directions, and, since  $a \times b$  = winding space factor,

$$k_a = k_b = \frac{k_i}{1 - \sqrt{sf}} \quad (62)$$

The value of  $k_i$  for solid insulating materials used in coil windings is usually between 0.0035 and 0.007 watt per cu in. per  $^\circ\text{C}$ ; but for coils wound with *round* cotton-covered wires, without extra insulation between layers, a good average value is  $k_i = 0.0025$ , whence, for *this particular condition*, the formula (62) becomes

$$k_a = k_b = \frac{1}{400(1 - \sqrt{sf})} \quad (62a)$$

#### 67. Illustrative Example. Temperature Rise in Armature Conductors.

The total thickness of the slot insulation around the conductors in the slotted armature of a d-c generator is 0.054 in. This consists of micanite and manila paper pressed tightly around the armature coil. The outside dimensions of the two insulated coil sides (in contact with the iron of the slot) are 0.5 in. wide by 1 in. deep. The total cross section of copper in the slot is 0.3 sq in. and the current density is 3,200 amp per sq in. Calculate the approximate difference of temperature between the copper conductors and the iron armature stampings, assuming that the amount of heat traveling longitudinally toward vent ducts or end connections is negligible.\*

By formula (53), p. 161, we have

$$t_d = R_h \times W$$

Before calculating the thermal resistance of the insulation we require a figure for the thermal resistivity or conductivity of the insulation. This conductivity will be lower than the figure obtained from tests on solid insulating materials, because, in the built-up insulation between copper and iron, there will usually be small air spaces which appreciably increase the heat resistivity. The thermal conductivity of the built-up insulation around armature conductors is usually  $k = 0.003$ , rising to  $k = 0.005$  watt per in. cube per  $^\circ\text{C}$  in high-voltage machines with thick,

\*The problem of local heating of armature conductors is not so simple as might be inferred from the solution here given, which neglects the longitudinal flow of heat from the center to the ends of the slots, the cooling effects of vent ducts, and the losses due to eddy currents in large solid conductors. For a more thorough study of this rather difficult problem, the reader is referred to C. J. Fehhheimer, Longitudinal and Transverse Heat Flow in Slot-wound Armature Coils, *Trans. AIEE*, vol. 40, p. 589, 1921, and W. V. Lyon, Heat Losses in the Conductors of Alternating Current Machines, *Trans. AIEE*, vol. 40, p. 1361, 1921. See also article by Fehhheimer, Heat Flow in Armature Coils, *Elec. World*, vol. 80, p. 1145, Nov. 25, 1922.



tightly compressed insulation. We shall take  $k = 0.003$  and calculate both  $R_h$  and  $W$  for a portion of the conductor 1 in. long. Thus

$$R_h = \frac{1}{0.003} \times \left( \frac{0.054}{3} \right)$$

where the heat path length  $l = 0.054$  in., and the area of the heat path per inch of longitudinal length of conductor is the perimeter of the two insulated coil sides, this being  $A = 3$  sq in.; and

$$\begin{aligned} W &= I^2 R = \Delta^2 \times \text{ohms per inch cube of copper} \times \text{volume of copper} \\ &\quad \text{in cubic inches} \\ &= (3,200)^2 \times (0.84 \times 10^{-6}) \times (1 \times 0.3) \end{aligned}$$

whence, by formula (53), we obtain the answer  $t_d = 15.5^\circ\text{C}$ .

### TEST PROBLEMS

1. Calculate the friction loss in watts at the surface of a commutator, given the following particulars: diameter of commutator = 14 in.; speed = 550 rpm; the machine is six-pole with six sets of brushes, each set consisting of four carbon brushes 1 by  $\frac{5}{8}$  in.; springs are adjusted to give a pressure of  $1\frac{1}{2}$  lb per sq in. between brush and commutator; coefficient of friction = 0.25. *Ans. 256 watts.*

2. The coils of the shunt-field winding of an eight-pole dynamo are connected in series across 492 volts. Each coil is 6 in. long and wound on a cylindrical core 5 in. in diameter to a total depth (or radial thickness) of 2 in. Calculate the current in the wire which will give a temperature rise of  $40^\circ\text{C}$ , given that the cooling coefficient is  $c = 0.0095$  watt per sq in. per degree centigrade rise of temperature. *Ans. 2.175 amp.*

3. Using the data and solution of Problem 2, calculate (a) the cross section of the wire in square inches, (b) the length of wire on one pole in feet, given that the winding space factor is 0.56 and that the temperature of the wire is  $60^\circ\text{C}$ , at which temperature the resistance of copper is 1 ohm per cir mil per in. *Ans. (a) 0.00203, (b) 6,070.*

4. When the two coils of a horseshoe type of lifting magnet are connected in series on 110 volts, the temperature rise is  $35^\circ\text{C}$ . Each coil is 8 in. long and  $2\frac{1}{4}$  in. thick, wound on a cylindrical core 4 in. in diameter. Calculate the current in the wire, given that the cooling coefficient is 0.006 watt per sq in. per degree centigrade rise of temperature. The operation of the magnet is intermittent, being "on" 10 sec and "off" 4 sec consecutively until the steady temperature of  $35^\circ\text{C}$  is attained. *Ans. 2.16 amp.*

5. Given that 55 watts are required to raise the temperature of 1 cu in. of copper  $1^\circ\text{C}$  in 1 sec, calculate the time during which the magnet coil of which particulars follow may be left in circuit with a limiting temperature rise of  $60^\circ\text{C}$ , neglecting the loss of energy by radiation from the surface of the coil, and the heat absorption by the insulating materials.

Number of turns of wire = 7,000

Mean length per turn = 24 in.

Cross section of wire = 0.001276 sq in.

Ohms per 1,000 ft = 7

Current density in wire = 4,000 amp per sq in.

*Ans. 4 min, 36 sec.*

6. The thermal conductivity of assembled armature stampings is forty times as great in the direction of laminations as in the direction perpendicular to the laminations. Calculate the watts that will be conducted across the laminations in a stack  $1\frac{1}{2}$  in. thick by 10 sq in. cross section with a difference of temperature of  $15^\circ\text{C}$ , given that a difference of temperature of  $5^\circ\text{C}$  will cause 32 watts to be conducted through a section 4 sq in. in area and  $\frac{1}{2}$  in. thick measured along the laminations. *Ans. 2 watts.*

7. A copper rod of  $\frac{3}{16}$ -in. diameter is insulated with a micanite tube which fits tightly around the rod and into the rotor slot of an induction motor. The walls of the insulating tube are  $\frac{1}{16}$  in. thick, and the thermal conductivity of the micanite is  $k = 0.003$  watt per in. cube per degree. Calculate the watts that will pass through the insulation from copper to iron per inch length of the conductor when the temperature of the latter is  $22^\circ\text{C}$  higher than that of the iron core. *Ans. 1.66 watts.*

8. The insulation between the field magnet coils of a dynamo and the pole core consists of a sheet of presspahn 0.08 in. thick, but, in addition to this, there is an air clearance between the presspahn and the iron pole core of 0.05 in. The thermal conductivity of presspahn is 0.004, and of the thin layer of still air 0.0013 watt per in. cube per degree centigrade difference of temperature. Calculate the watts per square inch that will pass from copper to pole core with a difference of temperature of  $40^\circ\text{C}$ . *Ans. 0.684 watt.*

9. Calculate the full-load efficiency of a d-c generator from the following data: terminal volts (flat-compounded) = 220; line current = 455 amp; sum of windage, friction, and iron losses = 2,500 watts; resistance of shunt field and rheostat = 25 ohms; resistance of armature (total) = 0.005 ohm; resistance of all series-field windings = 0.002 ohm; resistance of brush contacts (total) = 0.003 ohm. Assume the "long-shunt" connection. *Ans. 0.938.*



## CHAPTER 7

### ALTERNATING-CURRENT MACHINERY— SYNCHRONOUS GENERATORS

**68. Introductory.** The following chapters deal with a-c generators, motors, and transformers. They are written on the assumption that the student has an elementary knowledge of a-c theory and is familiar with the use of vectors to represent the magnitude and phase relations of quantities varying periodically according to the simple harmonic law. An effort will be made to keep the treatment as simple as possible without making unreasonable or unpractical assumptions which would seriously affect the accuracy of the calculated results. Sine-wave forms are assumed, and all higher harmonics are neglected unless special reference is made to irregular wave shapes. The reader is supposed to have a general knowledge of the elements already discussed, and problems in design will be worked out in less detail than in the earlier chapters.

The design of asynchronous generators will not be touched upon. This type of machine is essentially an induction motor reversed, the rotor, with its short-circuited windings, being mechanically driven.

Apart from the absence of commutator, the chief point of difference between an a-c and d-c generator is that the frequency of the former is specified, whereas, in the latter, this is a matter which concerns the manufacturer only. It follows that, for a given speed, the number of poles is determined by the frequency requirements, and this fact necessarily influences the design. The low frequencies of 25, 50, and 60 cycles are common to power and lighting services in the United States. Efforts are being made to establish 60 cycles as the standard for the country.

*Classification of Synchronous Generators.* It is well to distinguish between two classes of alternators:

1. Machines with salient poles, driven at moderate speeds by belt or direct-connected to reciprocating steam, gas, or oil engines, or to water turbines. The peripheral speed of the rotating part (usually the field magnets) will generally lie between the limits of 3,000 and 8,000 fpm.

2. Machines direct-coupled to high-speed steam turbines, in which the peripheral velocity usually exceeds 15,000 fpm and may attain

26,000 fpm. In these machines the field system is always the part that rotates; the number of poles is small, and, although salient poles are sometimes used on the lower speeds, the cylindrical field magnet with distributed windings is more common. The mechanical problems encountered in the design of these high-speed machines are relatively of greater importance than the electrical problems; but, since these are beyond the scope of this book, they will not be considered in detail.

*Number of Phases.* Whether a machine is to supply single-phase, two-phase, or three-phase currents does not appreciably affect the design procedure. The calculations on a machine for a large number of phases are not more difficult than when the number of phases is small. The theory of the single-phase generator is, in fact, somewhat less simple than that of the polyphase machine.

Whatever may be the type of machine, or number of poles, we may consider the armature conductors to be cut by the magnetic lines in the manner indicated in Fig. 76. Here we have a diagrammatic representation of single-phase, two-phase, and three-phase windings. In each case, the system of alternate pole pieces is supposed to move across the armature conductors in the direction indicated by the arrow. It will be noted that successive coils of each phase are connected to aid one another, each of the single-turn coils being similar in construction to those used in d-c armature windings.

At the instant represented by part (a), the maximum emf will be generated in the single-phase winding. In part (b), two distinct, similar windings *A* and *B* are so arranged that their effective emfs, although equal, will be out of phase in time by exactly the same number of electrical degrees as their 90° space displacement. Finally, the diagram of part (c) shows three distinct, similar windings *A*, *B*, and *C*, so arranged that their effective emfs, although equal, will be out of phase in time by exactly the same number of electrical degrees as their 120° space displacement.

*Usual Speeds of A-C Generators.* The student is referred to the table on page 16, which is applicable to a-c generators when they are driven by comparatively slow-speed engines. In hydroelectric work the generator is usually direct-coupled to the waterwheel, the speed of which will be high in the case of impulse wheels working under a high head. As an example, a Pelton waterwheel, to develop 1,500 hp under a head of 1,000 ft, would have a wheel about 5 ft in diameter, running at 500 rpm. This would be suitable for direct coupling to a 6-pole 25-cycle generator.

In the case of steam turbines—with a blade velocity of about 5½ miles per min—the speeds are always very high. Speeds from 1,200 to 3,600 rpm are usual.



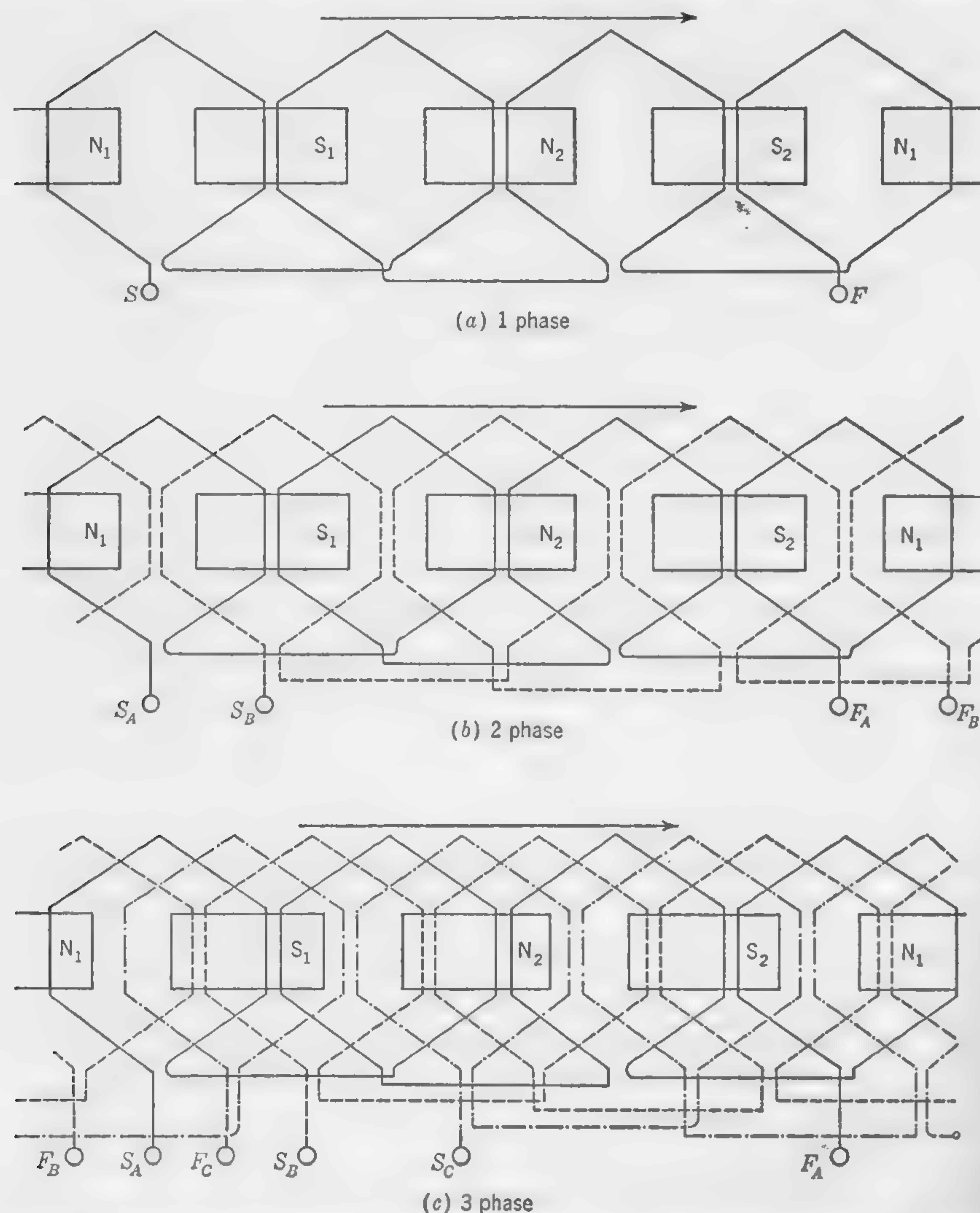


FIG. 76. Simple sketches illustrating single-, two-, and three-phase windings. (Single-turn coils are shown for convenience.)

### 69. Electromotive Force Developed in Windings.

Let  $\Phi$  = flux per pole in maxwells

$N$  = revolutions per minute

$p$  = number of poles

The flux cut *per revolution* is then  $\Phi \times p$  and the flux cut *per second* is  $\Phi p(N/60)$ . The average value of the emf developed in each armature

conductor must, therefore, be

$$E_c (\text{mean}) = \frac{\Phi p N}{60 \times 10^8} \quad \text{volts}$$

If the space distribution of the flux density over the pole pitch follows the sine law, the effective value of the emf is 1.11 times the mean value.

In other words, the *form factor*, or ratio  $\frac{\text{rms value}}{\text{mean value}}$ , is  $\frac{\pi}{2\sqrt{2}}$ , or 1.11, in the case of a sine wave.

*Concentrated and Distributed Windings.* If each coil side may be thought of as occupying a very small width on the armature periphery, and if the coil sides of each phase winding are spaced exactly one pole pitch apart, the arrangement would constitute what is usually referred to as a concentrated winding. With a winding of this kind, all conductors in series in one phase would always be similarly situated relatively to the center lines of the poles, and the curve of generated emf would necessarily be of the same shape as the curve of flux distribution over the armature surface. In practice, a winding with only one slot per pole per phase would be thought of as a concentrated winding. When there are two or more slots per pole per phase, the winding is said to be distributed; and, since the conductors of any one phase cover an appreciable space on the armature periphery, all the wires that are connected in series will not be moving in a field of the same density at the same instant of time. Except in the case of a sine-wave flux distribution, the form factor may depend largely upon whether the winding is concentrated or distributed. The wave shape of the developed voltage can always be determined when the flux distribution is known; but, in the preliminary stages of a design, it is usual to assume that the pole shoes are so shaped as to give a sinusoidal distribution of flux over the armature surface. The calculation of a correcting factor for distributed windings is then very simple. Thus, if there are two slots per pole per phase in a three-phase machine, there will be six slots per pole pitch, the angular distance between them being  $180^\circ/6 = 30^\circ$  electrical degrees. It is, therefore, merely necessary to add together, vectorially, two quantities having a phase displacement of  $30^\circ$ , each representing the emf developed in a single conductor. The result, divided by 2, will be the average voltage per conductor of the distributed winding. As an example, with three slots per pole per phase, the graphic construction would be as indicated in Fig. 77, where length  $AB = \text{length } BC = \text{length } CD$ , and what may be called the *distribution factor* is  $k = AD/3AB$ . The value of this distribution factor is, therefore, always either equal to, or less than, unity.

If  $Z$  is the total number of inductors in series *per phase*, the final



formula for the developed voltage is

$$E \text{ (per phase)} = \frac{kZ\Phi pN}{60 \times 10^8} \times \text{form factor} \quad (63)$$

On the sine-wave assumption, the form factor is 1.11, and the formula may, if preferred, be used in the form

$$E \text{ (per phase)} = \frac{2.22kf\Phi Z}{10^8} \text{ volts (on sine-wave assumption)} \quad (64)$$

Formula (65) may be used to determine the value of the distribution factor at fundamental frequency for any arrangement of slots and

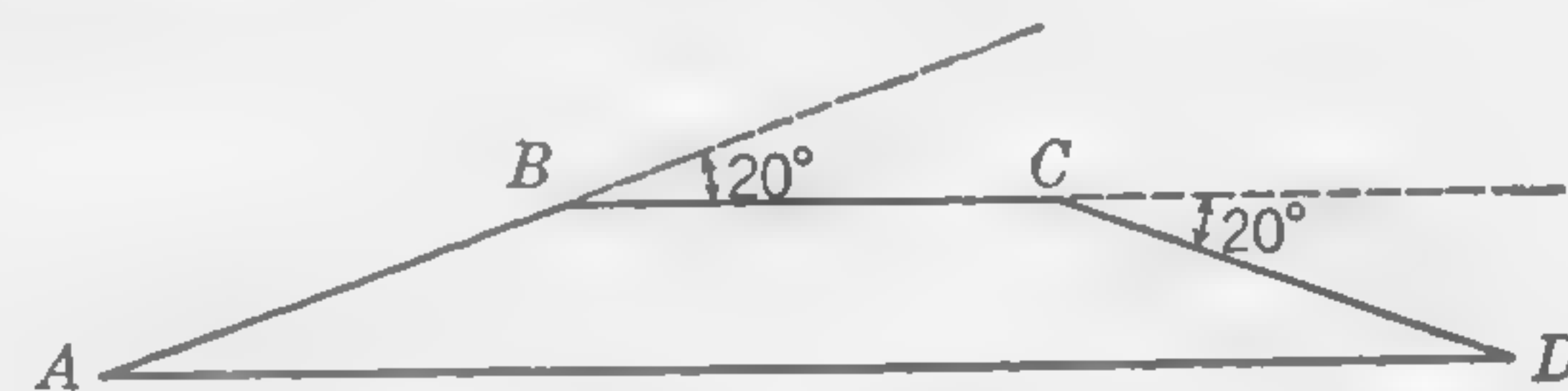


FIG. 77. Vector construction to determine distribution factor.

windings. If  $n_s$  is the number of slots per pole per phase, and  $\beta$  represents the number of electrical degrees between adjacent slots, then

$$k = \frac{\sin (n_s \beta / 2)}{n_s \sin (\beta / 2)} \quad (65)$$

With full-pitch, three-phase windings the distribution factor will have values shown in the following table.

DISTRIBUTION FACTORS FOR THREE-PHASE ALTERNATORS

Slots per pole	$n_s$	$\beta^\circ$	$k$
3	1	60	1.000
6	2	30	0.966
9	3	20	0.960
12	4	15	0.958
15	5	12	0.956
18	6	10	0.955

To determine the pitch factor at fundamental frequency, formula (66) may be used. Representing the *coil span*, in electrical degrees, by  $\gamma$ , then

$$k' = \sin \frac{\gamma}{Z} \quad (66)$$

The following table lists pitch factors for three-phase alternators having 3 to 15 slots per pole and coil spans  $\gamma$  of 180 to 120 electrical degrees.

PITCH FACTORS FOR THREE-PHASE ALTERNATORS

Slots per pole	Coil span $\gamma^\circ$										
	180°	168°	165°	160°	156°	150°	144°	140°	135°	132°	120°
3	1.0										0.866
6	1.0					0.966					0.866
9	1.0			0.985				0.940			0.866
12	1.0		0.991			0.966			0.924		0.866
15	1.0	0.995			0.978		0.951			0.914	0.866

The chief advantage of chorded windings, *i.e.*, fractional-pitch windings, is in machines of short axial length as compared with the pole pitch, because the end connections constitute a large percentage of the total length per turn. A coil span of 120 electrical degrees, for example, would be economical if the axial length of the armature core were no more than one-half to three-quarters of the pole pitch.

Formula (64), which was derived for a distributed, *full-pitch winding* ( $k = 1$ ), may now be modified to include *fractional-pitch* windings as well. Representing  $d$  as the winding factor, *i.e.*, the product of the distribution factor  $k$  and the pitch factor  $k'$  ( $d = k \times k'$ ), the general voltage equation becomes

$$E \text{ (per phase)} = 2.22 df\Phi Z \times 10^{-8} \text{ volts} \quad (64a)$$

*Star and Mesh Connections.* Each phase winding may be thought of as distinct from the other phase windings. It consists of starting and finishing ends between which all the coils of that particular phase are connected together to produce the required total emf per phase. The three phase windings of a three-phase generator are then joined together to form either the *mesh* ( $\Delta$ ) connection, or the *star* (Y) connection.

Figure 78 is a diagram of connections referring to a  $\Delta$ -connected three-phase generator, and Fig. 79 is the corresponding vector diagram, showing how the current in the external circuit may be expressed in terms of the armature current. The current leaving the terminal A (Fig. 78) is  $I_1 - I_2$ , and, since there will be a difference of 120 electrical degrees between the currents  $I_1$  and  $I_2$ , the vector construction of Fig. 79 gives  $OI$  as the line current. Its value is  $I = 2I_a \cos 30^\circ$ , or  $\sqrt{3} I_a$ , where  $I_a$  is the current in the armature conductors. The assumptions here made are that the load is balanced and that the current variations follow the simple harmonic law. It is well to bear in mind that vectors and



vector calculations can be used only when the variable quantities follow the sine law; when used in connection with irregular wave shapes, they must be supposed to represent an "equivalent" sine function, because under no other condition can the phase angle have any definite meaning.

If the starting ends of all the phase windings of a polyphase generator are connected to a common junction, or *neutral point*, the armature windings are said to be star-connected. In the three-phase machine this

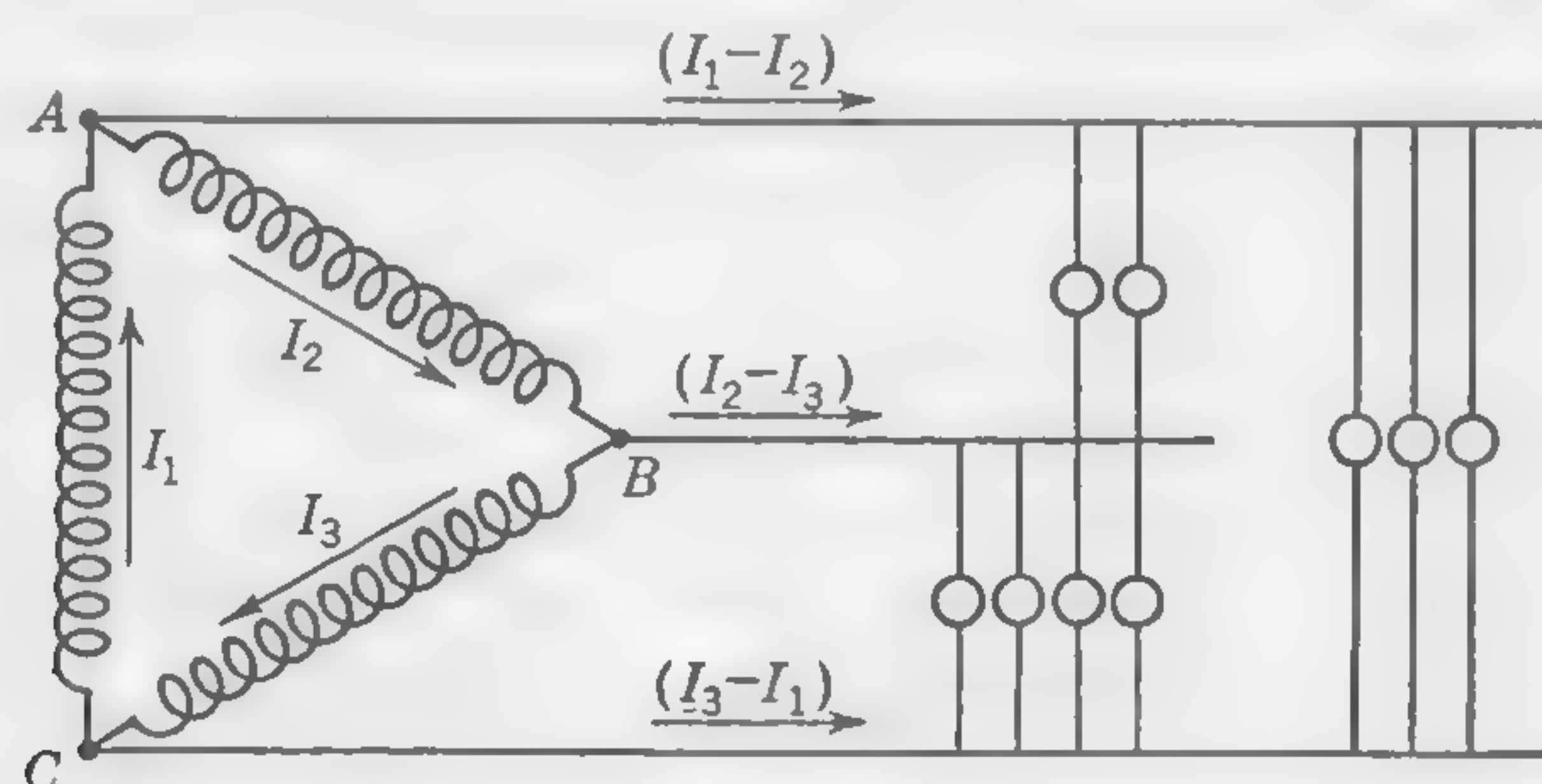


FIG. 78. Diagram of connections for  $\Delta$ -connected three-phase generator.

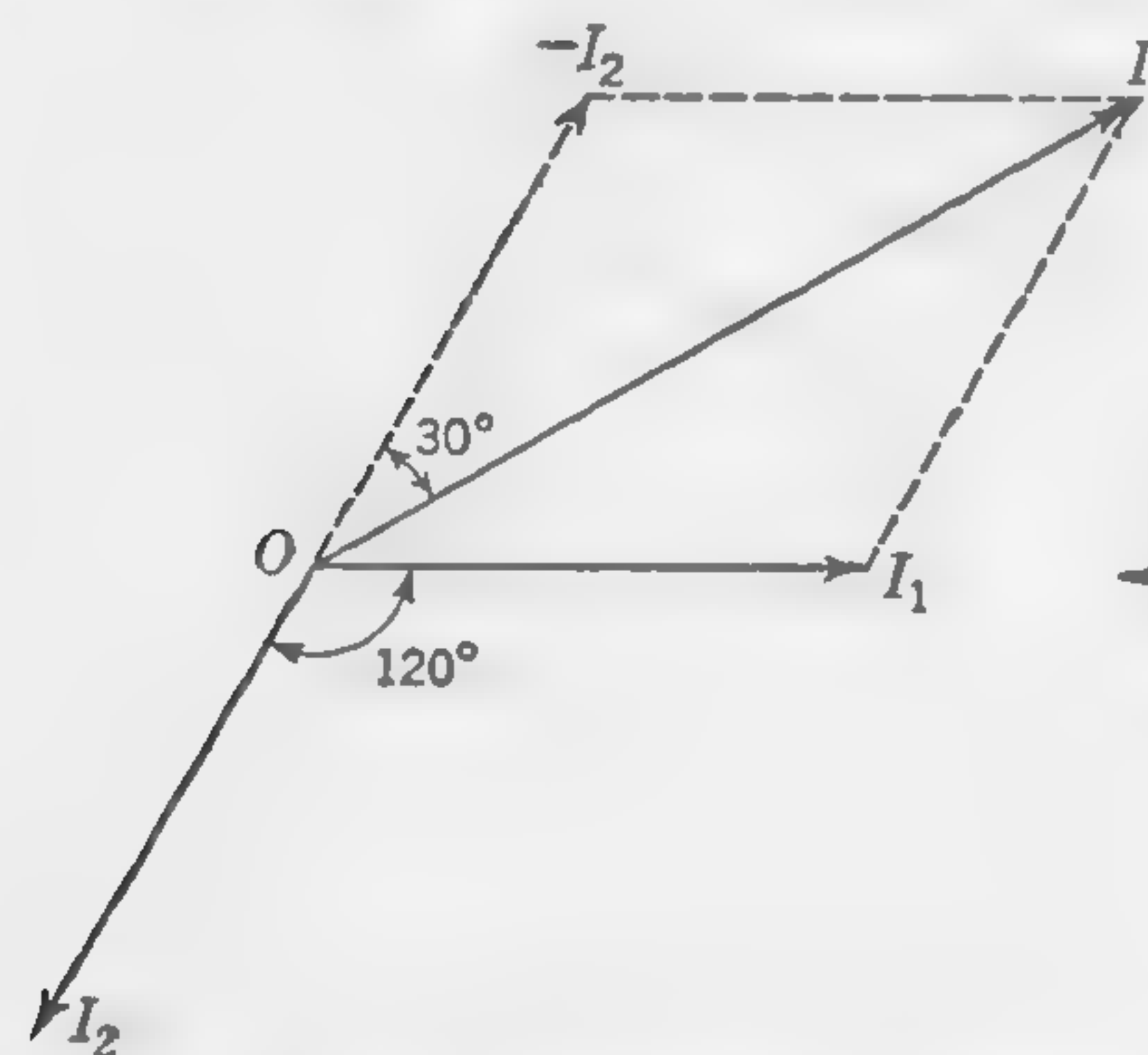


FIG. 79. Vector diagram of current relations in  $\Delta$ -connected three-phase generator.

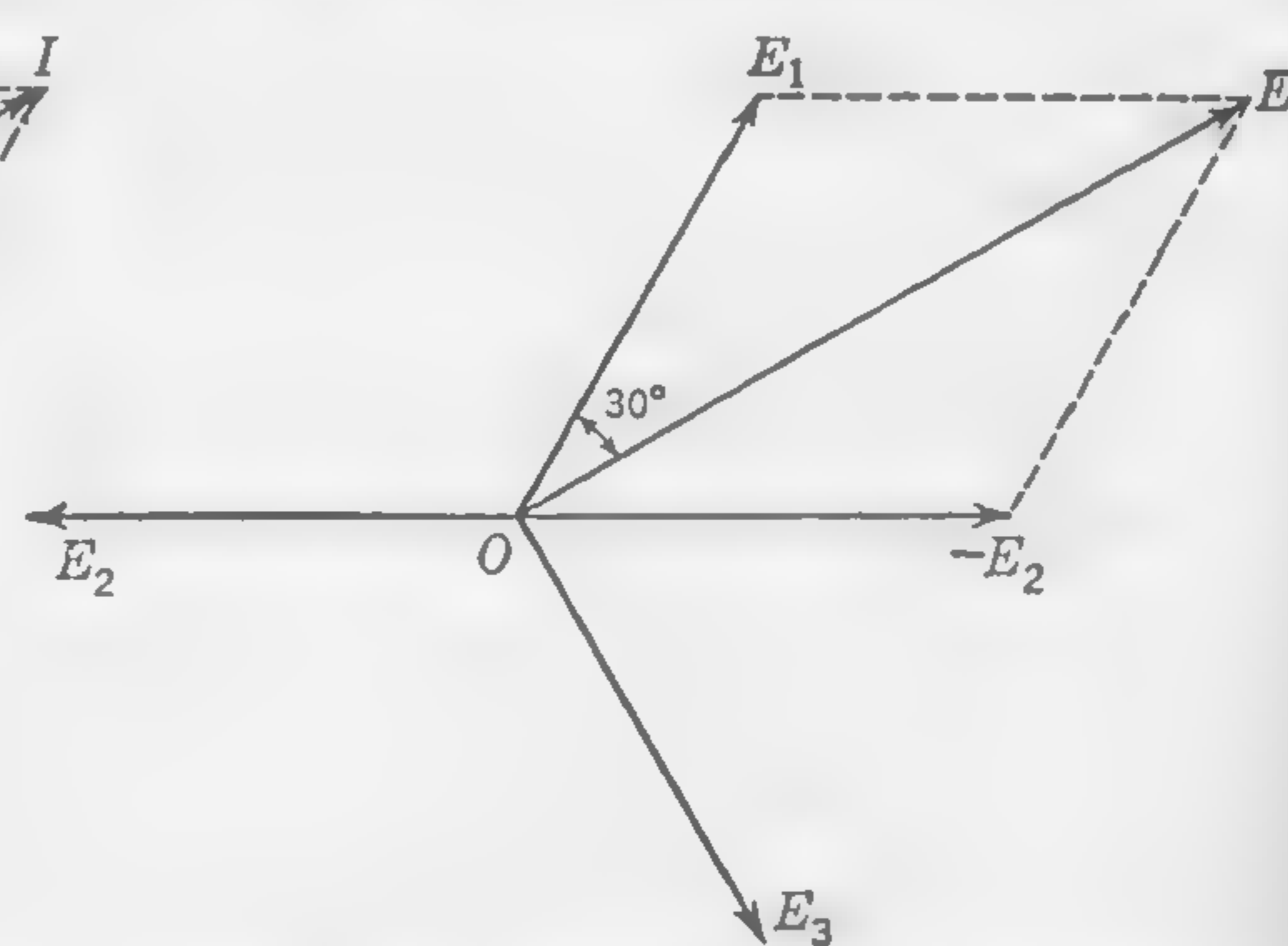


FIG. 80. Vector diagram showing voltage relations in Y-connected three-phase generator.

is also referred to as the Y connection. The outgoing lines being merely a continuation of the phase windings, it follows that, with a star-connected machine, the line current is exactly the same as the current in the armature windings. The voltage between terminals is, however, no longer the same as the phase voltage, as in the case of the previously considered mesh-connected machine. Referring to the vector diagram Fig. 80, it will be seen that the voltage between lines 1 and 2 is  $E_1 - E_2$ , which leads to the relation  $E = \sqrt{3} E_a$ , where  $E$  is the terminal voltage, and  $E_a$  the phase voltage as measured between any one terminal and the neutral point.

There is little to be said in regard to the choice of armature connections in a three-phase generator, except that, for the higher pressures, the Y connection has the advantage of a lower voltage per phase winding and, for heavy-current outputs, the  $\Delta$  connection has the advantage of a smaller current per phase winding.

**70. Power Output of Three-phase Generator.** Let  $E$  and  $I$  be the line voltage and line current, and let  $E_a$  and  $I_a$  be the phase voltage and armature current, respectively; then, in the  $\Delta$ -connected machine,

$$E = E_a \quad \text{and} \quad I = \sqrt{3} I_a$$

while, in the Y-connected machine,

$$E = \sqrt{3} E_a \quad \text{and} \quad I = I_a$$

Assuming unity power factor, we may write:

$$\begin{aligned} \text{Output of } \Delta\text{-connected machine} &= 3(E_a I_a) \\ &= 3E \times \frac{I}{\sqrt{3}} = \sqrt{3} EI \end{aligned}$$

and, similarly,

$$\begin{aligned} \text{Output of Y-connected machine} &= 3(E_a I_a) \\ &= 3 \frac{E}{\sqrt{3}} \times I = \sqrt{3} EI \end{aligned}$$

The total output is, of course, the same in both cases. If the power factor is not unity, the output in watts of the three-phase generator on a balanced load is

$$W = \sqrt{3} EI \cos \theta$$

where  $\theta$  is the angle of lag between terminal emf of a phase winding and current in the winding. The quantity  $\cos \theta$  is the power factor when both current and emf waves are sinusoidal.

Since the magnetic circuit of an a-c generator has to be designed for a certain flux to develop a given voltage, while the copper windings must be of sufficient cross section to carry a given current, the size of the machine will depend upon the product of volts and amperes, and not upon the actual power output. Alternating-current generators are, therefore, rated in kilovolt-amperes (kva), the actual output in kilowatts being dependent upon the power factor of the external circuit.

*Usual Voltages.* Owing to the absence of the commutator, a-c machines can be wound for higher voltages than d-c machines. Large a-c generators may be wound to give as high a pressure as 33,000 volts at the terminals, but it is rarely economical to develop much above



16,000 volts in the generator; when higher pressures are required, as for long-distance power transmission, step-up transformers are used. A common terminal voltage for three-phase generators to be used in connection with step-up transformers is 6,600 volts, but higher voltages are being adopted for the larger outputs, in order to avoid heavy currents in the machine and between the machine and the primary terminals of the transformer. By direct generation at moderately high voltages it is possible to do without step-up transformers at the sending end of the transmission line. Machines operating at 33,000 volts have already been built, and special designs for still higher pressures are constructed occasionally.

**71. Pole Proportions and Specific Loading.** Although there can be no sparking at the sliding contacts, as in d-c designs, with their commutation difficulties, the effects of field distortion and demagnetization are apparent in the voltage regulation of a-c generators. A very large pole pitch, involving as it does a large number of ampere-conductors per pole, is objectionable and should be avoided if possible. Where it is unavoidable, a large air gap or a high flux density in the teeth is necessary in order to keep the armature mmf from overpowering the field excitation; but this leads to increased cost.

The pole pitch  $\tau$  is a function of the peripheral speed and the frequency; thus

$$\tau = \frac{\pi D}{p}$$

where  $p$  = number of poles, and  $D$  = diameter of armature in inches. Also  $f = pN/120$  and

$$v = \frac{\pi DN}{12}$$

where  $v$  = peripheral velocity of armature in feet per minute. It follows that

$$\tau = \frac{v}{10f} \quad (67)$$

which explains why the pole pitch is always large in steam-turbine-driven alternators.

In 60-cycle machines running at moderate speeds, the pole pitch usually lies between 6 and 12 in., a pitch of 8 to 10 in. being very common. In 25-cycle generators, the pole pitch might measure from 10 to 20 in. The speed of the machine—which is usually a factor in determining the peripheral velocity—has an appreciable influence upon the choice of pole pitch; pole cores of approximately square section are not always feasible or economical, and the designer must make some sort of a com-

promise to get the best proportions. The output formula, as used for determining the proportions of dynamos, is not so readily applicable to the design of alternators, because the armature diameter in a-c machines will be determined largely by considerations of peripheral velocity and pole pitch, the proportions of the pole face being a secondary matter.

The value of the ratio  $\frac{\text{pole arc}}{\text{armature length}}$  is, therefore, determined largely by the limits of peripheral velocity, which may lead to a smaller diameter and greater axial length than would be strictly economical if the weight of copper in the field coils were the only consideration.

It is usual, when possible, to limit the armature ampere-turns per pole to 12,000, which will determine the maximum permissible value of the pole pitch; but this limit must sometimes be exceeded, as in the case of steam-turbine-driven machines, in which a pole pitch of 3 to 4 ft is by no means uncommon.

The pole arc is about the same portion of the total pitch as in continuous-current machines; the value of  $r$  (i.e., the ratio  $\frac{\text{pole arc}}{\text{pole pitch}}$ ) rarely exceeds 0.75. A very common value is 0.7, while it may frequently be as low as 0.6. The reason for the smaller circumferential space occupied by the pole face is partly to avoid excessive magnetic leakage, but mainly to provide a proper distribution of flux over the armature surface. An attempt is usually made to obtain sinusoidal distribution by the proper shaping and proportioning of the pole shoe.

*Specific Loading.* As in the case of d-c machines, the specific loading  $q$  is defined as the number of ampere-conductors per inch of armature periphery; i.e.,  $q = ZI_c/\pi D$ . However, since  $Z = nn_sC_s$  and  $\tau = \pi D/p$ , where  $n$  = number of phases,  $n_s$  = number of slots per pole per phase, and  $C_s$  = number of conductors per slot,

$$q = \frac{nn_sC_sI_c}{\tau} \quad (68)$$

Also,  $\tau/nn_s = \lambda$ , so that the specific loading is also

$$q = \frac{C_sI_c}{\lambda} \quad (69)$$

The conductors of all phases are counted, and the current considered is the effective, or rms, value of the armature current. The magnetizing effect of the armature as a whole will, at any moment, depend upon the instantaneous value of the currents in the individual conductors, but this matter will be taken up later.



The following are average values of  $q$ , as found in commercial machines:

Output of a-c generator, kva	Average value of $q$
50	450– 500
100	480– 550
200	530– 600
500	620– 700
1,000	700– 800
5,000	800– 900
10,000	900– 1,000

The proper value of  $q$  to be used in a given design will depend upon several factors. Apart from the fact that its value increases with the size of the machine, it will depend somewhat upon the following factors: (1) number of poles, (2) frequency, (3) voltage.

1. Machines with a small number of poles usually have a small armature diameter and a large pole pitch, calling for a *small* value of  $q$ . In modern steam-turbine-driven generators there is, however, a tendency to use high values of  $q$  in order to limit the length of the armature (and increase the critical speed).

2. With low frequency it is easy to keep the iron loss small, and either more copper or a greater current density in the conductors is permissible.

3. If the emf is low, the insulation occupies less space, and there is more room for copper without unduly reducing the cross section of the armature teeth.

The approximate figures given in the above table may be increased or reduced about 20 per cent, the highest values being used only when there is a combination of low voltage, low frequency, and large number of poles. In single-phase machines, the value of  $q$  may be about 20 per cent greater than in polyphase machines.

**72. Flux Density in Air Gap—Length of Air Gap.** Assuming the flux distribution over the pole pitch to be sinusoidal, the *maximum* value of the air-gap density will be  $(\pi/2)B_g$ , where  $B_g$  stands for the *average density over the pole pitch* (not under the pole face only, which is what this symbol stands for in Chap. 2 in connection with the design of d-c machines). When selecting a value for  $B_g$ , it is necessary to bear in mind the *maximum* air-gap density, because this will determine the maximum density in the iron of the teeth. The frequency being usually higher than in d-c machines, lower tooth densities must be used in order to avoid excessive loss. The allowable flux density in the air gap will depend upon the proportions of tooth and slot; but the following values may be used for preliminary calculations.

For a frequency of 25,  $B_g'' = 28,000$  to 40,000 lines per sq in.

For a frequency of 60,  $B_g'' = 21,000$  to 35,000 lines per sq in.

If  $\Phi$  = the total number of maxwells per pole, and the shape of the flux distribution over the pole pitch is assumed to be a sine wave, we have

$$\text{Area of pole pitch} = \frac{\Phi}{B_g''}$$

which determines the axial length of the armature core when its diameter and the number of poles have already been decided upon. The maximum air-gap density, on the above assumption, is  $(\pi/2)B_g$ , and, after the tooth and slot proportions are decided upon, it is advisable to see that this density will not lead to an unreasonable value for the apparent tooth density. As a check, it may be stated that the tooth density in alternators is rarely higher than 115,000 lines per sq in. in 25-cycle machines, and 100,000 lines per sq in. in 60-cycle machines. Higher densities are used in some steam-turbine-driven machines, with a view to reducing

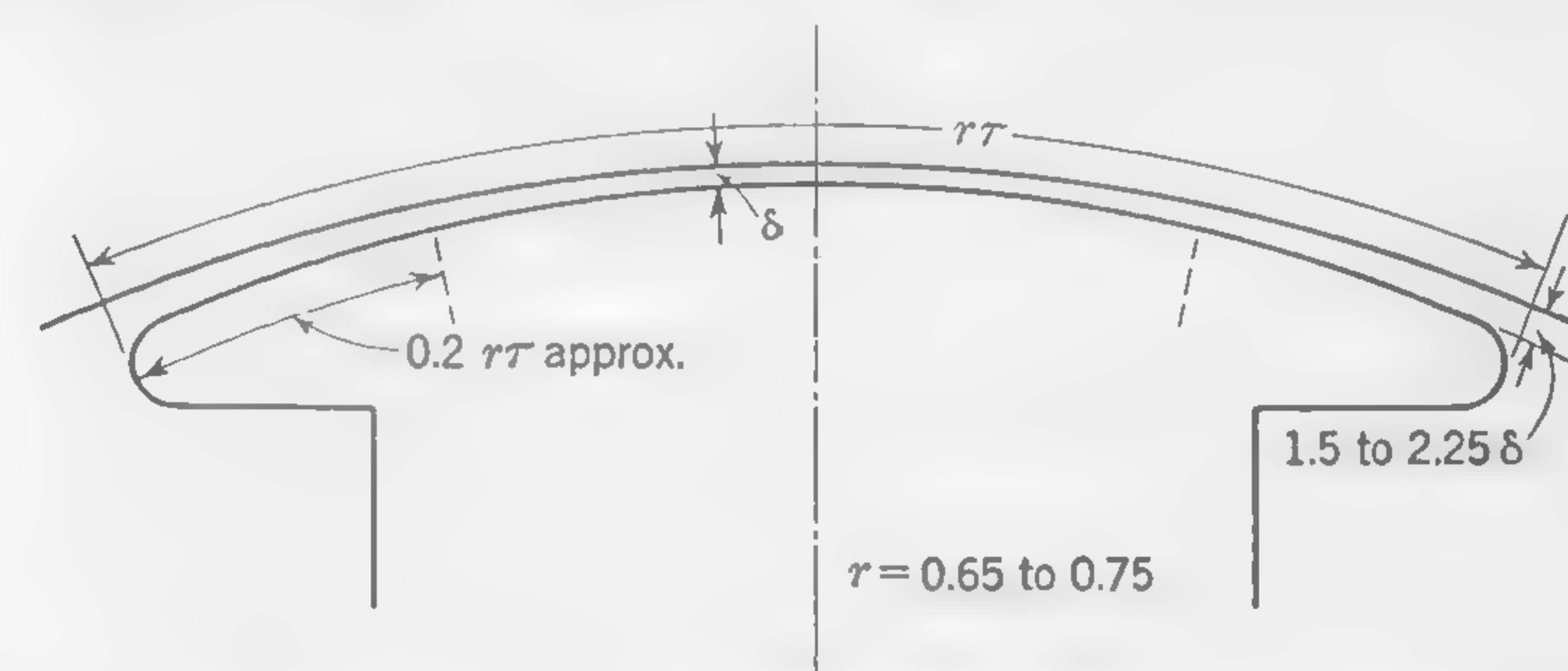


FIG. 81. Pole-shoe construction for synchronous machines.

the size of the rotor. A good system of forced ventilation is then imperative. Moreover, the fact that tooth densities limit the maximum permissible air-gap densities means that the latter are generally lower in the case of the high-voltage machines. This is because the slot space factor, *i.e.*, the ratio of copper area to total slot area, diminishes as the voltage to ground is raised; as a result, more slot space must be provided for insulation, thereby reducing the effective tooth area. Too low an air-gap density will, of course, result in an uneconomical use of iron in the magnetic circuit.

**Length of Air Gap—Inherent Regulation.** In a-c machines, just as in d-c machines, the length of air gap should depend upon the armature mmf and, therefore, on the pole pitch  $\tau$  and the specific loading  $q$ . In salient-pole machines, the air gap will not be of constant length but will increase from the center outward, in order to produce the required distribution of flux. Figure 81 illustrates a pole-shoe shape that will give a reasonably good flux-density distribution. Note that, beginning at about  $0.2 r\tau$  from the tips, the pole horns flare out so that the air gap at the tips is 50 to 125 per cent greater than it is at the center. This construction tends to



minimize the harmonic content in the generated voltage wave, although the higher harmonics, due to the presence of armature slots, may still be objectionable unless corrected in other ways. The minimum clearance to be allowed between pole face and armature surface at the center of the pole may be determined approximately by making it of such length that the open-circuit ampere-turns shall not be less than 1.25 to 1.75 times the full-load armature ampere-turns. In large turbo-alternators this ratio may be appreciably less in order to reduce the weight of copper on the rotor to keep the short-circuit current within reasonable limits. The distribution of armature mmf will be discussed later; but, for the purpose of estimating the air gap, the ampere-turns per pole may be taken as  $q\tau/2$ . If we assume the ampere-turns to overcome air-gap reluctance to be 1.5 times the armature ampere-turns per pole, and the "equivalent" air-gap under center of pole shoe to be 20 per cent greater than the actual air gap, an approximate expression for the minimum clearance between pole face and armature core is

$$\delta = 1.25 \frac{q\tau}{B_g''} \quad (70)$$

where  $\delta$  and  $\tau$  are in inches, and  $B_g''$  is the average air-gap flux density over the pole pitch, expressed in lines per square inch.

A large air gap has the effect of improving the regulation of the machine; but otherwise it is objectionable, as it leads to increased magnetic leakage and higher cost, due mainly to the greater weight of copper in the field coils.

The *inherent regulation* of a generator, at any given load, may be defined as the percentage increase in terminal voltage when the load is thrown off, the speed and field excitation remaining constant. Owing to the low power factors resulting from the connection of induction motors on a-c circuits, it is practically impossible to design a generator of which the inherent regulation is so good that auxiliary regulating devices are unnecessary. It is, therefore, uneconomical to aim at very good *inherent* regulation, especially as efficient automatic field regulators are now available. The inherent regulation of commercial machines usually lies between 5 and 10 per cent at full load on unity power factor, while it may easily be 20 per cent, or higher, on 85 per cent lagging power factor, with normal full-load current taken from the machine. This very marked effect of a low power factor will be explained later; but it may be stated here that the effect of a lagging armature current is very similar to that of a change of brush position in a continuous-current dynamo, causing the armature ampere-turns—which on unity power factor have merely a distorting effect—to become partly demagnetizing.

Not only must the magnetic effect of the armature be weak relatively

to the field, but the inductance of the armature windings should be small if the inherent regulation is to be good. Thus the regulating qualities of an alternating-current generator depend on both armature *reaction* and armature *reactance*; but, since these cannot be made so small as to dispense entirely with external regulating devices, the designer rarely aims at getting very good inherent regulation.

Good inherent regulation means that the current on short circuit may be very large, and this is sometimes objectionable. With the exception of high-speed, steam-turbine-driven units, the short-circuit current in modern a-c generators (with full field excitation) is about three to five times the normal full-load current; but in connection with the larger units, and on systems dealing with large amounts of energy, power-limiting reactances, external to the generator, are usually installed to prevent the current attaining a dangerous value before the automatic circuit breakers have had time to operate. Many of the larger units, driven at very high speeds by steam turbines, are purposely designed with large armature reaction and highly inductive windings, in order that they may be able to withstand momentary short circuits without mechanical injury.

**73. Armature Windings.** Elementary winding diagrams for single-, two-, and three-phase machines were illustrated by Fig. 76 and explained in Art. 68. Briefly extending the discussion of armature windings (this important topic, involving a great variety of constructions, arrangements, and connections, is properly considered in detail in special texts\*), several fundamental aspects of the subject will now be summarized.

When referring to windings in modern polyphase machines (single-phase units are rarely used) it is always implied that they are either two-phase or three-phase. This means, of course, that the *space* displacement of the two or three independent sections of the two- or three-phase windings in the stator core is electrically equivalent to the *time* displacement, 90° or 120°, respectively, of the generated emfs. Such windings may be arranged and constructed in many ways, but three general types are common to modern machines; these are (1) concentric-chain, (2) wave, and (3) lap. Each type has been found, by experience, to serve best under certain operating conditions, and these may be generalized as follows: concentric-chain windings are used most frequently in low-speed, large-diameter alternators; wave windings are ideal for the rotors of wound-rotor induction-type motors; lap windings have their widest fields of application in the stators of most high-speed synchronous machines and a-c motors. From the standpoint of construction the three types of winding differ in the following ways: concentric-chain

\* HIRKIND, C. S., "Alternating-current Armature Windings," McGraw-Hill Book Company, Inc., 1951.



windings are *single-layer*, *i.e.*, each slot contains one coil side, and several coil shapes and sizes are required; both lap and wave windings are nearly always double-layer; *i.e.*, each slot contains two coil sides one above the other, in which case there is an *even number* of conductors per slot and all coils of a given winding are identical in shape and size. Under some special conditions of winding design and construction, where there must be an *odd number* of conductors per slot (see Art. 82 and Fig. 93), a single-layer winding must be employed.

**Concentric-chain Windings.** Figures 82 and 83 illustrate two styles of concentric-chain winding in which the coils for one phase are shown in each. Note particularly the differing coil sizes and shapes and the manner in which they are interconnected to form magnetic poles. Moreover, the coils for each of the other two phases would be shaped still

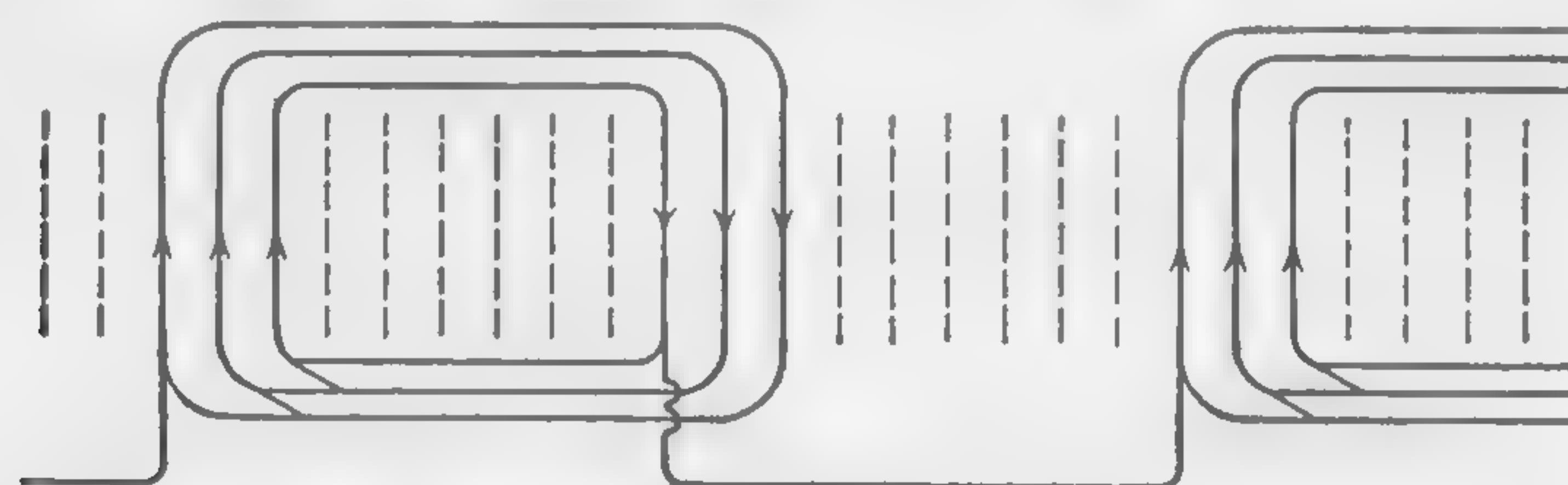


FIG. 82. Three-phase, single-layer winding; three slots per pole per phase.

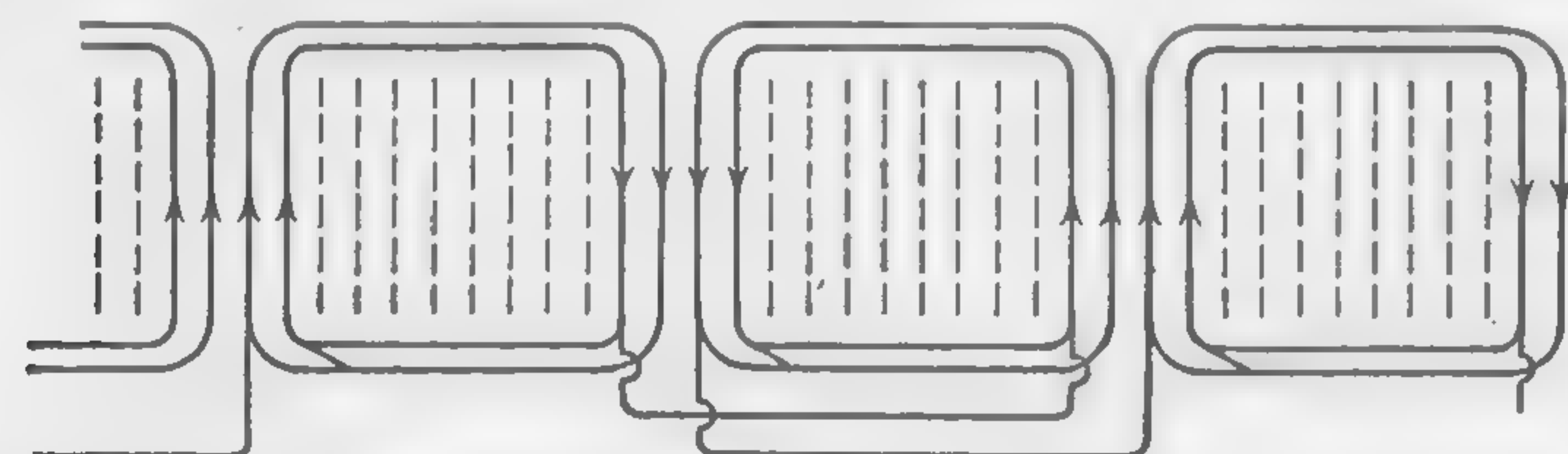


FIG. 83. Three-phase, single-layer winding; four slots per pole per phase.

differently from those shown because the end connections would have to be bent to clear one another. It is obvious, therefore, that such windings involve a larger number of special tools and formers and many more spare coils than do unit-construction windings of the lap and wave types. These disadvantages are, however, sometimes outweighed by the facts that the total number of coils in the machine is smaller and that good insulation is easily obtained because the end connections may be separated by large air spaces. Furthermore, when each phase is considered separately, the full number of turns per pole may encircle one pole only, as shown in Fig. 82, or they may be divided between a pair of poles, in two equal parts, as shown in Fig. 83. Also observe that there are three slots per pole per phase in Fig. 82, and four slots per pole per phase in Fig. 83. The coils of the other two phases in each diagram

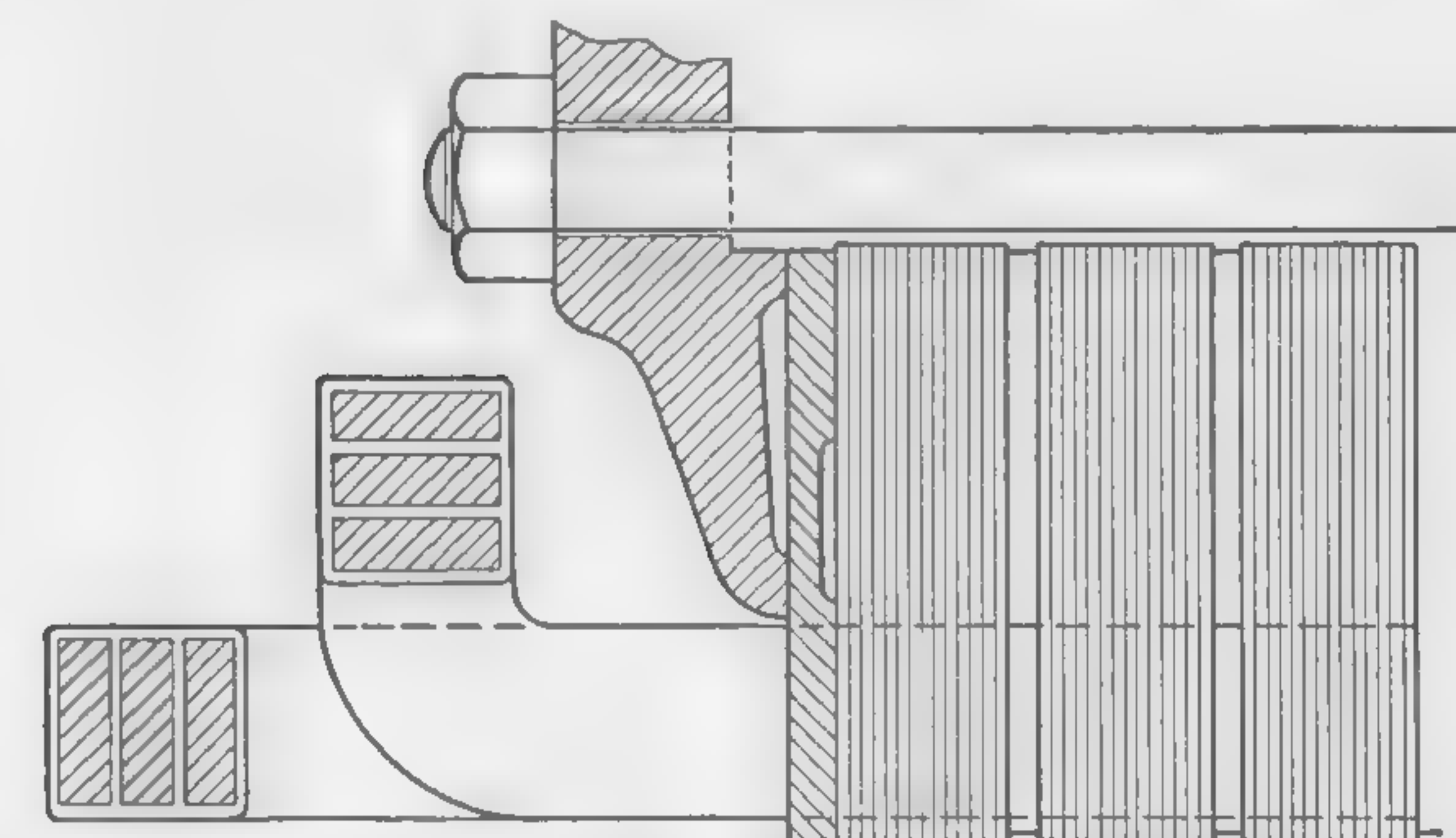


FIG. 84. End connections of single-layer armature winding.

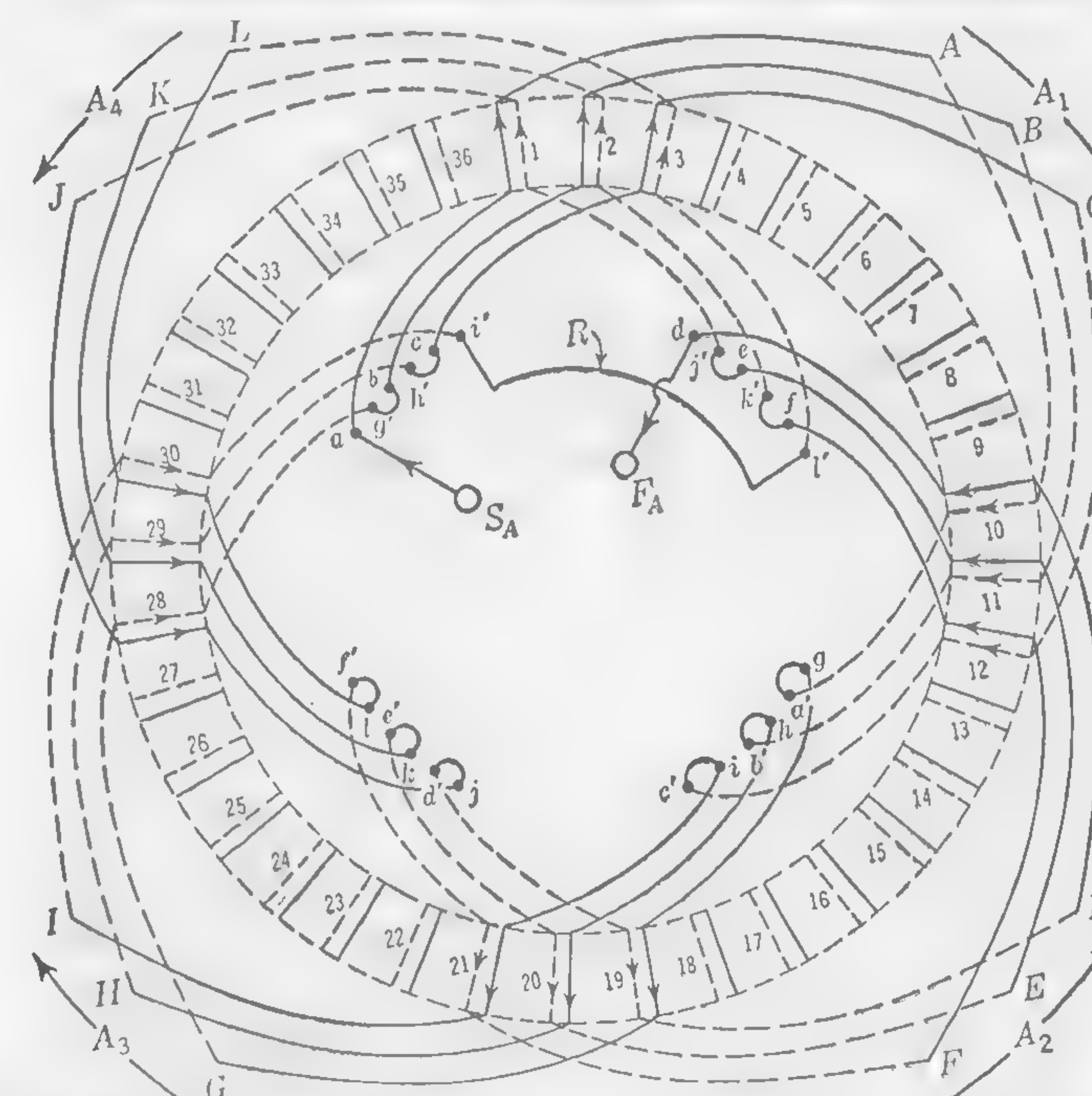


FIG. 85. Diagram showing one phase of a 36-slot 4-pole 3-phase wave winding, completely connected. Note that only one cross-connector  $R$  is used.

would be similarly arranged in the remaining slots, the ends projecting beyond the slots being shaped or bent so as to clear the other coils, generally as shown in Fig. 84.

**Wave Windings.** The coils used to construct a wave winding in an a-c machine are identical with those employed in a d-c winding (see Fig. 5). The coil ends of the latter are connected to commutator segments, while those in polyphase a-c windings are joined together to form properly arranged phases. Figure 85 represents a 36-slot core in which all the



coils of one of the three phases, *i.e.*, 12 coils, are shown properly located and connected for a four-pole winding. To avoid confusion and to simplify the drawing, single-turn coils are indicated. Note particularly that (1) all coils have exactly the same size and shape, in contrast to those used in concentric-chain windings (Figs. 82 and 83); (2) there are two coil sides per slot, which means that each slot must always have an even number of conductors; and (3) the coil ends are bent outward from the sides so that the proper coils may be joined together conveniently without the necessity of using jumpers. The completed phase may be traced from  $S_A$  to  $F_A$  for phase  $A$  by advancing through the coils in the following order:  $S_A$  to  $a$ , then through coils  $A, G, B, H, C$ , and  $I$  in a *clockwise* direction, next through reversing connector  $R$  to coil end  $U$ , and finally through coils  $L, F, K, E, J, D$  in a *counterclockwise* direction, ending at  $F_A$ . The other two phases would, of course, be inserted and connected in a similar way, care being taken to provide a 120-electrical-degree relationship between phases.

**Lap Windings.** The lap winding is the type most commonly employed on the stators of polyphase a-c machines. In appearance and construction the coils are identical with those used in d-c armatures. And, except for the fact that the coil ends are brought out near one of the "knuckle" bends, they are similar to wave coils. When the core has overhanging teeth, *i.e.*, partially closed slots, the coils are not taped when they are first made. Instead, the wire is wound on a former of the proper shape and dimensions, after which the individual wires of each coil are fed into the slots one or two at a time, through narrow openings between teeth; this practice applies equally to wave windings. A diagram showing one phase of a 3-phase 4-pole lap winding in a 36-slot core is illustrated by Fig. 86. Note particularly that, except for the interconnections between coils, it is quite similar to that of the wave winding of Fig. 85, in that the coils have the same shape and slot arrangement, with two coil sides per slot. It should also be pointed out that both windings, lap and wave, are shown with full-pitch coils ( $k' = 1$ ), although more common designs would involve the use of fractional-pitch coils. The completed phase may be traced from  $S_A$  to  $F_A$  by advancing through the coils in the following order:  $S_A$  to  $A, B, C$  in a clockwise direction,  $F, E, D$  in a counterclockwise direction, clockwise through  $G, H, I$ , and finally through  $L, K, J$ , and thence to  $F_A$  in a counterclockwise direction. The other two phases would, of course, be identical with phase  $A$ , but each one displaced by 120 electrical degrees with respect to the others.

A completely developed diagram for a 36-slot 4-pole machine is given in Fig. 87; this winding is shown with a coil pitch of 77.8 per cent (140 electrical degrees) so that  $k' = \sin 70^\circ = 0.910$ . For machines of rather

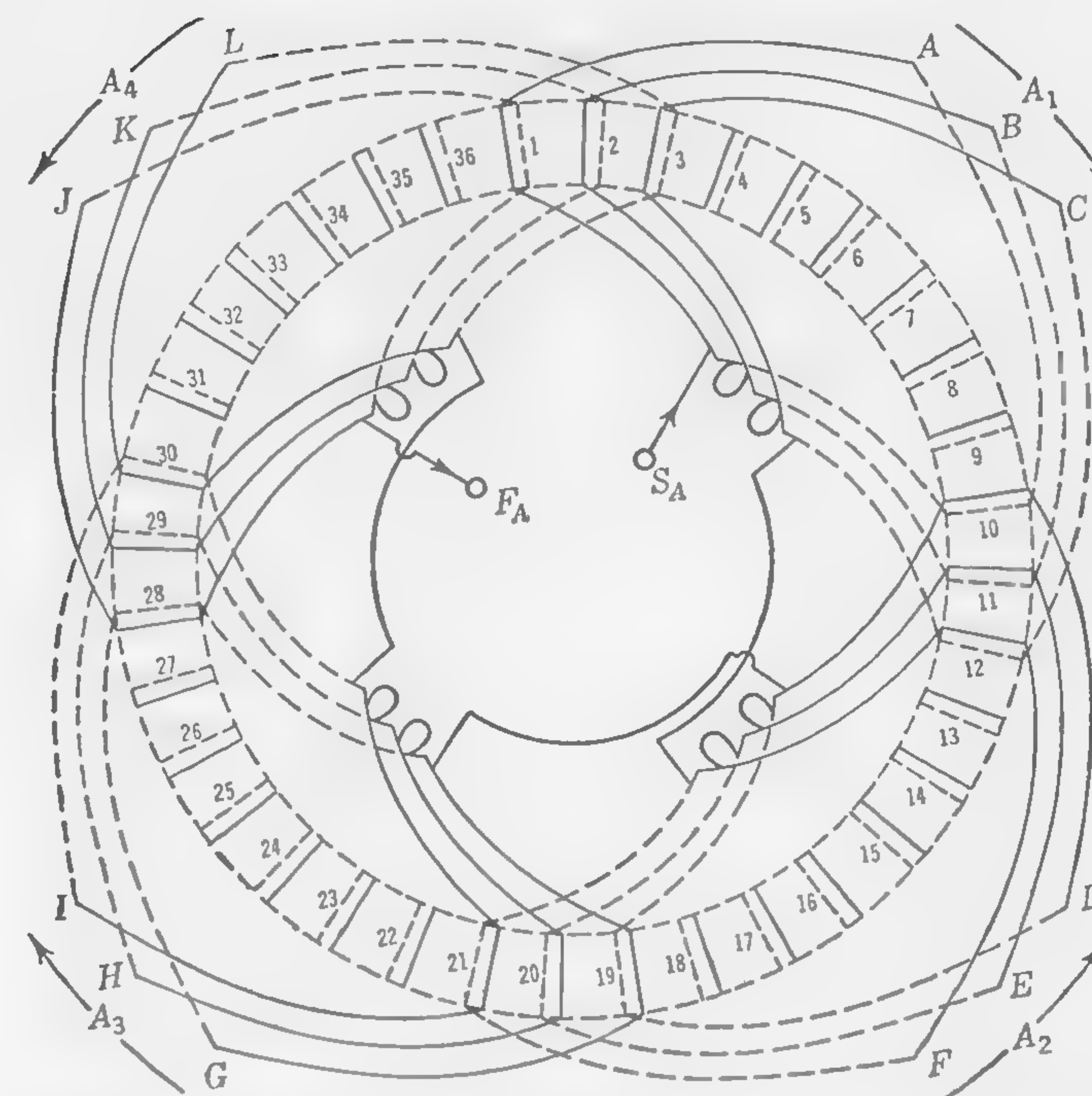


FIG. 86. Diagram showing one phase of a 36-slot 4-pole 3-phase lap winding, completely connected.

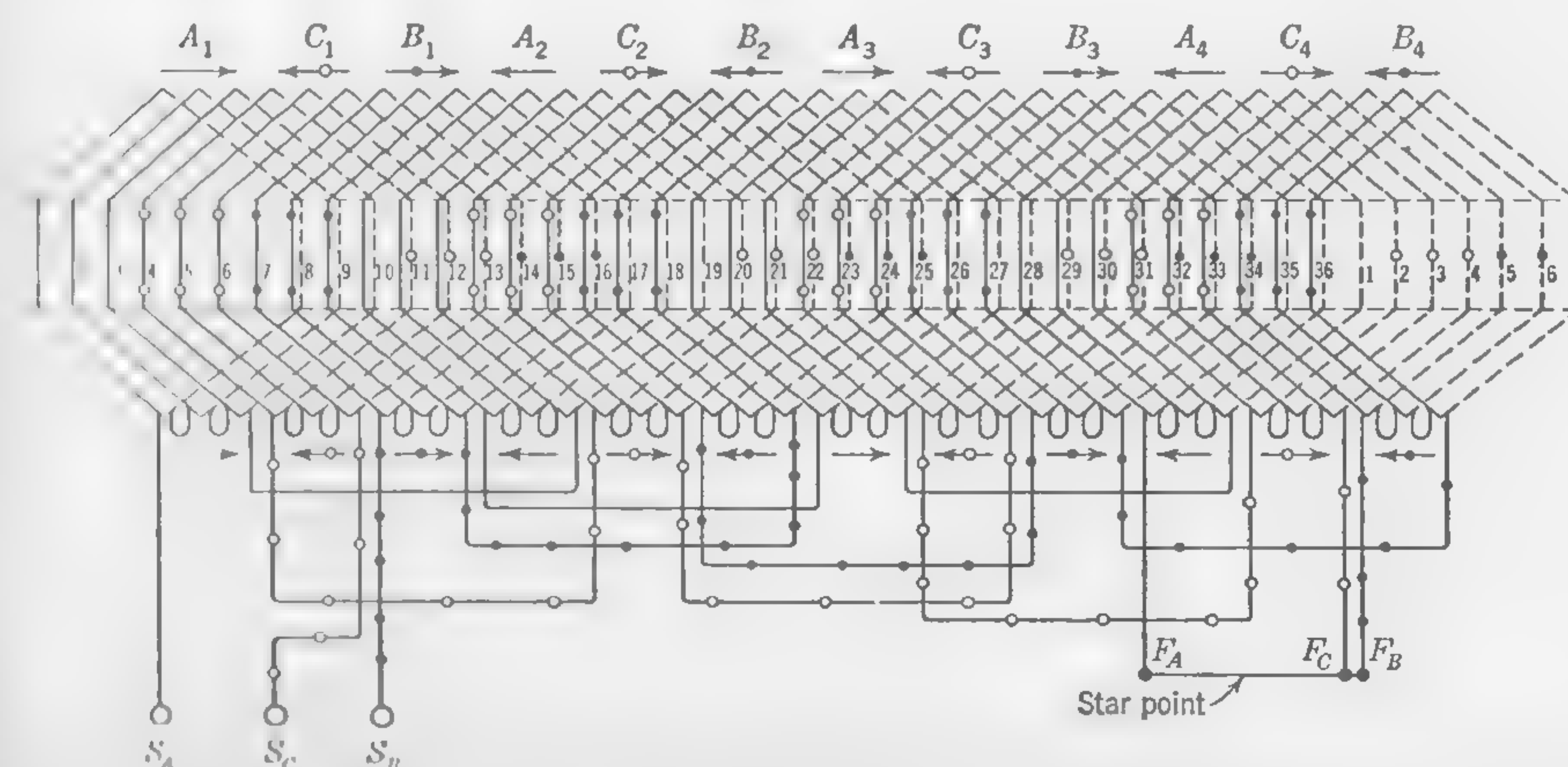


FIG. 87. Complete wiring diagram of a 4-pole 3-phase fractional-pitch star-connected lap winding in a 36-slot core. The coil pitch is slots 1 to 8; this is 140 electrical degrees, or 77.8 per cent.



high ratings many more slots and coils would be used, but the winding design and construction procedure would, in general, be similar to the foregoing.

**Spread of Windings.** In two-phase and three-phase machines, all the slots on the armature are utilized. With full-pitch windings,\* the number of slots per pole is divisible by 2 for a two-phase generator, and by 3 for a three-phase generator. Thus, with distributed windings (more than one slot per pole per phase), the "spread," or space occupied by each phase winding, is  $180/2 = 90$  electrical degrees for a two-phase machine, and  $180/3 = 60^\circ$  for a three-phase machine.

In single-phase machines, nothing is gained by winding all the slots on the armature surface; after a certain width of winding has been

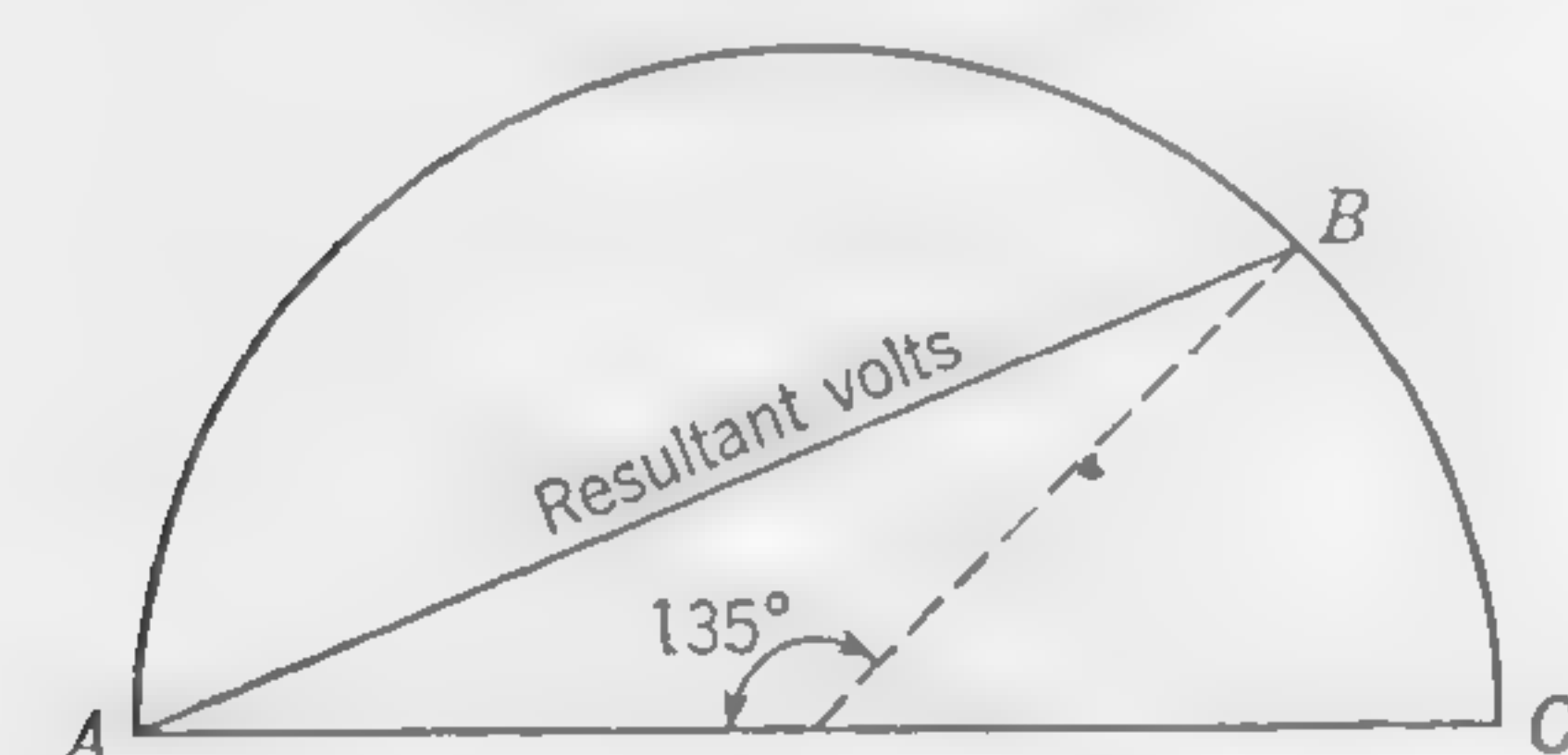


FIG. 88. Vector diagram illustrating "spread" of armature winding in single-phase alternator.

reached, the filling of additional slots merely increases the resistance and inductance of the winding, without any appreciable gain in the matter of developed voltage. This is made clear in the vector diagram (Fig. 88). The winding is supposed to be distributed in a very large number of slots, and the diameter of the semicircle represents the resultant generated emf if all the slots are filled with conductors (connected in series). If, as is usual in practice, only 75 per cent of the slots are utilized, the spread of the single-phase winding will be about 135 electrical degrees, the resultant emf will be  $AB$ , which is not much shorter than  $AC$ ; but the length and weight of copper in the two cases are in the proportion  $\frac{\text{arc } ABC}{\text{arc } AB}$ .

The fact that, in polyphase machines, the whole of the armature surface is available for the windings, while only a portion of this surface is utilized in the single-phase alternator, accounts for the fact that the output of the latter is less than that of the polyphase machine for the same size of frame. Given a three-phase machine, it is merely necessary to omit one of the phase windings entirely and connect the two remaining phases in series, to obtain a single-phase generator. The modified machine will be capable of giving something more than two-thirds of the output of the polyphase generator, the limit being reached when the copper losses become excessive.

\* Short-pitch windings are very common in two-pole machines, as they tend to simplify the end connections. In this case the double-layer winding, as in d-c machines, would be used. Fractional-pitch windings with coils having 50 per cent pitch are frequently used when construction difficulties are anticipated with longer coil pitches.

**74. Current Density in Armature Conductors.** Although the armature may be stationary, the permissible current density in the conductors will depend to some extent upon the peripheral speed of the rotating field magnets, because the fanning effect will be greater at the higher velocities. The cooling effect of the air thrown against the conductors by the rotation of the field magnets is not so great as when the armature rotates, and, moreover, the air is warmed to some extent in passing over the heated surface of the field coils. The current density in alternating-current armatures usually lies between 2,000 and 3,500 amp per sq in. of cross section. The general expression for determining the current density, previously used in the design of dynamo armatures, may be applied to the armature conductors of synchronous machines; this is formula (17), page 36, which is  $\Delta = (k/q) + (v/4)$ . However, values of  $k$  should range between 700,000 and 1,000,000 and  $q$  and  $v$  are, as before, specific loading and peripheral velocity, respectively.

**75. Tooth and Slot Proportions.** In deciding upon the number of teeth on the armature, a compromise must be made between a very small number of teeth—which involves the bunching of conductors, with consequent high internal temperatures and high inductance—and a large number of teeth, involving more space taken up by insulation, and a higher cost generally. Although larger slots are permissible in a-c machines than in d-c machines, a tooth pitch ( $\lambda$ ) greater than 2.5 in. is not recommended. The tooth pitch may be as small as  $\frac{3}{4}$  in. but it usually lies between the limits 1 and 2 in. In large turbo-alternators, the tooth pitch may be as large as 3 or even  $3\frac{1}{2}$  in., but in such cases a slot wedge built up of laminated iron plates is generally used, thus virtually reducing the slot opening and equalizing the flux distribution over the slot pitch. In a three-phase machine, the number of slots per pole per phase is usually from one to four; but in turbo-alternators, with large pole pitch, the number of slots may greatly exceed these figures.

The conductors must be so arranged that the width of slot is not such as to reduce the tooth section beyond the limit corresponding to a reasonable flux density in the iron of the tooth (see Art. 72); but, on the other hand, a deep slot is sometimes objectionable because it leads to a high value of slot-leakage flux. The depth of the slot should preferably not exceed three times the width, although deeper slots can be used and may, indeed, be desirable in cases where poor inherent regulation is deliberately sought.

**76. Length and Resistance of Armature Winding.** Apart from the pitch  $\tau$ , and the gross length of armature core  $l_a$ , the length per turn of the winding will depend upon the voltage and also upon the slot dimensions. The voltage will determine the amount by which the slot insulation should project beyond the end of the armature core, and the cross



section of the coil will be a factor in determining the length taken up in bends at the corners of the coil. A rough sketch of the coil should be made, and the length of a mean turn estimated as closely as possible for the purpose of calculating the resistance and weight. Although no definite rules can be laid down to cover all styles of winding, the straight projection of the coil side (and insulation) outside the slot, in inches, would be about  $0.5 + 0.35 \text{ kv}$ , where kv stands for the pressure between terminals in kilovolts. On the basis of an average size of slot, the actual overhang beyond end of core would have a mean value of about  $\frac{1}{2}[\text{kv} + 3 + (\tau/4)]$ , where  $\tau$  is the pole pitch in inches. On this basis, as a very rough estimate, the *mean length per turn* in inches would be

$$2l_a + 2.5\tau + (2 \times \text{kv}) + 6 \quad (71)$$

The cross section having been previously decided upon, the resistance per phase of the armature winding can readily be calculated.

**77. Full-load Developed Voltage.** The losses in the armature core at full load will depend upon the developed emf, which is not quite so

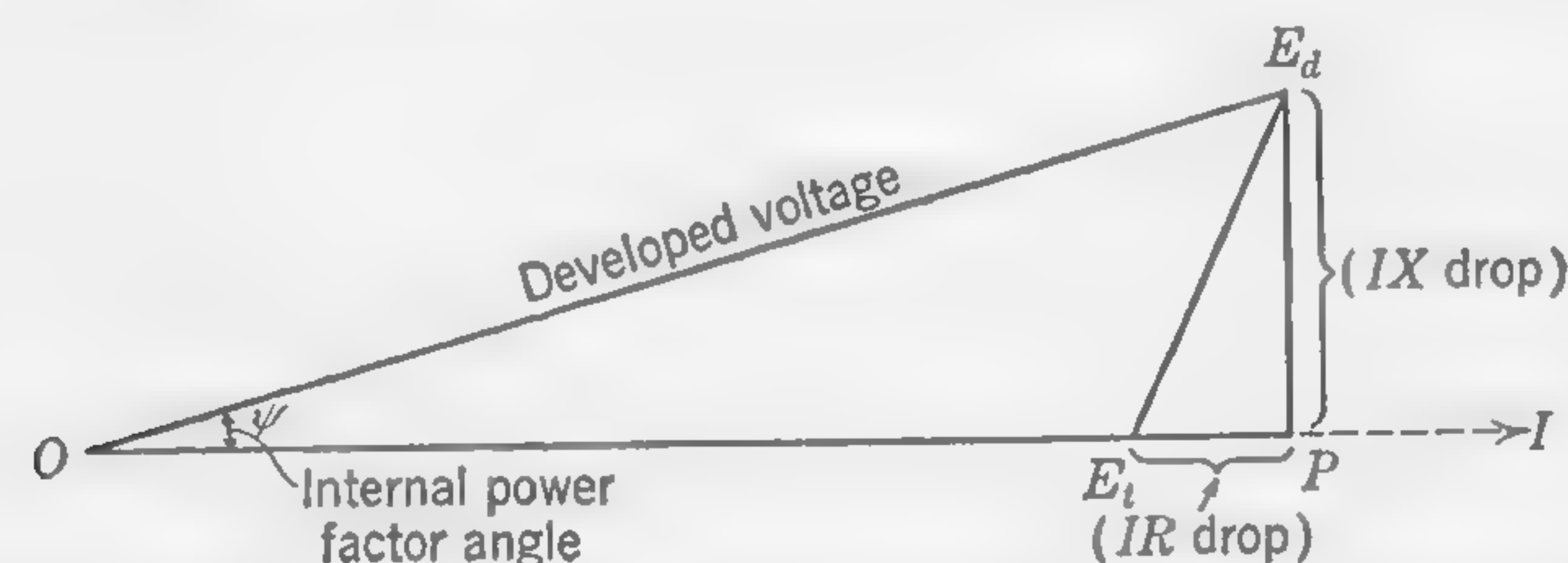


FIG. 89. Vector diagram for calculating developed emf—non-inductive load.

easily calculated as in the case of a d-c dynamo. The voltage that has to be generated in the armature windings of an alternator for a given terminal voltage will depend not only upon the  $IR$  pressure drop, but also on the  $IX$  drop. In other words, the inductance of the armature windings and the power factor of the load must be taken into account when calculating the developed voltage.

The vector diagram (Fig. 89) refers to a machine working on a load of unity power factor. The current is in phase with the terminal voltage  $OE_t$ ; but the developed volts are  $OE_d$  and not  $OP$ , as would be the case if the  $IR$  drop only had to be considered. The vector  $PE_a$  represents the emf component necessary to counteract the reactance drop in the armature windings. Although the external power-factor angle is zero, there is an angle  $\psi$  between the current vector and the vector of the developed emf, which may be termed the internal power-factor angle.

In Fig. 90, the external power-factor angle is  $\theta$  (power factor of load =  $\cos \theta$ ). The construction shows how the reactance voltage  $IX$  becomes a factor of greater importance on the lower power factors. The emf that

must be developed to obtain a constant terminal pressure must, therefore, be greater on low power factor. This, however, is not the chief cause of poor regulation on low power factors; it is the demagnetizing effect of armature ampere-turns which is chiefly accountable for poor regulation on all but unity power factor.

The vector diagrams should always be drawn to show the relation of the variable quantities in *one phase of the winding*, a balanced load being assumed. It does not then matter whether the phases are star- or delta-connected, except that, in the case of a star-connected generator, the vector  $OE_t$  would stand for the voltage between one terminal and the neutral point, and its numerical value would, therefore, be  $1/\sqrt{3}$  times the voltage between terminals.

The length of the vector  $E_tP$  (Figs. 89 and 90) is easily calculated, but the numerical value of  $IX$  (the vector  $PE_a$ ) is not so easily estimated. Consider first what is to be understood by the term "armature reactance."

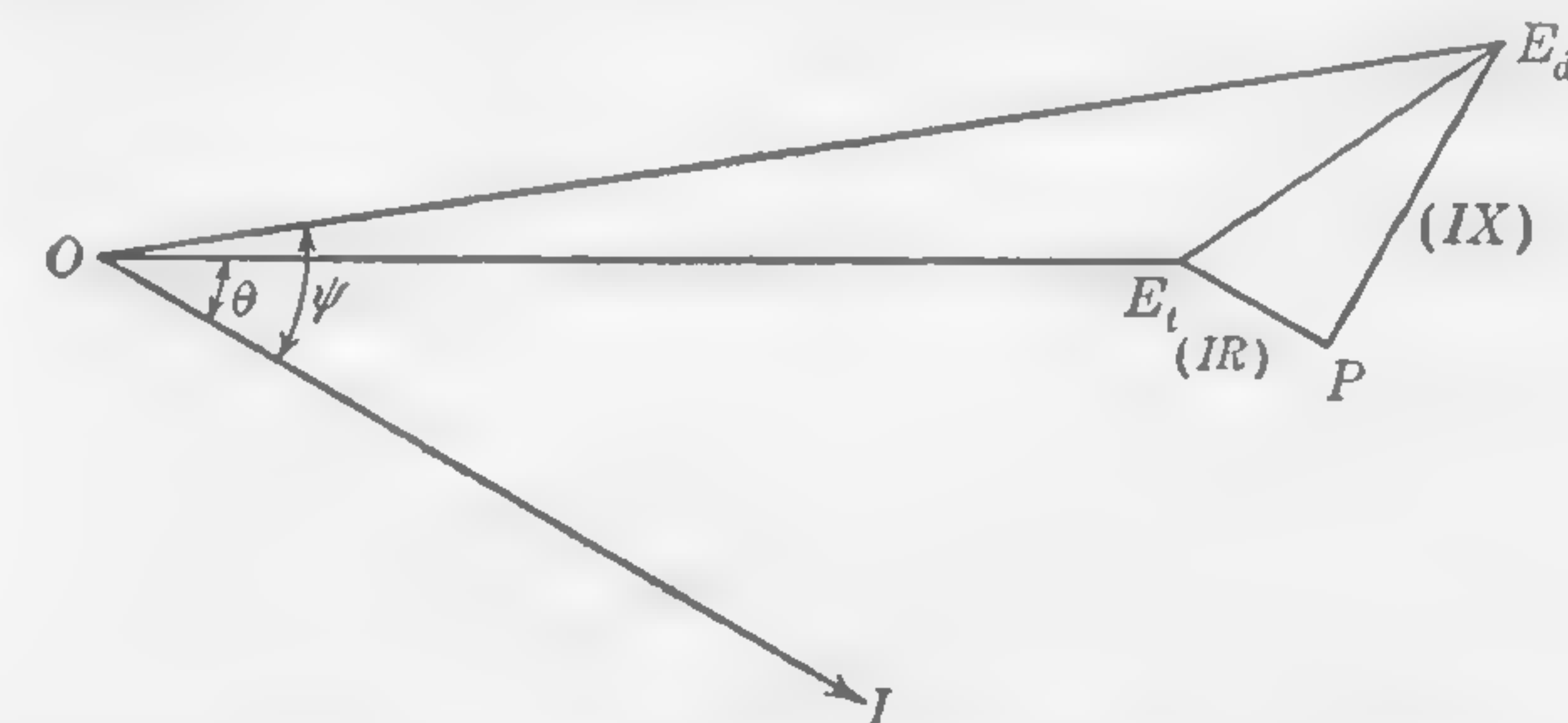


FIG. 90. Vector diagram for calculating developed emf—load partly inductive.

**78. Reactive Voltage Drop in A-C Armature Windings.** It is not always easy to separate armature reactance  $X$  from armature reaction (the demagnetizing effect of the armature ampere-turns). Both cause a drop of pressure at the terminals under load, especially on low power factors. By departing from the conventional methods of treating this part of the subject, and striving to keep in mind the actual physical conditions, by picturing the armature conductors cutting through the flux lines, the difficulties of the subject may, to a great extent, be removed.

What is usually referred to as the reactive voltage component (the vector  $E_dP$  in Figs. 89 and 90) is really due to the cutting of the end flux by the conductors projecting beyond the ends of the slots; the slot flux, being actually provided by the main poles, does not enter the armature core below the teeth, and, since the greater part of it is not cut by the armature inductors, this portion of the slot flux should not be thought of as producing an emf of self-induction in the windings. The amount of slot flux may be very large, especially on a heavy load of low power factor, and it will have an appreciable effect on the inherent regulation of the



machine. The mmf of the conductors in the slot accounts for the fact that a certain percentage of the flux in the air gap does not enter the armature core below the teeth; but the statement here made is that the slot-leakage flux does not induce a counter-emf in the armature windings.

The core loss will depend upon the flux necessary to develop the emf  $OE_d$  (Figs. 89 and 90), where the component  $E_dP$  is the reactance voltage drop due to the flux linkages of the end connections only; or, in other words, where  $E_dP$  is the emf induced in the conductors outside the slots by the cutting of the flux lines created by the currents in all the phase windings.

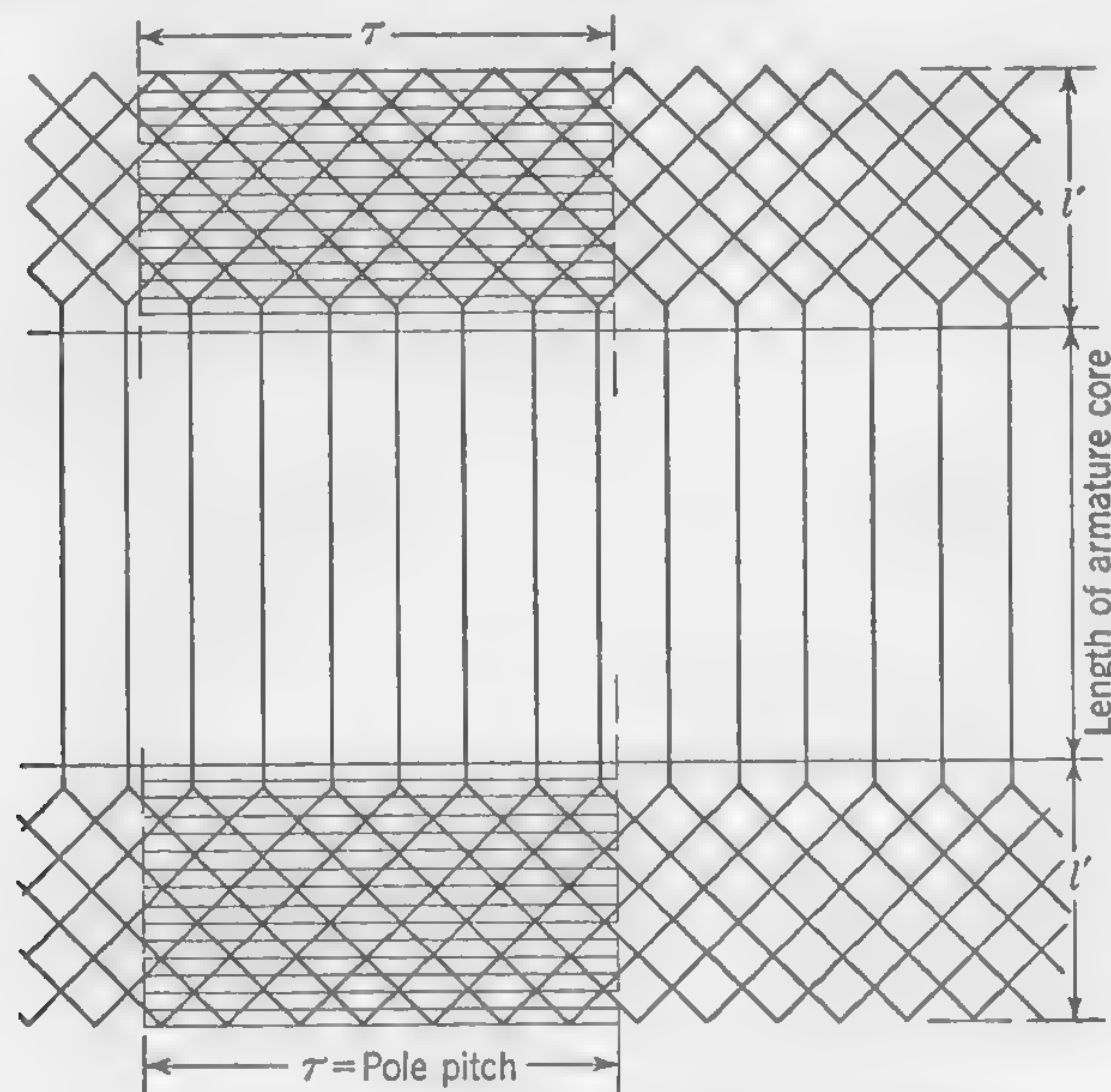


FIG. 91. Developed view of stator winding.

**Calculation of Armature  $IX$  Drop.** In Fig. 91, let  $\tau$  represent the pole pitch of a polyphase generator, and  $l'$  the average extension of the coils beyond the ends of the armature core. (Means of estimating the average equivalent projection of the armature windings beyond the ends of the core will be explained later.) If the total flux produced by the armature currents, in the space of width  $\tau$  and depth  $l'$ , as shown cross-hatched in Fig. 91, can be estimated, the voltage developed by the cutting of this flux can readily be calculated. A. Still has developed elsewhere\* formulas for estimating the amount of the end flux which is cut by the overhanging portion of the armature winding in the space  $2\tau l'$  as indicated in Fig. 91. The symbols used in these formulas are defined as follows:

\* STILL, ALFRED, End-connection Reactance of Synchronous Machines, *J. AIEE*, p. 535, July, 1930.

- $C_s$  = the number of conductors in each slot (each carrying the current  $I_c$  amp)
- $n_s$  = the number of slots per pole per phase
- $n$  = the number of phases
- $I_c$  = the rms value of the armature current, amperes
- $l'$  = the equivalent projection of the armature windings beyond the ends of the slots, expressed in centimeters (means of estimating this quantity will follow)
- $k$  = a correcting factor depending upon the type of machine, the type of winding, and the proximity of masses of iron tending to reduce the reluctance of the flux paths through the coils.

For single-layer windings, the end flux is

$$\Phi_e = knn_s C_s I_c l' \quad \text{maxwells} \quad (72)$$

For double-layer windings the amount of the end flux will be about  $2/\pi$  times the amount which links with the single-layer windings, whence

$$\Phi_e = \frac{2}{\pi} knn_s C_s I_c l' \quad \text{maxwells} \quad (72a)$$

Since the flux  $\Phi_e$  may be thought of as being "cut" by the projecting end connections exactly as the main flux entering the armature is cut by the inductors in the slots, it follows that the emf induced in the end connections, expressed as a percentage of the developed emf, is

$$\text{Percentage } (IX)_{\text{ends}} = 100 \frac{\Phi_e}{\Phi} \quad (73)$$

where  $\Phi$  stands for the flux per pole which enters the armature core.

If  $p$  is the number of poles of the machine, the total number of conductors per phase is  $pC_s n_s$ , and the average value of the voltage developed in the end connections by the cutting of the end flux will be  $2f\Phi_e pC_s n_s \times 10^{-8}$ . Assuming the form factor to be 1.11, which would be correct if the flux distribution were sinusoidal, the voltage component developed per phase, in a full-pitch winding, by the cutting of the end flux, is

$$(IX)_{\text{ends}} = \frac{\pi}{\sqrt{2}} f\Phi_e (n_s C_s p) 10^{-8} \quad (74)$$

This quantity is usually referred to as the reactive voltage drop per phase due to the inductance of the end connections; it appears as the vector  $I'E_d$  (Figs. 89 and 90).

Before substituting the calculated value of  $\Phi_e$ , another factor should be introduced to take account of the fractional-pitch windings which are



common in modern designs. Let  $d$  stand for the winding factor, which may take account of both coil pitch and width of phase belt. For example, with a coil pitch of two-thirds the pole pitch and a three-phase winding with four slots per pole per phase, the numerical value of this factor would be  $d = 0.958 \sin(120^\circ/2) = 0.83$ , where the multiplier 0.958 is the distribution factor due to the phase belt's being spread over four slots per pole and  $\sin(120^\circ/2)$  is the pitch factor. If the armature end connections were cutting a sinusoidal flux provided by an independent winding, the developed voltage would be  $d$  times the voltage given by formula (74); but since the flux cut is produced by the armature winding itself, the flux  $\Phi_e$  of formulas (72) and (72a) will have to be reduced to the same extent, so that it is the quantity  $d^2$  which must be introduced as a correcting factor in the final formula. With this addition

$$(IX)_{\text{ends}} = \frac{\pi}{\sqrt{2}} f \Phi_e (n_s C_s p) d^2 \times 10^{-8} \quad (74a)$$

Next, substituting the value of  $\Phi_e$  given by formula (72a) in formula (74a), and dividing by  $I_c$ , the final formula for *end-connection reactance per phase winding* for a polyphase synchronous machine with double-layer winding becomes

$$X_e = n \sqrt{2} k d^2 f (n_s C_s)^2 p l' \times 10^{-8} \quad \text{ohms} \quad (75)$$

where the number of phases  $n$  is three or more. For a single-layer winding, the reactance as calculated by formula (75) must be multiplied by  $\pi/2$ .

*Approximate Values for the Factor  $k$  and the Length  $l'$ .* The factor  $k$  in the above formulas depends upon the amount of iron in the path of the magnetic flux linking with the end connections. It cannot easily be calculated and is really an empirical coefficient. A. Still suggests the value  $k = 1.7$  for slow- and medium-speed salient-pole generators, and  $k = 3.5$  for high-speed turbo-generators.

In respect to the dimension  $l'$  which, in the formulas, is the overhang in centimeters beyond the ends of the iron core, the equivalent projection of a coil that is bent up to clear the coils of other phases might be considered equal to the projection of the same coil if flattened out. With  $\tau$  expressed in inches, an approximate value for  $l'$  is

$$l' = 1.27 \left( kv + 3 + \frac{\tau}{4} \right) \quad \text{cm} \quad (76)$$

This formula applies to the *single-layer* type of winding. With the *double-layer* winding, it is well to use a length for  $l'$  somewhat greater

than the straight overhang of the windings beyond the slot. In this manner, the necessary allowance can be made (1) for the flux linking with the bend at the ends of the coil, and (2) for the fact that the flux density does not fall off immediately after the coils leave the slots. This is explained in Fig. 92, where  $a$  is the straight projection beyond the slot of the two coil sides before the upper and lower layers of the winding branch off in different directions. The equivalent overhang for use in formula (72a), expressed in terms of the dimensions in Fig. 92, is

$$l' = b + \frac{\pi}{2} (a + c) \quad \text{cm} \quad (77)$$

**79. Total Losses to Be Radiated from Armature Core.** The losses in the iron stampings—teeth and core—are calculated as explained in Art. 52 (use curve of Fig. 67). The flux to be carried at full load by the core below the teeth is that which will develop the necessary emf as obtained from the vector construction of Fig. 90. The radial depth of the armature stampings is calculated by assuming a reasonable flux density in the iron. This will usually be between 50,000 and 60,000 lines per sq in. in 60-cycle machines, increasing to 65,000 or even 70,000 in 25-cycle generators.

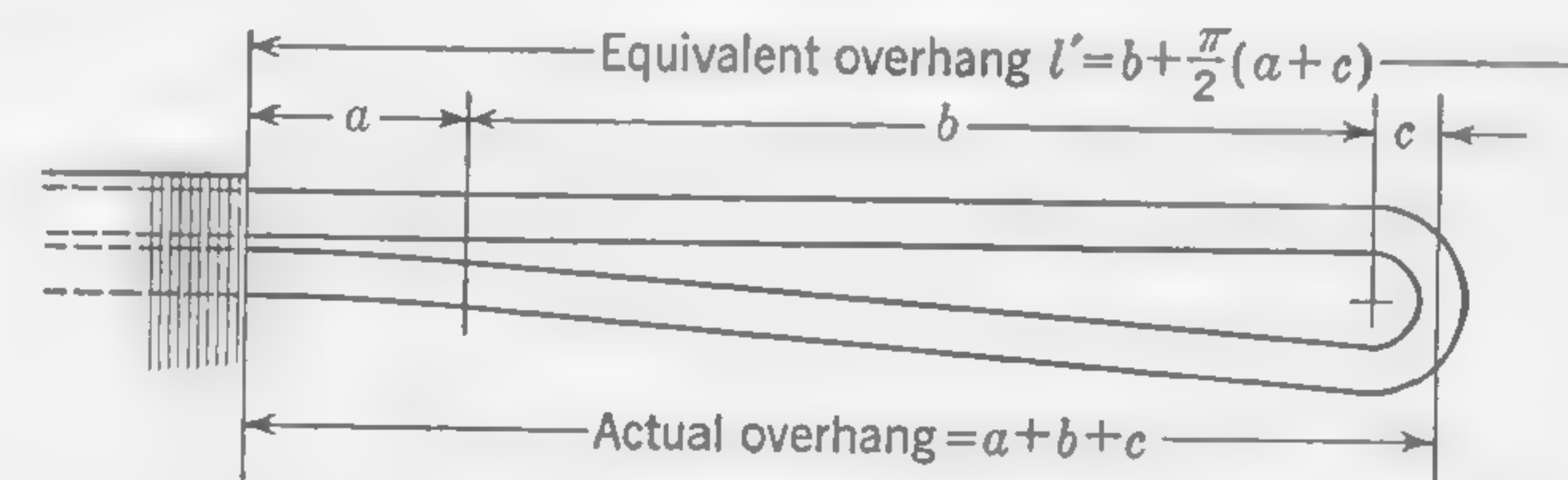


FIG. 92. Equivalent overhang of end connections in double-layer winding.

The permissible density in the teeth, as mentioned in Art. 72, rarely exceeds 100,000 lines per sq in. at 60 cycles and 115,000 lines per sq in. at 25 cycles. Higher densities may have to be used occasionally, but special attention must then be paid to the methods of cooling, in order to avoid excessive temperatures. The maximum value of the tooth density will depend upon the maximum value of the air-gap density, and this, in turn, is modified by armature distortion and slot leakage. The flux that must enter the core and be cut by the armature inductors is known, but the amount of flux entering the teeth under each pole face is greater, since it includes the slot-leakage flux in the neutral zone, the amount of which depends not only upon the current in the armature, but also upon its phase displacement (*i.e.*, upon the power factor of the load). Then, again, the maximum value of the air-gap flux density depends not only upon the average density, but also on the shape of the flux distribu-



tion over the pole pitch. It will not be necessary to go into details of this nature for the purpose of estimating the temperature rise of the armature, and a sinusoidal flux distribution may be assumed, making the maximum air-gap density  $\pi/2$  times the average value over the pole pitch. The calculation of slot-leakage flux will be explained later, and its effect may for the present be neglected.\*

As a check on the calculated core loss, the figure of Art. 52 may be used; but these values will depend upon whether the copper or the iron losses are the more important (*i.e.*, on the relative proportions of iron and copper in the machine). Iron losses 50 per cent in excess of the average values given on page 140 would not necessarily imply inefficiency or a high temperature rise.

When computing the total losses to be carried away, in the form of heat, from the surface of the armature core, the whole of the copper loss should not be added to the iron loss, but only the portion of the total  $I^2R$  loss which occurs in the buried part of the winding (*i.e.*, in the "active" conductors of length  $l_a$ ). In the case of large machines, it may be necessary to make some allowance for eddy-current loss in the armature conductors. This loss might be considerable if solid conductors were used; but it is usual to laminate the copper† in the slot so that the eddy-current loss due to the slot flux is very small. This point must not, however, be overlooked in large units; and special means may have to be adopted to avoid eddy-current loss in the armature conductors.

The eddy currents in the buried portions of the winding are due to two causes:

1. The flux entering the sides of the teeth through the top of the slot
2. The slot-leakage flux which the armature conductors themselves produce when the machine is delivering current to the circuit

The loss due to 1 is independent of the load and would be of importance in the case of solid conductors of large cross section in wide open slots. With narrow, or partially closed, slots, it is negligible; but occasion arises when it is advisable to laminate the conductors in the upper part of the slot to avoid appreciable loss due to this cause.

Item 2 may lead to very great additional copper losses if solid conductors of large cross section are used in narrow slots of considerable depth.

It is customary to calculate the  $I^2R$  losses at a temperature of 75°C and to include in the total copper losses an allowance to cover not only eddy-

\* The amount of the slot-leakage flux, expressed as a percentage of the total flux per pole, becomes of importance in well-designed machines only when the pole pitch is very small.

† Transposed Armature Coils in A-C Generators, by S. L. Henderson, *Elec. J.*, vol. 23, p. 348, July, 1926.

current losses in the armature winding itself, but all stray losses due to alternating magnetic fluxes which depend upon the load current. It is suggested that the calculated  $I^2R$  losses be increased from 20 to 30 per cent in the case of moderate-speed machines of medium size, but for large machines, especially steam-turbine-driven units of large output, the increase is usually not less than 50 per cent and may be as much as 100 per cent. With conductors of very large cross section, a considerable reduction in eddy-current losses due to skin effect is obtained with bars built up of a number of strips in parallel transposed so that each strip occupies in turn every position in the cross section of the slot. The manner in which the transpositions of the strands forming the conductor are obtained varies with different manufacturers.

**80. Cooling and Temperature Rise of Stators.** The temperature rise of stators of machines with salient-pole rotating field magnets is estimated by using formulas and proceeding generally as explained in the Illustrative Example of Art. 60. The cooling surfaces are calculated in a similar manner; but with the stationary armature and internal rotating field magnets, the belt of active conductors is the *inside* cylindrical surface of the armature; and this is cooled by the air thrown against it by the fanning action of the rotor. The cooling coefficient, containing the factor  $v$  (the peripheral velocity), may be used, just as if the armature were rotating instead of the field magnets. The external cylindrical surface of the armature core will have no air blown against it (in the self-ventilating machine), and the value of  $v$  in the formula will be zero. In regard to the radial vent ducts, the cooling is not quite so good as when the armature rotates, but a blast of air is driven through the ducts, and this is effective in carrying off the heat. The difficulty in determining cooling coefficients that will be applicable to all sizes and types of machine stands in the way of obtaining great accuracy in the calculation of temperature rise. It is, however, suggested that formulas (50) and (51) be used and that the temperature rise of stators, as calculated by the application of these formulas, be increased 20 per cent. A temperature rise of 45°C is usually permissible.

High-speed machines, such as turbo-alternators, when provided with forced ventilation, are usually totally enclosed, the air passages being suitably arranged to prevent the outgoing (hot) air being mixed with the incoming (cool) air. Large ducts must be provided for conveying the air to and from the machine. A safe rule is to provide ducts or pipes of such a cross section that the mean velocity of the air will not exceed 2,000 fpm.

Hydrogen gas as a cooling medium in place of air has been tried and found to give such satisfactory results that its use for the cooling of turbo-generators may be justified. A great many high-capacity alternators and synchronous condensers, which are totally enclosed in gas-



tight casings, are presently in service, with hydrogen as the cooling medium, in place of air.\*

**81. Illustrative Example. Forced Ventilation of Turbo-generator.** Calculate (a) the average velocity of the air through the vent ducts; (b) the approximate surface temperature rise; and (c) the weight of air required per hour of an 8,000-kw 6,600-volt 60-cycle a-c generator direct-coupled to a steam turbine running at 1,800 rpm. Assume the following dimensions and other particulars.

The machine is entirely enclosed and cooled by air forced through longitudinal ducts in rotor and stator. There are no radial ducts, and the cooling air passes from end to end of the machine in a direction generally parallel to the shaft. The total cross section of all air ducts, including the air gap between rotor and stator and also spaces between the outside of the stator stampings and the cast-iron casing, is 6.6 sq ft. The total surface area of all the ducts in contact with the cooling air is 130,000 sq in. The total of all the losses to be carried away by the circulating air amounts to 290 kw, which includes the losses in the laminated iron of the stator and the  $I^2R$  losses in both stator (armature) and rotor (field) windings.

*Calculation a.* On the basis of 100 cu ft of air per minute per kilowatt (Art. 58) the average velocity in the ducts is  $(290 \times 100)/6.6 = 4,400$  fpm.

*Calculation b.* In the absence of detailed particulars regarding the construction of the machine, and empirical data relating to the cooling coefficients for the different kinds of ducts and surface conditions, we may use formula (51) to calculate the average cooling coefficient. This will, however, give no more than a rough indication as to whether or not there is likely to be overheating of the surfaces in contact with the air. The approximate cooling coefficient is  $c_d = 4,400/100,000 = 0.044$  watt per sq in. per degree centigrade rise of temperature, whence the approximate surface temperature rise of the ducts is

$$\frac{290,000}{0.044 \times 130,000} = 50^\circ\text{C}$$

*Calculation c.* The weight of a cubic foot of air is about 0.072 lb, whence the weight of air passing through the machine per hour is  $60 \times (290 \times 100) \times 0.072 = 125,000$  lb, or  $62\frac{1}{2}$  tons. It is interesting to

\* KNOWLTON, RICE, and FREIBURGHOUSE, Hydrogen as a Cooling Medium for Electrical Machinery, *Trans. AIEE*, vol. 44, pp. 922-932, 1925; D. S. SNELL, The Hydrogen-cooled Turbine Generator, *Trans. AIEE*, vol. 59, pp. 35-45, January, 1940; R. B. ROBERTS, Hydrogen Cooling for Turbine Generators, *West. Eng.*, vol. 7, no. 5, pp. 138-142, September, 1947; C. J. FECHHEIMER, Liquid Cooling of A-C Turbine Generators, *Trans. AIEE*, vol. 69, pp. 165-170, 1950.

note that the weight of cooling air which passes through a steam-turbine-driven generator in 1 hr is frequently appreciably greater than the total weight of the machine.

**82. Illustrative Example. Design of Armature (Stator) of A-C Generator.** Design the armature of the turbo-generator described in the following specification:

Output, kva.....	8,000
Number of phases.....	3
Terminal voltage.....	6,600
Power factor of load.....	0.8
Frequency.....	60
Type of drive.....	Steam turbine
Speed, rpm.....	1,800
Inherent regulation.....	Within 25 per cent rise when full load is thrown off
Exciting voltage.....	130
Permissible temperature rise after 6-hr, full-load run (by thermometer).....	45°C
Ventilating fan.....	Independently driven (not part of generator)

Turbo-alternators have been built in America in sizes exceeding 100,000 kva output at 1,800 and 3,600 rpm. Machines of European design have been built in single units larger than 100,000-kva output at speeds of 1,500 and 3,000 rpm. With the great weight of the slotted rotors, carrying insulated exciting coils and traveling at very high peripheral velocities, new problems have arisen, and these problems should be seriously studied by anyone proposing to take up the design of modern electrical machinery. Engineering textbooks may constitute a basis of necessary knowledge; but, with the rapid advance in this field of electrical engineering, the information of greatest value (apart from what the manufacturing firms deliberately withhold) is to be found in current periodical publications, including the papers and discussions appearing in the journals of the engineering societies.

Since it will not be possible to discuss the mechanical details of turbo-alternator designs in these pages, a machine of small size (8,000 kva) has been chosen, and the peripheral speed of the rotor will not be permitted to exceed 18,000 fpm. The mechanical difficulties will, therefore, not be so great as in some of the larger machines running at higher peripheral velocities, and the electrical features of the design will be considered alone, reference being made to mechanical details only as occasion may

Although this problem deals with the design of an armature for a high-speed machine provided with a cylindrical field magnet, an attempt will be made to render it of use in the design of armatures for slow-speed



salient-pole machines, and, with this end in view, the items in the design sheet as shown on page 199 are arranged so as to cover both types of machine.

## CALCULATIONS

Items 1 to 12. With a frequency of 60 cycles per sec and a speed of 1,800 rpm, the number of poles is

$$p = \frac{2 \times 60 \times 60}{1,800} = 4$$

At a peripheral velocity of 18,000 fpm, the diameter of the rotor would be  $(18,000 \times 12)/(1,800 \times \pi) = 38.2$  in.

Since the air gap is not likely to be much less than 1 in., let us decide upon an internal diameter of the armature  $D = 40$  in. (item 11) and determine the exact dimensions of the rotor after the air gap has been decided upon.

The line current (item 4) is

$$I = \frac{8,000,000}{\sqrt{3} \times 6,600} = 700 \text{ amp}$$

and, if we select the star connection of phases, this is also the current per phase winding (item 8).

The volts per phase are  $6,600/\sqrt{3} = 3,810$ .

Referring to Art. 71 for values of the specific loading, we find that the average value there suggested is  $q = 860$ .

The pole pitch (item 12) is

$$\tau = \frac{\pi \times 40}{4} = 31.416 \text{ in.}$$

and since

$$(TI)_a = \left[ \left( \frac{\pi D}{p} \right) \left( \frac{Z' I_c}{\pi D} \right) \frac{1}{2} \right] = \frac{\tau q}{2}$$

the approximate armature ampere-turns per pole (item 9) will be

$$(TI)_a = \frac{31.42 \times 860}{2} = 13,500$$

Referring to Art. 72, we can get a preliminary idea of the required length of air gap. We shall, in this design, deliberately select a high value for the air-gap flux density and, if necessary, saturate the teeth of the rotor while keeping the density in the armature teeth within reasonable limits to prevent excessive hysteresis and eddy-current loss. Let us try  $B_g'' = 39,000$  lines per sq in., which is higher than the upper limit of

DESIGN SHEET FOR ARMATURE OF A-C GENERATOR  
(Dimensions in inches unless otherwise stated)

	Sym-bols	Assumed or approximate values	Final values
1 Number of poles.....	$p$	.....	4
2 Peripheral speed (fpm).....	$v$	18,000	
3 Diameter of rotor.....	.....	32.2	38.25
4 Line current.....	$I$	.....	700
5 Phase connection (star or delta).....	.....	Y	Y
6 Volts per phase.....	.....	.....	3,810
7 Specific loading.....	$q$	860	800
8 Current in armature conductors.....	$I_c$	.....	700
9 Armature ampere-turns per pole.....	$(TI)_a$	13,500	
10 Length of air gap at center.....	$\delta$	$\frac{7}{8}$	$\frac{7}{8}$
11 Internal diameter of stator (armature).....	$D$	40	40
12 Pole pitch.....	$\tau$	.....	31.416
13 Pole arc.....	.....	Distributed winding	
14 Percentage of armature covered by poles.....	.....	Distributed winding	
15 Number of inductors per phase.....	$Z$	51.5	48
16 Total number of inductors.....	$Z'$	.....	144
17 Number of armature slots per pole per phase.....	$n_s$	4	4
18 Total number of slots in armature.....	.....	.....	48
19 Slot pitch.....	$\lambda$	2.62	2.62
20 Number of inductors per slot.....	$C_s$	3	3
21 Flux per pole (no load).....	$\Phi$	$62.7 \times 10^6$	$62.7 \times 10^6$
22 Average flux density over pole pitch (open circuit).....	$B_g''$	39,000	38,800
23 Axial length of armature core (gross).....	$l_a$	51	51
24 Axial length of armature core (net).....	$l_n$	46.8	46.8
25 Type of winding.....	.....	Single-layer	
26 Current density in armature conductors.....	$\Delta$	2,000	2,000
27 Size of conductor.....	.....	.....	$4 \times \frac{5}{8} \times 0.14$
28 Slot width.....	$s$	.....	1
29 Slot depth.....	$d$	.....	$4\frac{1}{8}$
30 Apparent tooth density (no load) at center of tooth.....	$B_t''$	.....	92,000
31 Flux density in armature core, lines per sq in.....	.....	.....	55,500
32 Radial depth of armature core below slots.....	$R_d$	.....	14
33 Weight of iron in core, lb.....	.....	.....	28,000
34 Weight of iron in teeth, lb.....	.....	.....	4,900
35 Total core loss, including teeth (kw)—open circuit.....	.....	.....	100
36 Length mean turn of armature winding.....	.....	.....	210
37 Resistance per phase, ohms.....	.....	.....	0.01135
38 $I^2R$ drop per phase (full-load current), volts.....	.....	.....	8.4
39 Total armature copper loss (full-load current), kw.....	.....	.....	25
40 Amount of copper loss to be radiated from core.....	.....	.....	
41 Approximate temperature rise of armature.....	.....	.....	
42 $IX$ drop (ends), volts per phase winding.....	$E_{dP}$	(see Fig. 90)	150
43 Full-load developed, volts per phase winding.....	$O E_d$	(see Fig. 90)	3,910



the range suggested in Art. 72. The principal advantage of using high flux densities is that the axial length of the rotor can thus be reduced; but, if it is found later that the selected value of  $B_g''$  leads to unduly high flux density in the teeth, it will have to be modified. By formula (70) on page 180, we have

$$\delta = 1.25 \frac{860 \times 31.42}{39,000} = 0.866, \text{ or (say) } \frac{7}{8} \text{ in.}$$

In the case of medium-speed salient-pole designs, the peripheral velocity would not be decided upon by merely selecting the upper limit of 8,000 fpm as given in Art. 68. This has to be considered in connection with the pole pitch (see Art. 71), a preliminary diameter of rotor being selected in keeping with what seems to be a reasonable pole pitch. A few rough calculations will very soon show whether or not the tentative value of  $\tau$  will lead to a suitable axial length of armature core.

Items 15 to 20. On the basis of  $q = 860$ , the number of conductors per phase would be

$$Z = \frac{1}{3} \left( \frac{\pi D q}{I_c} \right) = 51.5$$

With four slots per pole per phase, and three conductors in each slot, we have  $Z = 3 \times 4 \times 4 = 48$ , which is close enough to the desired value. Furthermore, the fact that each slot will contain three conductors, an odd number, means that only a *single-layer* winding is possible; a double-layer winding always involves an even number of conductors per slot. Each of the eight coils per phase will, therefore, have three turns in series [ $48/(2 \times 8) = 3$ ]. To construct such a single-layer winding in a 48-slot core requires a coil span of 13 slots; i.e., the coil pitch must be from slot 1 to slot 14, from an odd-numbered to an even-numbered slot. Such a pitch, one slot beyond full pitch, is electrically equivalent to a fractional-pitch winding each of whose coils is one slot short of full pitch or 180 electrical degrees. Therefore,  $k' = \sin (165/2) = 0.991$ . Also, with three slots per pole per phase,  $k = 0.958$ . Hence  $d = 0.991 \times 0.958 = 0.950$ .

A complete diagram showing the coil arrangement and winding connections is given in Fig. 93.

For item 19 we have  $\lambda = 31.416/12 = 2.62$  in., giving a corrected value for peripheral loading of

$$q = \frac{700 \times 3}{2.62} = 800 \text{ (approx)}$$

Items 21 to 24. For the purpose of calculating the flux required on open circuit, we may use formula (61a) of Art. 69, where  $E_{\text{per phase}}$

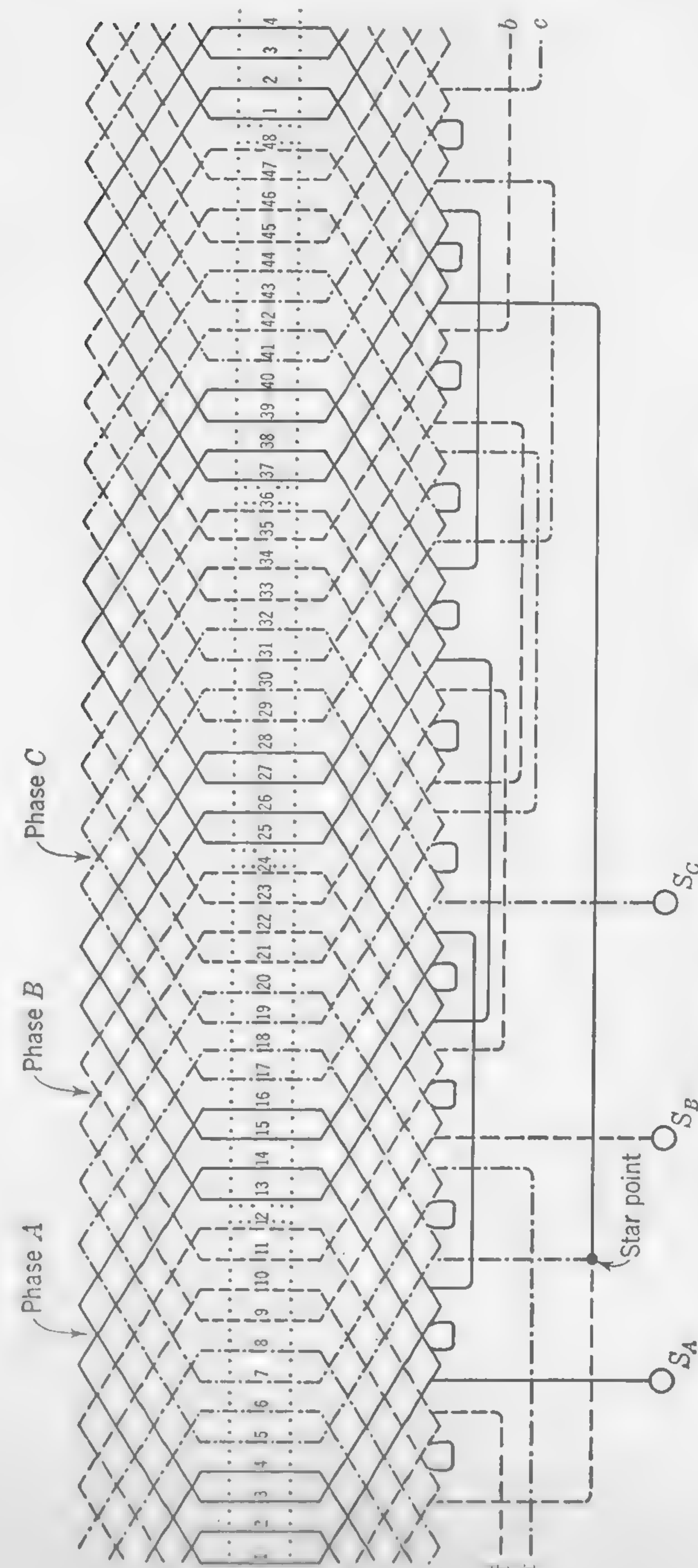


Fig. 93. Winding diagram for Illustrative Example of Art. 82.



6,600/ $\sqrt{3}$ . The required flux per pole is, therefore,

$$\begin{aligned}\Phi &= \frac{6,600 \times 10^8}{\sqrt{3} \times 2.22 \times 0.950 \times 60 \times 48} \\ &= 62.7 \times 10^6 \text{ maxwells}\end{aligned}$$

With the assumed value of 39,000 lines per sq in. for  $B''_o$ , the axial length of armature core will be

$$l_a = \frac{62.7 \times 10^6}{39,000 \times 31.42} = 51.2 \text{ in., or (say) 51 in.}$$

This is a short armature for a machine with a rotor 38.25 in. in diameter; but it is what we are aiming at, and, if the field winding can be accommodated in the space available, the design should be satisfactory.

We shall attempt to ventilate this generator by means of axial air ducts only, which is admittedly not in accordance with modern practice for the larger steam-turbine-driven generators but should be satisfactory in connection with this machine of comparatively small size. If, then, there are no radial air spaces, the net length of iron in the armature core will be approximately  $l_n = 0.92l_a = 46.8$  in. (Art. 16); but these dimensions cannot be finally decided upon until the slot proportions and tooth densities have been settled.

*Items 25 to 30.* As previously pointed out, a single-layer winding must be used (see Art. 73). The current density in the armature windings cannot be determined by the empirical formula of Art. 74, because this is not applicable to speeds higher than 8,000 fpm, and, in any case, the conditions of cooling in an enclosed machine with forced ventilation are not the same as for a self-ventilating generator. In a turbo-alternator there is usually plenty of room for the armature conductors, the chief trouble being with the rotor winding which may have to be worked at a high current density. There is no definite rule for the most suitable current density in the armature conductors, the permissible copper cross section being dependent on the length of armature core, the position and area of the vent ducts, and the supply of air that can economically be passed through the machine. The specific loading will obviously have some effect on the allowable current density in the copper; and, as a guide in making a preliminary estimate, we may use the formula

$$\Delta = \frac{1,600,000}{q}$$

which gives us for item 26 a current density of 2,000 amp per sq in. of armature copper.

It is well to laminate the conductors in a direction parallel to the slot-

leakage flux, and we may build up each conductor of four flat strips each  $\frac{5}{8}$  by 0.14 in., giving a total cross section of 0.35 sq in. per conductor.

There will be 12 copper strips in each slot, the total thickness, including the cotton insulation, being about 1.92 in. To determine the slot insulation, formula (16) in Art. 13 cannot be used since it applies to machine voltages below 2,000; for voltages between 6,000 and 14,000 a formula which agrees with modern practice is

$$\text{Thickness of slot insulation (one side) in mils} = 50 + \frac{E}{55}$$

The slot insulation will, therefore, be  $50 + (6,600/55) = 170$  mils, and the total slot space for winding and insulation will be 1 in. wide by  $2\frac{1}{4}$  in.

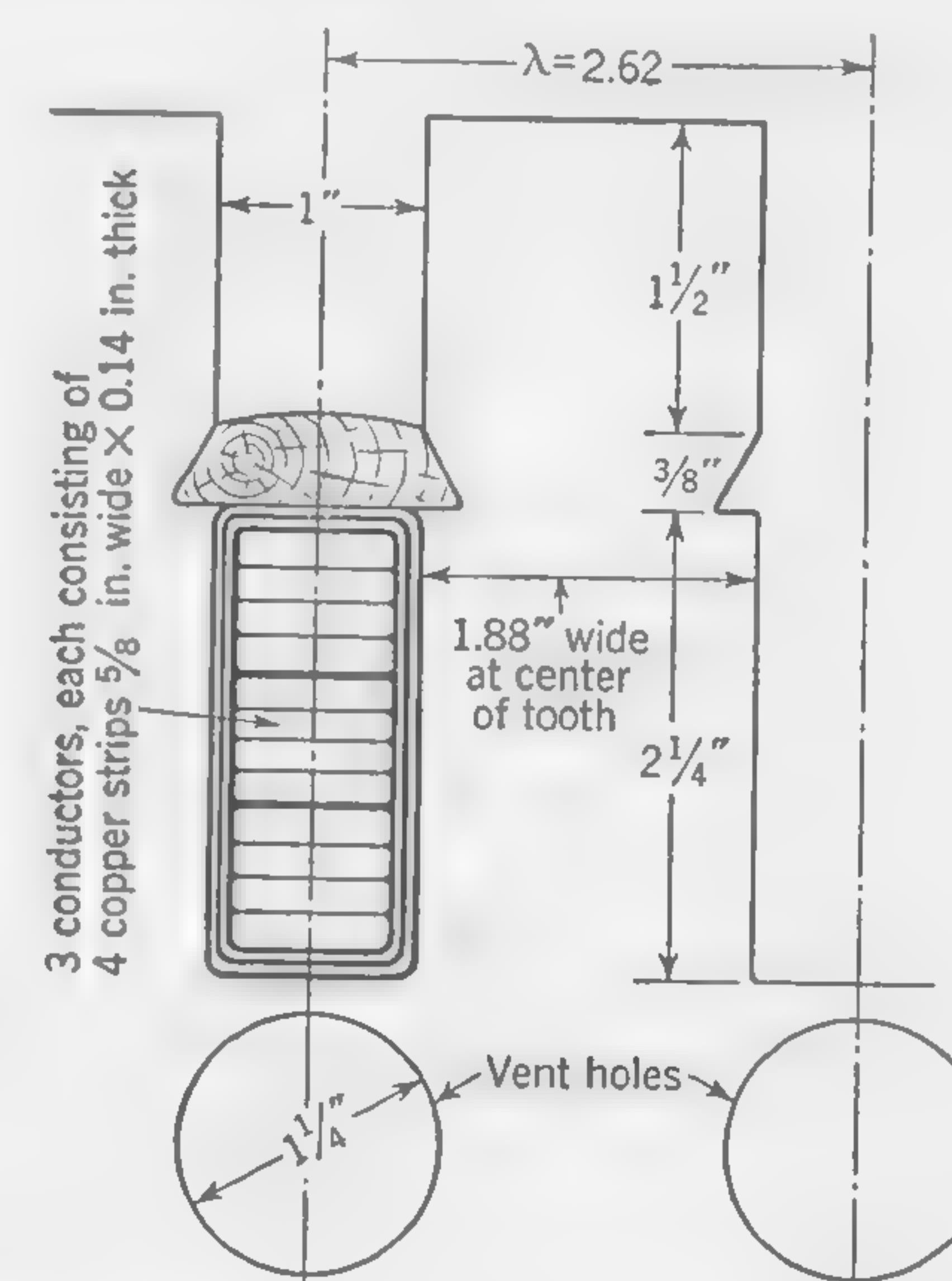


FIG. 94. Details of armature (stator) slot, Illustrative Example, Art. 82.

deep. The thickness of wedge might be  $\frac{3}{8}$  in., and we shall, in this design, allow an extra slot depth of  $1\frac{1}{2}$  in. above the wedge, with a view to increasing the slot inductance, and so limiting the instantaneous rush of current in the event of a short circuit. This increased armature inductance might have been obtained by using a smaller width and greater depth of copper conductor; but, inasmuch as the width of tooth will probably be sufficient, the proposed design of slot (as shown in Fig. 94) has the advantage that the eddy-current loss in the armature inductors will be very small.

The width of copper strip has been selected to fit into the 1-in. slot, because this seems to provide a suitable cross section for the stator tooth. Thus, a section halfway down the tooth, or (say) 2 in. from the top, will have a diameter of .44 in., and the average width of tooth will be  $[(\pi \times$



44)/48] - 1 = 1.88 in. On the basis of  $B_g'' = 38,800$  lines per sq in., and a sinusoidal flux distribution over the pole pitch, the "apparent" tooth density (item 30) would be

$$\frac{\pi}{2} B_g'' \frac{\lambda l_a}{t l_n} = \frac{\pi \times 38,800 \times 2.62 \times 51}{2 \times 1.88 \times 46.8} = 92,000 \text{ lines per sq in.}$$

which is not too high (see Art. 72).

Items 31 to 35. Assuming a flux density of 55,500 lines per sq in. in the armature core (see Art. 79), the net radial depth of stampings below the slots will be

$$\frac{62.7 \times 10^6}{2 \times 55,500 \times 46.8} = 12.1 \text{ in.}$$

The actual radial depth should be greater than this to allow for the reduction of section due to the presence of axial vent ducts. In this particular machine it is proposed to ventilate, if possible, with axial ducts only, and a fairly large cross section of air passages must, therefore, be allowed. An adequate supply of air will probably be obtained if the total cross section of air duct through the body of the stampings in square inches is not less than  $0.005 \times$  cubic inches of iron in stator below slots. In this case the volume of iron in the stator ring will be approximately  $\pi(48.25 + 12.1) \times 12.1 \times 46.8 = 107,500$  cu in.; and the total cross section of air ducts in the stampings should be  $0.005 \times 107,500 = 537.5$  sq in.

The actual radial depth of stamping below the teeth can be calculated by assuming that the air ducts reduce the gross depth by an amount equal to  $\frac{537.5}{\text{average circumference}}$ , or (say)  $\frac{537.5}{\pi \times 62} = 2\frac{3}{4}$  in. Let us make the depth  $R_d$  (item 32) = 14 in. and provide vent ducts arranged generally as shown in Fig. 95, where there are 10 holes per slot, each  $1\frac{1}{4}$  in. in diameter, making a total air duct cross section in the armature stampings of  $(\pi/4) \times (1.25)^2 \times 10 \times 48 = 589$  sq in.

The weight of iron in core (item 33), is

$$0.28 \times 46.8 \times \{\pi[(38.125)^2 - (24.125)^2] - 589\} = 28,000 \text{ lb (approx)}$$

The weight of the iron in the teeth (item 34) is

$$0.28 \times 46.8 \times \{\pi[(24.125)^2 - (20)^2] - (48 \times 1 \times 4.125)\} = 4,900 \text{ lb}$$

Taking the approximate flux densities as previously calculated (items 30 and 31), and referring to the iron-loss curve (Fig. 67), the iron loss per pound for carefully assembled high-grade armature stampings is found to be 6.35 and 2.45 watts in teeth and core respectively.\* The

\* The figures as read off the curve have been reduced 20 per cent.

loss in the teeth\* is, therefore,  $6.35 \times 4,900 = 31,100$  watts, and in the core below the slots,  $2.45 \times 28,000 = 68,600$  watts, making a total iron loss of (say) 100 kw, or 1.25 per cent of the rated kilovolt-ampere output.

Items 36 to 39. In a machine of so large an output as the one under consideration, the weight and cost of copper should be determined by making a drawing of the armature coils and carefully measuring the length

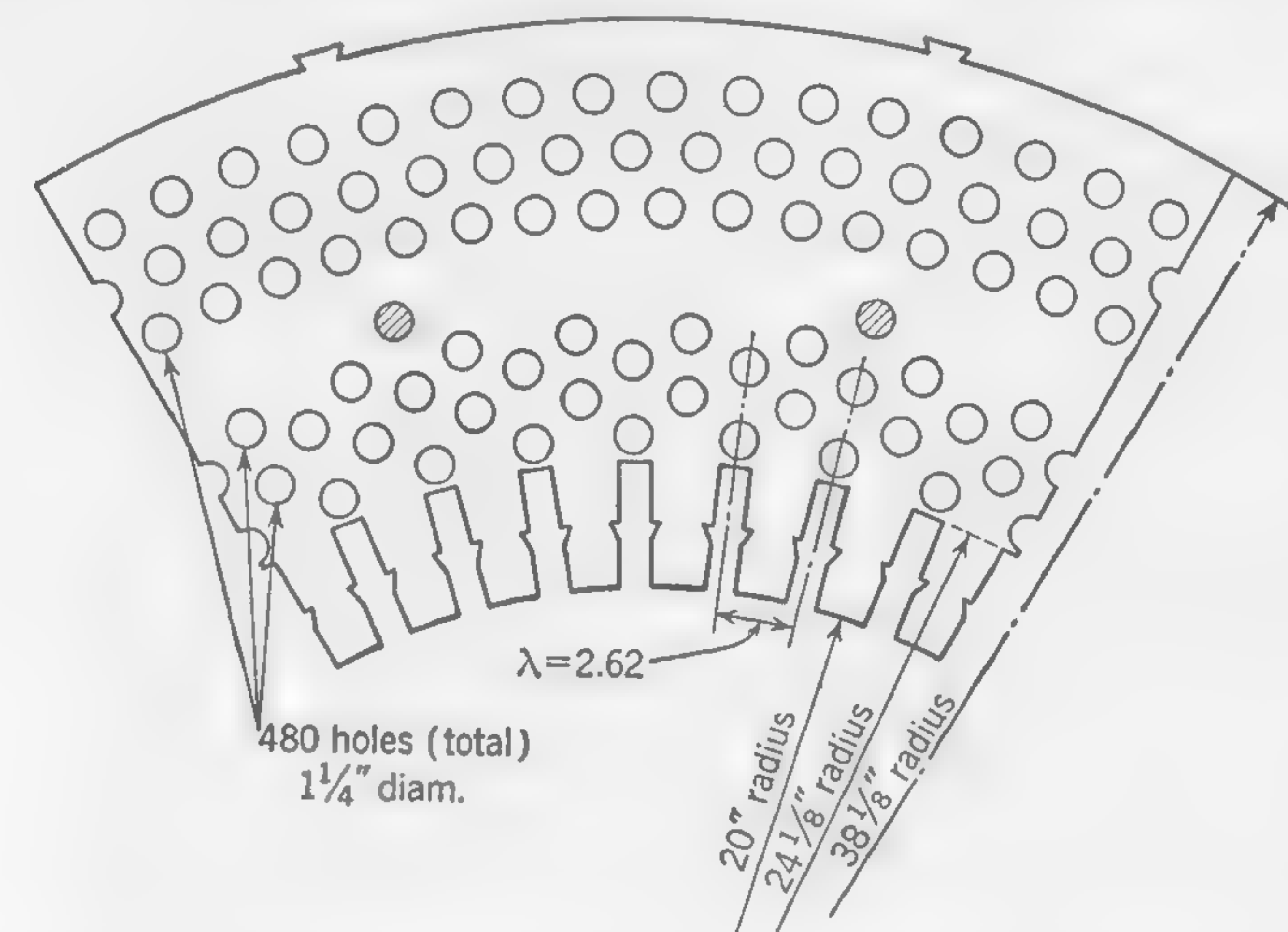


FIG. 95. Armature stamping of 8,000-kva turbo-alternator, Illustrative Example, Art. 82.

required. Since this design is being worked out for the purpose of illustration only, we shall use the formula (71) of page 188 and assume the length per turn of armature winding (item 36) to be

$$(2 \times 51) + (2.5 \times 31.42) + (2 \times 6.6) + 6 = 199.8 \text{ in.}$$

It will be safer to use the figure 210 in. for this mean length, because all the coils will probably be bent back and secured in position by insulated clamps in order to resist the mechanical forces which tend to displace or bend the coils when a short circuit occurs.

The cross section of the conductor (four strips in parallel) is 0.35 sq in., or 445,000 cir mils. The number of turns per phase is 24, and, since the resistance per circular-mil-inch at 60°C is 1 ohm, the resistance per phase at 60°C is  $(210 \times 24)/445,000 = 0.01135$  ohm. The  $IR$  drop per phase (item 38) is  $0.01135 \times 700 = 7.95$ , or (say) 8.4 volts, in order to include

\* It is here assumed that the apparent flux density at the center of tooth is about the same as the actual flux density at a point one-third of the slot depth measured from the narrow end of the tooth, which is the section recommended for tooth-loss calculations in Art. 52.



the effect of eddy currents in the conductors. The  $I^2R$  loss in armature winding (item 39) is  $3 \times 0.01135 \times (700)^2 = 16,700$  watts, which should be increased about 50 per cent (see Art. 79) to cover sundry indeterminate load losses. The total full-load armature copper loss may, therefore, be estimated at 25 kw, or 0.31 per cent of the rated full-load kilovolt-ampere output.

*Items 40 and 41.* These are included because they would be required in connection with the design of a self-ventilated, slow-speed, open-type generator for which the calculations are made generally as for a d-c generator (refer to Art. 60). In the case of a turbo-alternator cooled by forced ventilation, the necessary supply of air to be passed through the machine would be calculated after all the losses, including those in the rotor field windings, have been determined.

*Items 42 and 43.* The reactive voltage drop per phase due to the cutting of the end flux cannot be predetermined accurately; but we may use the empirical formula (75) of Art 78, wherein the symbols have the following numerical values:

$$n = 3, k = 3.5, d = 0.950, f = 60, n_s = 4, C_s = 3, p = 4$$

The equivalent average projection of the winding beyond the ends of the slots may be computed by noting that, with a mean length per turn of 210 in., the average projection beyond ends of slots will be

$$l' = \frac{210 - 2(51 + 31.42)}{4} \times 2.54 = 28.7 \text{ cm}$$

Since we have a single-layer winding, the factor  $\pi/2$  must be introduced into the formula (75), whence—with the current  $I_c = 700$ —the reactive voltage due to cutting of end flux, with full-load current per phase, is

$$700 \times \frac{\pi}{2} \times 3 \sqrt{2} \times 3.5(0.950)^2 60(4 \times 3)^2 4 \times 28.7 \times 10^{-8} \\ = (\text{say}) 150 \text{ volts}$$

We are now in a position to draw a vector diagram similar to Fig. 90 and calculate the length of the vector  $OE_d$  which represents the full-load developed voltage and is, therefore, a measure of the flux actually cut by the conductors at full load. (The flux entering the teeth through the air gap is somewhat greater, since it must include the slot-leakage flux which is not cut by the conductors and, therefore, does not produce an emf in the armature windings.) The numerical values of the component vectors are:

$$OE_t = 3,810 \quad E_t P = 8.4 \quad PE_d = 150$$

The angle  $\theta$  is  $36^\circ 0' 52''$ , since the power factor  $\cos \theta$  is specified as 80 per cent. Thus, the full-load developed voltage (item 43) is

$$OE_d = \sqrt{(OE_t \cos \theta + E_t P)^2 + (OE_t \sin \theta + PE_d)^2} \\ = 3,910 \text{ volts}$$

This is the last item called for in the design sheet, and all the quantities required in connection with this problem have been calculated.

The design of the field magnet (rotor) for this machine will be taken up at the close of the next chapter.

### TEST PROBLEMS

1. (a) At what speed must an 8-pole 60-cycle alternator be driven? (b) What is the pole pitch in inches, if the peripheral velocity is 6,000 fpm?

Ans. (a) 900 rpm, (b) 10.

2. An alternator runs at a peripheral speed of 6,600 fpm, and it has 8 poles. The speed is 900 rpm. Calculate (a) the frequency, (b) the pole pitch.

Ans. (a) 60 cycles, (b) 11 in.

3. A 12-pole alternator runs at 250 rpm and has a pole pitch of 16 in. Calculate (a) the frequency, (b) the peripheral velocity. Ans. (a) 25 cycles, (b) 4,000 fpm.

4. Given the following alternator data: axial length of armature (gross) = 15 in.; sinusoidal flux distribution over armature surface, with maximum value of 7,000 gauss; flux per pole = 3,600,000 maxwells. Calculate the pole pitch in inches. Ans. 8.35.

5. Given: alternator with maximum air-gap flux density of 7,400 gauss; pole pitch = 6.25 in.; axial length of armature = 10 in.; flux distribution sinusoidal. Calculate the flux per pole. Ans. 1,895,000 maxwells.

6. Calculate the output in kilowatts of a three-phase star-connected generator on a load of power factor 0.8, when the volts between line and neutral point are 3,200, and the current per phase is 110 amp. Ans. 845 kw.

7. A 3-phase 250-kva alternator is delivering power at 80 per cent power factor. All three phases are equally loaded, and the line voltage is 2,200. Calculate the full-load current in the armature windings (a) if the windings are delta-connected, (b) if the windings are star-connected. Ans. (a) 37.9 amp, (b) 65.6 amp.

8. Given: three-phase generator, specific loading = 573; armature diameter = 4 ft; star-connected windings; 12 poles; 2 slots per pole per phase; line current = 100 amp. Calculate the number of inductors per slot. Ans. 12.

9. The line current of a 2,200-volt 3-phase generator operating at 85 per cent power factor is 247 amp. Calculate (a) the output in kilowatts, (b) the armature current when the windings are delta-connected. Ans. (a) 800 kw, (b) 142.5 amp.

10. Given a 3-phase Y-connected 2,200-volt generator, with an armature diameter of 4 ft and specific loading of 400 amp-conductors per inch of armature periphery, delivering 100 kw on 70 per cent power factor. Calculate (a) the amperes per phase in the armature winding, (b) the number of inductors per phase. Ans. (a) 37.5 amp, (b) 536.

11. Given: flux per pole = 1,900,000 maxwells; pole pitch = 6.25 in.; gross length of armature core = 10 in. Calculate the maximum value of the air-gap density if the flux distribution is sinusoidal. Ans. 47,800 lines per sq in.

12. A certain 3-phase 2,200-volt star-connected generator has 7 inductors per slot, 2 slots per pole per phase, 36 poles, and is driven at 200 rpm. Calculate the no-load flux per pole on the assumption of sinusoidal flux distribution over the pole pitch. Ans. 1,960,000 maxwells.

13. A 3-phase 600-volt delta-connected 60-cycle 16-pole generator has 1 slot per



pole per phase with a total of 480 inductors per phase, the form factor being 1.15. Calculate the useful flux per pole. *Ans.* 905,000 maxwells.

14. Given: 3-phase star-connected, 2,200-volt 60-cycle generator, with 10 poles, 2 slots per pole per phase, a sine wave emf, and a flux per pole of 3,800,000 maxwells. Calculate the number of inductors in each slot. *Ans.* 13.

15. Given: flux per pole = 1,500,000 maxwells; sine-wave flux distribution; pole pitch = 8 in.; length of armature core (gross) =  $7\frac{3}{4}$  in.; length of armature core (net) =  $6\frac{1}{2}$  in.; tooth pitch = 2 in.; tooth width (average) = 1 in. Calculate the maximum value of the apparent flux density in the teeth. *Ans.* 90,700 lines per sq in.

16. Given: ampere-turns per pole to overcome air-gap reluctance = 7,000; average air-gap density over slot pitch at center of pole = 7,500 gauss; permeance of air gap over area of slot pitch at center of pole = 50; slot pitch =  $1\frac{1}{2}$  in. Calculate the gross length of armature core. *Ans.* 6.06 in.

17. Given: flux per slot pitch at center of pole = 580,000 maxwells; slot pitch = 1.5 in.; axial length of armature core (gross) = 10 in.; ampere-turns required to overcome reluctance of air gap at center of pole = 8,000. Calculate the average permeance per square centimeter of the air gap under center of pole. *Ans.* 0.597.

18. Given:  $\Delta = (700,000/q) + (v/5)$  being the current density (in amperes per square inch) in the armature conductors of a 3-phase star-connected 8-pole generator with pole pitch = 12 in.; frequency = 60; line current = 100 amp; 3 slots per pole per phase; 6 inductors per slot; gross axial length of armature = 12 in.; length of "active" copper = 50 per cent of total. Calculate (a) the size of armature wire in circular mils, (b) the resistance per phase winding. (Assume a temperature of 60°C.) *Ans.* (a) 42,500, (b) 0.0814 ohm.

## CHAPTER 8

### SYNCHRONOUS GENERATORS (Continued)

#### FIELD MAGNET DESIGN—ARMATURE REACTION

**83. The Magnetic Circuit.** Except for the fact that the field magnets usually rotate, the design of the complete magnetic circuit of an a-c generator differs little from that of a d-c dynamo. Given the ampere-turns required per pole, and the voltage of the continuous-current circuit from which the exciting current is obtained (usually about 125 volts), the procedure for calculating the size of wire required is the same as would be followed in designing any other shunt coils (see Illustrative Example of Art. 50). When estimating the voltage per pole across the field winding, a suitable allowance must be made for the pressure absorbed by the rheostat in series with the field windings. The exact amount of excitation required under any given condition of loading can, of course, be determined only after the complete magnetic circuit has been designed.

In the absence of reliable data on any particular type and size of self-ventilated machine, the curve of Fig. 96 may be used for selecting a suitable cooling coefficient. The cooling surface considered includes, as before, the inside surface near the pole core and the two ends, in addition to the outside surface of the coil. It is to be understood that the cooling coefficient obtained from Fig. 96 is approximate only, being an average of many tests on different sizes and shapes of coils on rotating field magnets.

In determining the amount by which the pole must project from the yoke ring, it is well to allow about 1 in. of radial length of winding space for every 1,500 amp turns per pole required at full load (*i.e.*, estimated maximum excitation). An effort should be made to keep the radial projection of the poles as small as possible in order to prevent excessive magnetic leakage (refer to Arts. 41 and 42).

The current density in the field-magnet windings of salient-pole, rotating-field, a-c generators is usually between 1,100 and 1,600 amp per sq in.

The required useful flux per pole being known, the flux to be carried by pole core and yoke may be calculated if the leakage factor is known. The leakage coefficient will be low in machines with large pole pitch, and high in the case of slow-speed engine-driven generators with a large num-



ber of closely spaced poles. The following approximate values may be used for estimating the flux in poles and yoke ring.

High values; to be selected when pole pitch is small, and radial length of pole core great in proportion to width.....	1.35 to 1.45
Average values; for pole pitch 8 to 12 in. and length of winding space about equal to width of pole core.....	1.25 to 1.35
Low values; for large pole pitch and small radial length of pole core....	1.15 to 1.25

Provided a reasonably high leakage factor has been used, the cross section of the poles and yoke of good dynamo steel may be calculated for a flux density of 85,000 to 100,000 lines per sq in.

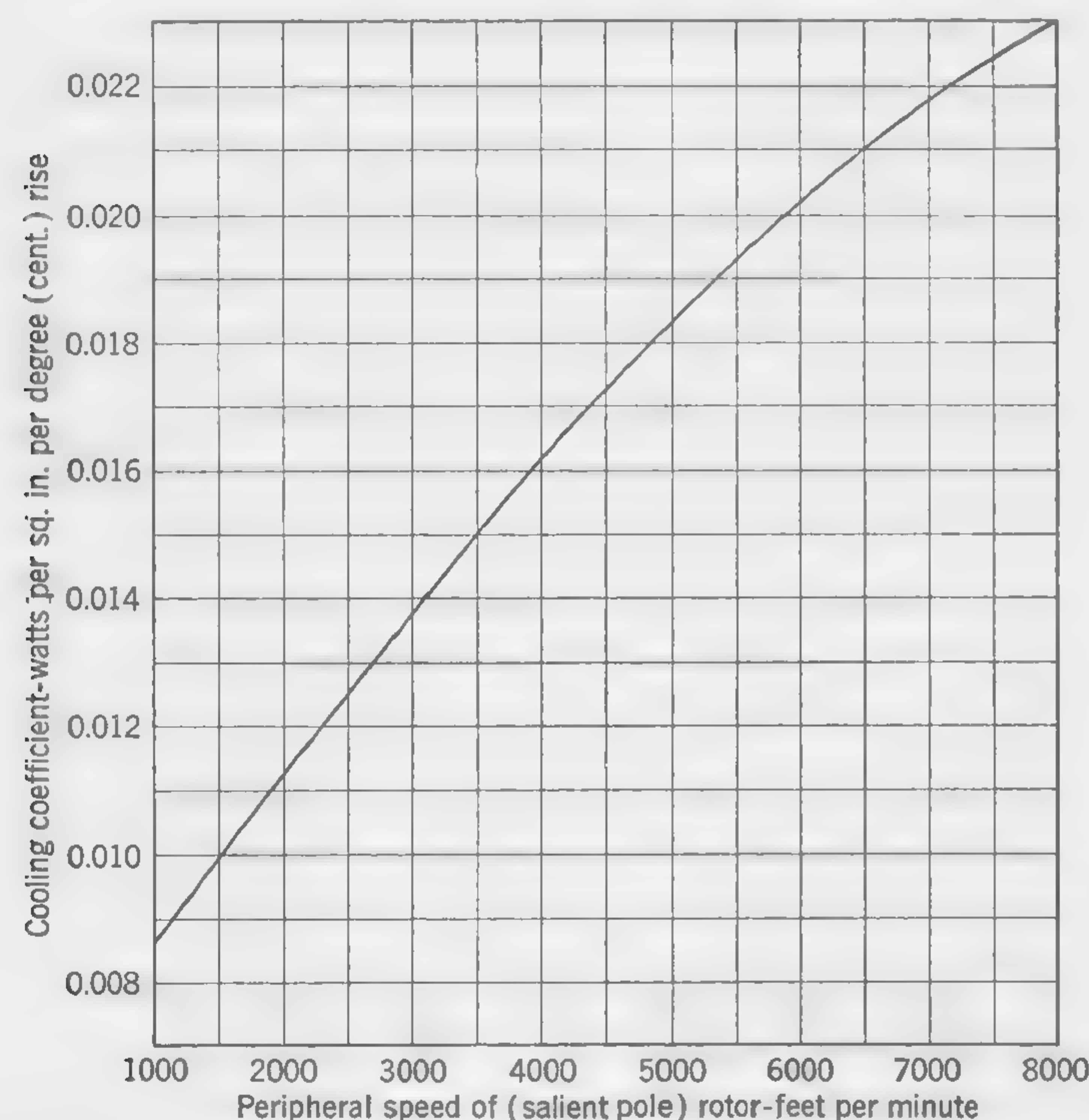


FIG. 96. Cooling coefficient for field windings of rotating field alternators.

Bearing in mind the above-mentioned points, the open-circuit saturation curve—connecting ampere-turns per pole and resulting terminal voltage—can be calculated and plotted exactly as in the case of a continuous-current dynamo with rotating armature and stationary poles (see Art. 49 and Illustrative Example of Art. 50).

**84. Shape of Pole Face—Distributed Field Windings.** When an alternator is provided with salient poles, the open-circuit flux distribution over the pole pitch can be made to approximate a sine curve by suitably

shaping the pole face. Figure 81 illustrates one pole-face shape that yields fair results. Another method, that of increasing the air-gap reluctance from the center outward, is illustrated in Fig. 97. The "equivalent" air gap  $\delta_e$  at center of pole face is calculated as explained in Art. 35 [formula (37a) or (37b)], and the equivalent gap at any other point under the pole is made equal to  $\delta_e / \cos \alpha$ , where  $\alpha$  is the angle in electrical space degrees between the center of pole and the point considered. The pole face would extend about 56 electrical degrees on each side of the center, the pole tips being rounded off with a small radius. In practice, the curve of the pole face would probably not conform exactly with this cosine law; it would generally be a circular arc, not concentric with the

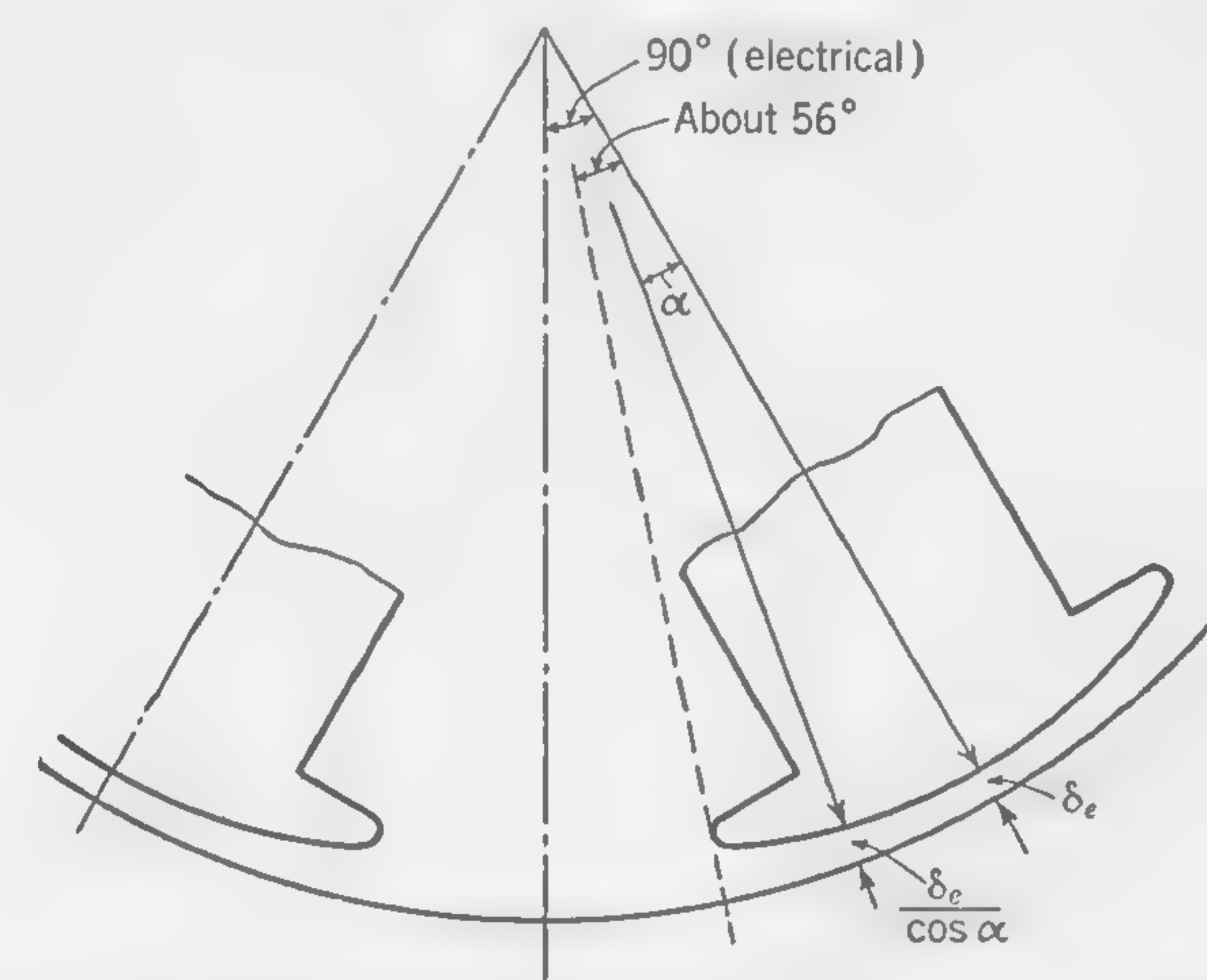


FIG. 97. Method of shaping pole face of salient-pole alternator.

bore of the armature, but with the center displaced so that the air gap near the pole tip would be approximately as determined by the method here described. When the length of the air gap does not increase so rapidly near the pole tips as when the shape of pole shoe follows this so-called cosine law, the pole arc may be somewhat greater, and a pole arc equal to 65 or even 70 per cent of the pole pitch is not uncommon in modern designs.

With the cylindrical field magnet it is not usual to shape the pole face. The clearance between the tops of the teeth on armature and rotor would have a constant value, the proper distribution of flux over the armature surface being obtained by spreading the field coils over the periphery of the cylindrical rotor. From 15 to 25 per cent of the pole pitch is left unwound at the center of the pole. This unwound portion is usually slot-  
ted, but it can be left solid if it is desired to reduce the reluctance of the air gap at the center of the pole face while yet retaining the cylindrical



form of rotor. One feature of equally spaced slots over the surface of the rotor is that there are no sudden changes in the air-gap permeance—the average value of which is then the same at all points on the periphery. An argument in favor of slotting the unwound portion of the pole face is that the field may be “stiffened” by using high flux densities in the teeth.

Figure 98 is a section through part of the slotted rotor of a four-pole turbo-alternator.

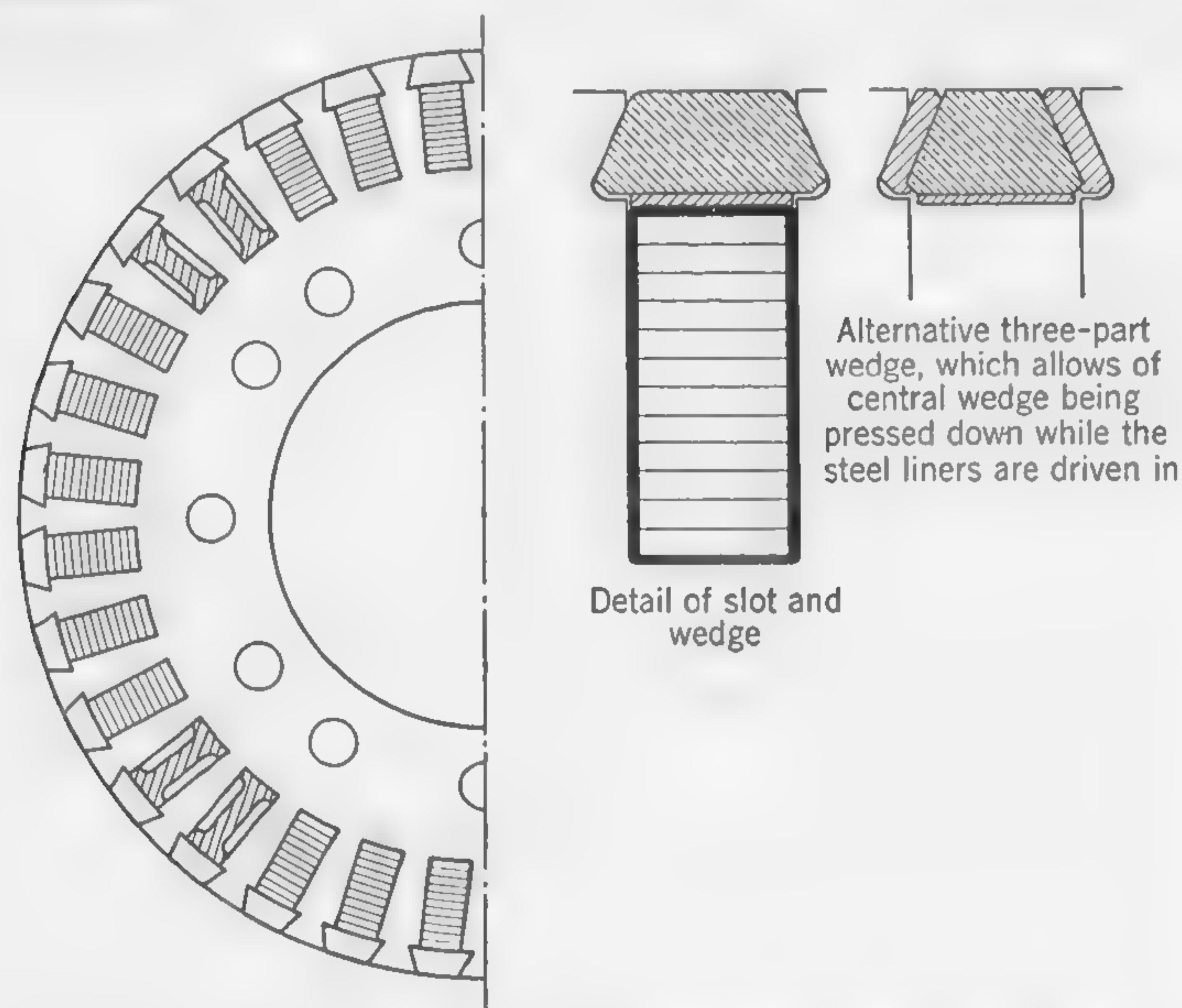


FIG. 98. Rotor of four-pole turbo-alternator, with radial slots.

**85. Magnetomotive Force and Flux Distribution with Cylindrical Field Magnet.** If the whole surface of the rotor is provided with equally spaced slots, the *average* permeance of the air gap between stator and rotor will have a constant value for all points on the armature periphery. This condition is represented in Fig. 99, if the center portion of the pole, of width  $W$ , is slotted as indicated by the dotted lines. This constant average air-gap permeance can be calculated within a close degree of approximation by making conventional assumptions in regard to the path of the magnetic lines, as was done in the case of the salient-pole machine when deriving formula (37) on page 92, giving the permeance at center of pole. The flux lines are supposed to be made up of straight lines and quadrants of circles; and, if the permeance over one tooth pitch is worked out for different relative positions of field and armature, very satisfactory results can be obtained by this method. It will usually suffice to make the calculations for one tooth pitch in the position of greatest permeance,

and again in the position of least permeance. The average of these calculated values, divided by the area of the tooth pitch in square centimeters, will give the average value of the air-gap permeance per square centimeter of the armature surface. More accurate results may be obtained by plotting the flux lines and equipotential surfaces as explained in Chap. 5 (see also Fig. 41).

Under this condition of constant air-gap permeance, the flux distribution on open circuit will follow the shape of the mmf curve; but, in any case, since  $B = \text{mmf} \times \text{permeance per square centimeter}$ , the air-gap flux distribution can always be obtained when the mmf distribution is

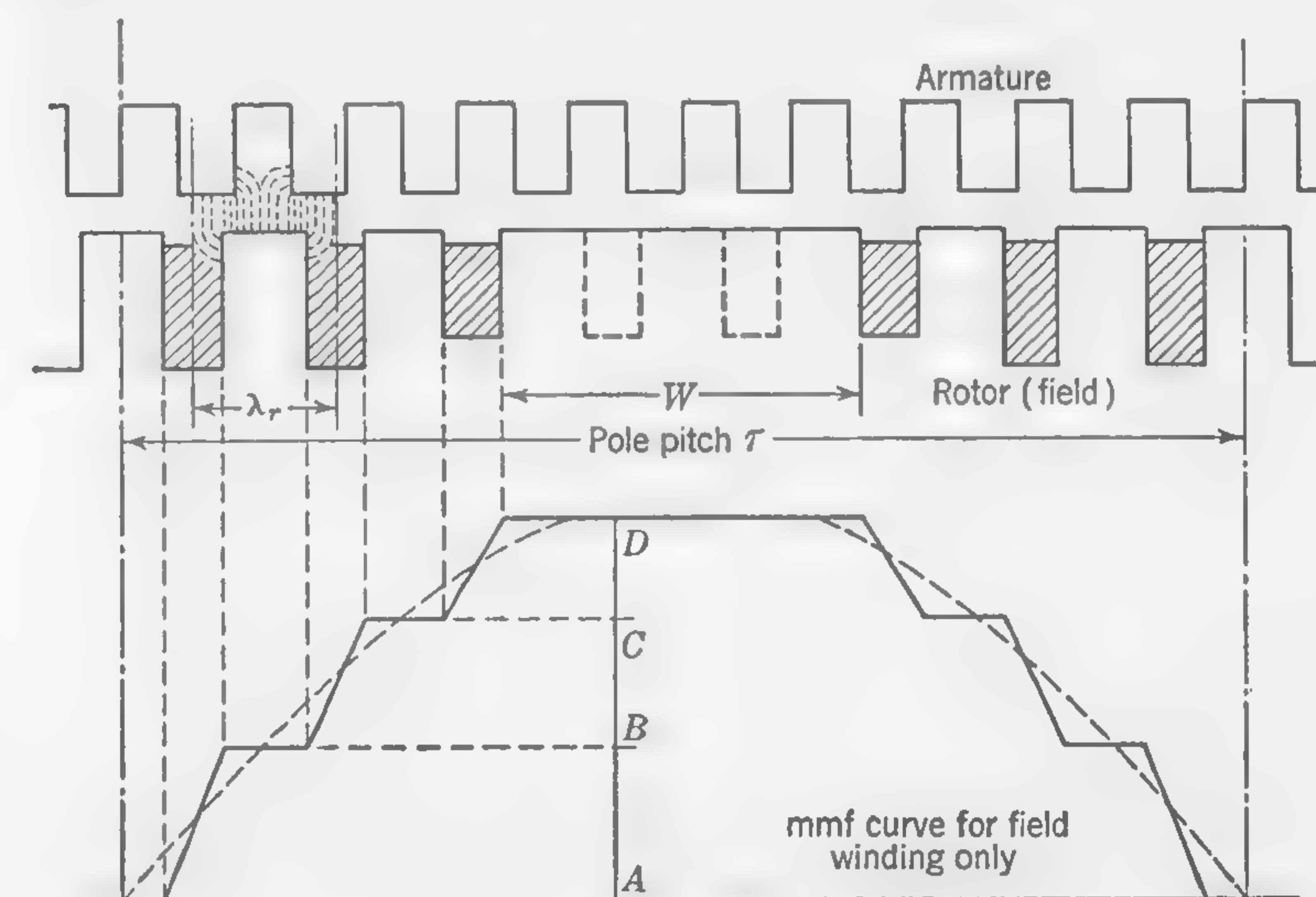


FIG. 99. Mmf over pole pitch, due to distributed field winding.

known. Thus, if the portion  $W$  of the pole (Fig. 99) is not slotted, the permeance curve, instead of being a straight line of which the ordinates are of constant value, would be generally as shown in Fig. 100. From these values of the permeance per square centimeter of armature surface, curves such as those of Fig. 50 can be drawn, so as to include the reluctance of the armature teeth. From all points on the armature between  $A$  and  $B$ , and  $C$  and  $D$  (Fig. 100), the average air-gap permeance would have the value  $AA'$ . Over the central portion  $W$  it would have the value  $EE'$ , while, in the neighborhood of the points  $B$  and  $C$ , it may be assumed to have an intermediate value as indicated by the ordinate  $BB'$ .

If the depth of the slots in the rotor has been decided upon and the number of ampere-conductors in each slot determined, the distribution of mmf over armature surface due to the field winding can readily be plotted, as in the lower sketch of Fig. 99. Thus the ampere-turns in the coil



nearest the neutral zone are represented by the height  $AB$ , those in the middle coil by  $BC$ , and those in the smallest coil by  $CD$ . The broken straight line so obtained is best replaced by the dotted curve, which takes care of fringing and represents the average effect. This curve, being the open-circuit distribution of mmf over armature surface for a given value of exciting current, must be combined with the curve of armature mmf to obtain the resultant mmf under loaded conditions.

**86. Armature MMF in A-C Generators.** In a continuous-current machine the current has the same value in all the armature conductors, and Fig. 51 shows how the armature mmf follows a straight-line law over a zone equal to the pole pitch, this being the distance between brushes referred to armature surface. In a-c and *polyphase* generators the curve of armature mmf can no longer be represented graphically by straight lines, as in Fig. 51, because the value of the current will not be the same in all the conductors included in the space of a pole pitch.

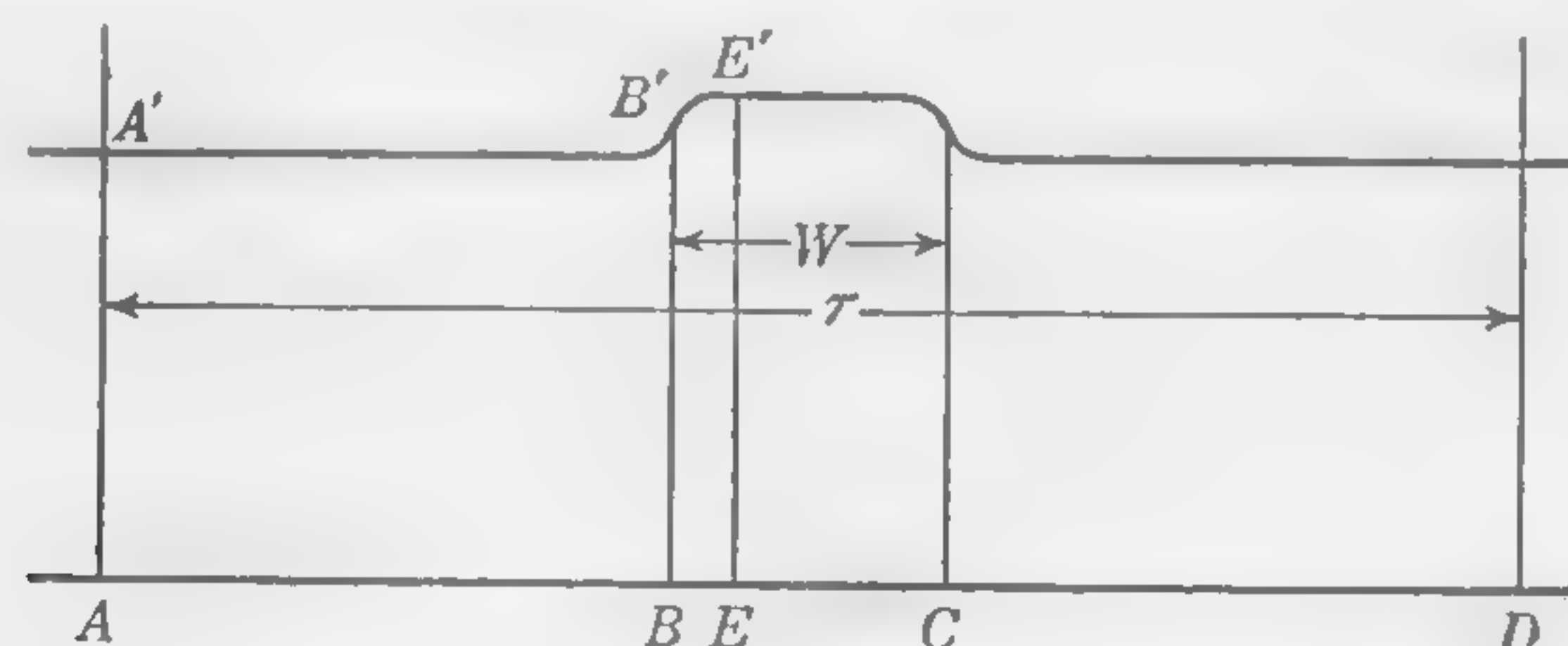


FIG. 100. Distribution of air-gap permeance in turbo-alternator when unwound portion of pole face is not slotted.

If the polyphase synchronous generator is considered first, and a sinusoidal current wave assumed, it is an easy matter to draw a curve representing the armature mmf at any particular instant of time, provided the phase displacement—or position of the conductors carrying the maximum current—relatively to the center line of the pole is known. If this be done for different time values, a number of curves will be obtained, all consisting of straight lines of varying slopes, the length of which in relation to the pole pitch will depend on the number of phases for which the machine is wound. The average of all these curves will be a sine curve of which the position in space relatively to the poles is constant and exactly 90 electrical space degrees behind the position of maximum current.

The method of drawing the curve of armature mmf for any instant of time is illustrated in Fig. 101, where the upper diagram shows the distribution of mmf over the armature periphery of a three-phase generator at the instant when the current in phase 2 has reached its maximum value. If the power factor is unity (load noninductive), the current maximum will occur simultaneously with the voltage maximum (*i.e.*,

when the belt of conductors is under the center of the pole face), as shown in the diagram. A low power factor would cause the current to attain its maximum value only after the center of the pole has traveled an appreciable distance beyond the center of the belt of conductors.

The vector diagram on the right-hand side of the upper figure shows how the value of the current in phases 1 and 3, at the instant considered,

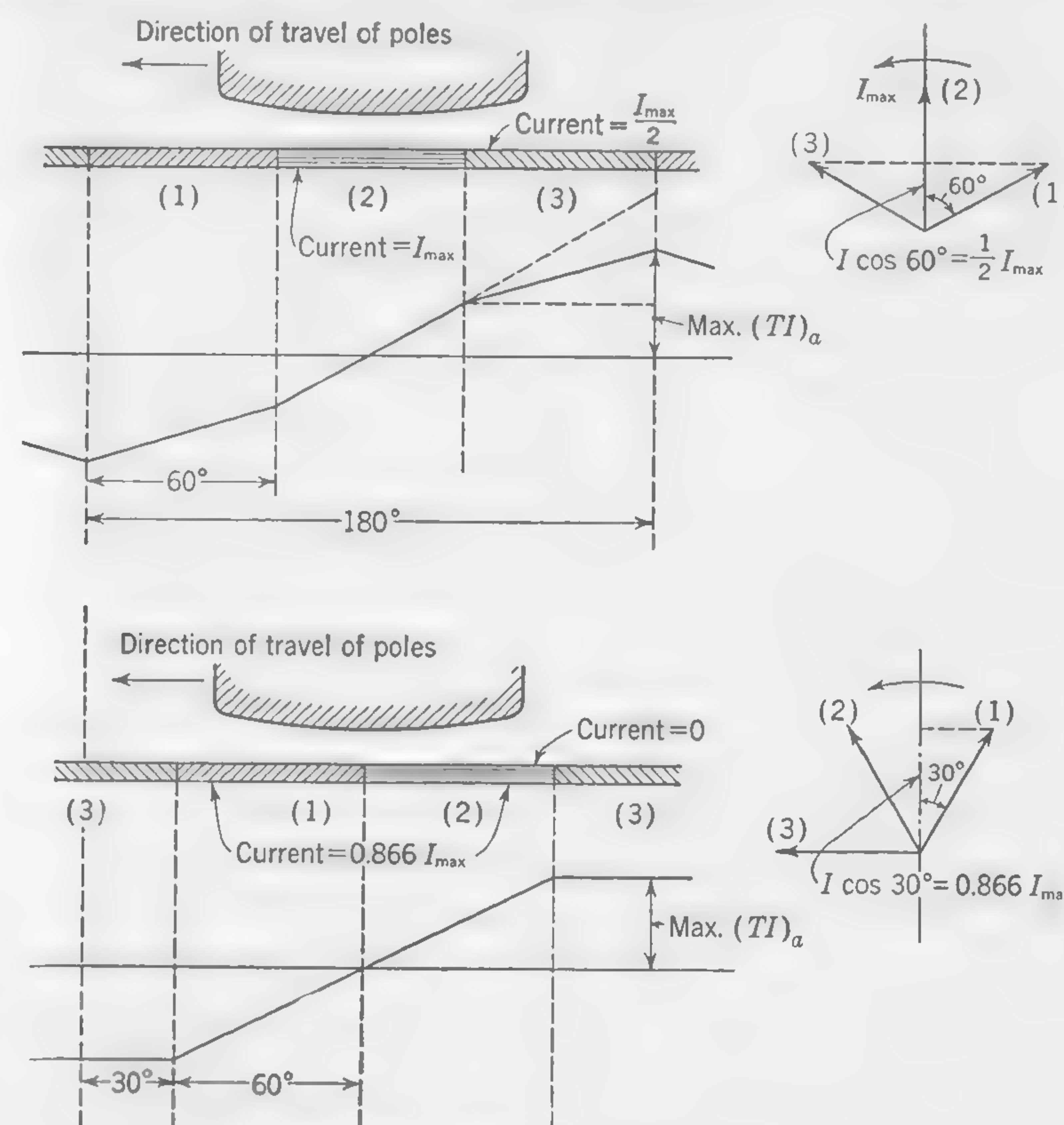


FIG. 101. Instantaneous values of armature ampere-turns.

will be exactly half the maximum value; and the magnetizing effect of phase 1 or 3 is, therefore, exactly half that of phase 2. The angle of  $60^\circ$  between vectors representing three-phase currents—with a phase displacement at terminals of  $120^\circ$ —is accounted for by the fact that the angular displacement between adjoining belts of conductors is only  $\frac{180^\circ}{3} = 60$  electrical degrees; but the connections between the phase windings are so made as to obtain the phase difference of  $120^\circ$  between the respective emfs. Thus, the reversal of the vector 1 in the diagram would cause it to lead vector 2 by  $120^\circ$  instead of lagging behind by  $60^\circ$ ;



The lower diagram of Fig. 101 shows the armature mmf one-twelfth of a period later (*i.e.*, when the poles have moved to the left, or the conductors to the right, 30 electrical space degrees). The current in phases 1 and 2 now has the instantaneous value  $i = I_{\max} \cos 30 = 0.866I_{\max}$ , while the current in phase 3 is zero. If several curves of this kind are drawn, it will be found that the instantaneous values of mmf at any point on the armature periphery (considered relatively to the poles) differ very little from the average value; in other words, the pulsations of flux due to cyclic changes in the mmf will, in a three-phase machine, be negligibly small. For this reason, and also in order to shorten and simplify the work, the armature mmf of a polyphase generator may conveniently be

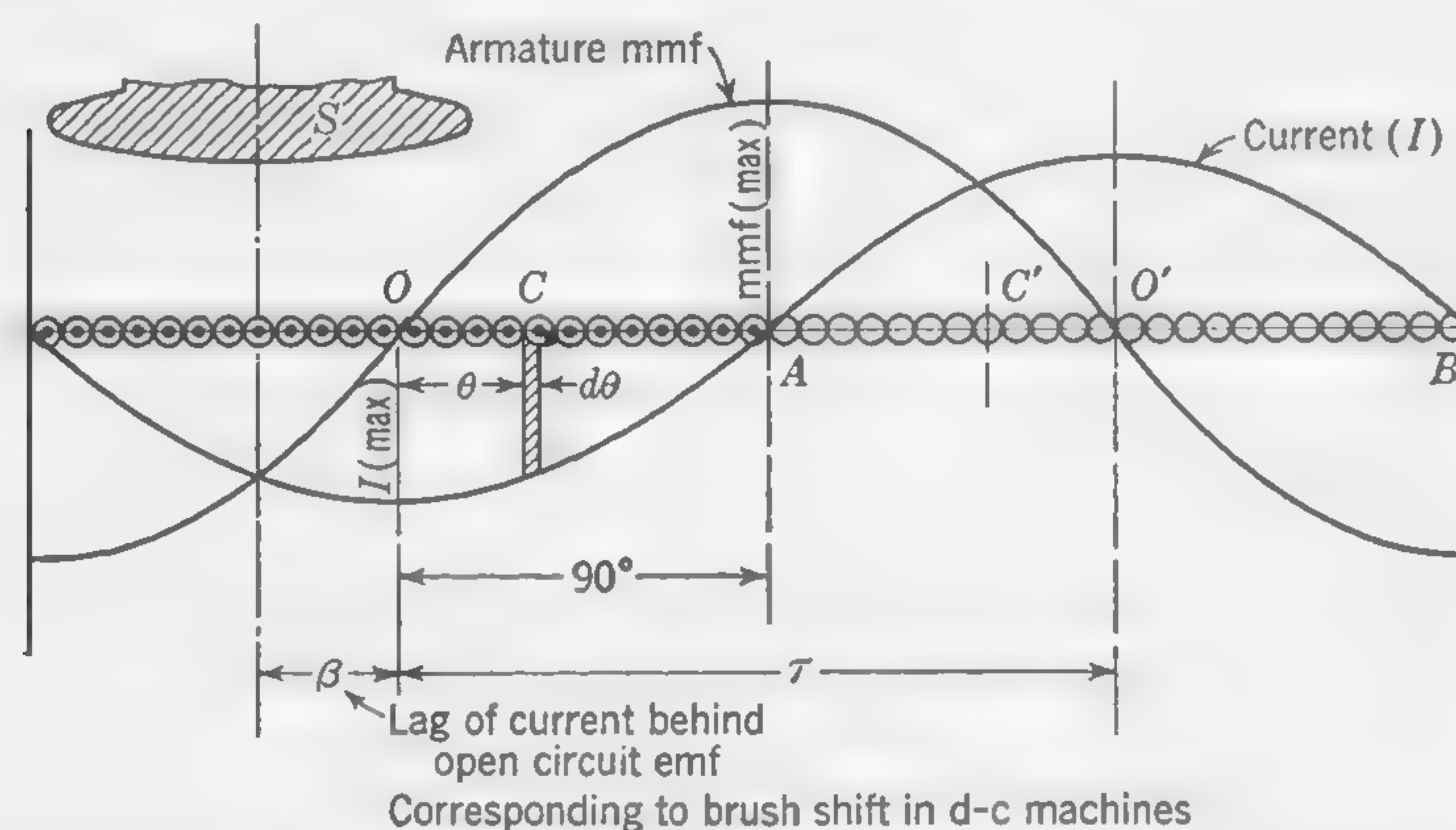


FIG. 102. Method of obtaining curve of armature mmf from curve of current distribution.

studied by assuming a large number of conductors, and a number of phases equal to the number of conductors in the space of one pole pitch. Thus, the ordinates of curve  $I$  of Fig. 102 (assumed to be a sine curve) give the value of the current in the various conductors distributed over the armature surface. It is understood that the current in each individual conductor varies according to the simple harmonic law; but it is constant in value for any given point on the armature surface *considered relatively to the poles*. The direction of the current in the conductors between the points  $A$  and  $B$  may be considered as being downward, while the direction of the current in the adjoining sections of width  $\tau$  would be upward. The maximum value of the armature mmf, therefore, occurs at the points  $A$  and  $B$ , where the current has zero value, while the zero value of mmf must occur at the points  $O$  and  $O'$ , where the current is a maximum.

The value of the armature ampere-turns per pole at any intermediate point  $C$  is equal to the *ampere-conductors* in the space  $OC$ , because the magnetizing effect of the (upward) current in the space  $CA$  is balanced by that of the (downward) current in the space  $AC'$  of equal width, leaving as the effective ampere-turns per pole at the point  $C$  a band  $OC$  of conductors, carrying currents in a positive direction, and an equal band  $C'O'$  of conductors carrying the same average amount of current in a negative direction. The ampere-conductors in the space of width  $d\theta$  are

$$I_{\max} \cos \theta \times \frac{Z' d\theta}{p\pi}$$

where  $Z'$  stands for the total number of inductors on the armature periphery (all phases), and  $\theta$  is expressed in radians. It should be noted that we are considering electrical space angles and  $\tau = 180^\circ = \pi$  radians, which accounts for the quantity  $p\pi$  in the denominator of the above quantity. Thus,

$$\left. \begin{array}{l} \text{Ampere-conductors} \\ \text{in space } OC \end{array} \right\} = I_{\max} \frac{Z'}{\pi p} \int_0^\theta \cos \theta \, d\theta = \frac{Z'}{\pi p} I_{\max} \sin \theta$$

This expression indicates that, with an unlimited increase in the number of inductors (and phases), the armature mmf curve of Fig. 102 will be a sine curve when the current variation follows the sine law.

The maximum value of the armature ampere-turns is obtained by putting  $\theta = \pi/2$ , whence

$$(TI)_a = \frac{Z'}{\pi p} I_{\max} = \frac{\sqrt{2} Z'}{\pi p} I_c \quad (78)$$

where  $I_e$  stands for the effective or rms value of the current in the armature conductors.

This formula may be compared with formula (10) on page 15, which refers to d-c machines. If  $C_s$  = number of series conductors per slot,  $n_s$  = number of slots per pole per phase, and  $n$  = number of phases, the total number of armature inductors is  $Z' = nn_s C_s p$ , and formula (78) may be written:

$$(TI)_a = \sqrt{2} I_c \frac{nn_s C_s}{\pi} \quad (78a)$$

Since the number of slots per pole

$$nn_s = \frac{\pi D}{\lambda p}$$

The formula may be expressed more conveniently in terms of the armature diameter  $D$  and the tooth pitch, as follows:

$$(TI)_a = \sqrt{2} I_c \frac{DC_i}{\lambda p} \quad (78b)$$



The angle of displacement  $\beta$  (Fig. 102) of the armature mmf curve relatively to the center line of pole depends upon the "internal" power factor, and also upon the displacement of the wave of developed emf, a displacement or distortion which is due to cross magnetization. The angle  $\beta$  is not very easily predetermined, but, once known or assumed, the curve of armature mmf can be drawn in the correct position in relation to the curve of field mmf; and the resultant mmf over the armature surface can thus be obtained. An approximate method of predetermining the displacement angle  $\beta$  for any load and power factor will be explained later.

**87. Armature MMF of Single-phase Alternator.** When single-phase currents are taken from an armature winding, the mmf due to this winding as a whole must necessarily be of zero value at the instant of time when the current is changing from its positive to its negative direction. This suggests that the magnetizing effect of the loaded armature will be pulsating; that it to say, it cannot be of constant strength at any given point considered relatively to the poles, whatever may be the phase displacement of the current relatively to the developed voltage. If the change of current in any given conductor be considered over a complete cycle, and if at the same time the position of this conductor relatively to the poles be noted, it will be seen that, *in relation to the field magnet system*, the armature windings produce a pulsating field of double the normal frequency. The actual flux component due to the armature currents will not, however, pulsate to any appreciable extent, because the tendency to vary in strength at comparatively high frequencies is checked by the damping effect of the field coils, even if the pole shoes and poles are laminated.

No modern single-phase alternator, unless of very small size, should be built without *amortisseur* windings, or damping grids. These consist of copper conductors in holes or slots, running parallel to the shaft, in the faces of the field poles. They are joined together at both ends by heavy copper connections and form a "squirrel cage" of short-circuited bars, which damp out the flux pulsations and also prevent the sweeping back and forth, or "swinging," of the armature flux due to "hunting" when synchronous a-c machines are coupled in parallel.

A simple form of damper is illustrated in Fig. 103, where a number of copper rods through the pole face—and on each side of the pole shoe—are short-circuited at both ends by heavy bands of copper. Any tendency to sudden or periodic changes of flux through any portion of the pole face is checked to a very great extent by the heavy currents that a small change of flux will establish in the short-circuited rods.

In Fig. 104, the windings of a single-phase alternator are shown covering 60 per cent of the armature surface, and the distance  $\tau$  is one pole

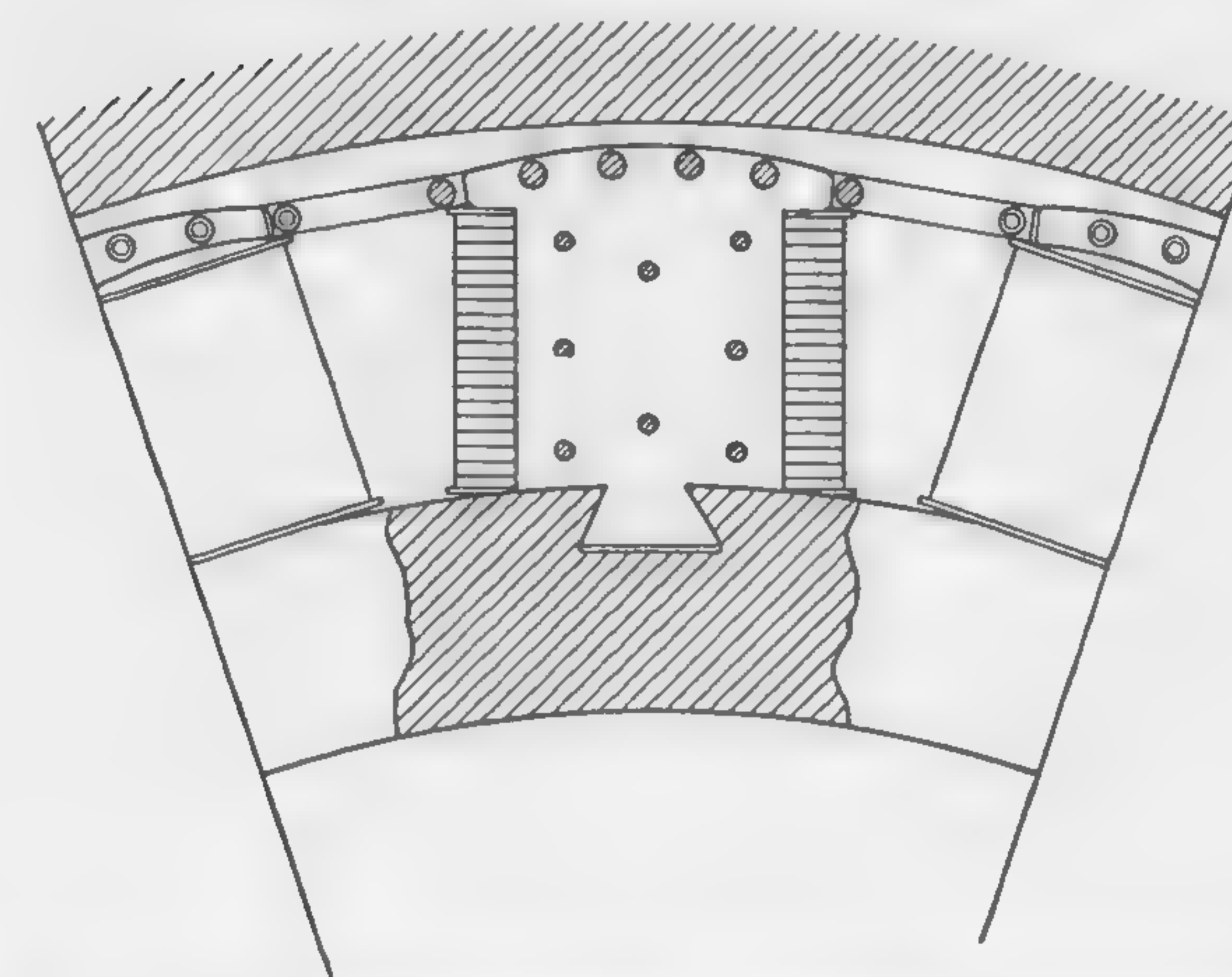


FIG. 103. Short-circuited damping bars in pole face of single-phase alternator.

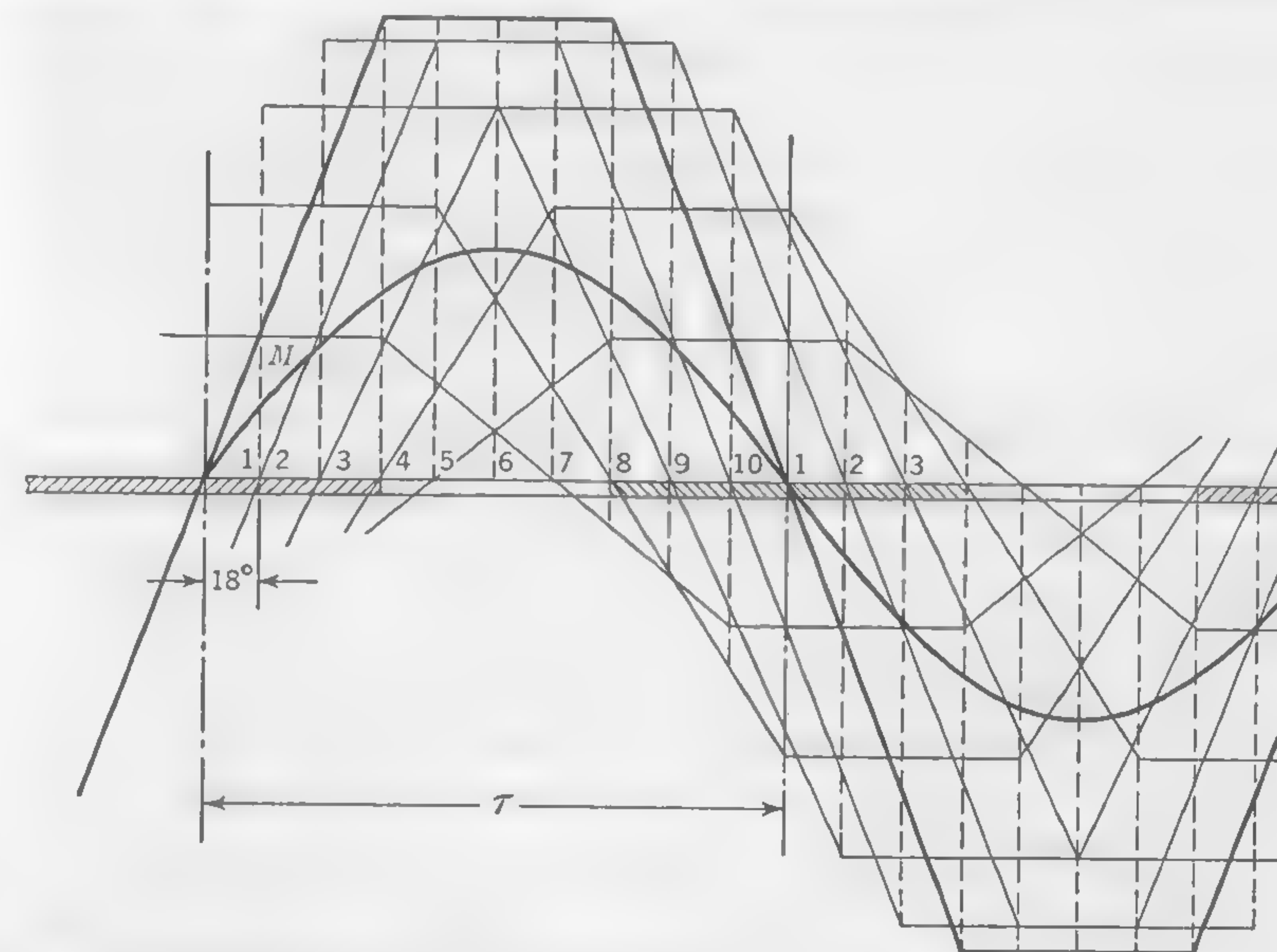


FIG. 104. Instantaneous and average values of armature mmf in single-phase alternator.

pitch. This distance is divided into 10 equal parts, each corresponding to 18 electrical degrees. The thick line represents the armature mmf when the current has reached its maximum value. The armature is then supposed to move  $18^\circ$  to the right of this position, and a second mmf curve is drawn, corresponding to this position of the windings. Its maximum ordinate is, of course, less than in the case of the first curve, because the current (which is supposed to follow the sine law) now has



a smaller value. This process is repeated for the other positions of the coil throughout a complete cycle, and the resultant mmf for any point in space (*i.e.*, in relation to the poles, considered stationary) is found by averaging the ordinates of the various mmf curves at the point considered. In this manner the curve  $M$  (Fig. 104) is obtained. It is seen to be a sine curve, of which the maximum ordinate is about half the instantaneous maximum mmf per pole of the single-phase winding, and it may be used exactly in the same manner as the armature mmf curve in Fig. 102 (representing armature mmf of a polyphase machine); that is to say, it can be combined with the field-pole mmf curve to obtain the resultant mmf at armature surface from which can be derived the flux-distribution curves under loaded conditions.

The maximum value of the resultant ampere-turns per pole is, therefore

$$(TI)_a = \frac{1}{2} I_{\max} \times \frac{Z}{2p} = \sqrt{2} I_c \frac{Z}{4p} \quad (79)$$

where  $Z$  is the total number of "active" conductors on the armature.\*

In single-phase alternators it is the pulsating nature of the armature mmf which leads to eddy-current losses that are practically inappreciable in the case of two- or three-phase machines working on a balanced load, that is to say, with the same current and the same voltage in each of the phase windings, and with the same angular displacement between current and emf in the respective armature circuits. Sometimes the polyphase load is not balanced, and in that case pulsations of the armature field occur as in the single-phase machines, the amount of the pulsating field being dependent upon the degree of unbalancing of the load. The effect is then as if an alternating field were superposed on the steady armature mmf because of the balanced components of the total armature current.

**88. Slot-leakage Flux.**† Referring again to Fig. 102, if we wish to derive a curve of resultant mmf over the armature periphery for any condition of loading, it will be necessary, before combining the curves of armature and field pole mmf, to determine the relative positions of these two curves. In the d-c machine, the position of maximum armature mmf coincides with the brush position; but the point  $A$  (Fig. 102) is not so easily determined. Its distance from the center of the pole is  $\beta + 90^\circ$ , a displacement which depends not only on the power factor of the load (*i.e.*, on the lag of the current behind the terminal potential difference), but also on the strength of the field relatively to the armature, because

\* If the "spread" of the winding is different from the 60 per cent assumed in this calculation, modified formulas can be derived in a similar manner.

† The explanation here given of the effects of slot-leakage flux is based upon A. Still's article, Slot Leakage in A. C. Generators, *J. Franklin Inst.*, vol. 210, No. 4, October, 1930.

this relation determines the position (in relation to the center of the pole) of the maximum emf developed in the conductors.

The field mmf will depend upon the flux in the air gap, and, since this includes the slot-leakage flux, it will be necessary to consider the meaning, and determine the value, of the slot flux before attempting to calculate the angle  $\beta$  (Fig. 102).

When there is no current in the conductors of a slotted armature, the magnetic flux in the air gap passes through the teeth into the armature core and is "cut" by that portion of the armature winding which is buried in the slots. Even if the flux density in the teeth is very high, causing an appreciable part of the total flux to pass into the core by way

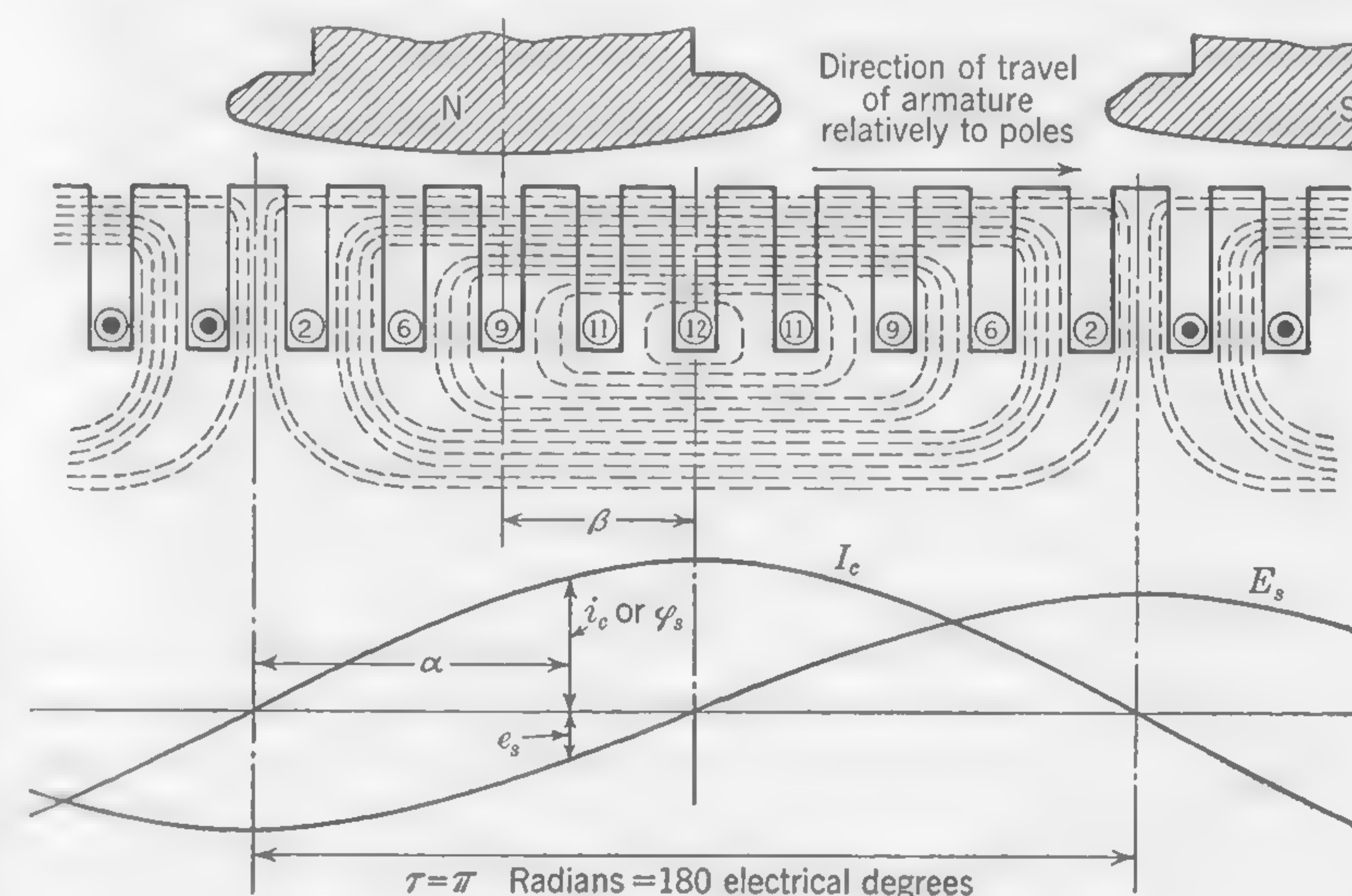


FIG. 105. Slot flux in polyphase generator.

of the slots, this does not alter the fact that, under open-circuit conditions, all the flux in the air gap under the poles is cut by the conductors and thus causes an emf, proportional to the air-gap flux, to be developed in the armature windings. But when current is drawn from the armature, an mmf proportional to the ampere-conductors in a slot will cause some flux to be diverted from tooth to tooth across the slot, and this flux will not be cut by *all* the armature conductors.

The effect of the slot-leakage flux is to cause a change in the number of flux lines cut by the active conductors, and the emf developed in the armature winding is not the same as it would have been if all the flux lines passing from pole face to armature had continued down into the core through the roots of the teeth or by a parallel path through the slots.

The dotted lines in Fig. 105 form a diagrammatic representation of the



slot flux in the armature of a synchronous a-c generator, assuming that this flux could be considered independently of the main flux entering the armature from the pole faces. Such a condition does not exist in an actual machine operating under load, and it could only be realized by passing current through the armature windings from an independent source while the machine is driven at normal speed with the field circuit disconnected. It is assumed that all the slot flux set up by the conductors in any one slot entirely surrounds these conductors; that is to say, all flux lines cross the slot in the space *above* the conductors, and the effect of leakage flux passing through the material of the conductors is, for the present, neglected.

Another assumption which will be made is that there are as many phases as there are slots in the space of one pole pitch. Thus, the generator of Fig. 105 must be thought of as a nine-phase machine. If the armature were that of a three-phase machine, there would be three slots per pole per phase, and the ampere-conductors in each slot of a group of three adjacent slots would have the same value at a given instant of time. The assumption of  $n$  phases in a machine with  $n$  slots per pole has been made in order to simplify the problem and justify the use of vector diagrams.

The distribution of current in the several conductors will depend upon the position of the slot in relation to the field system. It will be convenient to consider a stationary field system with rotating armature. The current is supposed to have its maximum value when the angular displacement of the slot relatively to the center line of the pole is  $\beta$ . On the assumption that the current variations follow the sine law, the figures on the diagram represent approximate current values for various slot positions in the space of one pole pitch. Since the slot-leakage flux is proportional to the ampere-conductors in the slot, a correct diagrammatic representation of this flux is obtained by making the number of lines which cross from tooth to tooth in each slot proportional to the current in the conductor. The reluctance of the iron in the path of the slot-leakage flux is considered negligible in relation to that of the air path between adjacent teeth.

If  $I_c$  stands for the rms value of the armature current, its maximum value is  $\sqrt{2} I_c$ , and the value of the current in a slot displaced by an angle  $\alpha$  from the position where  $i_c = 0$  is

$$i_c = \sqrt{2} I_c \sin \alpha \quad (80)$$

and, since the slot flux is proportional to this current, we may write

$$\phi_s = K I_c \sin \alpha \quad (81)$$

where  $K$  is a constant depending upon the slot dimensions and the num-

ber of conductors in a slot. The sine curve marked  $I_c$  (Fig. 105) may therefore stand for either the armature current or the slot flux for any position of the armature slot in relation to the field poles.

The instantaneous value of the emf developed in a single slot conductor due to the rate of change of the flux linkages is

$$e_s = -\frac{d\phi_s}{d\alpha} = -K I_c \cos \alpha \quad (82)$$

from which the curve marked  $E_s$  can be plotted. This is obviously a sine wave lagging behind the sine wave of current distribution by a quarter period.

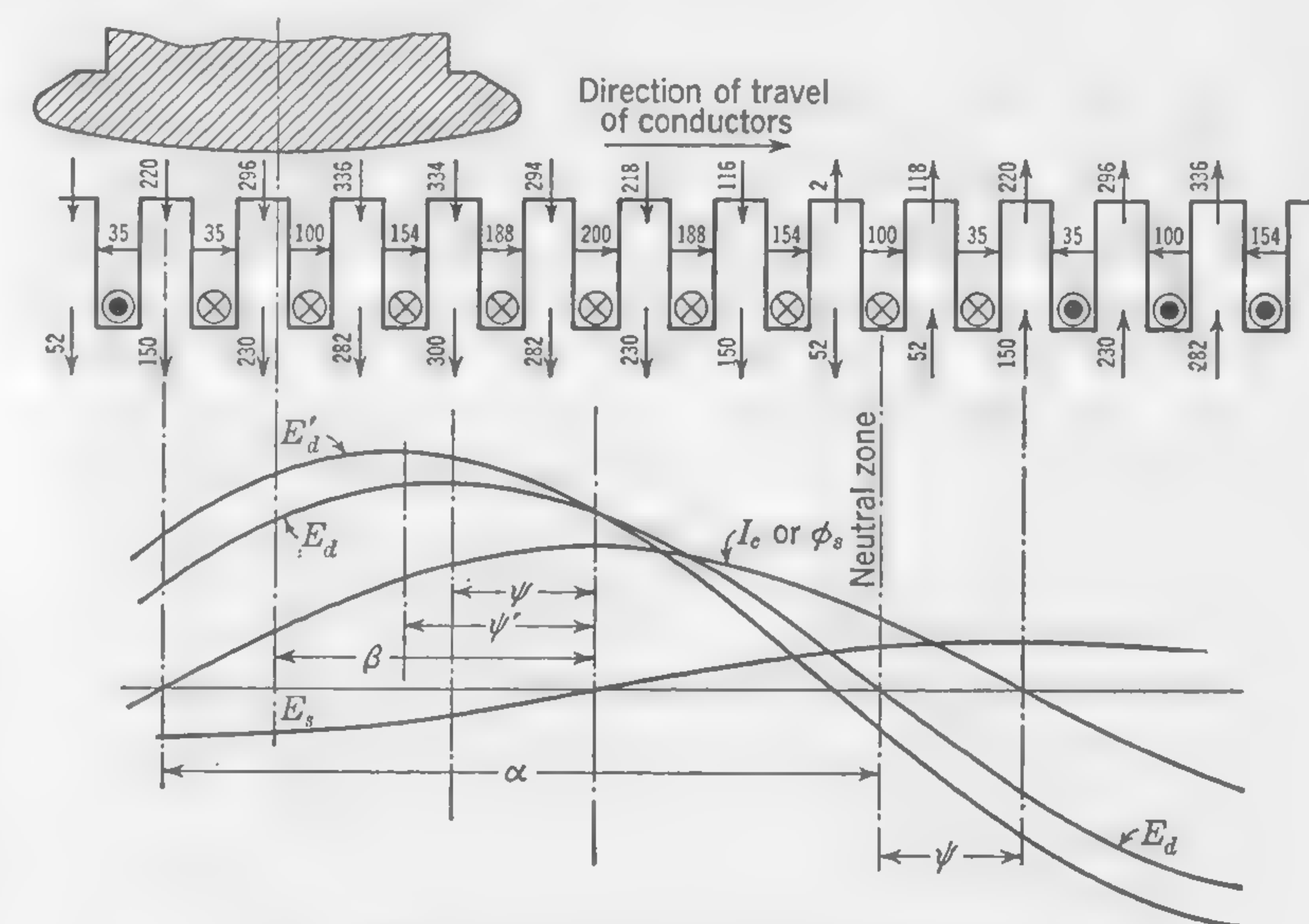


FIG. 106. Component curves of developed emf.

Bearing in mind that the flux represented diagrammatically by the dotted lines in Fig. 105 may be considered approximately stationary in space, while the slotted armature, carrying the conductors, is moving from left to right, the emf of formula (82), represented by the curve  $E_s$ , can be calculated by considering the rate at which the flux lines entering the armature core through the roots of the teeth are "cut" by the conductors in the slots.

In the diagram (Fig. 106), the same simplifying assumptions have been made as in connection with Fig. 105, namely, that there are as many phases as there are slots in one pole pitch, and that all the slot-leakage flux passes from tooth to tooth in the space above the conductors. No attempt has been made to show the actual paths of the flux lines, but



the figures on the arrows, indicating direction of flux in slots and teeth, are proportional to the number of flux lines entering the teeth from the air gap, passing across the slots and entering the armature core through the roots of the teeth.

It is assumed that the combined effect of field and armature ampere-turns is to produce a sinusoidal flux distribution over the armature surface\* as represented by the curve  $E'_a$ . The current distribution in the armature conductors is indicated by the curve  $I_c$ , which represents not only the current, but also the slot mmf and slot-leakage flux. Considering a particular tooth  $t$ , the fact that the slot ampere-conductors are greater in the adjacent slot on the right than in the adjacent slot on the left leads to a tooth mmf proportional to  $154 - 100 = 54$  which opposes the mmf tending to send flux through the tooth into the armature. The flux entering the armature core through this tooth is therefore not 336, which it would have been if the slot mmf had not caused more flux to leave the tooth on the right-hand side than enters it on the left, but  $336 + (100 - 154) = 282$ , as indicated on the arrow through the root of the tooth. If, therefore, we draw the curve marked  $E_s$ , of which the ordinates are a measure of the difference between the slot fluxes on the two sides of a tooth, and then add the ordinates of this curve to those of the curve  $E'_a$ , we obtain the curve  $E_a$ , which represents the flux entering the armature core through the roots of the teeth and is therefore also a measure of the emf actually developed in the armature conductors by the cutting of this flux.

It should be noted that the emf corresponding to the flux curve  $E_d$  has no real existence; it is a fictitious quantity which may be called the *apparent developed voltage*, being the emf that would have been developed in the armature windings if part of the flux entering the teeth from the air gap had not been diverted from tooth to tooth in the form of slot-leakage flux. The difference between the voltages  $E'_d$  and  $E_d$  is the voltage component that would have been developed if a certain amount of flux—equal to 100 in Fig. 106—had not been diverted from tooth to tooth in the neutral zone,† where it is not “cut” by the armature conductors.

The maximum value of the slot-leakage flux occurs where the armature current reaches its maximum value of  $\sqrt{2} I_c$ . This is the position in space where the angle  $\alpha$  is equal to  $90^\circ$  and the slot-leakage flux (Fig. 100) has the value 200. Note that half a pole pitch away, the current has

\* An assumption which may not always be justified in connection with salient-pole machines.

† The neutral zone is the position in space, or in relation to the field system, where the direction of the flux is parallel to the direction of travel of the armature conductors (*i.e.*, where no lines enter the armature in such a direction as to be "cut" by the conductors).

fallen to zero and all the leakage flux, in the slot where the current was a maximum, has passed into the armature core through the roots of the teeth comprised in the space of one-half the pole pitch. If  $\Phi_s$  = maximum value of leakage flux in one slot, and  $n$  = number of slots per pole, the *average* value of the slot flux which enters or leaves the armature through one tooth is  $2\Phi_s/n$ , and, since we are dealing with sine curves, the maximum amount of slot flux passing into or out of the armature core through one tooth is  $(\pi/2)(2\Phi_s/n) = (\pi/n)\Phi_s$ . This, therefore, is the height of the maximum ordinate of the curve marked  $E_s$  (Fig. 106).

The angles  $\psi$  and  $\psi'$  (Fig. 106) are the angles by which the current lags behind the actual and "apparent" developed voltages  $E_d$  and  $E'_d$ , respectively. It follows that the value of slot-leakage flux in the neutral zone, where  $\alpha = (180^\circ - \psi)$ , is:

$$\text{Slot flux in neutral zone} = \Phi_s \sin \psi \quad (83)$$

which, for the particular case of Fig. 106, is  $200 \times \sin [(180 \times 1.5)/9] = 100$ , as marked on the arrow across the slot in the neutral zone.

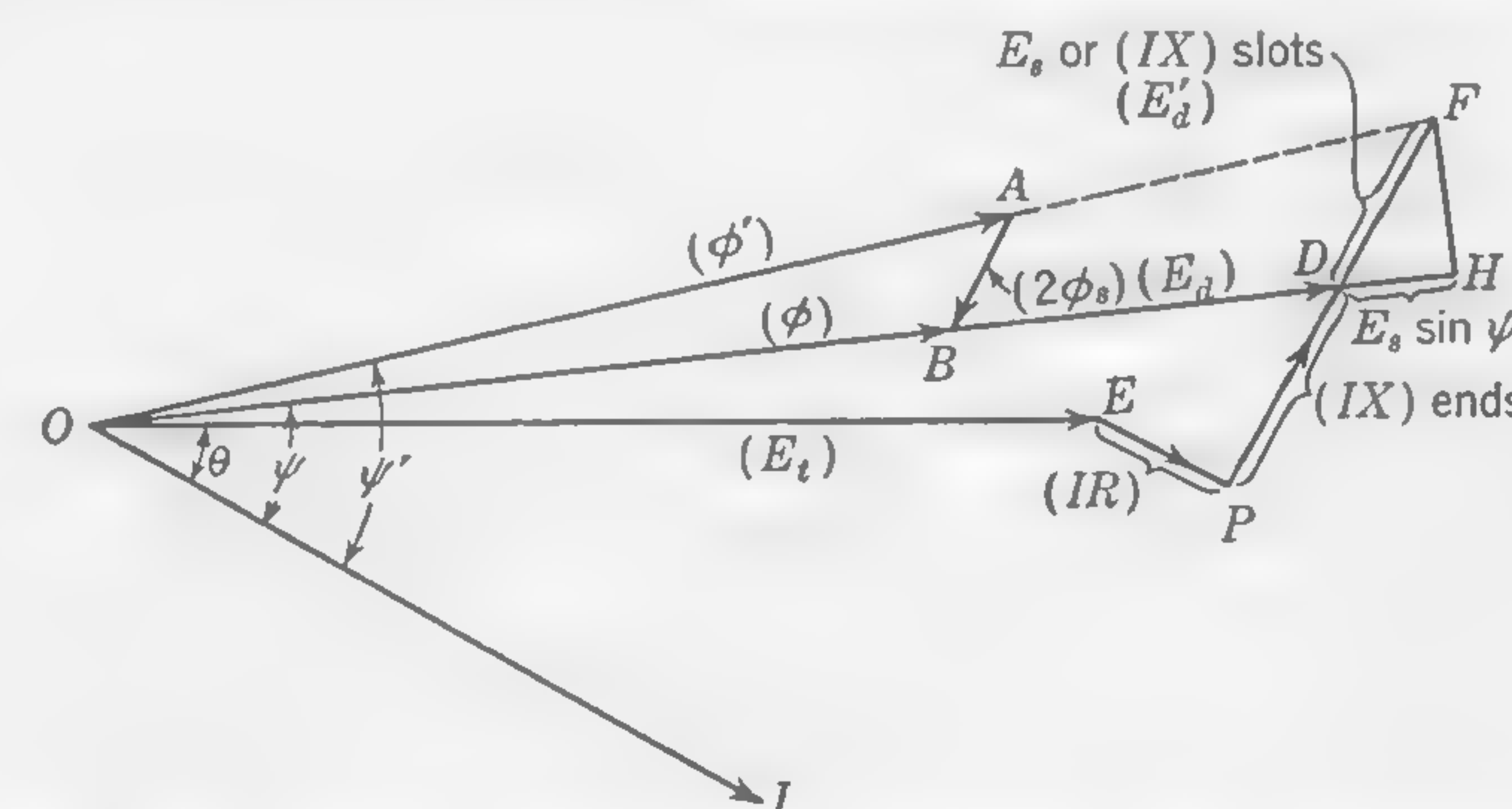


FIG. 107. Vector diagram including emf component due to slot-leakage flux.

*Vector Diagram Including the Effect of Slot Leakage.* The vector  $OE = E_t$  (Fig. 107) represents the voltage at the terminals of an a-c generator when the armature current, represented by the vector  $OI$ , lags behind this voltage by an angle  $\theta$ .

$EP$ , parallel to  $OI$ , is the voltage component to compensate for  $IR$  drop in the windings.

*PI*), leading *OI* by 90°, is the emf component to compensate for the *IX* drop due to the inductance of that portion of the armature winding which is outside the slots and may be considered as beyond the direct influence of the field system.

$OD \equiv E_d$  is the vectorial sum of  $E_i$ ,  $IR$ , and  $(IX)_{\text{cnda}}$ . It is the voltage actually developed in the slot conductors, and it leads the current by the angle  $\psi$ .



$FD = E_s$  is the emf component due to the inductance of that portion of the armature winding which is buried in the slots.

$OF = E'_a$  is the *apparent developed voltage* which leads the current by the angle  $\psi'$ .

$DH = -E_s \sin \psi$  is the emf component that would have been developed if slot flux equal in amount to  $\Phi_s \sin \psi$  had entered the armature core instead of being diverted from tooth to tooth in the neutral zone.

Considering the several components of the flux, we have:

$OA = \Phi'$  lines entering the tops of the teeth from the field poles in the space of one pole pitch.

$AB = 2\Phi_s$  lines, being slot leakage passing down the teeth into the armature core in the space of one pole pitch. This is the flux component marked  $E_s$  (Figs. 105 and 106). Since  $\Phi_s$  is the maximum leakage flux across one slot, and since we are now considering this flux independently of other flux components, it is necessary, as will be seen in Fig. 105, to take twice this value as the slot-flux component entering the armature core in the space of one pole pitch.

$OB = \Phi$  lines, is the vectorial sum of  $\Phi'$  and  $2\Phi_s$ , and it is, therefore, the flux actually cut by the conductors to develop the voltage  $E_a$  in the armature winding.

Although the diagrams used to illustrate this article show the current lagging behind the terminal voltage, the construction followed in Fig. 107 would be exactly the same for a generator supplying a *leading* current on a capacitor load. In this case, the vector  $OD$  would be greater than  $OF$ , that is to say, the mmf which sets up slot-leakage flux would cause more flux to enter the core through the roots of the teeth than passes from the air gap into the tops of the teeth, and the *apparent developed emf* would then be *less* than the emf actually developed in the armature.

**89. Calculation of Equivalent Slot Flux.** The diagrams, Figs. 105 and 106, assume that all the slot flux passes across the slot in the space above the conductors. In practice a large portion of this flux passes through the space occupied by the slot conductors, and, in order to develop a formula for calculating the component  $FD$  of Fig. 107 [or determining  $K$  in formula (81)], it will be convenient to determine the *equivalent slot flux*. This may be defined as a fictitious flux which, if cut by all the armature conductors, would develop an emf component equal to the emf which the actual slot-leakage flux would develop if it could be considered independently of other fluxes.

Figure 108a indicates the path of the magnetic lines in the neutral zone when the current in the slots occupying this particular position (in relation to the field system) is zero. Figure 108b is a diagrammatic

representation of the flux lines in the neutral zone when the current in the slot conductors has an appreciable value. Note that, of the nine lines entering the tooth top from the air gap, all are cut by the slot conductors under the condition *a* when there is no leakage flux; but under condition *b*, the flux lines  $\Phi_2$  and  $\Phi_3$  are no longer cut by the armature conductors and therefore develop no emf in the winding. The flux lines  $\Phi_1$ , which pass through the copper and through the space occupied by insulation between the upper and lower coil sides of a double-layer winding, are not cut by *all* the conductors in the slot. Figure 108c illustrates the method of calculating the equivalent slot flux for which the symbol  $\Phi_{es}$  will be used.

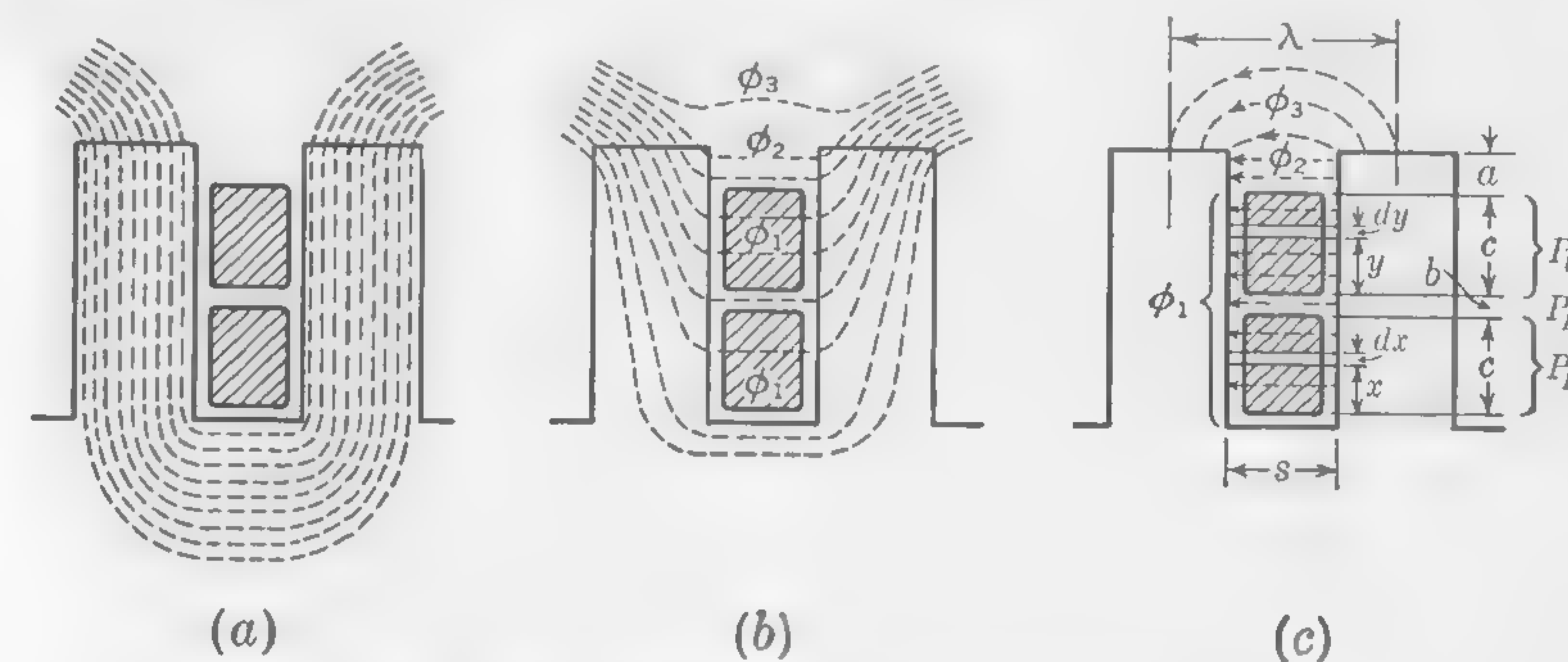


FIG. 108. Illustrating slot-flux calculations.

Let  $C_s$  = number of conductors per slot, and  $i_s$  = current per conductor in amperes; then if  $F$  stands for the total slot mmf tending to establish flux leakage across the slot, we have

$$F = 0.4\pi C_s i_s \quad (84)$$

and

$$\Phi_{es} = F \times l_a P_{es} \quad (85)$$

where  $l_a$  = gross length of armature core in centimeters, and  $P_{es}$  = equivalent permeance per centimeter length of slot. The authors believe that use of the gross length rather than the net length of the armature core is justified, since it includes an allowance for the fringing fluxes at the sides of vent ducts.

The permeance of the flux path of depth  $dx$  in Fig. 108c is  $dx/s$  per centimeter length of slot, but the amount of the flux in this space is not due to the total mmf  $F$ , but to  $F(x/2c)$ , and this element of flux fails to link with  $C_s(x/2c)$  conductors. The *equivalent permeance* of the element considered is therefore  $(dx/s)(x/2c)^2$ , and the equivalent permeance of the space occupied by the lower coil side is

$$P_L = \frac{1}{4sc^2} \int_0^c x^2 dx = \frac{c}{12s} \quad (86)$$



Similarly, for the upper coil side,

$$P_U = \int_0^c \frac{dy}{s} \left( \frac{c+y}{2c} \right)^2 = \frac{7c}{12s} \quad (87)$$

The equivalent permeance of the space of depth  $b$  between the two coil sides is

$$P_B = \frac{b}{s} \left( \frac{c}{2c} \right)^2 = \frac{b}{4s} \quad (88)$$

The equivalent permeances of the flux paths  $\Phi_2$  and  $\Phi_3$  are, of course, the same as the actual permeances of these paths. Using the symbols  $P_2$  and  $P_3$  for these permeances per centimeter of slot length, and summing up the equivalent permeances as expressed by formulas (86), (87), and (88), we obtain for the total equivalent slot permeance

$$l_a P_{es} = l_a \left[ \frac{8c + 3b}{12s} + P_2 + P_3 \right] \quad (89)$$

where  $l_a$  is the gross length of the armature core in centimeters. The equivalent slot flux is therefore

$$\Phi_{es} = 0.4\pi C_s i_s l_a \left[ \frac{8c + 3b}{12s} + P_2 + P_3 \right] \quad (90)$$

*Calculation of Permeances  $P_2$  and  $P_3$ .* Assuming parallel sides to the slot in the space of depth  $a$  above the coils, we have

$$P_2 = \frac{a}{s} \quad (91)$$

which must be modified if the sides of the slot are not parallel at this point. The flux component  $\Phi_3$  is supposed to account for the flux lines that cross from tooth to tooth in the air gap outside the slot. Any leakage flux beyond what is included between the center lines of the teeth on each side of the slot should not be treated as slot flux and will therefore be disregarded in these calculations. A convenient formula to use for calculating this portion of the slot-leakage permeance in salient-pole machines is Finnis's formula [see formula (35), p. 79] which assumes the flux paths to be semiellipses with the foci at the edges of the teeth. Putting  $r = \lambda/s$ , where  $\lambda$  = tooth pitch and  $s$  = slot width, as indicated on Fig. 108c, the tooth-top permeance per centimeter of slot length, for salient-pole machines, may be written

$$P_3 = \frac{1}{\pi} \log_e (r + \sqrt{r^2 - 1}) \quad (92)$$

In machines with cylindrical fields and a uniform air clearance ( $\delta$ ) not

only under the pole centers, but in the neutral zone also,

$$P_3 = \frac{\delta}{\lambda} \quad (93)$$

In order to determine the length of the vector  $DF$  (Fig. 107), it is necessary to calculate the emf component due to the "cutting" of the slot-leakage flux by the conductors.

Since  $2\Phi_{es}$  is the total amount of the slot flux which, if considered as a separate flux component, enters or leaves the armature core in the space of one pole pitch (see Figs. 105 and 106), the average value of the voltage component which would result from the cutting of these flux lines is

$$E_{avg} = \frac{2\Phi_{es} p N}{10^8 \times 60} (C_s n_s p) \quad (94)$$

where  $p$  = number of poles,  $N$  = revolutions per minute,  $C_s$  = number of conductors per slot, and  $n_s$  = number of slots per pole per phase. Or, in terms of frequency, since  $Np = 120f$ ,

$$E_{avg} = 4\Phi_{es} f (C_s n_s p) 10^{-8} \quad (95)$$

Since we are assuming sine-wave shapes, it is necessary to multiply the mean value by  $\pi/2 \sqrt{2}$  to obtain the rms value, and, if we substitute for  $i_s$  in formula (90) its maximum value  $\sqrt{2} I_c$ , the final expression for the fictitious reactive voltage component per phase due to slot inductance is

$$E_s = I_c \times 0.8\pi^2 f C_s^2 n_s p l_a \left[ \frac{8c + 3b}{12s} + P_2 + P_3 \right] 10^{-8} \text{ volts} \quad (96)$$

**90. Method of Determining Position of Maximum Armature MMF.** Turning again to Fig. 102, we are still unable to determine the angle  $\beta$ , or the displacement ( $\beta + 90^\circ$ ) of the maximum armature mmf beyond the center line of the pole, because the angle  $\psi'$  (Fig. 107) shows merely the lag of the current behind the apparent developed emf; but, owing to armature distortion, the full-load flux-distribution curve (from which the voltage  $OE'_d$  is derived) will not be symmetrically placed relatively to the center line of the pole; it will be displaced in the direction of motion of the conductors (*i.e.*, to the right in Fig. 102).

The effect of slot-leakage flux on voltage regulation is almost identical with that of armature reaction; that is to say, it causes a displacement of the resultant flux in relation to the center line of the field pole, and usually a change in the shape of the emf wave; but this minor effect is disregarded here since, in order to simplify the treatment, only the fundamental sine waves of the alternating quantities are considered.



The vector diagram (Fig. 109) explains how the slot-leakage flux is a factor in determining the field excitation required and, incidentally, it will explain how the angle  $\beta$  (Figs. 105 and 106) and the position of the neutral zone with reference to the center of the pole face ( $\beta - \psi + 90^\circ$ ) may be calculated. The assumption of sine-wave functions is still made, although, as previously stated, this may not always be justified because of the distortion of the flux-distribution curves, especially with salient-pole machines.

The vectors  $OI$ ,  $OE$ ,  $OD$ , and  $OF$  (Fig. 109) have the same meaning as in Fig. 107. The vector  $OM$ , in phase with  $OF$  (the "apparent" developed voltage  $E'_d$ ), represents the ampere-turns required to overcome air-gap and tooth reluctance when the air-gap flux is such that it would

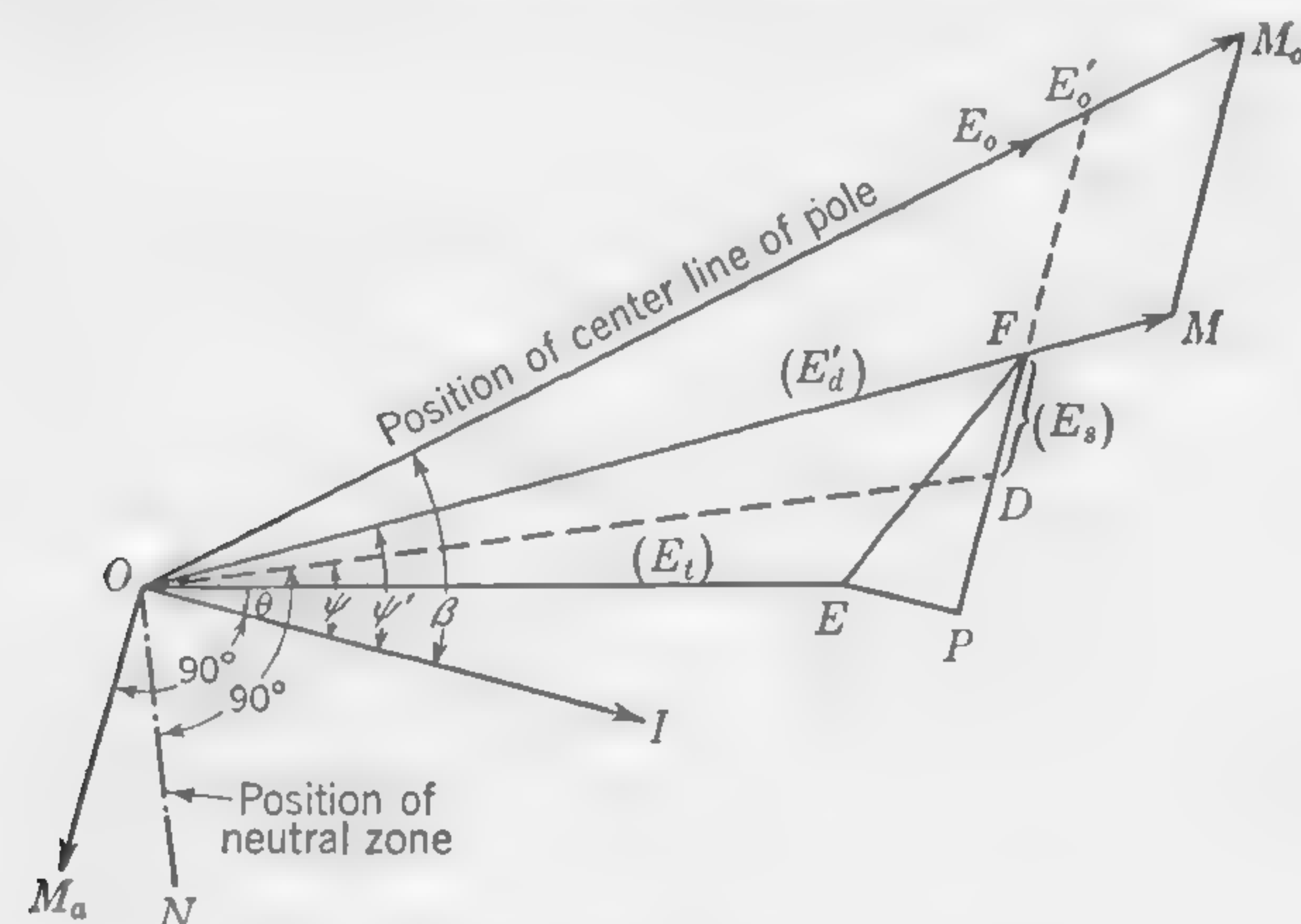


FIG. 109. Vector diagram for a-c generator.

develop  $E'_d$  volts per phase in the armature if it were cut by all the conductors. If we neglect the effect of increased tooth saturation, the vector  $OM$  may be defined as

$$OM = (\text{open-circuit field } TI \text{ per pole}) \times \frac{E'_d}{E_t}$$

the open-circuit field excitation being calculated as explained in Arts. 83 and 85. The vector  $OM_a$ , drawn exactly  $90^\circ$  behind  $OI$ , represents the maximum value of the armature ampere-turns per pole as calculated by formula (78) on page 217. This must be balanced by the field component  $MM_0$ , giving  $OM_0$  as the required field excitation under load. If the load is thrown off, the developed voltage will be  $OE_0$  with the point  $E_0$  on the vector  $OM_0$ . The length  $OE_0$  will usually be somewhat less than  $OE'_0$ , obtained by extending  $PF$  until it meets  $OM_0$ , because increased saturation of the iron in the magnetic circuit will prevent the developed emfs from being exactly proportional to the exciting ampere-turns.

When the load is thrown off, the maximum value of the voltage wave  $OE_0$  will occur immediately under the center line of the pole face, and  $\beta$ , as obtained from Fig. 109, is therefore the angular displacement from the center line of the pole of the slot conductors carrying the maximum current. The line  $ON$ , drawn  $90^\circ$  behind  $OD$ , is the position of the neutral zone in relation to the poles. The amount of slot flux passing from tooth to tooth in this zone determines the magnitude of the effect which slot leakage has upon the inherent voltage regulation of the machine. The diagram (Fig. 109) shows how not only the magnitude but also the direction of the component vector  $E_s$  affect the voltage regulation ( $OE_0 - OE$ ) of the machine. If the mmf distribution over the armature surface on open circuit is known (whether or not this is a sinusoidal distribution), the curve of full-load mmf distribution can be obtained by adding to the ordinates of the open-circuit curve the ordinates of the armature mmf curve which must be plotted with a lag of  $(90 + \beta)^\circ$  (see Fig. 102 and the vector diagram, Fig. 109). If the permeance between pole and armature is known for all points over the pole pitch, it is then possible to plot curves of flux distribution for both open-circuit and loaded conditions. This will be done in the example which follows.

**91. Illustrative Example. Design of Field Magnet (Rotor) of Turbo-generator.** Referring to the Illustrative Example of Art. 82, design the field magnet (rotor) of the 8,000-kva turbo-generator of which the armature (stator) was designed. Take all necessary data and particulars from the design sheet on page 199.

### CALCULATIONS

Items 1, 2, 3, and 4 are data taken from Art. 82.

Item 5, axial length of pole face, is made somewhat less than the gross axial length of the armature core (item 23, Art. 82). Refer to Art. 47. We may decide upon 49.5 in. for this dimension.

Items 6 and 7. In order to calculate the flux per pole which the rotor must provide under full-load conditions, it is necessary to know what has been referred to as the *apparent developed voltage* (i.e., the length of the vector  $OF$ , Fig. 107). The length of the vector  $OD$  was calculated in Art. 82 (item 43), and this determines the amount of flux in the armature core which is cut by the conductors. But the flux in the air gap between pole and armature teeth includes also the slot-leakage flux and we must, therefore, calculate this or the volts which would have been developed in the armature if the slot-leakage flux had been cut by the armature conductors. The dimensions used in the following calculations refer to the stator and stator slots and they are taken from Art. 82.

The loss of pressure due to the slot flux may be calculated as explained



in Art. 89, using formula (96), wherein the quantities have the following numerical values:  $f = 60$ ,  $p = 4$ ,  $C_s = 3$ ,  $n_s = 4$ ,  $I_c = 700$ ,  $l_a = 51 \times 2.54 = 129.5$  cm,  $b = 0$ ,  $2c = 2\frac{1}{8}$  in., and  $s = 1$  in. The permeances  $P_2$  and  $P_3$  of the flux path in the air spaces above the conductors can be

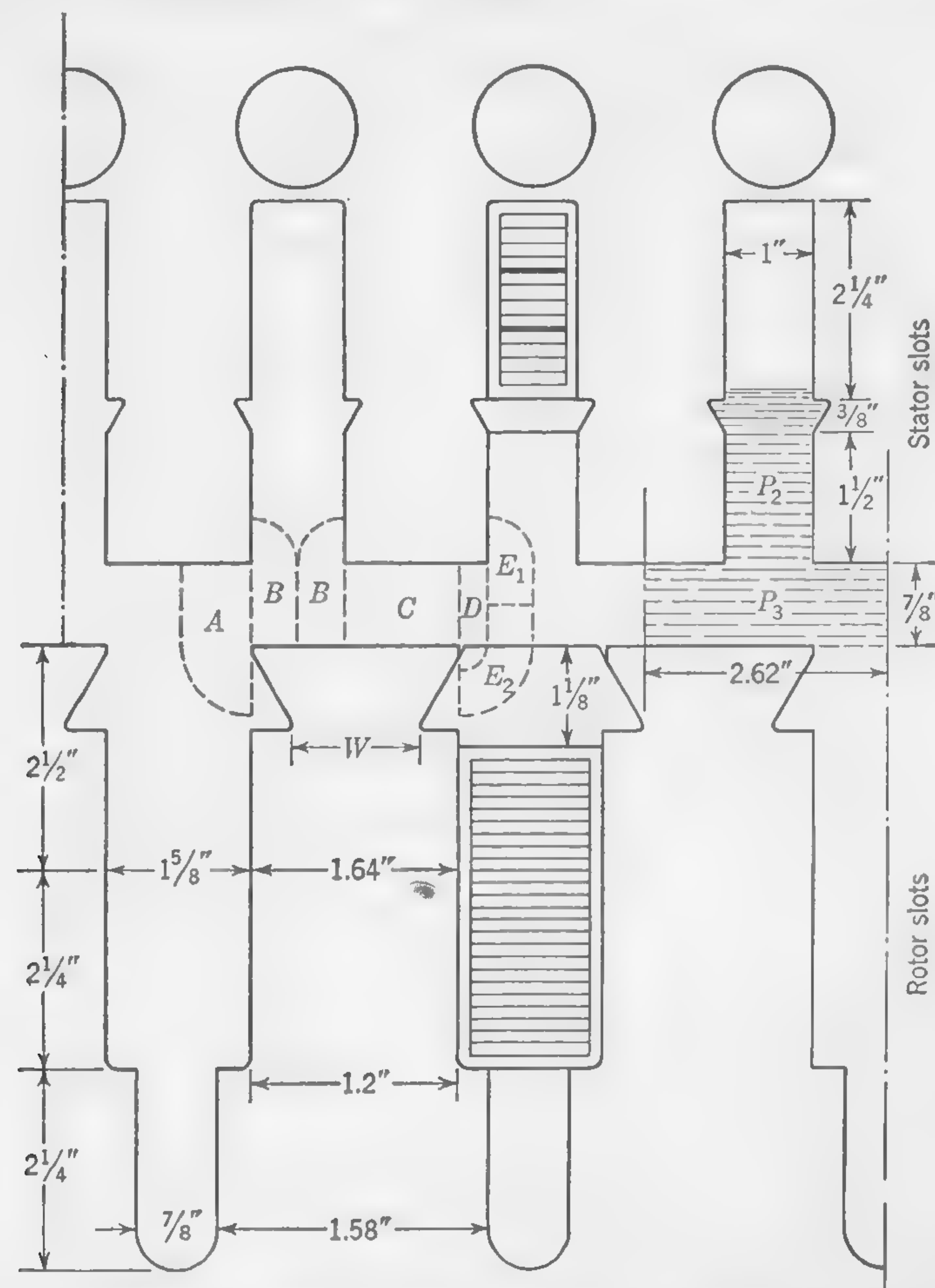


FIG. 110. "Developed" section through stator and rotor teeth of 8,000-kva turbo-generator.\*

calculated as follows. Neglecting the widening of the slot to accommodate the wedge, the permeance of the slot above the winding (see Fig. 110) is  $P_2 = (2 \times 1)/1 = 2$  per centimeter length of armature core measured parallel to the shaft. The permeance of the path from tooth top to tooth top may be calculated by assuming the mmf of one armature slot

\* Several tooth dimensions are not dimensionally correct because, for convenience in drawing, teeth are shown with parallel sides instead of properly tapered sides.

to set up the flux in an air space of radial depth  $\delta = \frac{7}{8}$  in., and of length  $\lambda = 2.62$  in. Thus  $P_3 = (7 \times 1)/(8 \times 2.62) = 0.334$ . This last quantity cannot have a numerical value smaller than that calculated by this method. If the rotor teeth were built up of thin plates like the stator, the numerical value of  $P_3$  would be greater than 0.334; but we are assuming a solid steel rotor (which is customary), and for this reason it will be

DESIGN SHEET FOR ROTOR OF TURBO-GENERATOR  
(Dimensions in inches unless otherwise stated)

	Sym-bols	Known or calculated values
1 Number of poles.....	$p$	4
2 Peripheral speed, fpm.....	$v$	18,000
3 Outside diameter.....		38.25
4 Flux per pole (no load), maxwells.....	$\Phi$	$62.7 \times 10^6$
5 Axial length of pole face.....		$49\frac{1}{2}$
6 $I\lambda$ drop (armature slots), volts per phase winding.....		190
7 Full-load flux per pole, maxwells.....		$66.3 \times 10^6$
8 Shape of pole face.....		Cylindrical
9 Number of slots per pole (rotor).....		8
10 Slot pitch (rotor).....	$\lambda_r$	3.76
11 Slot width (rotor).....		1.625
12 Permeance per sq cm of air gap (center).....		0.3408
13 Equivalent air gap at center of pole.....	$\delta_e$	1.25
14 "Actual" tooth density in terms of air-gap density.....		Fig. 111
15 Saturation curves for air gap and teeth.....		Fig. 112
16 Open-circuit flux-distribution curve.....		Fig. 114
17 Open-circuit mmf-distribution curve.....		Fig. 115
18 Full-load mmf and flux curves.....		
19 Completion of field-magnet design.....		
20 Flux-leakage coefficient.....	$l_f$	1.15
21 Amp-turns (per pole) on field (no load).....		27,000
22 Amp-turns (per pole) on field (full load).....		37,000
23 Field-magnet winding.....		$1\frac{1}{4} \times 0.12$
24 Current in field winding (no load).....		375
25 Current in field winding (full load).....		514
26 $I^2R$ loss (field) (full load).....		66 kw
27 Total cross section of air ducts—stator and rotor (forced ventilation).....		6.6 sq ft

best to neglect the flux paths through the iron of the rotor teeth. A sudden growth of leakage flux is impossible in solid iron, owing to the demagnetizing effect of the eddy currents produced, and the value for  $P_3$  as here calculated will be about right. The extra slot depth of  $1\frac{1}{2}$  in. above the wedge was deliberately provided to increase the permeance  $P_2$  and reduce the amount of the instantaneous current on a short circuit.



By inserting all these numerical values in formula (96), we get for the volts lost by slot leakage, when the armature conductors are carrying full-load current,  $E_s = 189$ , or (say) 190 volts.

We are now in a position to draw a vector diagram similar to Fig. 107 for any power-factor angle  $\theta$ , the calculated numerical values of the component vectors being:

$$\left. \begin{aligned} E_t &= OE = 3,810 \\ (IR) &= EP = 8.4 \\ (IX)_{\text{ends}} &= PD = 150 \\ E_s &= DF = 190 \end{aligned} \right\} \text{From Art. 82}$$

In order to calculate the full-load flux per pole with a load power factor of 0.8 (see Art. 88, Fig. 107) we have for the "apparent" developed voltage:

$$\begin{aligned} E'_d &= \sqrt{(E_t \cos \theta + EP)^2 + (E_t \sin \theta + PF)^2} \\ &= 4,030 \text{ volts} \end{aligned}$$

The full-load flux per pole (item 7) is, therefore,

$$\begin{aligned} \frac{62.7 \times 10^6 \times E'_d}{E_t} &= \frac{62.7 \times 10^6 \times 4,030}{3,810} \\ &= 66.3 \times 10^6 \text{ maxwells} \end{aligned}$$

*Item 8.* Since we are using a cylindrical rotor, the variation of flux density over the pole pitch must be obtained by distributing the field winding in slots on the rotor surface; but, in the design of salient-pole machines, the pole face should be shaped as explained in Art. 84, and approximate dimensions of the pole core should be decided upon with a view to providing sufficient space for the exciting coils. The cross section of the pole cores would be determined, as in the case of continuous-current dynamos, by calculating or assuming a leakage factor (see p. 210) and deciding upon a flux density in the iron (from 90,000 to 100,000 lines per sq in.).

*Items 9 to 11.* Let us try a rotor as shown in Fig. 98 (p. 212), with eight slots per pole, only six of which are wound, leaving two slots without winding at the center of each pole. The tooth pitch is, therefore,  $(\pi \times 38.25)/32 = 3.76$  in. This quantity, when measured on the inside bore of the stator, is  $(\lambda \times 12)/8 = 3.93$  in.

The slot width may be decided upon by arranging for a fairly high density in the rotor teeth. Thus, the open-circuit flux which passes through a total of eight teeth is  $62.7 \times 10^6$  maxwells. If  $t$  is the average width of rotor tooth in inches, the average tooth density in maxwells

per square inch is  $B'' = (62.7 \times 10^6)/(8 \times t \times 49.5)$ , which must be multiplied by  $\pi/2$  to obtain the approximate maximum density in the teeth near the center of the pole. Neglecting leakage flux, and assuming  $B''_{\text{max}} = 140,000$ , the tooth width will be 1.78 in., which indicates that a slot  $1\frac{5}{8}$  in. wide will probably be suitable.

Before deciding upon the depth of rotor slot, it will be advisable to calculate the equivalent air gap in order that the field ampere-turns and necessary cross section of copper may be determined.

The thickness of wedge for keeping the field windings in position might be about  $1\frac{1}{8}$  in., shown in Fig. 110; but as the centrifugal force exerted upon it by the copper in the slot may be very great on account of the high peripheral velocity, careful calculations should be made to determine the compression and bending stresses in the wedge. The allowable working stress for manganese bronze or phosphor bronze wedges is about 14,000 lb per sq in.

While discussing the matter of rotor slot design, the question of stresses in the rotor teeth should be mentioned. After the slot depth has been decided upon, the centrifugal pull on the rotor tooth should be calculated and the maximum stress in the steel determined, the slot proportions being modified if this stress exceeds 14,000 lb per sq in. for cast steel or 16,000 lb per sq in. for mild steel. Materials are now available for use in large modern turbo-generators in which the safe working stress is appreciable in excess of these figures. The total centrifugal pull at the root of one tooth is due to the weight of the tooth plus the contents of one slot, including the wedge, while the pull at the narrow section near the top of tooth (the width  $W$  in Fig. 110) is due to the contents of one slot plus the wedge and the portion of the tooth above the section considered (see numerical example, Art. 158).

*Items 12 and 13.* The calculation of the average permeance of the air gap between rotor and stator is carried out as explained in Art. 85. The approximate paths of the flux lines are shown in Fig. 110, which is a "developed" section through the stator and rotor teeth; that is to say, no account is taken of the curvature of the air gap, the tooth pitch on the rotor being made exactly equal to 1.5 times  $\lambda$ , namely, 3.93 in., or 10 cm. The actual air gap from tooth top to tooth top (from Art. 82) is  $\delta = 0.875$  in., and, if we neglect the slightly increased reluctance due to the angle of the tooth sides under the wedge, the component flux paths may be thought of as made up of straight lines, or of straight lines terminating in quadrants of circles. The permeance of each section of the flux path between stator and rotor over a space equal to the rotor slot pitch is easily calculated. The particular case of flux paths such as  $A$ ,  $B$ , and  $E$  of Fig. 110 is dealt with as explained in connection with the permeance  $P_2$  in



Art. 35. The calculated numerical values of the permeances per centimeter of air gap measured axially are:

$$\begin{aligned}\text{Path } A &= 0.5725 \\ \text{Path } B &= 0.4080 \\ \text{Path } B &= 0.4080 \\ \text{Path } C &= 1.4900 \\ \text{Path } D &= 0.2845 \\ \text{Path } E &= 0.2450 \\ \text{Total} &= 3.4080\end{aligned}$$

The permeance per square centimeter cross section of air gap is, therefore,  $3.408/10 = 0.3408$ , and the equivalent air gap is  $\delta_e = 1/0.3408 = 2.94$  cm, or 1.156 in. If great accuracy is required, a similar set of calculations should now be made with the relative position of rotor and stator teeth slightly changed so as to bring a rotor tooth opposite a stator slot instead of a rotor slot opposite a stator slot as shown in Fig. 110, and the mean of the two calculated values will more nearly correspond with the average air-gap permeance. Let us assume that this has been done and that a reasonable value for the average equivalent air gap is  $\delta_e = 1.25$  in.\*

*Item 14: Tooth Saturation Curves.* The curves of Fig. 111 have been constructed as explained in Art. 36 and illustrated by the example of Art. 38 (Fig. 49). A curve is required for the rotor teeth as well as for the stator teeth; indeed, in a turbo-alternator design, the effects of saturation are more noticeable in the rotor teeth, since it is here that the flux density usually attains the highest values. With the comparatively low flux densities in the teeth of a 60-cycle stator, we may use the simpler formula (40b) for calculating one point in the required curve and then draw a straight line through the zero point of the diagram. For the higher densities in the rotor teeth, the more accurate formula (40) must be used. The numerical values for use in these formulas are given below. In the first place, the depth of the slot in the rotor must be approximately determined.

With an equivalent air gap,  $\delta_e = 1.25$  in., and an assumed sinusoidal flux distribution, the field ampere-turns on open circuit to overcome the reluctance of air gap only will be

$$TI = \frac{62.7 \times 10^6 \times \pi}{(51 \times 31.42 \times 6.45) \times 2} \times \frac{1.25 \times 2.54}{0.4\pi} = 24,000$$

\* Should any difficulty be experienced in calculating the permeance of a flux path such as  $E$ , with curved flux lines at both ends, it is generally permissible to divide it in two parts as indicated by the letters  $E_1$  and  $E_2$  (Fig. 110), the permeance of each part being calculated separately. Thus, in the example which has just been worked out, the permeance of  $E_1$  is 0.655, and the permeance of  $E_2$  is 0.39. The total of 0.245 is obtained by taking the reciprocal of the sum of the reluctances.

which makes the ampere-conductors per slot  $24,000/3 = 8,000$ . This does not include the ampere-turns to overcome the reluctance of the teeth and the remainder of the magnetic circuit, neither does it take into account the considerable increase of excitation with full-load current on a power factor less than unity. The current density in the copper may, however, be carried up to 2,500 or even 3,000 amp per sq in. of copper cross section, and it is probable that a slot  $4\frac{3}{4}$  in. deep will provide sufficient space for the field winding.

The dimension  $d_e$  in formula (40) is the actual slot depth less the difference between the equivalent and actual air gap. This difference amounts to  $\frac{3}{8}$  in.; but, since it is caused by the slotting of both the stator and the rotor surfaces, we shall halve this amount and make  $d_e = d - \frac{3}{16}$  in., whether the depth  $d$  refers to the stator or rotor slots.

The ratio  $l_a/l_n$  for the stator is taken—together with the other stator data—from Art. 82. In the case of the rotor, it should be observed that we are considering the air-gap density over the surface of the *stator*, and, for this reason, the slot pitch for the rotor tooth calculations should be taken as  $\lambda = 3.93$  in., being  $1\frac{1}{2}$  times the stator slot pitch (this is the ratio between number of stator and number of rotor teeth). There will be no radial vent ducts in the rotor, and the ratio  $l_a/l_n$  may be taken as

$$\frac{\text{Gross axial length of armature}}{\text{Axial length of rotor}} = \frac{51}{49.5} = 1.03$$

The numerical values of all the symbols used in formulas (40) and (40b) are as follows:

Stator:

$$\begin{aligned}\delta_e &= 1.25 \text{ in.} \\ \lambda &= 2.62 \text{ in.} \\ d_e &= 3.94 \text{ in.} \\ t &= 1.88 \text{ in. (at center of tooth)} \\ l_a/l_n &= 1.09 \\ \lambda &= 3.93 \text{ in.} \\ d_e &= 4.56 \text{ in.}\end{aligned}$$

Rotor:

$$\begin{aligned}t &= 1.64 \text{ in. (at center of tooth)} \\ l_a/l_n &= 1.03\end{aligned}$$

The value of  $\mu$  for use in formula (40) is obtained from the  $B$ - $H$  curve (Fig. 48). Note that the densities read from Fig. 111, and referred to in the following calculations, are in gauss. They must be multiplied by 0.45 if the student prefers to work with flux densities expressed in maxwells per square inch.



Item 15. The saturation curve for air gap, teeth, and slots is constructed as explained in Illustrative Example of Art. 38 in connection with the design of a d-c dynamo (Fig. 49). The ampere-turns per inch length of tooth are read from Figs. 47 and 48; and Simpson's rule [see Art. 37, formula (42)] is used in calculating the ampere-turns required for the rotor teeth at the higher densities. In regard to the stator teeth,

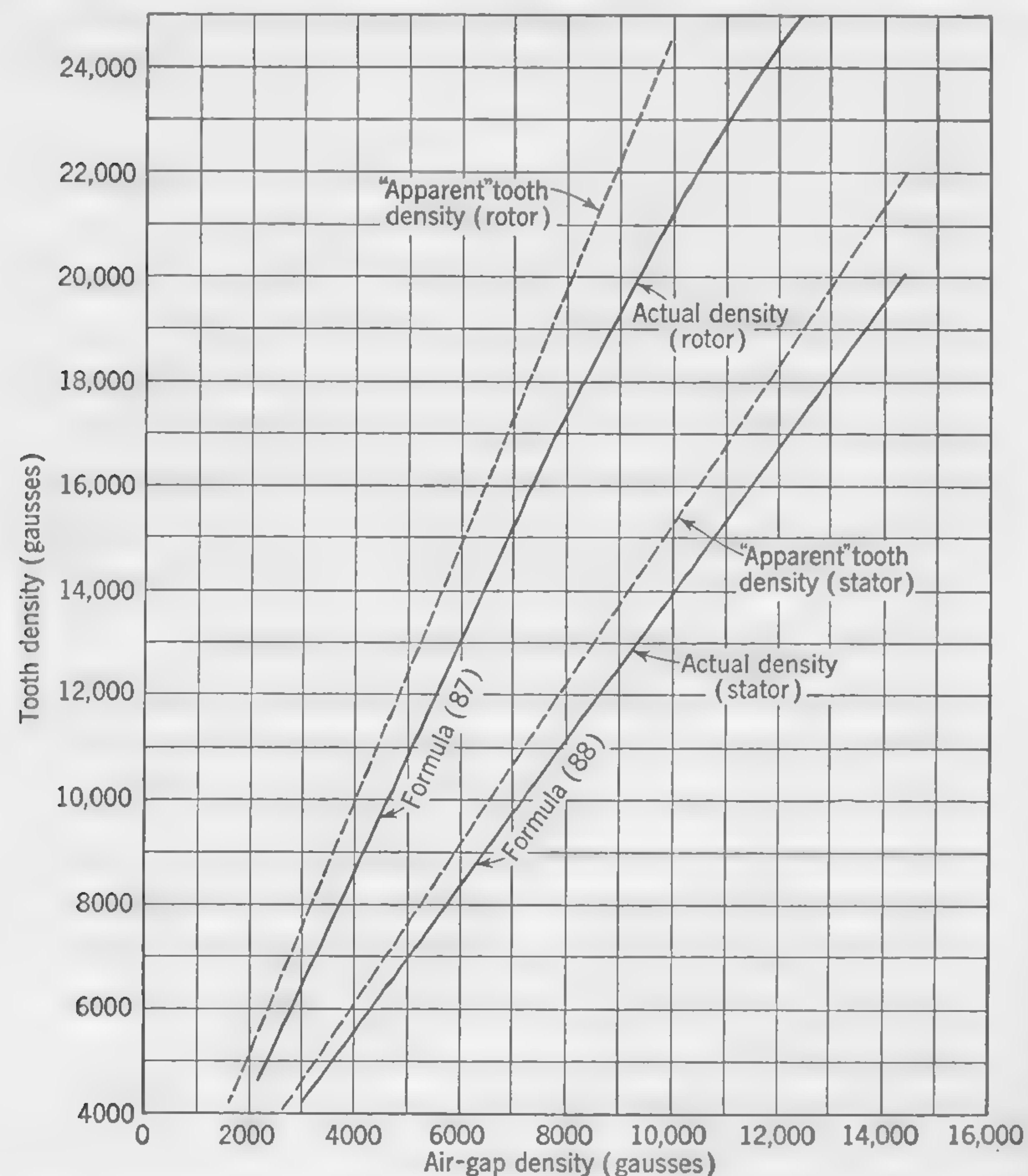


FIG. 111. Tooth densities in terms of air-gap density—8,000-kva turbo-generator.

the mean value of the tooth density may be used in determining the ampere-turns required, the application of Simpson's rule being, in this case, an unnecessary refinement. In calculating the tooth reluctance for plotting the saturation curve, Fig. 111, no correction for leakage flux has been made. It is true that the total flux in the body of the rotor is somewhat greater than the useful flux entering the armature; but the omission of this correction may be set against the fact that the tooth

density calculations make no allowance for the flux lines which pass from the sides of the tooth into the iron at the bottom of the slot, thus causing the actual density at the narrowest part of the tooth to be something less than the calculated value.

The curve marked *air gap, teeth, and slots* (Fig. 112) shows what excitation is required to produce a particular density in the air gap. The departure from the air-gap line (the dotted straight line) is due almost entirely to saturation of the rotor teeth, the reluctance of the stator teeth being negligible as compared with that of the  $1\frac{1}{4}$ -in. air path. The upper curve for center of pole face will be referred to later.

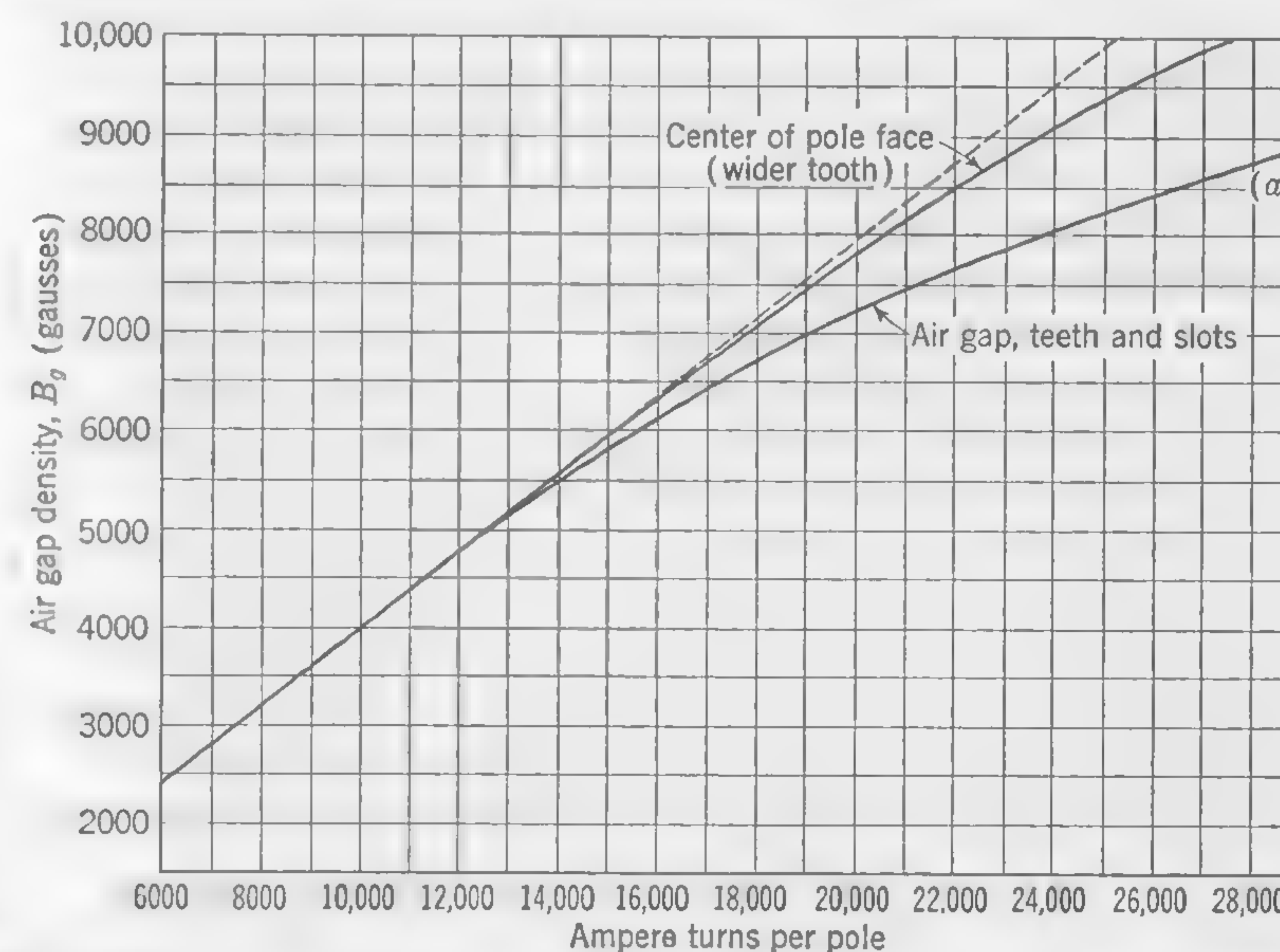


FIG. 112. Saturation curves for air gap, teeth, and slots—8,000-kva turbo-generator.

Items 16 and 17. The upper curve of Fig. 113 shows the ideal flux-distribution curve for open-circuit conditions. It is a sine curve of which the average ordinate is

$$B_g = \frac{62.7 \times 10^6}{6.45 \times 31.416 \times 51} = 6,070 \text{ gauss}$$

and of which the maximum value is, therefore,  $(\pi/2) \times 6,070 = 9,520$  gauss. The area of this curve is a measure of the total air-gap flux on open circuit. The pole pitch—represented by 180 electrical degrees—has been divided into eight parts, and the height of the vertical lines is a measure of the flux density in the air gap over the center of a rotor tooth.

By providing a datum line and vertical scale of ampere-turns immediately below the no-load flux curve, it becomes a simple matter to plot



an ideal curve of mmf distribution over the pole pitch, the shape of this curve being such as to produce the desired flux distribution (see Art. 85). It is merely necessary to read off the curve of Fig. 112 the ampere-turns corresponding to the required air-gap density and to plot this over the center of the corresponding tooth. In this manner the lower curve of

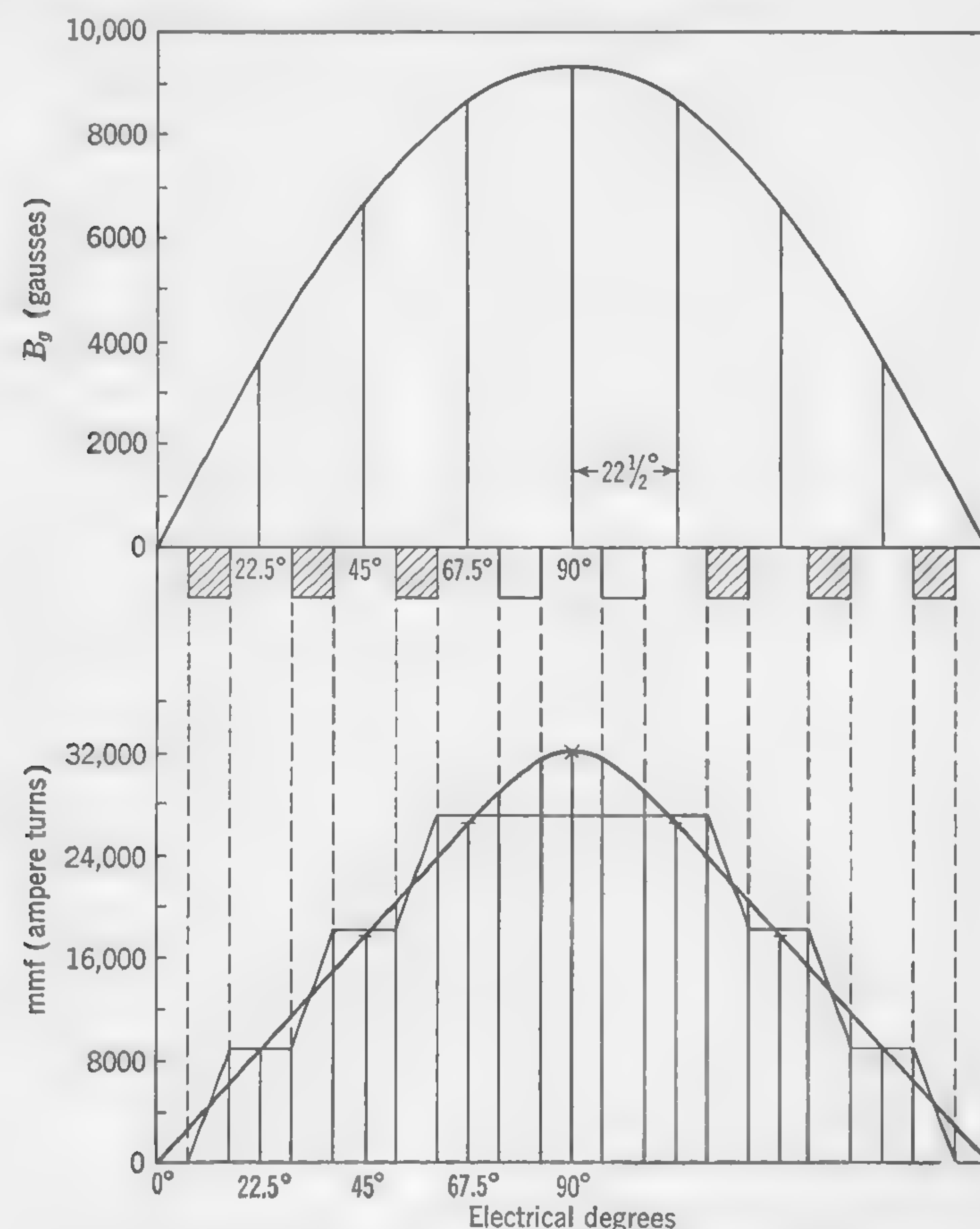


FIG. 113. Ideal flux-distribution and mmf curves—8,000-kva turbo-generator.

Fig. 113 is obtained. The practical approximation to this ideal mmf distribution would be the arrangement shown by the stepped curve, with 9,000 amp conductors in each slot. This would produce a flat-topped flux distribution curve, a condition which might be remedied by putting 5,000 amp-turns in the empty slots at the center of the pole face; but such a procedure would be very uneconomical and unsatisfactory. The best thing to do will be to increase the permeance of the center tooth, either by reducing the width of the two slots on each side of the center tooth or

by partly filling up these slots with iron wedges so shaped as to produce the effect of a tooth with parallel sides. These slots should, in any case, be filled with material equal in weight to the copper and insulation in the wound slots, in order to improve the balance and equalize the stresses at high speeds; and the proportion of magnetic to nonmagnetic metal can be so adjusted as to obtain any desired tooth reluctance. If we provide wedges having a thickness of  $\frac{1}{2}$  in. at the bottom of the slot, we can get the equivalent of a center tooth 2.2 in. wide with parallel sides. This calls for an additional curve in Fig. 112, which can be calculated in the same manner as the curve previously drawn, except that the correction for taper of teeth (Simpson's rule) has not to be applied.

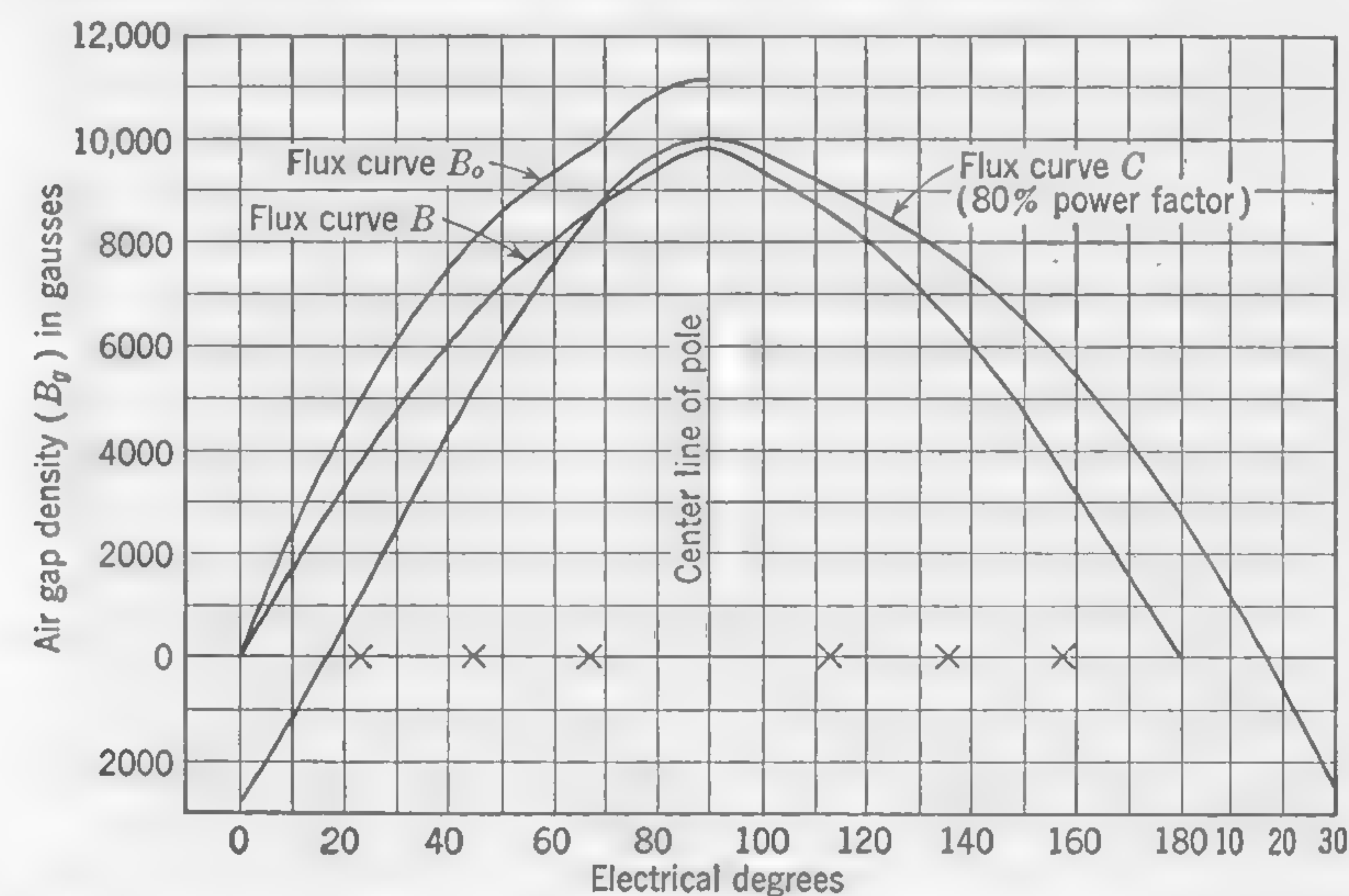


FIG. 114. Air-gap flux-distribution curves—8,000-kva turbo-generator. (Note: Flux curve  $B_0$  is referred to in Chap. 9.)

If we decide upon a rotor winding with 9,000 amp-conductors per slot, as indicated by the stepped curve in the lower part of Fig. 113, we shall obtain an open-circuit flux curve  $B$  as plotted in Fig. 114. This curve would be exactly similar in shape to the flux curve of Fig. 113, if it were not for the fact that the widening of the tooth at the center of the rotor pole face has lowered the reluctance at this point rather more than would have been necessary in order to obtain the perfect sine curve of flux distribution. The slightly higher ordinate at the center of the new flux curve adds so little to the area of this curve that we shall not trouble to measure this. It is evident that the proposed excitation with 9,000 amp-conductors per slot will generate the required open-circuit voltage.

The mmf curve corresponding to the flux curve  $B$  has been redrawn in Fig. 115, the stepped curve of Fig. 113 being replaced by a smooth curve.



In this connection it should be noted that the "fringing" of flux at the tooth tops tends to round off the sharp corners of the flux-distribution curves and so justifies the use of smooth curves in any graphical method of study. At the same time, it will generally be possible to detect in oscillograph records of the emf waves the irregularities or "ripples" due to the tufting of the flux at the tooth tops; but these minor effects will be neglected.

Item 18. The vector diagram (Fig. 116) is constructed as explained in Art. 90 in connection with Fig. 109; the "apparent" developed voltage at full load being  $OE'_d = 4,030$  volts, as calculated under item 7.

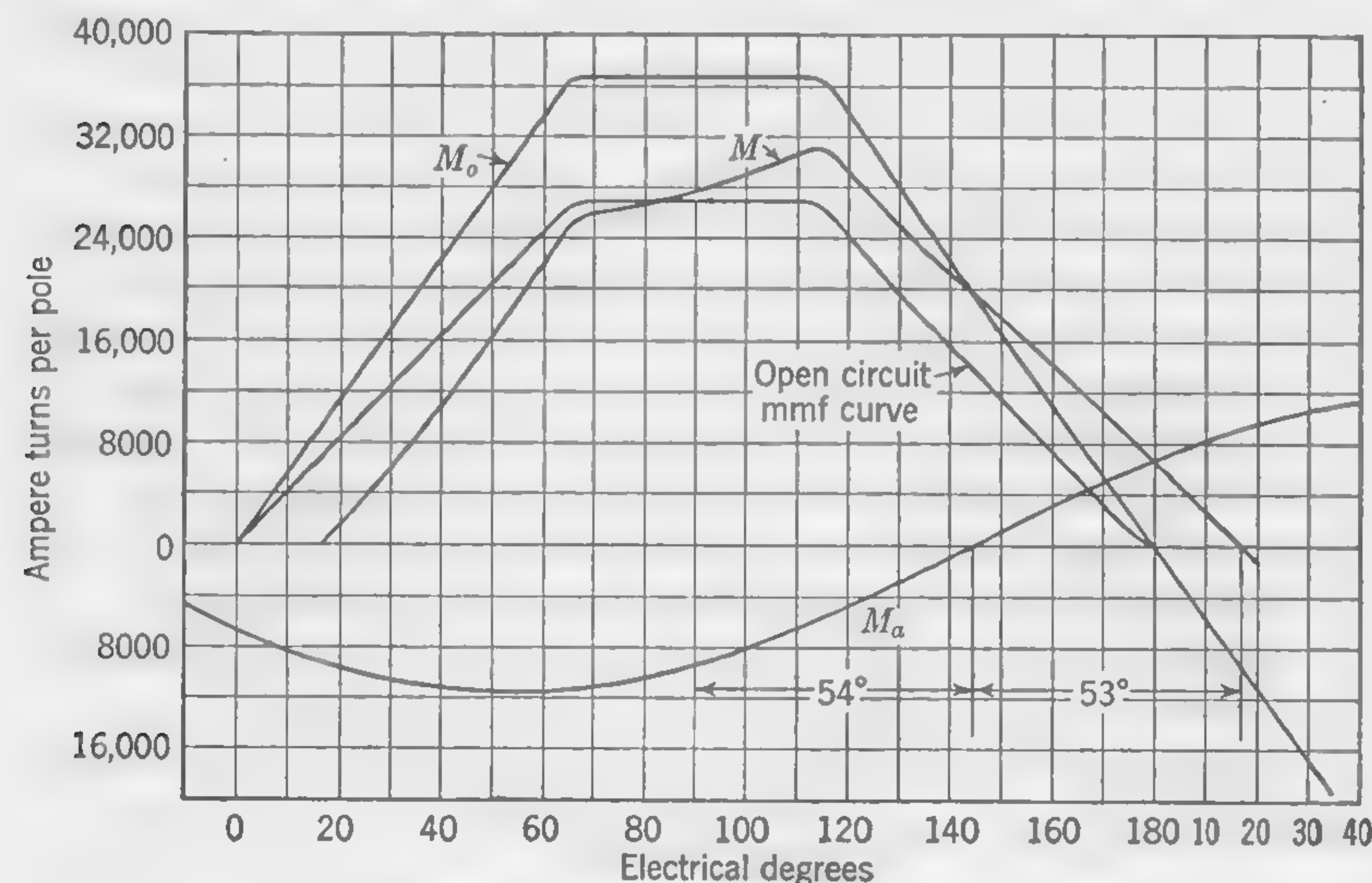


FIG. 115. Mmf curves for 8,000-kva turbo-generator.

In order to determine the field excitation necessary to provide the required flux with full-load current taken from the machine on a power factor of 0.8, it is necessary to know the maximum armature mmf and also the position on the armature surface (considered relatively to the field poles) at which this maximum occurs. It was shown in Art. 86 that the armature mmf can be represented by a sine curve of which the maximum value [by formula (78)] is

$$(TI)_a = \frac{(48 \times 3) \times 700 \times \sqrt{2}}{\pi \times 4} = 11,340 \text{ amp-turns per pole}$$

The displacement of this mmf curve relatively to the center of the pole is obtained approximately by calculating the angle  $\beta$  as explained in Art. 90. The vectors representing the component mmfs have been drawn in Fig. 116, the angle  $\psi'$  being calculated from the previously ascertained

values of the voltage vectors. Thus

$$\cos \psi' = \frac{(0.8 \times 3,810) + 8.4}{4,030} = 0.76$$

Whence  $\psi' = 40^\circ 0' 30''$ .

Since 27,000 amp-turns per pole (or 9,000 amp-conductors per slot) are required to develop 3,810 volts per phase, and since the saturation curve does not depart appreciably from a straight line, the mmf vector  $OM$  to

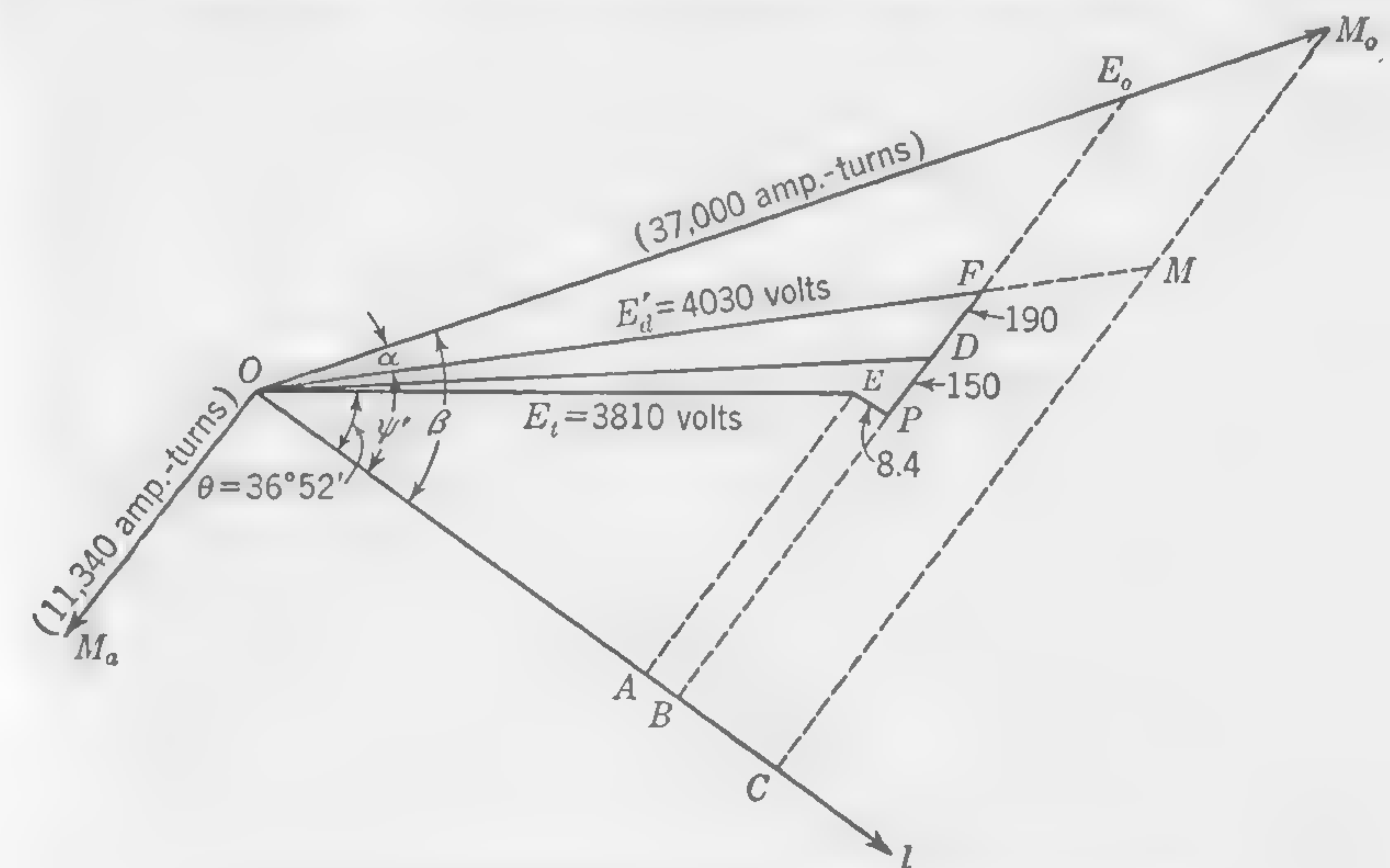


FIG. 116. Vector diagram for 8,000-kva turbo-generator.

develop  $E'_d$  (i.e., 4,030 volts) must represent approximately  $(27,000 \times 4,030)/3,810 = 28,600$  amp-turns, and the required angle is,

$$\beta = \tan^{-1} \frac{CM_o}{OC}$$

where

$$CM_o = CM + MM_o = OM \sin \psi' + 11,340 = 29,940$$

and

$$OC = OM \cos \psi' = 21,700$$

The angle  $\beta$  is thus found to be  $54^\circ 4'$ , or (say)  $54^\circ$ .

The sine curve  $M_a$ , representing armature mmf, can now be drawn in Fig. 115, with its maximum value displaced  $(54 + 90)^\circ$  beyond the center of the pole. The required field ampere-turns are given approximately by the length of the vector  $OM_o$  (Fig. 116), which does not take account



of increased tooth saturation. The length  $OM_o$  is  $OC/\cos \beta = 21,700/0.588 = 36,900$ . An excitation slightly in excess of this amount will probably suffice,\* because, if the average density over the pole pitch is raised from 6,070 gauss to  $6,070 \times (4,030/3,810) = 6,420$  gauss, the average effect of increased tooth reluctance, as shown by Fig. 112, is small, and we shall try 37,000 amp-turns on the field. This full-load field excitation is represented by the curve  $M_o$  (Fig. 115). Now add the ordinates of  $M_o$  and  $M_a$ , and obtain the resultant mmf curve  $M$ . Using this new mmf curve, we can obtain from Fig. 112 the corresponding values of air-gap flux density and plot in Fig. 114 the full-load flux curve  $C$  of which the area, as measured by planimeter, is found to be 113.8 unit squares. In order to check this figure and determine whether or not the full-load flux is sufficient to generate the required voltage in the windings, note that the base of the curve (the pole pitch) measures 18 divisions and that the height of each unit square represents 1,000 gauss. The required average density in the air gap over the pole pitch is 6,420 gauss, and the total flux required (item 7) is  $66.3 \times 10^6$  maxwells. The required area under the full-load flux curve is, therefore,  $18 \times 6.42 = 115.6$  unit squares, which checks fairly well with the measured area. It follows that a field excitation of approximately 37,000 amp-turns will provide the right amount of flux to give the required terminal voltage when the machine is delivering its rated full-load current at 80 per cent power factor.

In the design of slow-speed machines with salient poles shaped to give approximately a sinusoidal flux distribution on open circuit, curves of mmf and flux distribution can be plotted generally as explained in connection with the distributed field winding in this problem. The work is, however, less simple and more tedious because of the variations in the air-gap reluctance for different points on the armature surface relatively to center line of pole (refer to Art. 43).

*Item 19.* This applies mainly to the salient-pole type of machine, the procedure in proportioning the field poles and yoke ring being then similar to that followed in d-c design. The depth of iron below the slots in the rotor of a turbo-alternator is usually more than sufficient to carry the flux, including the leakage lines. In the particular design under consideration we shall be able to provide air ducts at the bottom of the rotor slots as shown in Figs. 110 and 117 and still leave enough section of iron to carry the flux. We shall assume a solid-forged rotor in this design, which may be either in one piece with the shaft (tapering from about 13 to  $10\frac{1}{2}$  in. in the bearings) or provided with shaft projections bolted to the two ends.

\* This method of estimating the full-load field ampere-turns is not scientifically sound, especially in the case of salient-pole machines, because the mmf distribution over the armature surface, due to the field-pole excitation, is rarely sinusoidal as here assumed.

*Item 20: Leakage Coefficient.* The amount of the leakage flux at the two ends of the rotor is not easily estimated; but when expressed as a percentage of the useful flux it is never large in extra high-speed machines with wide pole pitch; the greater the axial length of rotor, in respect to the diameter, the smaller will be the percentage of the flux leaking from pole to pole at the ends. The rotor leakage which occurs from tooth to tooth, and in the air gap, over the whole length of the machine, is shown diagrammatically in Fig. 117. This sketch shows a total of four lines of

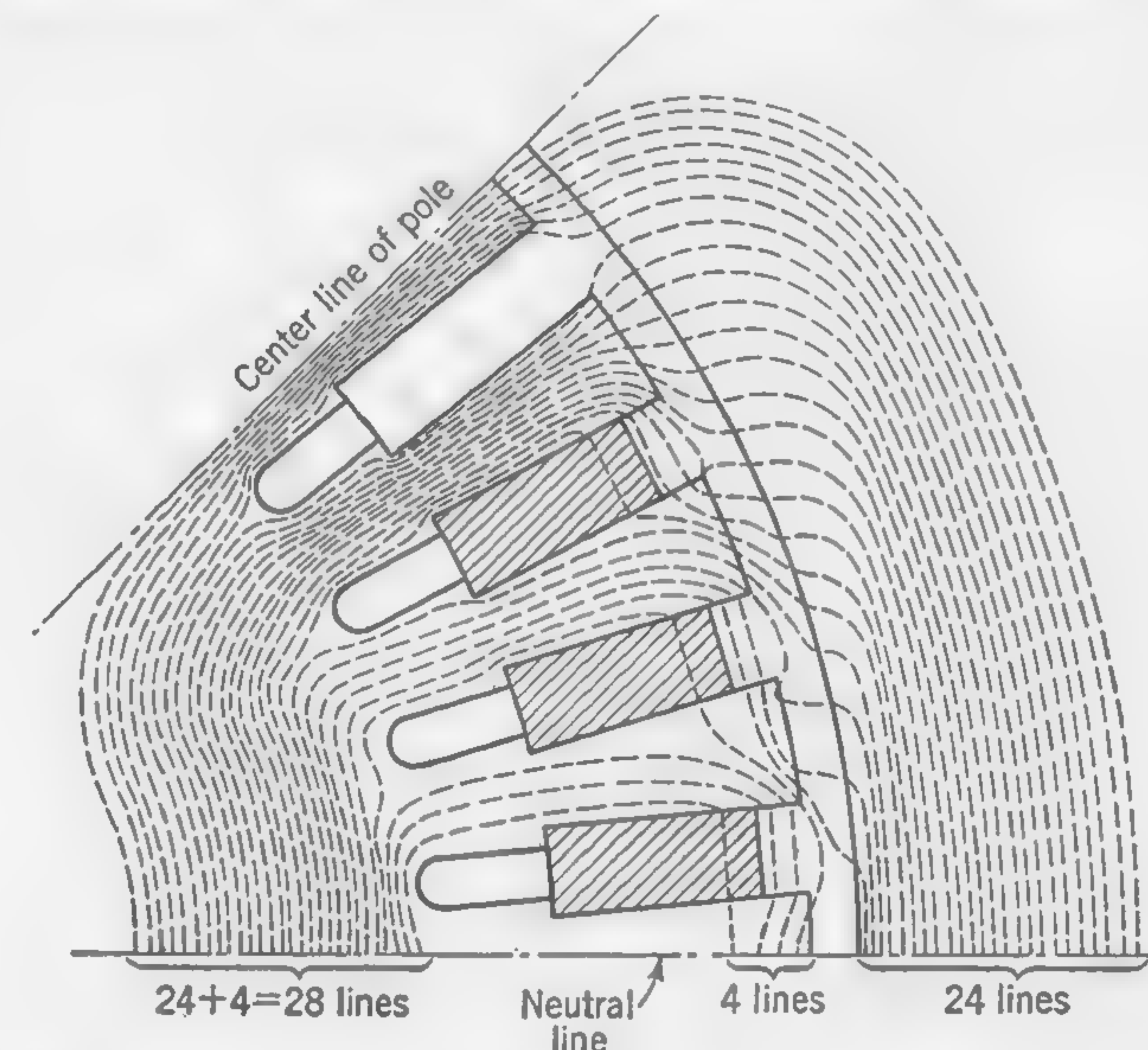


FIG. 117. Illustrating leakage flux in rotor of turbo-generator.

leakage flux which pass through the body of the rotor but do not enter the armature. This leakage flux will not appreciably affect the flux density in the rotor teeth near the neutral zone, because it will follow the path of least reluctance and be distributed between several teeth.

The calculation of the rotor slot flux may be carried out as for the stator windings. Thus, at full load, with  $37,000/3 = 12,300$  amp-conductors per slot, the flux passing from tooth to tooth below the wedge is

$$\underbrace{\frac{0.4\pi \times 12,300}{2}}_{\text{Average mmf}} \times \underbrace{\frac{(3.5 \times 49.5) \times 2.54}{1.625}}_{\text{Permeance}} = 2,100,000 \text{ maxwells}$$

The flux in the space occupied by the wedge and insulation above the copper, including an allowance for the spreading of the flux lines into the air gap above the wedge (tooth top leakage), is approximately

$$0.4\pi \times 12,300 \times \frac{(1.75 \times 49.5) \times 2.54}{1.8} = 1,900,000 \text{ maxwells}$$



where the figure 1.75 is the assumed radial depth in inches of the flux path, and 1.8 is the assumed average length of the flux lines (somewhat greater than the width of slot below the wedge).

The sum of these two flux components is 4,000,000 maxwells, making the total slot flux for both sides of the pole face equal to twice this amount, or 8,000,000 maxwells. As a rough estimate, we may assume the end leakage to be about one-sixth of this, making a total of 9,300,000 maxwells. The full-load leakage coefficient is, therefore,  $(66.3 + 9.3)/66.3 = 1.141$ , or (say) 1.15.

The maximum number of flux lines in the rotor which cross the section below the slots (represented by 28 lines in Fig. 117) is

$$\frac{6,630,000}{2} \times 1.15 = 38,100,000$$

The radial depth of iron below vent ducts to center of rotor is  $12\frac{1}{8}$  in., whence the cross section is  $12\frac{1}{8} \times 49\frac{1}{2} = 600$  sq in., which makes the average flux density 63,500 lines per sq in. The section of iron below the slots is, therefore, sufficient, and the reluctance of the body of the rotor is a negligible quantity in comparison with that of the teeth and air gap.

*Items 21 to 26.* With a density of 55,500 lines per sq in. in the stator core (Art. 82), and ample iron section in the rotor, the additional ampere-turns required to overcome reluctance of armature and field cores will probably not exceed 200, and the curves of Fig. 112 may be thought of as applying to the machine as a whole. The ampere-turns at no load and at full load (items 21 and 22) will, therefore, be taken at 27,000 and 37,000, respectively, as previously calculated.

The slot insulation will be appreciably thicker than as given by the formula used in items 25 to 30 of Art. 82. It should be not less than 0.1 in. thick, and the field winding might be in the form of copper strip  $1\frac{1}{4}$  in. wide laid flat in the slot. Allowing  $\frac{3}{4}$ -in. total depth of insulation—preferably of mica or asbestos fabric—between the layers of the winding, the total cross section of copper in one slot will be  $2\frac{7}{8} \times 1\frac{1}{4} = 3.6$  sq in., making the current density at full load  $\Delta = 12,300/3.6 = 3,420$  amp per sq in. This is a high, but not necessarily an excessive, figure.

The mean length per turn of the rotor winding should be measured off a drawing showing the method of bending and securing the end connections. We shall assume this length to be 156 in. All the turns will be in series, and the mean length per turn for the four poles in series will be  $156 \times 4 = 624$  in. Assuming the potential difference at the slip rings to be 120 volts, the cross section of the winding, at 60°C, is  $(m) = (624 \times 37,000)/120 = 192,500$  cir mils, or 0.1512 sq in. If we use a copper strip

0.12 in. thick, the number of conductors in each slot will be  $2.875/0.12 = 24$ , making the turns per pole  $24 \times 3 = 72$ .

The current per conductor at full load must be  $37,000/72 = 514$  amp.

The total length of copper strip is  $(72 \times 4 \times 156)/12 = 3,740$  ft. The resistance (hot) will be about 0.250 ohm, and the required pressure at slip rings will be  $0.25 \times 514 = 128.5$  volts. The  $I^2R$  loss is, therefore,  $128.5 \times 514 = 66$  kw, or 0.825 per cent of the rated output. This may be compared with the figures on page 259 in the following chapter which refer to average exciter capacities required with modern a-c generators.

*Item 27: Cooling Ducts.* The cooling air, which enters at one end of the machine, is supposed to travel through the longitudinal vent ducts to the other end of the machine, no radial ducts being provided. Such an arrangement leads to the temperature of one end of the machine being higher than that of the other end; but systems of ventilation designed to obviate this are usually less simple, and the straight-through arrangement of ducts has much to recommend it. In machines larger than the one under consideration, it might be necessary to have the cold air enter at both ends, in which case one or more radial outlets would be provided at the center.

In addition to the ducts, of which mention has already been made, we may provide a number of spaces between the stator iron and the casing to allow of air being passed over the outside of the armature core. Let us suppose that there are 12 such ducts, each 10 in. wide by 1 in. deep; the total cross section of the air ducts is then made up as follows:

	Sq In.
Outside stator stampings.....	$12 \times 10 \times 1 = 120$
Holes punched in stator stampings (Fig. 95, Art. 82).....	$= 590$
Spaces above wedge in stator slots (Fig. 110)....	$48 \times 1.5 \times 1 = 72$
Clearance between stator and rotor.....	$\frac{7}{8} \times \pi \times 39\frac{1}{8} = 108$
Spaces in rotor forging below slots.....	$32 \times 1.94 = 62$
Total.....	$= 952$

or 6.6 sq ft.

Calculations regarding the amount and velocity of the cooling air in this machine were made in the Illustrative Example of Art. 81. Efficiency calculations and methods of predetermining regulation and the probable amount of the short-circuit current will be taken up at the end of the following chapter.

TEST PROBLEMS

The contents of this chapter do not readily lend themselves to being reviewed by a number of short problems similar to those with which previous chapters have been concluded, but an attempt will be made in the problems and questions at the end of Chap. 9 to include some of the subjects which have been presented in this chapter and illustrated by the Illustrative Example of Art. 91.



## CHAPTER 9

## SYNCHRONOUS GENERATORS (Concluded)

## REGULATION AND SHORT-CIRCUIT CURRENT

**92. Voltage Regulation.** The curves in Fig. 118 may be considered as having been plotted from actual test data. The upper curve is the open-circuit saturation characteristic, giving the relation between the number of ampere-turns of field excitation per pole and the pressure at

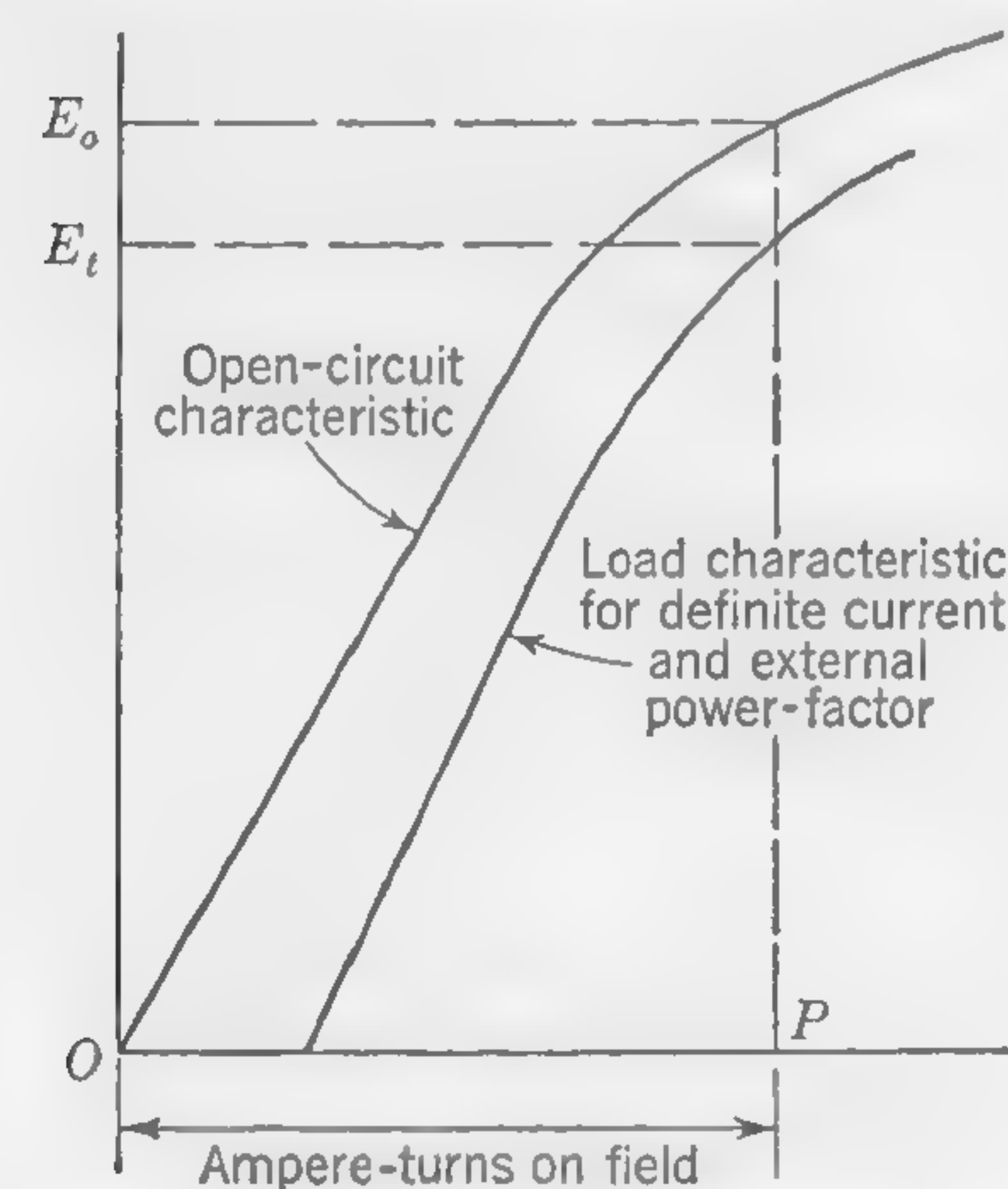


FIG. 118. Inherent regulation obtained from open-circuit and load-saturation curves.

degree of accuracy within which curves, such as those shown in Fig. 118, can be drawn before the machine has been built and tested.

The factors which influence the terminal voltage of a generator driven at constant speed with constant field excitation are:

1. The total or resultant flux actually cut by the armature windings (this involves the flux linkages producing armature reactance)
2. The ohmic resistance of the armature windings
3. The wave shape of the generated emf. This means that the measured terminal voltage depends not only upon the amount of flux cut by the conductors, but also upon the distribution of flux over the pole pitch,

the terminals, which in this case is the same as the emf actually developed in the armature windings. The lower curve is the load characteristic corresponding to a given armature current and a given external power factor. The inherent regulation when the field excitation is of the constant value  $OP$  is, therefore, the difference of terminal voltage  $E_oE_t$  divided by the load voltage  $E_t$ , or, expressed as a percentage of the lower voltage,

Inherent regulation

$$= \frac{OE_o - OE_t}{OE_t} \times 100$$

Thus the error in predetermining the inherent regulation depends upon the

because the amount of flux cut determines the average value of the developed voltage, while the form of the emf wave determines the relation between the mean value and the virtual or rms value.

By far the most important items are included under item *a*, and it is proposed to consider exactly how the resultant flux cut by the armature windings varies when load is put on the machine.

Considering first the flux cut by the active belt of conductors under the pole face, this is not usually the same under load conditions as on open circuit (the field excitation remaining constant), for the following reasons. The current in the armature windings produces a magnetizing effect which, together with the field pole mmf, determines the resultant mmf and the actual distribution of the flux in the air gap. When the power factor of the load is approximately unity, the armature current produces cross-magnetization and distortion of the resultant field, accompanied usually by a reduction of the total flux, owing to increased flux density in the armature teeth where the air-gap density is greatest. This effect is, however, less marked in a-c than in d-c generators, because in the former the tooth density is rarely so high as to approach saturation. On low power factor, with lagging current, the armature mmf tends to oppose the field mmf, and on zero power factor its effect is wholly demagnetizing, thus greatly reducing the resultant air-gap flux. With a leading current, the well-known effect of an increased flux and a higher voltage is obtained. The effect known as "armature reaction," as distinguished from "armature reactance," is, therefore, dependent not only on the amount of the armature current but also largely upon the power factor.

The effect of the individual conductors in producing slot leakage was discussed in Art. 88 and illustrated by Figs. 105 and 106, wherein it is shown that, as current is taken out of the armature, the total flux cut by the active conductors is less than at no load (with the same field excitation) by the amount of the slot flux—or equivalent slot flux—which passes from tooth to tooth in the neutral zone.

Turning now to the flux cut by the end connections (*i.e.*, by those portions of the armature winding which project beyond the ends of the slots), this flux is set up almost entirely by the mmf of the armature windings and is negligible on open circuit. For a given output and power factor, the end flux in a polyphase generator is fixed in position in relation to the field poles, being stationary in space if the armature revolves (see Art. 78). The maximum value of the armature mmf occurs at the point where the current in the conductors is zero, and, on the assumption of a sinusoidal flux distribution, the emf generated by the cutting of these end fluxes may be represented correctly as a vector drawn  $90^\circ$  behind the current vector (refer to the vector diagrams of Figs. 89 and 90). It is, therefore,



permissible to consider this emf component as a reactive voltage such as would be obtained by connecting a choking coil in series with the "active" portion of the armature windings; and if the inductance  $L_e$  of the end windings is known, and a sinusoidal flux distribution assumed, the emf developed by the cutting of the end fluxes under load conditions is given by the well-known expression  $2\pi f L_e I_c$ , where  $I_c$  is the effective value of the current in the armature windings and  $f$  is the frequency.

This quantity was calculated in Art. 78 and expressed in formula (74), the calculation being based upon an amount of end flux per pole ( $\Phi_e$ ) given by the formula (72) or (72a).

**93. Regulation on Zero Power Factor.** In practice, any power factor below 20 per cent is usually considered to be equivalent to zero, so that

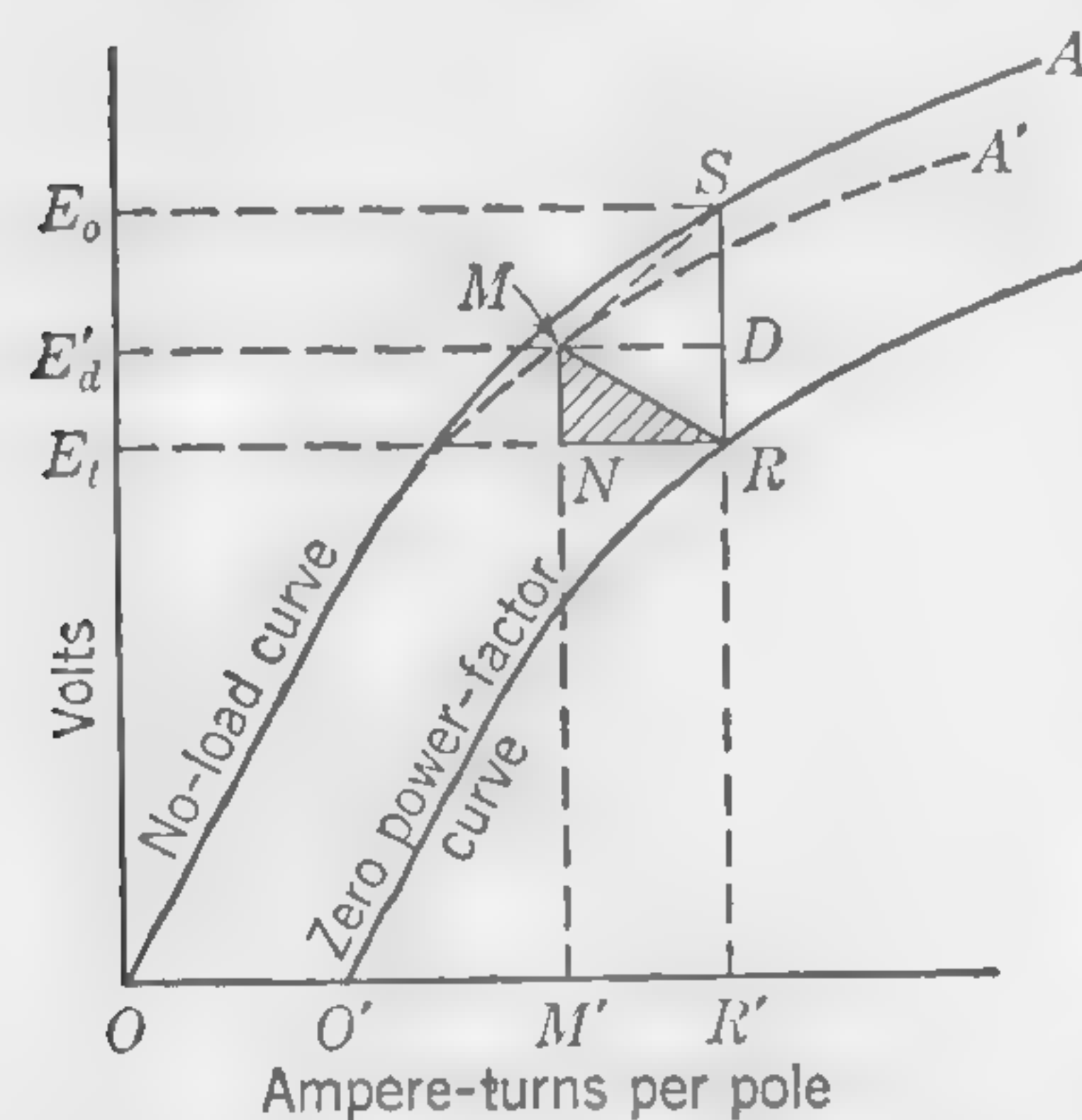


FIG. 119. Method of constructing saturation curve for zero power factor.

the calculations can be checked when the machine is built, by providing as a load for the generator a suitable number of induction motors running light. On these low power factors with lagging current, the phase displacement of the armature current causes the armature mmf to be almost wholly demagnetizing, that is to say, it directly opposes the mmf due to the field windings, the distortional or cross-magnetizing effect being negligible. Its maximum value per pole is given by formula (78) of Art. 86 and its effect in reducing the flux in the air gap is readily compensated (on zero power factor) by increasing the field excitation so that the resultant ampere-turns remain unchanged.\*

Let curve  $A$  (Fig. 119) be the open-circuit saturation curve of the machine, referred to in Art. 92; it is the curve for the complete machine and can be plotted only after the magnetic circuit external to the armature has been designed.

Knowing the increase of flux in pole and frame, the mmf absorbed in

\* This statement is not strictly correct, because the increased ampere-turns on the field poles give rise to a greater leakage flux, and this alteration should not be overlooked, especially when working with high flux densities in the iron of the magnetic circuit. If the estimated leakage flux for a given developed voltage on open circuit is  $\Phi_l$  maxwells, then, for the same voltage with full-load current on zero power factor, the leakage flux would be approximately  $\Phi_l' = \Phi_l [(M + M_a)/M]$ , where  $M$  is the number of field ampere-turns on open circuit, and  $(M + M_a)$  is the number of field ampere-turns with full-load current in the armature, the power factor being zero. The quantity  $M_a$  is the demagnetizing ampere-turns per pole due to the armature current, as given by formula (78).

overcoming the increased reluctance of these parts can be calculated, and in this way the dotted curve  $A'$  (Fig. 119) can be drawn. This is merely the open-circuit saturation curve corrected for increased leakage flux due to the additional field current required to balance the demagnetizing effect of a given armature current.

Assuming all the alternating quantities to be simple harmonic functions, the vector diagram (Fig. 120) can be drawn as explained in connection with Fig. 107 (Art. 88). It shows the voltage components for one phase of the winding, the vector  $PE_t$  being the  $IR$  drop, while  $E_dP$  and  $E_d'E_d$  stand for the reactance voltage drop due to end flux and slot flux respectively. The numerical value of  $E_dP$  can be obtained from formula (74) on page 191, and of  $E_d'E_d$  from formula (96) on page 229.

The apparent developed voltage  $E_d'$ , obtained from Fig. 120, gives the point  $M$  on the corrected no-load saturation curve  $A'$  (Fig. 119), and the distance  $E_d'M$  or  $OM'$  shows what exciting ampere-turns are required to develop this emf. The terminal voltage is, however, only  $E_t$ , which gives

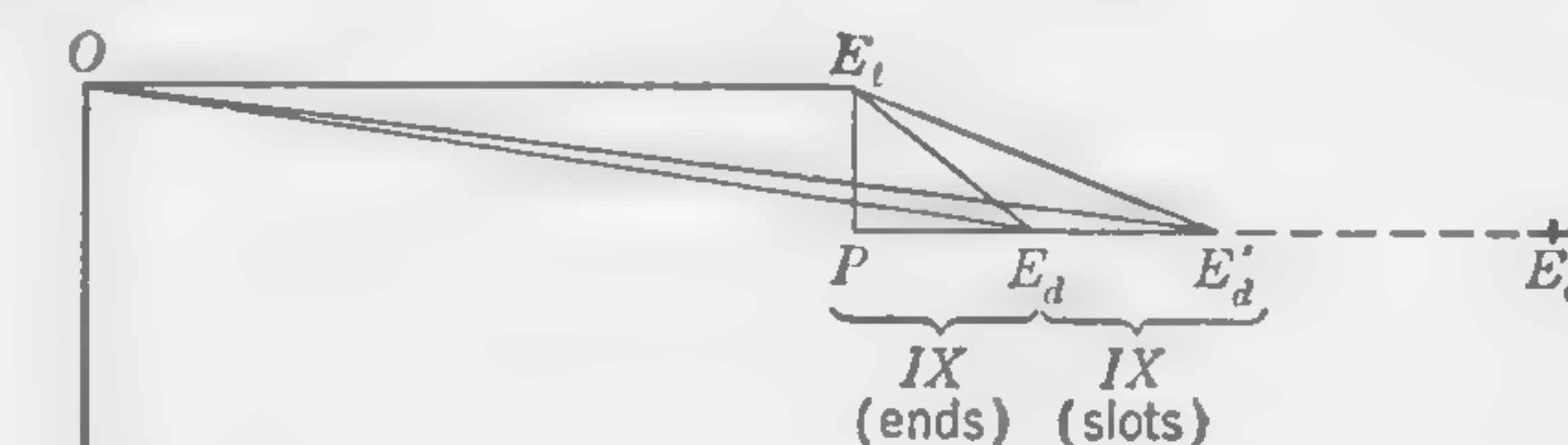


FIG. 120. Vector diagram for zero power factor.

the point  $N$  of the triangle  $MNR$ . Now draw  $NR$  parallel to the horizontal axis to represent the total number of ampere-turns per pole due to the armature current, which, as previously explained, will be entirely demagnetizing and must, therefore, be compensated by an equal number of ampere-turns on the field pole. Thus  $E_tR$  or  $OR'$  is the field excitation necessary to produce  $E_t$  volts at the terminals of the machine. If the load is now thrown off, the terminal pressure will rise to  $E_o$  and the percentage regulation for this particular current output on zero power factor will, therefore be  $100(RS/R'R)$ . This simple construction enables the designer to predetermine with but little error the regulation on zero power factor, provided he can correctly calculate the reactances required for the vector quantities of Fig. 120. The complete load characteristic  $O'R$  is quickly obtained by sliding the triangle  $MNR$  along the corrected no-load saturation curve. The difference of pressure  $SR$ , corresponding to any particular value  $OR'$  of field excitation (Fig. 119), is called the *synchronous reactance drop*, because, although it is made up partly of real reactance drop and partly of armature reaction, it may conveniently be treated as if it were due to an equivalent or fictitious reactance capable of producing the same total loss of pressure if the mmf of the armature



had no demagnetizing or distortional effect. Thus, by producing the line  $PE'_d$  to  $E_o$  (Fig. 120), so that  $PE_o$  is equal to  $RS$  (Fig. 119), the vector diagram shows the difference between the open-circuit pressure  $OE_o$  and the terminal pressure  $OE_t$  under load conditions at zero power factor when the field excitation is maintained constant. The additional (fictitious) reactance drop  $E_oE'_d$  is correctly drawn at right angles to the current vector, because on zero power factor the effect of the armature mmf is wholly demagnetizing; in other words, it tends to set up a magnetic field displaced exactly  $90^\circ$  (electrical space) behind the current producing it; hence, when the load is thrown off, the balancing mmf component on

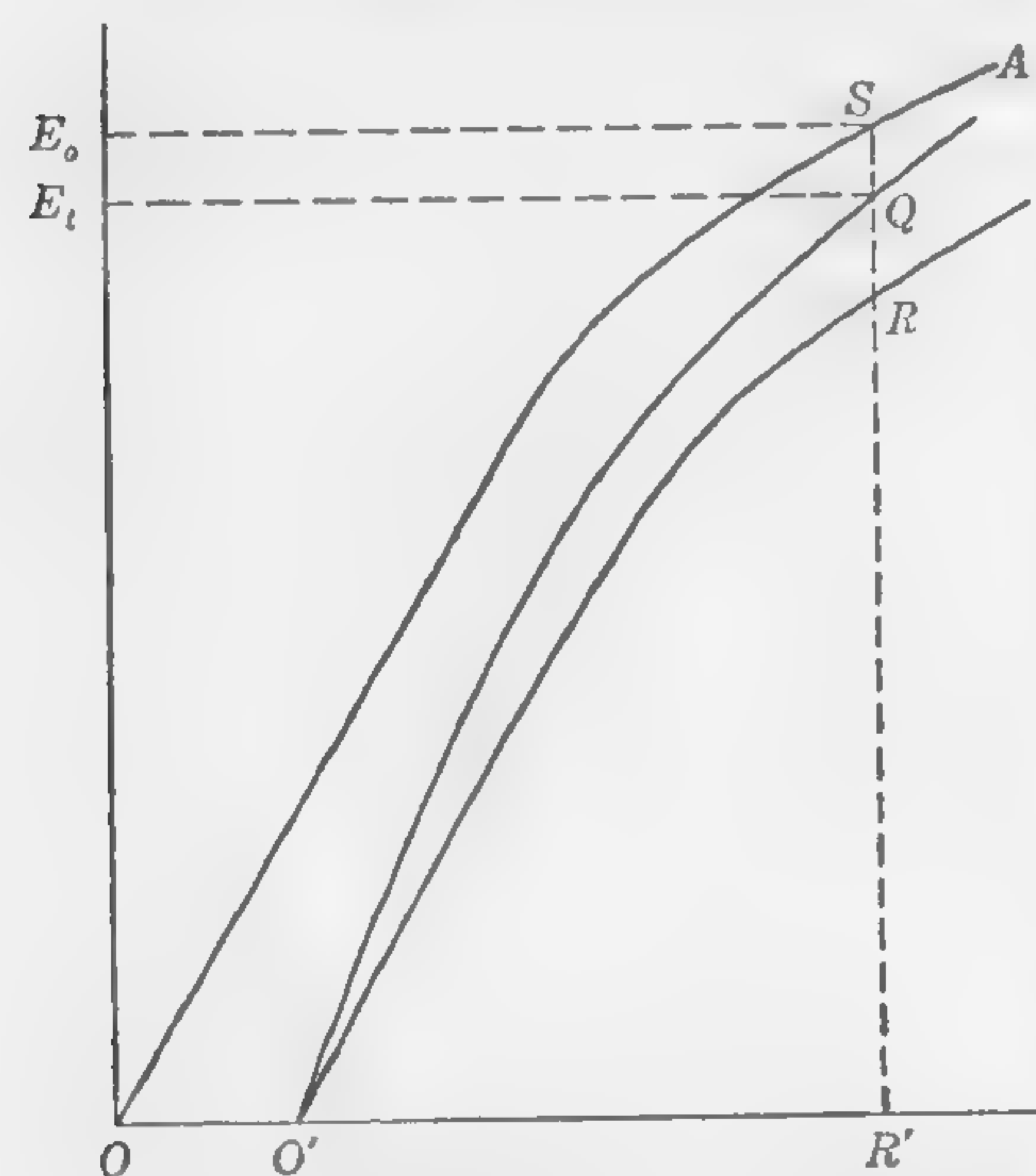


FIG. 121. Saturation curve for any power factor.

the field poles will generate the additional voltage in the phase  $OE_o$ . It should be realized that the fictitious reactance drop  $E_oE'_d$  (Fig. 120) cannot be predetermined until the whole of the magnetic circuit of the machine has been designed. The distance  $DR$  (Fig. 119) is the loss of voltage corresponding to  $E'_dP$  (Fig. 120) and is approximately constant for a given armature current. The portion  $SD$ , however, of the total difference of voltage depends on the slope of the line  $MS$  and is thus some function of the degree of saturation of the iron in the magnetic circuit. It is far from being constant (except over the straight

part of the open-circuit saturation curve) and must be measured off the diagram for each different value of the field excitation. This diagram (Fig. 119) shows very clearly the advantage of high flux densities (magnetic saturation) in some portion of the magnetic circuit, if good inherent regulation is aimed at.

**94. Regulation on Any Power Factor.** Unless the effects of cross-magnetization are taken into account, it is impossible to predetermine the regulation accurately when the power factor differs appreciably from zero, but by the intelligent use of vector quantities (involving as they do the assumption of simple harmonic curves) very satisfactory results can be obtained. Let the external power factor be  $\cos \theta$ , and  $OR'$  (Fig. 121) the constant field excitation which would, on open circuit, develop the pressure  $E_o$ , represented by  $R'S$ . The full-load current zero-power-factor saturation curve  $O'R$  has been drawn as previously described. If, then, it is possible to determine the point  $Q$  on the full-load saturation curve

for power factor  $\cos \theta$ , required percentage regulation may be expressed as  $100(QS/R'Q)$ .

In Fig. 122, draw the right-angled triangle  $E_tPE_o$  in such a way that  $PE_t$  represents the armature resistance drop per phase with full-load current, and  $E_oP$  the corresponding synchronous reactance drop, as given by  $SR$  (Fig. 121). From  $E_t$  draw the line  $E_tm$  of indefinite length and so that  $mE_tP$  is the required power-factor angle  $\theta$ . From  $E_o$  as center describe the arc of a circle of radius  $R'S$  (Fig. 121) equal to the open-circuit voltage, and cutting  $mE_t$  produced at  $O$ . Then  $OE_t$  will be the required terminal voltage, which may be plotted as  $R'Q$  (Fig. 121). This construction provides for the proper angle  $\theta$  between terminal voltage and current; and, in regard to the relation between the terminal voltage  $E_t$  and the open-circuit voltage  $E_o$  when load is thrown off, it will be seen that the total synchronous reactive drop has been used in the impedance

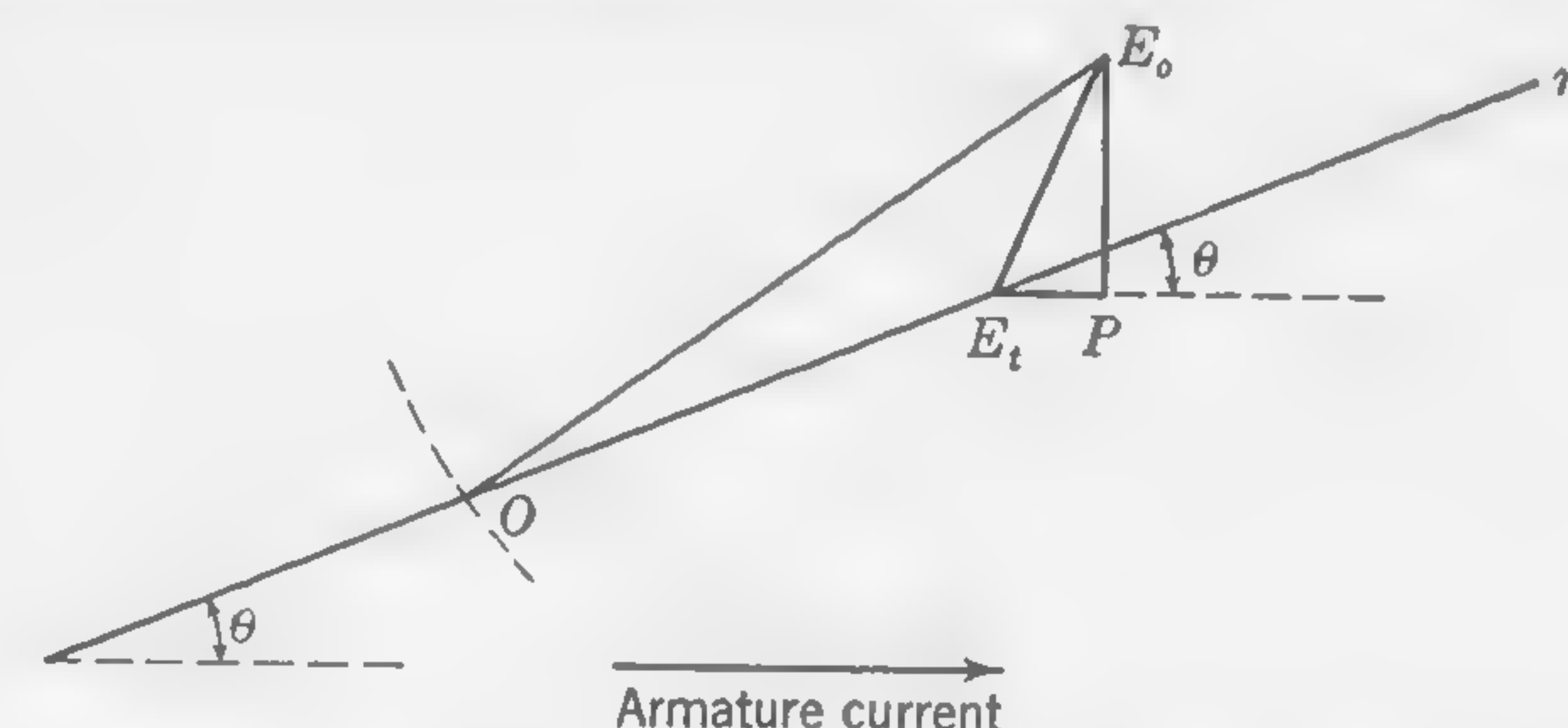


FIG. 122. Diagram for calculating developed voltage for load of power factor  $\cos \theta$ .

triangle  $E_tPE_o$  (Fig. 122). This virtually assumes the demagnetizing and distortional effects of the armature current to be equivalent to a fictitious reactance drop capable of being treated vectorially like any other reactance drop, and of which the direct effect on regulation is proportional to the sine of the angle of lag—a not unreasonable assumption, though scientifically inaccurate. This gives good results in machines of normal design. It is when departures are made from standard practice that such approximations are likely to be abused.

**95. Short-circuit Current.** The maximum value of the armature current at the instant a short circuit occurs depends mainly on the inductance of the armature windings; but, when the armature mmf has had time to react on the field and has actually reduced the flux of induction in the air gap, the resulting current may be fairly accurately calculated by using the construction indicated in Figs. 123 and 124.

The vector triangle (Fig. 123) is constructed for any assumed value  $I_c$  of the armature current. It shows that when the terminal voltage is zero—all three phases of the machine being short-circuited—the flux in the air gap must be such that the pressure  $OE'_d$  would be developed in



the armature conductors on open circuit. The value  $OF$  (Fig. 124) of the ampere-turns necessary to produce this flux in the air gap is thus obtained, the ordinate  $OE'_a$  being the voltage developed in the windings as deter-

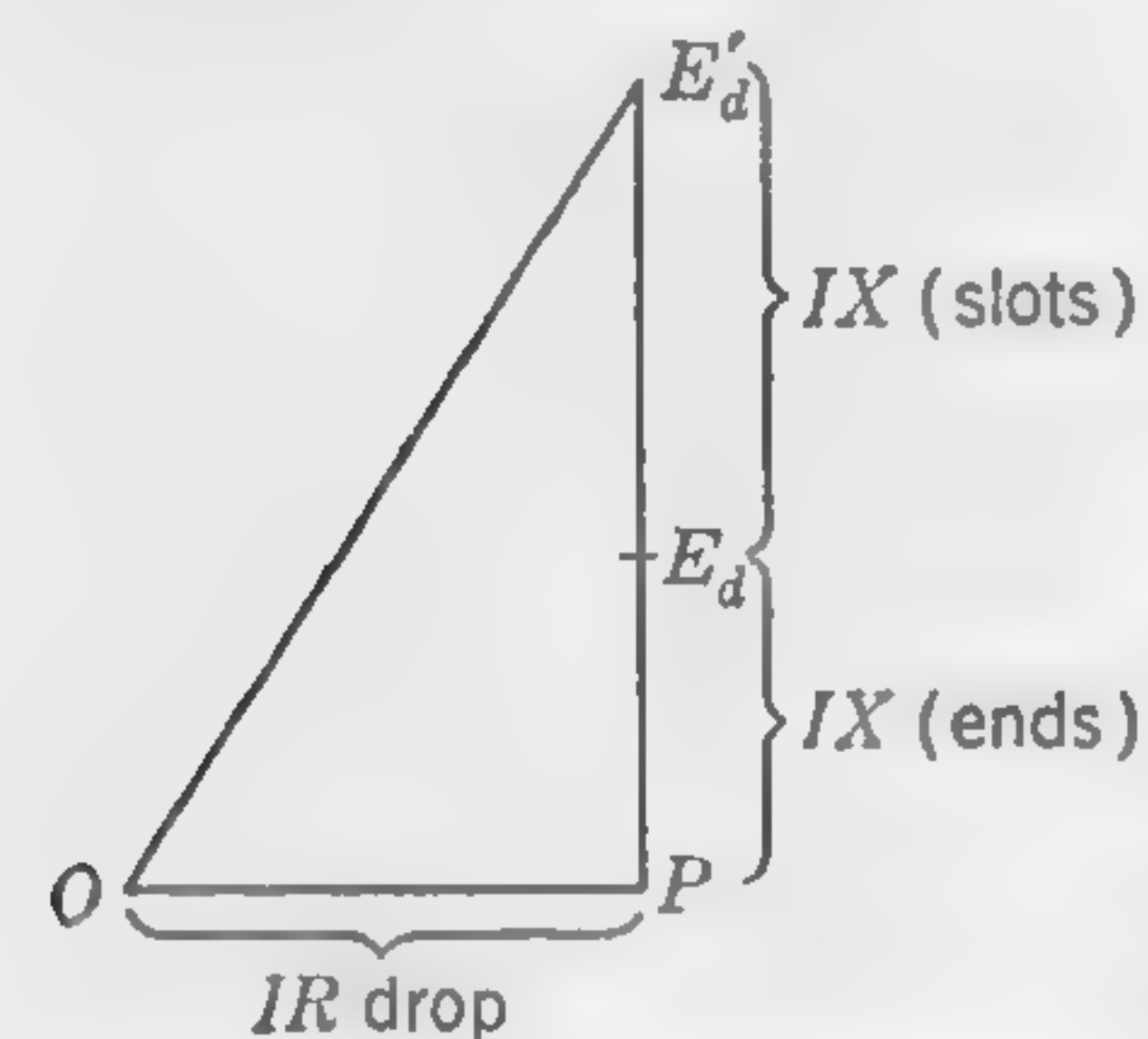


FIG. 123. Vector diagram of short-circuited armature.

mined by the vector diagram. Now since the mmf of the armature windings will be almost wholly demagnetizing, it is correct to assume that the field excitation must be increased by an amount equal to the maximum armature ampere-turns per pole in order that the resultant excitation may be  $OF$ . Thus  $FG$  (Fig. 124) is made equal to the maximum value of the armature ampere-turns, and, by drawing, to a suitable scale, the ordinate  $GJ$  equal to the assumed armature current  $I_c$ , the point  $J$  on the short-circuit current curve is obtained.

By repeating the construction for any other assumed value of the current it will be seen that so long as  $E'_a$  lies on the straight portion of the no-load

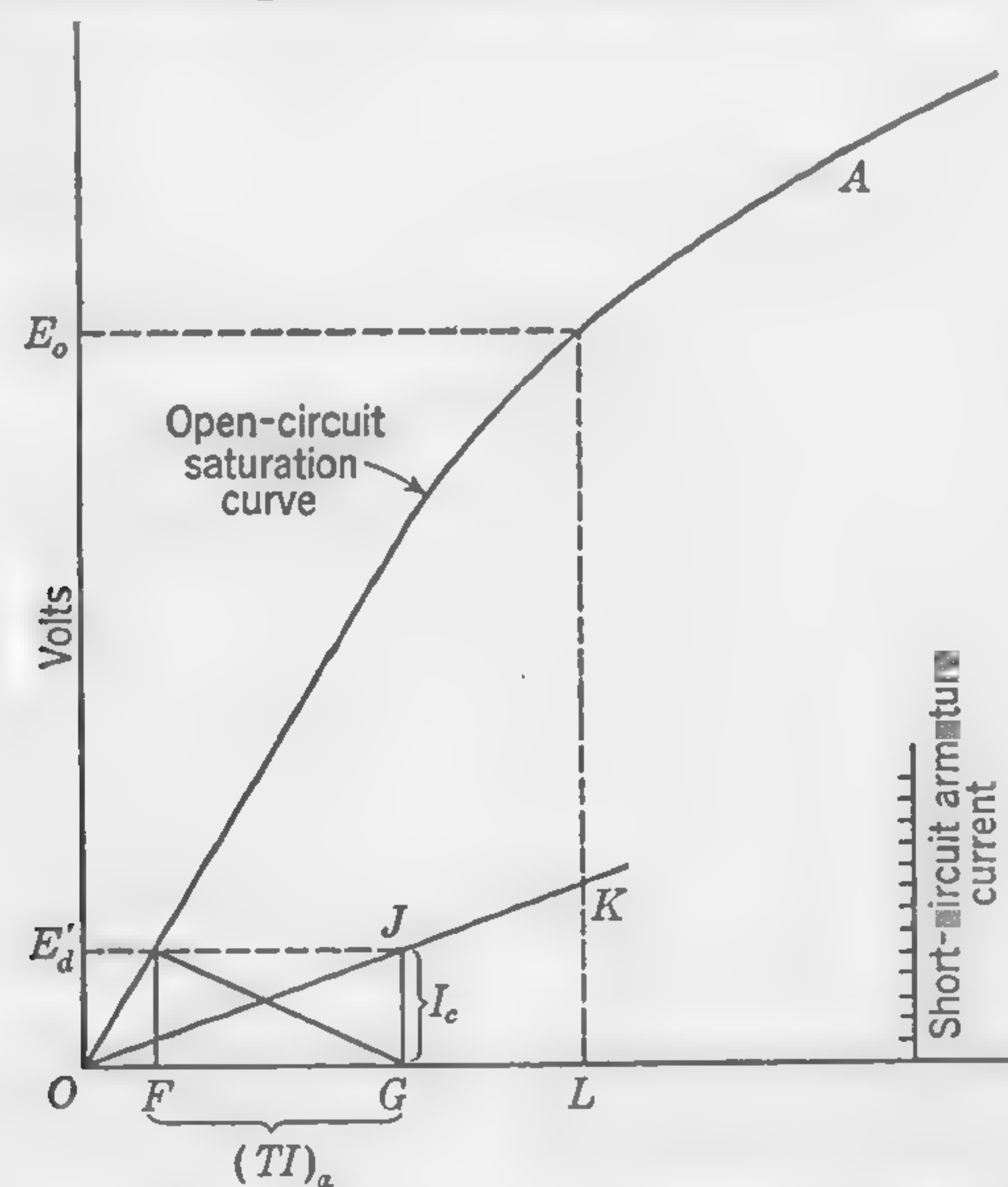


FIG. 124. Method of constructing curve of armature current on short circuit.

characteristic, the relation between the short-circuit current and the field-pole excitation is also represented by a straight line. When the field excitation is  $OL$ , giving a pressure  $OE_0$  on open circuit, the short-circuit current will be  $LK$ .\*

\* The effects of single-phase short circuits on three-phase generators are discussed by H. B. Dwight, Sustained Short Circuits, *Elec. World*, vol. 90, p. 1243, Dec. 17, 1927. See also W. M. Hanna, Calculation of Short-circuit Currents in A-C Networks, *Gen. Elec. Rev.*, March, April, June, and August, 1937.

An important factor that must be taken into account in synchronous alternator design is the so-called *short-circuit ratio*. This ratio refers to the relation between the field ampere-turns that are responsible for rated terminal emf on open circuit, and the field ampere-turns required for a generated emf sufficient to circulate rated current through the armature winding when the latter is short-circuited. Thus, if  $I_e$  in Fig. 124 represents full-load armature current, the field must develop  $OF + FG = OG$  ampere-turns on short circuit if voltage  $E'_a$  is to be generated internally; the open-circuit ampere-turns, to generate  $E_o$  volts, is obviously  $OL$ . It follows, therefore, that the short-circuit ratio is  $OL/OG$ ; it is a reasonably good measure of the ratio of the field strength to the armature strength. When, in the interest of economy, both the air gap and the volume of field copper are small, the short-circuit ratio will also be low; under this condition poor inherent regulation will result, and considerable field-excitation change will be required with change in load. Conversely, a large short-circuit ratio will involve a large air gap and a rather large expensive field winding; under this condition the inherent voltage regulation will be low, *i.e.*, good. In practice, synchronous generators will have short-circuit ratios that vary between values of 0.66 and 1.2.

*Initial Short-circuit Current.* The problem is different when it is desired to predetermine the *initial* short-circuit current or the amount of the armature current at the instant a short circuit occurs (*i.e.*, before the increased armature mmf has had time to react upon the field and reduce the amount of magnetic flux in the air gap). There will be nothing but the impedance of the armature windings to check the growth of the current, and, since the resistance of the windings is usually a small percentage of their reactance, we may consider the  $IR$  drop to be negligible. It should be observed that the slot reactance, which, under normal operating conditions, is correctly treated as a fictitious reactance, now becomes a real reactance similar to that of the end connections. (The end-connection reactance of the armature of a synchronous machine may be calculated by formula (75) on page 192.) The initial short-circuit current may, therefore, be calculated by assuming the full voltage developed in the armature at the time of the short circuit to be applied across a choke coil of reactance ( $X_{\text{ends}} + X_{\text{slots}}$ ). The quantity  $X_{\text{slots}}$  can be obtained from formula (96) on page 229, by assuming the current  $I_c$  to be 1 amp. This would be the correct value to use when all the phases are short-circuited. When only one or two phase-windings of a polyphase machine are short-circuited, a correction must be made in evaluating the amount of the self-induced flux which links with the windings.

*Core-surface Reactance in Salient-pole Machines.* In salient-pole machines there is yet another component of the total reactance to consider; this is the reactance of the flux paths over the cylindrical surface of the armature in the air space between the pole tips. This has not



previously been considered because, under normal operating conditions, the tendency of the belt of armature conductors between the pole tips to establish flux from tooth to tooth and from pole tip to pole tip is accounted for in any proper scheme for dealing with armature reaction. However, when a sudden short circuit occurs, this core-surface leakage flux\* may be an important factor in determining the short-circuit current, and the reactance of the leakage paths over the armature surface between pole tips should be considered as a real reactance to be added to those of the slots and end connections.

In order to calculate the leakage flux  $\Phi_B$  (Fig. 125), the following simplifying assumptions will be made: (1) The portion of the armature face between pole tips is a plane surface. (2) The position of the conductors carrying maximum current is halfway between pole tips. This is not

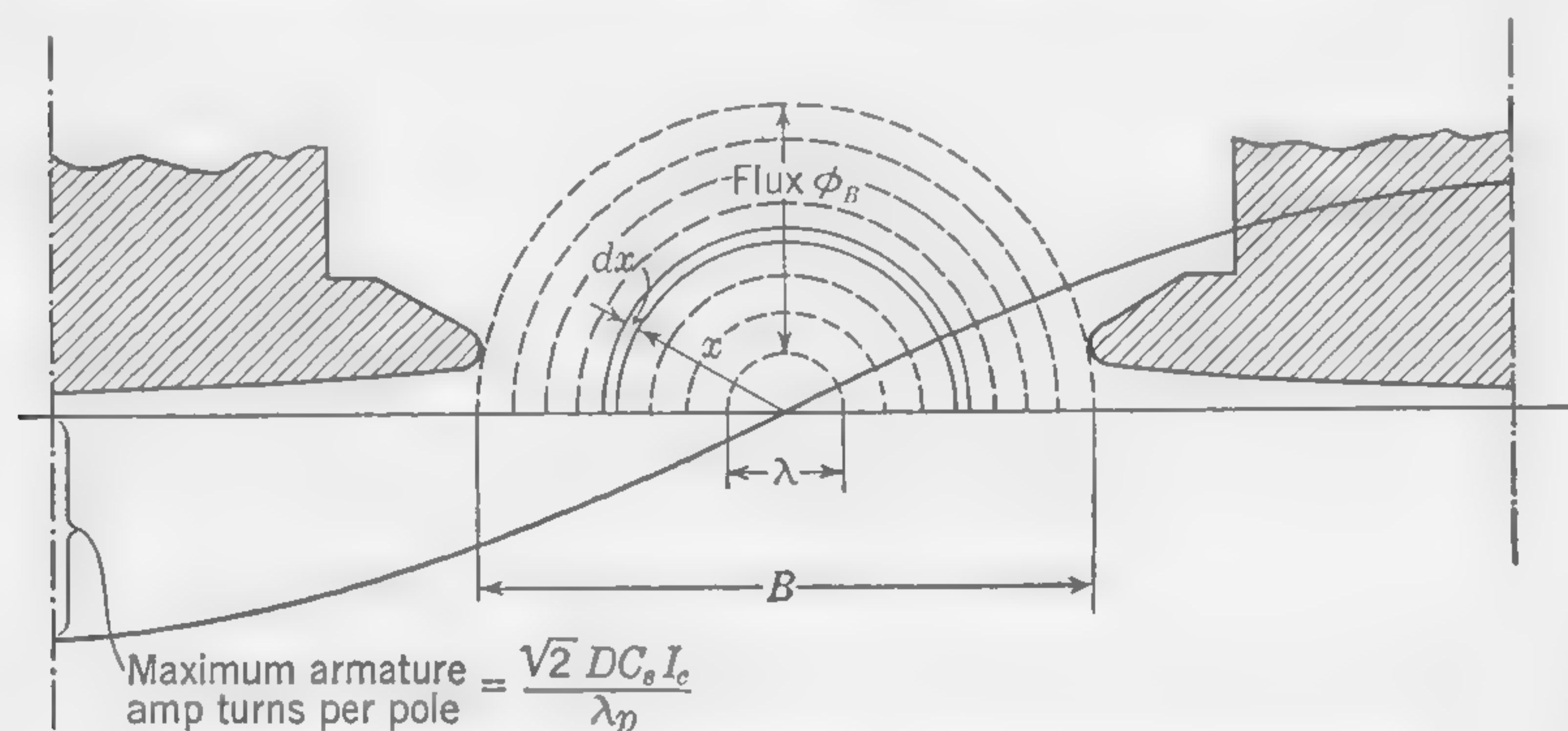


FIG. 125. Illustrating calculation of core-surface leakage flux.

unreasonable inasmuch as the power factor is nearly zero when a short circuit occurs. (3) The distribution of current in the conductors is sinusoidal over the armature periphery. This assumption is as previously made; it involves the idea of very narrow "belts" of conductors, or a large number of slots with as many phases as there are slots. (4) The armature has a smooth surface, the fact that this surface is actually broken up by a succession of teeth and slots being disregarded. (5) The flux paths in air are semicircular arcs described from a center on the armature periphery midway between pole tips. (6) The reluctance of the iron core is negligible. The symbols used are:

$D$  = diameter of armature core in inches

$l_a$  = gross length of armature core in inches

$p$  = number of poles

$B$  = distance between pole tips in inches

\* Sometimes referred to as zigzag leakage and belt leakage, being flux due to current in the armature windings which is not accounted for as slot flux or end flux.

$\lambda$  = tooth pitch in inches

$C_s$  = number of conductors per slot

$n_s$  = number of slots per pole per phase

$I_c$  = rms value of current in armature windings in amperes

With a sinusoidal current distribution having its maximum midway between poles, the distribution of armature mmf will also be sinusoidal and its maximum will occur under the center of the poles where its value is  $0.4\pi$  times the ampere-turns as given by formula (78b) of Art. 86. Thus,

$$F = 0.4\pi \frac{\sqrt{2}DC_s I_c}{\lambda p} \quad \text{gilberts} \quad (97)$$

At a distance  $x$  from the position of zero mmf, the armature mmf per pole is  $F \sin x$ , and the permeance of a flux path in air of width  $dx$  is  $2.54l_a dx / \pi x$ , whence

$$d\Phi_B = 2F \sin x \frac{2.54l_a dx}{\pi x}$$

The lower limit of integration is  $\lambda/2$  because the flux for smaller values of  $x$  is included in the formula for slot-leakage flux. The upper limit is  $B/2$ , but, since both these quantities are in inches they must be multiplied by  $p/D$  to express them in radians. Therefore,

$$\Phi_B = \frac{2 \times 2.54l_a}{\pi} F \int_{p\lambda/2D}^{pB/2D} \frac{\sin x}{x} dx$$

The average value of the distance  $x$  between the limits considered is small, and no appreciable error will be introduced by assuming that  $\sin x$  is equal to  $x$ , whence

$$\Phi_B = \frac{2 \times 2.54l_a}{\pi} F \left( \frac{p}{2D} \right) (B - \lambda)$$

Substituting the value of  $F$  given by formula (97), we get

$$\Phi_B = 1.44C_s I_c l_a \left( \frac{B - \lambda}{\lambda} \right) \quad \text{maxwells} \quad (98)$$

The voltage component or  $IX$  drop due to the "cutting" of this flux by the armature conductors may be calculated in the same manner as when developing formula (95) for the slot-flux emf component (p. 229); thus, on the sine-wave assumption,

$$IX_{\text{core surface}} = 4.44\Phi_B f(C_s n_s p) 10^{-8}$$

Substituting  $\Phi_B$  from formula (98) we get

$$IX_{\text{core surface}} = I_c 6.4 f C_s^2 n_s p l_a \left( \frac{B - \lambda}{\lambda} \right) 10^{-8} \quad \text{volts} \quad (99)$$



wherein the core length  $l_a$  is expressed in inches. It is well to remember that this is *not* a component of the total voltage developed in the armature windings under normal operating conditions.

If, instead of a reactive voltage component, the expression for the reactance  $X_{\text{core surface}}$  is needed in order to add this to  $X_{\text{ends}}$  and  $X_{\text{slots}}$ , and so obtain the total reactance in ohms, which determines the amount of the initial short-circuit current, omit  $I_c$  from the formula (99).

**96. Efficiency.** In estimating the efficiency of an a-c generator before it is built, the same difficulties occur as in the case of the dynamo. There are always some losses, such as windage, bearing friction, and eddy currents, which cannot easily be predetermined, and it is, therefore, necessary to include approximate values for these in arriving at a figure for the total losses. Very little need be added to what has already been said in Art. 61 and the Illustrative Example of Art. 63. In the ratio *efficiency*

$= \frac{\text{output}}{\text{output} + \text{losses}}$ , it is the actual output of the generator at a given power factor with which we are concerned, and not the rated kilovolt-ampere output.

Efficiency depends upon the speed at which the machine runs, and also upon the power factor of the load. In large machines, direct-coupled to the prime mover, the windage and bearing friction losses are generally a rather small percentage of the full-load output. As a rough indication of the magnitude of these friction losses, the following figures may be useful.

APPROXIMATE WINDAGE AND FRICTION LOSSES EXPRESSED AS PERCENTAGE OF FULL-LOAD OUTPUT

	Kva output	Windage and bearing friction, per cent
Open-type, self-ventilated a-c generators.....	50	1.5
	200	1.0
	500	0.7
	Larger	0.5
Turbo-alternators; forced ventilation (exclusive of power to drive fan).....	5,000	1.5
	10,000	1.1
	20,000	0.8
	40,000	0.6

The power required to drive the ventilating fan for turbo-alternators will generally be from 0.35 to 0.5 per cent of the rated full-load output of the generator.

The brush-friction loss is usually small. If  $A$  is the total area of con-

tact in square inches between brushes and slip rings, and  $v$  is the peripheral velocity of the slip rings in feet per minute, the brush-friction loss will be approximately  $vA/100$  watts.

The figures in the following table give usual (approximate) percentage efficiencies of synchronous generators on full load at 0.8 power factor, together with usual excitation losses (size of exciter) expressed as a percentage of the kilovolt-ampere output of the generator.

Kva rating	Efficiency, per cent	Exciter capacity, per cent
50	90.2	5
100	91	3.5
500	93.8	2.0
1,000	95	1.6
5,000	96.7	1.0
10,000	97.2	0.6

Very large modern generators, using high-grade steel for the armature cores, have been built with efficiencies between 0.98 and 0.985.

**97. Illustrative Example. Regulation and Short-circuit Current of Turbo-alternator.** Calculate the inherent regulation, the short-circuit current, and the efficiency of the 8,000-kva turbo-alternator designed in Illustrative Example of Art. 82 (stator) and Illustrative Example of Art. 91 (rotor). All necessary particulars are to be taken from the design sheets of these problems, the quantities to be calculated from the design data being:

- a. The percentage inherent regulation (full-load current) when the full load (80 per cent power factor) is thrown off
- b. The short-circuit current (per phase winding) with full-load excitation—both instantaneous and steady values
- c. The efficiency at full load and specified power factor of 80 per cent

*Item a: Inherent Regulation.* With varying degrees of tooth saturation—especially when, as in this design, all the rotor teeth are not of the same cross section—the only correct method of predetermining the open-circuit saturation curve (similar to Fig. 118, Art. 92) is to plot the flux distribution for different values of the exciting ampere-turns and calculate the emf developed in each case. It is not necessary to calculate a large number of values in this manner; two or three points taken with fairly high values of the exciting current will show how the tooth saturation affects the resulting flux; and a curve can be drawn connecting the known



straight part of the saturation curve with these ascertained values for the higher densities.

The saturation curve for zero power factor can be drawn as explained in Art. 93 (Fig. 119), and the construction of Figs. 121 and 122 can be applied for obtaining curves giving the approximate connection between terminal volts and exciting current for any other power factor. We shall confine ourselves here to calculating the inherent regulation by the more correct but more tedious method of plotting flux curves.

We know that, although 27,000 amp-turns per pole will develop the specified terminal voltage when no current is taken from the machine, this excitation must be increased to 37,000 amp-turns to give the same terminal voltage under full-load conditions (80 per cent power factor). If, then, we can calculate the voltage, with this greater field excitation, when the load is thrown off, the inherent regulation can be predetermined, and, incidentally, we shall obtain a point on the open-circuit characteristic corresponding to a fairly high value of the excitation.

The required flux curve, marked  $B_o$ , has been plotted in Fig. 114. It is derived, like any other flux curve, from the mmf curve  $M_o$  of Fig. 115 by using the saturation curves of Fig. 112 which must be extended beyond the limits of the diagram in order to read the flux values for the higher degrees of excitation. Careful measurements of the flux curve  $B_o$  give an area over the pole pitch of 129 unit squares, and, if we assume the form factor of the resulting emf wave (not plotted) to be the same as for the open-circuit wave at normal voltage, the emf corresponding to the flux  $B_o$  will be

$$\frac{3,810 \times 129}{108} = 4,550 \text{ volts}$$

where 108 is the area of flux curve  $B$  (Fig. 114) and 3,810 is the terminal voltage divided by  $\sqrt{3}$ , because the three windings on the armature are star-connected. The inherent regulation at 80 per cent power factor is, therefore,

$$\frac{4,550 - 3,810}{3,810} = 19.5 \text{ per cent}$$

which is the answer *a*.

*Item b: Short-circuit Current.* On the assumption that the inductance of the armature windings can be correctly calculated, the short-circuit current corresponding to any given field excitation can readily be determined by the method described in Art. 95. The curve marked *volts* (Fig. 126) is the open-circuit characteristic of the machine, the scale of ordinates being on the left-hand side of the diagram. The construction shows that, in order to develop the flux necessary to produce full-load current (700 amp) in the short-circuited windings, 1,900 amp-turns per pole are

required. This is the excitation which will develop an "apparent" emf equal to the sum of  $IX$  drop (ends) and  $IX$  drop (slots), the effect of the  $IR$  drop being negligible. The armature mmf is almost directly demagnetizing, and the ampere-turns per pole must, therefore, be  $1,900 + 11,340 = 13,240$  (the figure 11,340 is calculated on page 242). The current curve, within the range of the diagram, will be a straight line, and, with the full-load excitation of 37,000 ampere-turns, the short-circuit current will be 1,950 amp, or 2.8 times normal. This is the steady value which the short-circuit current would attain if the field excitation were gradually brought up to full-load value; but at the instant of the occurrence of a short circuit with full-load excitation, the current would be limited only by the impedance of the stator windings, which must set

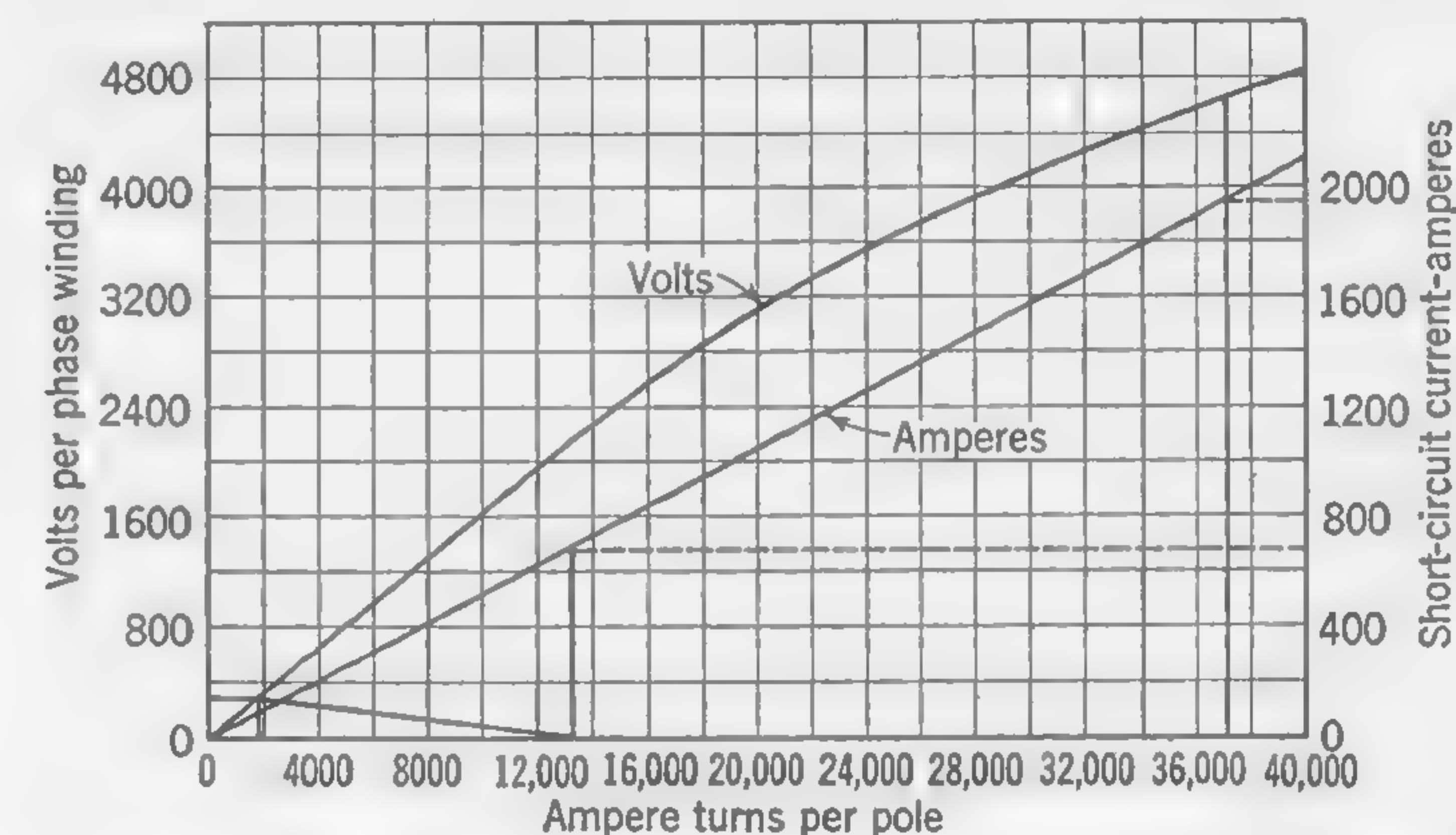


FIG. 126. Curves of open-circuit voltage and short-circuit current—8,000-kva turbo-generator.

up a flux of self-induction equal to the total flux. If we neglect the effect of iron saturation and the changes in the paths of the flux leakage lines, the momentary current might be  $700 \times (4,030/340) = 8,300$  amp, or nearly 12 times normal-load current. The number 4,030 is  $OE'_a$  of Fig. 116, and the denominator 340 is the sum of the  $IX$  voltage drops, which, on account of the  $IR$  drop being relatively negligible, is the same as  $OE'_a$  of Fig. 123.

The momentary short-circuit current might even be greater than this, depending upon the instantaneous value of the generated emf when the short circuit occurs, and the windings should be arranged, if possible, to withstand without injury the mechanical forces exerted on the coils under this condition. If this cannot be done, reactance coils external to the machine must be provided; but the tendency today is to design machines, even of the largest sizes, with sufficient internal magnetic leakage to prevent mechanical injury due to excessive magnetic forces on short circuit (refer to Art. 153).



When calculating the initial short-circuit current for machines with salient poles, the impedance of the armature windings is still further increased by what has been called the core-surface reactance, which produces the  $IX$  drop, as given by formula (99) on page 257. The reason why a leakage-flux component equivalent to the flux  $\Phi_B$  (Fig. 125) is not calculated for the design with cylindrical rotor now under consideration is that the flux lines in the air gap have been included in the slot-leakage flux. These are the dotted lines shown in the space marked  $P_3$  in Fig. 110. It is assumed that the solid iron teeth of the field magnet (rotor) will oppose the sudden growth of a magnetic field through the teeth or the body of the rotor. If the rotor teeth were laminated, it would be reasonable to assume a reduction of the short-circuit current on account of what would be called *zigzag* or *belt-leakage* flux.

*Item c: Efficiency.* The calculation of efficiency under different conditions of loading was illustrated in the Illustrative Example of Art. 63 in connection with the design of a d-c dynamo. In this problem we shall determine the full-load efficiency only.

The windage and bearing friction loss is very difficult to estimate, but some approximate figures were given in the Illustrative Example of Art. 63. We shall assume 1.1 per cent of the total kilovolt-ampere output for the loss due (mainly) to the friction of the air passing through the axial ducts, and also to friction in the outside bearing. It is assumed that the losses in the bearing on the side of the prime mover are included in the steam-turbine efficiency. The power necessary to drive the blower is not included in the above estimate of the windage and friction loss.

For the calculation of iron losses, the student is referred to Art. 52, and the Illustrative Example of Art. 53, where the method of determining the tooth losses was explained; but, since the maximum air-gap density under full-load conditions, as indicated by curve  $C$  of Fig. 114, does not differ appreciably from the maximum of the open-circuit curve  $B$ , we shall not trouble to correct the tooth losses as previously calculated.

With reference to the iron in the body of the stator, the flux indicated by the area of the load flux curve  $C$  (Fig. 114) does not all enter the core below the slots, because this total flux includes the slot-leakage flux, as explained in Art. 88. The position of the conductors carrying the maximum current coincides with the zero point on the armature mmf curve. The point where the resultant mmf curve crosses the datum line is the neutral zone, under the given load conditions. This is the position 17" (Figs. 114 and 115); and the current in the conductor will be approximately  $700 \times \cos 53^\circ = 420$  amp. The slot-leakage flux corresponding to this particular current—the *total* not the "equivalent" flux—can be calculated as explained in Art. 89, when deriving formula (90) which, however, gives the equivalent and not the total slot-leakage flux. If  $\Phi_s$  is

the calculated slot flux, and  $\Phi$  is the total flux per pole in the air gap, then the flux actually carried by the section of the armature iron below the slots is  $(\Phi/2) - \Phi_s$ . This correction is a refinement which need not be applied in the case of a turbo-alternator, in which the pole pitch is always large, causing  $\Phi_s$  to be small in relation to  $\Phi$ ; but in machines with a small pole pitch—especially if there is only one slot per pole per phase—the correction should be made.

The full-load flux per pole is  $66.3 \times 10^6$  maxwells as against  $62.7 \times 10^6$  on open circuit. With the increase of flux density, the loss per pound of iron will be about 2.75 instead of 2.45 watts, and the full-load iron loss will, therefore, be  $0.3 \times 28,000 = 8.4$  kw more than on open circuit, thus bringing the total iron loss up to (say) 109 kw.

The loss at the slip rings may be calculated by the approximate formula given in Art. 96. The diameter of the slip rings will probably not be less than 15 in., so that the rubbing velocity will be  $[(\pi \times 15)/12] \times 1,800 = 7,100$  fpm. The contact area of the two sets of brushes (to carry 514 amp) might be 5 sq in., making the loss from this cause  $[(7,100 \times 5)/100] = 355$  watts, which is negligible in comparison with the other losses.

Adding up the separate losses, we have:

	Kw
Windage and friction.....	88
Stator iron.....	109
Stator copper (Illustrative Example, Art. 82).....	25
Rotor copper (Illustrative Example, Art. 91).....	66
Total.....	288

The kilowatt output is  $0.8 \times 8,000 = 6,400$  and the efficiency, excluding losses in exciter and in air blower external to the generator, is, therefore,  $[6,400/(6,400 + 288)] = 0.957$ .

# TEST PROBLEMS

(Chaps. 8 and 9)

It is not an easy matter to illustrate the contents of this and the preceding chapter with short numerical problems, and the few problems here given do not adequately cover the contents of the last two chapters. It is suggested that, in order to make the best use of the text, actual designs should be worked through to completion. Thus, assuming the armature of a machine to have been designed generally as in Illustrative Example of Art. 82, the calculations for the complete machine should be made and its performance and efficiency predetermined by following item by item the procedure of Illustrative Examples of Arts. 91 and 97.

1. Given: salient-pole alternator; exciter volts = 125; per cent drop in field rheostat = 20; field ampere-turns per pole = 10,000; number of poles = 12; diameter of (cylindrical) pole core = 10 in.; depth of field winding = 2 in.; current density in field wire = 1,510 amp per sq in. Calculate (a) the cross section of the wire in circular



mils, (b) the number of turns per pole of the field winding (assume resistance per circular mil per inch = 1 ohm). *Ans. (a) 45,500, (b) 185.5.*

2. Given: current per armature conductor = 141 amp; number of inductors per slot = 13; number of slots per pole per phase = 2; number of poles = 12. Calculate the maximum value of the armature ampere-turns. *Ans. 4,950.*

3. Given a three-phase delta-connected generator; external power factor = 0.866; terminal volts = 2,200;  $IR$  drop per phase winding = 50 volts;  $IX$  drop (ends and slots) per phase winding = 200 volts; resultant ampere-turns to develop "apparent" voltage in armature = 9,000; armature ampere-turns per pole (maximum value) = 4,000. Calculate (a) the angle  $\beta$  between current vector and open-circuit emf vector, (b) approximate ampere-turns on field pole under the above conditions. *Ans. (a) 48°, 15 min.; (b) 11,700.*

4. Given: 1,000-kva 2,200-volt 3-phase Y-connected generator having a resistance per phase winding of 0.1 ohm, and a total reactance per phase winding of 0.2 ohm. The flux per pole on open circuit is 5,000,000 maxwells. Calculate the flux per pole under full-load conditions. *Ans. 5,200,000 maxwells.*

5. Given: the full-load curve of flux distribution in air gap of three-phase generator is a sine wave of maximum value 7,000 gauss; full-pitch winding with 2 slots per pole per phase; 12 poles; 60 cycles; armature diameter = 45 in.; gross length of armature core = 18 in.; number of inductors per phase = 256. Calculate the mean value of the full-load "apparent" generated voltage per phase winding. *Ans. 1,810 volts.*

6. Given: 100-kva generator; iron loss = 2,100 watts; windage and friction loss = 700 watts;  $I^2R$  (armature) = 1,200 watts with full-load current;  $I^2R$ , field, at full load on 0.8 power factor = 1,200 watts;  $I^2R$  loss, field, at no load = 900 watts (assume straight-line law between and beyond these limits). Calculate efficiency at 0.8 power factor with  $1\frac{1}{4}$  full-load current. *Ans. 0.945.*

## CHAPTER 10

### POLYPHASE INDUCTION MOTORS—DESIGN OF THREE-PHASE MOTOR

**98. Introductory.** In a three-phase generator, the rotation of the field magnet system generates three-phase currents in the armature windings. If the field system is removed and replaced by a laminated iron cylinder, a rotating magnetic field will be produced in the cylinder (through the air gap) when the armature (stator) windings are excited from a three-phase supply. If the laminated cylinder (rotor) is provided with slots containing copper bars short-circuited at both ends, it will be dragged round by the rotating field, because, if the rotor conductors are not allowed to follow the field, heavy currents will be generated in them, and these will develop magnetic poles that tend to make the rotor rotate in the same direction as the revolving field. It is only when the speed of the rotor is exactly the same as that of the field (synchronous speed) that there will be no emf generated in the short-circuited conductors. Thus it is the "slip" of the rotor, or difference between field revolutions and rotor revolutions, which causes emfs to be generated and currents to flow in the rotor windings. This, in brief, is the principle of operation of the rotating-field, polyphase induction motor with which the student is supposed to be generally familiar.

The most scientific method of studying the theory underlying the performance of induction motors is to consider this type of motor as a special case of the a-c transformer. Thus, whether the rotor coils are moving slowly or fast, we should, properly, consider separately the two components of emf generated in them, the one being the emf due to *transformer action* (the pulsating fluxes set up by the magnetizing currents in the stationary—primary windings), and the other being the emf of *rotation* due to the cutting of the (pulsating) fluxes as the rotor rotates. Since the effect of these actual pulsating flux components of a polyphase stator field is equivalent to that of a resultant field rotating at a particular speed known as the "synchronous speed," it is permissible to substitute this rotating field for the actual component pulsating fields, and the design of an induction motor may, therefore, be carried out on lines almost identical with those on which other dynamo-electrical machines have



been designed in preceding chapters of this book. We shall, therefore, think of the rotor conductors being cut by the flux set up by the stator windings as in a dynamo or a-c generator, except that the rate of cutting will not be directly proportional to the speed of the machine, but to the *difference* between the speed of the rotating field and that of the rotor. The rate of cutting of the *stator* conductors by the rotating field is constant, and equal to the inside periphery of the stator stampings multiplied by the synchronous speed.

**99. Design of Induction Motors.** Much of what has been said in connection with alternator and dynamo design is applicable to the design

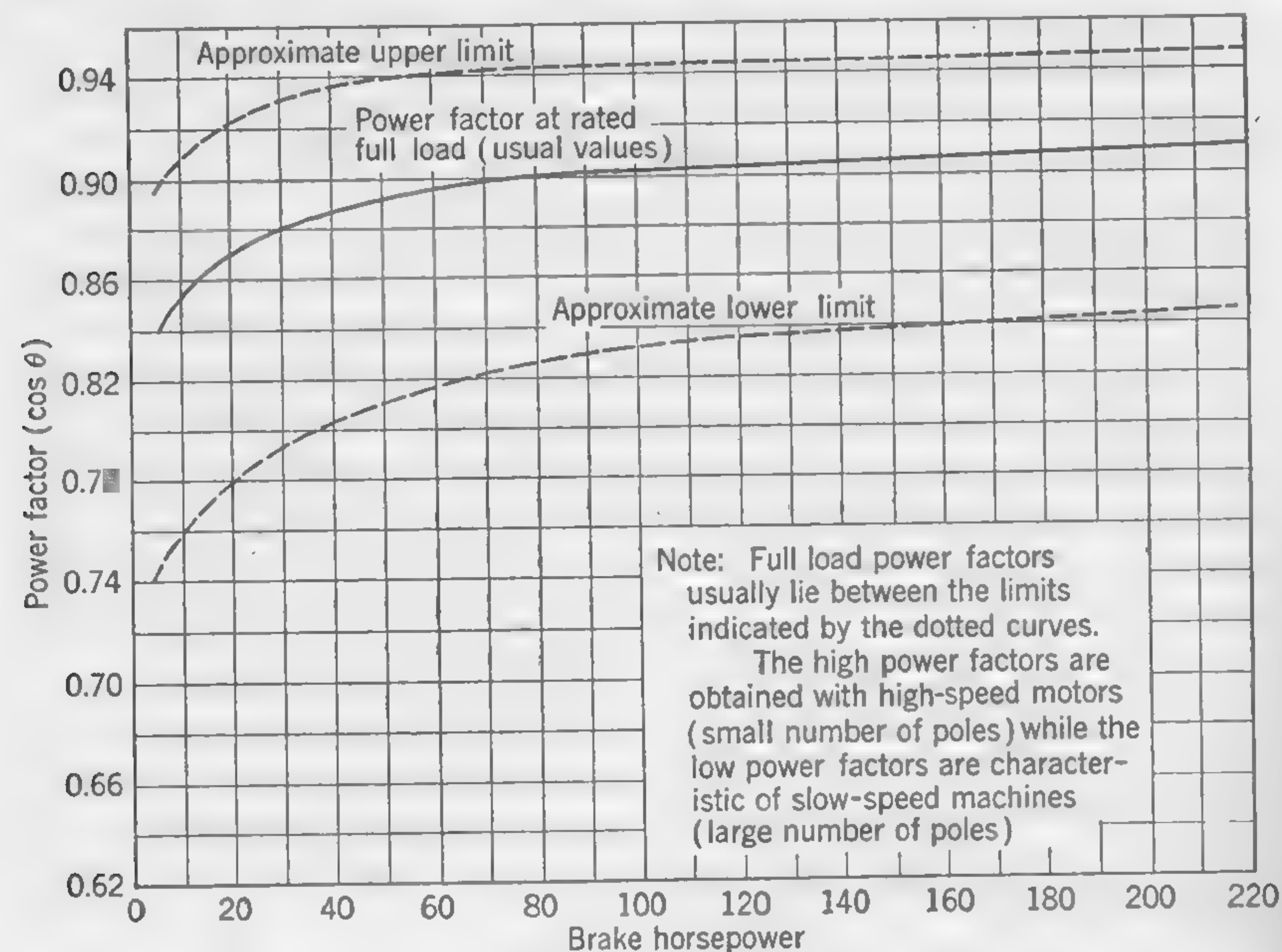


FIG. 127. Power factor of three-phase induction motors.

of induction motors. We shall consider a certain flux of  $\Phi$  maxwells per pole in the air gap, resulting from the magnetizing currents in all the windings on the stator. This flux revolves around the axis of the machine at synchronous speed and is cut by the stator conductors (to which it owes its existence) and also by the rotor conductors when the rotor speed is not exactly the same as that of the field. By synchronous speed is meant the speed in revolutions per minute at which the magnetic field in the air gap appears to rotate. This is, obviously,  $N$  in the formula  $f = (p/2) \times (N/60)$  as used in dynamo and alternator design.

We shall assume a sinusoidal distribution of flux density in the air-gap, and sine-wave emf and current quantities, the maximum values of which are  $\pi/2$  times the mean values. The air gap in induction motors is made

as small as possible to keep down the amount of the magnetizing component of the stator current which gives rise to the flux, and we shall not, at first, concern ourselves with the excitation necessary to establish the magnetic field.

**Usual Values of Efficiency and Power Factor.** In order to estimate the probable input and current per phase for a machine of which the *mechanical output* is specified, some approximate figures are required. The curves of Fig. 127 may be used to estimate the probable full-load power factor of a three-phase induction motor, while Fig. 128 gives usual full-load efficiencies. Also, the accompanying tables represent actual performance data for 60-cycle general-purpose squirrel-cage and wound-rotor induction motors; the values given may be used to check design calculations.

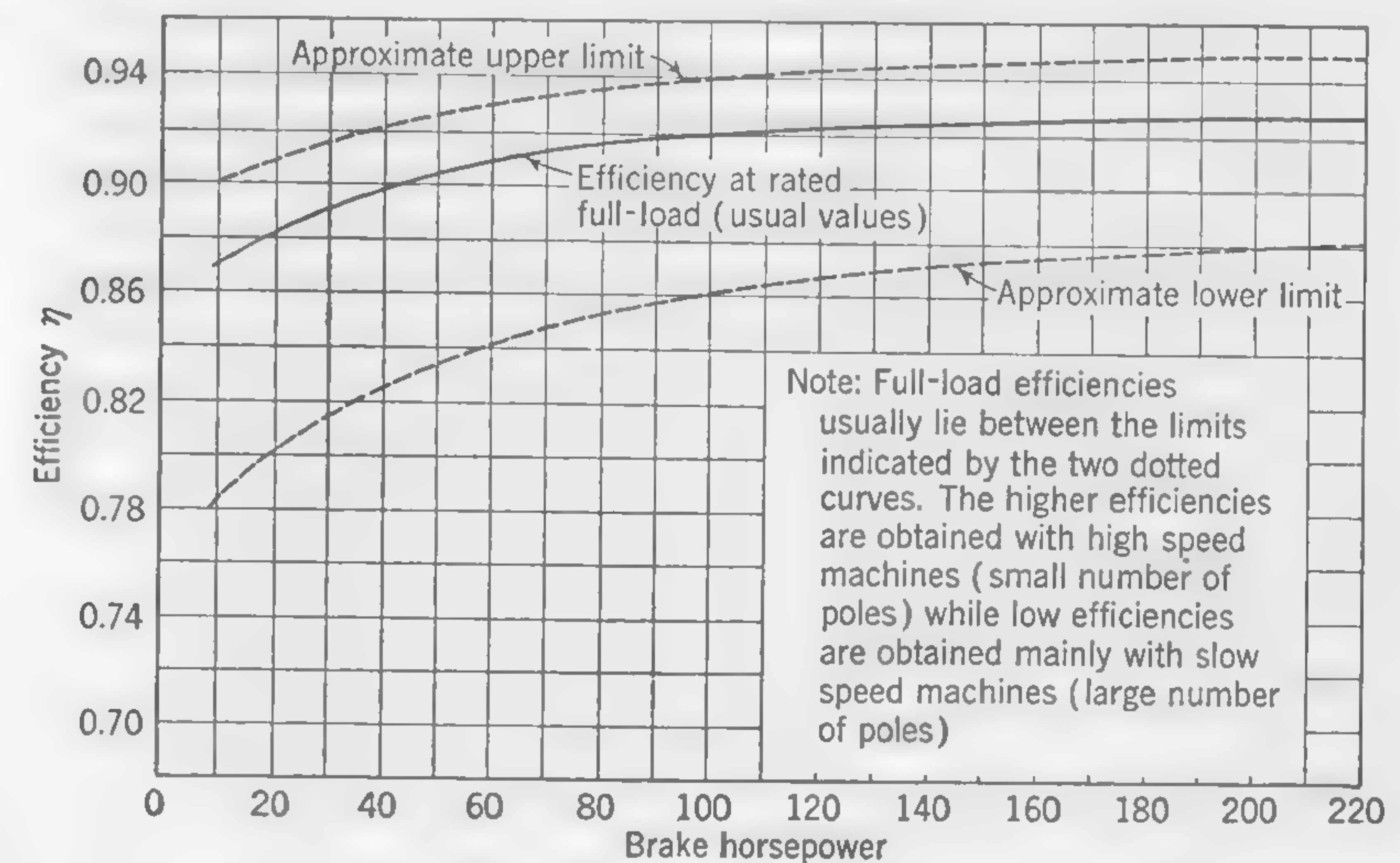


FIG. 128. Efficiency of three-phase induction motors.

**100. Usual Values of Flux Density and Specific Loading.** The average value of the flux density over the pole pitch is defined as  $B_g'' = \Phi / \tau l_a$ , where  $\Phi$  is the total number of maxwells per pole of the rotating field,  $\tau$  and  $l_a$  are the pole pitch and the gross (axial) length of the stator, both in inches, the density  $B_g''$  being the average air-gap density in lines per square inch. On the sine-wave assumption, the maximum value of the air-gap flux density is  $(\pi/2)B_g$ , and it is important that this should not be so high as to cause magnetic saturation of the teeth. The maximum tooth density is  $B_t = (\pi/2)B_g(\lambda l_a / l_n)$  where  $\lambda$ ,  $t$ , and  $l_n$  stand, respectively, for tooth pitch, tooth width, and net length of stator core. Thus  $B_g$  is seen to depend upon the relation of  $t$  and  $\lambda$ , and on the maximum permissible flux density in the teeth. In practice, the usual range



TABLE OF PERFORMANCE DATA FOR  
60-CYCLE GENERAL-PURPOSE SQUIRREL-CAGE INDUCTION MOTORS

Hp	Poles	Rpm at full load	Amp at full load		Locked rotor amp at 220 volts	Torque, lb-ft			Per cent effi- ciency at full load	Power factor at full load
			220 volts	440 volts		Full load	Max	Start- ing		
1	2	3,450	2.9	1.45	25	1.52	4.5	2.6	82	0.82
	4	1,750	3.2	1.6		3.00	9.0	5.9	80	0.76
	6	1,160	3.6	1.8		4.53	12.4	9.0	80	0.68
	8	870	4.0	2.0		6.04	15.0	9.0	78	0.63
2	2	3,500	5.4	2.7	45	3.0	8.2	5.2	83	0.87
	4	1,750	5.8	2.9		6.0	18.0	15.0	83	0.81
	6	1,160	6.6	3.3		9.1	22.7	16.0	82	0.72
	8	870	7.6	3.8		12.1	27.4	18.0	79	0.65
3	2	3,500	7.8	3.9	60	4.5	11.2	7.8	85	0.89
	4	1,750	8.4	4.2		9.0	25.0	23.0	85	0.82
	6	1,160	9.6	4.8		13.6	34.0	24.0	84	0.73
	8	870	10.8	5.4		18.1	40.7	27.9	84	0.65
5	2	3,500	13.0	6.5	90	7.5	16.8	11.0	85	0.89
	4	1,750	13.6	6.8		15.0	33.7	28.0	85	0.85
	6	1,160	15.0	7.5		22.7	51.0	36.0	85	0.77
	8	870	16.4	8.2		30.2	68.0	39.0	84	0.71
7½	2	3,500	19.2	9.6	120	11.3	24.0	17.0	85	0.90
	4	1,750	20.0	10.0		22.5	48.0	39.0	85	0.87
	6	1,160	21.6	10.8		34.0	73.0	51.0	85	0.80
	8	870	23.0	11.5		45.3	97.0	56.0	84	0.76
10	2	3,500	25.6	12.8	150	15.0	30.0	22.0	85	0.90
	4	1,750	26.4	13.2		30.0	60.0	52.0	85	0.87
	6	1,160	28.0	14.0		45.3	90.0	68.0	85	0.82
	8	870	30.0	15.0		60.4	120.0	75.0	85	0.77
15	2	3,500	38.0	19.0	225	22.5	45.0	34.0	86	0.90
	4	1,750	39.0	19.5		45.0	90.0	74.0	86	0.88
	6	1,160	40.0	20.0		68.0	136.0	95.0	86	0.85
	8	870	43.0	21.5		90.0	181.0	113.0	86	0.79
20	2	3,500	50.0	25.0	295	30.0	60.0	45.0	87	0.90
	4	1,750	51.0	25.5		60.0	120.0	90.0	87	0.88
	6	1,160	53.0	26.5		90.6	181.0	122.0	87	0.85
	8	870	56.0	28.0		121.0	242.0	151.0	87	0.80
25	2	3,500	62.0	31.0	365	37.5	75.0	56.0	88	0.90
	4	1,750	62.0	31.0		75.0	150.0	112.0	88	0.89
	6	1,160	64.0	32.0		113.0	226.0	152.0	88	0.87
	8	870	69.0	34.5		151.0	302.0	188.0	88	0.81

TABLE OF PERFORMANCE DATA FOR  
60-CYCLE GENERAL-PURPOSE SQUIRREL-CAGE INDUCTION MOTORS.—  
(Continued)

Hp	Poles	Rpm at full load	Amp at full load		Locked rotor amp at 220 volts	Torque, lb-ft			Per cent effi- ciency at full load	Power factor at full load
			220 volts	440 volts		Full load	Max	Start- ing		
30	2	3,500	74	37	435	45	90	67	89	0.90
	4	1,750	74	37		90	180	135	89	0.89
	6	1,160	76	38		136	272	183	89	0.87
	8	870	82	41		181	362	226	88	0.82
40	2	3,500	90	49	575	60	120	81	89	0.90
	4	1,750	90	49		120	240	180	89	0.90
	6	1,160	100	50		181	362	244	89	0.88
	8	870	106	53		242	484	302	88	0.84
50	2	3,500	122	61	725	75	150	93	89	0.90
	4	1,750	122	61		150	300	225	89	0.90
	6	1,160	126	63		227	454	306	89	0.88
	8	870	132	66		302	762	377	88	0.84
75	2	3,500	182	91	1,075	113	226	124	90	0.90
	4	1,750	182	91		225	450	337	90	0.90
	6	1,160	188	94		240	680	458	90	0.88
	8	870	192	96		453	906	565	89	0.86
100	2	3,500	242	121	1,450	150	300	165	90	0.90
	4	1,750	242	121		300	600	375	90	0.90
	6	1,160	248	124		453	906	565	90	0.88
	8	870	256	128		604	1,208	755	89	0.86
125	4	1,750	300	150	1,800	375	750	410	90	0.90
	6	1,160	306	153		566	1,132	705	90	0.90
	8	870	316	158		755	1,510	940	89	0.89
	10	690	324	162		951	1,902	1,140	89	0.89
150	4	1,750	354	177	2,175	450	900	405	91	0.91
	6	1,160	360	180		680	1,360	850	91	0.91
	8	870	366	183		906	1,812	1,130	90	0.90
	10	690	380	190		1,141	2,282	1,370	89	0.89
200	4	1,750	474	237	2,900	600	1,200	600	91	0.91
	6	1,160	480	240		906	1,812	1,130	91	0.91
	8	870	488	244		1,208	2,416	1,510	90	0.90
	10	690	506	253		1,522	3,044	1,825	89	0.89
250	4	1,750	590	295	3,600	750	1,500	750	91	0.91
	6	1,160	596	298		1,133	2,266	1,415	91	0.91
	8	870	604	302		1,510	3,020	1,855	90	0.90
	10	690	618	309		1,903	3,806	2,280	90	0.90



TABLE OF PERFORMANCE DATA FOR  
60-CYCLE WOUND-ROTOR INDUCTION MOTORS

Hp	Poles	Rpm at full load	Full-load amp at 220 volts		Torque, lb-ft		Per cent efficiency at full load	Power factor at full load
			Stator	Rotor	Full load	Max		
1	6	1,100	3.85	10	4.8	9.2	73	0.70
	8	845	3.85	10	6.2	16.4	73	0.69
2	4	1,700	6.2	17.2	6.2	14.0	78	0.82
	6	1,115	7.1	18.0	9.5	19.0	77	0.72
	8	850	7.7	18.0	12.3	31.5	76	0.67
3	4	1,700	8.8	21.0	9.3	19.0	81	0.83
	6	1,140	9.5	21.0	13.9	28.0	80	0.78
	8	855	10.8	22.0	18.4	40.7	80	0.68
5	4	1,700	13.6	30.5	15.5	33.0	84	0.86
	6	1,140	14.8	27.5	23.0	46.0	82	0.81
	8	855	16.5	30.0	30.7	62.0	83	0.72
7½	4	1,700	19.9	28.0	23.2	47.0	85	0.87
	6	1,140	21.0	27.7	34.4	72.0	85	0.83
	8	870	26.9	29.2	45.0	100	85	0.64
10	4	1,725	25.9	28.0	30.5	90	88	0.86
	6	1,145	27.4	30.0	45.9	91	85	0.84
	8	840	30.0	52.5	62.0	150	83	0.78
15	4	1,700	43.0	57.0	46.3	110	87	0.86
	6	1,125	41.6	60.5	70.0	160	85	0.83
	8	840	44.0	64.0	94.0	200	85	0.79
20	4	1,720	52.0	61.0	61.0	150	87	0.87
	6	1,145	53.0	62.5	91.0	220	86	0.85
	8	835	57.0	104	126.0	230	85	0.81
25	4	1,720	64	66	77	195	86	0.87
	6	1,130	67	97	116	300	86	0.85
	8	840	70	103	158	225	86	0.82
30	4	1,740	78	70	90	300	86	0.88
	6	1,145	79	93	137	350	87	0.85
	8	850	82	132	185	375	86	0.83
40	4	1,740	101	79	121	360	87	0.88
	6	1,145	102	138	184	400	87	0.87
	8	850	106	141	245	500	86	0.85

TABLE OF PERFORMANCE DATA FOR  
60-CYCLE WOUND-ROTOR INDUCTION MOTORS.—(Continued)

Hp	Poles	Rpm at full load	Full-load amp at 220 volts		Torque, lb-ft		Per cent efficiency at full load	Power factor at full load
			Stator	Rotor	Full load	Max		
50	4	1,720	91	123	152	360	87	0.91
	6	1,170	85	128	225	750	90	0.85
	8	870	82	135	300	850	89	0.81
	10	685	80	140	385	950	87	0.80
75	4	1,755	183	145	225	560	90	0.89
	6	1,165	188	148	338	900	90	0.87
	8	870	193	145	453	1,200	89	0.85
	10	695	200	146	565	1,350	88	0.80
100	4	1,760	244	142	300	750	90	0.90
	6	1,165	246	192	450	1,050	90	0.88
	8	870	256	150	600	1,500	90	0.85
	10	695	265	207	755	1,525	88	0.83
	12	580	314	164	905	2,000	88	0.73
125	4	1,760	304	131	375	1,100	90	0.90
	6	1,170	306	200	560	1,300	91	0.88
	8	875	316	210	750	1,700	90	0.86
	10	695	325	228	945	1,900	89	0.84
	12	580	350	170	1,130	2,400	89	0.79
150	4	1,760	360	134	450	1,200	90	0.90
	6	1,170	367	152	675	1,500	91	0.89
	8	875	373	217	900	2,000	90	0.88
	10	695	387	220	1,135	2,275	90	0.84
	12	580	400	225	1,350	3,000	89	0.80
200	4	1,760	480	175	600	1,300	90	0.90
	6	1,170	484	173	900	2,000	91	0.88
	8	875	490	237	1,200	2,500	91	0.88
	12	580	500	240	1,800	4,250	90	0.87

of maximum densities in the minimum section of the iron of induction motor teeth, expressed in lines per square inch, is as follows:

For  $f = 25$ ,  $B_t''$  lies between 90,000 and 125,000, a common value being  $B_t'' = 100,000$ .

For  $f = 60$ ,  $B_t''$  lies between 75,000 and 105,000, a common value being  $B_t'' = 85,000$ .

The flux density in the stator core below the teeth will generally be



between 50,000 and 85,000 lines per sq in. in 60-cycle induction motors, the usual range for 25-cycle machines being from 65,000 to 100,000 lines. These figures refer to the maximum density of the rotating flux, that is to say, of the resultant flux in the stator ring due to the combined magnetizing effect of all the phase windings.

The air-gap density may have to be kept below what would be permissible if the resulting tooth densities alone were considered. It is usually desirable to keep the magnetizing component of the stator current as small as possible, which involves not only a small air gap, but low flux

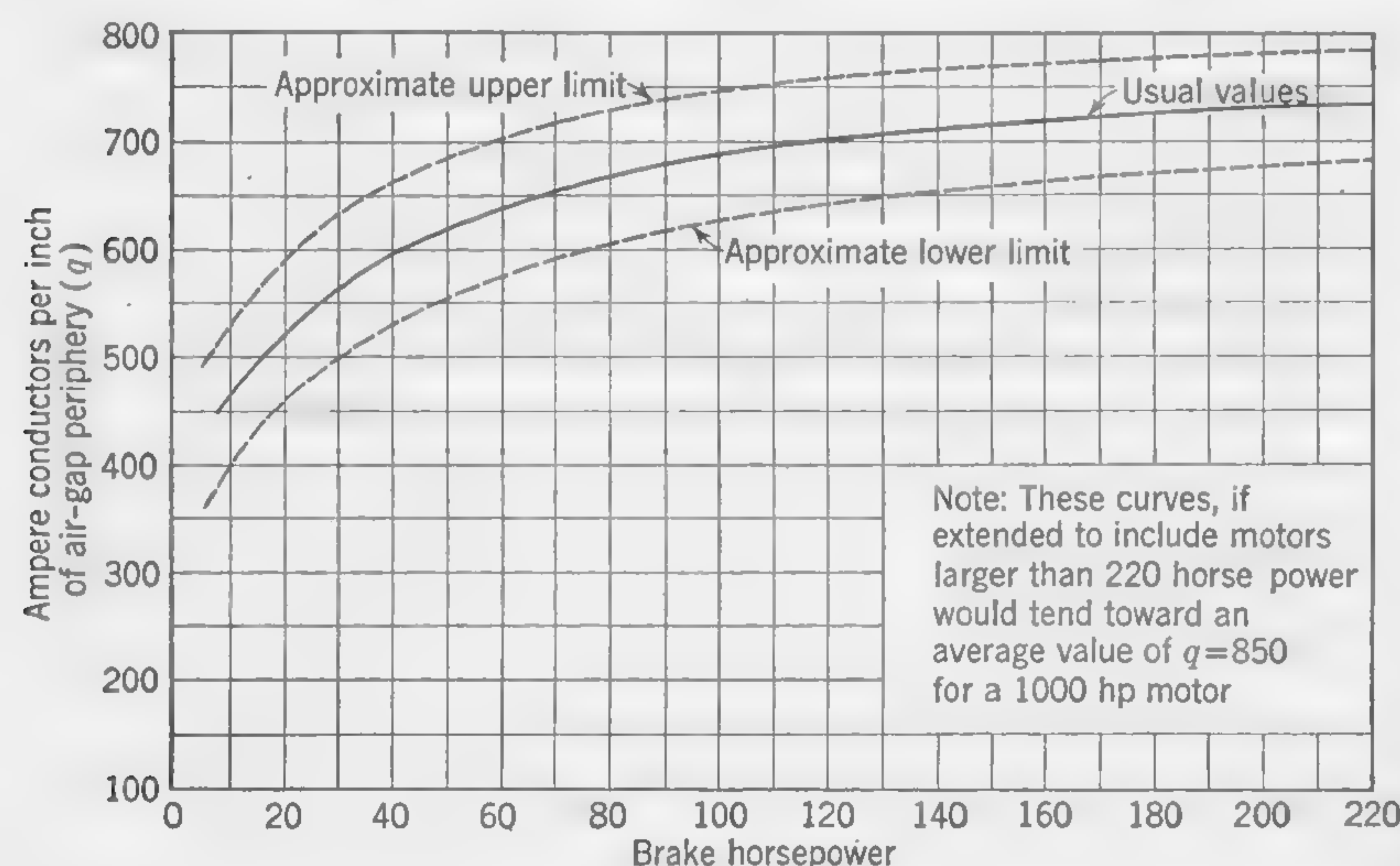


FIG. 129. Curves giving approximate values for the stator ampere-conductors per inch of air-gap periphery of induction motor.

densities in air gap and teeth. Usual values for the average air-gap density over the pole pitch, expressed in lines per square inch, are as follows:

For  $f = 25$ ,  $B_g''$  lies between 28,000 and 45,000, a common value being around 35,000.

For  $f = 60$ ,  $B_g''$  lies between 23,000 and 38,000, a common value being around 26,000.

The higher values of air-gap density occur in machines of large output, large diameter of rotor, low voltage, and small number of poles.

**Specific Loading.** This is the quantity  $q$  as used in dynamo and alternator design. It is the ampere-conductors per inch of air-gap periphery the length around the air gap being practically the same whether measured on the outside of the rotor or inside of the stator, because of the very small clearance between the two. Thus, in a three-phase motor,  $q = 3ZI_c/\pi D$ , where  $Z$  is the number of face conductors per phase,  $I_c$  is the current per conductor, and  $D$  is the air-gap diameter in inches. Usual values of  $q$  are given in the curves of Fig. 129.

**101. Usual Values of Slot Pitch.** The slot pitch  $\lambda$  is equal to the pole pitch divided by the number of slots per pole. The designer has no definite rules to guide him in deciding upon the number of slots per pole. Generally speaking, a large number of slots is desirable; but this increases the amount of space taken up by insulation, and it increases the weight and cost of the machine. The number of slots in the stator should be divisible by 2 for two-phase motors, and by 3 for three-phase motors. It is usual to provide a number of slots which is also divisible by the number of poles, but windings can be devised for stators having a fractional number of slots per pole. Machines with 8 and 10 slots per pole are suitable only for two-phase motors. The table shown below gives the usual number of slots per pole for different values of the pole pitch. As a general rule, it is desirable to make the width of the slot approximately equal to the tooth width at the internal diameter of the stator.

Pole pitch $\tau$ in.	Number of slots per pole
3 to 4	6 or 8
5	8 or 9
6	8, 9, or 10
7	9 or 10
8 to 9	9, 10, or 12
10	10 or 12
12 to 14	12 or 15

The slot depth ranges from about 1 up to 3 in. in very large motors. A 100-hp motor would generally have a depth of slot not exceeding 2 in.

**102. The Output Equation.** Expressed in horsepower, the output of a polyphase motor is

$$\text{hp} = EI_c \cos \theta \times \frac{n\eta}{746}$$

where  $E$  = volts per phase winding, being  $1/\sqrt{3}$  times the supply voltage if the stator is three-phase star-connected

$I_c$  = effective current (rms value) per stator conductor

$\cos \theta$  = power factor of motor

$\eta$  = efficiency

In order to make this formula of use in determining the leading dimensions of the machine, certain substitutions must be made. The quantity  $E$  may be expressed by formula (64a) which was developed in Art. 69 dealing with a-c generators; thus, on the sine-wave assumption,

$$E = 2.22f\phi dZ \times 10^{-8}$$

But

$$f = \frac{pN}{120} \quad \text{and} \quad \phi = B_g'' \frac{\pi D L_a}{p}$$



Therefore,

$$E = 2.22 \left( \frac{pN}{120} \right) \left( B_g'' \frac{Dl_a}{p} dZ \times 10^{-8} \right) \\ = 5.81 NB_g'' D l_a dZ \times 10^{-10}$$

Also,

$$q = \frac{nZI_c}{\pi D} \quad \text{and} \quad \Phi I_c = \frac{q\pi D}{nZ}$$

Substituting the values of  $E$  and  $I_c$  in the formula for horsepower,

$$\text{hp} = 5.81 (NB_g'' D l_a dZ \times 10^{-10}) \left( \frac{q\pi D}{nZ} \right) \cos \theta \times \frac{n\eta}{746}$$

Hence,

$$D^2 l_a = \frac{4.07 \times \text{hp} \times 10^{11}}{B_g'' q N d \eta \cos \theta} \quad (100)$$

where  $D$  and  $l_a$  are the diameter and axial length of the air gap expressed in inches, and  $d$  is the winding factor, *i.e.*, the product of the distribution factor  $k$  and the pitch factor  $k'$ , formulas (65) and (66), respectively.

As the output equation properly shows, the quantity  $D^2 l_a$ , which is actually a *measure* of the physical volume of the machine, depends, among other things, upon the horsepower per revolution. This is particularly significant because it indicates that, for a given value of  $D^2 l_a$ , *i.e.*, size, the horsepower output of a motor increases as the speed is raised. Or, to put it another way, this implies that two-pole motors are generally smaller and less expensive to build than are those designed for multipolar operation. Moreover, since present-day motors are manufactured in accordance with National Electrical Manufacturers Association (NEMA) frame sizes and standards, it is important to recognize that motor manufacturers may employ each lamination design for several combinations of horsepower output and speed.

**Ratio of Air-gap Diameter to Axial Length.** It is not possible to lay down hard-and-fast rules regarding the relation of the diameter of rotor (or stator) to the length measured parallel to shaft (*i.e.*, the total thickness of stampings in the iron core, including vent ducts and insulation between stampings). The number of poles is an important consideration and, for a definite relation between pole pitch and axial length, we would have  $l_a \propto D/p$ , the condition for a square polar area being  $l_a = \tau = \pi D/p$ ; but large variations are permissible. There are many factors governing this ratio, which include economical considerations, such as the labor cost of assembling the parts, even when alternative designs show no appreciable difference in material cost. The peripheral velocity must also be considered and kept within reasonable limits, but the proper diameter  $D$  is rarely determined on this basis. It is obvious that, if we

can decide upon a suitable value for either  $\tau$  or  $l_a$ , the other dimension is obtained from the output equation (100). The pole pitch  $\tau$  will evidently depend somewhat upon the horsepower *per pole* and will be considerably larger in a machine of large output and few poles than in a machine of small output and many poles. On the basis of the same output *per pole*, the area of the air gap ( $\tau \times l_a$ ) must be larger for a low-frequency than for a high-frequency machine, because of the slower rate of cutting of the flux by the conductors in the slots. (This slower rate of cutting is not entirely compensated for by the fact that slightly higher flux densities are permissible with the lower frequencies.) Thus, the pole pitch  $\tau$  will generally be greater in 25-cycle motors than in 60-cycle motors. The values of  $\tau$  found in commercial machines are the result of considering all the controlling factors. The following dimensions are usual, but considerable departures therefrom are permissible. It will, of course, be understood that, since the pole pitch is equal to  $\pi D/p$ , it is not usually an exact number of inches, and the figures here given are approximate only.

APPROXIMATE USUAL VALUES OF POLE PITCH ( $\tau$ )

Hp per pole	$f = 60$		$f = 25$	
	$\tau$ , in.	$v$	$\tau$ , in.	$v$
1	4	2,400	5	1,250
2	5	3,000	6¼	1,560
4½	6	3,600	7½	1,875
8	7	4,200	8¾	2,190
15	8	4,800	10	2,500
25	9	5,400	11¼	2,810
40	10	6,000	12½	3,130
60	11	6,600	13¾	3,440
85	12	7,200	15	3,750
120	13	7,800	16	4,000

**103. Peripheral Velocity—Ventilating Ducts.** The peripheral velocity of the rotor in feet per minute is  $v = \pi DN/12$ . However, since  $N = 120/f/p$  (very nearly, for induction motors) and  $\tau = \pi D/p$ , the peripheral speed may be expressed in terms of frequency and pole pitch as follows:

$$v = 10f\tau \quad (101)$$

Thus, for a given frequency, the peripheral speed is directly proportional to the pole pitch, and it, therefore, increases with the *output per pole*. Values for  $v$  corresponding to particular pole-pitch dimensions are given in the foregoing table.



**Ventilating Ducts.** Radial vent ducts are provided in the stator core as in the armature cores of a-c generators (refer to Arts. 16 and 58). They should be about  $\frac{3}{8}$  to  $\frac{1}{2}$  in. wide, and their number will depend

Peripheral velocity $v$ , fpm	Thickness of stack, in.
1,500	$1\frac{1}{2}$ to 2
3,000	2 to $2\frac{1}{2}$
4,500	$2\frac{1}{2}$ to 3
6,000	3 to $3\frac{1}{4}$

somewhat upon the peripheral velocity of the rotor. Experience shows that the thickness of the stack of stampings between air ducts should not exceed the figures given in the above table.

**104. Losses in Stator Core and Teeth.** American practice favors open slots in the stator stampings, with closed or nearly closed slots in the rotor. Such slots reduce the cost of winding and also improve the electrical and mechanical features of the stator coils. With semiclosed slots in the stator as well as in the rotor, the core losses are less because the high-frequency flux variations known as tooth pulsations are very greatly reduced. With open slots in the stator, these additional core losses due to high-frequency flux pulsations and eddy currents may be considerable.\* It is suggested that the total core losses in induction motors with closed or partially closed slots in both stator and rotor may be read, without reduction, directly from the curve, Fig. 67; but, when open slots are used in the stator, the loss per pound as read from the curve should be increased about 25 per cent.

**105. Stator Windings—Current Density.** There is no essential difference between the windings on the stator of an induction motor and those on the armature of an a-c generator. The student is, therefore, referred to Art. 73, where armature windings are briefly discussed. There are many forms of winding, for both generator armatures and induction-motor stators, which will not be described in this book, but some comments will be made concerning two general types used in the stators of design problems which follow. In one of them, the so-called *single-layer* “mush” winding, the coils are all similar and usually are taped at the ends before being put into position. The straight portion of the coil is left untaped, so that the wires may be inserted one by one into previously insulated slots of the semiclosed type. The ends of the coils outside the slots are bent and twisted in such shape as to clear each other. In this type of winding (sometimes referred to as *full-overlap* winding) the total

\* SPOONER, T., and C. W. KINCAID, No-load Induction Motor Core Losses, *Trans. AIEE*, vol. 48, p. 645, 1929; SPOONER, T., Squirrel-cage Induction Motor Core Losses, *Trans. AIEE*, vol. 44, p. 155, 1925; SPOONER, T., Tooth Pulsations in Rotating Machines, *Trans. AIEE*, vol. 43, p. 252, 1924.

number of slots counted around the periphery must be a multiple of 4. The manner in which the coils would be arranged on the stator of a small, three-phase induction motor with 36 slots is shown in Fig. 130.

The approximate mean length per turn of the winding on induction motor stators for use on circuits up to 600 volts may be calculated by the formula

$$\text{Mlt in inches} = 2l_a + 2.3\tau + 6 \quad (102)$$

where  $\tau$  is the pole pitch, or “throw” of the coil in the case of a chorded or short-pitch winding.

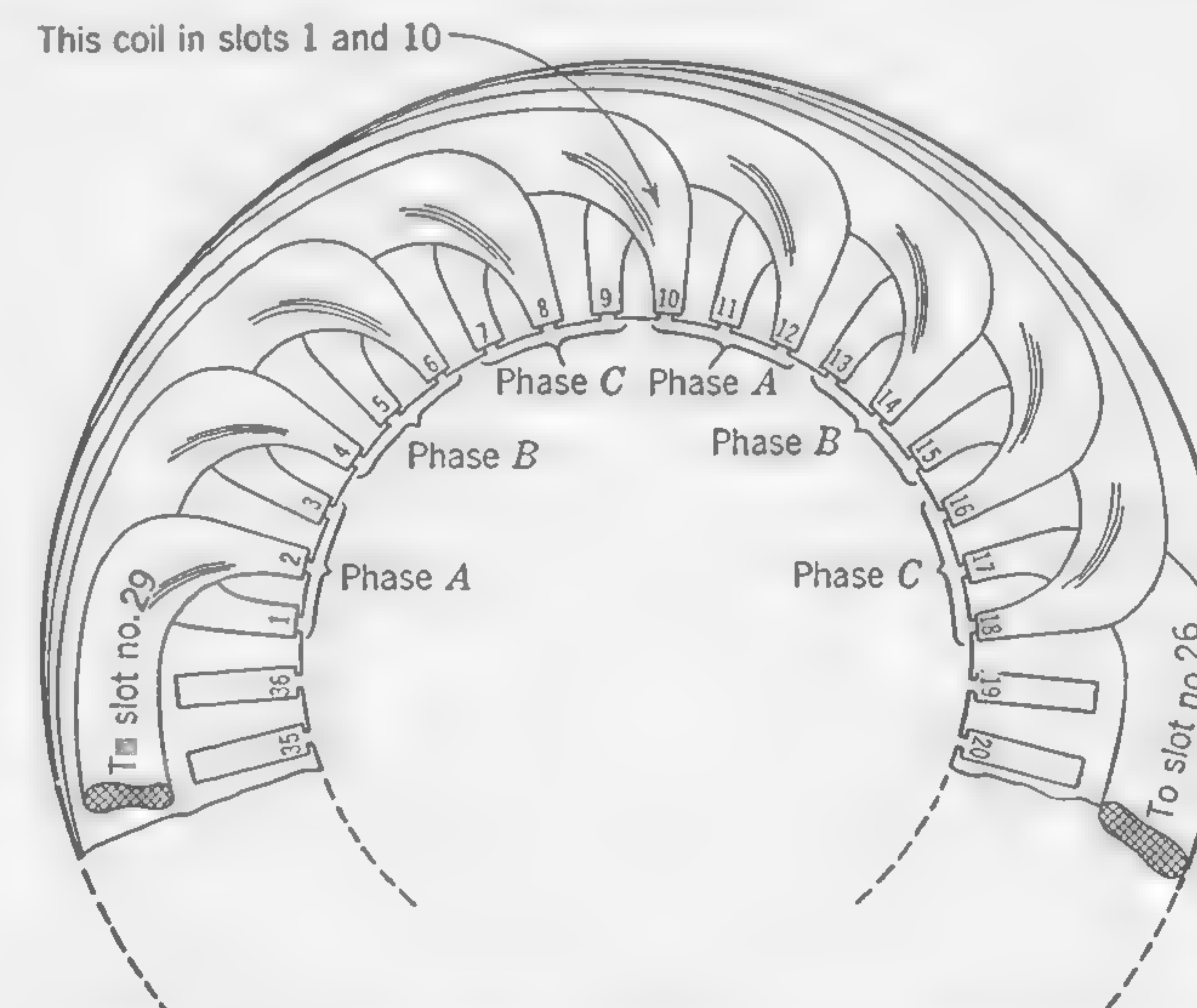


FIG. 130. Portion of full-overlap single-layer winding on stator of three-phase induction motor (4-pole—36 slots—3 slots per pole per phase).

**Current Density.** The current density in the stator windings is usually between 1,500 and 3,300 amp per sq in. It depends upon the peripheral velocity of the rotor and is usually higher on the lower-voltage machines because of the smaller thickness of insulation required and the greater facility for getting rid of the heat. A common value for the current density  $\Delta$  in amperes per square inch is from 2,000 to 3,000, with 3,500 as a usual value in motors used intermittently, as for the operation of elevators. The current density in the rotor conductors may generally be about 15 to 30 per cent higher than in the stator windings.

A more common type of stator winding, and one that is used almost exclusively in standard motors, is the two-layer lap winding in which all coils, similar in shape and size for a given machine, are usually preformed on special machines before they are inserted in the slots of the core.



When the stator has open slots, and this is particularly true of some of the larger motors, the coils are dipped in insulating varnishes and baked before the actual winding procedure is started. Unlike single-layer windings, whose coil pitches are limited to certain spans that are determined by the number of slots, poles, and phases, double-layer windings can have any desired fractional pitch; this is an important design advantage when the coil pitch must be adjusted to provide a definite number of *effective* turns per coil. Figure 86 illustrates one of the phases of such a winding with full-pitch coils, while Fig. 87 shows a complete lap-winding diagram with a fractional pitch of  $\frac{7}{9}$ , *i.e.*, 140 electrical degrees.

**106. Rotor Windings—Current Density.** The great majority of present-day induction motors are manufactured with squirrel-cage rotors, a common practice being to employ windings of cast aluminum. In this construction the assembled rotor laminations are placed in a mold after which molten aluminum is forced in, under pressure, to form the bars and end rings; often cooling fins are formed as extensions of the end rings. In other designs, copper or brass bars, of round or rectangular shape to fit the rotor slots tightly, are driven into the slots, projecting a short distance from each end of the core; end rings of the same material, with holes lining up with the projecting conductors, are then forced over the latter, after which conductors and end rings are soldered, welded, or brazed.

For induction motors requiring speed control or extremely high values of starting torque, the wound-rotor construction is frequently employed. An insulated winding, generally of the modified wave type (see Fig. 85), is used and, for three-phase service, is connected star or delta, with the phase ends brought out to three slip rings; as in the stator winding the coils may be either full-pitch or fractional pitch.

Essentially, there is little difference between the squirrel-cage and wound rotors, the object of the latter being merely to bring out the ends of a polyphase winding to slip rings in order that additional external resistance may be connected in series to improve the starting torque. The squirrel-cage rotor may be thought of as being provided with short-circuited, single-turn, full-pitch coils, equal in number to one-half the number of rotor bars. It is a winding of many phases. The wound rotor, on the other hand, is usually provided with a three-phase winding, in order to limit the number of slip rings.

The relation between torque and slip, as affected by rotor resistance, is discussed in Art. 108 and again in Art. 119, wherein the circle diagram is used to show how the starting torque is influenced by both the leakage reactance and the resistance of the windings. The effect of rotor resistance on starting torque may, however, be explained briefly as follows. Assuming very small rotor losses ( $R_r$  nearly zero), the current at starting

(rotor at rest) would be large, but it would be *out of phase* with the rotating field which produces the back emf in the stator windings, and the starting torque would be small. By increasing the resistance of the rotor circuits, the amount of the starting current may be reduced, but a larger component of this current will be in phase with the flux, and, since torque depends upon the product of magnetic field and the current component in phase with it, the starting torque will be improved. Obviously, there is a particular value of resistance which will give the best starting torque, and any resistance in excess of this will so reduce the total current that the torque will be less, although the phase of the current will be more nearly the same as that of the magnetic field.

The slip-ring motor permits of a low-resistance winding which will give high efficiency under running conditions, with the means of inserting extra resistance to give large torque under starting conditions. The chief difference in construction is that insulated rotor slots are necessary and there is less room for the copper than in the squirrel-cage rotor. Wound rotors are usually provided with double-layer wave windings. The coil connections are generally such as to provide a three-phase star winding with the free ends brought out to the three slip rings, although in the case of high-voltage motors (Art. 110 and Fig. 138) the delta connection may be employed to limit the voltage between slip rings. It is important to see that the thickness of the tooth at the root is sufficient for mechanical strength, even if the flux density is not excessive. The maximum tooth density may be from 100,000 to 125,000 lines per sq in. in the rotor teeth.

By using special designs of squirrel-cage rotor, it is possible to obtain a performance approaching that of machines with wound rotor, namely, good starting torque with low current, combined with reasonably high efficiency under running conditions. Double squirrel-cage windings\* are sometimes used, with an inner winding (bottom of slots) of low resistance and high reactance, and an outer winding (upper part of slots) of high resistance and low reactance. When starting the motor, with rotor at rest, the outer winding is effective in providing the large starting torque, but, as the speed increases, the frequency of the rotor currents decreases and the inner winding becomes effective in providing good full-load efficiency and small slip. The distribution of current between the two windings is automatic and exactly in accordance with requirements. A magnetic bridge is usually provided between the upper and lower bars in the slot. This increases the reactance of the inner winding.

By providing deep narrow slots in the rotor punchings, and using a squirrel-cage winding of thin flat copper bars, fairly good full-voltage

\*B. S. L. CHANG, General Theory of Multiple-cage Induction Motors, *Trans. AIEE*, Vol. 68, part 2, pp. 1139-1143, 1949.



starting may be obtained without much sacrifice of full-load efficiency. With the large slot-leakage flux passing through the copper bars at a high frequency with rotor at rest, eddy currents are induced which increase the apparent resistance of the rotor winding and ensure a good starting torque. Under running conditions, with low frequency in the rotor, the copper losses—and therefore the slip—are not excessive.

An important aspect of squirrel-cage design is the proper selection of the number of slots with respect to that on the stator; the number of slots on rotor and stator must never be the same, but either may be more than the other. Although the analysis and principles underlying stator and rotor slot combinations are beyond the scope of this book,\* it should be pointed out that certain improper combinations will cause the motor to cog, develop synchronous cusps in the torque-speed curve, or operate noisily. Cogging may result when the starting torque varies widely for different rotor positions with respect to the stator; in fact, in certain positions the locking torque may be sufficient to prevent the motor from starting. When synchronous cusps develop, the motor speed increases to a fraction—one-seventh, for example—of synchronous speed, and continues to operate at the subsynchronous speed; in some designs the synchronous cusps may be so pronounced that the normal starting torque may not be sufficient to accelerate the unloaded motor to normal speed. The objectionable characteristics indicated are brought about by certain combinations of stator and rotor slots that cause flux harmonics in the air gap. Noise and vibration should, of course, be avoided, where this is possible, in the original design. In addition to the careful choice of slot combinations it should be pointed out that such faulty operation may be minimized by the use of equalizer connections† in the stator winding and good mechanical construction.

Concerning stator and rotor slot combinations, the following general rules should be followed: (1) to avoid cogging the *difference* between the number of stator and rotor slots should not be equal to or a multiple of  $3p$  for three-phase machines, nor equal to or a multiple of  $2p$  for two-phase motors; (2) to avoid synchronous cusps in the torque-speed curve the *difference* between the number of stator and rotor slots should not be equal to  $p$ ,  $2p$ , or  $5p$  for three-phase machines, nor to  $p$  for two-phase motors; (3) to avoid noisy operation the *difference* between the number of stator and rotor slots should not be equal to 1, 2,  $(p + 1)$ , or  $(p + 2)$ .

\* MORRILL, W. J., Harmonic Theory of Noise in Induction Motors, *Trans. AIEE*, vol. 59, p. 474, 1940; DREESE, E. E., Synchronous Motor Effects in Induction Machines, *Trans. AIEE*, vol. 49, p. 1033, 1930; GRAHAM, Q., Dead Points in Squirrel-cage Motors, *Trans. AIEE*, vol. 59, p. 637, 1940.

† SISKIND, C. S., "Alternating-current Armature Windings," Chap. 15, McGraw-Hill Book Company, Inc., 1951.

*Rotor-bar Skew.* Another rather general practice is to provide the squirrel cage with skewed slots, *i.e.*, slots that are *not* parallel to the shaft axis. When carefully done, rotor-bar skew will effectively reduce motor noise and vibration, and will minimize cogging and synchronous cusps; other advantages resulting from the choice of a *proper* angle of "twist" are increased starting torque and reduced starting current.

Because of the presence of slots and teeth in both stator and rotor, space ripples are superimposed upon the normal sinusoidal flux-density distribution. Harmonic rotor voltages induced by such ripples then tend to develop corresponding harmonic rotor currents which, in turn, react with the flux wave to produce such undesirable effects as noise and dips in the torque-speed curve. To subdue a particularly objectionable  $n$ th harmonic the rotor bars should be skewed by an angle that is just sufficient to cause the induction of *two equal and opposite emfs in each bar*; such harmonic emf cancellation will then eliminate the very harmonic *current* that normally reacts with its corresponding component in the flux wave to produce noise and dips in the torque-speed characteristic. For example, if it is deemed desirable to nullify the effect of the seventh harmonic in the flux wave of a four-pole machine (the seventh harmonic develops 28 poles in a four-pole motor), the rotor bars must be skewed one-fourteenth of  $360^\circ$ , or  $25.7^\circ$ ; thus, with 28 harmonic poles, a skew of  $25.7$  mechanical degrees or  $360$  electrical degrees, each bar will be acted upon equally by alternate harmonic poles of the *same* polarity. (In a d-c generator, this would be equivalent to an armature-winding coil span of  $360$  electrical degrees, a condition that would result in zero generated voltage.) Under certain manufacturing conditions it is sometimes found desirable to skew the stator slots, instead of those of the rotor. When this is done the skew in stator slot pitches must be equivalent, in terms of electrical degrees, to that calculated for the rotor bars.

*Current Density.* Current densities in the bars of squirrel-cage rotors may be 2,500 to 4,500 amp per sq in. In deciding upon the section of the conductor, the rotor resistance of bars and end rings must be proportioned so that the motor develops the required starting torque.

When the rotor has a wire-wound winding the mean length per turn is approximately equal to that in the stator, and is given by formula (102).

**107. End-ring Current in Squirrel-cage Rotors.** The actual current distribution in the bars and end rings of squirrel-cage rotors is complicated because (1) the magnitudes and directions change in the individual conductors from instant to instant as the rotor revolves; (2) for any given instant the magnitudes and/or directions differ in all the conductors over one pole pitch; and (3) the current variations do not follow a simple sinusoidal function. A reasonably good approximation may, however, be obtained for the end-ring current if the space and time variations are



assumed to be sinusoidal. Considering a group of rotor conductors in one pole pitch, one-half of them send current into an end ring while the other half receive a like amount of current from the same end ring. At the instant when a conductor near the center of the group is carrying maximum current, those at the two extremes of the pole pitch will carry no current. It follows, therefore, that the *maximum* current occurring in the end rings which short-circuit the rotor bars is the sum of the *average* currents in one-half of the number of bars under one pole. Thus, the maximum end-ring current

$$I_{e(\max)} = \frac{\text{bars}}{2p} \times I_{r(\text{avg})}$$

Since  $I_{r(\text{avg})} = I_r \times 1.11$ , where 1.11 is the form factor for a sine wave and  $I_r$  stands for the rms value of the rotor-bar current,

$$I_{e(\max)} = \frac{\text{bars}}{2p} \times \frac{I_r}{1.11}$$

But  $I_{e(\max)} = I_e \sqrt{2}$ . It follows, therefore, that

$$I_e = \frac{\text{bars} \times I_r}{2\sqrt{2} \times 1.11p} = \frac{\text{bars} \times I_r}{\pi p} \quad (103)$$

**108. Relation between Slip and Rotor Resistance.** With no external load on the motor, and negligible friction and windage losses, the rotor would rotate at the same speed as the field; and, since the rotor conductors would not be cut by the rotating flux, there would be no voltage generated in these conductors, and, consequently, no rotor current. When the motor is called upon to do mechanical work, the motor will slow down until the "slip revolutions" are just sufficient to develop a voltage in the rotor conductors which will overcome the ohmic resistance and produce the particular current which will make the torque developed by the rotor exactly equal to the torque exerted by the load (including friction and windage losses in the motor itself). The *slip revolutions* are the difference between the synchronous rpm and the actual rpm of the rotor.

The *slip* of an induction motor is defined as the ratio

$$s = \frac{\text{synchronous rpm} - \text{actual rpm}}{\text{synchronous rpm}} \\ = \frac{\text{slip revolutions}}{\text{synchronous revolutions}}$$

The slip revolutions (the numerator in this expression) must obviously be proportional to the volts necessary to overcome the rotor resistance, or to  $I_r R_r$ , while the synchronous revolutions (the quantity in the denominator) are proportional to the voltage generated by transformer action *i.e.*, by the same (imaginary) revolving field cutting the rotor conductors at *synchronous speed*. This ratio may be more clearly expressed in terms of power input and output.

*Relations between Torque, Speed, and Power.* The force which causes the rotor to rotate and transmit mechanical power to the shaft is the sum of all the tangential forces due to the currents in the rotor conductors acting upon the magnetic field in which they are moving. The force exerted by each conductor at a given instant is proportional to the product of current and density of magnetic flux. Thus the torque may be said to be proportional to the product of magnetic flux and the rotor current component in phase with it. This may be expressed in pound-feet, or as the pull in pounds which, when acting at a radius of 1 ft, will produce the same turning effect as the summation of all the smaller forces acting at the periphery of the rotor on the individual conductors.

Power is the product of torque and speed. The field revolves at synchronous speed, and the emf induced in the rotor by transformer action—the stator winding being the primary and the rotor winding the secondary—may be thought of as being due to a flux *rotating at synchronous speed*. In the rotor, or secondary, winding, there is also a back emf produced due to the rotation of the rotor.

Let  $\Phi$  stand for the flux which actually enters the rotor core. It may be defined as that component of the total flux in the stator which is in phase with the rotor current  $I_r$  and is "cut" by the rotor winding of resistance  $R_r$ . We may therefore think of the current  $I_r$  in the rotor as being in phase with the emf generated by the cutting of the flux  $\Phi$ .

If  $E_r$  = voltage generated in rotor due to the "slip" revolutions,

$$E_r = K\Phi(N_s - N_r) = I_r R_r$$

where  $N_s$  = synchronous rpm,  $N_r$  = rotor rpm, and  $K$  is a constant. Thus,

$$I_r R_r = K\Phi N_s - K\Phi N_r \quad (a)$$

Expressed in words, this means that the rotor  $IR$  drop is equal to the difference between the emf developed by the rotation of the field,  $K\Phi N_s$ , and the emf developed by the rotation of the rotor,  $K\Phi N_r$ . If the rotor were to run at synchronous speed, there would be no emf developed in the rotor windings.

Multiplying both sides of Eq. (a) by  $I_r$ , we get

$$I_r^2 R_r = (KI_r \Phi) N_s - (KI_r \Phi) N_r \quad (b)$$

in which the quantity  $(KI_r \Phi)$  is proportional to torque.

Expressed in words, Eq. (b) means that the power lost in the rotor is equal to the difference between the power input to rotor,  $KI_r \Phi N_s$ , and the power output from rotor,  $KI_r \Phi N_r$ , which is obviously true. It should be noted that the friction and windage losses and the small amount of iron loss in the rotor core are here considered as part of the motor load.

By definition, the slip is  $s = (N_s - N_r)/N_s$  and, by substitution from Eq. (b), this leads to



s = (K I\_r \Phi (N\_s - N\_r) / (K I\_r \Phi N\_s)) = (I\_r^2 R\_r / (N\_s (K I\_r \Phi))) = (rotor copper loss / rotor input) (104)

It also follows that

(Rotor input / Rotor output) = (synchronous speed / rotor speed) = (1 / (1 - s)) (105)

When the rotor is of the squirrel-cage type, the starting characteristics (to be considered later) will not be good if the rotor resistance is very small. It is, therefore, customary to design squirrel-cage rotors with a certain amount of resistance which will be a compromise between the high resistance required to give good starting torque and the low resistance required to give high efficiency under running conditions. Since rotor resistance and slip are connected as indicated by Eq. (104), it is merely necessary to decide upon a reasonable value for the slip at full load. Usual values for motors with squirrel-cage rotors are given below. Approximate values for the friction and windage losses are also given, for use in calculating efficiency.

Horsepower output	Slip, per cent	Windage and friction, per cent of output
1	5.0	5.5
2	4.6	4.3
5	4.2	3.2
10	4.0	2.5
30	3.6	1.8
100	3.2	1.2
200	3.0	1.0

109. Illustrative Example. Design of Squirrel-cage Induction Motor. Design a 10-hp 3-phase 220-volt 60-cycle 1,800-srpm induction motor, the rotor to be of the squirrel-cage type.

In this problem it is not proposed to aim at any specified performance; but, by following usual practice and adopting reasonable values for current and flux densities, a normal design should be produced. An investigation of the performance of the machine, as designed, and the determination of power factor, starting torque, and other characteristics of the design will form the subject of another problem at the conclusion of the following chapter.

CALCULATIONS

Items 1 and 2: Number of Poles. p = (2 x 60 x 60 / 1,800) = 4

Volts per phase (star): E = (220 / sqrt(3)) = 127

DESIGN SHEET FOR INDUCTION MOTOR (Dimensions in inches unless otherwise stated)

Item No.	Specifications: 10-hp 3-phase motor, with squirrel-cage rotor; 220 volts; 60 cycles; 1,800 rpm, (synchronous)	Sym-bol	Numerical values
1	Number of poles.....	p	4
2	Volts per phase (use star connection).....	E	127
3	Estimated full-load power factor.....	cos θ	0.86
4	Estimated full-load efficiency.....	η	0.87
5	Full-load current in stator winding (amp).....	I <sub>c</sub>	26.2
6	Average flux density in air gap (lines per sq in.).....	B <sub>g</sub> ''	23,900
7	Specific loading of stator.....	q	515
8	Distribution factor (pitch factor = 1).....	k	0.96
9	The quantity D <sup>2</sup> l <sub>a</sub> (in. units).....		258
Stator Design			
10	Internal diameter of stator.....	D	7
11	Peripheral velocity of rotor (approx) (fpm).....	v	3,300
12	Pole pitch (on stator).....	τ	5.5
13	Gross length of stator core.....	l <sub>a</sub>	5 1/4
14	Number and size of vent ducts (1/2 in. wide).....		1
15	Net length of iron in stator core.....	l <sub>n</sub>	4.27
16	Number of slots per pole per phase.....	n <sub>s</sub>	3
17	Number of slots per pole.....		9
18	Slot pitch.....	λ	0.612
19	Number of stator conductors per slot.....	C <sub>s</sub>	12
20	Number of stator conductors in series per phase.....	Z	144
21	Air-gap flux per pole.....	Φ	690,000
22	Maximum "apparent" tooth density (lines per sq in.).....	B <sub>t</sub> ''	91,200
23	Tooth width (narrow end).....	t	0.31
24	Slot width.....	s	0.302
25	Current density in windings.....	Δ	2,550
26	Thickness of slot insulation.....		0.035
27	Size of wire.....	Two No. 12 B & S in parallel	
28	Depth of stator slots.....	d	1.34
29	Length per turn of stator winding.....		29.15
30	Ohms per phase (hot).....		0.161
31	IR drop per phase (volts).....		4.22
32	Total stator copper loss (watts).....	W	332
33	Flux density in iron of stator core (lines per sq in.).....		57,200
34	Outside diameter of stator stampings.....		12 1/2
35	Weight of iron in stator core (lb).....		58.7
36	Weight of iron in stator teeth (lb).....		24.4
37	Losses in stator core (watts).....		194
38	Losses in stator teeth (watts).....		126
39	Total stator iron loss (watts).....		320
Rotor Design (squirrel-cage)			
40	Number of slots.....	n <sub>r</sub>	31
41	Slot pitch.....	λ <sub>r</sub>	0.71
42	Current per rotor bar (amp).....		311
43	Current density in rotor bars (amp per sq in.).....		2,600
44	Dimensions of rotor bar.....		0.2 x 0.6
45	Width of rotor slot.....	s <sub>r</sub>	0.2
46	Depth of rotor slot.....	d <sub>r</sub>	0.67
47	Maximum flux density in rotor teeth (lines per sq in.).....		87,000
48	I <sup>2</sup> R loss in rotor bars (watts).....		132
49	Current in end rings (amp).....		765
50	Current density in end rings (amp per sq in.).....		2,930
51	Dimensions of end rings (sq in.).....		0.261
52	I <sup>2</sup> R loss in end rings (watts).....		268
53	Total I <sup>2</sup> R loss in rotor (watts).....	W <sub>r</sub>	400
54	Slip at full load (per cent).....		5.1
55	Full-load speed (rpm).....		1,708
56	Calculated efficiency [compare with item (4)].....	η	0.856



Items 3 and 4. These are estimated with the aid of the curves of Figs. 127 and 128 (Art. 99).

Items 5, 6, and 7. The current in stator windings is obtained from the equation

$$H_p \times 746 = 3EI_c \cos \theta \times \eta$$

whence  $I_c = 26.2$  amp.

For  $B'_g$  we shall select 26,000 lines per sq in. (refer to Art. 100).

For the specific loading we select  $q = 470$  from Fig. 129 (Art. 100); but this is subject to correction when the winding details have been worked out.

Item 8. The winding factor depends upon the number of slots per pole per phase and on the pitch of the coils, that is to say, whether or not we have a short pitch of chorded winding. This factor was discussed in Art. 69. The probable number of slots per pole per phase is obtained by referring to the table in Art. 101, although this assumes the pole pitch to be known. In a 10-hp motor running at 1,800 rpm the pole pitch is not likely to be less than 5 or more than 7 in., so that the proper number of slots per pole for a three-phase winding is almost certain to be nine. With a full-pitch winding,  $k' = 1$ , which is likely to be used in a small motor such as this one, the value of  $d$  is 0.96.

Item 9. Inserting numerical values in Eq. (100) of Art. 102, we have

$$D^2 l_a = \frac{4.07 \times 10^{11} \times 10}{0.87 \times 0.86 \times 0.96 \times 26,000 \times 470 \times 1,800} = 258$$

#### STATOR DESIGN

Items 10 to 13. Refer to Art. 102. The output *per pole* is  $10/4 = 2.5$  hp, and from the table on page 275 it appears that a suitable pole pitch will be about  $5\frac{1}{4}$  in. This would require a stator diameter (internal) of  $(4 \times 5.25)/\pi = 6.67$  in. Since the table on page 275 is to be used merely as a guide in deciding upon dimensions, and since considerable departures from the suggested values are permissible, we shall try a stator diameter of 7 in., which makes the pole pitch ( $\tau$ ) 5.5 in. (item 12).

The peripheral velocity of the rotor (the diameter of which is only very little smaller than 7 in.) is approximately, by formula (101),

$$v = 10 \times 60 \times 5.5 = 3,300 \text{ fpm}$$

which is not excessive.

The gross length of the stator core (or the length of the air gap measured parallel with shaft) is

$$l_a = \frac{258}{(7)^2} = 5.27 \text{ in., or (say) } 5\frac{1}{4} \text{ in.}$$

the figure 258 being item 9.

Items 14 and 15. Refer to Art. 102. With a gross length of stator of only  $5\frac{1}{4}$  in., one  $\frac{1}{2}$ -in. vent duct should be sufficient. Then, if the stacking factor is taken as 0.9, the net length of iron is

$$l_n = 0.9(5.25 - 0.5) = 4.27 \text{ in.}$$

Items 16 to 20. When discussing item 8 we assumed 9 slots per pole. This may be checked and compared with other possible numbers of slots by constructing a table as follows:

Number of slots per pole per phase ( $n_s$ )	Number of slots per pole	Slot pitch ( $\lambda$ )	Number of inductors per slots ( $C_s$ )		Specific loading ( $q$ ) corrected
			Calculated	Selected for trial	
2	6	0.917	16.4	16	457
3	9	0.612	11.0	12	515
4	12	0.458	8.2	8	457

The figures in the third column are the slot pitch  $\lambda$ , which results from dividing the pole pitch of 5.5 in. by the number of slots per pole; the calculated number of conductors per slot, by formula (69), in the fourth column, is

$$C_s = \frac{q\lambda}{I_c} = \frac{470}{26.2} \times \lambda$$

With only two slots per pole per phase, the slot pitch is rather large for so small a diameter of stator. With  $n_s = 4$  and a total number of 12 slots per pole, there is a possible advantage in that the stator can be wound for two-phase operation if desired, and also that three-phase windings could be put on in the form of two parallel circuits which might be connected in series for operation on 440 volts. However, nine slots per pole seems best if we have merely to consider the machine as specified, and we shall decide upon a stator with 36 slots. Then the number of conductors in series per phase (item 20) is

$$Z = C_s \times n_s \times p = 144$$

Items 21 to 24. Having decided upon the number of conductors, the necessary flux per pole should be calculated so as to check the air-gap and tooth densities. By formula (64a) on page 173 we have

$$\Phi = \frac{127 \times 10^8}{2.22 \times 0.96 \times 60 \times 144} = 690,000 \text{ maxwells}$$



The corrected value of air-gap density (average value) is

$$B''_a = \frac{\Phi}{\tau l_a} = \frac{690,000}{5.5 \times 5.25} = 23,900$$

The maximum value (sine-wave assumption) is

$$\frac{\pi}{2} \times 23,900 = 37,600 \text{ lines per sq in.}$$

In order to calculate the minimum permissible tooth width, a tooth density must be assumed (refer to Art. 100). Let us try  $B'_t = 85,000$ , then

$$t = \frac{37,600 \times 0.612 \times 5.25}{85,000 \times 4.27} = 0.333 \text{ in.}$$

which would make  $s = \lambda - t = 0.279$  in. Usually the slot width  $s$  is about the same as the tooth width  $t$  and, since  $B'_t = 85,000$  is the "apparent" density in the narrowest part of the tooth, the actual density at the center of the tooth will be appreciably less and a somewhat narrower tooth is permissible. Let us try  $t = 0.31$  in. at the narrow end; then  $s = 0.612 - 0.31 = 0.302$  in., which is the slot width as measured in the punching; but, owing to slight inequalities, the finished slot, when ready for the insulation, will not be quite so wide as this. Allowing 0.012 in. for "slot tolerance," the actual width of slot space available for conductors and insulation will be 0.29 in.

The corrected maximum "apparent" tooth density (item 22) is

$$B'_t = 85,000 \times \frac{0.333}{0.310} = 91,200$$

Before deciding upon the depth of slot, it is necessary to consider the dimensions of the conductors and space taken up by insulation.

*Items 25 to 28.* For the current density (see Art. 105) we shall try  $\Delta = 2,400$  amp per sq in.; whence area of conductor cross section =  $26.2/2,400 = 0.0109$  sq in. A single wire of this cross section would be too stiff for so small a motor and we shall try two No. 12 wires in parallel. The area is  $2 \times 0.00513 = 0.01026$ ; whence  $\Delta = 2,550$ , which is probably not too high. The thickness of slot insulation by formula (16) on page 34, is 34.3 mils, or about 0.035 in., so that the width of slot available to accommodate the wires is  $0.29 - (2 \times 0.035) = 0.22$  in., and, since a No. 12 B & S wire measures about 0.093 in. over the cotton (see Table I, p. 431), there will be ample room for two wires side by side, but not for three. Since  $C_s = 12$ , we have 24 of the single No. 12 wires to accommodate in one slot and, therefore, 12 wires in depth. If we adopt the "full overlap" type of "mush" winding as illustrated in Fig. 130, there will

be only one coil side per slot, and the total depth of slot may be computed as follows:

Slot lining.....	0.035
12 wires.....	1.116
Slot lining and wedge.....	0.065
Tooth thickness.....	0.070
Allowance for spaces between wires.....	0.054
Total slot depth.....	1.34 in.

Ratio  $d/s = 4.43$ , which is somewhat on the high side, but not objectionable. This ratio is commonly between  $3\frac{1}{2}$  and  $4\frac{1}{2}$ . The tooth and slot dimensions are shown in Fig. 131. The connections between stator coils must be made in any convenient manner which will cause all the emfs due to rotation of the flux to be additive. A greatly simplified sketch of one of the phase windings is shown in Fig. 132, and a complete diagram of the single-layer three-phase star-connected lap winding is given in Fig. 133.

*Items 29 to 32.* By formula (102) on page 277, the mean length per turn of the stator winding is, approximately,

$$(2 \times 5.25) + (2.3 \times 5.5) + 6 = 29.15 \text{ in.}$$

The number of turns in series per phase is 72 and the length per phase winding (of the two wires in parallel) is 175 ft. The resistance per phase winding is

$$\frac{175}{1,000} \times \frac{1.846}{2} = 0.161 \text{ ohm}$$

where the figure 1.846 is obtained from Table I (p. 431) for an assumed temperature of 60°C.

The  $IR$  drop per phase (item 31) is  $26.2 \times 0.161 = 4.22$  volts. The total copper loss in stator (item 32) is  $3 \times 4.22 \times 26.2 = 332$  watts.

*Items 33 to 35.* Referring to Art. 100, we shall try a density of 60,000. The amount of leakage flux is small and, assuming the flux in stator core to be one-half the flux in the air gap, the radial depth of core below the slots should be

$$\frac{690,000}{2 \times 60,000 \times 4.27} = 1.345 \text{ in.}$$

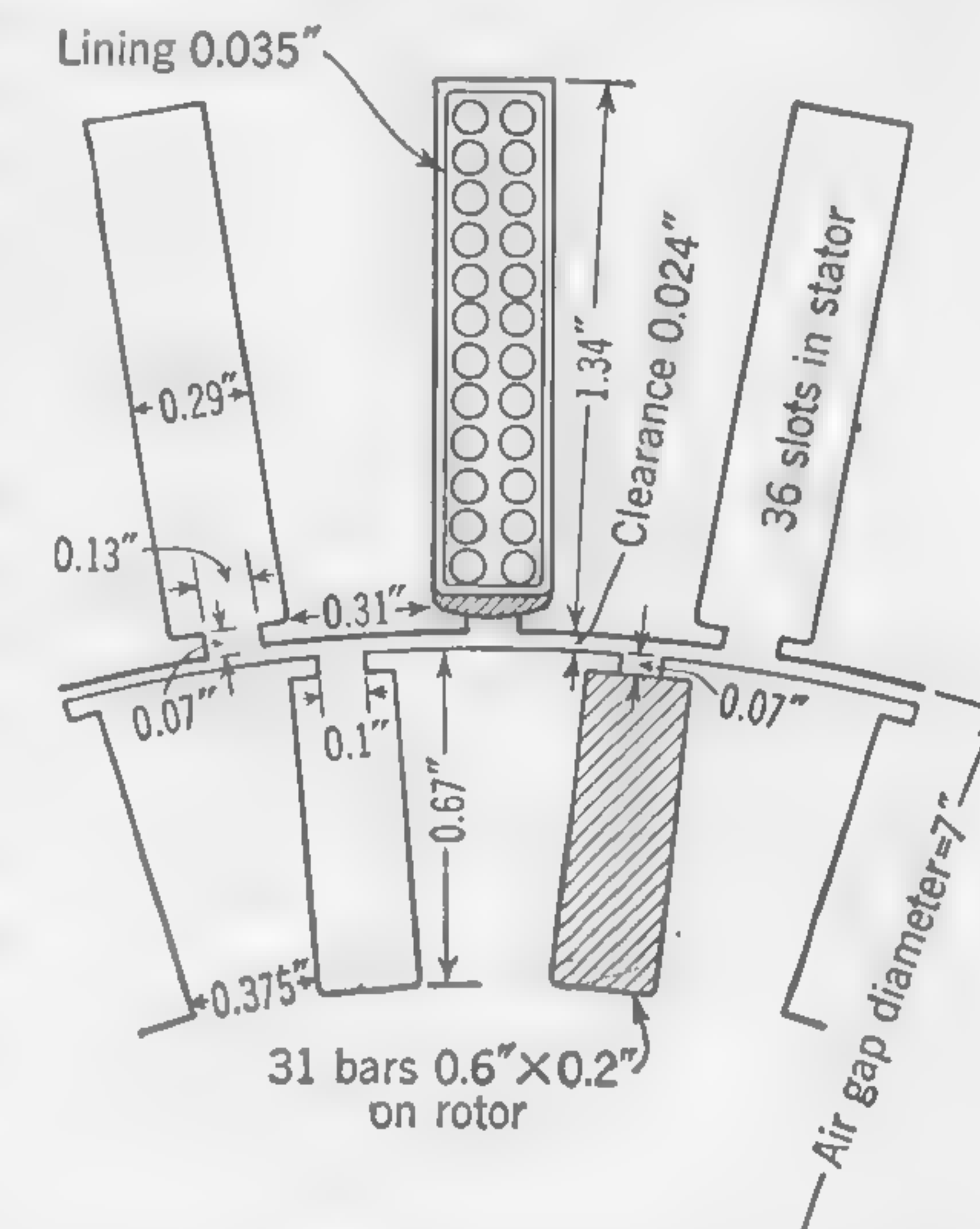


FIG. 131. Slot dimensions for induction motor, Illustrative Example of Art. 109.



This makes the outside diameter of stator stampings 12.37 in. Let us make this exactly  $12\frac{1}{2}$  in., which makes the corrected value of the maximum flux density in the core approximately 57,200.

The weight of iron in stator core, not including teeth (item 35), is  $0.28 \times \pi(12.5 - 1.41) \times 1.41 \times 4.27 = 58.7$  lb.

Items 36 to 39. The width of the stator teeth at the narrow end (near the air gap) on a circle of about 3.5-in. radius is 0.3 in. The slot is 0.302

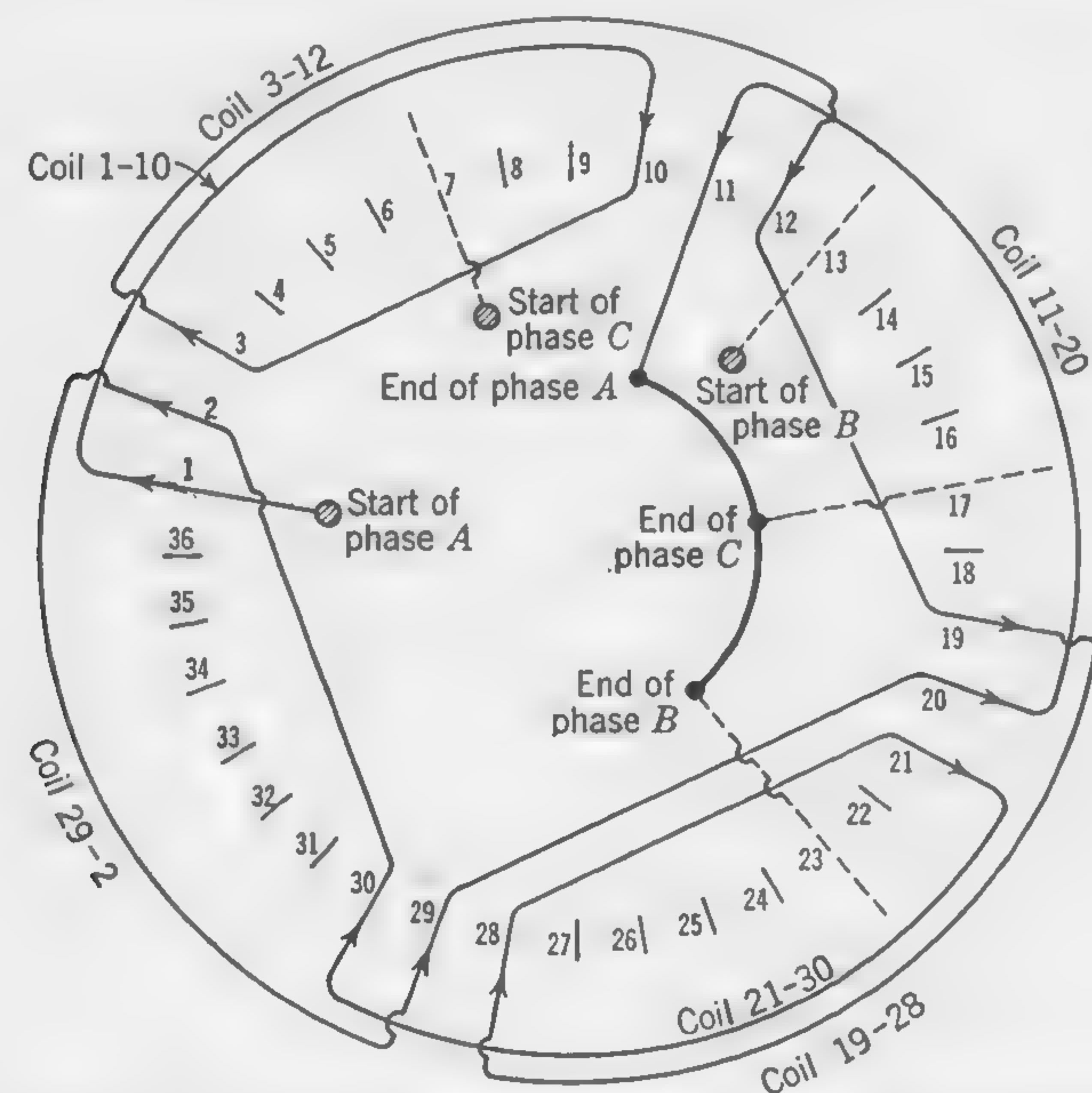


FIG. 132. Series-star stator coil connections for one phase of a four-pole motor (36 slots). See Art. 109.

in. wide, which makes the tooth width 0.544 in. near the bottom of the slot, the average width being 0.422 in. The weight of iron in the teeth is, therefore,

$$0.28 \times 0.422 \times 1.34 \times 4.27 \times 36 = 24.4 \text{ lb}$$

In order to calculate the losses in the teeth, we first calculate the flux density at a section one-third up from the narrow end (see Art. 52). The width here is 0.388 in. and the density is, therefore,  $91,200 \times (0.31/0.388) = 72,800$  lines per sq in. This is not the true maximum density, because the figure 91,200 (item 22) is the "apparent" density at the narrow end. The true density may be calculated as explained in Art. 30 by means of formula (40), but, since the density is fairly low, this would be a refinement which need not be introduced here.

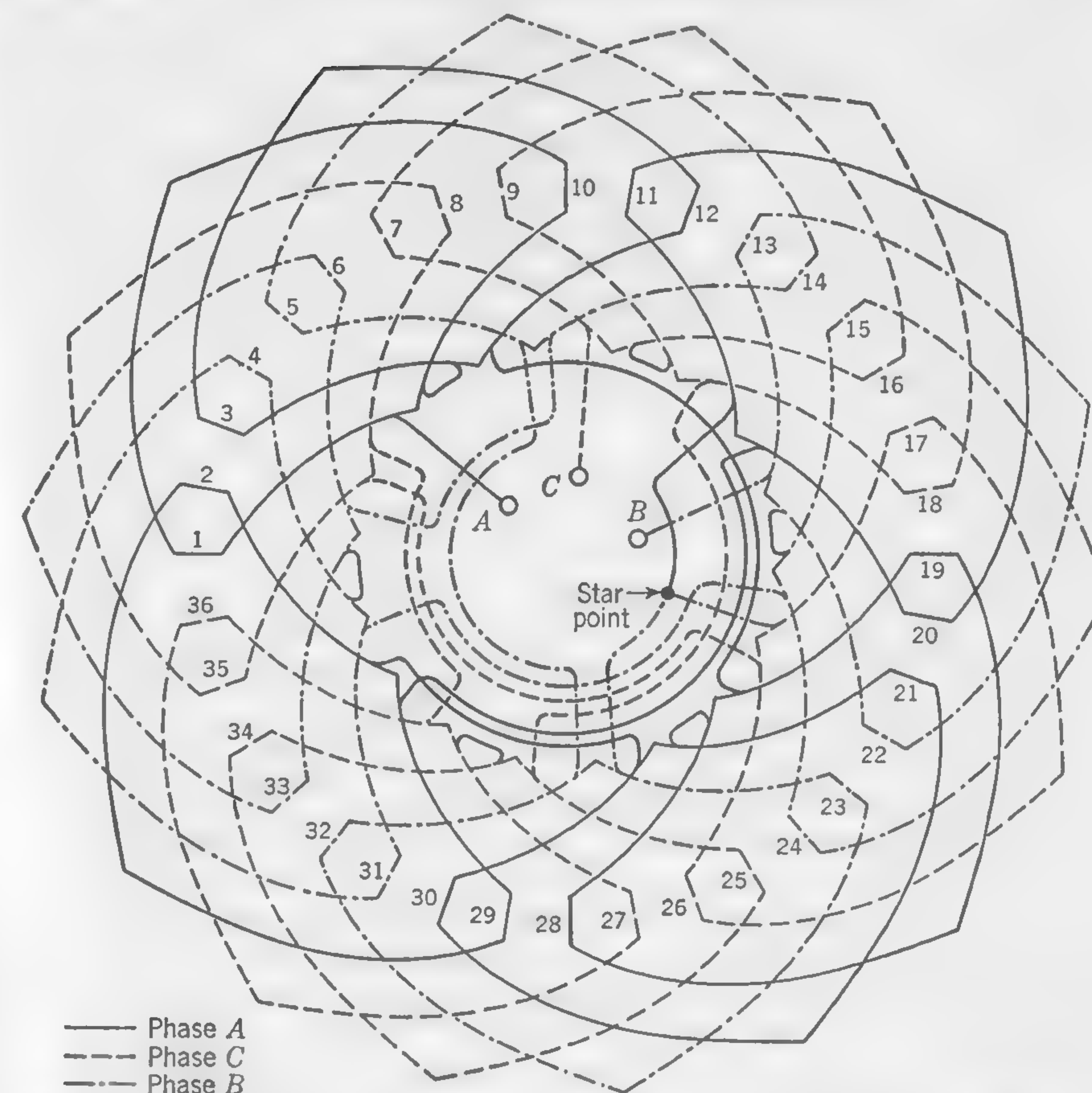


FIG. 133. Complete diagram of single-layer lap winding for Illustrative Example of Art. 109. Refer to Fig. 132 for simplified sketch of phase A.

Using the curve of Fig. 67 we have

$$\text{Watts lost in stator core} = 0.055 \times 60 \times 58.7 = 194$$

$$\text{Watts lost in stator teeth} = 0.085 \times 60 \times 24.7 = 126$$

$$\text{Total} = 320 \text{ watts}$$

#### DESIGN OF SQUIRREL-CAGE ROTOR\*

Items 40 and 41. Referring to Art. 106, the number of squirrel-cage bars will be made 31. With a difference of  $(36 - 31) = 5$  between stator and rotor slots, this will fulfill conditions (1) and (2) indicated in that article concerning cogging and synchronous cusps, although not  $(p + 1)$

\* MORRILL, W. J., Harmonic Theory of Noise in Induction Motors, *Trans. AIEE*, vol. 59, p. 474, August, 1940.



for noisy operation; the latter is not particularly objectionable if the rotor is provided with a stiff shaft and skewed slots. This makes the slot pitch  $\lambda_r = 0.71$  in.

*Items 42 to 48.* Since the total ampere-conductors on the rotor are about the same as on the stator, the current in each of the 31 rotor bars is easily calculated. The total primary (stator) current is 26.2 amp (item 5), but part of this is required for excitation and to supply stator losses. About 85 per cent of the full-load primary current would be required to "balance" the secondary (rotor) current, or, equating the primary and secondary ampere-conductors, we have

$$I_r \times 31 = (0.85 \times I_e) \times (3Z)$$

whence the current in each rotor conductor is

$$I_r = \frac{0.85 \times 26.2 \times 3 \times 144}{31} = 311 \text{ amp}$$

The current density in the rotor bars and ring connections may be calculated so as to give a definite "slip" (see Art. 108), but the adjustment of rotor resistance is best done in the end rings. For the bars in the slots, the current density may be somewhat higher than in the stator windings, and we shall try  $\Delta = 2,600$  amp per sq in. This gives a bar cross section of  $311/2,600 = 0.12$  sq in. (approx). We shall try a section  $0.2 \times 0.6$  and see if the tooth density is not too high. Since the frequency of flux reversal in the iron of the rotor is very low (it is the slip frequency), the rotor iron losses are practically negligible and densities as high as 115,000 lines per sq in. in the teeth are permissible.

Allowing 0.07 in. for thickness of tooth over the conductor (see Fig. 131) and neglecting the air-gap clearance, the width of rotor tooth at the root is

$$\frac{2\pi (3.5 - 0.67)}{31} - 0.2 = 0.375$$

whence, if the *net* core length is the same as in the stator,

$$\text{max tooth density} = \frac{\pi}{2} \times \frac{(4 \times 690,000)}{31 \times 4.27 \times 0.375} = 87,000 \text{ lines per sq in.}$$

which is considerably lower than the permissible maximum tooth density. The hole in the rotor core stampings may be  $3\frac{3}{4}$  in. in diameter without forcing the flux density in the iron above about 90,000 lines per sq in. The  $I^2R$  loss in the rotor bars (item 48) may now be calculated for an operating temperature of  $60^\circ\text{C}$ .

Allowing  $1\frac{1}{2}$  in. for skewing the rotor bars one slot pitch (0.71 in.) and for the distance between the ends of the rotor core and the short-circuiting rings, the length of each rotor bar is  $5\frac{1}{4} + 1\frac{1}{2} = 6\frac{3}{4}$  in. and the resistance per rotor bar is

$$\frac{6.75}{0.2 \times 0.6 \times \frac{4}{\pi} \times 10^6} = 4.42 \times 10^{-5} \text{ ohm}$$

whence the  $I^2R$  loss in the slot conductors is

$$31 \times (311)^2 \times 4.42 \times 10^{-5} = 132 \text{ watts}$$

*Items 49 to 55.* Referring to Art. 107 and formula (103), the current in the end rings

$$I_e = \frac{31 \times 311}{4 \times \pi} = 765 \text{ amp}$$

The current density in the end rings, and the material used, will depend upon the resistance required. This, together with the rotor-bar resistance, will determine the starting torque (to be discussed in the next chapter) and the slip under running conditions (see Art. 108). From the table on page 284 we see that a slip of 4 per cent is a usual value for a 10-hp squirrel-cage rotor; but, in order to obtain a good starting torque, we shall aim at about 5 per cent slip, although this necessarily involves some loss of efficiency. In order to produce this slip, the rotor copper losses must have a definite value to satisfy Eq. (104) of Art. 108. Let  $x$  be the total rotor  $I^2R$  loss; then

$$0.05 = \frac{x}{7,460 + x}$$

whence  $x = 392$ , or (say) 400 watts; which leaves  $400 - 132 = 268$  watts to be dissipated from the end rings. The resistance of each of the two short-circuiting rings should, therefore, be  $\frac{1}{2}[268/(765)^2]$  ohm. The mean length of the current path of the ring is about  $\pi \times 6$ , or (say) 19 in. Assume that the alloy of which the end rings are cast has four times the resistivity of copper. The resistance of the two end rings will, therefore, be

$$R_e = \frac{(2 \times 19) \times 4}{(m)} = \frac{152}{(m)}$$

Since the total end-ring copper loss is 268 watts,  $I_e^2 R_e = 268 = (765)^2 \times [152/(m)]$ , whence

$$(m) = \frac{(765)^2 \times 152}{268} = 332,000 \text{ cir mils}$$

The cross section of each ring (at  $60^\circ\text{C}$ ) thus becomes 0.261 sq in.

The current density in the end rings (item 50) will be  $765/0.261 = 2,930$  amp per sq in., which is not excessive. By using an alloy of high specific resistance for the cast rings, a larger cross section may be used without reducing the amount of the rotor losses.



The slip at full load, by Eq. (104), is

$$s = \frac{400}{7,460 + 400} = 0.051$$

The "slip revolutions" are  $1,800 \times 0.051 = 92$  (approx) which makes the full-load speed (item 55) equal to  $1,800 - 92 = 1,708$  rpm.

Item 56: Efficiency. The efficiency of a motor is

$$\eta = \frac{\text{output}}{\text{output} + \text{losses}} = 1 - \frac{\text{losses}}{\text{output} + \text{losses}}$$

The losses must include an estimate for friction and windage loss (refer to table on p. 284). The iron loss in rotor is almost negligible under running condition (when the speed is near synchronous speed) but may be estimated at about 5 per cent of the stator iron loss.

#### SUMMARY OF LOSSES

Stator copper	=	332 (item 32)
Rotor copper	=	400 (item 53)
Stator iron	=	320 (item 39)
Rotor iron	=	16 (5 per cent of stator iron loss)
Friction and windage	=	185 (assumed 2.5 per cent of output)
Total	=	1,253 watts

whence efficiency  $= 1 - [1,253/(7,460 + 1,253)] = 0.856$ .

Figure 134 shows the general arrangement and gives the over-all dimensions of the motor as designed.

**110. Illustrative Example. Design of Stator for Wound-rotor Induction Motor.** Design the stator for a 50-hp 3-phase 2,200-volt 25-cycle 500-srpm induction motor, the rotor to be of the wound-rotor type. A standard *double-layer winding* is to be used on the stator.

The design will be carried on in much the same way as in the Illustrative Example of Art. 109; an important departure will, however, include a commonly used double-layer type of lap winding.

#### CALCULATIONS

Items 1 and 2: Number of Poles and Volts per Phase.

$$p = \frac{120 \times 25}{500} = 6$$

$$E = \frac{2,200}{\sqrt{3}} = 1,270 \text{ (using a star connection)}$$

Items 3 and 4: Power Factor and Efficiency. For a comparatively high voltage machine it will be desirable to have preformed, completely insulated coils; such coil construction will necessitate the use of open slots

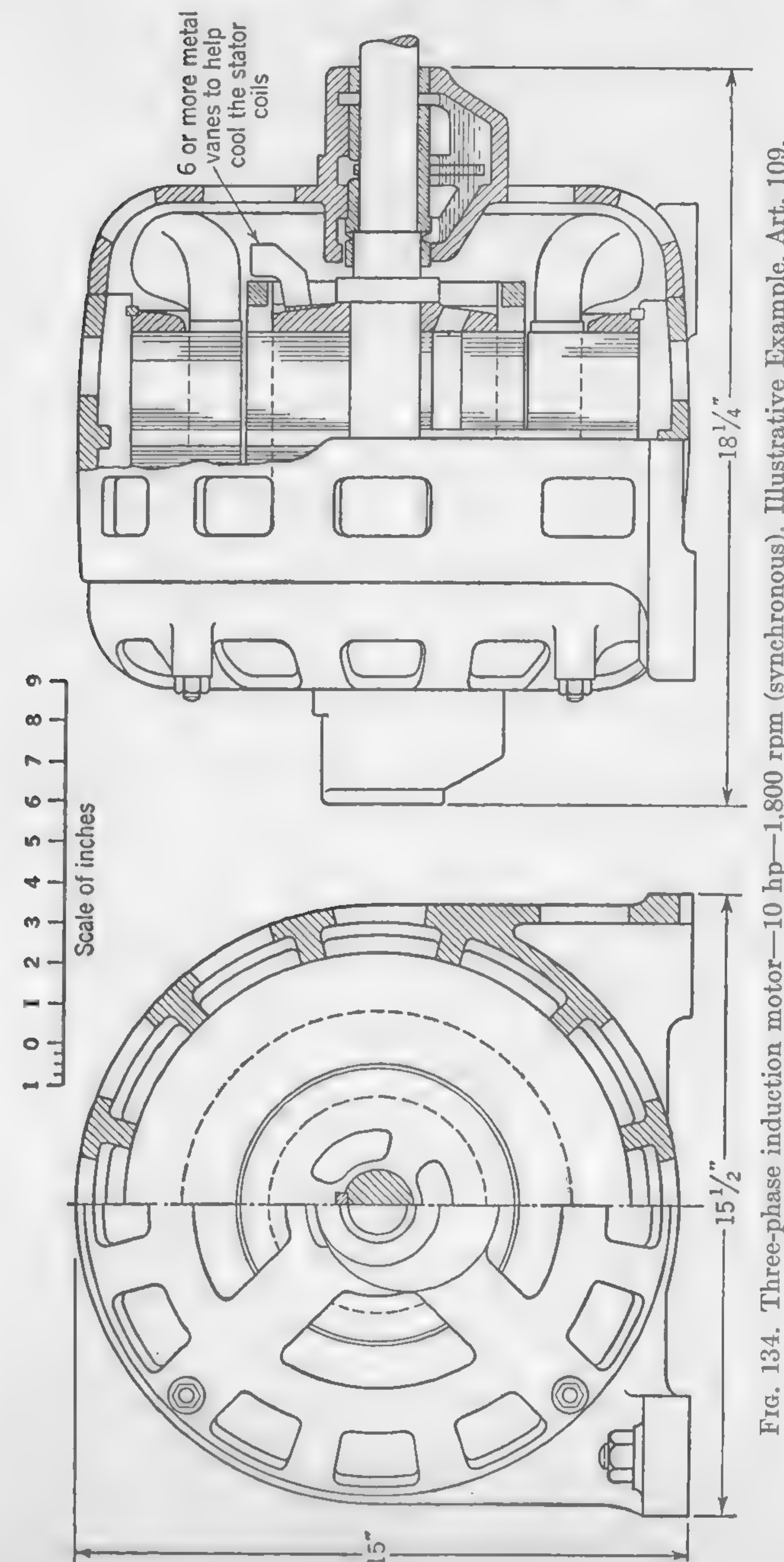


Fig. 134. Three-phase induction motor—10 hp—1,800 rpm (synchronous), Illustrative Example, Art. 109.



The magnetizing component of the no-load current can, therefore, be expected to be high, for which reason the motor power factor and efficiency will be rather low. It is estimated that the power factor and efficiency will be 0.81 and 0.83, respectively.

Items 5, 6, and 7. The full-load stator current will be

I\_c = (50 \* 746) / (3 \* 1,270 \* 0.81 \* 0.83) = 14.6 amp

Preliminary values of B'' = 32,000 lines per sq in. and q = 530 amp-conductors per in. will be assumed.

Item 8: Winding Factor. The winding factor is the product of the distribution factor k and the pitch factor k'. The first of these, k, is a function of the number of slots per pole per phase, which in turn depends upon the pole pitch (see Art. 101). For a machine with the given specifications it is probable that the pole pitch will be about 9 (hp/pole = 8 1/3), so that four slots per pole per phase should be about right; after the internal diameter of the stator has been decided upon the slot pitch can be calculated, and this value should indicate whether or not the number of slots has been properly chosen. The distribution factor k is therefore 0.958 (see Art. 69). A standard double-layer fractional-pitch lap winding will be used in the stator, and the coil span will arbitrarily be made one slot short of 180 electrical degrees, i.e., 165 electrical degrees. The pitch factor k' thus becomes sin (165/2) = 0.991, and the winding factor d is 0.958 \* 0.991 = 0.95.

Item 9. It is now possible to determine the preliminary value of D^2l\_a, using given and assumed quantities. Thus by formula (100)

D^2l\_a = (4.07 \* 50 \* 10^11) / (32,000 \* 530 \* 500 \* 0.95 \* 0.83 \* 0.81) = 3,760

STATOR DESIGN

Items 10 to 13. As previously indicated, hp per pole is 8 1/3 so that the pole pitch should be about 9 in.; the internal diameter of the stator D is, therefore, about 9 \* 6/π = 17.2 in. Since the voltage of this machine is rather high the required thick slot insulation will reduce the slot space factor. Thus, to provide sufficient effective copper area without the necessity of narrowing the tooth width (to increase the tooth density) and deepening the slot (to increase the leakage flux), the internal stator diameter will be made 18 in.

The peripheral velocity of the rotor is, therefore,

v = (π \* 18 \* 500) / 12 = 2,350 fpm

DESIGN SHEET FOR INDUCTION MOTOR  
(Dimensions in inches unless otherwise stated)

Item No.	Specifications: 50-hp 3-phase motor, with wound rotor; 2,200 volts; 25 cycles; 500 rpm (synchronous)	Sym- bol	Numerical values
1	Number of poles.....	p	6
2	Volts per phase (use star connection).....	E	1,270
3	Estimated full-load power factor.....	cos θ	0.81
4	Estimated full-load efficiency.....	η	0.83
5	Full-load current in stator winding (amp).....		14.6
6	Average flux density in air gap (lines per sq in.).....	B_g''	31,600
7	Specific loading of stator.....	q	522
8	Winding factor (k × k').....	d	0.95
9	D^2l_a (in. units).....		3,888
Stator Design			
10	Internal diameter of stator.....	D	18
11	Peripheral velocity of rotor (approx) (fpm).....	v	2,350
12	Pole pitch (on stator).....	τ	9.42
13	Gross length of stator core.....	l_a	12.0
14	Number and size of ventilating ducts (3/8 in. wide).....		4
15	Net length of iron in stator core.....	l_n	9.45
16	Number of slots per pole per phase.....	n_s	4
17	Number of slots per pole.....		12
18	Slot pitch.....	λ	0.785
19	Number of stator conductors per slot.....	C_s	28
20	Number of stator conductors per phase.....	Z	672
21	Air-gap flux per pole.....	Φ	3.58 × 10^6
22	Maximum apparent tooth density (lines per sq in.)...	B_t''	123,500
23	Tooth width (narrow end).....	t	0.40
24	Slot width.....	s	0.385
25	Current density in windings.....	Δ	1,890
26	Thickness of slot insulation.....		0.07
27	Dimensions of conductor.....		0.081 × 0.102
28	Depth of stator slots.....	d	1.72
29	Length per turn of stator winding.....		51.5
30	Ohms per phase (hot).....		1.76
31	IR drop per phase (volts).....		25.7
32	Total stator copper loss (watts).....	W	1,125
33	Flux density in yoke of stator core (lines per sq in.).....		75,000
34	Outside diameter of stator stampings.....		26.5
35	Weight of iron in stator core (lb).....		504
36	Weight of iron in stator teeth (lb).....		140
37	Losses in stator core (watts).....		1,135
38	Losses in stator teeth (watts).....		875
39	Total stator iron loss (watts).....		2,010



The gross length of the stator core is  $l_a = D^2 l_a / D^2 = 3,760 / (18)^2 = 11.6$ , but this will be increased to 12 in. to make sure that the tooth density is not excessive; later calculations will verify the desirability of doing this.

The corrected value of  $D^2 l_a$  is  $(18)^2 \times 12 = 3,888$ , and the pole pitch is  $\tau = \pi \times 18 / 6 = 9.42$  in.

*Items 14 and 15.* Only four ventilating ducts, each one  $\frac{3}{8}$  in. wide, will be used in the stator, although the low peripheral velocity of the rotor and its 12-in. length would indicate that more duct area is desirable; this decision was made to keep the tooth density within reasonable limits, and added cooling will be provided by a fan on the rotor. The net length of iron is

$$l_n = 0.9 [12 - (4 \times \frac{3}{8})] = 9.45 \text{ in.}$$

*Items 16 to 20.* With four slots per pole per phase there will be 12 slots per pole, and a total of 72 slots in the stator. The slot pitch will, therefore, be

$$\lambda = \frac{\pi \times 18}{72} = 0.785 \text{ in.}$$

A preliminary value of conductors per slot will be calculated, using the assumed specific loading  $q$  of 530. Thus

$$C_s = \frac{q\lambda}{I_c} = \frac{530 \times 0.785}{14.6} = 28.5$$

Since the winding is double layer, an even number of conductors per slot must be used. Therefore,  $C_s$  will be made 28, and each coil will contain 14 turns. The number of conductors per phase becomes

$$Z = C_s \times n_s \times p = 28 \times 4 \times 6 = 672$$

The corrected value of  $q = (672 \times 3 \times 14.6) / (\pi \times 18) = 522$ .

*Items 21 to 24.* The next step is to determine the preliminary dimensions of the tooth and slot widths, although these may need some revision when conductor size, slot depth, and tooth density are calculated. The flux per pole is

$$\Phi = \frac{1,270 \times 10^8}{2.22 \times 0.95 \times 25 \times 672} = 3,580,000 \text{ maxwells}$$

The corrected value of the average air-gap flux density is

$$B_g'' = \frac{\Phi}{\tau l_n} = \frac{3,580,000}{9.42 \times 12} = 31,600 \text{ lines per sq in.}$$

and the *maximum* air-gap flux density (assuming a sine wave) is

$$B_{g(\max)} = \frac{\pi}{2} \times 31,600 = 49,600 \text{ lines per sq in.}$$

To calculate the minimum permissible tooth width (near the inside periphery of the stator core), a tooth density of 120,000 lines per sq in. will be assumed. Thus

$$t = \frac{49,600}{120,000} \times \frac{0.785 \times 12}{9.45} = 0.412 \text{ in.}$$

This dimension will be reduced slightly to 0.40 in. to provide a little extra space for the slot width to accommodate the heavy insulation. The slot width is, therefore,  $s = \lambda - t = 0.785 - 0.40 = 0.385$ , and the corrected tooth density is

$$B_t'' = 120,000 \times \frac{0.412}{0.40} = 123,500 \text{ lines per sq in.}$$

This is rather high, but permissible, in view of the fact that a wider tooth would result in a very deep slot.

When the stator laminations are assembled, slight irregularities will make the finished slot width of the stack a little less than actual slot width; an 0.015-in. allowance will, therefore, be made for stacking, and this will leave  $0.385 - 0.015 = 0.37$  in. for copper and insulation.

*Items 25 to 28.* Since the ability of the machine to cool itself will be somewhat restricted (the peripheral velocity of the rotor is low, the insulation will be heavy, and only four ventilating ducts are used), a current density of about 1,900 amp per sq in. will be assumed. The area of cross section will be about  $14.6 / 1,900 = 0.00768$  sq in.

To determine the slot insulation a formula that is satisfactory for voltages between 1,500 and 6,000 is

$$\text{Thickness of slot insulation (one side) in mils} = 30 + \frac{E}{55}$$

The slot insulation will, therefore, be  $30 + (2,200 / 55) = 70$  mils. This leaves  $0.37 - (2 \times 0.07) = 0.23$  in. for copper and its covering of insulation. With 28 conductors per slot it will be desirable to use rectangular dee copper ribbon, with 2 conductors in width and 14 conductors in depth. Consulting Table III, page 434, it is found that a conductor  $0.081 \times 0.102$  in., having an area of 0.00773 sq in., will be satisfactory. This conductor has insulated dimensions of  $0.094 \times 0.114$  in. The actual current density will be  $14.6 / 0.00773 = 1,890$  amp per sq in.; also, the width of copper and insulation will be  $2(0.07 + 0.114) = 0.368$ , which is just about right for the 0.37-in. slot.



Figure 135 illustrates the arrangement of the conductors in the slot and the important dimensions. The slot depth is determined as follows:

Slot wedge	= 0.125
Insulation below wedge	= 0.080
Insulation between coil sides	= 0.070
Insulation in bottom of slot	= 0.070
14 conductors ( $14 \times 0.094$ )	= 1.316
Allowance for spaces between wires	= 0.059
Total	= 1.72 in.

Ratio  $d/s = 1.72/0.385 = 4.45$ , which is high but acceptable.

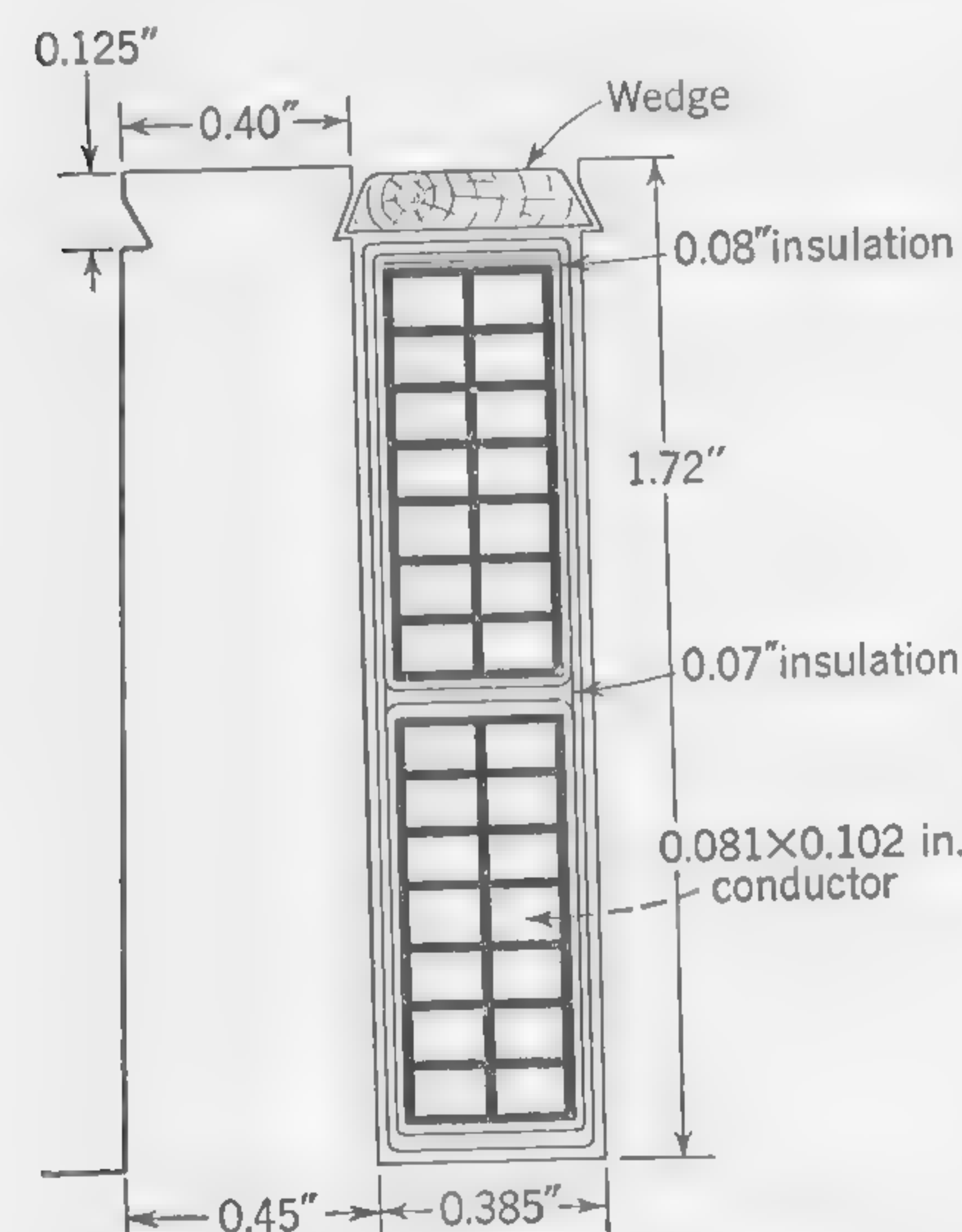


FIG. 135. Tooth and slot details for Illustrative Example of Art. 110.

Items 29 to 32. The mean length of each turn of the stator-winding coil is, by formula (102), approximately

$$(2 \times 12) + (2.3 \times 9.42) + 6 = 51.5 \text{ in.}$$

With 14 turns per coil and 24 coils per phase, all connected in series, the total length of wire per phase is

$$\frac{14 \times 24 \times 51.5}{12} = 1,432 \text{ ft, or (say) } 1,440 \text{ ft}$$

allowing for connecting wires.

Referring again to Table III, the resistance per 1,000 ft of  $0.081 \times 0.102$  conductor is 1.28 ohms at  $75^\circ\text{C}$ .

At  $60^\circ\text{C}$  it would be  $1.28 \times (294.5/309.5) = 1.22$  ohms per 1,000 ft.

The resistance per phase is, therefore,  $1.44 \times 1.22 = 1.76$  ohms, and the  $IR$  drop is  $14.6 \times 1.76 = 25.7$  volts per phase. The total stator copper loss is  $3 \times 25.7 \times 14.6 = 1,125$  watts.

Items 33 to 35. The depth of the stator laminations below the slots the yoke—and the over-all dimension may be determined by assuming a reasonable flux density; estimating the latter at about 75,000 lines per sq in., neglecting any leakage flux, and remembering that the yoke flux is one-half the air-gap flux per pole, the radial dimension of the core below the slots is

$$\frac{3,580,000}{2 \times 75,000 \times 9.45} = 2.53 \text{ in.}$$

This makes the outside diameter of the stator lamination  $18 + 2(1.72 + 2.53) = 26.5$  in.

The weight of the stator iron, not including the teeth, is

$$0.28 \times \pi(26.5 - 2.53) \times 2.53 \times 9.45 = 504 \text{ lb}$$

Items 36 to 39. The width of the stator teeth at the air-gap diameter is 0.4 in., and the tooth width at the root (at the bottom of the slot) is  $[\pi(18 + 3.44)/72] - 0.385 = 0.45$  in.; the average width is, therefore, 0.425 in. This makes the weight of the iron in the teeth

$$0.28 \times 0.425 \times 1.72 \times 9.45 \times 72 = 140 \text{ lb}$$

The iron loss in the yoke iron will be based on a density of 75,000 lines per sq in. Using the curve of Fig. 67, the watts per lb per cycle is 0.09; this loss is, therefore,

$$0.09 \times 504 \times 25 = 1,135 \text{ watts}$$

The iron loss in the teeth will be based on an "apparent" density one-third up from the narrow end; the width here is 0.417 in., and the density is  $123,500(0.4/0.417) = 118,500$  lines per sq. in. For this density the watts per lb per cycle is 0.25; this loss is, therefore,

$$0.25 \times 140 \times 25 = 875 \text{ watts}$$

The total stator core loss is  $1,135 + 875 = 2,010$  watts.

Diagrams showing the coil arrangement and the schematic connections of the three-phase double-layer fractional-pitch lap winding are given in Fig. 136.

No attempt will be made here to design completely the rotor core and the winding for this machine since the procedure would, except for certain restrictions and limitations, follow that given for the stators of Arts. 109 and 110. Several additional points should, however, be made concerning wound-rotor design, and these are briefly summarized as follows:

1. The number of rotor slots should generally be about 10 per cent less than in the stator. For this specification, with 72 stator slots, the rotor should probably have 63 slots. Although this number of slots will require a so-called *fractional-slot* winding, since slots/poles  $\times$  phases is not an integer,  $(63/6 \times 3 = 3\frac{1}{2})$ , a satisfactory winding is possible, as will subsequently be shown.

2. It is generally desirable to employ partially closed slots in the rotor; this practice tends to reduce the equivalent air gap and thus minimize the magnetizing component of the no-load current. However, when partially closed slots are used the conductor width must be somewhat narrower than the opening between the projecting tips of the teeth, because the individual wires of the coils must be fed into the slots one or two at a time; in such cases, the coils are untaped, although partly formed, before they are inserted in the slots.



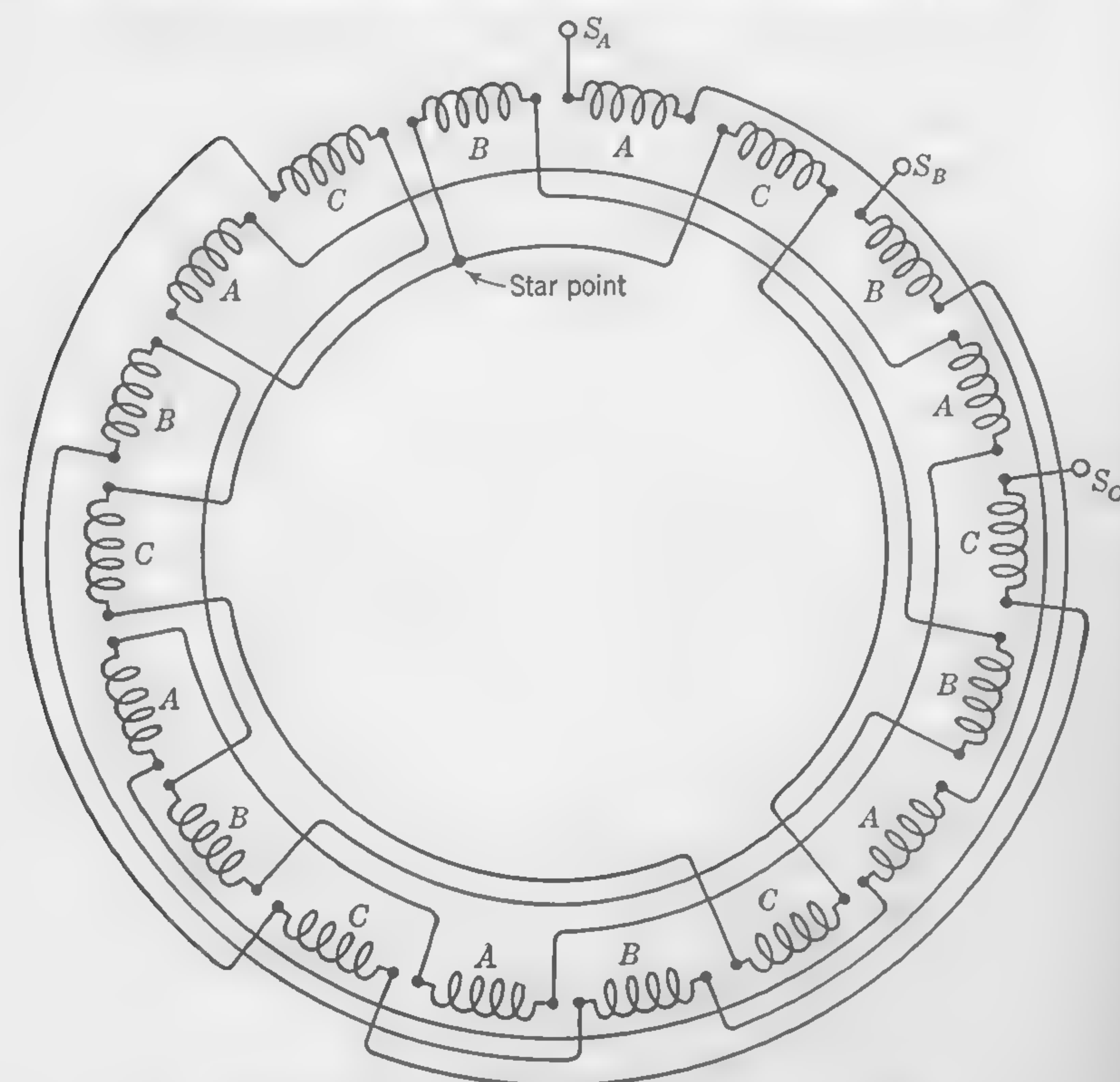
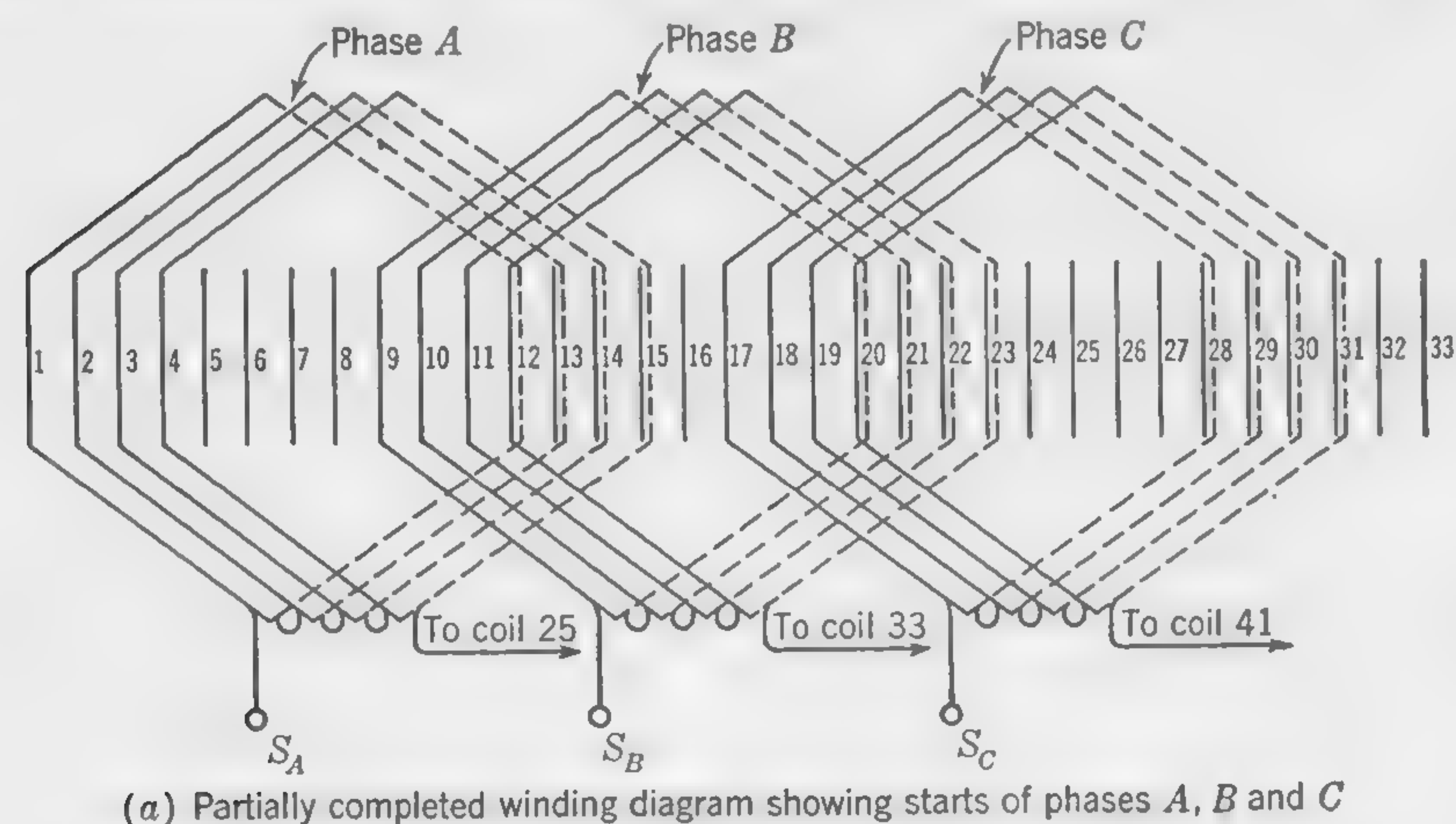


FIG. 136. Winding diagram for Illustrative Example of Art. 110.

3. In designing the rotor winding it is necessary to remember that the latter represents the secondary of a transformer and that the voltage between slip rings is a maximum when the rotor is at rest. Therefore, to keep the slip-ring voltage down to acceptable values the effective stator to rotor *turn ratio* must be properly adjusted, where the term *effective* takes the distribution and pitch factors into account. This ratio is usually such as to limit the slip-ring voltage to about 440 volts in normal-voltage general-purpose motors. For high-voltage motors, as in the design of this article, the slip-ring potential may be somewhat more than the value given; also, in the case of large machines with many rotor



FIG. 137. Schematic sketch showing succession of series-connected coils for the 63-slot 6-pole wave winding in the rotor of the Illustrative Example of Art. 110.

ampere-turns there must not be too few rotor turns, as this would require the use of excessively large conductor sections. Moreover, if a delta-connected rotor winding is employed the slip-ring voltage will be the phase voltage, and 173 per cent of the phase voltage when the winding is connected series-star. In equation form, the stator to rotor *phase-voltage ratio* may be written as follows:

$$\frac{E_s}{E_r} = \frac{k_s k'_s T_s}{k_r k'_r T_r} \quad (106)$$

where the subscripts *s* and *r* refer to the stator and rotor quantities, respectively, and *E* and *T* stand for phase voltage and series-turns per phase. For a delta-connected rotor winding, *E<sub>r</sub>* is also the voltage



between rings. However, if a star connection is used, and this is customary in low-voltage machines, the ring potential is

$$E_{\text{rings}} = \sqrt{3} E_s \frac{k_r k'_s T_r}{k_s k'_s T_s} \quad (106a)$$

4. Insulation thickness will, of course, depend upon the maximum ring

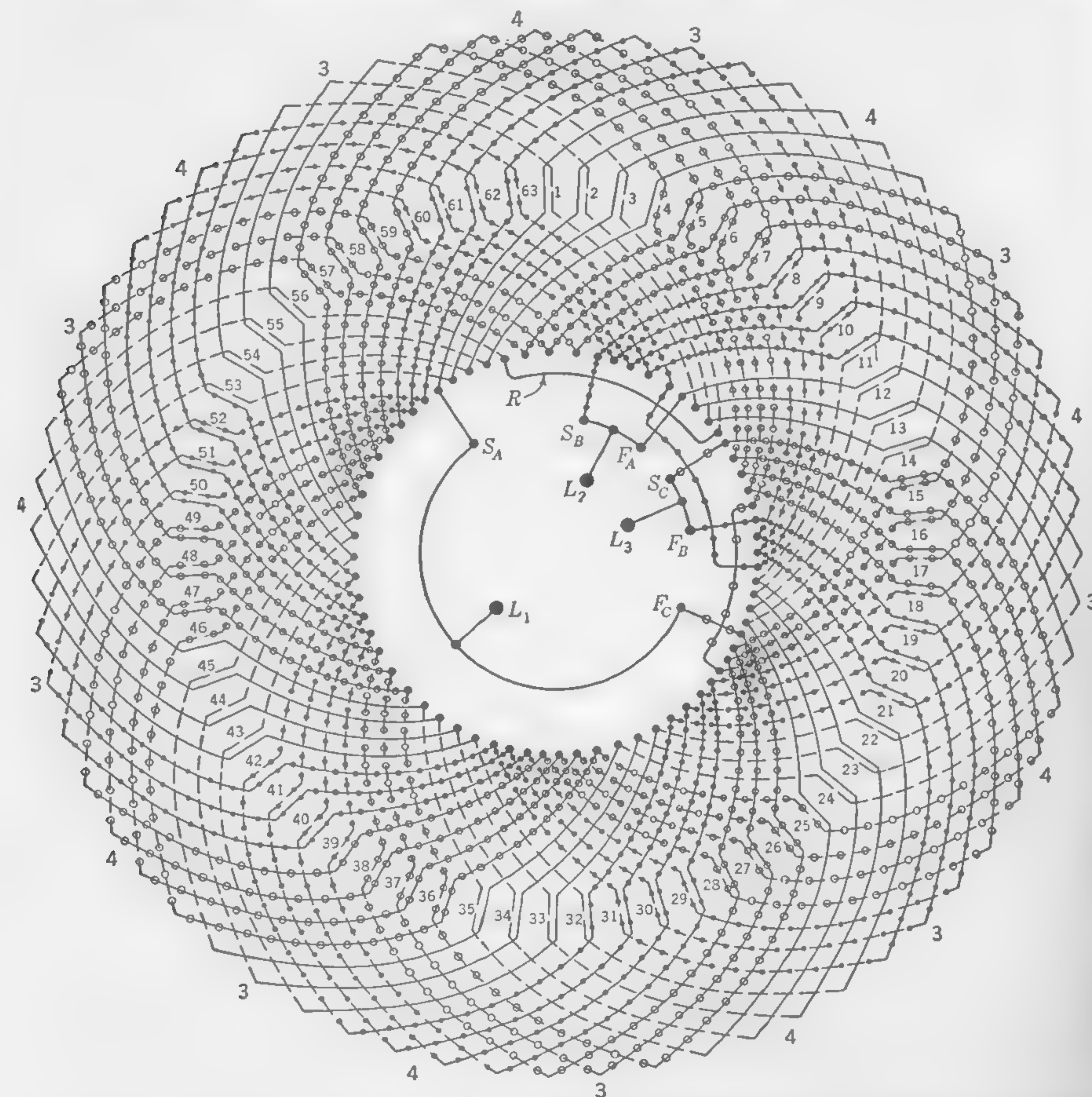


FIG. 138. Complete diagram of double-layer fractional-slot delta-connected wave winding for the rotor of Illustrative Example of Art. 110.

voltage as in stator design, and the empirical formulas, previously given, may be used.

Assuming a 63-slot rotor, as indicated in item (1) above, the rotor slot pitch  $\lambda_r$  will be  $\pi \times 18/63 = 0.897$ ; this is reasonable. A standard three-phase delta-connected double-layer wave winding will be used, and this means that there will be a total of 63 coils, or 21 coils per phase. With six poles, the theoretical number of coils per phase per pole is  $2\frac{1}{6} = 3\frac{1}{2}$ . Since fractional coils are not practicable it will be necessary to have three

groups of four coils in series and three groups of three coils in series; the total number of coils in series per phase will, therefore, be  $(3 \times 4) + (3 \times 3) = 21$ . Figure 137 shows a schematic diagram of a satisfactory arrangement of the coils in which the numbers of coils per group are clearly indicated for the three phases A, B, and C.

Following the schematic of Fig. 137, a complete double-layer delta-connected wave winding diagram is given in Fig. 138. The student will find it worthwhile to trace the drawing carefully, noting especially that, beginning at the start of a phase such as  $S_A$ , the winding progresses clockwise through all the four-coil groups and then, passing into reverse connector  $R$ , proceeds in a counterclockwise direction through the three-coil groups, finishing at  $F_A$ .

### TEST PROBLEMS

The few problems which follow do not cover thoroughly the contents of this chapter. A varied collection of problems relating to induction motors—although not having any particular reference to design—will be found in several texts dealing with the principles of a-c machines. See, for example, Fitzgerald and Kingsley, "Electric Machinery," pp. 434–439, McGraw-Hill Book Company, Inc., 1952; Mueller, "Alternating-current Machines," pp. 266–271, McGraw-Hill Book Company, Inc., 1952.

1. A certain three-phase induction motor runs at a speed of 750 rpm when connected to a 25-cycle circuit. What would be the speed of the same motor if it were connected to a 60-cycle circuit after the stator winding had been altered to produce twice the number of poles?

Ans. 900 rpm.

2. Given a six-pole induction motor connected to a 60-cycle 3-phase circuit. Calculate the air-gap diameter (rotor diameter), given that the peripheral velocity at synchronous speed is 4,090 fpm.

Ans. 13 in.

3. An induction motor has a rotor diameter (air-gap diameter) of 18 in., and the stator is wound to produce a six-pole field. Calculate the gross axial length of the stator core, given that the average flux density in the air gap is 4,000 gauss when the total flux per pole is 2,550,000 maxwells.

Ans.  $10\frac{1}{2}$  in.

4. Given an induction motor in which the stator tooth at the narrow end is exactly half the tooth pitch, and in which the ratio of net to gross axial length of the stator core is 0.8, calculate the maximum value of the apparent tooth density when the average air-gap density is 3,900 gauss (sine-wave flux distribution assumed).

Ans. 15,350 gauss.

5. A three-phase induction motor has an air-gap diameter (inside bore of stator) of 7 in. The stator has a 4-pole winding with 3 slots per pole per phase, and 12 conductors in each slot. Calculate the current in the stator windings, given that the specific loading (in ampere-conductors per inch of periphery) is 530.

Ans. 27 amp.

6. Calculate the full-load current in the stator windings of a 40-hp star-connected 3-phase induction motor connected to a 220-volt circuit, given that the power factor of the motor is 0.89 and the efficiency is 0.9.

Ans. 97.8 amp.

7. The synchronous speed of an induction motor is 1,800 rpm and the slip at full load is 5 per cent. Calculate (a) the full-load speed of the motor, (b) the  $I^2R$  losses in the rotor windings, given that the power developed by the rotor (including what is required to provide for bearing friction and windage losses) is 10 hp.

Ans. (a) 1,710 rpm, (b) 393 watts.



## POLYPHASE INDUCTION MOTORS (Continued)

**111. The Circle Diagram.** Although the student is supposed to be generally familiar with the circle diagram\* as used for studying the performance of induction motors, it is proposed to review briefly the manner in which such a diagram may be constructed from test data, before considering how the designer must proceed in order to draw the circle diagram from the dimensions and other particulars of the design.

- a. The volts, amperes, and watts (or power factor) per phase when the machine is running light at synchronous speed
- b. The volts, amperes, and watts (or power factor) per phase with the rotor locked and rotor windings short-circuited (in the case of a wound rotor with slip rings)
- c. The resistance per phase of the stator winding†

The test *b* with rotor at rest is usually made by adjusting the voltage to pass about full-load current through the stator coils. The short-circuit current with normal operating voltage at terminals is then calculated on the assumption that the current is proportional to the voltage at terminals. The frequency of supply must be the same as that on which the motor operates under normal working conditions.

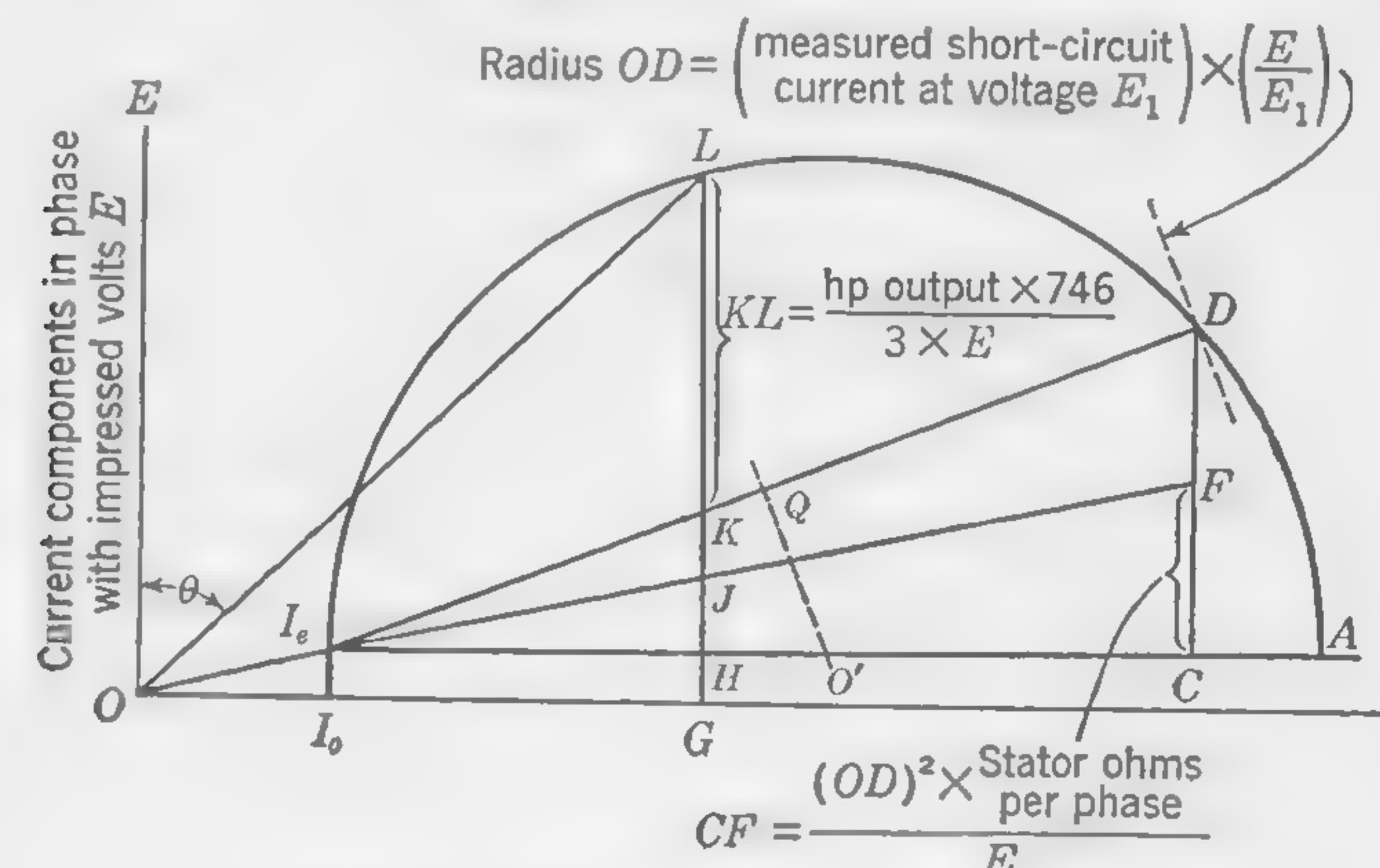
\* JEFFREY, F., Circle Diagram and the Induction Motor, *Allis-Chalmers Elec. Rev.*, vol. 4, p. 5, September, 1939.

† For a star-connected winding, the resistance per phase is one-half the resistance measured between adjacent terminals whatever may be the number of phases. For a mesh-connected winding (which is infrequently used) the "equivalent" star resistance per phase must be calculated. The equivalent star resistance is the resistance of a star winding in which the  $I^2R$  losses would be the same as in the actual mesh winding.

This is equal to  $\left[ \frac{n}{4(n-1) \sin^2(180/n)} \right] R_t$ , where  $n$  is the number of phases and  $R_t$  is the resistance measured between adjacent terminals. In the special case of a delta-connected three-phase stator winding, this becomes  $\frac{1}{2} R_t$ , which is the same as the resistance per phase of a star-connected winding.

current components are drawn longer than they would be in the diagram of an actual machine. In this vector diagram the vertical lines represent current components in phase with the applied stator voltage, while the horizontal lines represent the “wattless” or “reactive” current components.

Draw  $OI_e$  to represent the exciting current as measured under no-load conditions. The angle  $EOI_e$  is the power-factor angle, and in a three-



Phase of reactive stator current components  
FIG. 139. Circle diagram of three-phase induction motor.

phase motor the vector  $I_o I_e$  is equal to

$$\frac{\text{One-third of open-circuit losses}}{\text{Volts per phase winding}}$$

Draw  $I_e A$  parallel to the base line.\* With  $O$  as a center, describe the dotted arc of radius  $OD$ ,† representing the stator current per phase winding at normal voltage with rotor locked. Thus

$$OD = \text{measured current with locked rotor} \times \frac{\text{normal operating voltage}}{\text{test voltage}}$$

The angle  $EOD$  is the power-factor angle, the vector  $CD$  being the in-phase current component which, for a three-phase motor, is obtained by dividing one-third of the total loss in watts, obtained from test  $b$ ,<sup>‡</sup> by the volts across each phase winding. To locate the center of the circle,

\* The assumption here made is that the losses due to windage, bearing friction, hysteresis, and eddy currents in the laminated iron cores are constant at all loads and equal to the losses measured on the no-load test.

† Since the line  $OD$  would almost coincide with  $OI, D$  and tend to complicate the diagram, it has been omitted from Fig. 139.

† Since the test with locked rotor is usually made with greatly reduced voltage, the losses in the iron are very small and may be neglected.



bisect  $I_e D$  at  $Q$  and erect the perpendicular  $QO'$  on  $I_e D$ . The center  $O'$  of the circle lies on the line  $I_e A$ . Draw the semicircle passing through  $I_e$  and  $D$ .

In order to separate the stator and rotor losses, another line  $I_e F$  must be drawn at such a slope that

$$\frac{CF}{FD} = \frac{\text{stator losses}}{\text{rotor losses}}$$

The point  $F$  may be located by making the in-phase current component  $CF$  equal to

$$\frac{\text{Watts per phase of stator copper loss}}{\text{Volts per phase winding}}$$

or

$$\frac{(OD)^2 \times \text{ohms per phase of stator winding}}{\text{Volts across the windings of one phase}}$$

Then for any stator current  $OL$  we have

$$KL = \frac{\text{the in-phase current representing useful work} = \text{horsepower} \times 746}{\sqrt{3} \times \text{line volts}}$$

$$JL = \text{the in-phase current representing power supplied to rotor}$$

$$GL = \text{the in-phase current representing power supplied to the motor}$$

$$HJ = \text{the in-phase current representing stator copper losses}$$

$$JK = \text{the in-phase current representing rotor copper losses}$$

$$\text{ratio } \frac{KL}{GL} = \text{efficiency}$$

$$\text{ratio } \frac{JK}{JL} = \text{slip [refer to formula (104) on p. 284]}$$

With a star-connected three-phase stator, any vertical line representing in-phase amperes per phase may be converted into *watts* by multiplying by  $\sqrt{3}$  times the line voltage.

The manner in which the starting torque is read from the circle diagram, and the relation between torque and leakage flux, will be discussed later.

If the circle diagram is to be drawn from design particulars instead of test data, it is necessary to calculate certain quantities which will provide us with the same information as may be obtained from an actual machine by making the tests referred to at the beginning of this article. The stator resistance as obtained from test *c* is easily calculated, but, in order to calculate all the quantities determined by tests *a* and *b*, we require to know:

1. The magnetizing current (without which the power factor of the motor running light cannot be calculated)

2. The leakage flux (to enable us to calculate the reactive voltage drop and the power factor when the windings are carrying heavy currents)

**112. Magnetizing Current of Induction Motor.** In order to calculate the amount of current in the stator windings required to establish a given flux (or flux density) in the air gap, we must know the length of the equivalent air gap and express the resultant magnetizing mmf in terms of the number of conductors in the stator slots and the current per conductor.

*Air-gap Clearance.* This is usually made as small as possible and is, therefore, determined largely by mechanical considerations. A small clearance means a good power factor and small reactive drop (as in a transformer with small separation between primary and secondary windings). If the gap is very small, there is, however, a possibility of increased losses through flux pulsations and eddy currents in the teeth. If the diameter of the rotor is large and the peripheral velocity high, a larger air gap is necessary than with a rotor of smaller diameter or of the same diameter but running at a lower peripheral velocity. Obviously, a stiff shaft and rigid framework are required when the air gap is reduced to a mere mechanical clearance, and great length axially should be avoided so that the bearings shall not be too far apart. The following formula gives the approximate air-gap clearance for induction motors of normal design with the usual peripheral speeds:

$$\delta = 15 + D \quad (107)$$

where  $D$  is the rotor diameter in inches, and  $\delta$  is the air-gap clearance in mils.

*Equivalent Air Gap.* The equivalent air gap is the length of air gap between rotor and stator which would cause the same exciting ampere-turns to establish the same amount of flux in the gap *if the slotted surface of both stator and rotor were replaced by smooth surfaces*. The manner in which the equivalent air gap may be calculated is explained in Art. 35 and in calculating items 12 and 13 in the Illustrative Example of Art. 91.

A simple way to determine the equivalent air-gap length, which takes account of the slots in stator and rotor, is to consider the reduction in the area of the cylindrical iron surfaces due to the slot openings, a suitable allowance being made for the "fringing" of the flux at the edges of the teeth. Thus, if there are  $n_s$  slot openings on the stator, each of width  $w$ , and  $n_r$  slot openings on the rotor, each  $w_r$  wide, the average reduction of the iron surface measured around the air gap is  $(n_s w + n_r w_r)/2$ , and, if we



allow 15 per cent for "fringing,"\* the reluctance of the air gap will be increased in the ratio

$$\frac{\pi D}{\pi D - \left( \frac{n_1 w + n_2 w_r}{2} \times 0.85 \right)}$$

which is the quantity by which the actual air-gap clearance  $\delta$  must be multiplied to obtain the equivalent length of air gap  $\delta_e$ .

**Magnetizing Ampere-turns of Three-phase Stator Winding.** The magnetizing effect of the three-phase winding on the stator of an induction motor is the same as that of the armature windings of a three-phase generator, and we may use the formula (78) on page 217. This may be put in the form

$$\left. \begin{array}{l} \text{Resultant maximum ampere-turns per} \\ \text{pole, produced by three-phase distrib-} \\ \text{uted winding} \end{array} \right\} = (TI)_\phi = \frac{1}{2.22} \times \frac{Z' I_0}{p} \quad (108)$$

where  $Z'$  = the total number of inductors in stator slots, being three times the number of inductors per phase

$I_0$  = the rms value of the magnetizing current

$p$  = the number of poles

In order to solve for  $I_0$ , we must first calculate the ampere-turns required to establish the flux across the air gap.

Let  $B_g''$  be the average air-gap density over the pole pitch, in lines per square inch (see Art. 100), then  $(\pi/2)B_g''$  is the *maximum value* of the flux density (sine-wave distribution assumed). Thus

$$(TI)_\phi = 0.313 \times \frac{\pi}{2} B_g'' \times \delta_e \quad (109)$$

where  $\delta_e$  is the equivalent air gap in inches. This formula gives the ampere-turns required to overcome the air-gap reluctance only. The reluctance of the iron portions of the magnetic circuit of an induction motor is always comparatively small, and it is usual to assume that the air gap represents from 70 to 85 per cent of the total reluctance. On the assumption that the total ampere-turns of excitation are  $m$  times the ampere-turns required for the air gap, we may put  $m$  times the quantity given in formula (109) equal to the quantity of formula (108) and solve for  $I_0$ . This gives

$$\left. \begin{array}{l} \text{Approximate rms value of magnetizing} \\ \text{component of exciting current in stator} \\ \text{windings} \end{array} \right\} = I_0 = m \times 1.095 \frac{p B_g'' \delta_e}{Z'} \quad (110)$$

\* This allowance for fringing is intended to correct for the fact that the spreading of the flux lines at the edges of the slot openings causes the effective slot openings to be somewhat less than the actual opening.

where the multiplier  $m$  depends upon the relative reluctance of iron and air portions of the magnetic circuit. The numerical value of  $m$  is usually between 1.2 and 1.4. Expressed in terms of the full-load stator current  $I_c$ , the magnetizing component  $I_0$  of the no-load current usually approximates to the values given below:

Hp of motor	Ratio $I_0/I_c$
1	0.45
5	0.35
20	0.30
50	0.27
100 and larger	0.25

These figures apply to 60-cycle motors. In 25-cycle motors the magnetizing current is usually rather greater, but, on the other hand, the  $IX$  drop is less on the lower frequency.

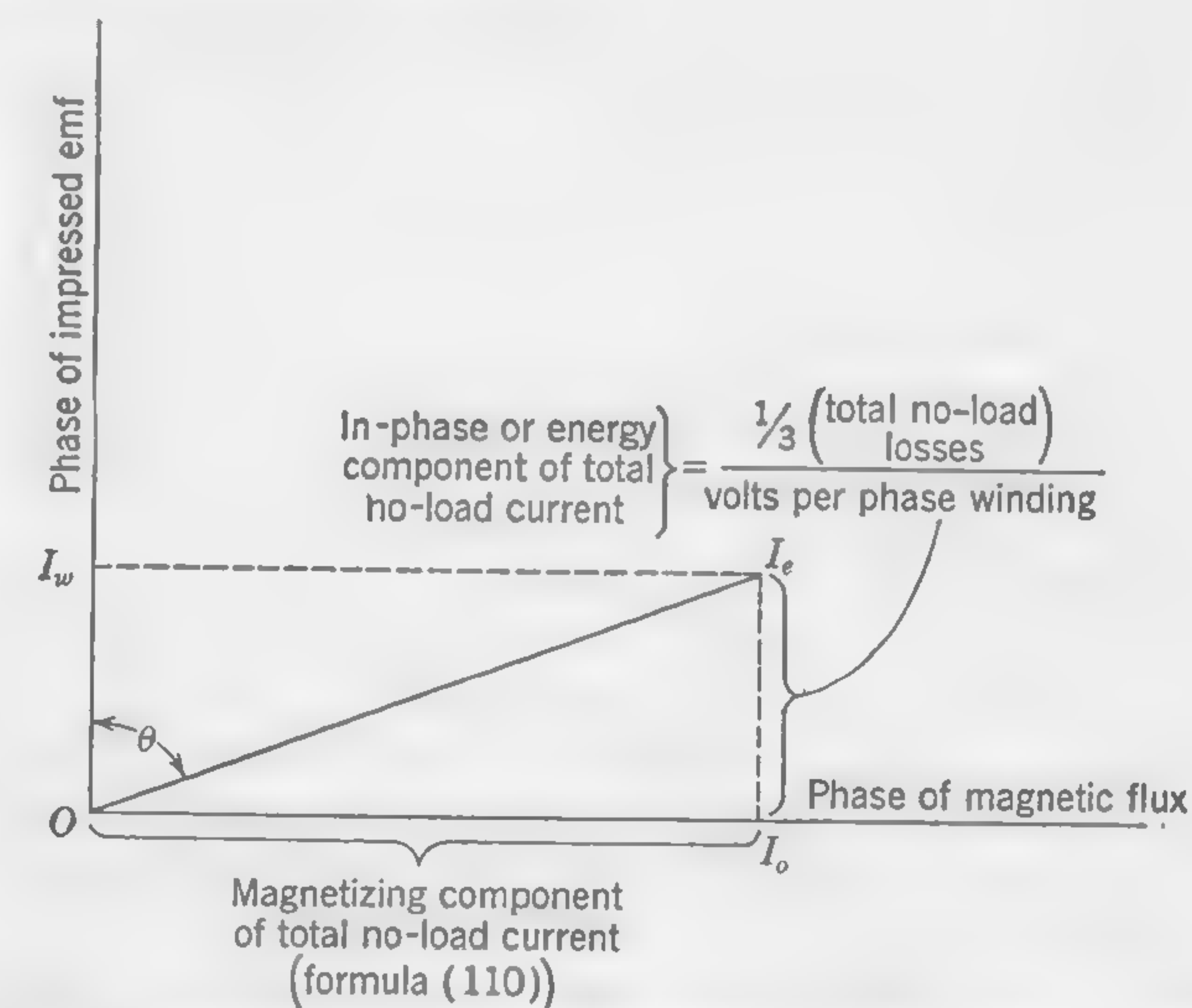


FIG. 140. Vector diagram showing components of no-load stator current of three-phase induction motor.

**113. Total No-load Current in Stator Windings.** The current  $I_0$ , as given by formula (110), is only the magnetizing component of the total current in the stator windings required to run the motor at approximately synchronous speed without external load. The total current is the (vectorial) sum of this "wattless" component and the in-phase or "energy" component which supplies the friction and iron losses. This is illustrated in Fig. 140 where the current component in phase with the applied emf is drawn at right angles to the component  $I_0$ . Its length is easily calculated by dividing one-third of the total no-load losses by the volts across the windings of one phase.



The power factor with rotor running light and full voltage across stator terminals is  $\cos \theta = I_w/I_e$ , the value of  $I_e$  being  $I_e = \sqrt{I_0^2 + I_w^2}$ .

**114. Leakage Flux in Induction Motors.** Although a knowledge of the magnitude and phase of the exciting current is necessary for the construction of the circle diagram, it is not possible to complete the diagram and predict the performance of the motor without knowing the amount of the leakage flux.

With the rotor locked and normal operating voltage impressed on the stator windings, the conditions are similar to those in a static transformer with secondary short-circuited. Calculations of leakage flux reactance

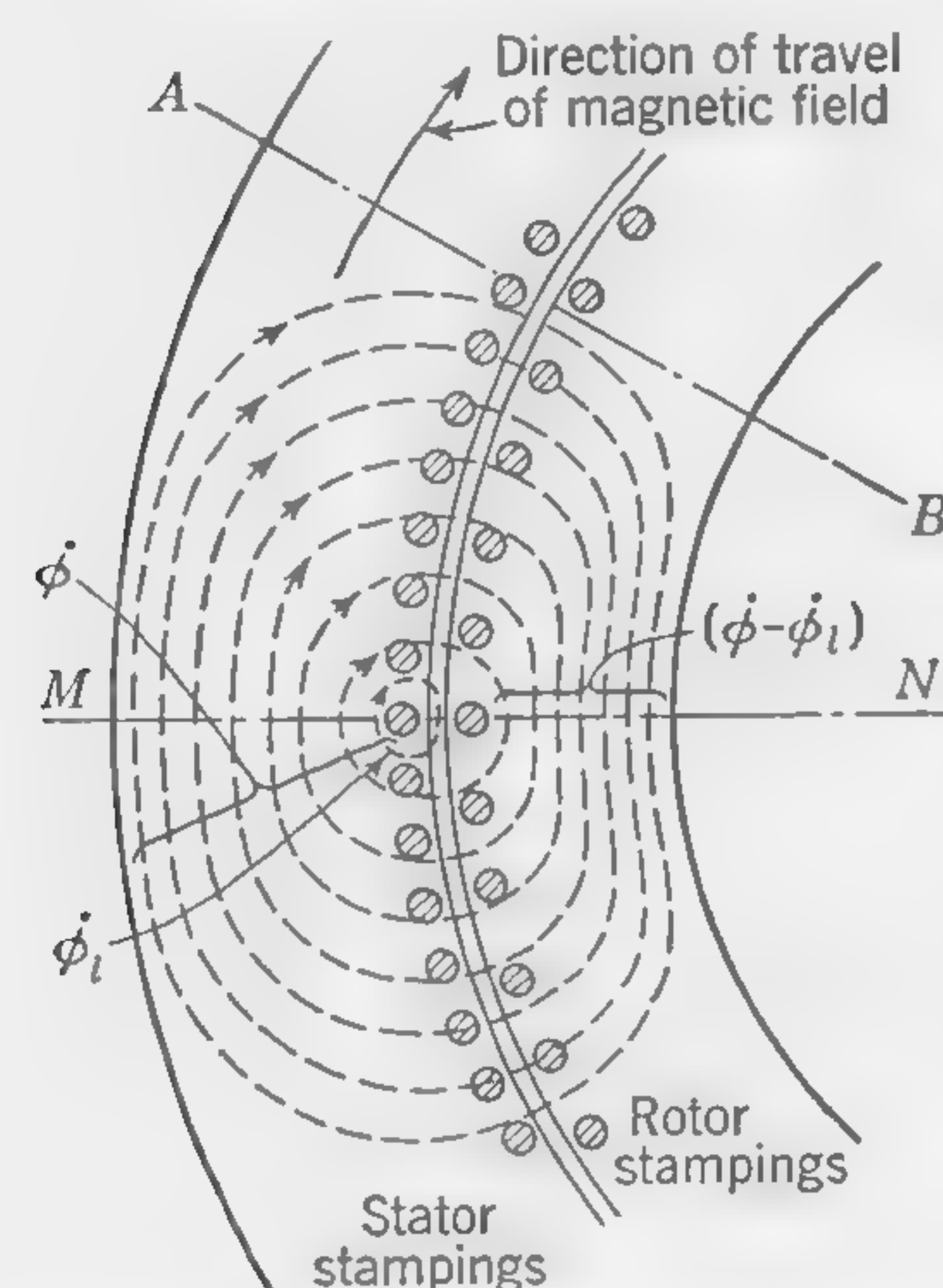


FIG. 141. Flux lines in induction motor.

and the reactive component of the total primary voltage can, therefore, be made as for a transformer (see Art. 137). If it is desired to retain the picture of a rotating field, we must consider this field rotating at synchronous speed ("slip" = 100 per cent with locked rotor) and note that the rotor conductors are not cut by the whole of the flux which cuts the stator conductors, but only by that portion of the total flux which is not leakage flux. The amount of flux cut by the rotor conductors is just sufficient to generate an emf equal to the  $IR$  drop in the rotor.

Figure 141 shows the flux due to the magnetizing effect of the three-phase star winding in the space of one pole pitch.  $\Phi$  is the flux in the stator ring (equal to

one-half the flux per pole) and  $\Phi_l$  is the leakage flux which links with the stator winding (primary) but *not* with the rotor winding (secondary). The difference between  $\Phi$  and  $\Phi_l$  is the flux in the rotor stampings below the slots. It is this flux which cuts the rotor conductors and generates an emf in them.

When the machine is running light (no external load), the leakage flux  $\Phi_l = 0$ . If the machine could operate under load on unity power factor, the rotor current would reach its maximum value in the conductors under the center of the pole (*i.e.*, on the line  $AB$  in Fig. 141) and the effect of magnetic leakage would be practically negligible, but, with rotor locked so that it cannot rotate with the field, the in-phase component of the voltage (required to circulate the rotor current) will be relatively small and the condition in the stator winding will be as indicated by the vector diagram (Fig. 142). The vector  $OP$  will be small in comparison with  $OE$  and the power factor  $\cos \theta$  with rotor locked will, therefore, be of low

value. The angle  $\theta$  will approach its limit of  $90^\circ$  and cause the phase of the leakage flux  $\Phi_l$  to be very nearly the same as that of the flux which cuts the rotor conductors. The rotor current will have its maximum value in the conductors near the neutral zone (the line  $MN$  of Fig. 141)\* and the loss of pressure due to magnetic leakage will, therefore, be a maximum. The manner in which this maximum reactive voltage drop (the vector  $EP$  of Fig. 142) may be calculated is explained in the following articles.

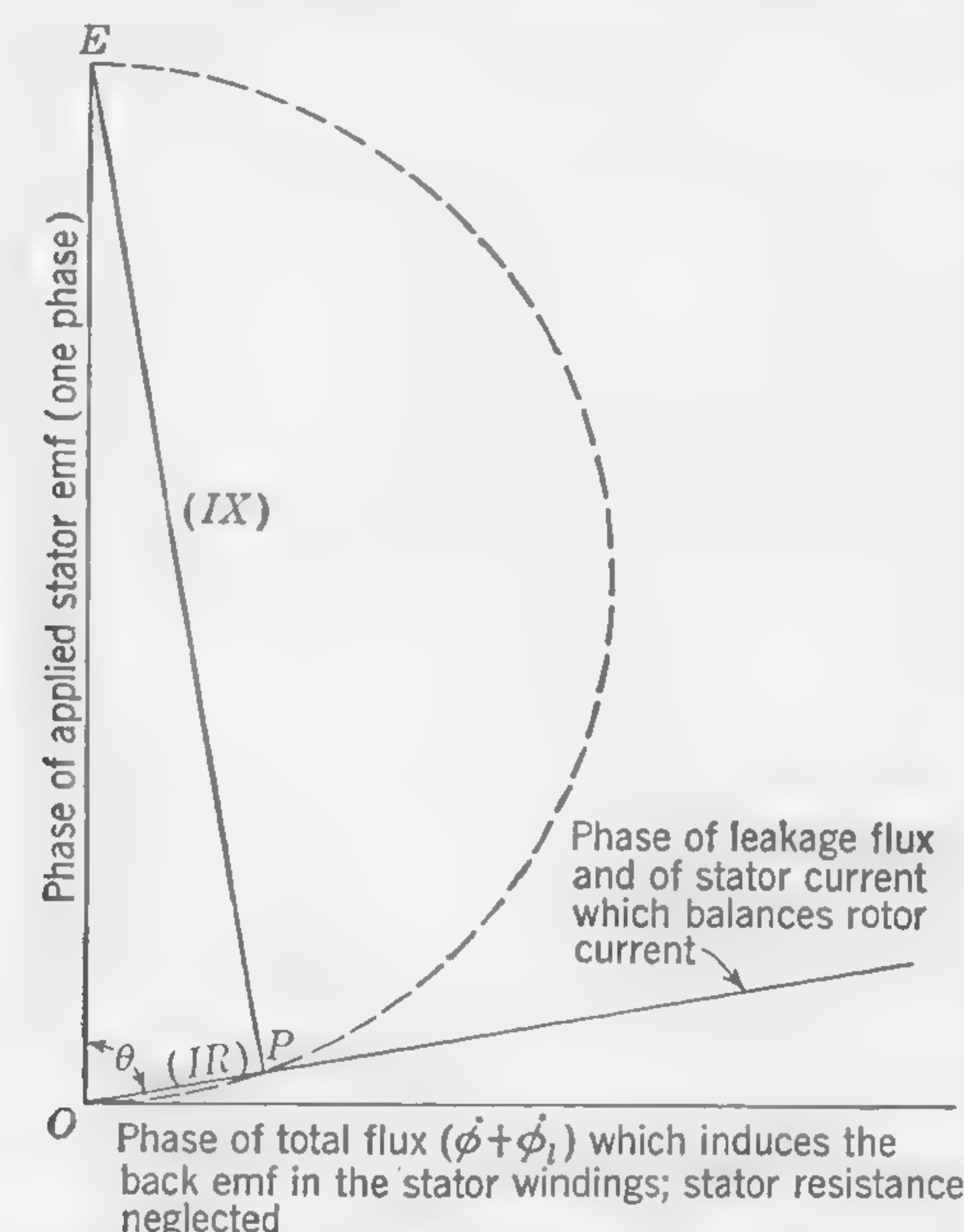


FIG. 142. Vector diagram for induction motor with locked rotor.

**115. Calculation of Leakage Flux in Slots and Air Gap.** Figure 143 is an enlarged representation of the leakage paths in the neutral zone (*i.e.*, on the line  $MN$  of Fig. 141).

The reactive voltage drop is the loss of pressure which is due to the magnetizing effect of the heavy currents in the stator and rotor windings. These currents cause a certain portion of the total flux, which links with the primary (stator) windings, to pass in the spaces between the primary and secondary windings, so that all the flux which generates a back emf in the primary is not available to generate an emf in the secondary. Thus, the emf which gives rise to the current in the secondary (rotor) circuit is due to the cutting of the flux which enters the rotor core, and

\* The manner in which the power factor affects the position of the conductor carrying maximum current was discussed in connection with alternator design. The displacement referred to is the angle  $\beta$  of Fig. 102.



this is the difference between the total primary flux and the leakage flux. The reactive voltage drop  $IX$  in the primary (stator) circuit is the emf due to the cutting of the *leakage component* of the total flux. This is easily calculated if the amount of the leakage flux is known.

The several paths taken by the slot and air-gap leakage flux, as indicated by the broken lines in Fig. 143, are

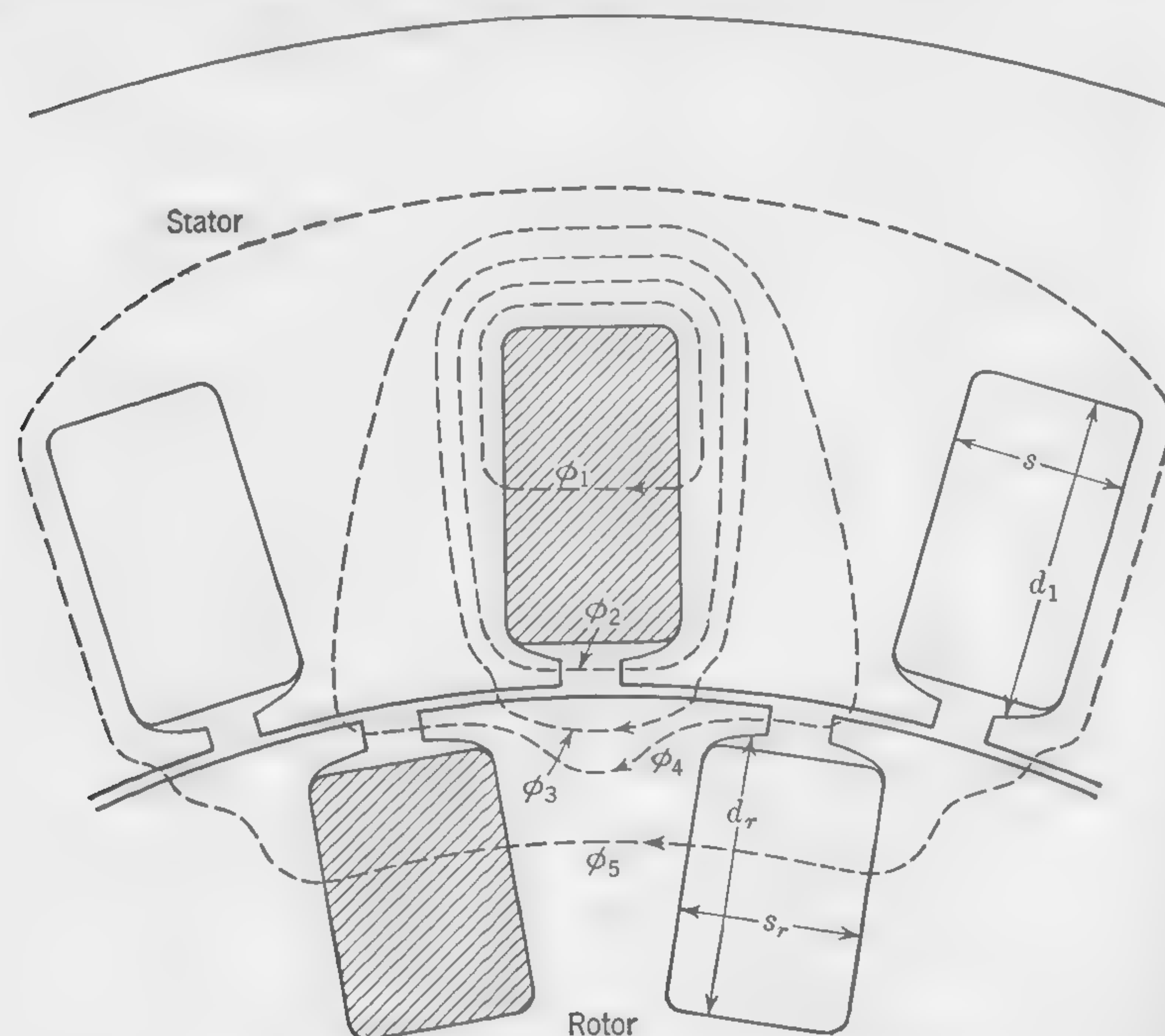


FIG. 143. Paths of leakage flux in induction motor.

Path 1. Across the stator slots through the copper

Path 2. Across the opening above the windings in the stator slots

Path 3. In the air gap (usually referred to as the *zigzag leakage path*)

Path 4. Across the opening above the windings in the rotor slots

Path 5. Across the rotor slots through the copper

*Equivalent Flux in Path 1.* Use formula (90) developed in Art. 80, which, for the stator winding of Fig. 143, simplifies into

$$\Phi_{1(\text{equivalent})} = 0.4\pi(C_s i) \times \frac{d_1}{3s} \quad (111)$$

this being the equivalent flux *per centimeter of slot length* when the ampere-conductors in one slot are  $(C_s i)$ . [In making the substitution in formula (90),  $b = 0$  and  $c = d/2$ .]

*Flux in Path 2.* The flux per centimeter of slot length is

$$\Phi_2 = 0.4\pi(C_s i) \times P_2$$

where the permeance  $P_2$  can be calculated from the dimensions of the slot opening.

*Flux in Path 3.* This is the zigzag leakage per centimeter length of slot. The position of the rotor tooth opposite the opening of the stator slot, as shown in Fig. 144, corresponds to the condition of maximum permeance of the path followed by the air-gap (or zigzag) leakage flux. The maximum leakage flux in the air gap due to the ampere-conductors  $(C_s i)$  in one

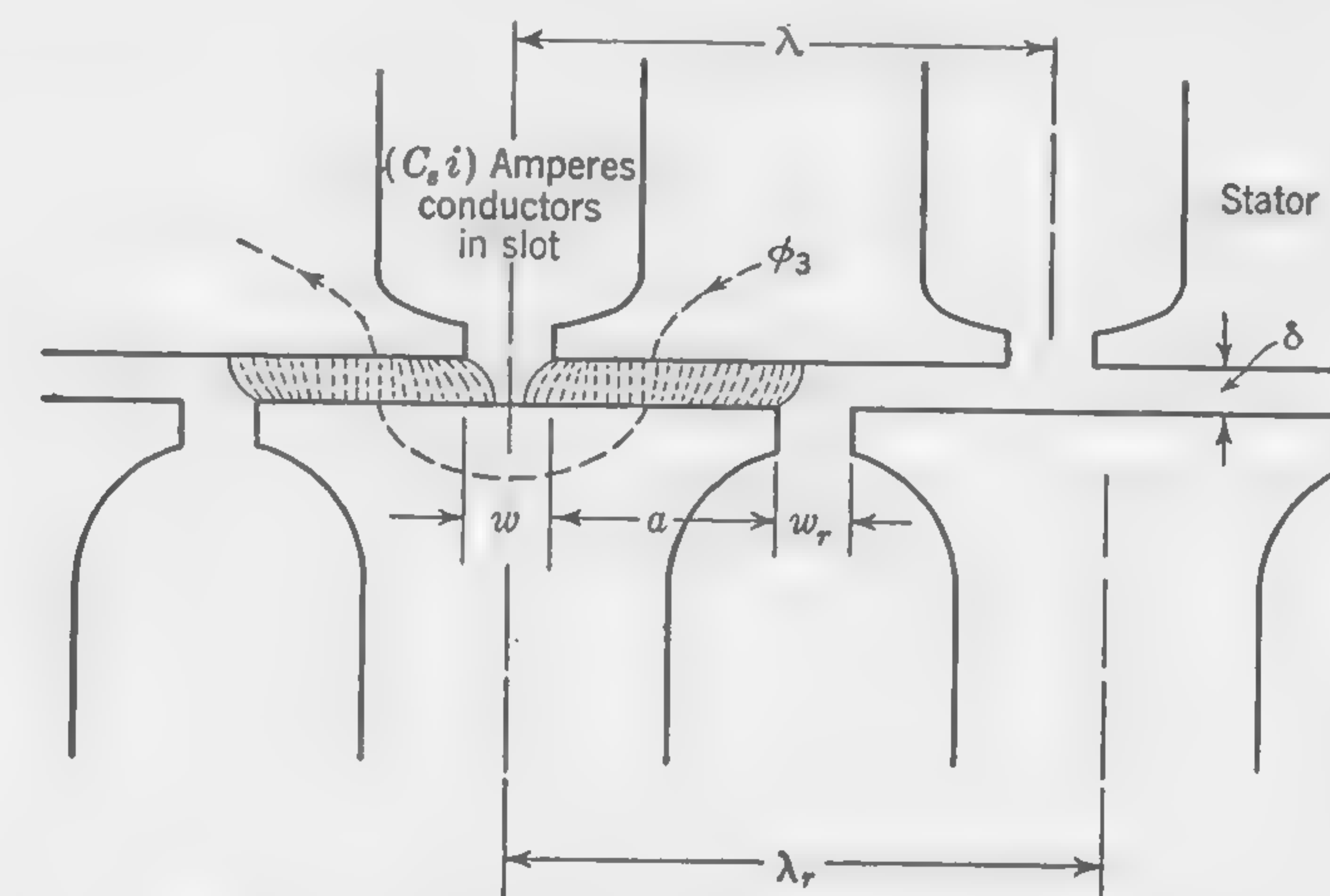


FIG. 144. Leakage flux in air gap of induction motor.

stator slot will depend upon the permeance of a path of width  $a$  (see Fig. 144) and length  $2\delta$ . If we assume that the effect of fringing of flux at the edges of the slot opening is to make the effective cross section of the path  $c$  times greater than if there were no fringing of flux, the permeance of the path considered (per centimeter length of slot) is  $P_3 = (a/2\delta)c$ , and, since the permeance of this path will be very small (almost zero) when a rotor slot is exactly opposite a stator slot, we shall assume the average permeance to be half the above value, whence

$$P_{3(\text{avg})} = \frac{c \times a}{4\delta}$$

The value of  $a$  in terms of the rotor slot pitch  $\lambda_r$  and the width  $w$  and  $w_r$  of the slot openings in stator and rotor, respectively, is

$$a = \frac{(\lambda_r - w_r) - w}{2}$$



whence

$$P_{3(\text{avg})} = \frac{\lambda_r - (w + w_r)}{8\delta} \times c \quad (112)$$

or, if we assume  $c = 1.14$ ,

$$P_{3(\text{avg})} = \frac{\lambda_r - (w + w_r)}{7\delta} \quad (112a)$$

and the average value of the zigzag leakage flux per centimeter length of the slot is, approximately,

$$\Phi_3 = 0.4\pi(C_s i)P_3$$

*Flux in Path 4.* This flux component is calculated in the same manner as the flux in path 2, except that the ampere-turns per slot will depend upon the relative number of slots in stator and rotor. Let  $r = \frac{\text{number of stator slots}}{\text{number of rotor slots}}$ , then the flux in path 4, per centimeter length of slot, is

$$\Phi_4 = 0.4\pi(C_s i)r \times P_4$$

where the permeance  $P_4$  depends upon the dimensions of the openings in the rotor slots. If there are no openings, the flux in the thin bridge of iron over the slots may be calculated by assuming a fairly high value of flux density at this point.

*Flux in Path 5.* A formula similar to that used for the flux in the stator slots is applicable to rotor slots also, although this formula assumes many small wires in the slot, while the rotor winding frequently consists of solid rods of copper or aluminum. From Fig. 143, it is seen that the reactive voltage drop is caused by the flux line  $\Phi_1$  linking with a certain portion of the stator winding near the bottom of the slot, while in the case of the flux line  $\Phi_5$  the loss of voltage is due to the fact that this flux line does *not* link with a certain portion of the rotor winding near the bottom of the slot. It is for this reason that the equivalent slot-leakage flux may be calculated in the same manner for both stator and rotor slots. Using the same ratio  $r$  for correcting the ampere-conductors per slot as in calculating  $\Phi_4$ , the expression for the flux per centimeter of slot length in path 5 is\*

$$\Phi_{5(\text{equivalent})} = 0.4\pi(C_s i)r \times \frac{d_r}{3s_r} \quad (113)$$

Summing up these several flux components, the expression for the total equivalent leakage flux in air gap and slots is

$$\Phi_l = (2.54l_a)0.4\pi(C_s i)[P_1 + P_2 + P_3 + r(P_4 + P_5)] \quad (114)$$

\* This formula does not include the reluctance of the air gap and the iron in the path of the flux component  $\Phi_5$ , but this is negligible in comparison with the reluctance of the slot.

where  $l_a$  = gross axial length of stator core in inches

$(C_s i)$  = ampere-conductors in one stator slot

$$r = \frac{\text{number of stator slots}}{\text{number of rotor slots}} = \frac{\text{rotor slot pitch}}{\text{stator slot pitch}} = \frac{\lambda_r}{\lambda}$$

$P_1 = d_1/3s$  [from formula (111)]

$P_3$  = the permeance as given by formula (112) or (112a)

$P_5 = d_r/3s_r$  [from formula (113)]

**116. Reactive Voltage Drop in Induction Motor.** The leakage flux represented by the line  $\Phi_l$  (Fig. 141) may be calculated by the formula (114) which was developed in the preceding article. Note that *twice* this amount of flux is the total number of maxwells *per pole* cut by the primary (stator) windings, but not by the secondary (rotor) windings; and this is the cause of the reactive voltage drop. The leakage flux is merely a component of the total flux which is cut by the stator slot conductors. It may be considered as rotating at synchronous speed relatively to the stator conductors, so that the amount of leakage flux which cuts each stator slot conductor *per second* is  $(2\Phi_l) \times 2f$ , and, since there are  $C_s n_s p$  slot conductors per phase winding, the *average* value of the reactive emf is

$$4f\Phi_l(C_s n_s p)10^{-8} \quad \text{volts}$$

This must be multiplied by  $\pi/2 \sqrt{2}$  to obtain the rms value (on the sine-wave assumption). Thus

$$IX_{\text{slots and air gap}} = \frac{2\pi f}{\sqrt{2}} \Phi_l(C_s n_s p)10^{-8}$$

Before substituting for  $\Phi_l$  its value as expressed by formula (114), note that the current  $i$  in the slot conductors in the neutral zone is a maximum on zero power factor (short-circuited and locked rotor) when it is equal to  $\sqrt{2}$  times the rms value of the stator current, or  $i = \sqrt{2} I_c$ . The final expression for reactive voltage drop due to slot and air-gap leakage is

$$IX_{\text{slots and gap}} = 2\pi f \times 0.4\pi C_s^2 n_s p \times 2.54l_a[P] \times I_c \times 10^{-8} \quad (115)$$

where  $[P]$  stands for the sum of the five permeances, or "equivalent" permeances, *per centimeter length of stator core*, as calculated in connection with formula (114).

*Reactive Voltage Drop Due to Inductance of End Connections.* In order to obtain a figure for the total reactive drop in the windings, it is necessary to increase the amount given by formula (115) by the voltage drop due to the reactance of the portion of the stator windings outside the slots.\*

\* It is almost impossible to consider the end-connection reactance of the rotor winding independently of the stator winding. With the squirrel-cage rotor, the reactance of the end rings and the short lengths of bar outside the slots is usually negligible. With a wound rotor, the end-connection reactance, if considered independently of the stator, would be greater than that of the squirrel-cage rotor, but,



This reactance may be calculated by formula (75) on page 192, as used in connection with the armature windings of synchronous generators.

**117. Equivalent Resistance of Windings.** Since the circle diagram is drawn to represent conditions in the primary (stator) circuit, all quantities calculated for the secondary (rotor) circuit must be expressed in terms which shall be directly comparable with the quantities of the primary circuit. Thus, although the resistance of a wound rotor may be measured or calculated, the quantity we wish to know is the *equivalent* primary resistance. In other words, we require to calculate the amount by which the primary resistance would have to be increased, if the secondary had no resistance, to produce in the primary circuit the same effect as is produced by the actual secondary resistance. With squirrel-cage rotor, the resistance is not easily measured, and it will, therefore, be convenient to express the equivalent primary resistance in terms of the copper losses.

Let  $I_c$  = current in primary windings  
 $W$  = total watts lost in stator copper  
 $W_r$  = total watts lost in rotor copper

Then, in a three-phase motor, the equivalent resistance per phase winding is

$$R_{\text{equivalent}} = \frac{1/3(W + W_r)}{I_c^2} \quad \text{ohms} \quad (116)$$

**118. Construction of Circle Diagram from Design Data.** In Art. 111 the construction of the circle diagram (Fig. 139) from test data was explained. The manner in which a similar diagram (Fig. 145) may be constructed from calculations based on design particulars will now be considered.

Calculate the exciting current per phase ( $I_e$ ) at normal operating voltage, as explained in Art. 113, and draw  $OI_e$  at the proper angle relatively to the phase of the impressed stator voltage  $OE$ . Draw  $OM$  at right angles to  $OE$  and of such a length as to represent to the same scale as  $OI_e$  the calculated maximum current per phase with locked rotor *assuming the resistance of the windings to be zero*. Thus,

$$OM = \frac{\text{volts per stator phase winding}}{\text{equivalent total reactance per phase}} = \frac{E}{X_{\text{equivalent}}}$$

since the currents in the rotor windings tend to counteract the magnetizing effect of the current in the stator windings, the total or equivalent end-connection reactance will not necessarily be any greater with the wound rotor. In either case, the frequency of flux reversal in the secondary, being proportional to the slip revolutions, is only a small percentage of the supply frequency, and it is suggested that formula (75) used for salient-pole synchronous generators will give the approximate total amount of end-connection reactance in an induction motor.

where  $X_{\text{equivalent}}$  is the sum of the reactances calculated as explained in Art. 116. It is the quantity calculated by formula (115) with the current  $I_c$  omitted, plus the quantity calculated by formula (75). Erect the perpendicular  $MB$  at  $M$ . Draw  $I_e A$  parallel to  $OM$  and meeting  $MB$  at  $A$ . Describe a semicircle of diameter  $I_e A$ . Locate the point  $B$  by making

$$AB = I_e A \times \frac{R_{\text{equivalent}}}{X_{\text{equivalent}}}$$

Join  $I_e B$ , which locates the point  $D$  on the semicircle. Then  $OD$  is the total stator current with locked rotor, and  $I_e D$  is the component of the

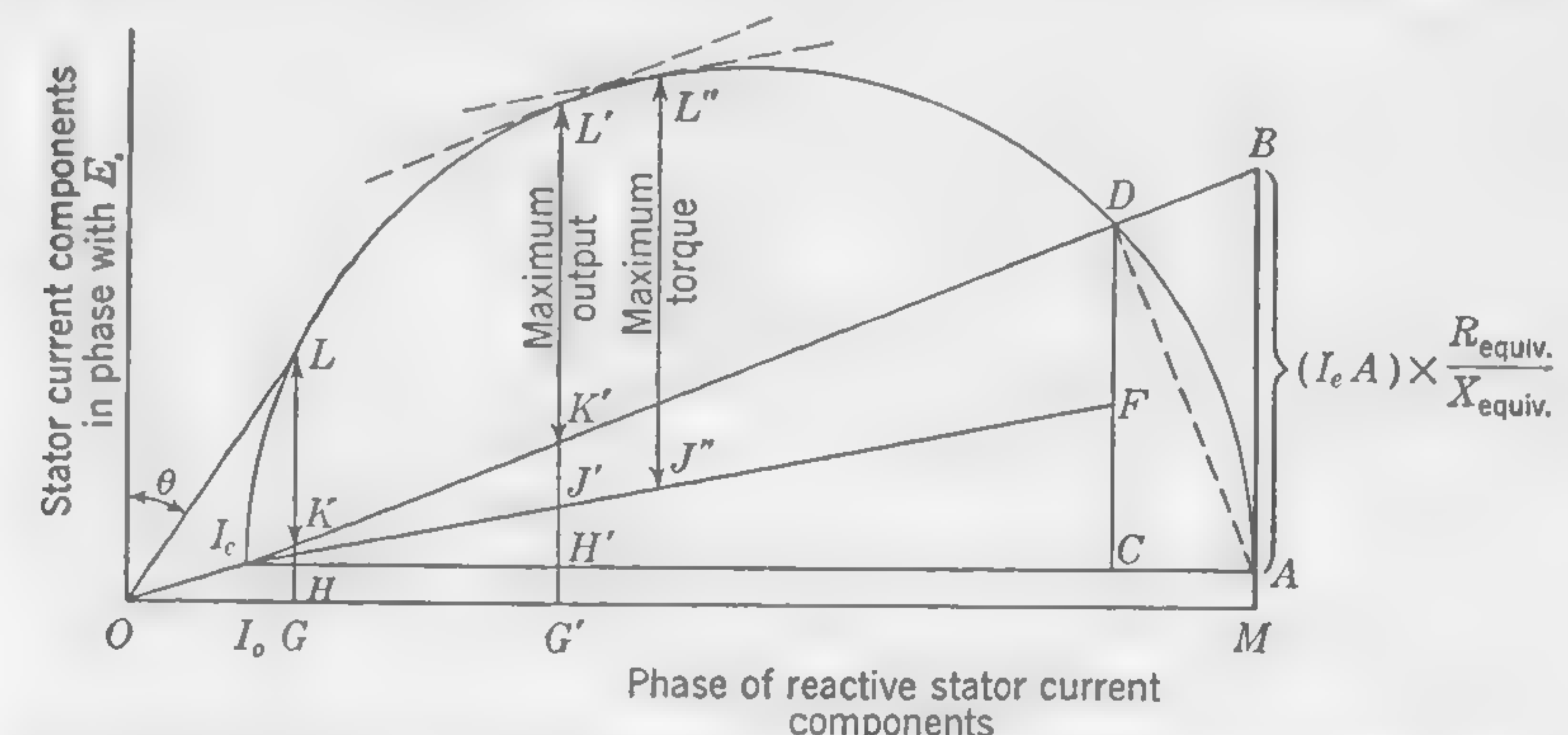


FIG. 145. Circle diagram for induction motor constructed from design data.

total current which balances the rotor current. The in-phase component of this current is  $CD$ , and it is the current component in the primary circuit which supplies all the copper losses under the condition of locked and short-circuited rotor.\*

\* The right-angled triangles  $I_e B A$  and  $I_e A D$  are similar; therefore,

$$\frac{I_e D}{I_e A} = \frac{I_e A}{I_e B} \quad \text{and} \quad I_e D = \frac{(I_e A)^2}{I_e B}$$

On account of the construction of the diagram,  $I_e B$  may be expressed in terms of  $I_e A$  and the calculated quantities  $R$  and  $X$ . Its value is

$$I_e B = \frac{I_e A}{X} \sqrt{X^2 + R^2}$$

whence

$$I_e D = \frac{X(I_e A)}{\sqrt{X^2 + R^2}}$$

Note that, when constructing the diagram, the length  $OM$  was determined by the equation  $X(OM) = \text{impressed volts}$ . Therefore,  $X(I_e A)$  is the impressed voltage less what is required to establish the magnetic field, and the last equation may be expressed in words as

$$\left. \begin{array}{l} \text{Current component in stator which} \\ \text{balances the rotor currents} \end{array} \right\} = \frac{\text{emf}}{\text{impedance}}$$

which proves the correctness of the construction.



In order to draw the line  $I_e F$ , we must divide the line  $CD$  into two parts,  $CF$  and  $FD$ , which shall represent the current components supplying the stator and rotor losses, respectively. Thus

$$CF = CD \times \frac{\text{stator copper loss}}{\text{total copper loss in stator and rotor}}$$

The manner in which the circle diagram indicates the performance of the motor under different loads was explained in Art. 111. For the condition of maximum output, the point  $L'$  must be located where the length of the vector  $K'L'$  will be a maximum. This may easily be done by drawing a tangent to the circle parallel to  $I_e D$ .

**119. Use of Circle Diagram in Calculating Torque.** The manner in which torque is related to the slip revolutions and the resistance of the rotor windings was briefly discussed in Art. 108. We shall now see how torque may be read off the circle diagram, and discuss the conditions necessary to ensure a good starting torque.

The product torque  $\times$  speed is a measure of power, and we may write

$$\text{Torque} \propto \frac{\text{power transmitted to shaft}}{\text{actual rpm}}$$

or

$$\text{Torque} \propto \frac{\text{rotor input}}{\text{synchronous rpm}}$$

and, since the synchronous speed is constant,

$$\text{Torque} \propto \text{rotor input}$$

Therefore, with constant impressed voltage,

$$\text{Torque} \propto \begin{cases} \text{the current component in phase with impressed volts which} \\ \text{represents rotor output, plus the current component rep-} \\ \text{resenting losses in rotor} \end{cases}$$

or

$$\text{Torque} \propto \text{the vector } JL \text{ on circle diagram}$$

The maximum torque is proportional to the current component  $J''L''$ , the point  $L''$  being located by drawing a tangent to the circle parallel to the line  $I_e F$ . This maximum torque does not depend upon the rotor resistance, but the speed (or slip) at which maximum torque occurs does depend upon the rotor resistance. Thus, in order to obtain maximum torque at starting, the rotor resistance would have to be increased so as to bring the point  $D$  to coincide with  $L''$ , because slip would then be 100 per cent (rotor at rest), while the in-phase current component in the rotor

would be a maximum. This condition can be obtained with wound rotors provided with slip rings by inserting resistance of the proper amount when starting the motor, the slip rings being short-circuited when the motor is running.

The factor of importance in determining the maximum torque obtainable in an induction motor is the leakage flux, or rather the leakage reactance  $X$ , because, as  $X$  becomes smaller (less magnetic leakage), the diameter of the circle increases and this also increases the length of the vector  $J''L''$ , which is a measure of the maximum torque.

**Effect of the Ratio ( $X/R$ ) on Starting Torque.** The torque obtained at starting (i.e., with slip = 100 per cent) is proportional to the length  $FD$  on the circle diagram. It depends not only upon the rotor resistance, but also upon the total impedance of the windings.

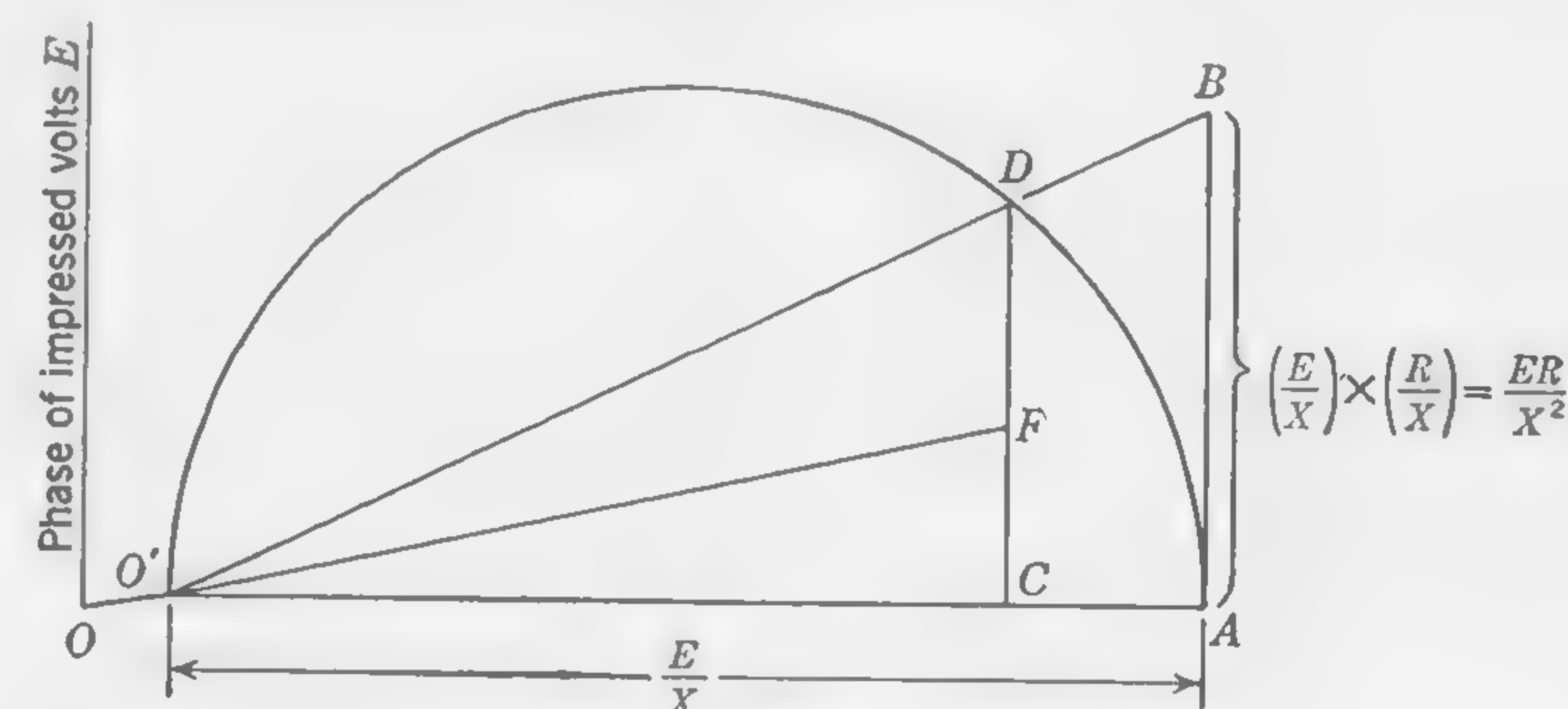


FIG. 146. Diagram for study of starting torque.

For the purpose of calculating the starting torque, it is usually permissible to neglect the exciting current component  $I_e$ , which is small in comparison with the short-circuit current. We shall, therefore, assume that the diameter of the circle  $O'A$  (Fig. 146) is simply  $(E/X)$ , where  $E$  = voltage, per phase, impressed upon the stator windings, and  $X$  = reactance, per phase, due to leakage flux—usually referred to as the equivalent reactance and expressed in ohms. Then by construction,

$$AB = O'A \left( \frac{R}{X} \right) = \frac{ER}{X^2}$$

where  $R$  stands for the equivalent resistance per phase as defined in Art. 117. The starting current (on the assumption of negligible exciting current component) is

$$O'D = \frac{E}{\sqrt{R^2 + X^2}}$$

as proved in the footnote on page 319.



It has been shown that the starting torque is proportional to the length of the vector  $FD$ , which may be expressed in terms of  $E$ ,  $R$ , and  $X$ . Thus,

$$\begin{aligned}\text{Current component } FD &= \frac{\text{watts lost in rotor per phase}}{E} \\ &= \frac{(O'D)^2 \times R_r}{E} \\ &= \frac{E^2}{R^2 + X^2} \times \frac{R_r}{E}\end{aligned}$$

which may be written

$$FD = \frac{ER_r}{R^2[1 + (X/R)^2]} \quad (117)$$

where  $R_r$  stands for the equivalent rotor resistance.

If we assume  $E$ ,  $R$ , and  $R_r$  to be constant in value, it follows that

$$\text{Starting torque} = A \text{ constant} \times \frac{1}{1 + (X/R)^2} \quad (118)$$

which shows how a reactance which is large relatively to the resistance of the windings will cause the starting torque to be small; whence the importance of keeping down the amount of the leakage flux if a large starting torque is desired.

If it is desired to express starting torque in pound-feet, we have

$$\frac{2\pi (\text{torque in lb-ft}) \times N}{33,000} = \text{horsepower imparted to rotor}$$

where  $N$  is the synchronous speed in revolutions per minute, because, although the rotor is at rest, the field which produces the torque is rotating at synchronous speed. In the case of a three-phase motor, the horsepower is

$$\begin{aligned}\text{Hp} &= 3 \times \frac{\text{in-phase component of current} \times \text{volts per phase}}{746} \\ &= 3 \times \frac{(FD) \times E}{746}\end{aligned}$$

whence

$$\text{Starting torque in lb-ft} = 21.1 \frac{E}{N} (FD) \quad (119)$$

Inserting for  $FD$  its value as given by formula (117), we get

$$\text{Starting torque} = 21.1 \frac{E^2 R_r}{N(R^2 + X^2)} \text{ lb-ft} \quad (120)$$

**120. Illustrative Example.** Characteristics of Induction Motor Determined from Design Data and Circle Diagram. Calculate the following quantities and construct the circle diagram for the 10-hp 3-phase induc-

tion motor designed in the Illustrative Example of Art. 109; obtain all necessary data from the design sheet on page 285:

- The exciting current
- The power factor with motor running light
- The circle ratio
- The horsepower output, total copper losses, efficiency, power factor, and slip, for the condition of maximum output
- The power factor when operating under normal full-load condition (10-hp output)
- The horsepower output at which the power factor is a maximum
- The ratio of maximum torque to full-load torque, and the slip corresponding to maximum torque
- The amount of the starting torque and the ratio of starting torque to full-load torque

All data required for these calculations, taken from Art. 109, are here assembled for convenience of reference. The numbers in parentheses are the item numbers as taken from the design sheet of page 285.

*Calculations for Items a and b: The Exciting Current and No-load Power Factor.* Before calculating the magnetizing component of the total exciting current, it is necessary to decide upon the air-gap clearance between rotor and stator cores. From formula (107) on page 309, we have  $\delta = 15 + 7 = 22$  mils. This is approximate only, and we shall select 0.024 in. as a suitable value.

The equivalent air gap (refer to Art 112) is

$$\begin{aligned}\delta_e &= \frac{\pi \times 7}{\pi \times 7 - \left[ \frac{(36 \times 0.13) + (31 \times 0.1)}{2} \times 0.85 \right]} \times 0.024 \\ &= 0.0282 \text{ in.}\end{aligned}$$

The average value of the flux density in the air gap is 23,900 lines per sq in.; whence, by formula (109) on page 310, the maximum value of the required ampere-turns per pole is

$$\begin{aligned}(TI)_p &= 0.313 \times \frac{\pi}{2} \times 23,900 \times 0.0282 \\ &= 331 \text{ amp-turns}\end{aligned}$$

The current per stator winding which will produce these magnetizing ampere-turns is given by formula (110) on page 310. Thus if we assume the air-gap reluctance to be 75 per cent of the total reluctance of the magnetic path, the numerical value of the factor  $m$  would be 1.33, and

$$\begin{aligned}I_0 &= 1.33 \times 1.095 \times \frac{4 \times 23,900 \times 0.0282}{432} \\ &= 9.1 \text{ amp}\end{aligned}$$



DATA FOR ART. 120 TAKEN FROM ART. 109  
(All dimensions in inches unless otherwise stated)

(10)	Diameter of rotor.....	$D$	7
	Number of slots in stator ( $3n_s \times p$ ).....	$n_1$	36
(Fig. 131)	Width of slot opening (stator).....	$w$	0.13
(40)	Number of slots in rotor.....	$n_r$	31
(Fig. 131)	Width of slot opening (rotor).....	$w_r$	0.1
(6)	Average flux density in air gap (lines per sq in.).....	$B_g$	23,900
(1)	Number of poles.....	$p$	4
	Total number of stator conductors ( $3 \times 144$ ).....	$Z'$	432
(5)	Full-load current in stator winding (amp).....	$I_c$	26.2
(39)	Iron loss in stator core and teeth (watts).....		320
(30)	Resistance per phase (stator) (ohm).....		0.161
(2)	Volts per phase across stator winding.....	$E$	127
(Fig. 131)	Depth of stator slots (1.34-0.07).....	$d_1$	1.27
	Width of stator slots.....	$s$	0.302
	Depth of rotor slots (0.67-0.07).....	$d_r$	0.6
	Width of rotor slots.....	$s_r$	0.2
(41)	Slot pitch (rotor).....	$\lambda_r$	0.71
(19)	Number of conductors per stator slot.....	$C_s$	12
(16)	Number of stator slots per pole per phase.....	$n_s$	3
(13)	Gross length of stator core.....	$l_a$	5½
(12)	Pole pitch.....	$\tau$	5.5
(29)	Mean length per turn of stator winding.....		29.15
(32)	Full-load stator copper loss (watts).....	$W$	332
(53)	Full-load rotor copper loss (watts).....	$W_r$	400
	Total losses at full load (watts).....		1,253
	Synchronous speed (rpm).....	$N$	1,800

The ratio of magnetizing current to full-load primary current is, therefore,

$$\frac{I_0}{I_c} = \frac{9.1}{26.2} = 0.347$$

which compares favorably with the usual values for this ratio as given in Art. 112.

The in-phase or energy component of the no-load exciting current is calculated from the estimate of total no-load losses. These are:

Stator iron loss.....	320
Rotor iron loss (estimated as 5 per cent of stator loss).....	16
Copper loss (from estimated primary current of 9.2 amp) = $3 \times (9.2)^2 \times 0.161$ .....	41
Windage and friction loss.....	185
Total.....	562 watts

Whence the in-phase component of the exciting current (see Fig. 140)

$$I_w = \frac{562}{3 \times 127} = 1.48 \text{ amp}$$

and the total exciting current is

$$I_e = \sqrt{(9.1)^2 + (1.48)^2} = 9.22 \text{ amp} \qquad \text{Ans. a.}$$

The power factor is

$$\cos \theta = \frac{I_w}{I_e} = \frac{1.48}{9.22} = 0.1605 \qquad \text{Ans. b.}$$

*Calculations for Item c: The Circle Ratio.* The quantity obtained by dividing the diameter of the circle in the circle diagram by the magnetizing current component is called the "circle ratio." It is of use in comparing different designs of motor. We shall, therefore, make whatever calculations may be necessary to determine the diameter of the circle in the circle diagram.

*Calculation of Leakage-flux Reactance.* (Refer to Arts. 115 and 116.) If we omit the term  $I_c$  in formula (115) on page 317, we obtain an expression for the equivalent reactance in ohms due to the leakage flux in air gap and slots. The equivalent permeance  $[P]$  will first be calculated.

From formula (111) we have  $P_1 = \frac{d_1}{3s} = \frac{1.27}{3 \times 0.302} = 1.4$

From dimensions in Fig. 131 we have  $P_2 = \frac{0.07}{0.13} = 0.54$

By formula (112a),  $P_3 = \frac{0.71 - (0.1 + 0.13)}{7 \times 0.024} = 2.86$

The factor  $r$ , which occurs in formula (114), is the ratio

$$\frac{\text{number of stator slots}}{\text{number of rotor slots}} = \frac{36}{31} = 1.16$$

whence, from the dimensions of Fig. 131, we have

$$r \times P_4 = 1.16 \times \frac{0.07}{0.1} = 0.81$$

From formula (113) we have

$$r \times P_5 = 1.16 \times \frac{0.6}{3 \times 0.2} = 1.16$$

The total equivalent permeance of these leakage paths is the sum of the above quantities; whence

$$[P] = 6.77$$

By formula (115), omitting the term  $I_c$ , the equivalent reactance due to the leakage flux in air gap and slots is

$$X_{\text{air gap and slots}} = 2\pi \times 60 \times 0.4\pi(12)^2 \times 3 \times 4(2.51 \times 5.25) \times 6.77 \times 10^{-8}$$

= 0.74 ohm



An approximate value for the reactance of the portion of the stator winding which is outside the slots is given by formula (75) on page 192. In order to estimate the average projection  $l'$  of the coils beyond the ends of the slot, we have

$$l_s = \text{mean length per turn} - 2l_a = 29.15 - 10.5 = 18.65 \text{ in.}$$

and

$$l' = \frac{l_s - 2\tau}{4} = \frac{18.65 - (2 \times 5.5)}{4} = 1.92 \text{ in.} = (\text{say}) 5 \text{ cm}$$

The winding factor for full-pitch coils with three slots per pole per phase is  $d = 0.96$ ; whence

$$X_{\text{ends}} = \frac{\pi}{2} \times 3 \times \sqrt{2} \times 1.7(0.96)^2 60(3 \times 12)^2 4 \times 5 \times 10^{-8} = 0.16 \text{ ohm}$$

The total equivalent reactance per phase is, therefore,

$$X = 0.74 + 0.16 = 0.9 \text{ ohm}$$

The length  $OM$  in the circle diagram (see Fig. 145) is  $E/X = 127/0.9 = 141$  amp, and the diameter of the circle is

$$I_s A = OM - OI_s = 141 - 9.1 = 132 \text{ amp}$$

The *circle ratio* is, therefore,  $132/9.1 = 14.5$ , which is the *answer c*.

In order to obtain the other quantities asked for in this problem, we must first calculate the equivalent resistance and then construct the circle diagram.

**Calculation of Equivalent Resistance.** (Refer to Art. 117.) At full load, when the stator current is  $I_s = 26.2$ , the stator copper loss is  $W = 332$  watts, and the rotor copper loss is  $W_r = 400$  watts. Whence, by formula (116), the equivalent resistance of the windings is

$$R = \frac{(332 + 400)}{3 \times (26.2)^2} = 0.355 \text{ ohm}$$

**Construction of Circle Diagram.** This is carried out exactly as explained in Art. 118 in connection with Fig. 145. Any convenient scale divided into tenths may be used, and the vectors plotted in amperes. Thus  $OM = 141$  amp, and  $I_s A = 132$  amp. The length of the construction line  $AB$  is  $132 \times (0.355/0.9) = 52.1$ .

The position of the point  $F$  on  $CD$  is found by making

$$CF = CD \times \frac{\text{stator copper loss}}{\text{total copper loss}} = CD \times \frac{332}{732} = 0.453CD$$

The required quantities, as obtained from the diagram, for the condition of maximum output, being the *answers d*, are

$$\text{Horsepower output} = \frac{3E \times K'L'}{746}$$

$$= \frac{3 \times 127 \times 45}{746} = 23$$

$$\text{Total copper losses} = 3E \times H'K' = 6,300 \text{ watts}$$

$$\text{Efficiency} \frac{K'L'}{G'L'} = \frac{45}{63} = 0.715$$

$$\text{Power factor} \frac{G'L'}{OL'} = 0.755$$

$$\text{Slip} \frac{J'K'}{J'L'} = 16.5 \text{ per cent}$$

**Power Factor under Full-load Conditions.** The circle diagram is of little use for studying the behavior of a lightly loaded motor and even of a

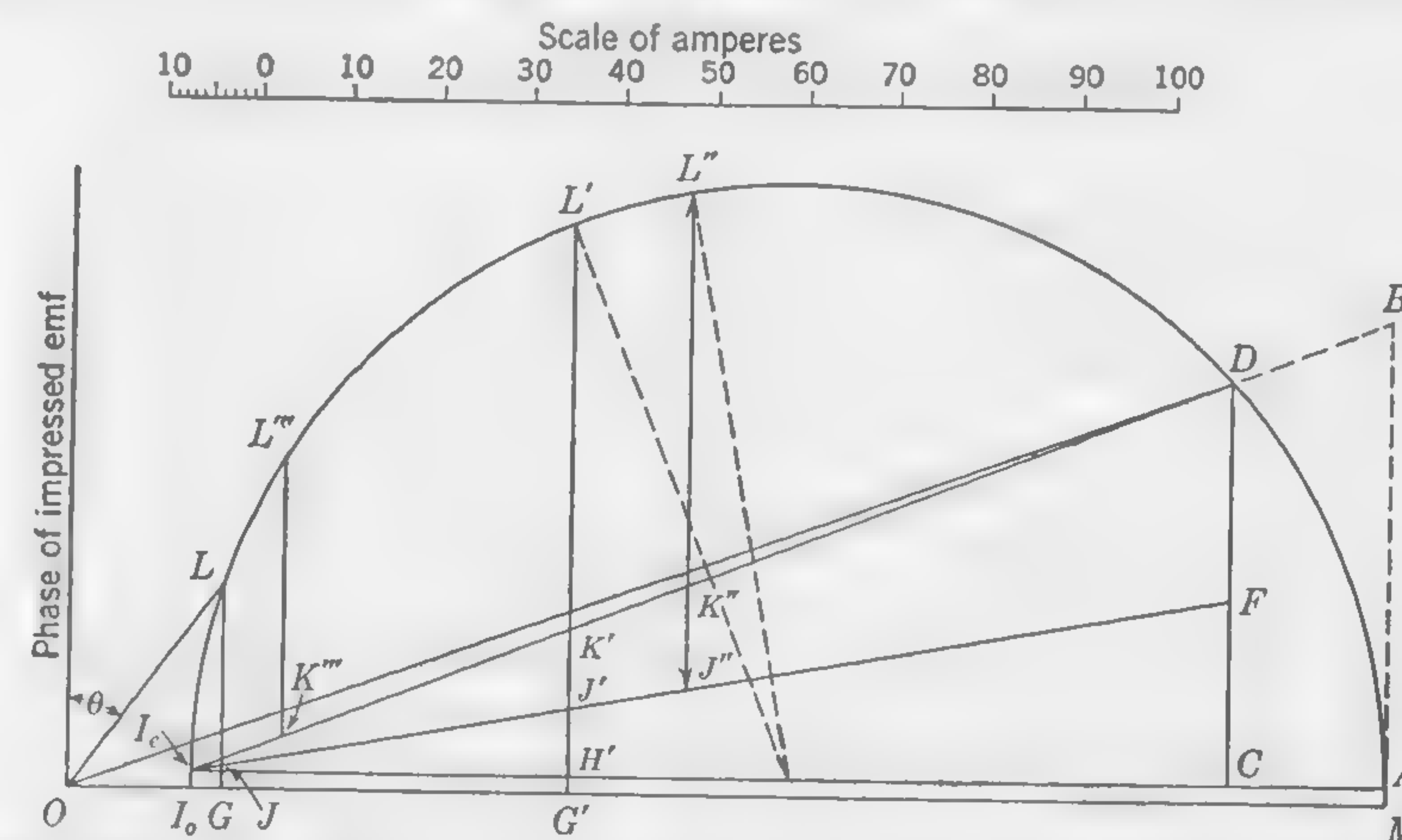


FIG. 147. Circle diagram of motor designed in Illustrative Example, Art. 109.

motor operating under full-load conditions. The full-load losses and efficiency have been calculated in Art. 109, but the circle diagram may be used to obtain an approximate value for the full-load power factor. The point  $L$  on the circle (Fig. 147) must be found where the in-phase current component  $GL$  corresponds to the calculated input. The input, being output plus losses, is  $7,460 + 1,253 = 8,713$  watts; whence

$$GL = \frac{8,713}{3 \times 127} = 22.9 \text{ amp}$$

The total current  $OL$  as scaled off the diagram is 28 amp. Therefore, the power factor when working on full load is  $\cos \theta = 22.9/28 = 0.82$ , which is the *answer c*.



*Output Corresponding to Maximum Power Factor.* From the point  $O$  draw a tangent to the circle so as to locate the point  $L'''$  which will be the end of the primary current vector corresponding to minimum value for the angle  $\theta$ . Drop a perpendicular from  $L'''$  onto the base line. Then

$$\begin{aligned}\text{Horsepower output} &= \frac{3E(K'''L''')}{746} \\ &= \frac{3 \times 127 \times 31.3}{746} = 16\end{aligned}$$

which is the answer  $f$ .

*Torque from Circle Diagram.* For the answers to item  $g$  we have

$$\text{Ratio maximum to full-load torque} = \frac{J''L''}{JL} = 2.7$$

$$\text{Slip at maximum torque} = \frac{J''K''}{J''L''} = 21.2 \text{ per cent}$$

For the answer to item  $h$  we have, by formula (119),

$$\text{Starting torque} = 21.1 \times \frac{127}{1,800} \times FD = 36.5 \text{ lb-ft}$$

$$\text{Ratio } \frac{\text{starting torque}}{\text{full-load torque}} = \frac{FD}{JL} = 1.2 \text{ (nearly)}$$

The results of these calculations, together with some of the quantities calculated in Art. 109, are here assembled to facilitate the comparison of similar quantities under different conditions of loading.

#### SUMMARY OF CIRCLE DIAGRAM CALCULATIONS— 10-HP INDUCTION MOTOR DESIGNED IN ART. 109

##### No-load conditions:

Windage and friction loss.....	185 watts
Total losses.....	562 watts
Total exciting current (per phase).....	9.22 amp
Power factor.....	0.16

##### Full-load conditions (rated output):

Total losses.....	1,253 watts
Efficiency.....	0.856
Power factor.....	0.82
Slip (per cent).....	5.1

##### Maximum output conditions:

Output.....	23 hp
Total copper losses.....	6,300 watts
Total losses.....	6,821 watts
Efficiency.....	0.715
Power factor.....	0.755
Slip (per cent).....	16.5

##### Torque ratios:

Ratio maximum to full-load torque.....	2.7
Ratio starting to full-load torque.....	1.2
Slip (per cent) at maximum torque.....	21.2

**121. Circle-diagram Limitations.** Although the circle diagram, discussed in Arts. 111, 118, 119, and 120, is extremely helpful to the student and designer in his analysis of general operating *trends*, it does not yield motor performance information that is considered sufficiently accurate; calculated values do not always check too closely with those obtained from actual tests. However, the unique advantage of the circle-diagram method is that it clearly indicates how certain constants affect operating characteristics, *i.e.*, horsepower output, torque, power factor, and efficiency, and how *changes* in one or more parameters *should be properly made* if modification or improvement is to be accomplished.

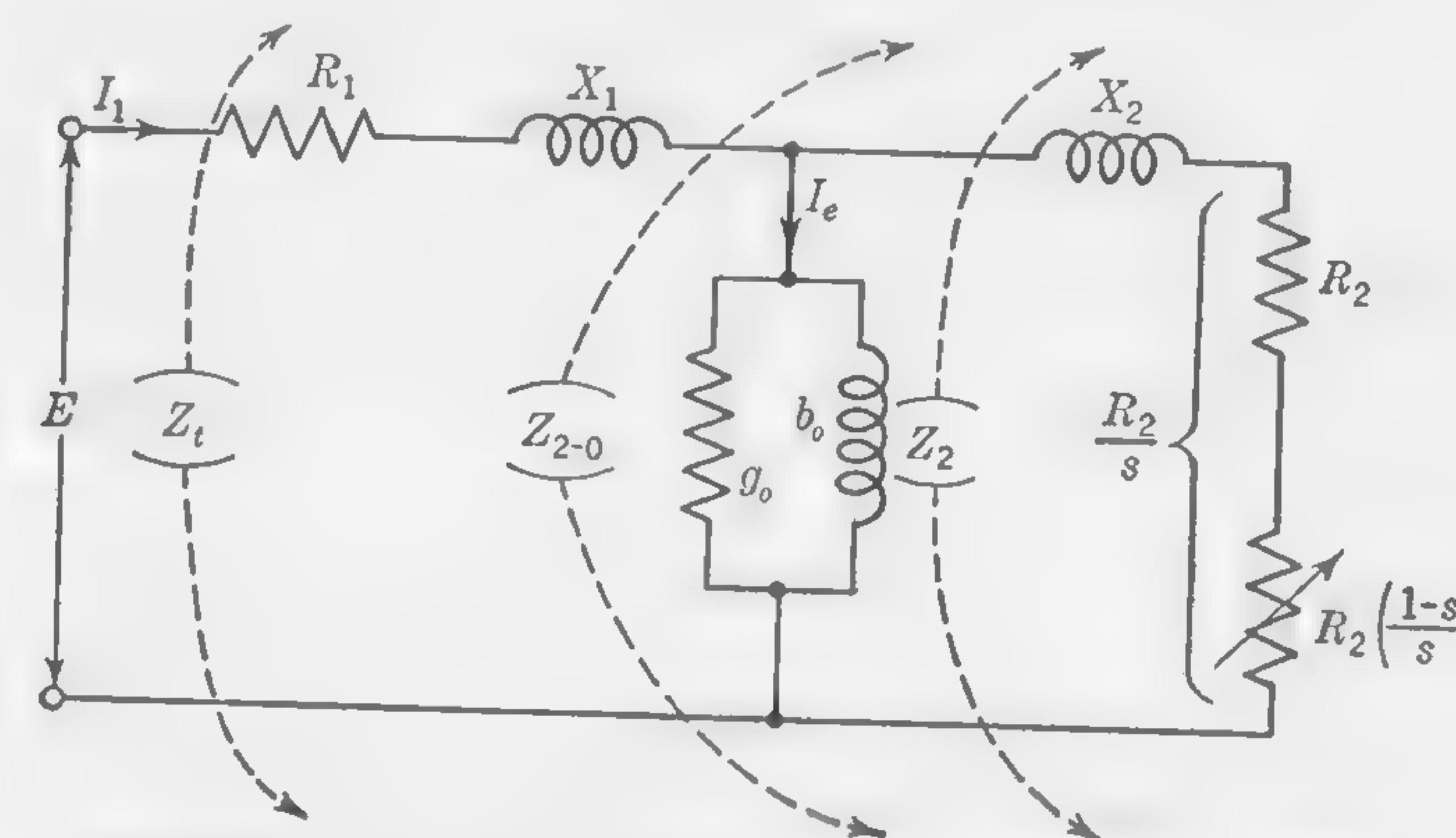


FIG. 148. Equivalent-circuit diagram of induction motor.

The most serious difficulty in the use of the circle diagram lies in the fact that the operating points usually fall in a very small section of a rather large circle, *i.e.*, in the portion  $OLG$  of Fig. 147; since most of the data for the calculation of the motor performance are found in this limited area, the accuracy is, therefore, poor, particularly if extreme care is not taken when the circle is drawn and when distances are scaled off. Moreover, the circle diagram is based upon the so-called *approximate equivalent* circuit of the induction motor (not the *exact equivalent* circuit), and this arbitrary simplification implies that the equivalent rotor circuit is directly in series with the stator circuit, an assumption that leads to considerable error in motors—especially small ones—requiring comparatively large values of no-load current. It should, therefore, be understood that the calculated values obtained in the Illustrative Example of Art. 120 are to be considered only as fair approximations of the machine's operating characteristics. A much more accurate procedure, involving the solution of the *exact* equivalent circuit, is given in succeeding articles.

**122. The Equivalent Circuit.** Figure 148 is a diagram representing the exact equivalent circuit of the induction motor, with which the student is



assumed to be familiar from his study of basic alternating-current machine theory; all symbols indicated thereon are on a per-phase basis and in stator terms. They are defined as follows:

- $R_1$  = stator resistance per phase
- $X_1$  = stator reactance per phase (assumed to equal  $X/2$ )
- $X_2$  = rotor reactance per phase (assumed to equal  $X/2$ )
- $R_2$  = rotor resistance per phase
- $R_2[(1-s)/s]$  = equivalent resistance per phase of mechanical load on motor
- $R_2/s$  = equivalent resistance per phase of rotor circuit
- $g_o$  = conductance per phase of exciting circuit
- $b_o$  = susceptance per phase of exciting circuit
- $Z_2$  = impedance per phase of rotor circuit
- $Z_{2-o}$  = impedance per phase of rotor and exciting circuits in parallel
- $Z_t$  = total impedance per phase of equivalent circuit of motor
- $I_1$ ,  $I_2$ , and  $I_o$  are respectively the stator, rotor, and exciting currents per phase
- $E$  = volts per phase

Before proceeding with a solution of the equivalent circuit to determine the motor characteristics, it is generally desirable to list the values of all items necessary for the calculation of impedances, currents, and other required data. The only parameters not previously found are  $g_o$  and  $b_o$ , and these may be evaluated as follows:

$$g_o = \frac{\text{total iron loss}}{3 \times (E_{\text{induced}})_{n.l.}^2} \quad (121)$$

$$b_o = \frac{I_o}{(E_{\text{induced}})_{n.l.}} \quad (122)$$

where  $(E_{\text{induced}})_{n.l.} = E - I_e X_1$

A table should next be prepared listing the various items of calculation in logical sequence under headings of arbitrarily assumed values of slip; this has been done for the illustrative example that follows. Summarizing the results of such a table in connection with Fig. 148, it should be noted that:

- a.  $Y_2 = G_2 - jB_2$  = admittance for the rotor circuit
- b.  $Y_{2-o} = (G_2 + g_o) - j(B_2 + b_o)$  = admittance for the rotor and exciting circuits
- c.  $Z_{2-o} = R_{2-o} + jX_{2-o}$  = impedance for the rotor and exciting circuits

d.  $Z_t = (R_1 + R_{2-o}) + j(X_1 + X_2)$  = total equivalent impedance of motor circuit

e.  $I_1 = E/Z_t$  = stator current

f. Stator copper loss =  $3I_1^2 R_1$

g.  $I_2 = (I_1 \times Z_{2-o})/Z_2$  = rotor current

h. Rotor copper loss =  $3I_2^2 R_2$

i. Rotor power developed =  $3 \times I_2^2 R_2 [(1-s)/s]$

j. Power output = (rotor power developed) -  $(W + F)$

k. Hp output =  $\frac{\text{power output}}{746}$

l. Rpm = srpm  $(1-s)$

m. Torque =  $(\text{hp} \times 5,250)/\text{rpm}$

n. Total losses =  $(W + F) + (\text{Fe}) + (\text{stator cu loss}) + (\text{rotor cu loss})$

o. Power input = (power output) + (total losses)

p. Power factor =  $\frac{\text{power input}}{3 \times E \times I_1}$

q. Per cent efficiency =  $\frac{\text{power output}}{\text{power input}}$

**123. Illustrative Example. Characteristics of Induction Motor Determined from Design Data and Equivalent-circuit Diagram.** Following the procedure outlined in Art. 122, determine the operating characteristics for the 10-hp 220-volt 3-phase induction motor designed in the Illustrative Example of Art. 109, obtaining all necessary data from the design calculations; assume slips of 0.02, 0.035, 0.05, and 0.06. After completing the table, plot characteristic curves of line current, slip, torque, efficiency, and power factor *versus* horsepower output. Also determine the slip for maximum torque, and the maximum torque.

#### SUMMARY OF DATA TAKEN FROM ART. 120

Windage + Friction  $(W + F)$  loss = 185 watts

Iron (Fe) loss = 336 watts

Equivalent resistance of windings  $R = 0.355$  ohm

Stator resistance  $R_1 = 0.161$  ohm

Equivalent reactance  $X = 0.90$  ohm

Total exciting current  $I_o = 9.22$  amp

Magnetizing component of exciting current = 9.1 amp

Using the information from the foregoing table, calculations will now be made for the unknown equivalent-circuit constants. These are:

$$R_2 = R - R_1 = 0.355 - 0.161 = 0.194 \text{ ohm}$$

$$X_1 = X_2 = X/2 = 0.9/2 = 0.45 \text{ ohm}$$



$$\text{Induced voltage at no load} = E - (I_e X_1) = 127 - (9.22 \times 0.45) = 122.9$$

$$g_o = \frac{336}{3 \times (122.9)^2} = 0.00743 \text{ mho} \quad [\text{formula (121)}]$$

$$b_o = \frac{9.1}{122.9} = 0.074 \text{ mho} \quad [\text{formula (122)}]$$

With these data properly identified on the equivalent-circuit diagram of Fig. 149, the accompanying table of calculations was prepared in accordance with the procedure previously outlined in Art. 122. Note particularly the orderly arrangement of the various items under the arbitrarily assumed values of slip equal to 0.02, 0.035, 0.05, and 0.06.

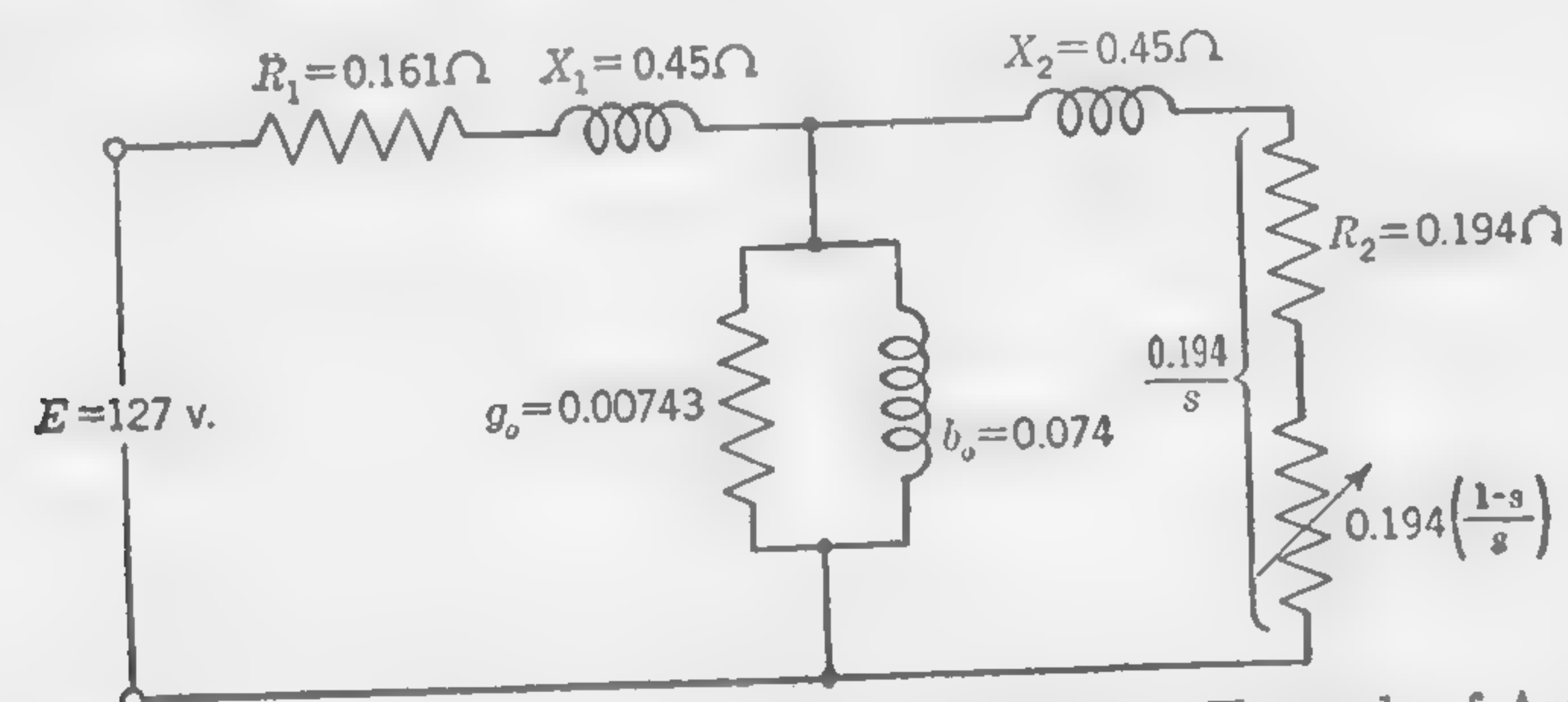


FIG. 149. Equivalent-circuit diagram for Illustrative Example of Art. 123.

With the results of the table plotted in the curves of Fig. 150, the motor develops the following characteristics when operating at full load, *i.e.*, 10 hp:

$$\text{Rpm} = 1,800(1 - 0.028) = 1,750$$

$$\text{Torque} = 30 \text{ lb-ft}$$

$$\text{Line amperes} = 25.3$$

$$\text{Per cent efficiency} = 86.5 \text{ (compare with item 4, p. 297)}$$

$$\text{Power factor} = 0.882 \text{ (compare with item 3, p. 297)}$$

A reasonably accurate empirical formula that gives the slip at which maximum torque occurs is

$$s_{mt} = \frac{R_1}{\sqrt{R_2^2 + X^2}} \quad (123)$$

Thus

$$s_{mt} = \frac{0.194}{\sqrt{(0.161)^2 + (0.90)^2}} = 0.212$$

which implies that the speed at which maximum torque occurs is

$$\text{rpm} = (1 - 0.212)1,800 = 1,420$$

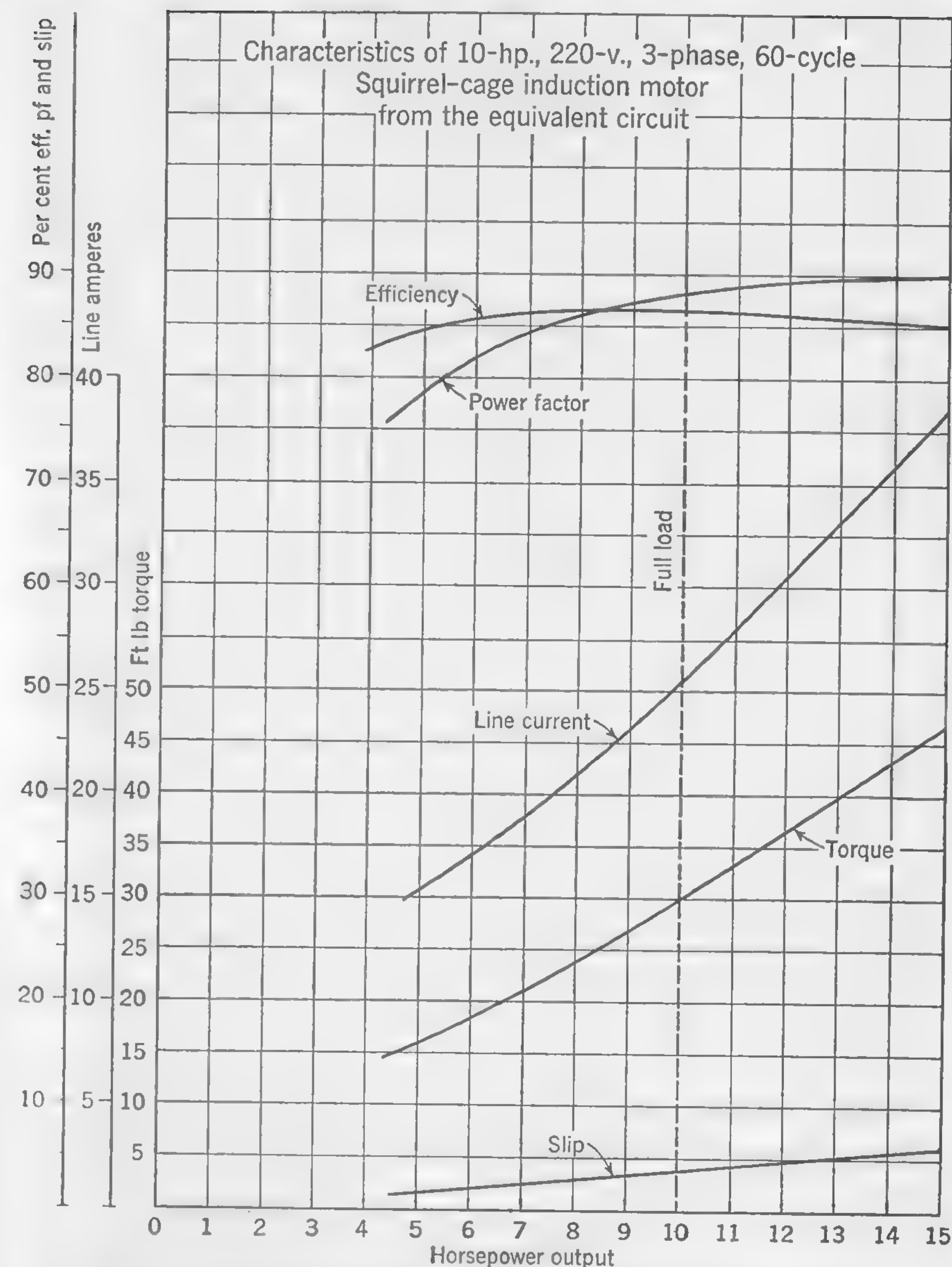


FIG. 150. Characteristic curves for Illustrative Example of Art. 123.



TABLE OF CALCULATIONS FOR SQUIRREL-CAGE INDUCTION MOTOR BY EQUIVALENT-CIRCUIT METHOD  
Specifications: 10 hp; 3 phase; 220 volts; 60 cycles; 1,800 rpm (synchronous)

Item No.	Circuit	Quantity	Formula	Slip, s			
				0.02	0.035	0.05	0.06
1	Rotor	$R_2/s$		9.70	5.55	3.88	3.23
2		$Z_2$	$(R_2/s) + jX_2$	$9.7 + j0.45 = 9.7$	$5.55 + j0.45 = 5.56$	$3.88 + j0.45 = 3.9$	$3.23 + j0.45 = 3.26$
3		$G_2$	$(R_2/s)/Z_2^2$	0.103	0.180	0.255	0.304
4		$B_2$	$X_2/Z_2^2$	0.0048	0.0146	0.0296	0.0422
5	Rotor and exciting in parallel	$Y_{2-o}$	$(G_2 + g_o) - j(B_2 + b_o)$	$0.110 - j0.079 = 0.135$	$0.187 - j0.089 = 0.207$	$0.262 - j0.104 = 0.282$	$0.311 - j0.116 = 0.332$
6		$R_{2-o}$	$(G_2 + g_o)/Y_{2-o}^2$	6.02	4.36	3.29	2.83
7		$X_{2-o}$	$(B_2 + b_o)/Y_{2-o}^2$	4.33	2.08	1.31	1.05
8		$Z_{2-o}$	$R_{2-o} + jX_{2-o}$	$6.02 + j4.33 = 7.42$	$4.36 + j2.08 = 4.82$	$3.29 + j1.31 = 3.53$	$2.83 + j1.05 = 3.02$
9	Total	$R_t$	$R_1 + R_{2-o}$	6.18	4.52	3.45	2.99
10		$X_t$	$X_1 + X_{2-o}$	4.78	2.53	1.76	1.50
11		$Z_t$	$R_t + jX_t$	$6.18 + j4.78 = 7.8$	$4.52 + j2.53 = 5.17$	$3.45 + j1.76 = 3.87$	$2.99 + j1.50 = 3.34$
12		$I_t$	$127/Z_t$	16.3	24.6	32.8	38.0
13	Stator	Cu loss	$3 \times I_1^2 \times R_1$	128	292	520	697
14		$I_1$	$I_t \times Z_{1-o}/Z_2$	12.5	21.4	29.7	35.2
15	Total			91	266	514	722

TABLE OF CALCULATIONS FOR SQUIRREL-CAGE INDUCTION MOTOR BY EQUIVALENT-CIRCUIT METHOD.—(Continued)

Item No.	Circuit	Quantity	Formula	Slip, s			
				0.02	0.035	0.05	0.06
16	Stator	Power developed	$3 \times I_1^2 R_2 [(1-s)/s]$	4,460	7,350	9,750	11,300
17		Power output	$(16) - (W + F)$	4,275	7,165	9,565	11,115
18		Hp output	$(17)/746$	5.73	9.6	12.8	14.9
19		Rpm	$1,800(1-s)$	1,764	1,737	1,710	1,692
20	Total	Torque	$(hp \times 5,250)/rpm$	17.1	29.0	39.3	46.2
21		Losses	$(F + W) + (Fe) + (13) + (15)$	740	1,079	1,555	1,940
22		Power input	$(17) + (21)$	5,015	8,244	11,120	13,055
23		Power factor	$\frac{(22)}{3 \times 127 \times (12)}$	0.808	0.880	0.890	0.902
24		Per cent efficiency	$[(17)/(22)] \times 100$	85.3	86.8	86.0	85.2



Proceeding with calculations for maximum torque,

$$\frac{R_2}{s} = \frac{0.194}{0.212} = 0.915 \text{ ohm}$$

$$Z_2 = 0.915 + j0.45 = 1.02$$

$$G_2 = \frac{0.915}{(1.02)^2} = 0.88$$

$$B_2 = \frac{0.45}{(1.02)^2} = 0.432$$

$$Y_{2-o} = (0.887 - j0.506) = 1.02$$

$$R_{2-o} = \frac{0.887}{(1.02)^2} = 0.852$$

$$X_{2-o} = \frac{0.506}{(1.02)^2} = 0.486$$

$$Z_{2-o} = 0.852 + j0.486 = 0.985$$

$$Z_i = 1.013 + j0.936 = 1.38 \text{ ohms}$$

$$I_1 = \frac{127}{1.38} = 92.0 \text{ amp}$$

$$\text{Stator cu loss} = 3(92)^2 \times 0.161 = 4,080 \text{ watts}$$

$$I_2 = \frac{92 \times 0.985}{1.02} = 88.8 \text{ amp}$$

$$\text{Rotor cu loss} = 3(88.8)^2 \times 0.194 = 4,590 \text{ watts}$$

$$\text{Power developed} = 4,590 \times \frac{1 - 0.212}{0.212} = 17,050 \text{ watts}$$

$$\text{Power output} = 17,050 - 185 = 16,865 \text{ watts}$$

$$\text{Hp output} = \frac{16,865}{746} = 22.6$$

$$\text{Torque} = \frac{22.6 \times 5,250}{1,420} = 83.5 \text{ lb-ft}$$

**124. Heating of Induction Motors.** The predetermination of the temperature attained by any piece of electrical apparatus or machinery involves the use of empirical constants which should be determined from tests on apparatus generally similar to the design under consideration. The student is referred to Art. 58 and Illustrative Example of Art. 60 where the manner of the probable temperature rise of the dynamo and alternator armatures was discussed. In the event of no data being available from tests on the particular type of induction motor in which the designer is interested, he may calculate the temperature rise of the stator as suggested on page 195 in connection with stationary armatures.

Generally speaking, if the current densities in the windings and the flux densities in the iron do not exceed the usual maximum values given in Chap. 10, the final temperature rise of the stator under full-load conditions is not likely to exceed 40 to 50°C, which is permissible in modern motors. The rotor core losses are negligible (on account of low frequency) and it is not usual to calculate the temperature rise of the rotor

The final temperature rise will depend largely upon the size and disposition of the ventilating openings in the frame, and also upon the efficiency of the vanes (if any) that are provided on the rotor to improve the air circulation.

Some designers prefer to use a formula based on the outside dimensions of the motor and a cooling coefficient which depends partly upon the peripheral velocity of the rotor. In the formula  $t = w/cS$ ,  $t$  is the temperature rise of stator (by thermometer) in degrees centigrade;  $w$  is the total of all losses in watts;  $S$  is the external surface in square inches being equal to  $\pi DL$ , where  $D$  is the outside diameter of casing and  $L$  is the outside axial length not including projections for bearings. The cooling coefficient  $c$  is in the form  $c = (a + v)/b$ , where  $a$  and  $b$  are numerical constants depending upon the type of machine and means of ventilation employed, and  $v$  is the peripheral velocity of the rotor in feet per minute. This formula for the cooling coefficient is similar to (50) on page 150, which is used for calculating the temperature rise of d-c armatures.

Using numerical values for  $a$  and  $b$  which give good results for medium-size induction motors of standard design, we have

$$t = \frac{40,000W}{(3,000 + v) DL} \quad ^\circ\text{C} \quad (124)$$

In fan-cooled motors the temperature rise will be about 90 per cent of that given by formula (124).

With totally enclosed motors, the temperature rise depends less upon the peripheral velocity,  $v$ ; but it would probably be about  $2\frac{1}{2}$  times the rise as calculated by formula (124).

**125. Illustrative Example. Temperature Rise of Induction Motor.** Calculate the probable maximum temperature rise (by thermometer) of the motor designed in the Illustrative Example of Art. 109. The required particulars obtained from the design sheet on page 285 are as follows:

Total losses in stator iron = 320 watts]

Total losses in stator copper = 332 watts

Gross axial length of stator core =  $5\frac{1}{4}$  in.

Number of cooling ducts = 1

Mean length per turn of stator winding = 29.15 in.

Inside diameter of stator core = 7 in.

Outside diameter of stator core =  $12\frac{1}{2}$  in.

Peripheral velocity of rotor = 3,300 fpm

Following the method of calculation outlined in Art. 58, the portion of the total copper loss to be radiated from the core surface is  $332 \times [(2 \times 5.25)/29.15] = 120$  watts, whence the total loss to be radiated is  $320 + 120 = 440$  watts. The three cooling surfaces to be considered are:



- a. The inside cylindrical surface  $= \pi \times 7 \times 5.25 = 115.5$  sq in.  
 b. The outside cylindrical surface  $= \pi \times 12.5 \times 5.25 = 206$  sq in.  
 c. The ducts and end surfaces  $= \frac{\pi}{4} [(12.5)^2 - 7^2] \times 4 = 338$  sq in.

The cooling coefficients are calculated on the assumption that the inside cylindrical surface of the stator is moving with a peripheral velocity equal to that of the rotor; but, since no air is thrown against the *outside* cylindrical surface, its peripheral velocity ( $v$  in the formula) is put equal to zero.

The cooling coefficients are, therefore,

- a. For the inside surface, by formula (50),  $c = (1,500 + 3,300)/100,000 = 0.048$ .  
 b. For the outside surface, by formula (50),  $c = 1,500/100,000 = 0.015$ .  
 c. For the ducts and ends, by formula (51),  $c = 3,300/(3 \times 100,000) = 0.011$ .

The watts that can be dissipated from the cooling surfaces *per degree rise of temperature* are:

$$\begin{array}{rcl} 0.048 \times 115.5 & = & 5.55 \\ 0.015 \times 206 & = & 3.09 \\ 0.011 \times 338 & = & 3.72 \\ \text{Total} & & \underline{12.36} \end{array}$$

whence, the calculated temperature rise is

$$t = \frac{440}{12.36} = 35.6^\circ\text{C}$$

as a check by formula (124), we have

Total full-load loss (from the table on page 294),  $W = 1,253$   
 Dimensions from Fig. 134,  $D = 15$  in.,  $L = 12\frac{1}{2}$  in.; whence

$$t = \frac{0.9 \times 40,000 \times 1,253}{(3,000 + 3,300)15 \times 12.5} = 38^\circ\text{C}$$

### TEST PROBLEMS

The subject of induction motor performance, as treated in this chapter, cannot easily be illustrated or elucidated by means of short problems.

*References:* The student who wishes to go further into the design of induction motors is referred to the following articles: Test Code for Polyphase Induction Motors, *AIEE*, No. 500, 1937.

WARE, D. H., Measurement of Stray-load Loss in Induction Motors, *Trans. AIEE*, vol. 64, p. 194, April, 1945.

LIWSCHITZ, M. M., Harmonics in Induction Motors, *Trans. AIEE*, vol. 62, p. 100, November, 1942.

HILDEBRAND, L. E., et al., Hot-spot Temperatures in Induction Motors, *Trans. AIEE*, vol. 64, p. 124, March, 1945.

American Standard for Rotating Electrical Machinery, ASA C50-1943.

## CHAPTER 12

### ALTERNATING-CURRENT TRANSFORMERS

**126. Introductory.** In order to provide a further illustration of the applications of electrical machine design as presented in the earlier chapters of this book, the calculations for the design of small, single-phase distribution transformers will be explained. Before this can be done, it will be necessary to discuss briefly a few essential matters which have not been covered in previous chapters; but it is assumed that the student is generally familiar with the construction and principles of operation of a-c transformers. Compared with a rotating machine, the static transformer would appear to present fewer difficulties to the designer because the interrelations between electric and magnetic circuits are less complex or variable. Transformer design does, nevertheless, involve manifold problems relating to core and winding proportions, insulation for high-voltage service, core materials, construction arrangements, protection against surges, tap changing, temperature rise, and other factors. Such details can obviously not be treated in one short chapter, but this introductory material will be extremely helpful to the student should he desire to pursue his studies further in books\* dealing exclusively with the subject.

**127. Theory of the Transformer.** The two separate sets of coils, known as the primary and secondary windings, respectively, are linked with the same magnetic flux† because they are wound on the same laminated iron core. It follows, therefore, that the emf induced by the alternating flux in the primary and secondary coils will be directly proportional to the number of turns in the respective windings. Also, since the  $IR$  drop in the primary windings is always small in relation to the impressed primary voltage, the emf induced in the primary must, necessarily, be almost exactly equal, but opposite in phase, to the impressed voltage.

Suppose, in the first place, that the two ends of the primary winding are connected to constant pressure mains, and that no current is taken from the secondary terminals. The total flux of  $\Phi$  maxwells increases twice from zero to its maximum value, and decreases twice from its

\* STILL, ALFRED, "Principles of Transformer Design," John Wiley & Sons, Inc., 1926.

† The effects of magnetic leakage will be considered later.



maximum to zero value, in the time of one complete period. The flux cut per second is, therefore,  $4\Phi f$ , and the *average* value of the induced emf in the primary is

$$E_{avg} = \frac{4\Phi f T_p}{10^8} \quad \text{volts}$$

where  $T_p$  stands for the number of turns in the primary winding.

If we assume the flux variations to be sinusoidal, the form factor is  $\pi/2 \sqrt{2} = 1.11$ , and the effective value of the induced primary voltage will be

$$E_1 = \frac{4.44f\Phi T_p}{10^8}$$

Further, since the only difference between the back emf in the primary and the potential difference applied across the primary terminals is due to the relatively negligible  $IR$  drop in the primary windings due to the exciting current, we may write

$$E_p = \frac{4.44f\Phi T_p}{10^8} \quad (\text{approx}) \quad (125)$$

and, similarly,

$$E_s = \frac{4.44f\Phi T_s}{10^8} \quad (\text{approx}) \quad (125a)$$

where  $E_p$  = primary impressed voltage

$E_s$  = secondary terminal voltage

$T_p$  = number of series turns in primary

$T_s$  = number of series turns in secondary

whence

$$\frac{E_p}{E_s} = \frac{T_p}{T_s} \quad (126)$$

which is approximately true in all well-designed transformers, even under load, unless a large current is drawn from the secondary, when the relative amount of the  $IR$  and  $IX$  voltage components may become appreciable. The total number of turns  $T_s$  in the secondary, when this is the low-voltage winding, should usually be divisible by 4 in order that the coils may be efficiently grouped for series or parallel connection.

Since the  $IR$  drop in the primary is comparatively small, and, indeed, frequently negligible, it follows that the flux linking with the primary must be approximately the same at full load as at no load, and the magnetizing ampere-turns necessary to establish this flux must, therefore, remain approximately the same whether or not current is drawn from the secondary. Thus, when current is taken from the secondary, there must always be a current in the primary of which the magnitude and phase will be such as almost exactly to balance and counteract the magnetizing effect

of the secondary ampere-turns. If  $I_p$  and  $I_s$  stand, respectively, for the primary and secondary currents, we may, therefore, write

$$I_p T_p = I_s T_s \quad (\text{approx})$$

whence

$$\frac{I_p}{I_s} = \frac{T_s}{T_p} \quad (\text{approx}) \quad (127)$$

**128. Classification and Types of Transformers.** We are here concerned merely with the piece of apparatus known as the static transformer, which is used for converting power represented by a high voltage and small current into power at a lower voltage and larger current, or vice versa. Such transformers may be classified according to number of phases, method of cooling, terminal voltage, or output; but from the point of view of the designer, it will be better to consider the use to which the transformer—whether single-phase or polyphase—will be put. This leads to the two classes:

1. Power transformers
2. Distribution transformers

**Power Transformers.** This term is here used to include all transformers of large size as used in central generating stations and substations for transforming the voltage at each end of a power transmission line. They may be designed for maximum efficiency at full load, because they are usually arranged in banks and can be thrown in parallel with other units or disconnected at will.

**Distribution Transformers.** These are of the self-cooling type and are almost invariably oil-immersed. They are continuously in circuit, whether or not current is drawn from the secondary windings, and the iron losses should be smaller relatively to the full-load copper losses than would be necessary in power transformers. In other words, they must be designed for good "all-day" efficiency and not for highest efficiency at full load.

Every transformer consists of a magnetic circuit of laminated iron with which the electric circuits (primary and secondary) are linked. A distinction is usually made between *core-type* and *shell-type* transformers. Figures 151 and 152 illustrate single-phase transformers of the core and shell types, respectively. The former shows a closed laminated circuit with the windings on two of the limbs. Each limb is wound with both primary and secondary circuits in order to reduce the magnetic leakage

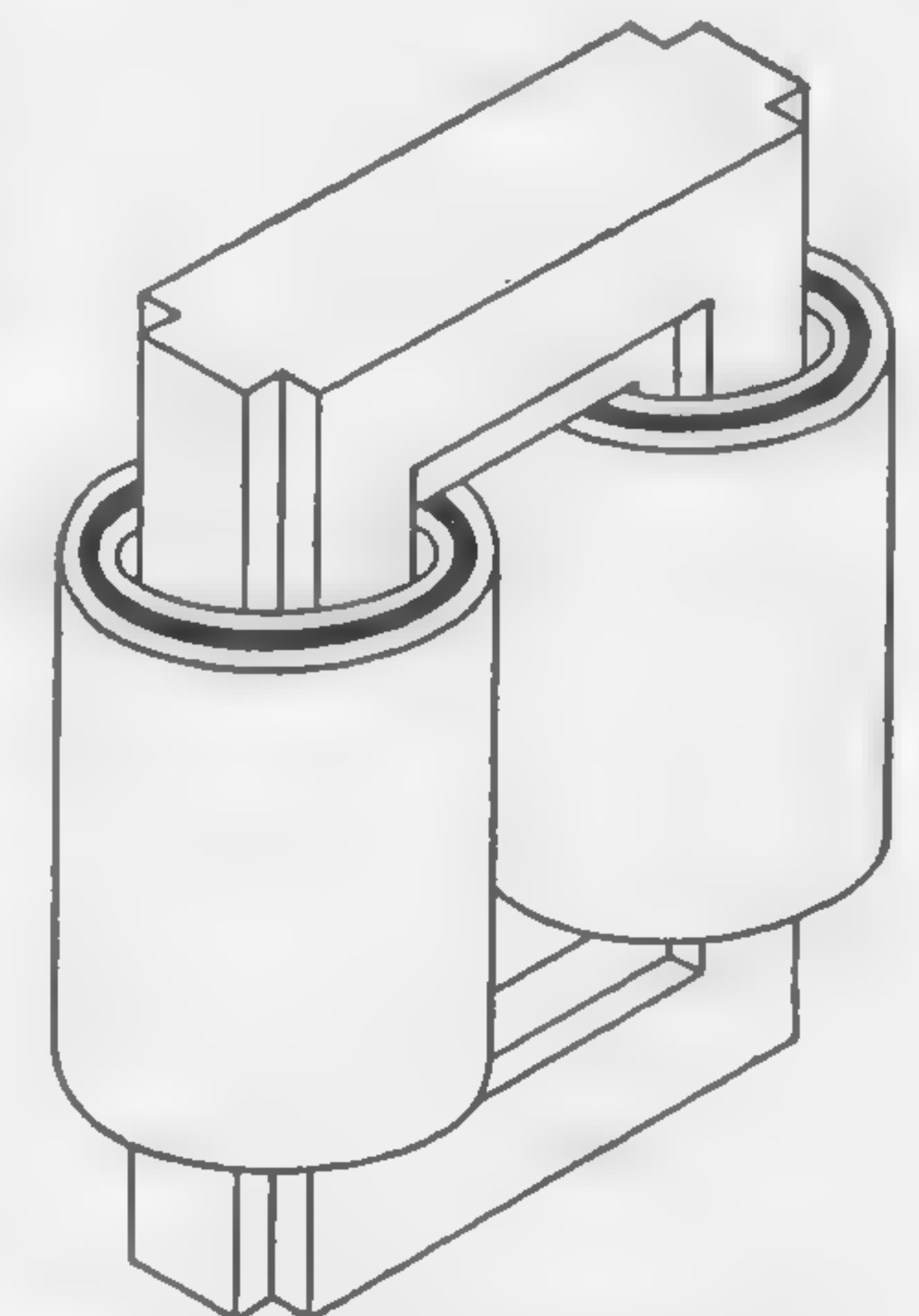


FIG. 151. Core-type transformer.



which would otherwise be excessive. The coils may be cylindrical in form and placed one inside the other with the necessary insulation between them, or the windings may be "sandwiched," in which case flat rectangular or circular coils, alternately primary and secondary, are stacked one above the other with the requisite insulation between.

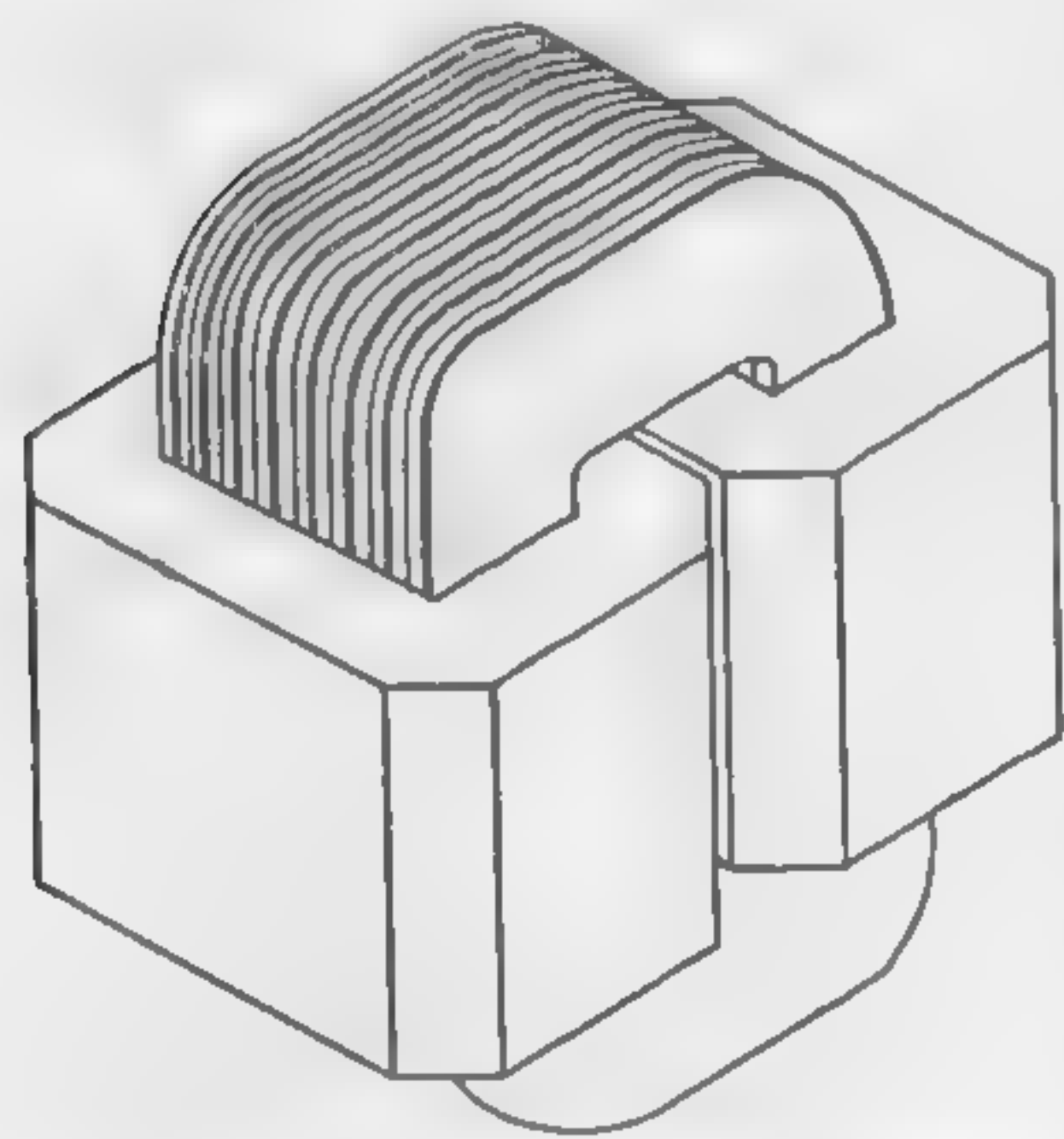


FIG. 152. Shell-type transformer.

Figure 152 shows a single set of windings on a central laminated core, which divides after passing through the coils and forms what may be thought of as a shell of iron around the copper. The manner in which the core is usually built up in shell-type transformers is shown in the two sketches of Fig. 153. Either 29-gage (0.014 in.) or 26-gage (0.0185 in.) laminations are generally used, the thicker plates being permissible when the frequency is low. A very usual thickness for transformers

working on 25- and 60-cycle circuits is 0.014 in. The arrangement of the stampings is reversed in successive groups of stampings, in order to cover the joints and so reduce the magnetizing component of the primary current. The stampings are usually stacked in pairs, the joints being covered on each side of every group of two stampings. A very thin coat of varnish is

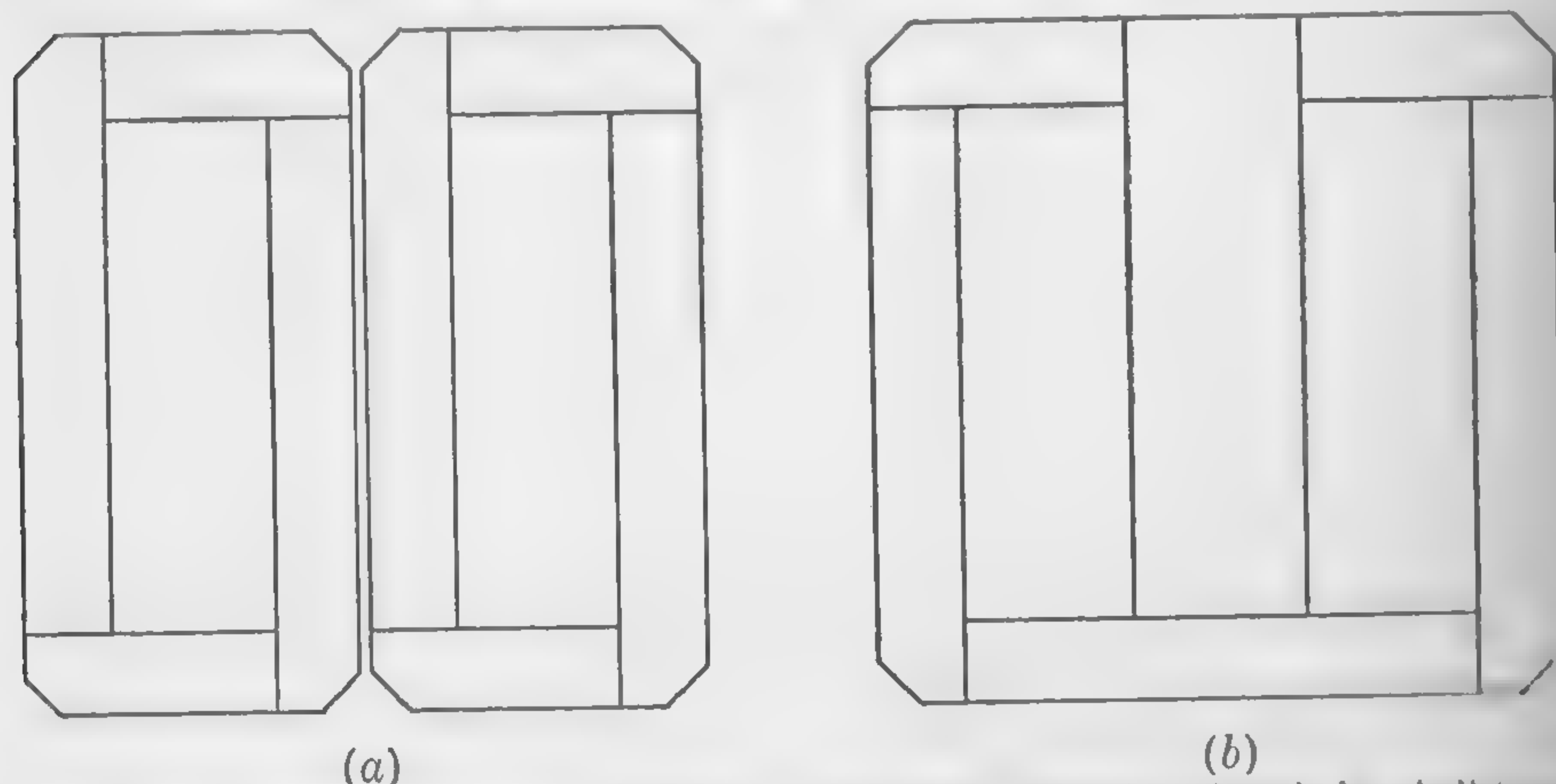


FIG. 153. Two methods of assembling stampings (straight pieces) in shell-type transformers.

sometimes used to provide insulation between laminations and reduce eddy-current loss, but usually the oxide on the surface of the iron affords adequate insulation, the voltage tending to establish circulating current from plate to plate being very small. Alloyed iron or silicon-steel is used for the cores of modern transformers. An alloy of nickel and iron

has better magnetic properties than silicon-steel and is used for the cores of instrument transformers, but its high cost renders it uneconomical for power or distribution transformers.

The choice of type—whether core or shell—will not greatly affect the efficiency or cost of the transformer. The shell type appears to be well adapted for low-voltage transformers of large output, while the core type is generally preferable for high-voltage transformers of small output.

**129. The Output Equation—Volts per Turn of Winding.** The volt-ampere input of a single-phase transformer is  $E_p I_p$ , and, if we substitute for  $E_p$  its value as given by formula (125), we have

$$\text{Volt-amperes} = \frac{4.44f}{10^8} \times \Phi \times T_p I_p$$

But  $T_p I_p = T_s I_s$  approximately, and, if we put  $(TI)$  to represent ampere-turns of either primary or secondary windings, we have

$$\text{Volt-amperes} = \frac{4.44f}{10^8} \times \Phi \times (TI) \quad (128)$$

There is no limit to the number of designs which will satisfy this equation; the total flux  $\Phi$  is roughly a measure of the cross section of the iron core, while the quantity  $(TI)$  determines the cross section of the windings. The problem before the designer is to proportion the parts and dispose the material in such a way as to obtain the desired output and specified efficiency at the lowest cost. The temperature rise is also a matter of importance which must be watched, and light weight is occasionally more important than cost.

If a suitable value for  $T$  in formula (128) could be determined or assumed, the amount of the flux  $\Phi$  could be calculated and we would have a starting point from which the leading dimensions of a preliminary design could be determined. Let  $V_t$  = volts per turn (of either primary or secondary winding); then

$$V_t = \frac{E}{T} = \frac{EI}{(TI)} = \frac{\text{volt-ampere output}}{(TI)}$$

Also, by formula (125) or (125a),

$$V_t = \frac{4.44f\Phi}{10^8}$$

Multiplying both values of  $V_t$  we may, therefore, write

$$V_t^2 = \frac{4.44}{10^8} \times \frac{f\Phi}{T} \times EI = k_1 \times \frac{f\Phi}{T} \times \text{volt-amperes}$$



whence

$$V_t = \frac{1}{k \sqrt{TI/f\Phi}} \times \sqrt{\text{volt-amperes}}$$

An analysis of the terms under the radical in the denominator of the above equation shows that, for a given frequency  $f$ , the ampere-turns are directly proportional to volt-amperes, while the flux  $\Phi$  is inversely proportional to volt-amperes. This means that the denominator has an approximately constant value for an efficient and economical design of a given type, without reference to the output. This permits of the formula being put in the form

$$V_t = \frac{1}{c} \times \sqrt{\text{volt-ampere output}} \quad (129)$$

The following numerical values are the usual limits for the coefficient  $c$ . An average value may be assumed for preliminary designs.

Core type (distribution).....	$c = 40$ to $70$
Core type (power).....	$c = 30$ to $55$
Shell type (distribution).....	$c = 25$ to $40$
Shell type (power).....	$c = 20$ to $30$

The *low* values of the coefficient  $c$  correspond to *low* voltages and *high* frequencies.

**130. Usual Limits of Flux Density and Current Density.** As a guide for use in preliminary designs, usual values of  $B''$  (maxwells per square inch) are given below:

APPROXIMATE VALUES OF  $B''$  IN TRANSFORMER CORES

	$f = 25$	$f = 50$ or $60$
Distribution transformers.....	75,000 to 90,000	70,000 to 85,000
Power transformers.....	85,000 to 95,000	80,000 to 95,000

Curves giving the total watts per pound of built-up transformer stampings are given in Fig. 154.

**Current Density in Windings.** Even with well-ventilated coils (air-blast), or improved methods of producing good oil circulation, the permissible current density in the copper windings is limited by local heating. If the watts lost per pound of copper exceed a certain amount, there will be danger of internal temperatures sufficiently high to cause injury to the insulation. As a rough guide in deciding upon suitable values for final dimensions in a preliminary design, the following approximate figures may be used:

AVERAGE VALUES OF CURRENT DENSITY ( $\Delta$ )  
IN COMMERCIAL TRANSFORMERS

Type of transformer	Amp per sq in.
Standard distribution transformers (oil-immersed, self-cooled) .....	900 to 1,600
Transformers for use in central generating stations, or substations (oil-cooled, or air-blast).....	1,500 to 2,100
Large, carefully designed transformers, oil-insulated, with forced circulation of oil, or with water-cooling coils.....	1,800 to 2,600

Since copper has a resistivity of 1 ohm per cir-mil in. at 60°C, it will be  $(234.5 + 75)/(234.5 + 60) = 1.05$  ohms at 75°C. Also, 1 cu in. of

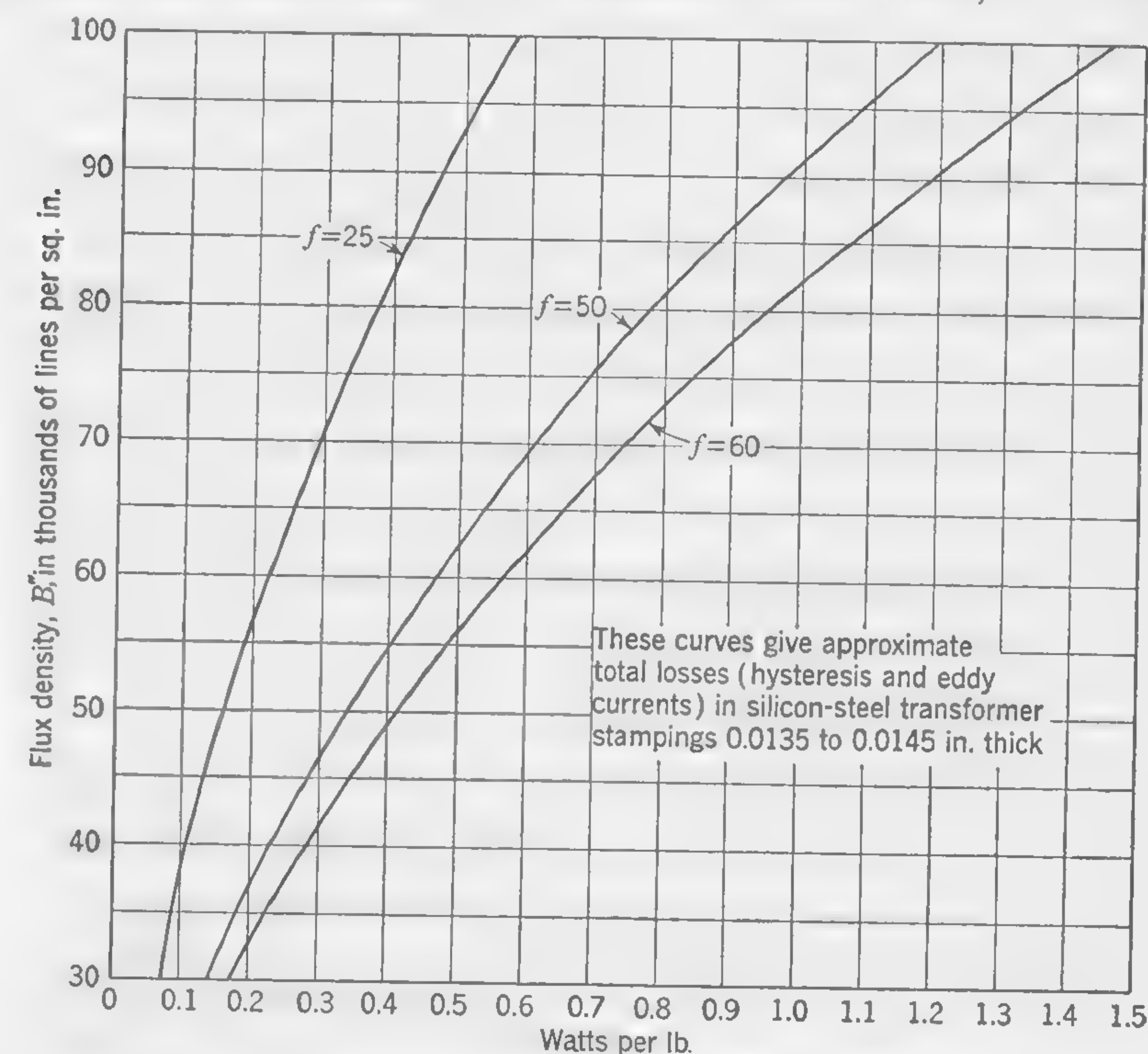


FIG. 154. Curves for calculating core loss in transformers.

copper, 1 in. long and 1 sq in. in cross section, has an area of  $(4/\pi) \times 10^6$  cir mils; moreover, the current  $I$  and the current density  $\Delta$  are numerically equal for a cross section of 1 sq in. It follows, therefore, that

$$\text{Watts lost per cubic inch of copper} = \frac{\Delta^2 \times 1.05}{4/\pi \times 10^6} = \frac{0.825\Delta^2}{10^6} \quad (130)$$

and since 1 cu in. of copper weighs 0.32 lb

$$\text{Watts lost per pound of copper} = \frac{0.825\Delta^2}{0.32 \times 10^6} = \frac{2.57\Delta^2}{10^6} \quad (131)$$



Both Eqs. (130) and (131) may be used to make rapid calculations regarding the probable copper loss when selecting a suitable value of  $\Delta$ .

**131. Insulation.** The solid materials used to insulate transformer windings must be mechanically strong, must have high dielectric strength, and must not be soluble in oil.\* For comparatively low voltages, these materials, including cotton tape, empire cloth, micanite, pressboard, horn paper, and other special products used to separate the windings from the core or framework, should have a total thickness of approximately the following values:

Voltage	Insulation thickness, mils
220	40
440	45
1,000	55
2,400	80

Modern transformers are nearly all of the oil-immersed type. Mineral oil is generally used, its main function (apart from its good insulating qualities) being to transfer the heat by convection from the heated surfaces to the outside walls of the containing case, or to the water-cooling coils when these are provided. Dry oil will withstand pressures up to 50,000 volts alternating between metal disks 0.5 in. in diameter with a separation of 0.2 in. However, since the presence of an extremely small percentage of water reduces the insulating properties of oil considerably (about 25 parts of water per million by volume lowers the dielectric strength approximately 50 per cent), the National Electrical Manufacturers Association specifies that "Transformer oils shall be capable of withstanding at commercial frequencies, 22,000 volts between 1 in. disc-terminals spaced 0.10 in. apart." The good insulating qualities of oil suggest that only small clearances would be required in transformers, even for high voltages; but, since the form of the surfaces separated by the layer of oil will have a considerable effect upon the *concentration* of the dielectric flux density, and, therefore, upon the voltage gradient, it is generally necessary to apply a reasonable factor of safety to the values previously given. For example, if 100,000 volts breaks down a layer of oil between two parallel flat electrodes 4 in. in diameter with a separation of 1 in., the same pressure will spark across a distance of about 3.5 in. between a disk and a needle point.

Partitions of solid insulation, such as pressboard or fuller board, are always advisable in the spaces occupied by the oil, since they will prevent the lining up of particles consisting of partly conducting impurities along

\* MINER, D. F., "Insulation of Electrical Apparatus," pp. 207-215, McGraw-Hill Book Company, Inc., 1911.

the lines of force and so reduce the total clearance which would otherwise be necessary.

With one or more partitions of solid insulating material to keep the width of any one oil duct between the limits of  $\frac{3}{16}$  and  $\frac{5}{16}$  in., a practical formula for determining the total insulation space (including oil) between the high-voltage windings and the low-voltage windings or laminated core is

$$\text{Insulation thickness (inches)} = 0.2 + 0.035 \text{ kv} \quad (132)$$

where kv stands for the rms value of the kilovolts that may exist between the windings or between windings and grounded metal. With carefully designed insulation the total thickness may be somewhat less than that given by formula (132) for extra-high-voltage transformers.

With coils that are rectangular in shape, or when there are corners or projections on one or both metallic surfaces separated by the insulation, the depth of insulation should be increased by about 25 per cent because the higher flux concentrations lead to higher voltage gradients.

For oil-immersed insulation, a practical rule for determining the creepage distance, in inches, is

$$\text{Surface distance (under oil)} = 0.25 + 0.07 \text{ kv} \quad (133)$$

where kv, as before, is in operating pressure in kilovolts.

Concerning high-voltage transformers, *i.e.*, 6,900 volts and higher, it is especially important that the end turns be insulated against the possibility of breakdown due to surges. Suggested recommendations are that 2.5 per cent of the windings at the end be given special insulation treatment up to 10,000 volts, and that  $\frac{1}{2}$  per cent be added for each increase of 10,000 volts, up to a total of about 15 per cent for 220,000-volt transformers.

In concluding this article on insulation design, it may be well to point out that it is very much more difficult to predetermine the behavior of high-voltage insulation from design data than the performance of an electromagnetic device or a rheostat under specified conditions. Usually, much experimental work has to be done, and modifications must be made in preliminary designs before the best and most economical insulation is obtained for any new type or size of high-voltage apparatus. The voltage gradient where the stress is greatest is not easy to determine except for a few simple shapes of electrodes, and, even when we are able to calculate this, there is no definite value for the "disruptive gradient" of solid insulation. The breakdown voltage or disruptive gradient is really a function of the temperature. Heating is caused by the application of the electrostatic stress (whether a-c or d-c) and, even, with high enough pressures to puncture the insulation, a certain time lag occurs between the



application of the voltage and the breakdown of the dielectric. The reason why the volts *per mil of thickness* which will puncture a sheet of any given insulating material are less for thick sheets than for thin sheets is that, with the thinner sheets, much of the heat is conducted away to the metal; but, with the thicker insulation, the heat is not so easily dissipated and the voltage gradient which will cause puncture is, therefore, lowered. The economical design of insulation for use on high-pressure systems is thus seen to be a matter involving the careful investigation of many special problems, backed by a large amount of experimental data.

**132. Space Factors.** The copper space factor is the ratio between the cross section of copper in a given space and the total cross section

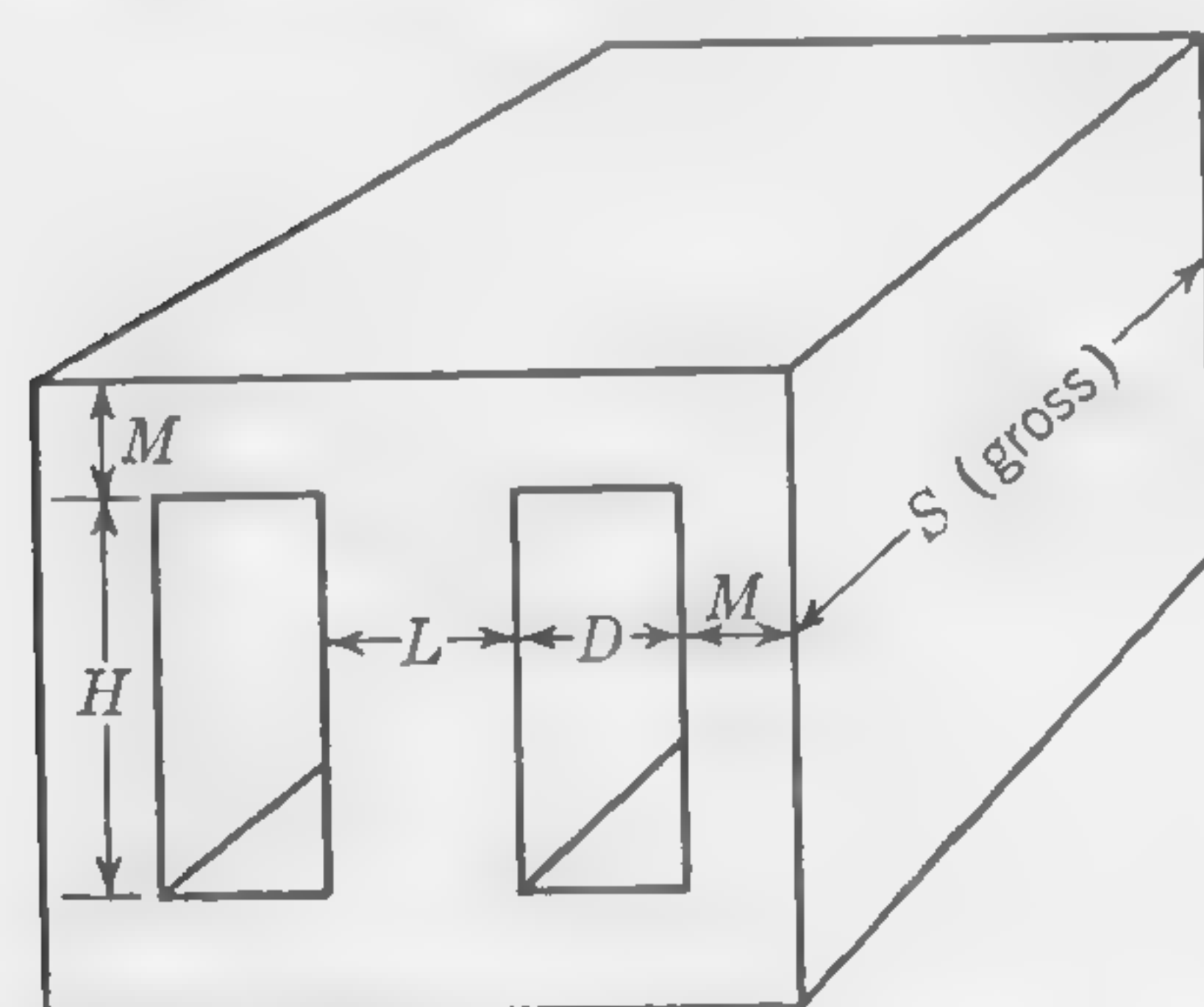


FIG. 155. Assembled stampings of single-phase shell-type transformer.

including the insulation and air or oil spaces. If we can estimate a space factor before going into the details of insulation, this will enable us to determine the probable dimensions of the "window" which must accommodate the windings and insulation. The amount of insulation and clearance space between high-tension windings and grounded core, or between the primary and secondary coils, will depend upon the voltage. The copper space factor will depend upon the voltage of both the primary and secondary windings and also upon the size, or output, of the transformer. The formula

$$sf = \frac{10}{30 + kv} \quad (134)$$

in which  $kv$  stands for the kilovolts at the high-tension terminals, will give approximate values of the winding space factor for transformers between 50- and 200-kva output. This factor will be larger for large transformers and smaller for small transformers. It might have to be 20 per cent larger than that calculated by formula (134) for transformers of 1,000 kva or more, and 20 per cent smaller for transformers having ratings up to about  $7\frac{1}{2}$  kva output.

**133. Usual Proportions of Built-up Cores.** Figure 155 shows the assembled iron stampings of a single-phase shell-type transformer. The area of the window opening for the two sets of coils is

$$H \times D = \frac{2(TI)}{\Delta \times sf}$$

and the height of the opening  $H$  is usually from  $2\frac{1}{2}$  to  $3\frac{1}{2}$  times the width  $D$ . For the assembled core the usual proportions are

$$S = 2 \text{ to } 3 \text{ times } L$$

$$M = 0.5 \text{ to } 0.75 \text{ times } L$$

The reason why  $M$  is frequently made greater than  $\frac{1}{2}L$  is that the length per turn of the winding may be kept small by forcing the flux density to fairly high values in the core inside the coils, while permitting a lower flux density (to avoid too great a loss in the iron) in the portion of the magnetic circuit outside the coils. Figure 156 shows the assembled iron stampings

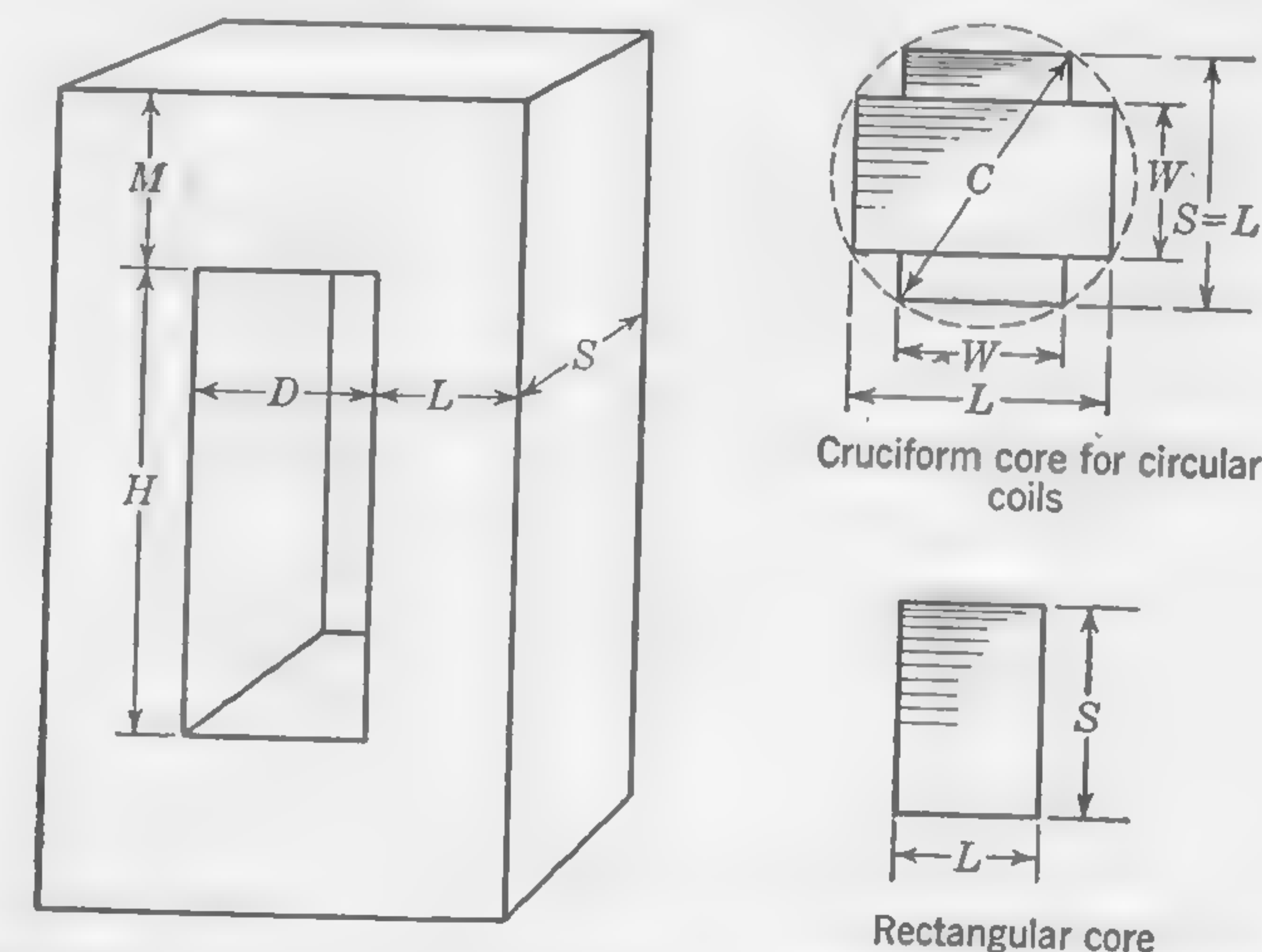


FIG. 156. Assembled stampings of single-phase core-type transformer.

of a single-phase core-type transformer. The dimensions for the window are determined by making the ratio  $H/D = 2.5$  to  $3.5$ . If circular coils are used (which is customary in high-voltage distribution and large power transformers of this type); the cruciform section of core limb, as illustrated in Fig. 156, is preferable to a square section, because it allows a greater cross section of iron within the coil. The relations between the dimensions  $C$ ,  $W$ , and  $L$  to give the largest core cross section for a constant diameter  $C$  (where the cruciform has one notch, *i.e.*, one step), as measured across corners, may be obtained as follows. The gross area of cross section is  $2WL - W^2$ . If we differentiate and put the result equal to zero, we have,

$$2 \left( W \frac{dL}{dW} + L \right) - 2W = 0 \quad (a)$$

Also,  $W^2 + L^2 = C^2$ , from which we can obtain a value for  $dL/dW$  to substitute in Eq. (a). Thus,

$$2WdW + 2LdL = 0$$



whence

$$\frac{dL}{dW} = -\frac{W}{L}$$

Substituting in Eq. (a) and solving for  $W$  in terms of  $L$  or  $C$ , we get

$$W = 0.618L \quad \text{and} \quad W = 0.525C$$

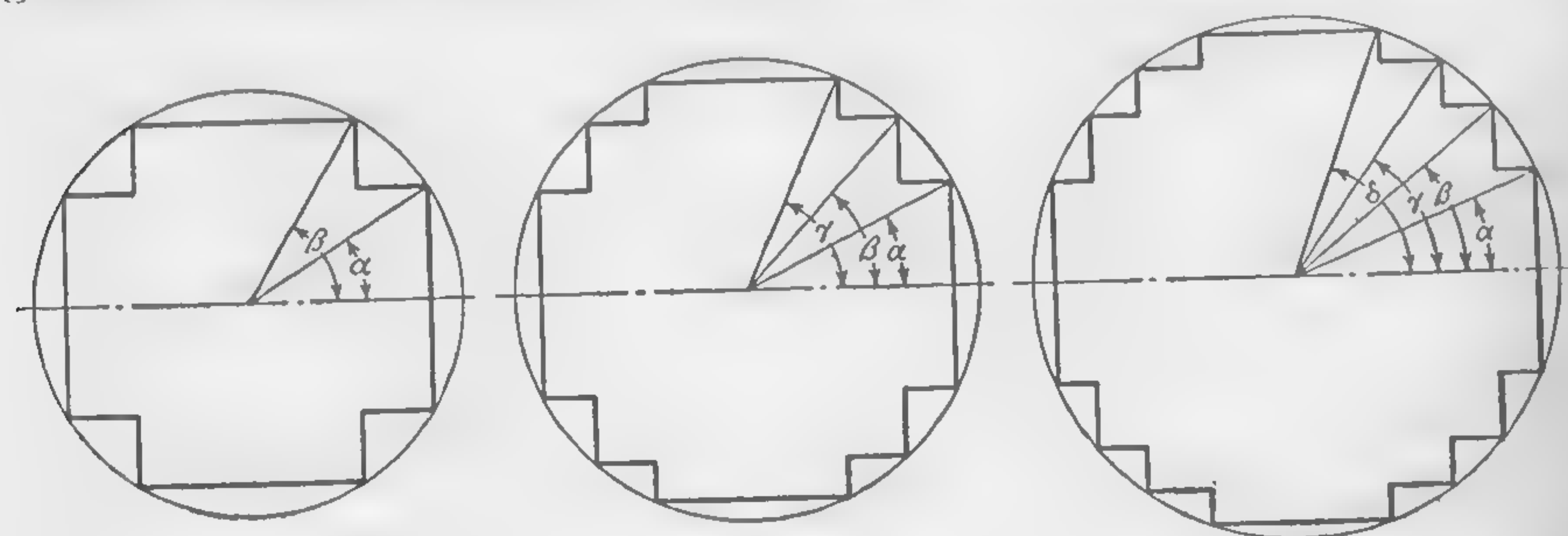
Also, the value of  $L$  in terms of  $C$  is

$$L = 0.85C$$

If it is more convenient to lay out the cruciform in terms of  $\alpha$  and  $\beta$ , Fig. 157a, these are

$$\alpha = \tan^{-1} \frac{\frac{1}{2}W}{\frac{1}{2}L} = \tan^{-1} \frac{0.525}{0.85} = 31.7^\circ \quad \text{and} \quad \beta = \tan^{-1} \frac{0.85}{0.525} = 58.3^\circ$$

For large transformers requiring comparatively large core areas it is generally more economical to design the cruciform sections with two,



$$(a) \alpha = 31.7^\circ \quad \beta = 58.3^\circ$$

$$(b) \alpha = 25.7^\circ \quad \beta = 45.7^\circ \\ \gamma = 64.3^\circ$$

$$(c) \alpha = 21.9^\circ \quad \beta = 38.3^\circ \\ \gamma = 53.5^\circ \quad \delta = 68.1^\circ$$

FIG. 157. One-, two-, and three-step cruciform sections, showing the important angular dimensions for their construction.

three, or more notches, *i.e.*, steps. Derived equations, similar to those given for the one-notch cruciform, indicate that for maximum cross sections, the various angles  $\alpha$ ,  $\beta$ ,  $\gamma$ , and  $\delta$  are as shown on the sketches of Figs. 157b and c.

It is important to remember that the *net* cross section of the core is obtained by multiplying the gross cross section by the stacking factor which usually lies between 0.86 and 0.9 if there are no air or oil ducts between sections of the core. In large transformers it is usual to provide such ducts from  $\frac{1}{4}$  to  $\frac{1}{2}$  in. wide to avoid excessive temperatures in the core, and the necessary correction must then be made in calculating the net cross section.

In small transformers of the core type, the cruciform core section would be too costly, and it is generally preferable to use a rectangular section, in which case a good proportion is  $S = 1.5L$ . If  $H$  is made equal to

about  $2.5D$ , this will be found to be a good proportion for the opening in this type of transformer for small outputs when wound for the usual voltages of lighting circuits. The dimension  $M$  is from 1 to 1.5 times  $L$ .

**134. Arrangement of Coils—Leakage Reactance.** The arrangement of the coils in the space  $H \times D$  will have a considerable influence upon the amount of the leakage flux and, therefore, upon the  $IX$  drop and voltage regulation. (The manner in which the  $IX$  drop may be calculated is explained in Art. 137.) For small shell-type transformers (up to 15 or 20 kva) the arrangement of Fig. 158 is satisfactory. This shows

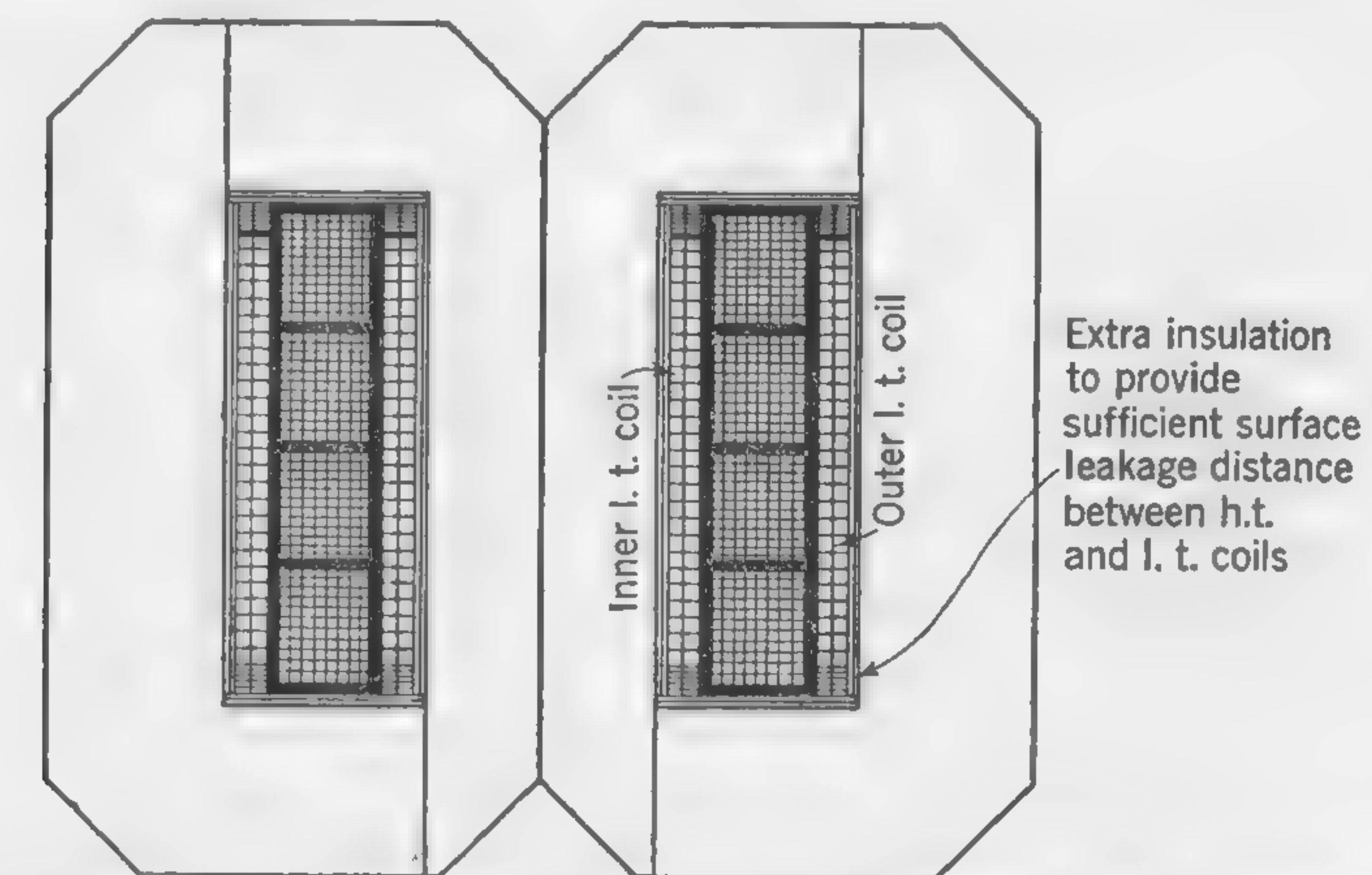


FIG. 158. Cross section through small shell-type transformer (solid insulation between windings).

the high-tension winding between two low-tension coils, which provides what is known as two *high-low sections*, because there are two gaps between primary and secondary windings which will be paths for leakage-flux lines. *The greater the number of high-low sections, the smaller will be the reactive voltage drop*, not because there are more paths for the leakage flux, but *because there are fewer ampere-turns setting up flux in these paths*. It will be observed that the high-voltage coil is divided into several sections (in this instance, four). This is done to reduce the difference of potential which would otherwise exist between the layers of the winding. The volts per coil, even in high-voltage transformers, rarely exceed 5,000.

Many designers prefer the arrangement of coils shown diagrammatically in Fig. 163, for both large and small shell-type transformers. This consists of two groups of high-voltage coils "sandwiched" between three groups of low-voltage coils, the center group having twice the number of turns of either of the two outside groups. The mean length per turn of all the coils is the same, and the arrangement provides four equal high-low sections.



Core-type transformers may have the coils arranged as in Fig. 159a, providing a total of four high-low sections, or as in Fig. 159b, providing a total of two high-low sections. The reactive voltage drop will be less with the arrangement as at (a), but it is not usually excessive with the simpler arrangement as at (b), in which less space is taken up by the insulation. The high-voltage winding will usually consist of two or more coils stacked one above the other, as shown in Fig. 158.

**135. Calculation of Exciting Current.** When calculating the magnetizing current for an induction motor (refer to Art. 112), the reluctance of

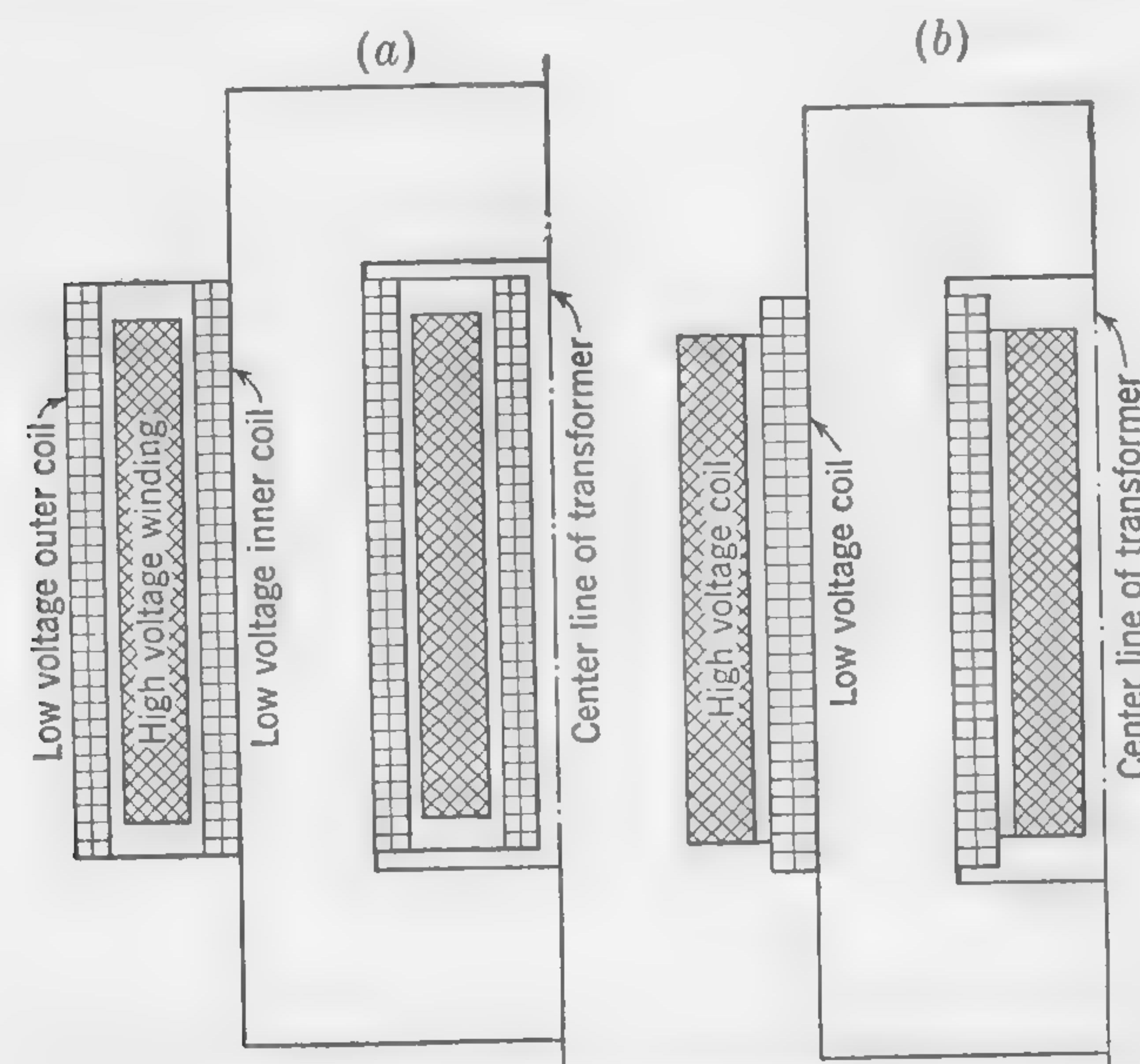


FIG. 159. Alternative arrangement of windings in core-type transformer.

the iron was estimated, being small in comparison with that of the air gap; but in a transformer, with its closed iron circuit, the reluctance of the iron is the important factor.

The exciting current  $I_e$  may be thought of as consisting of two components: (1) the magnetizing component  $I_o$  in phase with the magnetic flux, and (2) the "energy" component  $I_w$  leading  $I_o$  by one-quarter period, and, therefore, opposite in phase to the induced emf.

The magnitude of the  $I_w$  component depends on the amount of the iron losses only, because the very small copper losses may be neglected.

If these components could be considered sine waves, the vector construction of Fig. 160 would give correctly the magnitude and phase of the total exciting current  $I_e$ . For values of flux density above the knee of the  $B$ - $H$  curve, the instantaneous values of the magnetizing current

are no longer proportional to the flux, and this component of the total exciting current cannot, therefore, be regarded as a sine wave, even if the flux variations are sinusoidal. The error introduced by using the construction of Fig. 160 is, however, usually negligible, because the exciting current is a very small fraction of the total primary current.

The notes on Fig. 160 are self-explanatory, but reference should be made to Fig. 161, from which the ampere-turns per inch of the iron core may be read for any value of the (maximum) flux density; in practice, it is generally customary, and more accurate, to refer to the magnetization curves provided by the manufacturer of the steel used in the construction of the transformer. The flux density is given in maxwells per

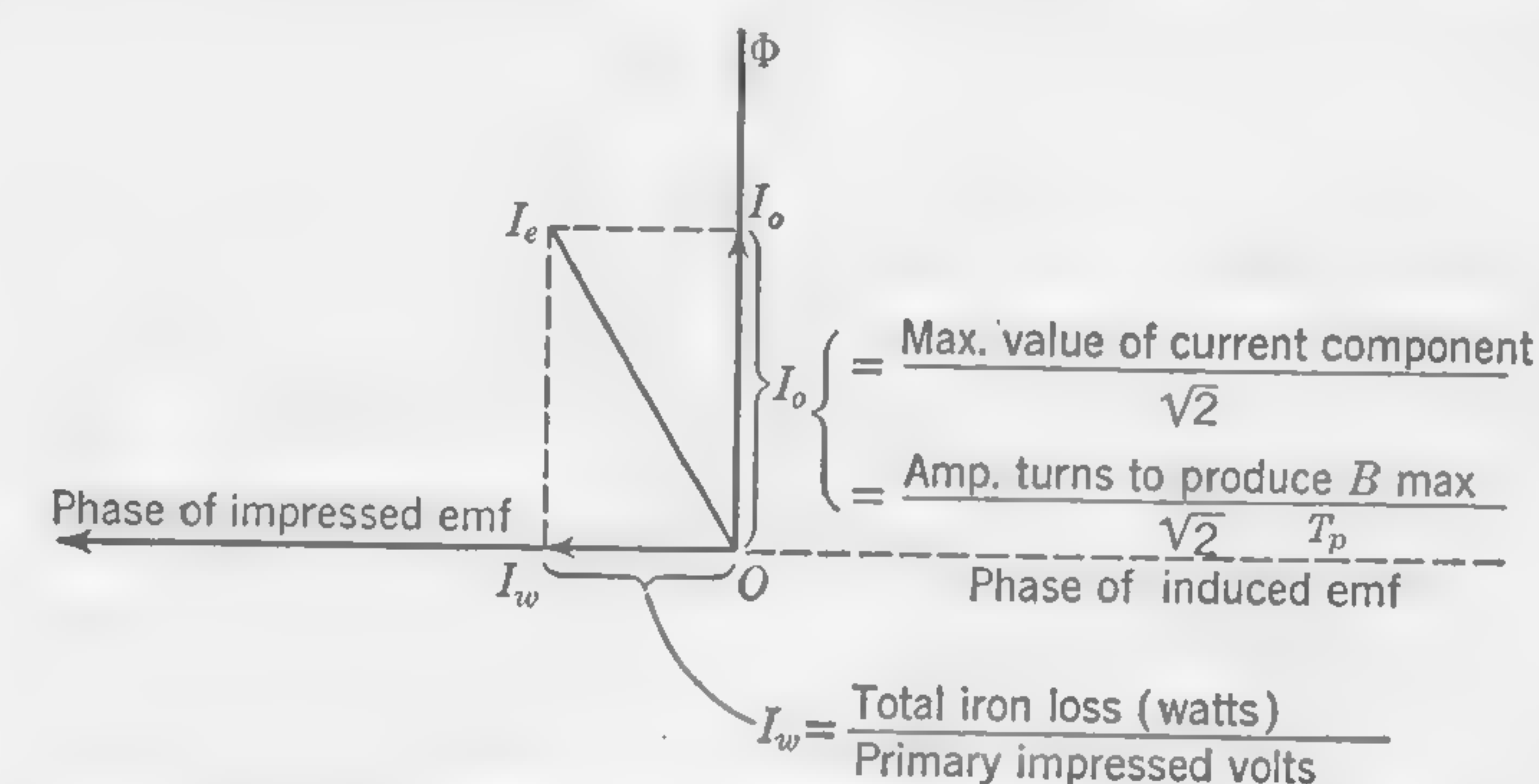


FIG. 160. Vector diagram showing components of exciting current.

square inch equal to the number read from the curve multiplied by the mean length of path of the flux which links with both primary and secondary coils.

**Ampere-turns for Joints.** The joints in the magnetic circuit may be thought of as consisting of very short air paths in parallel with iron paths, as indicated by the sketch (Fig. 162). This accounts for the shape of the curves of Fig. 162 which give the approximate ampere-turns for one joint. The total additional ampere-turns required to overcome the reluctance of the joints are obtained by multiplying the figure read off the curve by the number of joints in series in the magnetic circuit. The quantity  $B''$  is the maximum value of the flux density in the iron of the core on each side of the joint.

**136. Magnetic Leakage in Transformers—Voltage Regulation.** Assuming the voltage applied to the terminals of a transformer to remain constant, it follows that the flux linkages necessary to produce the required back emf can readily be calculated. The (vectorial) difference between the applied volts and the induced volts must always be exactly equal to the ohmic drop of pressure in the primary winding. Thus, the total primary flux linkages (which may include leakage lines) must be



such as to induce a back emf very nearly equal to the applied emf—the primary  $IR$  drop being comparatively small.

When the secondary is open-circuited, practically all the flux linking with the primary turns links also with the secondary turns; but when the

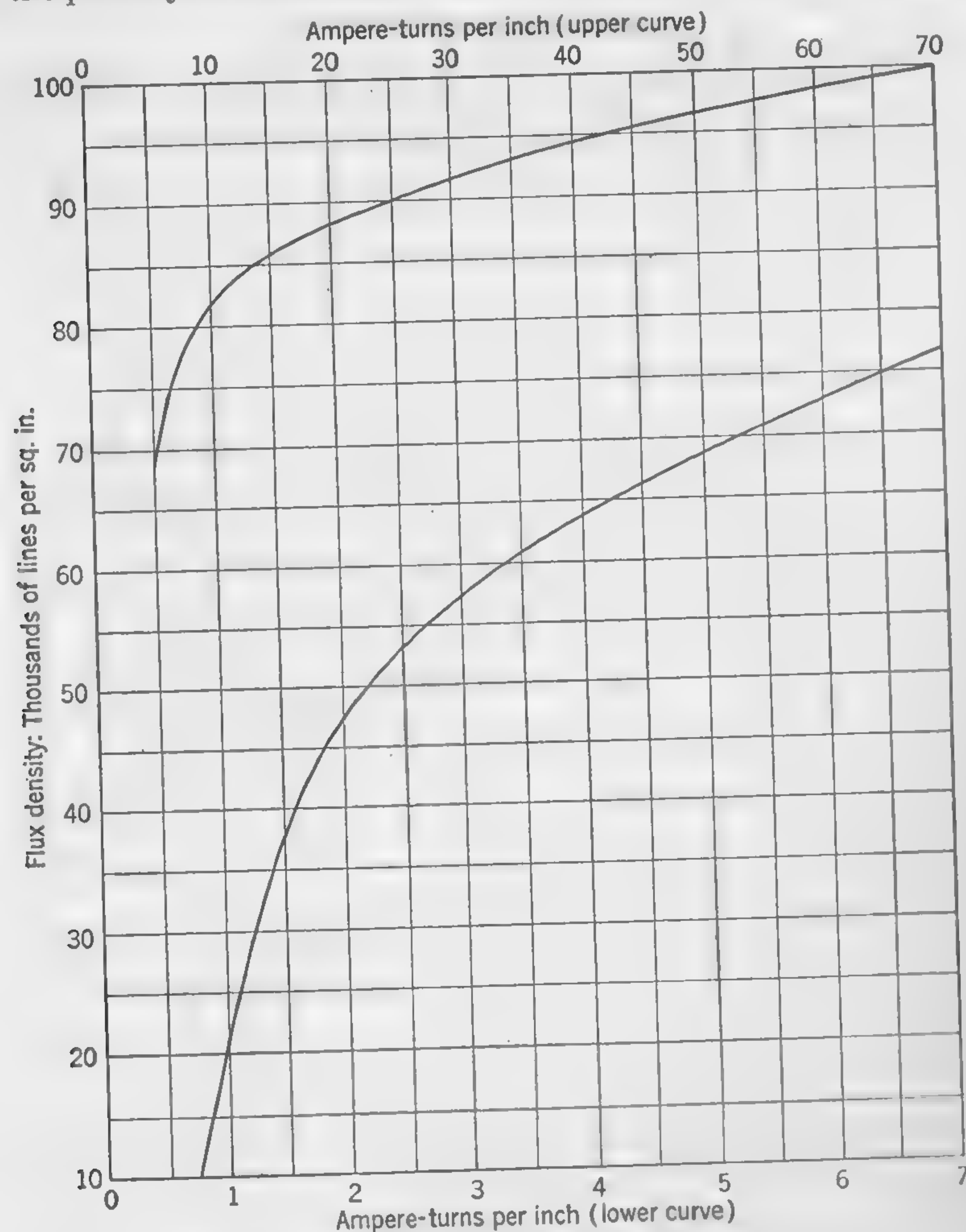


FIG. 161. Magnetization curves for transformer iron.

transformer is loaded, the mmf due to the current in the secondary winding has a tendency to modify the flux distribution, the action being as follows:

The mmf due to a current  $I_s$  flowing in the secondary coils would have an immediate effect on the flux in the iron core if it were not for the fact that the slightest tendency to change the number of flux lines through the primary coils instantly causes the primary current to rise to a value

$I_p$ , so that the resultant ampere-turns (the vector difference between  $I_p T_p$  and  $I_s T_s$ ) will produce the exact amount of flux required to develop the necessary back emf in the primary winding. Thus, the total amount of flux linking with the primary turns will not change appreciably when current is drawn from the secondary terminals; but the secondary mmf—together with an exactly equal but opposite primary magnetizing effect—will cause some of the flux which previously passed through the secondary core to “spill over” and avoid some, or all, of the secondary turns. This reduces the secondary volts by an amount exceeding what can be accounted for by the ohmic resistance of the windings.

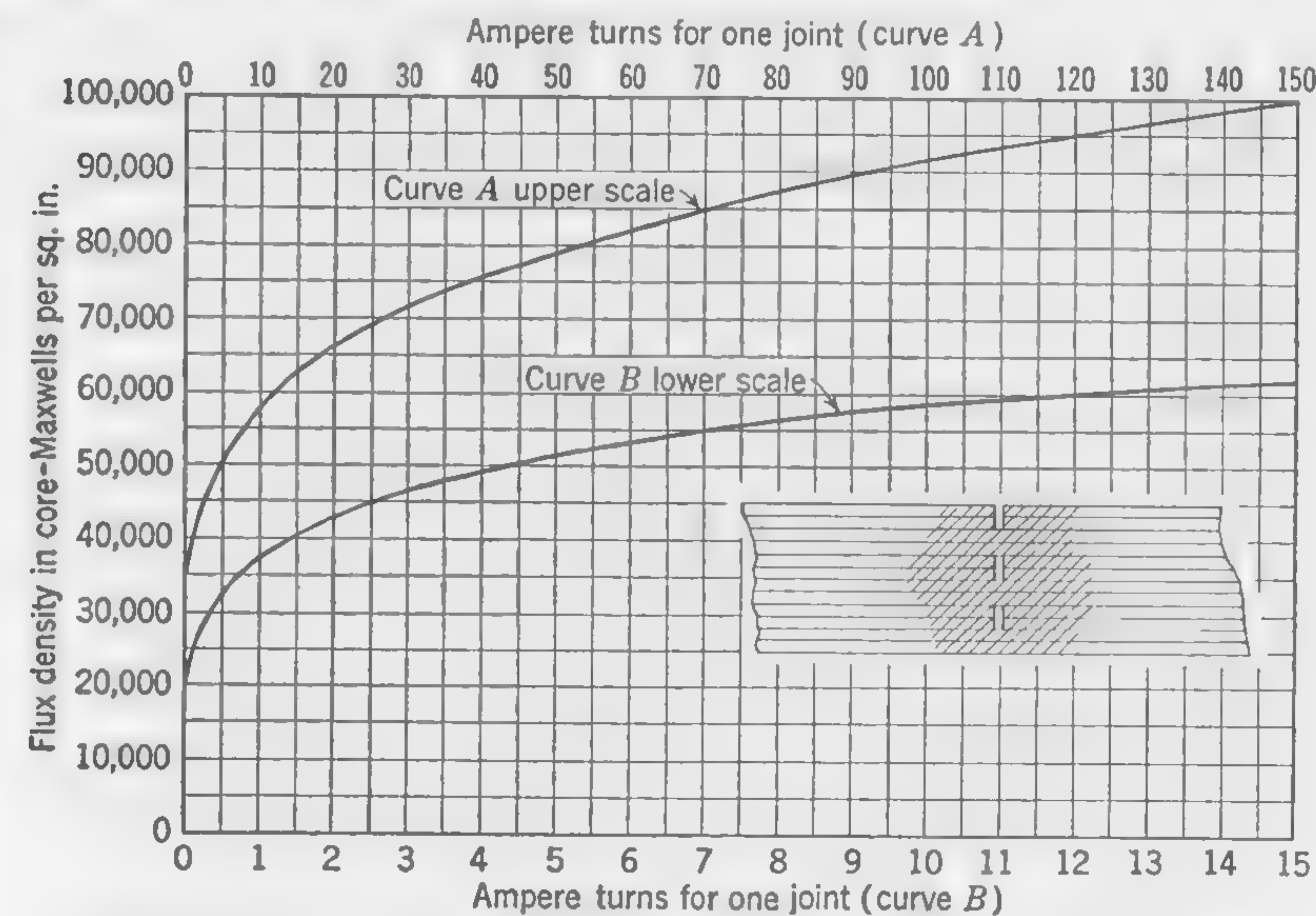


FIG. 162. Ampere turns of excitation for joints in transformer cores.

In order to predetermine the probable reactive voltage drop caused by magnetic leakage, the amount of the leakage flux must be calculated. What we actually desire to know is the amount of an equivalent flux which may be thought of as linking with all the primary turns while failing to link with any of the secondary turns. An alternative method of determining the effect of leakage flux on the voltage is to consider each small element of leakage flux as linking or not linking with a particular number of turns of the primary and secondary windings, and then adding together all these small elements of the total  $IX$  drop. The manner in which this may be done is explained in the following article.

**137. Calculation of Reactive Voltage Drop.** The windings on any transformer, because of their symmetrical arrangement, can usually be divided into a number of *equal* high-low sections; that is to say, a number of sections each consisting of a high- and a low-tension coil, or a



portion of a high- and a portion of a low-tension coil, with a space between them occupied by the insulation—whether oil, air, or solid material. These unit high-low sections are indicated in Fig. 163, which refers to a shell-type transformer with two groups of high-voltage and four groups of low-voltage coils (two of these being put together at the center). This

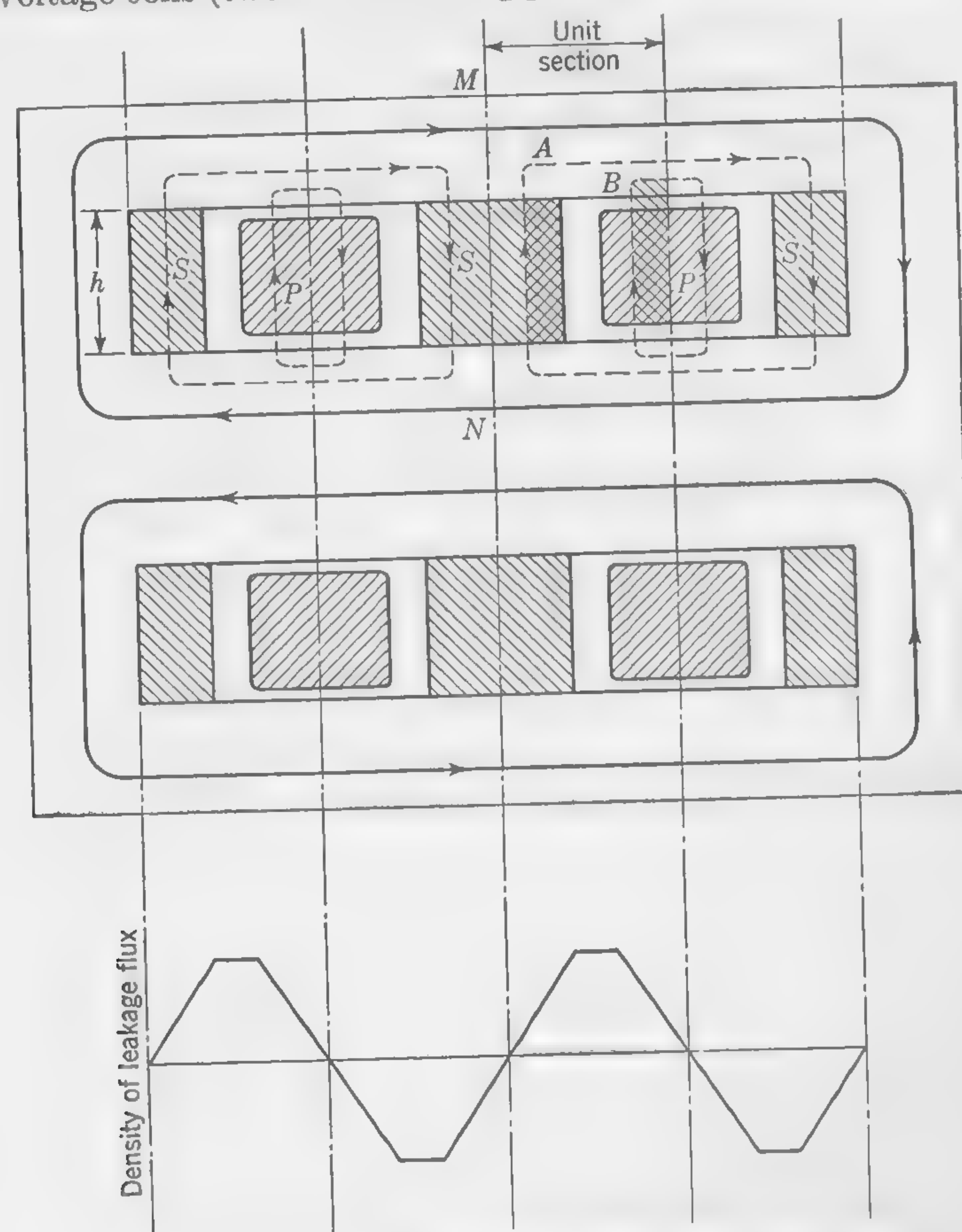


FIG. 163. Section through coils of shell-type transformer.

provides a total of four similar high-low sections in which the ampere-turns are all of the same amount, so that it is merely necessary to calculate the voltage drop in one such unit section and then multiply the result by 4 in order to obtain the total  $IX$  drop due to leakage flux.

The broken line at the bottom of Fig. 163 indicates the distribution of leakage-flux density through the coils and in the spaces between the coils.

The effect of all leakage lines in the gap between coils is to produce a back emf in the primary without affecting the voltage induced in the secondary by the main component of the total flux (represented by the

full line linking with all the primary and secondary coils). Of the other leakage lines,  $B$  links with only a portion of the primary turns and has no effect upon the primary turns which it does not link with; while  $A$  links not only with all the primary turns, but also with a certain number of secondary turns. Note that if the line  $A$  were to coincide with the dotted center line  $MN$ , marking the limit of the unit section under consideration, it would have no effect upon the transformer regulation, because flux which links equally with primary and secondary is not leakage flux. Actually, the line  $A$  links with all the primary turns of the half coil in the section under consideration, but with only a portion of the secondary turns in the same section. Its effect is, therefore, exactly as if

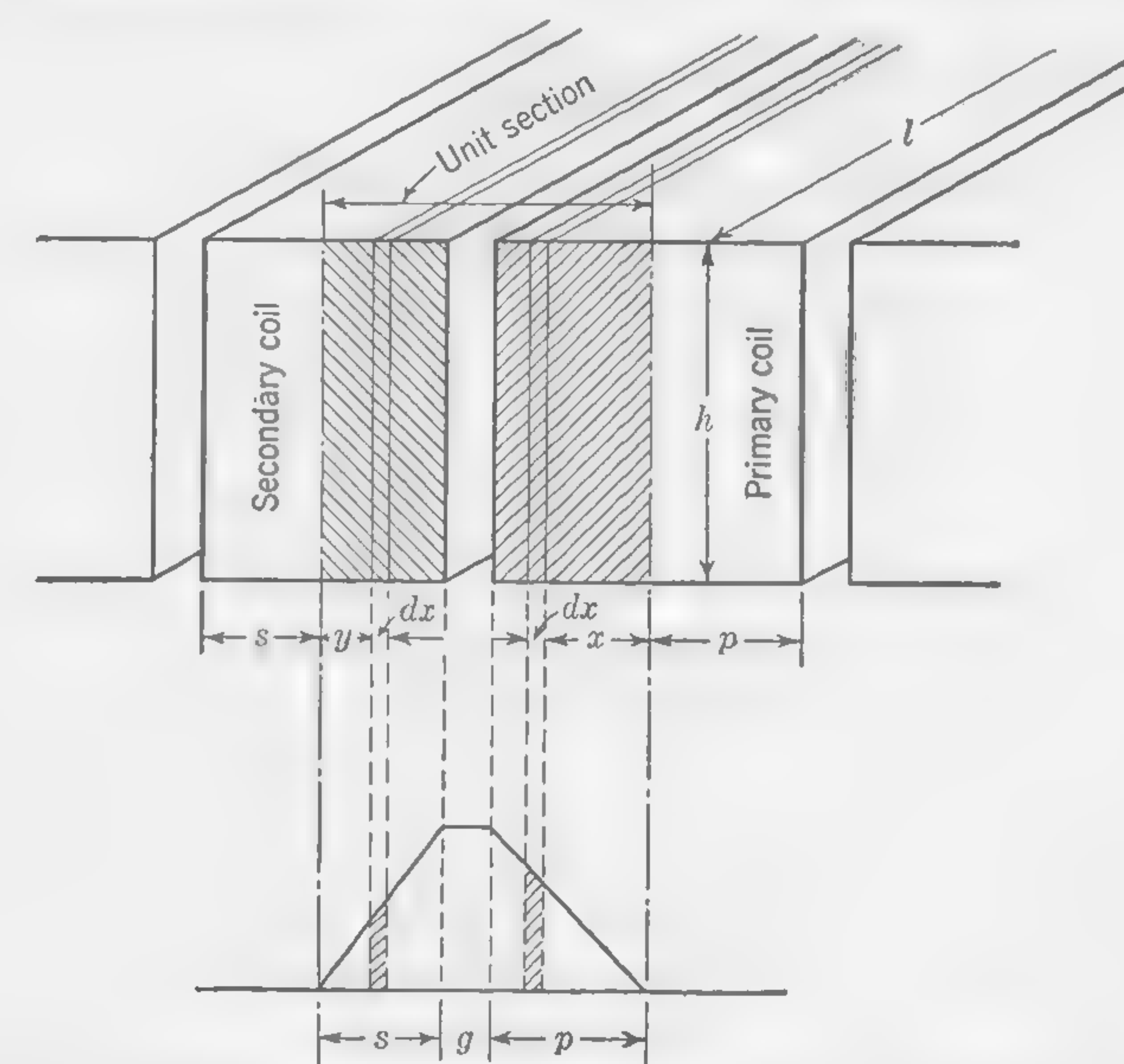


FIG. 164. Representing one high-low section of transformer winding.

it linked with only a fractional part of the primary. The mathematical development which follows is based on these considerations.

Figure 164 is an enlarged view of the unit section of Fig. 163, the length of which—measured perpendicularly to the cross section—is  $l$  cm. All the leakage is supposed to be along parallel lines perpendicular to the surface of the iron core above and below the coils. It is desired to calculate the reactive voltage drop in a section of winding of length  $l$  cm, depth  $h$  cm, and total width  $(s + g + p)$  cm,

where  $p$  and  $s$  = thickness of primary and secondary parts, respectively, of one unit high-low section (in Fig. 164 these symbols stand for half the thickness of a coil)

$g$  = the space between primary and secondary coils



The dimension  $h$  should be taken to include the insulation, being the height of the opening from iron to iron, as indicated in Fig. 163.

The voltage drop caused by the leakage flux in the spaces  $g$ ,  $p$ , and  $s$  will be calculated separately and the results added together to obtain the total reactive voltage drop.

The volts induced by an alternating flux of  $\Phi$  maxwells linking with  $T$  turns of wire are given by formula (125) on page 340 which may be put into the form

$$IX = 4.44f\Phi T \times 10^{-8} \quad (a)$$

but

$$\begin{aligned} \Phi &= \text{mmf} \times \text{permeance} \\ &= 0.4\pi TI_{\max} \times P \\ I &= 0.4\pi T(\sqrt{2}I)P \end{aligned} \quad (b)$$

Substituting formula (b) in formula (a)

$$\begin{aligned} IX &= \left( \frac{4.44 \times 0.4\pi \times \sqrt{2}f}{10^8} \right) (TI)P \times T \\ &= \frac{7.88f}{10^8} (TI)P \times T \end{aligned}$$

Putting  $7.88f/10^8 = m$ , the general formula for reactive drop becomes

$$IX = m(TI)P \times T \quad (c)$$

The symbols  $T_1$  and  $T_2$  will be used to denote the number of turns in the primary and secondary windings, respectively, of a unit high-low section. The meaning of the variables  $x$  and  $y$  is indicated in Fig. 164.

For the section  $g$  we have

$$(IX)_g = m(T_1 I_1) \frac{lg}{h} \times T_1 \quad (d)$$

In the section  $p$ , the mmf producing the element of flux in the space of width  $dx$  is due to the current  $I_1$  in  $(x/p)T_1$  turns, and, since this element of flux links with only  $(x/p)T_1$  turns, we have

$$\begin{aligned} d(IX)_p &= m \left[ \left( \frac{x}{p} \right) T_1 I_1 \right] \frac{ldx}{h} \times \left( \frac{x}{p} \right) T_1 \\ (IX)_p &= m \left[ \frac{T_1^2 I_1 l}{p^2 h} \right] \int_0^p x^2 dx \\ &= m(T_1^2 I_1) \times \frac{lp}{3h} \end{aligned} \quad (e)$$

In the section  $s$ , the mmf producing the small element of flux in the space of width  $dy$  is due to the current  $I_s$  in  $(y/s)T_s$  turns, and, since the

may be considered as *failing* to link with  $(y/s)T_1$  turns, we may write

$$\begin{aligned} d(IX)_s &= m \left[ \left( \frac{y}{s} \right) T_s I_s \right] \frac{ldy}{h} \times \left( \frac{y}{s} \right) T_1 \\ (IX)_s &= m \left[ \frac{(T_s I_s) T_1 l}{s^2 h} \right] \int_0^s y^2 dy \\ &= m(T_s^2 I_s) \times \frac{ls}{3h} \end{aligned} \quad (f)$$

in which the secondary quantities  $T_s$  and  $I_s$  have been eliminated by putting  $(T_1 I_1)$  in place of  $(T_s I_s)$ .

The final expression for the inductive voltage drop in the unit section considered is obtained by adding the quantities in formulas (d), (e), and (f). Thus

$$I_1 X_1 = mx \frac{T_1^2 I_1 l}{h} \left( g + \frac{p+s}{3} \right) \quad (g)$$

wherein the dimensions are in centimeters.

If  $n$  stands for the number of high-low sections, the total  $IX$  drop is  $n(I_1 X_1)$ , and the percentage  $IX$  drop is  $(nI_1 X_1/E_p) \times 100$ . Thus

$$(IX) \text{ per cent} = nx \left( \frac{7.88f}{10^8} \right) \left( \frac{T_1^2 I_1 l}{h} \right) \left( g + \frac{p+s}{3} \right) \frac{2.54 \times 100}{E_p} \quad (h)$$

wherein all dimensions are in inches.

But

$$nT_1 I_1 = T_s I_s \quad (i)$$

Also

$$\frac{nT_1}{T_s} = \frac{E_p}{E_s}$$

so that

$$\frac{T_1}{E_p} = \frac{T_s}{nE_s} \quad (j)$$

Substituting the values of formulas (i) and (j) in formula (h)

$$(IX) \text{ per cent} = \left( \frac{7.88f}{10^8} \right) \left( \frac{T_s I_s l}{h} \right) \left( \frac{T_s}{nE_s} \right) \left( g + \frac{p+s}{3} \right) (2.54 \times 100)$$

Hence

$$(IX) \text{ per cent} = \frac{2fT_s^2 I_s l}{nhE_s \times 10^8} \left( g + \frac{p+s}{3} \right) \quad (135)$$

Note particularly, in formula (135), that the leakage reactance drop is *inversely proportional* to the number of high-low sections  $n$ ; this obviously



means that the greater the degree of subdivision and interlinking, the more closely the individual sections, the high-low sections, of the primary and secondary windings are linked together.

The reluctance of the leakage-flux paths for the parts of the winding which are outside the iron is not easily calculated, but if the length  $l$  in formula (135) is taken equal to the mean length per turn of the windings—expressed in the same units as  $h$ —the formula will yield results which will usually check up fairly closely with test measurements made on the completed transformer.

**138. Transformer Vector Diagram Showing Effects of Leakage Flux.** The sketch of a transformer in Fig. 165 shows primary and secondary

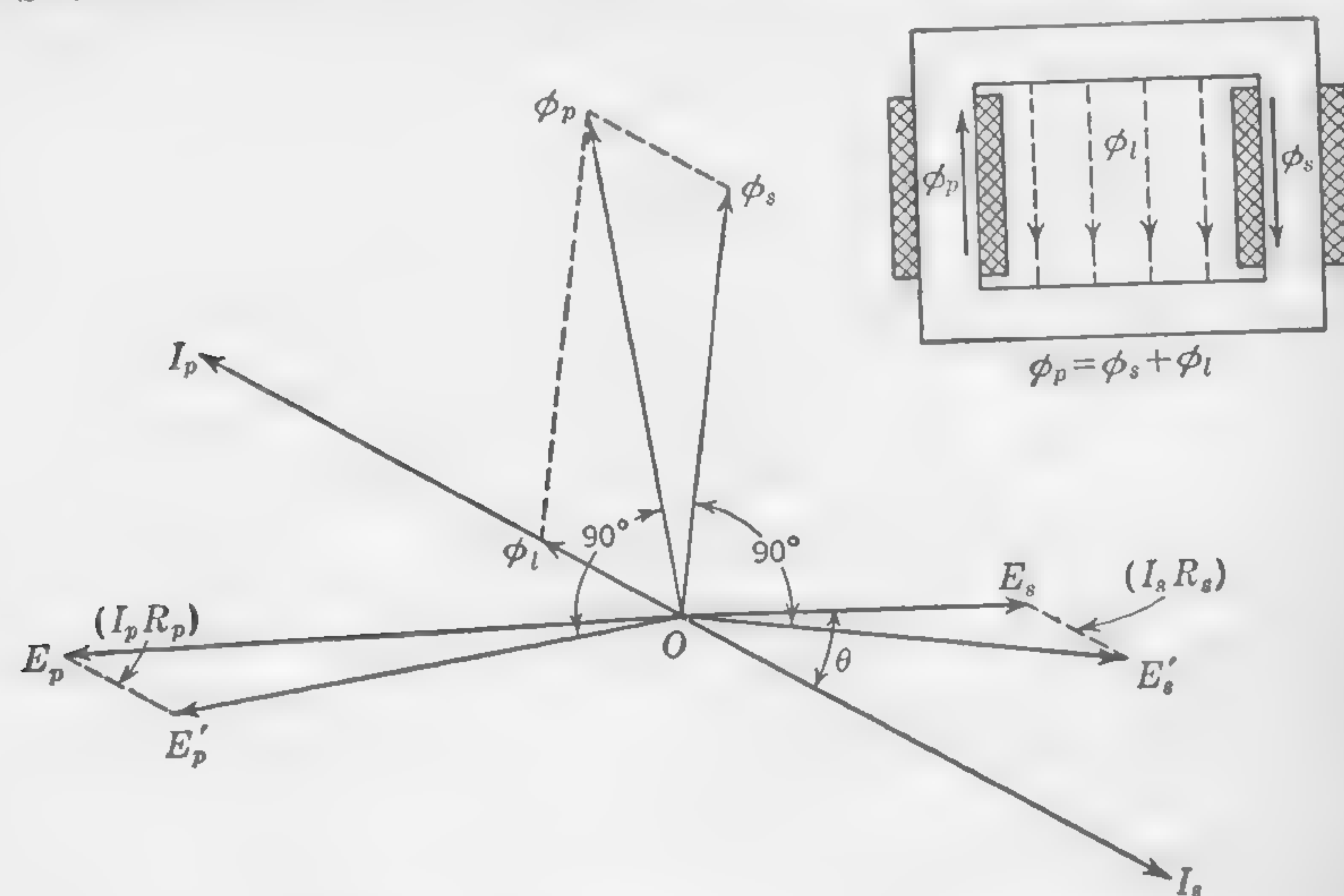


FIG. 165. Vector diagram of transformer with magnetizing component of primary current omitted.

windings on separate limbs of the core, which would be unsatisfactory in practice on account of the excessive amount of the leakage flux. The sketch is intended merely to show, in the simplest manner, the relation between the flux components and to facilitate the explanation of the vector diagram. There are  $\Phi_p$  flux lines linking with the primary,  $\Phi_s$  linking with the secondary, and the leakage flux is  $\Phi_l$ . Obviously, the vectorial sum of  $\Phi_s$  and  $\Phi_l$  must be equal to  $\Phi_p$ . We shall neglect the magnetizing component of the primary current—a very usual and permissible assumption—and construct the vector diagram for a 1 to 1 ratio transformer, assuming that the flux components, or their relative magnitudes, are known.\*

\* If the actual ratio is not 1 to 1, the correction in reading the diagram is made when the transformation ratio is known.

Draw  $OE_s$  and  $OI_s$  to represent the (known) secondary terminal voltage and current with the angle  $\theta$  between them corresponding to a load power factor of  $\cos \theta$ . The other vectors are drawn in the following order:

$E_s E'_s$  parallel to  $OI_s$  and of the proper length to represent the ohmic drop of  $I_s R_s$  volts in the secondary windings

$OE'_s$ , the emf which must be induced in the secondary windings

$O\Phi_s$ , drawn  $90^\circ$  in advance of  $E'_s$ , is the flux which links with the secondary windings

$OI_p$ , equal and opposite to  $I_s$ , is the primary current

$O\Phi_l$ , in phase with  $I_p$ , is the leakage flux

$O\Phi_p$ , the resultant obtained by the vectorial addition of  $\Phi_s$  and  $\Phi_l$ , is the flux which links with the primary windings

$OE'_p$ , drawn  $90^\circ$  in advance of  $\Phi_p$ , is the component of the impressed primary emf necessary to balance the emf induced in the primary windings by the flux  $\Phi_p$

$E'_p E_p$ , parallel to  $I_p$  and of the proper length to represent the ohmic drop of  $I_p R_p$  volts in the primary windings

$OE_p$ , the voltage which must be impressed at primary terminals to produce the secondary conditions which have been assumed

**139. Formulas for Voltage Regulation.** The vector diagram (Fig. 165) may be greatly simplified for the purpose of determining the voltage regulation by omitting the vectors representing magnetic flux, and by substituting for the actual secondary resistance an *equivalent secondary resistance* (refer to Art. 117, where the equivalent resistance of the rotor of an induction motor was discussed) which may be added to the primary resistance and so permit the diagram to be drawn to represent conditions in the primary circuit only. Thus, if  $R$  stands for the total equivalent primary resistance, we may write

$$I_p R = I_p R_p + I_s R_s \left( \frac{T_p}{T_s} \right)$$

but

$$I_s = I_p \left( \frac{T_p}{T_s} \right)$$

therefore

$$R = R_p + R_s \left( \frac{T_p}{T_s} \right)^2 \quad (136)$$

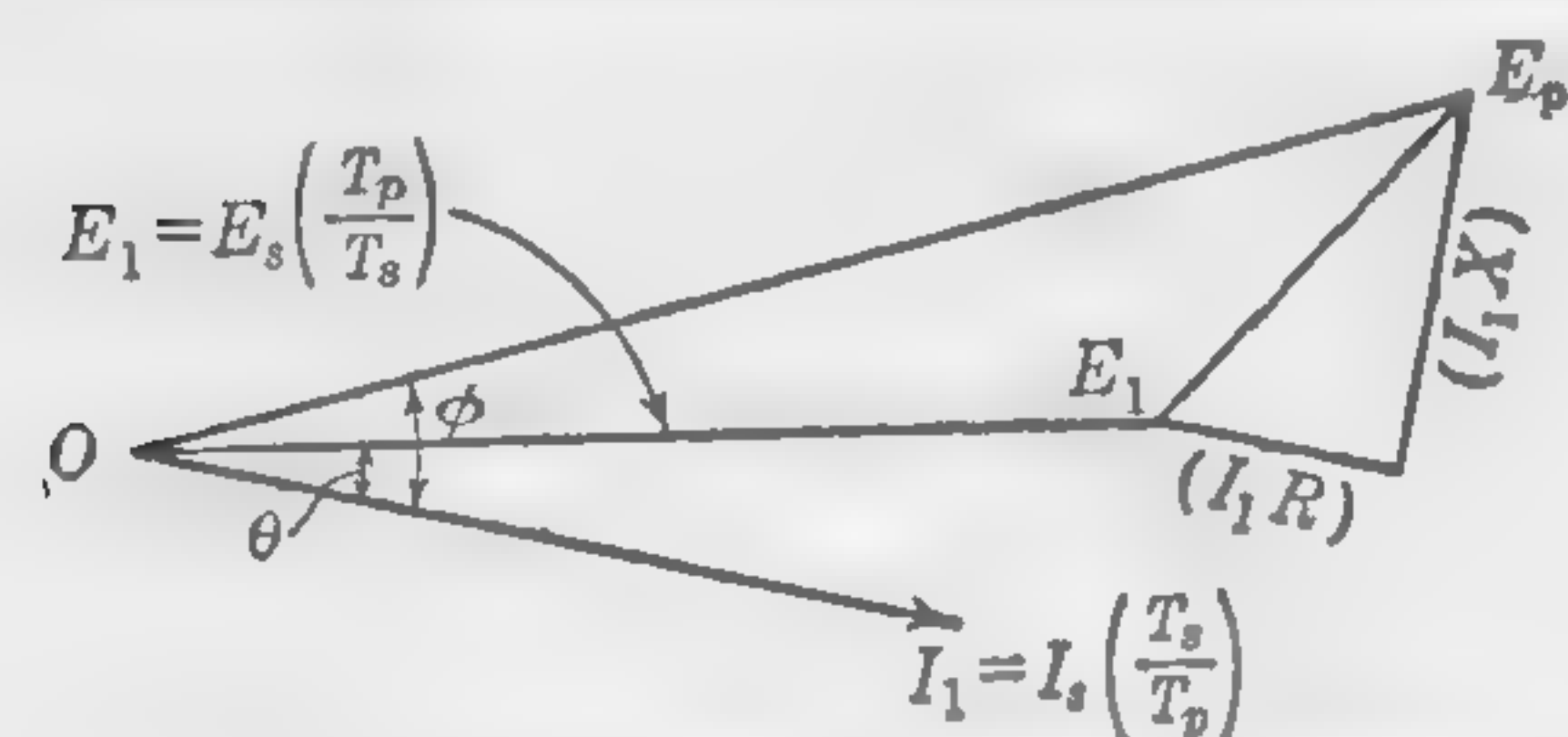
The simplified vector diagram for the condition of lagging power factor is shown in Fig. 166, wherein  $R$  is the quantity of formula (136) and  $(I_p X)$  is the total reactive voltage drop which is equal to the quantity of formula (9) on page 350 multiplied by the number of high-low sections.



From an inspection of Fig. 166 it is seen that

$$E_p = \frac{(I_1 R) + E_1 \cos \theta}{\cos \phi}$$

where  $\cos \theta$  is the power factor of the external load, and  $\cos \phi$  is the power factor on the primary side of the transformer. The angle  $\phi$  can be calculated from the expression



$$\tan \phi = \frac{(I_1 X) + E_1 \sin \theta}{(I_1 R) + E_1 \cos \theta}$$

FIG. 166. Simplified vector diagram for calculating transformer regulation. The percentage regulation is  $100 \times [(E_p - E_1)/E_1]$  and, if the ohmic drop of pressure is expressed as a percentage of the lower pressure  $E_1$ , we may write

$$\text{Per cent regulation} = \frac{\text{per cent equivalent } IR \text{ drop} + 100 (\cos \theta - \cos \phi)}{\cos \phi} \quad (137)$$

A more convenient formula, as used by practical designers, which is very nearly as accurate as formula (137), is

$$\begin{aligned} \text{Per cent regulation} = & (\text{per cent } IR) \cos \theta + (\text{per cent } IX) \sin \theta \\ & + \frac{(\text{per cent } IX \cos \theta - \text{per cent } IR \sin \theta)^2}{200} \quad (138)^* \end{aligned}$$

For unity power factor this becomes

$$\text{Per cent regulation on unity power factor} = \text{per cent } IR + \frac{(\text{per cent } IX)^2}{200} \quad (139)$$

The last term in formula (138) is usually so small as to be negligible, in which case we have

$$\begin{aligned} \text{Per cent regulation (approx)} \\ = & (\text{per cent } IR) \cos \theta + (\text{per cent } IX) \sin \theta \quad (140) \end{aligned}$$

If the transformer is connected to a load having a leading power factor the + sign in this formula must be changed to a - sign.

**140. Efficiency.** The output of a single-phase transformer in watts is  $W = E_s I_s \cos \theta$ ; and if  $w$  = total losses (iron + copper), we may write

$$\text{Efficiency} = 1 - \frac{w}{W + w} \quad (141)$$

\* Proof of formula (138) is given in books dealing with the principles of a-c machines.

whence the total losses are

$$w = \frac{1 - \text{efficiency}}{\text{efficiency}} \times W \quad (142)$$

If  $\eta$  stands for the efficiency of a transformer on a particular load of unity power factor, the efficiency on the same load but of power factor  $\cos \theta$  is

$$\text{Efficiency} = \frac{\cos \theta}{\cos \theta + \left( \frac{1 - \eta}{\eta} \right)} \quad (143)$$

In order to furnish complete information concerning the losses in a given transformer, the iron and copper losses must be stated separately, or the efficiency must be known for more than one condition of loading.

Let  $W$  = full-load output, watts

$a$  = efficiency at full load

$x$  = full-load copper loss, watts

$y$  = core loss, watts

$w$  = total loss at full load

Then

$$w = (x + y) = \left( \frac{1 - a}{a} \right) W \quad (144)$$

Let  $b$  = efficiency when the output is  $n$  times full-load output

$nW$  = output, watts

$n^2x$  = copper loss, watts

$w_n$  = total loss when the load is  $nW$

Whence,

$$w_n = (n^2x + y) = \left( \frac{1 - b}{b} \right) nW \quad (145)$$

Subtracting formula (145) from (144), we get

$$w - w_n = x - n^2x$$

whence,

$$\text{Full-load copper loss} = x = \frac{w - w_n}{(1 - n^2)} \quad (146)$$

**All-day Efficiency.** This may be defined as

Secondary output in watt-hours

Secondary watt-hours + watt-hours iron loss + watt-hours copper loss

the power output and losses being calculated for a period of 24 hr. The assumption commonly made in the case of distribution transformers is that the actual all-day loading is equivalent to 4-hr full load and 20-hr no load.



*Usual Transformer Efficiencies and Regulations.* A-c transformers are extremely efficient. Moreover, they incur extremely small voltage-drop change with changes in load; this means, of course, that the per cent regulation, formula (138), is generally low. The following tables indicate

PERFORMANCE DATA FOR 60-CYCLE SINGLE-PHASE DISTRIBUTION TRANSFORMERS, 2,400 OR 4,800 VOLTS TO 120/240 OR 240/480 VOLTS

Kva	Loss, watts, at 75°C		Per cent efficiency		Per cent regulation	
	Core	Copper	Full load	¼ full load	PF = 1.0	PF = 0.8
1½	20	48	95.8	94.2	3.2	4.48
3	27	71	96.8	96.0	2.4	3.36
5	37	104	97.2	96.6	2.2	3.08
7½	50	142	97.5	96.9	2.0	2.80
10	59	183	97.6	97.2	1.9	2.66
15	80	253	97.8	97.5	1.8	2.52
25	120	376	98.0	97.7	1.6	2.25
37½	155	495	98.3	98.0	1.4	1.96
50	190	605	98.4	98.1	1.3	1.82
75	290	905	98.4	98.1	1.3	1.82
100	380	1,175	98.5	98.2	1.3	1.82
150	575	1,670	98.5	98.2	1.3	1.82
200	820	2,050	98.6	98.1	1.2	1.70

PERFORMANCE DATA FOR 25-CYCLE SINGLE-PHASE DISTRIBUTION TRANSFORMERS, 2,400 OR 4,800 VOLTS TO 120/240 OR 240/480 VOLTS

Kva	Loss, watts, at 75°C		Per cent efficiency		Per cent regulation	
	Core	Copper	Full load	¼ full load	PF = 1.0	PF = 0.8
1½	25	61	94.5	92.8	4.1	5.74
3	38	91	95.8	94.4	3.1	5.34
5	51	155	96.0	95.3	3.1	5.34
7½	80	184	96.6	95.3	2.5	3.50
10	101	235	96.7	95.6	2.4	3.36
15	125	330	97.0	96.2	2.2	3.08
25	180	505	97.3	96.7	2.1	2.94
37½	230	750	97.4	97.1	2.1	2.94
50	280	1,055	97.5	97.3	2.1	2.94
75	410	1,430	97.6	97.4	2.1	2.94
100	460	1,910	97.7	97.7	2.0	2.80
150	1,225	1,325	97.7	97.7	1.9	2.66
200	1,460	1,790	97.7	97.7	1.8	2.52

cate what efficiencies and regulations may be expected of well-designed transformers at the present time.

Comparing the data for the 60-cycle and 25-cycle transformers it is well to note that the efficiencies and regulations are better for the higher-frequency units.

With an increase in voltage, the efficiencies are usually not quite so good. Thus, if the high-tension coils are wound for 13,200 volts, the total losses will be about 10 to 15 per cent greater, with the core loss about 25 to 40 per cent of the total losses.

**141. Temperature Rise of Oil-immersed Transformers.** When a transformer of small output is immersed in an insulating oil, the natural circulation of this oil, as it rises from the heated surface of core and windings and then flows downward near the sides of the iron-containing tank, carries the heat to where the cooling effect of the air surrounding the tank will keep the temperature rise within the required limits. The permissible temperature rise of the oil, being the difference in temperature between the hottest part of the oil and the air outside the tank, is usually about 50°C. The cooling coefficient for transformer tanks with smooth (not corrugated) surfaces is about  $c = 0.0041$  for a 30°C rise in temperature,  $c = 0.005$  for a 40°C rise, and  $c = 0.0057$  for a 50°C rise, this coefficient being, as before, the watts per square inch per degree centigrade rise of temperature, defined as

$$c = \frac{W}{tS}$$

The surface to be considered in applying this cooling coefficient is the total area of the (vertical) sides *plus* one-half the area of the lid, unless the oil is in contact with the lid, in which case the whole area of the lid should be taken. The cooling effect of the bottom of the containing tank is small and this area is not included in the cooling surface  $S$ .

*Example.* Suppose the tank of a self-cooling transformer measures 2 by 2 by 3½ ft high, the surface for use in temperature rise calculations is  $S = (3.5 \times 8) + 2 = 30$  sq ft. Then, if the temperature rise of the oil is not to exceed 40°C, the maximum permissible loss in the transformer is  $W = 0.005 \times 40 \times 30 \times 144 = 864$  watts. If the actual losses are greater than this, a larger tank must be provided, or the tank must be constructed with sides of corrugated sheet iron. When the losses are greater than a tank of reasonable dimensions with corrugated sides will get rid of, an arrangement of pipes or radiators may be attached to the tank to increase the cooling surface in contact with the heated oil, but, where there is no objection to cooling by water circulation, this method is more effectual in carrying off the heat losses.



Figure 167 shows a small size of distribution transformer in welded sheet-iron case, and Fig. 168 shows details of the insulating bushings through which the leads enter the transformer case.

The standard specifications for distribution transformers call for a temperature rise at the continuous rated kilovolt-ampere output not exceeding  $55^{\circ}\text{C}$  as determined by the resistance method.

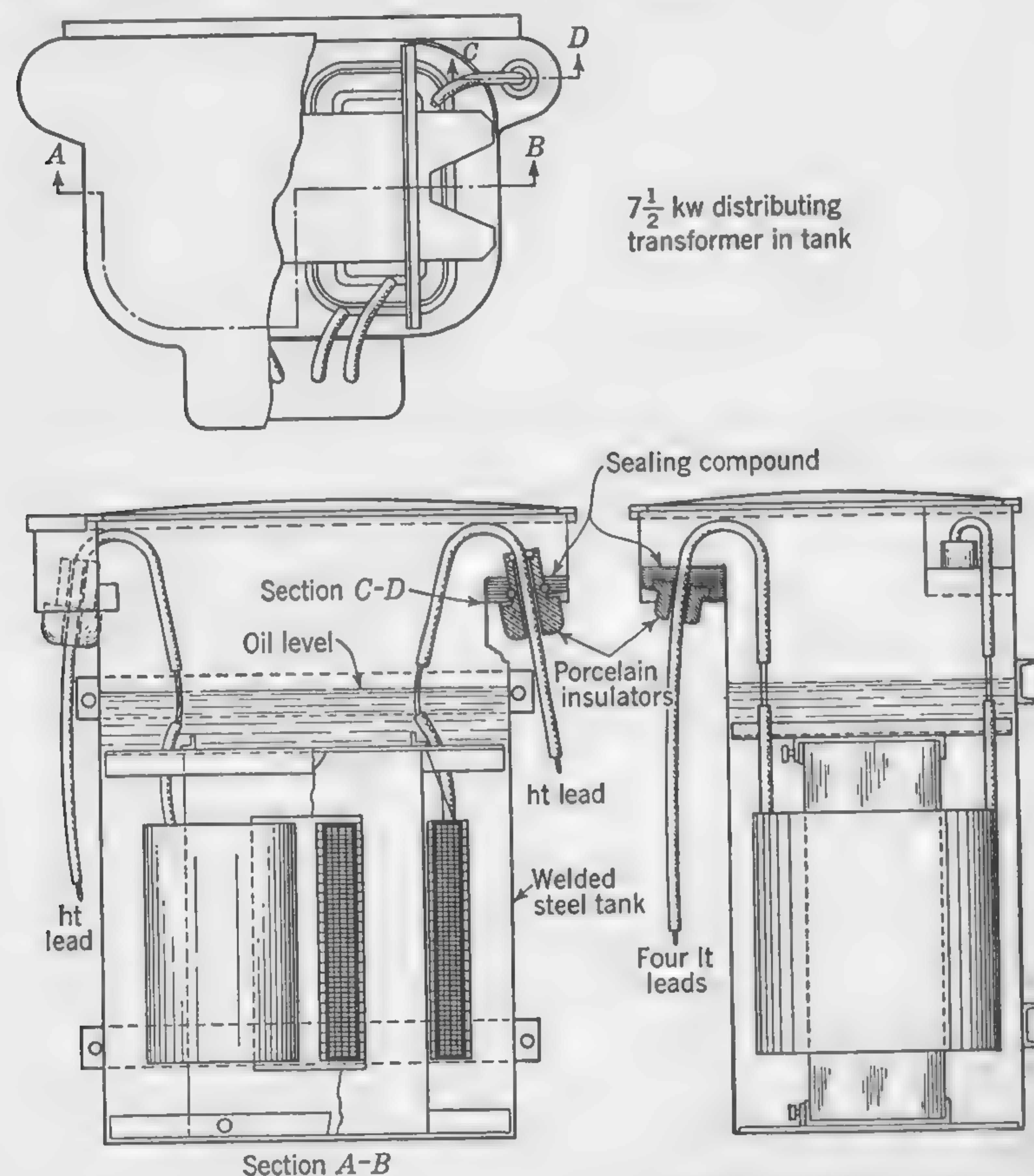


FIG. 167. Small core-type transformer in welded sheet-iron tank.

**142. Effect of Corrugations in Vertical Sides of Containing Tank.** The use of corrugated sheet-iron tanks in place of tanks with smooth sides for oil-insulated transformers or other apparatus will not lead to a reduction of temperature proportional to the increase of tank surface. The watts dissipated per square inch of surface when the tank is provided with corrugated sides will always be less than when the tank has smooth sides.

It is practically impossible to develop formulas which will take account of all factors involved, and recourse must therefore be had to empirical formulas based on test data. If  $\lambda$  is the pitch of the corrugations, measured on the outside of the tank, and  $l$  is the surface width of the tank sides per pitch (see the sketch in Fig. 169), the ratio of the actual tank surface to the surface of a tank without corrugations is  $l/\lambda$ . It is con-

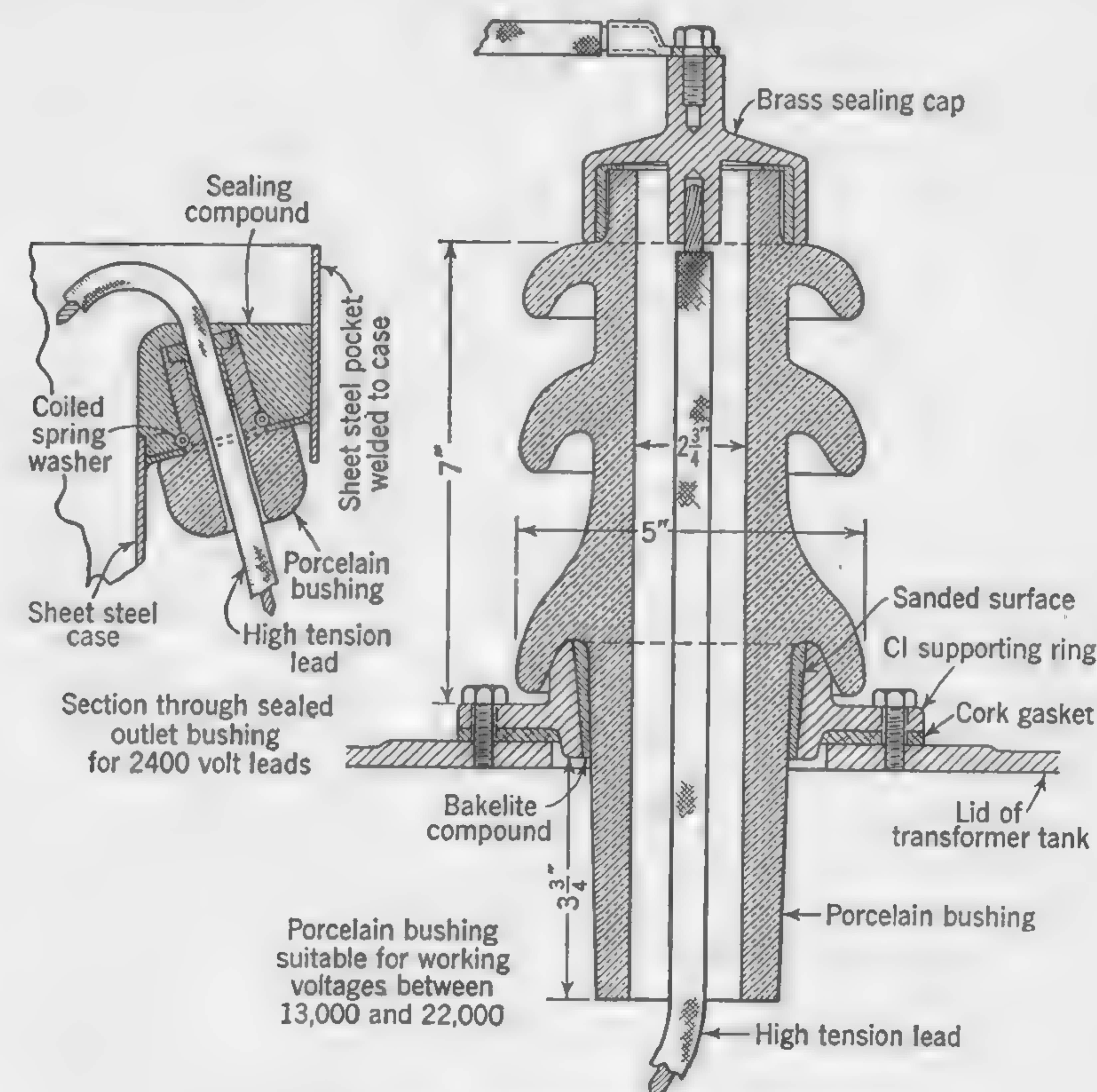


FIG. 168. Porcelain bushings for transformer leads.

venient to think of the surface of an equivalent smooth tank which will give the same temperature rise of the oil as will be obtained with the actual tank. If we apply a correction to the actual pitch  $\lambda$  and obtain an equivalent pitch  $\lambda_e$ , the ratio  $k = \lambda_e/\lambda$  is a factor by which the tank surface (without corrugations) must be multiplied in order to obtain the *equivalent* or *effective* surface. A. Still proposes the formula

$$\lambda_e = \lambda + (l - \lambda) \left( \frac{2\lambda}{l + \lambda} \right) \quad (147)$$



wherein the additional surface provided by the corrugations is reduced in the ratio  $2\lambda/(l + \lambda)$  which becomes unity when  $l = \lambda$ . It follows that

$$k = \frac{\lambda_e}{\lambda} = 1 + \frac{2(l - \lambda)}{l + \lambda} \quad (148)$$

or, if  $\lambda/l = n$ ,

$$k = 1 + 2 \left( \frac{1 - n}{1 + n} \right) \quad (149)$$

**Numerical Example.** What would have been the permissible power loss in the transformer if, instead of the smooth-side tank of the preceding example, Art. 141, a tank of the same internal dimensions had been provided, with corrugations 2 in. deep, spaced  $1\frac{1}{2}$  in. between centers?

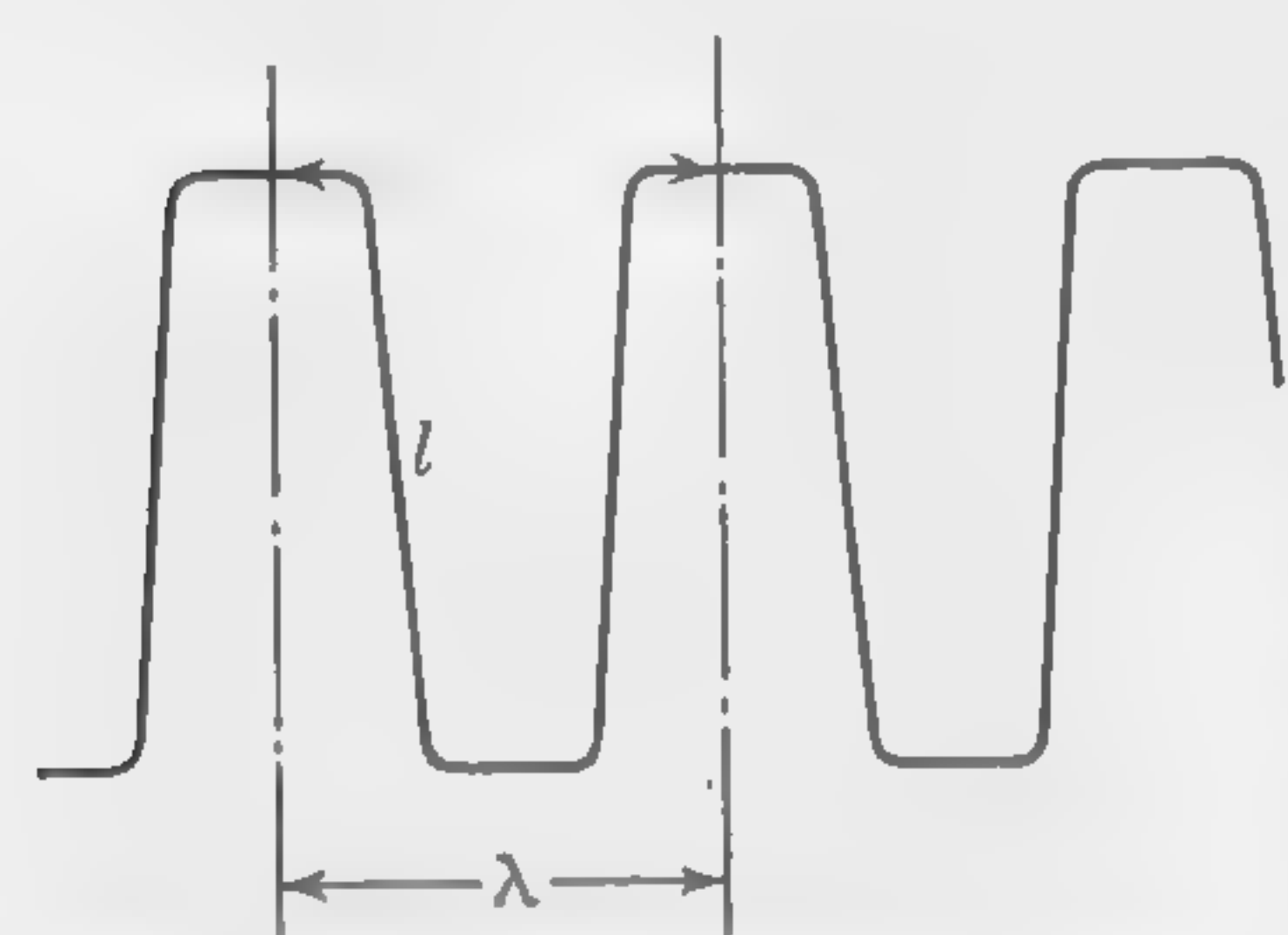


FIG. 169. Tank corrugation dimensions.

The approximate value of  $l$  is  $1.5 + 4 = 5.5$  whence  $n = 1.5/5.5 = 0.273$ ; and, by formula (149),  $k = 1 + 2(0.727/1.273) = 2.14$ . The equivalent tank surface is  $S = (3.5 \times 8 \times 2.14) + 2 = 60$  sq ft, which is just double that of the tank with smooth sides capable of dissipating 864 watts with a temperature rise of  $40^\circ\text{C}$ . It follows that the tank with corrugated sides would be suitable for a transformer having total losses amounting to 1,728 watts.

**143. Cooling Oil in Transformer Tanks by Water Circulation.** Transformer units of large size are effectually cooled by providing them with pipe coils through which cold water is circulated.\* The cooling coils should be constructed preferably of seamless copper tube placed in the top of the tank just below the surface of the oil. The water passing through the tubes carries away the heat at the rate of 1,000 watts for every  $3\frac{3}{4}$  gal flowing per minute when the difference of temperature between ingoing and outgoing water is  $1^\circ\text{C}$ . Allowing for a temperature rise of the water of  $15^\circ\text{C}$ , the amount of water required will be  $\frac{1}{4}$  gal per min per kw, which is a usual allowance. The rate of heat transfer from the oil to the water through the sides of the thin metal tube will depend upon the area of tube in contact with the oil and also upon the surface condition. The temperature rise of the oil above the temperature of the outside air will obviously be considerably greater than the temperature rise of the circulating water, but it is difficult to calculate this accurately because the rate of heat transfer from oil to water may be

\* MEADOR, J. R., Temperature Rise of Water-cooled Transformers, *Trans. AIEE*, vol. 65, pp. 18-21, January, 1946.

from 2 to  $2\frac{1}{2}$  times as great when the pipes are new as after they have become coated with scale. An allowance of 1 sq in. of coil surface per watt is customary and is generally sufficient, but it may be necessary to clean the pipes out occasionally with acid to avoid the danger of high oil temperatures.

**Example.** Given a transformer in which the total losses are 6 kw, but of which it is estimated that 2 kw are radiated from the tank surface, we shall calculate the necessary coil surface and quantity of cooling water.

On the basis of 1 watt per sq in., the total coil surface must be  $6,000 - 2,000 = 4,000$  sq in. Assuming a tube diameter of  $1\frac{1}{4}$  in., the total length of tube in the coil must be

$$\frac{4,000}{12 \times 1.25 \times \pi} = 85 \text{ ft}$$

The quantity of water required will be approximately  $0.25 \times 4 = 1$  gal per min.

**144. Hottest-spot Temperature of Transformer Coil.** Another aspect of the general problem of heat transfer and temperature rise in transformers concerns the hottest-spot temperature of the copper windings; this was discussed in Art. 66, to which the student is referred before proceeding with the example to follow. Practice has indicated that hot spots may be avoided and that reasonably good temperature uniformity may be attained by subdividing the windings so that individual coils do not have thicknesses greater than 1 in.; also, in the case of the larger sizes, it is usually necessary to provide ducts for the free passage of the circulating oil.

**Example.** Calculate the hottest-spot temperature of a transformer coil of which particulars follow, given that the outside surface is maintained at a temperature of  $75^\circ\text{C}$ .

Size of wire, square  $0.25 \times 0.25$  in., insulated with cotton 0.01 in. thick

Insulation between layers, 0.008 in. fuller board

Number of turns per layer = 7

Number of layers = 12

Current density in copper,  $\Delta = 1,400$  amp per sq in.

As defined in Art. 66, the thickness per inch *along* the layers of the winding  $a = 0.25/(0.25 + 0.02) = 0.926$ . The thickness of the copper per inch measured *across* the layers of the winding  $b = 0.25/(0.25 + 0.02 + 0.008) = 0.9$ . The space factor is, therefore,  $a \times b = 0.926 \times 0.9 = 0.833$ .

Using formula (61), page 164, and assuming that the thermal conductivity of the insulation  $k_i = 0.0035$ , the value of  $k_a = k_i/(1 - a) = 0.0035/0.074 = 0.017$ , and that of  $k_b = k_i/(1 - b) = 0.0035/0.1 = 0.035$ .



Also, the coil dimensions (see Fig. 75) are  $l = 7 \times 0.27 = 1.89$  in., and  $w = 12 \times 0.278 = 3.34$  in.

Instead of calculating the total watts lost in the coil as required for formula (59), it will be desirable to rewrite this formula in terms of the current density  $\Delta$  in the copper. If  $(n \times 10^{-6})$  be the resistance of copper in ohms per inch cube, the watts lost *per inch* measured normally to the cross section of the coil are

$$\frac{W}{m} = (n \times 10^{-6}) \Delta^2 \times lw \times (ab)$$

where  $(ab)$  is the winding space factor. By substituting in formula (59), we get

$$t_a = \frac{n \times 10^{-6} \Delta^2 lw (ab)}{8 [k_a(w/l) + k_b(l/w)]} \tag{150}$$

By formula (131),  $n = 0.825$  at  $75^\circ\text{C}$ ; therefore, at  $80^\circ\text{C}$   $n = [(234.5 + 80)/(234.5 + 75)] 0.825 = 0.84$ . Using formula (150) to calculate the *difference of temperature* between the center of the coil and the outside surface, we get

$$t_a = \frac{0.84 \times 10^{-6} (1,400)^2 \times 1.89 \times 3.34 \times 0.833}{8 [(0.047 \times 1.77) + (0.035 \times 1.77)]} = 12^\circ\text{C}$$

It follows that the hottest-spot temperature will be greater by  $12^\circ\text{C}$  than the outside temperature of  $75^\circ\text{C}$ , or  $12 + 75 = 87^\circ\text{C}$ .

**145. Illustrative Example. Design of Distribution Transformer.**  
Design a transformer to meet the following specifications:

- Output in kilovolt-amperes = 5
- Primary (high-tension) volts = 2,300
- Secondary (low-tension) volts = 115/230
- Frequency = 60 cycles
- Efficiency at unity power factor  $\begin{cases} \text{Full load} = 0.972 \\ \frac{1}{4} \text{ full load} = 0.966 \end{cases}$
- Temperature rise not to exceed  $55^\circ\text{C}$

*Item 1.* It is proposed to design a core-type transformer with rectangular coils. A subsequent design, Art. 147, will be devoted to the calculation of a cruciform-core type of transformer.

*Description.* This is a distribution transformer of standard type for maximum output rating. It is oil-immersed and self-cooling, without taps for voltage adjustment.

*Insulation tests* (in tank with oil); voltage applied for 1 min

- H.T. winding to L.T. winding and core, 10,000 volts
- L.T. winding to core, 4,000 volts

DESIGN SHEET FOR TRANSFORMER  
Single-phase Distribution Type (High All-day Efficiency)  
Guaranteed losses, watts  $\begin{cases} \text{Copper (full load)} & \dots\dots\dots 107 \\ \text{Iron} & \dots\dots\dots 37 \end{cases}$

Item No.	Summary of calculation		
1	Volts per turn: from formula = 1.22; actual = 1.175		
Windings		H.T.	L.T.
2	Total number of turns.....	1,960	196
3	Number of coils.....	2	4
4	Turns per coil.....	980	49
5	Full-load current, amp.....	2.17	21.7
6	Current density, amp per sq in.....	850	912
7	Cross section of each conductor, sq in.....	0.00256	0.0238
8	Dimension of conductors.....	No. 15	$0.14 \times 0.17$
9	Number of turns per layer per coil.....	112	49
10	Number of layers per coil.....	9	1
11	Taps.....	None	None
12	Volts per coil.....	1,150	57.5
13	Volts between layers.....	263	
14	Length of winding layer.....	$7\frac{3}{4}$ in.	8 in.
15	Length of layer including insulation.....	$8\frac{1}{2}$ in.	$8\frac{1}{2}$ in.
16	Insulation between layers, in.....	0.01	
17	Insulation on wire.....	dcc	dcc
18	Length per turn, ft.....	1.39	1.09
19	Total length, all turns in series, ft.....	2,720	214
20	Weight in copper, lb.....	26.8	19.6
21	Resistance at $75^\circ\text{C}$ —all coils in series, ohms. . .	10.6	0.09
22	<i>IR</i> drop, volts.....	23.0	1.95
23	Full-load copper loss (compare with guarantee). .	50	42.3

The Magnetic Circuit

24	Dimensions of "window," in.....	$8\frac{1}{2} \times 3\frac{1}{4}$
25	Total flux, maxwells.....	440,000
26	Flux density in core under windings, lines per sq in.....	66,700
27	Cross section of iron in core under windings.....	6.6 sq in.
28	Width of stampings in core under windings.....	$2\frac{1}{4}$ in.
29	Gross thickness of core.....	$3\frac{1}{4}$ in.
30	Total weight of iron in core, lb.....	72.7
31	Watts lost in iron (compare with guarantee).....	36.9
32	Total full-load losses, watts.....	129.2



Efficiency and Exciting Current		
33	Efficiency at unity power factor:	
	At $1\frac{1}{4}$ load.....	0.9718
	At full load.....	0.9748
	At $\frac{3}{4}$ load.....	0.9769
	At $\frac{1}{2}$ load.....	0.9766
	At $\frac{1}{4}$ load.....	0.9668
34	All-day efficiency (4-hr full load).....	0.9420
35	Primary exciting current, amp.....	0.059
REGULATION		
36	Total equivalent $IR$ drop, per cent.....	1.846
37	Total reactive drop, per cent.....	2.2
38	Regulation on unity power factor, per cent.....	1.846
39	Regulation on 0.80 power factor, per cent.....	2.82
DESIGN OF TANK—TEMPERATURE RISE		
40	Effective cooling surface of tank, sq in.....	960
41	Watts per sq in. of tank surface.....	0.135
42	Approximate temperature rise of oil, °C.....	33

The specified temperature rise of 55°C means that the temperature of the windings, as measured by the resistance method, after the transformer has been operating continuously at full load, will not be more than 55°C above the temperature of the surrounding air.

The transformer is not guaranteed against overloading.

#### CALCULATIONS

*Guaranteed Losses.* Before proceeding with the design it is well to determine the amount of the iron and copper losses corresponding to the specified efficiencies.

By formula (144),

$$\text{Total loss at full load} = \frac{1 - 0.972}{0.972} \times 5,000 = 144 \text{ watts}$$

By formula (145),

$$\text{Total loss at } \frac{1}{4} \text{ load} = \frac{1 - 0.966}{0.966} \times \frac{5,000}{4} = 44 \text{ watts}$$

By formula (146),

$$\text{Full-load copper loss} = \frac{144 - 44}{1 - \frac{1}{16}} = 107 \text{ watts}$$

and the guaranteed core loss is  $144 - 107 = 37$  watts.

The copper loss will be a maximum when the transformer is hot. In calculating the resistance of the windings to determine the full-load copper loss, a temperature of 75°C will be assumed.

In making the calculations, it is not possible to follow the exact sequence of the items as recorded in the design sheet shown on page 371, but the items covered by the calculations are referred to in the margin to facilitate reference.

Assuming  $c = 58$  in formula (129) of Art. 129, we have

$$V_i = \frac{\sqrt{5,000}}{58} = 1.22 \text{ volts}$$

*Items 2 to 5.* Since the high-tension winding is the primary and the low-tension winding the secondary, the number of secondary turns is  $230/1.22 = 189$ , or (say) 188 turns in four coils of 47 turns each. It is usual to have not less than four coils on the low-tension side in both large and small transformers. The number of primary turns will be 1,880. Before proceeding further, it should be pointed out that the numbers of primary and secondary turns here calculated are preliminary values and may require modification should the copper and iron losses differ greatly from the guaranteed losses; this is, in fact, actually the situation, as the results of items 6 to 15 indicate. This winding may consist of two coils (one on each limb) in a small transformer for as low a voltage as 2,300, but the winding on each limb may consist of two or more coils connected in series. Refer to Art. 134 for discussion of coil arrangements in both core- and shell-type transformers.

The full-load secondary current is  $5,000/230 = 21.7$  amp, and, since the ratio of transformation is 10 to 1, the primary current (neglecting the exciting current component) is 2.17 amp.

*Items 6 to 15.* Before deciding upon the sizes of wire in the windings, it will be advisable to determine the probable dimensions of the opening, or window, which must accommodate both primary and secondary windings. By formula (134) on page 348 the winding factor is  $sf = 10/(30 + 2.3) = 0.309$ , or (say) 0.3 for an approximate winding space factor. The current density (Art. 130) will be assumed at 1,000 amp per sq in.; whence the area of the window opening (Fig. 156) is,

$$H \times D = \frac{2(188 \times 21.7)}{1,000 \times 0.3} = 27.2 \text{ sq in.}$$

Using the ratio ( $H/D$ ) 2.5, as suggested in Art. 133, we may try  $D = 3\frac{1}{2}$  and  $H = 8\frac{1}{2}$  in. for the length of the limbs upon which the coils will be placed. Before proceeding further, it will be advisable to make a rough estimate of the core dimensions and iron loss.



By formula (125a) on page 340, the flux in the iron is

$$\Phi = \frac{10^8 \times 230}{4.44 \times 60 \times 188} = 459,000$$

From Art. 130 we select 70,000 lines per sq in. as a trial density in the limbs under the windings. Whence, with the proportion  $S = 1.5L$  (see Art. 133) and a stacking factor of 0.9, we have

$$0.9L \times 1.5L = \frac{459,000}{70,000} = 6.56 \text{ sq in.}$$

whence the width of the stampings under the windings is  $L = 2.21$ , or (say)  $2\frac{1}{4}$  in., and the total thickness of the stack of laminations is  $S = 3\frac{1}{4}$  in.

For preliminary calculations we shall assume  $M = L$  in Fig. 156. In other words, assume the same cross section of iron and the same flux density in the end portions of the core as in the limbs under the windings. Changes can be made later if the core losses are too high. The dimensions of the core will be as shown in Fig. 170, and the weight of iron is  $0.28(0.9 \times 3\frac{1}{4} \times 2\frac{1}{4}) \times 2(8\frac{1}{2} + 2\frac{1}{4} + 3\frac{1}{4} + 2\frac{1}{4}) = 60$  lb. From Fig. 154 we find the watts per pound for  $B'' = 70,000$  to be 0.75; whence the total core loss is  $0.75 \times 60 = 45$ , which exceeds the required loss of 37 watts. Before correcting the iron loss it is usually advisable to calculate the approximate copper loss because changes in the design can then be made to correct iron and copper losses simultaneously.

**Approximate Copper Losses.** The approximate mean length per turn of winding on rectangular limbs of core-type transformers, as illustrated in Fig. 170, is  $2(L + S + D)$  which includes an allowance for insulation and clearances around the iron core. Thus *mean length per turn* (m.l.t.) =  $2(2\frac{1}{4} + 3\frac{1}{4} + 3\frac{1}{4}) = 17\frac{1}{2}$  in. The cross section of copper in both windings is  $[2(188 \times 21.7)/1,000] = 8.17$  sq in., and the weight of copper is  $0.32 \times 17.5 \times 8.17 = 45.7$  lb. The watts lost per pound at 75°C are given by formula (131) on page 345, whence *total copper loss* =  $45.7[2.57(1000)^2/10^6] = 117$  watts. This is also in excess of the required loss, which is 107 watts.

By making slight changes in the design, it will now be possible to proceed with the final calculations and approximate the losses required to give the specified efficiencies.

An increase of turns in the windings will reduce the core losses even if no change is made in the dimensions of the core, but this will increase the copper loss unless the current density in the copper is reduced. We may try increasing the core cross section in the end portions so as not to increase the mean length per turn of the windings.

The copper losses can be kept within the desired limit by selecting sizes of wire which will cause the current density to be less than in the preliminary estimate.

By building the core to the dimensions of Fig. 171, and increasing the number of turns to 1,960 and 196 in primary and secondary, respectively, the core losses should be considerably reduced.

**Recalculation of Core Losses.** The total flux is

$$\Phi = 459,000 \times \frac{188}{196} = 440,000 \text{ maxwells}$$

The losses in the limbs under the windings and in the end sections must be calculated separately. The net cross section of the limbs is  $0.9 \times$

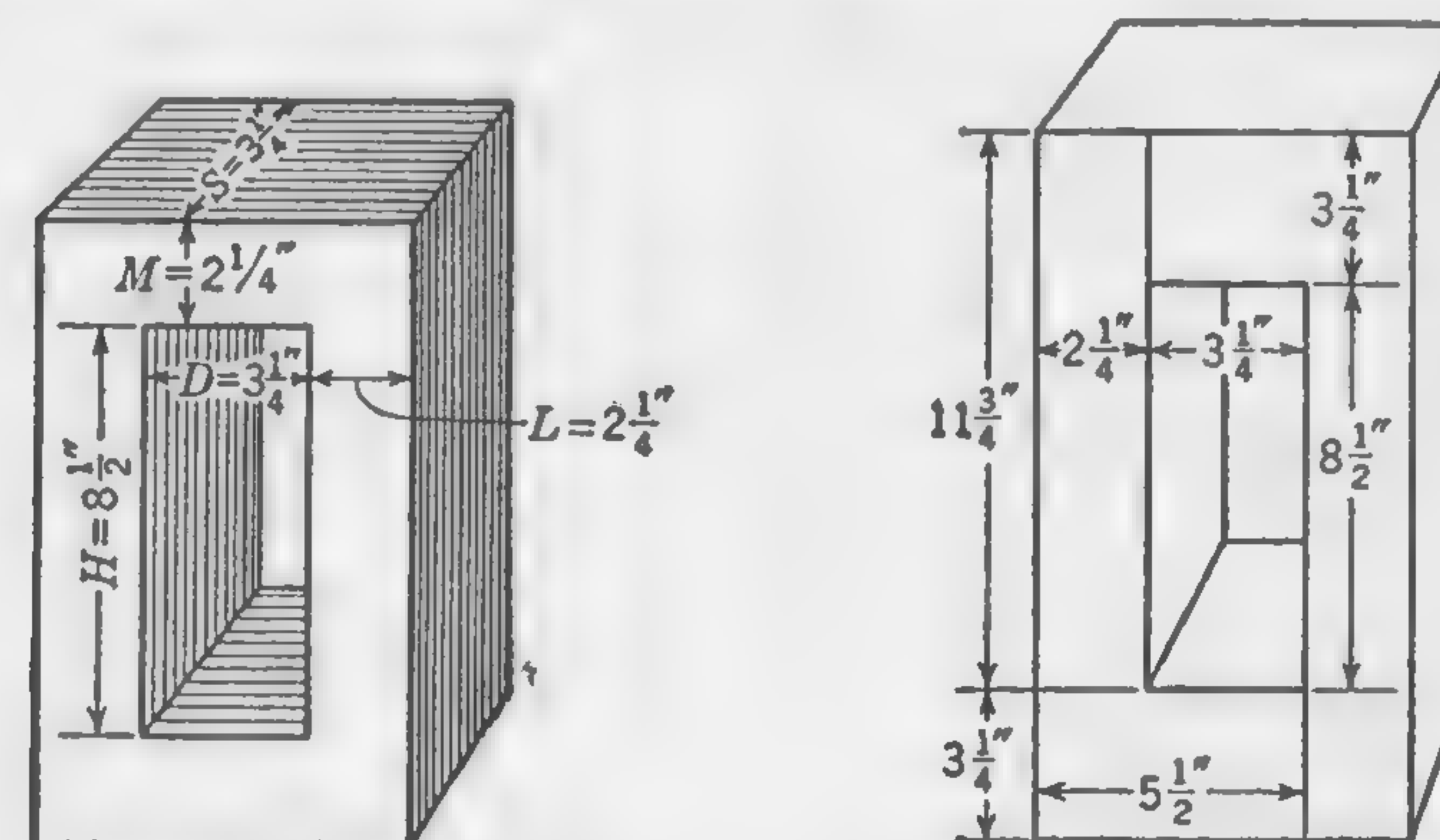


FIG. 170.

FIG. 171.

FIGS. 170 and 171. Core dimensions for transformer of Illustrative Example of Art. 145.

$3\frac{1}{4} \times 2\frac{1}{4} = 6.6$  sq in., whence  $B''$  in the limbs is  $440,000/6.6 = 66,700$  lines per sq in. From Fig. 154 we read *watts loss per pound* = 0.69. The weight of the two limbs is  $0.28 \times 6.6 \times 8.5 \times 2 = 31.5$  lb; whence the loss in the core sections under the windings is  $0.69 \times 31.5 = 21.7$  watts.

The losses in the end sections are calculated in a similar manner. Net cross section = 9.5 sq in. Flux density  $B'' = 46,200$ . Watts per pound = 0.37. Weight of both end sections = 41.2 lb. Loss in both end sections =  $0.37 \times 41.2 = 15.2$  watts. The total core loss is, therefore,  $21.7 + 15.2 = 36.9$  watts which is practically the specified loss of 37 watts.

**Sizes of Wire and Winding Particulars.** It is desirable to make a sketch such as Fig. 172 showing a cross section through the windings in the window opening of dimensions  $H = 8\frac{1}{2}$  in. and  $D = 3\frac{1}{4}$  in.

Two coils of the secondary or low-tension winding will be wound next to the core on each limb. Each coil may consist of 40 turns in a single



layer. The size of a suitable conductor of rectangular section may be calculated as follows. The cross section for a current density of (say) 900 amp per sq in. is  $21.7/900 = 0.0241$  sq in. Allowing  $\frac{1}{4}$  in. at each end of the layer for clearance and insulation, the available length of winding space in the layer is 8 in., and  $\frac{8}{49} = 0.163$  in., which is the width of one conductor including insulation. The cotton covering will account for 20 mils, leaving 0.143 for the width of copper. We shall make this 0.14 in. The thickness must be  $0.0241/0.14 = 0.172$ , or (say) 0.17 in.,

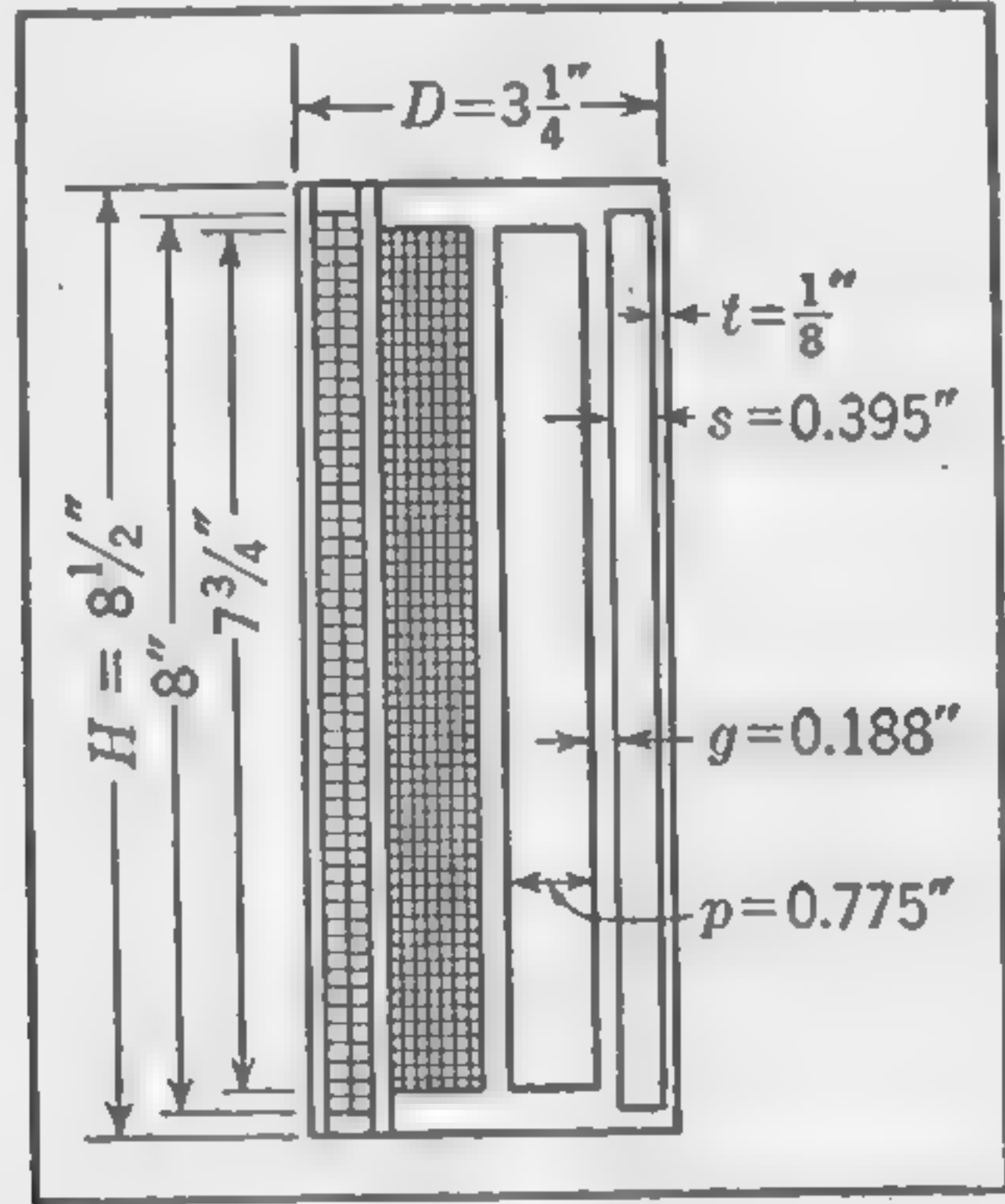


FIG. 172. Cross section of windings in window opening of core-type transformer, Illustrative Example, Art. 145.

so that a rectangular conductor 0.14 by 0.17 in. wound on edge will be suitable.

For the high-tension side we may select from the wire table on page 431 No. 15 dcc wire in which the current density will be  $2.17/0.00256 = 850$  amp per sq in.

Assuming the length of the winding layer to be  $7\frac{3}{4}$  in., the number of wires per layer will be about  $7.75 \times 14.5 = 112$ , where the figure 14.5 is obtained from the wire table on page 431. A total of nine layers of wire will be required for a single coil of 980 turns on each of the two limbs.

The greatest difference of potential between layers will be  $1,150 \times [(2 \times 112)/980] = 263$  volts (rms value) which is permissible if ample insulation is provided between layers. It is usual to limit the potential difference between layers to about 200 to 300 volts which can generally be accomplished without difficulty by subdividing the winding into a sufficient number of separate coils and providing adequate insulation between the coils.

Items 16 to 23. (The student should review Art. 131, which treats of insulation problems; but the formula there given for clearances in oil has reference to apparatus for considerably higher pressures than the trans-

former with which this problem is concerned.) With the core dimensions  $2\frac{1}{4}$  by  $3\frac{1}{4}$  in., the winding former would be about  $2\frac{1}{2}$  by  $3\frac{9}{16}$  in., with slightly rounded corners. As a check on the space  $D = 3\frac{1}{4}$  in. provided for the windings (Fig. 172) the total thickness of copper and insulation is computed as follows:

Material	Radial thickness, in.	
Cotton tape binding assembled laminations.....	0.018	$t = 0.125$
Varnished cambric.....	0.010	
Pressboard.....	0.030	
Clearance.....	0.067	
Inner L.T. coil (one layer) including cotton on wire.....	0.190	$s = 0.395$
Parchment paper (0.010) between coils; allow.....	0.015	
Outer L.T. coil (one layer).....	0.190	
Pressboard around outer L.T. coil.....	0.020	$g = 0.188$
Spacers of treated wood to form oil ducts*.....	0.125	
Pressboard.....	0.020	
Two layers cotton tape.....	0.018	
Parchment paper with crimped edges on which primary coil will be wound.....	0.005	
Nine layers of No. 15 dcc round wire.....	0.612	$p = 0.755$
Two thicknesses of 0.005 paper between layers.....	0.080	
Cotton tape, half lapped.....	0.018	
Allowance for bulging† ( $0.02 \times 3\frac{1}{4}$ ).....	0.065	
Total.....	1.483	

The space available to accommodate this total thickness of copper and insulation is  $3.25/2 = 1.625$ , so that the space provided as shown in sketch (Fig. 172) would seem to be sufficient to allow of a small clearance between the windings on the two limbs for insulation and oil circulation.

Calculation of Copper Losses. In these calculations we may neglect the magnetizing component of the total primary current, as this adds very little to the  $I^2R$  loss in the primary at full load.

\* For proper circulation of oil, these spacers should be thicker than  $\frac{1}{8}$  in.; but in so small a transformer as 5 kva there will be no danger of high internal temperatures, and the insulation is more than sufficient. It would be quite permissible to omit the oil channels and simply provide solid insulation of a total thickness as given in Art. 131. In larger transformers, and even in small transformers for the higher voltages, the oil duct should be at least  $\frac{3}{16}$  in. and preferably  $\frac{1}{4}$  in.; the total thickness of insulation (including oil ducts) between high-tension and low-tension windings being calculated by formula (132) on page 317.

† The allowance for bulging is here assumed to be equal to 2 per cent of the core thickness. With cores of cruciform cross section, the coils are circular, and no allowance for bulging is required.



Referring to Fig. 173, the mean length per turn (m.l.t.) of the windings, as designed, is computed as follows:

$$\text{Secondary m.l.t.} = \frac{2(2.25 + 3.25) + \pi(0.25 + 0.395)}{12} = 1.09 \text{ ft}$$

$$\text{Primary m.l.t.} = \frac{2(2.25 + 3.25) + \pi(0.25 + 0.79 + 0.775)}{12} = 1.39 \text{ ft}$$

The total lengths of wire are:

$$\text{Secondary winding length} = 196 \times 1.09 = 214 \text{ ft}$$

$$\text{Primary winding length} = 1,960 \times 1.39 = 2,720 \text{ ft}$$

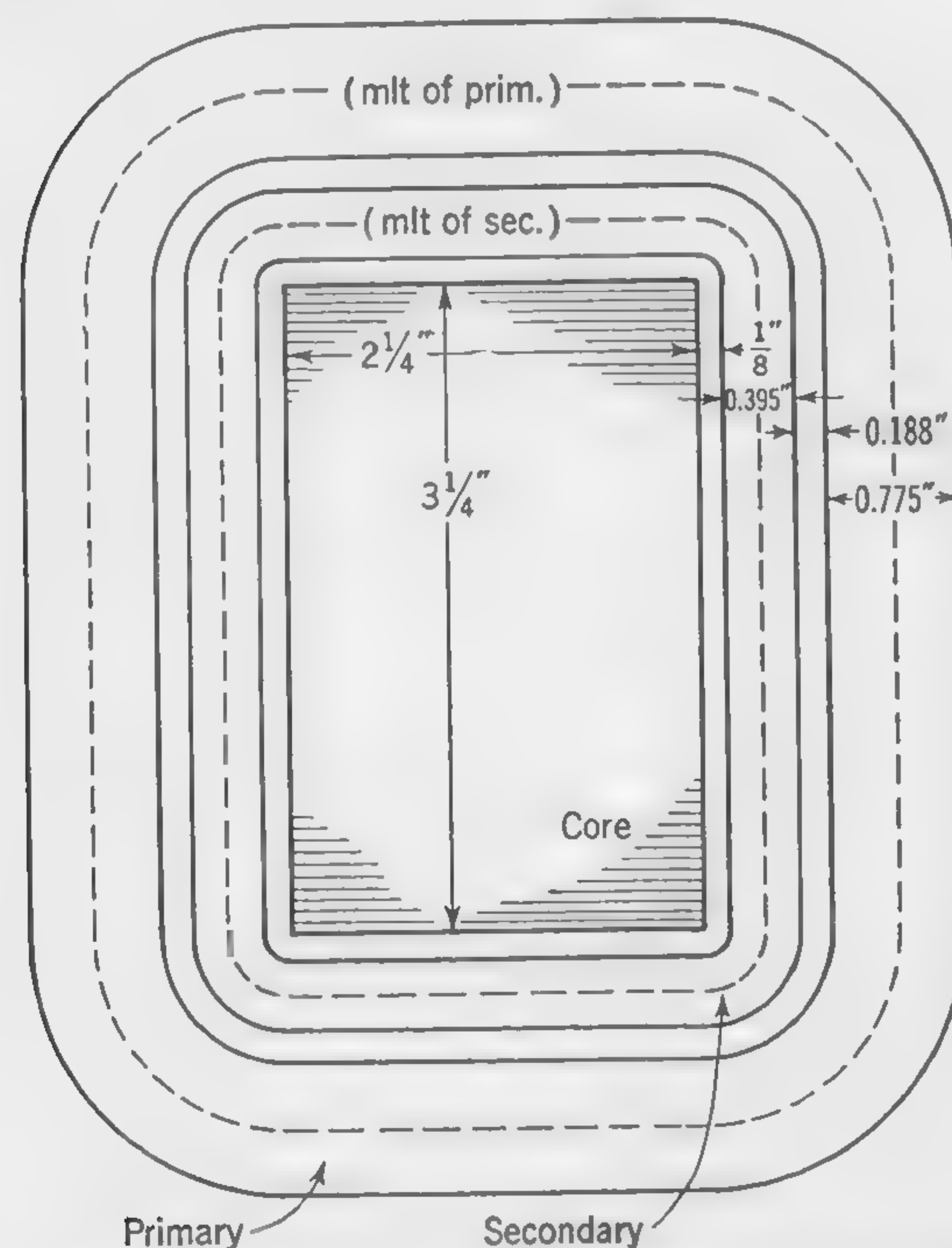


FIG. 173. Sketch showing arrangement of primary and secondary coils over one leg of core, and the mean length of turn of each winding.

The weight of the copper is:

$$\text{In the secondary coils, } 0.32(0.14 \times 0.17 \times 214 \times 12) = 19.6 \text{ lb}$$

$$\text{In the primary coils (No. 15), } 9.86 \times 2.72 = 26.8 \text{ lb}$$

Since the resistance per 1,000 ft of No. 15 wire at 60°C is 3.702 ohms (Table I, page 431), at 75°C, it will be

$$3.702 \left( \frac{234.5 + 75}{234.5 + 60} \right) = 3.9 \text{ ohms}$$

The total resistance of the high-voltage winding (hot) is therefore  $3.9 \times 2.72 = 10.6$  ohms.

$$IR = 2.17 \times 10.6 = 23 \text{ volts (i.e., 1 per cent) and } I^2R = 50 \text{ watts}$$

The cross section of the low-tension winding is 0.0238 sq in., as against 0.00256 for the high-tension wire. Therefore the resistance (hot) of all low-tension coils in series is

$$3.9 \left( \frac{0.00256}{0.0238} \right) \times \frac{214}{1,000} = 0.09 \text{ ohm}$$

$$IR = 21.7 \times 0.09 = 1.95 \text{ volts (i.e., 0.847 per cent), and } I^2R = 42.3 \text{ watts.}$$

The total copper loss is  $50 + 42.3 = 92.3$  watts, which is slightly less than the guaranteed copper loss as calculated from the specified efficiencies.

Items 24 to 32. The core dimensions as given in Fig. 171 are suitable and may be adopted. The total full-load losses (item 32) are  $36.9 + 92.3 = 129.2$  watts.

Item 33. (Refer to Art. 140.) By formula (141) the efficiencies at unity power factor are:

$$\text{At full load, } 1 - \frac{(36.9 + 92.3)}{5,000 + 129.2} = 0.9748$$

$$\text{At half-load, } 1 - \frac{(36.9 + 23.1)}{2,500 + 60.0} = 0.9766$$

The calculated values for other loads are:

$$\text{At 25 per cent overload, } 0.9718$$

$$\text{At three-quarters full load, } 0.9769$$

$$\text{At one-quarter full load, } 0.9668$$

The maximum efficiency occurs when the total copper losses are equal to the core loss, under which condition the fraction of rated load is

$$\sqrt{\frac{\text{core loss}}{\text{F.L. copper loss}}}. \text{ Thus, at the point of maximum efficiency the load is } 5 \sqrt{36.9/92.3} = 3.16 \text{ kva, and the maximum efficiency is}$$

$$1 - \frac{36.9 + 36.9}{3,160 + 73.8} = 0.9772$$

Item 34. On the basis of 4-hr full load and 20-hr no load, the all-day efficiency, as defined in Art. 140, is

$$\frac{5,000 \times 4}{(5,000 \times 4) + (36.9 \times 21) + (92.3 \times 4)} = 0.942$$



*Item 35.* (Refer to Art. 135.) The magnetizing component  $I_o$  of the total exciting current is calculated by making use of the  $BH$  curve (Fig. 161) and estimating the approximate mean lengths of the flux paths wherein the flux density is approximately of constant value throughout the length of path considered (refer to Fig. 171). Thus, for the two limbs under the windings, we have  $B'' = 66,700$ ; mean length = 17 in.; whence  $(TI) = 17 \times 4.6 = 78.2$ .

For the two ends of the core (outside the windings)  $B'' = 46,200$ ; mean length = about  $15\frac{1}{4}$  in., whence  $(TI) = 15.25 \times 2 = 30.5$ .

In order to estimate the ampere-turns required for the four joints in the core as shown in Fig. 171, we refer to Fig. 162.

For the two joints with core density  $B'' = 66,700$ , we have  $(TI) = 2 \times 21 = 42$ , and, for the two joints with core density  $B'' = 46,200$ , we have  $(TI) = 2 \times 3 = 6$ , making a total of 156.7 amp-turns. The magnetizing component of the primary current is, therefore,

$$I_o = \frac{156.7}{1,960 \times \sqrt{2}} = 0.0565 \text{ amp}$$

The "energy" component is  $I_w = 36.9/2,300 = 0.016$  amp and the total exciting current component is  $\sqrt{(0.0565)^2 + (0.016)^2} = 0.059$  amp.

*Items 36 to 39: Regulation.* The percentage  $IR$  drop in the two windings is the same as the total copper loss expressed as a percentage of the kilovolt-ampere output. Whence *per cent IR drop* =  $(92.3 \times 100)/5,000 = 1.846$ , which checks with the resistance drops previously calculated. Note that this quantity is also given by the expression  $(I_p R/E_p) \times 100$ , where  $I_p$  is the primary current (2.17 amp),  $E_p$  is the primary pressure (2,300 volts), and  $R$  is the *equivalent resistance* of the two windings, as given by formula (136) of Art. 139.

The numerical values of the quantities in formula (135) required for the calculation of the  $IX$  drop are as follows:  $f = 60$ ,  $T_s = 196$ ,  $I_s = 21.7$ ,  $E_s = 230$ ,  $n = 2$ .

The length of  $l$  may be taken as  $12 \times [(1.09 + 1.39)/2] = 14.9$  in., where the numbers 1.09 and 1.39 are the mean lengths per turn of low- and high-tension windings, respectively. The remaining dimensions are taken from Fig. 172, where  $h = H = 8.5$ ,  $g = 0.188$ ,  $p = 0.775$ , and  $s = 0.395$ .

The calculated  $IX$  drop is 2.2 per cent, which is equivalent to a reactive drop of  $2,300 \times 0.022 = 50.6$  volts in the primary winding. This would be the length of the vector marked  $(I_l X)$  in Fig. 166, which is used for determining the voltage regulation.

For calculating items 38 and 39, we may use the approximate formula (140); whence the regulation on unity power factor is the same as the

percentage  $IR$  drop, namely, 1.846 per cent. On 80 per cent power factor we have  $(1.846 \times 0.8) + (2.2 \times 0.6) = 2.82$  per cent (nearly).

*Items 40 to 42.* The temperature rise of the windings as measured by the resistance method must not exceed the specified  $55^\circ\text{C}$ . The permissible temperature rise of the oil near the top of the tank (where it is hottest) must be something less than this. The student is referred to Art. 66 and the Illustrative Example of Art. 144, where the manner in which the difference of temperature between the coil where the heat is generated and the oil on the outside of the insulation is explained. We shall here assume that if the temperature rise of the oil does not exceed  $50^\circ\text{C}$ , the temperature at the hottest part will not be excessive. In Art. 141 the cooling coefficient for self-cooling transformers was given as  $c = 0.0057$  watt per sq in. per  $^\circ\text{C}$  rise of temperature. The total outside area of tank surface should, therefore, not be less than

$$S = \frac{129.2}{50 \times 0.0057} = 454 \text{ sq in.}$$

The case to accommodate this transformer may be generally of the type illustrated in Fig. 167; the minimum dimensions would be about  $12\frac{1}{2}$  by 9 by 21 in. high, and the effective cooling surface, computed as explained in Art. 141, is  $21(25 + 18) + \frac{1}{2}(12.5 \times 9) = 960$  sq in.; whence the probable maximum temperature rise of the oil is

$$t = \frac{129.2}{0.0041 \times 960} = 33^\circ\text{C}$$

**146. Transformers with Ribbon Cores.** Improvement in transformer performance, particularly in small distribution units, is made possible by the use of a special silicon-iron alloy that possesses permanent nonaging characteristics. This material differs from ordinary silicon steel not so much in the elements it contains as in how it is made. In its manufacture it is rolled so that the individual magnetic crystals are "oriented," that is, lined up with their cube edges parallel to each other and to the direction of rolling, like bricks in a wall; this is in contrast to the pattern incidental to ordinary silicon steel, as used in the core of the Illustrative Example of Art. 145. The effect of such crystal orientation is to permit the steel to carry more flux with the same applied magnetizing force than it could if the crystals were haphazardly placed. This means simply that the knee of the magnetization curve is lifted to a higher flux density, with the result that increased flux densities, about 30 per cent more, are possible without change in core loss.

To take full advantage of the oriented steel it is necessary that the strips be sheared parallel to the grain of rolling; moreover, a construction



must be employed that causes the flux paths to be *with* the grain. This is accomplished in several ways by different manufacturers, in one of which a special machine winds the *steel ribbon* spirally through the winding openings and the outside of the coils. Transformers constructed in this way (1) are smaller in size for a given kilovolt-ampere rating; (2) pre-

DESIGN SHEET FOR TRANSFORMER  
Single-phase Distribution Core Type with Cruciform Section  
Guaranteed losses, watts { Copper (full load)..... 104  
Iron..... 73

Item No.	Summary of calculation		
1	Volts per turn: from formula = 2.07		
Windings		H.T.	L.T.
2	Total number of turns.....	1,160	116
3	Number of coils.....	4	4
4	Turns per coil.....	290	29
5	Full-load current, amp.....	3.12	31.2
6	Current density, amp per sq in.....	965	960
7	Cross section of each conductor, sq in.....	0.00323	0.0325
8	Dimension of conductors.....	No. 14	0.129 × 0.258
9	Number of turns per layer per coil.....	49	29
10	Number of layers per coil.....	6	1
11	Taps.....	None	None
12	Volts per coil.....	600	60
13	Volts between layers.....	200	
14	Length of winding layer including insulation, in.....	3 <sup>13</sup> / <sub>16</sub>	8
15	Insulation between layers, in.....	0.0075	
16	Insulation on wire.....	dee	dee
17	Length per turn, in.....	19.35	15.65
18	Total length, all turns in series, ft.....	1,870	151
19	Weight of copper, lb.....	18.9	23.2
20	Resistance at 75°C—all coils in series, ohms...	5.77	0.016
21	IR drop, volts.....	18.0	1.41
22	Full-load copper loss (compare with guarantee)	56	46

The Magnetic Circuit

23	Dimensions of "window," in.....	3 <sup>5</sup> / <sub>16</sub> × 8 <sup>1</sup> / <sub>2</sub>
24	Total flux, maxwells.....	7.78 × 10 <sup>8</sup>
25	Flux density in core under windings, lines per sq in.....	83,000
26	Cross section of iron in core under windings, gross.....	10.1
27	Widths of ribbon strips in cruciform section, in.....	2.14 and 3.6
28	Total weight of iron in core, lb.....	97
29	Watts lost in iron (compare with guarantee).....	71
30	Total full-load losses, watts.....	127

DESIGN SHEET FOR TRANSFORMER.—(Continued)  
Efficiency and Exciting Current

31	Efficiency at unity factor: At 1 <sup>1</sup> / <sub>4</sub> full load.....	0.976
	At full load.....	0.977
	At <sup>3</sup> / <sub>4</sub> full load.....	0.977
	At <sup>1</sup> / <sub>2</sub> full load.....	0.973
	At <sup>1</sup> / <sub>4</sub> full load.....	0.959
32	All-day efficiency (4-hr full load).....	0.9877
33	Primary exciting current, amp.....	0.467

Regulation

34	Total equivalent IR drop, per cent.....	1.35
35	Total reactive drop, per cent.....	0.892
36	Regulation at unity power factor, per cent.....	1.354
37	Regulation at 0.8 power factor, per cent.....	1.615

Design of Tank-temperature Rise

38	Effective cooling surface of tank, sq in.....	1,164
39	Watts per sq in. of tank surface.....	0.151
40	Approximate temperature rise of oil, °C.....	34.3

sent a more rigid core; (3) have lower iron losses at higher flux densities; (4) have reduced strains in the iron, normally set up by clamps; and (5) are cheaper to manufacture.

In parallel with the improvement in the core material itself, a new type of coating has been developed. This consists of a chemical change that is induced in the surface of the sheet during manufacture. The altered surface is able to withstand annealing temperatures and punching and has the further merit of being thinner than enameled coatings. The stacking factor of a core with the new surface insulation is 0.97, as against 0.90 to 0.92 for enamel-insulated punchings.

The design in the following article will involve the use of an oriented steel ribbon core with a cruciform section.

147. Illustrative Example. Design of Distribution Transformer. Design a transformer to meet the following specifications:

- Output in kilovolt-amperes = 7.5
- Primary (high-tension) volts = 2,400
- Secondary (low-tension) volts = 120/240
- Frequency = 60 cycles
- Efficiency at unity power factor { Full load = 0.977  
  { <sup>1</sup>/<sub>4</sub> full load = 0.959
- Temperature rise not to exceed 55°C.



*Item 1.* It is proposed to design a core-type distribution transformer with circular coils. The core is to have a one-step cruciform section (see Fig. 157a) and is to be constructed with ribbon-oriented steel, U.S.S. Transformer 58 grade, 29-gage, the core-loss curve for which is given in *Engineering Manual No. 3 (U.S.S. Electrical Steel Sheets)\** on page 30. It is to be oil-immersed and self-cooling, without taps for voltage adjustment.

*Insulation tests* (in tank with oil); voltage applied for 1 min; H.T. winding to L.T. winding and core, 10,000 volts; L.T. winding to core, 4,000 volts.

The specified temperature rise of 55°C implies that the winding temperature, as measured by the resistance method, after the transformer has been operating continuously at full load, will not be more than 55°C above the ambient temperature.

#### CALCULATIONS

##### Guaranteed Losses.

$$\text{Total loss at full load} = \frac{1 - 0.977}{0.977} \times 7,500 = 177 \text{ watts}$$

$$\text{Total loss at } \frac{1}{4} \text{ full load} = \frac{1 - 0.959}{0.959} \times \frac{7,500}{4} = 80 \text{ watts}$$

$$\text{Full-load copper loss} = \frac{177 - 80}{1 - \frac{1}{16}} = 104 \text{ watts}$$

$$\text{Core loss} = 177 - 104 = 73 \text{ watts}$$

After several preliminary trials of approximate calculations of losses, the value of  $c = 41.8$  was selected. Thus

$$V_t = \frac{\sqrt{7,500}}{41.8} = 2.07$$

*Items 2 to 4: Primary and Secondary Turns.* It will be desirable to use four primary and four secondary coils in this design, which means that the total number of turns on both primary and secondary must be a multiple of four. Thus,

$$\text{Total secondary turns} = \frac{240}{2.07} = 116$$

$$\text{Total primary turns} = 10 \times 116 = 1,160$$

$$\text{Turns per secondary coil} = \frac{116}{4} = 29$$

$$\text{Turns per primary coil} = 10 \times 29 = 290$$

\* Published by Carnegie-Illinois Steel Corp. See Appendix 2, p. 437.

*Item 5: Full-load Current.* These are

$$I_p = \frac{7,500}{2,400} = 3.12 \text{ amp} \quad I_s = \frac{7,500}{240} = 31.2 \text{ amp}$$

*Items 6 to 16.* The window opening, to accommodate the primary and secondary windings, will next be determined, but before doing this it will be necessary to assume an approximate winding space factor and current density. Using formula (134),  $sf. = 10/(30 + 2.4) = 0.309$ , but this will be arbitrarily reduced to about 0.24, because, with circular coils, there will be some loss of winding space between the flat sides of the core and the low-tension windings, and also because of the extra insulation required between the low-tension coils on each leg (see Fig. 176). A current density of 1,100 will be selected, subject to later modification should space requirements, copper losses, and the need for selecting standard wire sizes for primary and secondary make this necessary. Thus

$$H \times D = \frac{2(116 \times 31.2)}{0.24 \times 1,100} = 27.4$$

Making  $H$  equal to about  $2.5D$ ,  $D = \sqrt{27.4/2.5} = 3.31$ , or (say)  $3\frac{5}{16}$  in. Also,  $H = 27.4/3.31 = 8.27$ , or (say)  $8\frac{3}{8}$  in.

Before proceeding further, it will be advisable to estimate the core dimensions and the iron loss. The maximum flux in the core is

$$\Phi = \frac{240 \times 10^3}{4.44 \times 60 \times 116} = 7.78 \times 10^5$$

Assuming a core density  $B'' = 83,000$  and a stacking factor of 0.9, the gross section of the iron will be

$$A_{\text{gross}} = \frac{7.78 \times 10^5}{83,000 \times 0.9} = 10.4 \text{ sq in.}$$

Referring to Art. 133 and Figs. 156 and 157,  $A_{\text{gross}} = 2WL - W^2$ , so that

$$10.4 = 2(0.525C \times 0.85C) - (0.525C)^2$$

from which  $C = 4.1$  in.,  $W = 2.16$  in.,  $L = 3.5$  in.

Since the core is wound *through* the coils with ribbon of two widths, one of them  $W = 2.16$  in., and the other  $L = 3.5$  in., proper allowances must be made as indicated by Fig. 174.

The length of the mean magnetic flux path is, therefore,

$$\begin{aligned} \text{M.m.p.} &= 2[H + (D - 2R)] + \pi(L + 2R) \\ &= 2(8.375 + 3.13 - 1) + \pi(3.5 + 1) = 35 \text{ in. (approx)} \end{aligned}$$

The total weight of the iron core is  $0.28(0.9 \times 10.4 \times 35) = 92$  lb.

Referring next to the curves from the *U.S.S. Manual* previously mentioned, or Appendix 2, the watts per lb at 83,000 lines per sq in., for oriented



steel strips sheared parallel to the grain of rolling, is 0.81; whence the core loss is  $0.81 \times 92 = 74.5$  watts, which exceeds the guaranteed loss of 73 watts slightly.

*Approximate Copper Losses.* In making calculations for the *approximate* copper losses in both primary and secondary it will be assumed that the current densities in the two windings are the same, although this is

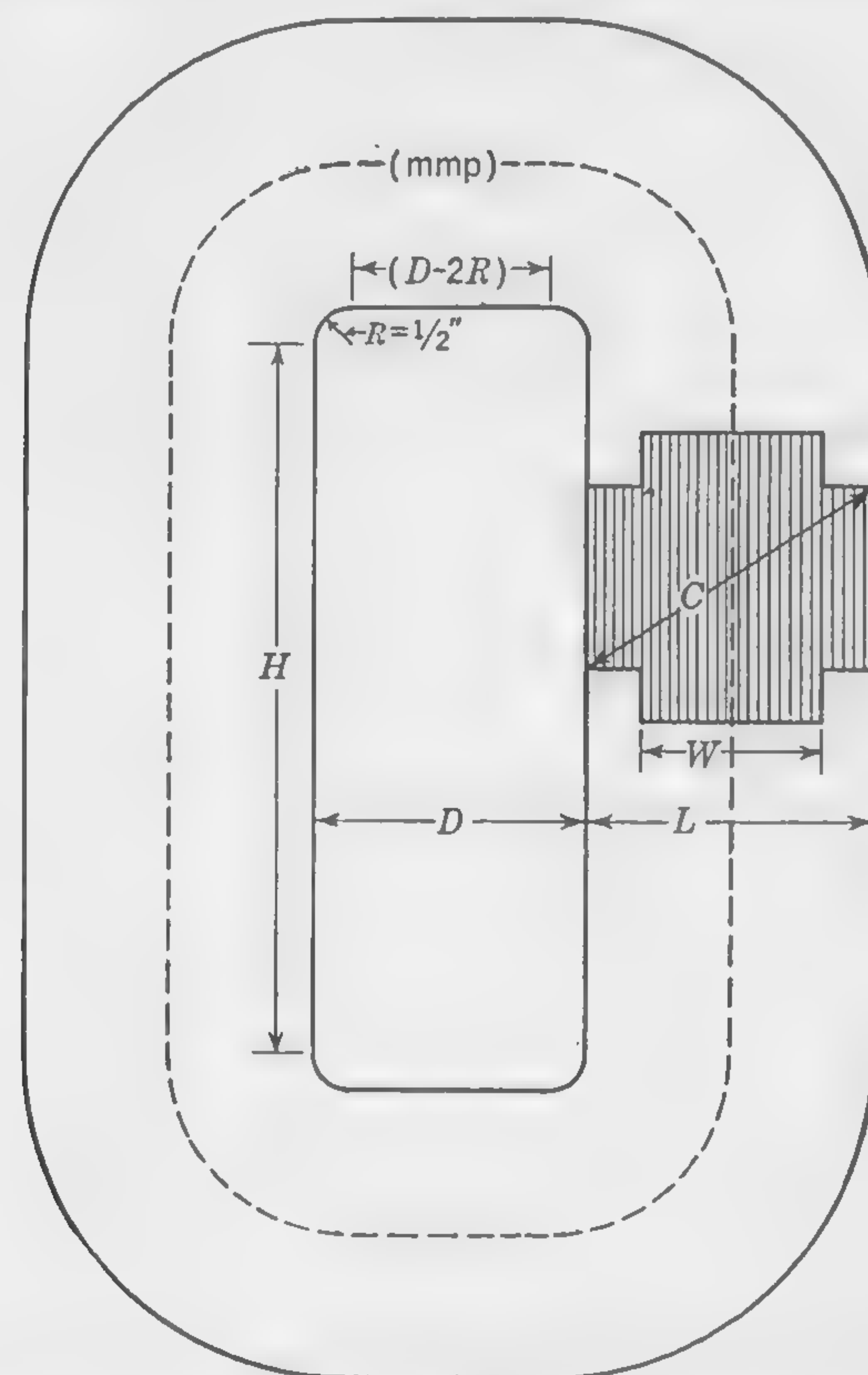


FIG. 174. Sketch showing core dimensions, window opening, and mean magnetic path for Illustrative Example of Art. 147.

generally not the case when standard wire sizes must be selected. Neglecting the small separation between the outer coils in the window opening (see Fig. 176), the average mean length of turn (m.l.t.) of the circular coils will be the average of the inner circumference  $\pi C$  and the outer circumference  $\pi(D + L)$ ; i.e.,  $\text{m.l.t.} = \pi/2(C + D + L)$ . Thus,

$$\text{M.l.t.} = \pi/2(4.1 + 3.31 + 3.5) = 17 \text{ in. (approx)}$$

The cross section in both windings is  $[2(116 \times 31.2)]/1,100 = 7.25 \text{ sq in.}$ , and the weight of copper is  $0.32 \times 17 \times 7.25 = 39.4 \text{ lb.}$  By formula

(131) the watts lost per pound is  $2.57\Delta^2/10^6$ , whence

$$\text{Total copper loss} = \frac{2.57(1,100)^2}{10^6} \times 39.4 = 123 \text{ watts}$$

This is also somewhat in excess of the guaranteed loss of 104 watts, but will be reduced to a satisfactory value later when wire sizes, yielding lower current densities than 1,100 amp per sq in., are selected.

*Size of Wire and Winding Particulars.* Figure 175 shows the general arrangement of the core and its surrounding windings. Note particularly the cruciform corner molds, and the tube forms around which the windings are placed and properly insulated before the transformer is

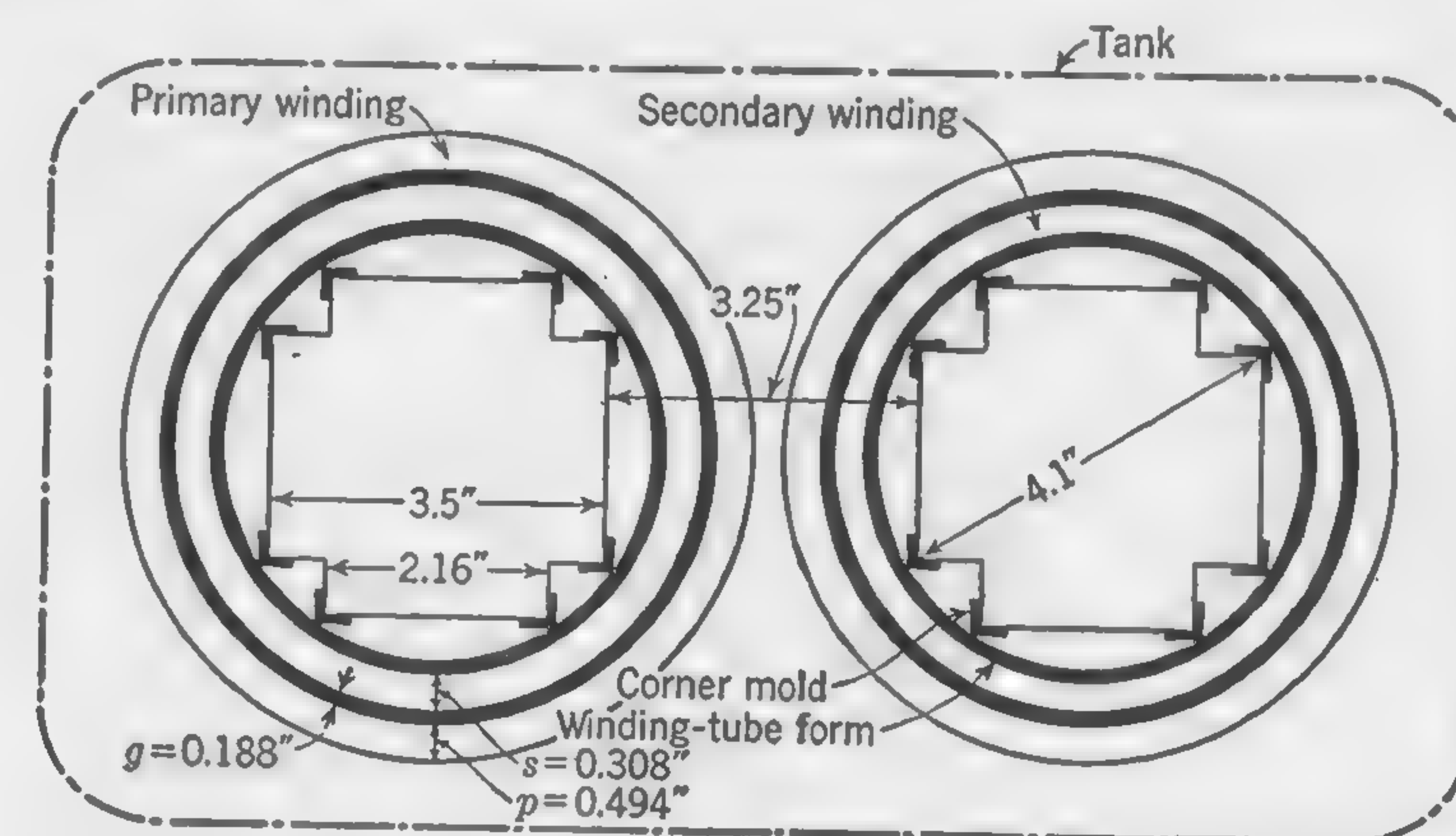


FIG. 175. Sketch showing the coil and insulation arrangement over the cruciform core for the Illustrative Example of Art. 147.

assembled. Another sketch illustrating the manner in which the windings are arranged in the window opening is given in Fig. 176.

The four secondary coils, two on each leg, will be wound directly over the insulating tube forms; each of the latter will be  $\frac{1}{8}$  in. thick, and will be covered with a 40-mil tape before the winding is started. The size of a suitable conductor of rectangular section may be calculated as follows. For a current density of about 1,100 amp per sq in. the cross section will be  $31.2/1,100 = 0.0284 \text{ sq in.}$  Assuming a winding layer of about 8 in., and with 29 conductors to the layer, each conductor should have a total width, including insulation, of  $\frac{8}{29} = 0.276 \text{ in.}$  The cotton covering will account for 18 mils, leaving 0.258 in. for copper. Consulting Table III, page 435, it is found that an area of 0.0325 sq in. would be suitable; this slightly larger area will be satisfactory because the current density and the resulting secondary copper loss will be reduced. The thickness of the wire, including insulation, will, therefore, be 0.140 in.



Thus, the active secondary current density will be  $31.2/0.0325 = 960$  amp per sq in. Finally, the total radial width of both secondary coils, allowing 10-mil paper between coils, will be  $(2 \times 0.149) + 0.01 = 0.308$  in. (see Fig. 176).

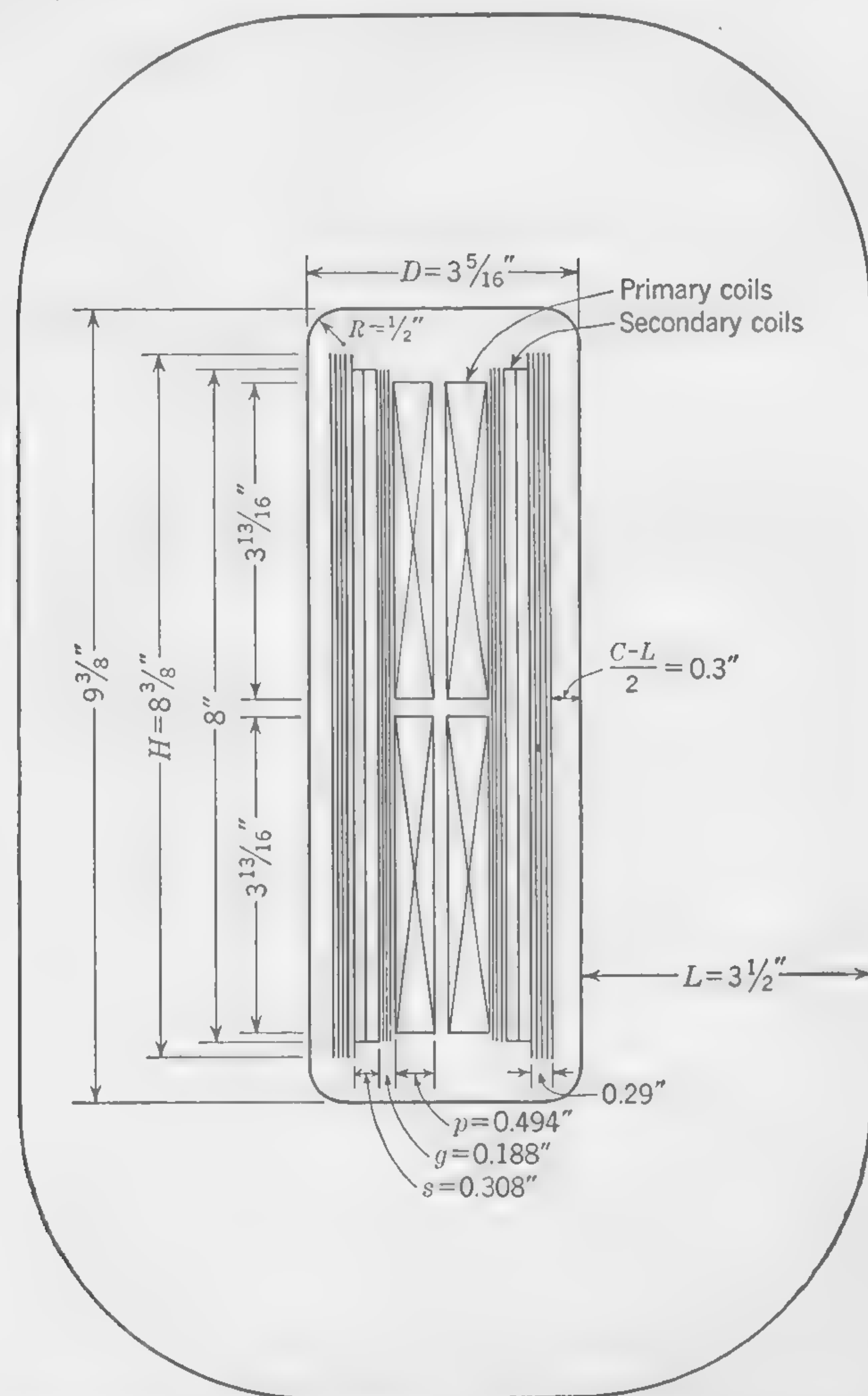


FIG. 176. Cross section of the windings and insulation in the window opening for the Illustrative Example of Art. 147.

Continuing radially, suitable insulating materials are placed over the outer low-tension coil; this will be about the same as that given in the table on page 377 for the Illustrative Example of Art. 145, so that  $g = 0.188$  in. There will be four primary coils as shown in Fig. 176, each one containing 290 turns. For a current density of about 1,100 amp per sq

in., the conductor area should be  $3.12/1,100 = 0.00284$  sq in. The size of standard round wire that would be suitable is No. 14 (see Table I, page 431), which has an area of 0.00323 sq in.; this is again slightly larger than that indicated above, so that the actual primary current density will be  $3.12/0.00323 = 965$  amp per sq in. Allowing  $7\frac{13}{16}$  in. in height for both coils on each leg, and  $\frac{3}{16}$  in. between coils to properly insulate them from each other, each coil will be  $(7\frac{13}{16} - \frac{3}{16})/2 = 3\frac{13}{16}$  in. high. Since No. 14 dcc wire winds 13 wires to the inch, there will be 49 wires in each layer. With 290 turns per coil there would, therefore, be 5 layers of 49 conductors and a final layer of 45 conductors; i.e., total turns per coil =  $(5 \times 49) + (1 \times 45) = 290$ . Using  $7\frac{1}{2}$ -mil paper between layers, the total radial width of the primary coil will be  $(6 \times 0.076) + (5 \times 0.0075) = 0.494$  in. (see Fig. 176).

The greatest difference of potential between layers will be twice the volts per layer. With 600 volts per coil in the high-tension winding, this will be  $(600/6) \times 2 = 200$  volts, which is satisfactory; note particularly that the volts between layers would have been twice this value if two primary coils had been used.

It will next be desirable to determine if there is sufficient clearance between the high-tension coils at the center of the window; if not it is generally customary to widen the dimension  $D$  sufficiently without increasing the iron loss perceptibly. Referring to Fig. 176, which shows the coil and insulation arrangement in the window, the following radial dimensions may be noted:

$(C - L)/2 \times 2 = 4.1 - 3.5 =$	0.600
(Corner mold) $\times 2 = 0.125 \times 2 =$	0.250
(Insulating tube) $\times 2 = 0.125 \times 2 =$	0.250
(Insulating tape on tube) $\times 2 = 0.04 \times 2 =$	0.080
Secondary winding plus insulation	0.616
Insulation between primary and secondary— $g =$	0.376
Primary winding plus insulation	0.988
Total	3.160

Subtracting 3.16 in. from the dimension  $D = 3.313$  leaves 0.153 in., which is ample for the separation of the primary coils at the center of the window.

*Items 17 to 22: Voltage Drop and Copper Losses.* Since the magnetizing component of the primary current is small it may be neglected in these calculations. Referring to Fig. 176, the mean lengths of turn of the windings, as designed, are:

$$\text{Secondary, m.l.t.} = \pi[C + (2 \times 0.29) + s] = \pi(4.1 + 0.58 + 0.308) = 15.65 \text{ in.}$$

$$\begin{aligned} \text{Primary m.l.t.} &= \pi[C + (2 \times 0.29) + 2s + 2g + p] \\ &= \pi(4.1 + 0.58 + 0.616 + 0.376 + 0.494) = 19.35 \text{ in.} \end{aligned}$$



The total lengths of the windings are:

$$\text{Secondary length} = (15.65/12) \times 116 = 151 \text{ ft}$$

$$\text{Primary length} = (19.35/12) \times 1,160 = 1,870 \text{ ft}$$

The weights of the windings are:

$$\text{Secondary weight} = 0.32 \times 0.0325 \times 151 \times 12 = 18.9 \text{ lb}$$

$$\text{Primary weight} = 0.32 \times 0.00323 \times 1,870 \times 12 = 23.2 \text{ lb}$$

The resistances of the windings at 75°C are:

$$\text{Secondary resistance} = 0.305 \times \frac{151}{1,000} = 0.046 \text{ ohm}$$

$$\text{Primary resistance} = \left( 2.936 \times \frac{309.5}{294.5} \right) \times \frac{1,870}{1,000} = 5.77 \text{ ohms}$$

where the number 0.305 is the resistance per 1,000 ft of the secondary conductor at 75°C, and the number 2.936 is the resistance per 1,000 ft of the primary conductor at 60°C.

The voltage drops in the windings are:

$$\text{Secondary } IR \text{ drop} = 31.2 \times 0.046 = 1.44 \text{ volts}$$

$$\text{Primary } IR \text{ drop} = 3.12 \times 5.77 = 18.0 \text{ volts}$$

The copper losses in the windings are:

$$\text{Secondary } I^2R \text{ loss} = 31.2 \times 1.44 = 45 \text{ watts}$$

$$\text{Primary } I^2R \text{ loss} = 3.12 \times 18.0 = 56 \text{ watts}$$

The total copper loss is 101 watts, which is slightly less than the guaranteed loss of 104 watts.

Items 23 to 30. The core dimensions and other data concerned with the core are given in Fig. 176 and in items 6 to 16.

The total full-load losses, item 30, are  $74.5 + 101 = 175.5$  watts.

Item 31: *Efficiencies*. Refer to Art. 140. The efficiencies at unity power factor are:

$$\eta_{1\frac{1}{2}\%} = 1 - \frac{74.5 + 158}{9,375 + 232.5} = 0.976$$

$$\eta_{1\%} = 1 - \frac{74.5 + 101}{7,500 + 175.5} = 0.977$$

$$\eta_{\frac{3}{4}\%} = 1 - \frac{74.5 + 57}{5,625 + 131.5} = 0.977$$

$$\eta_{\frac{1}{2}\%} = 1 - \frac{74.5 + 28}{3,750 + 102.5} = 0.973$$

$$\eta_{\frac{1}{4}\%} = 1 - \frac{74.5 + 7}{1,875 + 81.5} = 0.959$$

The maximum efficiency occurs when the iron loss is equal to the copper loss, and this takes place when the

$$\text{kva}_{\eta=\max} = \text{kva}_{\text{rated}} \sqrt{\frac{\text{iron loss}}{fl \text{ copper loss}}} = 7.5 \sqrt{\frac{74.5}{101}} = 6.43$$

The maximum efficiency is, therefore,

$$\eta_{\max} = 1 - \frac{74.5 + 74.5}{6,430 + 149} = 0.9774$$

Item 32: *All-day Efficiency*. On the basis of 4-hr full load and 20-hr no load, the all-day efficiency is

$$\eta_{\text{ad}} = 1 - \frac{(74.5 \times 24) + (101 \times 4)}{(7,500 \times 4) + (2192)} = 0.9318$$

Item 33: *Primary Exciting Current*. Referring again to the *U.S.S. Manual No. 3* for steel sheets, on page 29, or Appendix 2, it is found that the magnetizing force, for a density of 83,000 lines per sq in., is 14.5 amp-turns per in. Also, consulting Fig. 162, the number of ampere-turns per joint at the same density is about 63. (There is only one joint in the magnetic circuit of a ribbon-wound core.) The maximum value of the total number of ampere-turns required to magnetize the core will, therefore, be

$$TI = (14.5 \times 35) + 63 = 571$$

where the figure 35 is the mmp as determined on page 385. The magnetizing component of the primary current—the rms value—thus becomes

$$I_o = \frac{571}{\sqrt{2} \times 1,160} = 0.35 \text{ amp}$$

The “energy” component is

$$I_w = \frac{74.5}{2,400} = 0.31 \text{ amp}$$

so that the total exciting current is

$$I_e = \sqrt{(0.35)^2 + (0.31)^2} = 0.467 \text{ amp}$$

Items 34 to 37: *Regulation*. The percentage *IR* drop in the two windings is the total copper loss, item 22, expressed as a percentage of the rated kva output. Thus

$$\text{Per cent } IR \text{ drop} = \frac{101}{7,500} \times 100 = 1.35$$



The numerical values of the quantities in formula (135) required for the calculation of the per cent leakage reactance drop are as follows:  $f = 60$ ,  $T_s = 116$ ,  $I_s = 31.2$ ,  $n = 2$ . The length  $l$  may be taken as the average of the mean lengths per turn of the high- and low-tension windings; thus, from item 17,  $l = (19.35 + 15.65)/2 = 17.5$  in. The remaining dimensions are taken from Fig. 176, where  $h = 9\frac{3}{8}$  in.,  $g = 0.188$  in.,  $p = 0.494$  in., and  $s = 0.308$  in. Substituting these values in the formula,

$$\text{Per cent } IX = \frac{2 \times 60 (116)^2 \times 31.2 \times 17.5}{2 \times 9.375 \times 240 \times 10^5} \left( 0.188 + \frac{0.494 + 0.308}{3} \right) = 0.892$$

This is equivalent to a reactive drop of  $0.00892 \times 2,400 = 21.4$  volts in the primary winding.

Using formula (139),

$$\text{Per cent regulation (at PF} = 1.0) = 1.35 + \frac{(0.892)^2}{200} = 1.354$$

Using formula (138),

$$\begin{aligned} \text{Per cent regulation (at PF} = 0.8) &= (1.35 \times 0.8) + (0.892 \times 0.6) \\ &+ \frac{[(0.892 \times 0.8) - (0.6 \times 1.35)]^2}{200} = 1.615 \end{aligned}$$

*Items 38 to 40: Temperature Rise.* In designing a tank for the transformer, it is important to bear in mind that the oil temperature near the top must be somewhat less than the specified temperature rise of the windings. It is, moreover, desirable to have a reasonable clearance between the outside surface of the coils and the inside surface of the tank; for this design the clearance should be about  $\frac{3}{4}$  in., so that the tank outline will be approximately as shown in Fig. 175. Assuming an average temperature rise of about  $35^\circ\text{C}$ , for which the cooling coefficient  $c = 0.0044$  (see Art. 141), the total effective outside area of the tank should be about  $S = 175.5/(0.0044 \times 35) = 1,140$  sq in. Remembering that the surface to be considered is the area of the vertical sides plus one-half the area of the lid, a rectangular tank having dimensions  $8 \times 15$  in. and a height of 24 in. should be suitable. The cooling surface will, therefore, be

$$S = 2(8 + 15) \times 24 + \frac{1}{2}(8 \times 15) = 1,164 \text{ sq in.}$$

whence the probable maximum temperature rise of the oil is

$$t = \frac{175.5}{0.0044 \times 1,164} = 34.3^\circ\text{C}$$

**148. Design of High-voltage Power Transformers.** The transformer designs illustrated by Arts. 145 and 147 omit much that would have to be taken into account when designing larger transformers, especially for use

on high-pressure systems. The distribution of the total losses between the iron and copper would generally be such as to give maximum efficiency at full load. This condition is attained when the copper losses at full load are equal to the core losses.

Self-cooling transformers of large size are made by providing corrugated sides or cooling ribs to the tank, so as to increase the cooling surface (see Art. 142). When this area is insufficient to dissipate all the heat losses, external radiators, through which the oil can circulate, are provided. By directing an air blast against the radiators, their effectiveness for a given cooling surface may be greatly increased. The method of oil cooling by circulating water in pipes was discussed in Art. 143.

Although there are no moving parts in the a-c transformer, mechanical forces of considerable magnitude may cause displacement or distortion of the windings unless proper mechanical bracing is provided. These forces are due to the strong magnetic fields which may exist outside the iron core on heavy overloads or short circuits. The manner in which the mechanical effects of these stray magnetic fields may be calculated will be explained in the next chapter.

The biggest problem in the design of large power transformers for use on high-pressure circuits is the provision of adequate insulation, to withstand the very high voltages, while keeping the space between the windings and between the high-tension coils and ground metal as small as possible; also due account must be taken of the fact that the end turns are subjected to extremely high stresses during surge periods. In this connection a knowledge of the fundamental laws of the electrostatic circuit is essential. It is, moreover, important to recognize the need for specially designed high-voltage bushings to bring out the terminal ends of the high-voltage windings.

**149. Design of Instrument Current Transformers.** These transformers are usually of small size, their function being to provide a current for measuring instruments which shall be as nearly as possible proportional to the line current which passes through the primary winding. The secondary current is usually around 5 amp, but the primary current may be very much larger. Even when the ratio of transformation is not large, current transformers may be used on high-voltage circuits to avoid having to insulate the instruments for high voltages.

A current transformer does not differ fundamentally from a potential transformer, but, since the primary windings are in series with the primary circuit, the voltage across both primary and secondary terminals will not be approximately constant, as in a potential transformer, but will follow the changes in the primary current. For a given current in the secondary circuit, the voltage across the primary terminals will depend upon the impedance of the secondary circuit. For any known



or assumed secondary burden, it is possible to construct the vector diagram for a current transformer in exactly the same manner as for a potential transformer.

For use on an ammeter, the essential feature of a good current transformer is that the ratio between primary and secondary currents shall remain approximately the same over the whole range of currents to be measured; but when used on a watt-meter, it is equally important that the phase-angle error be also very small. This means that, under all conditions of load, the primary and secondary currents should be as nearly as possible in the same (or opposite) phase.

**150. Calculation of Phase Angle and Current Ratio.** The vector diagram (Fig. 177) has been drawn for a particular secondary burden of

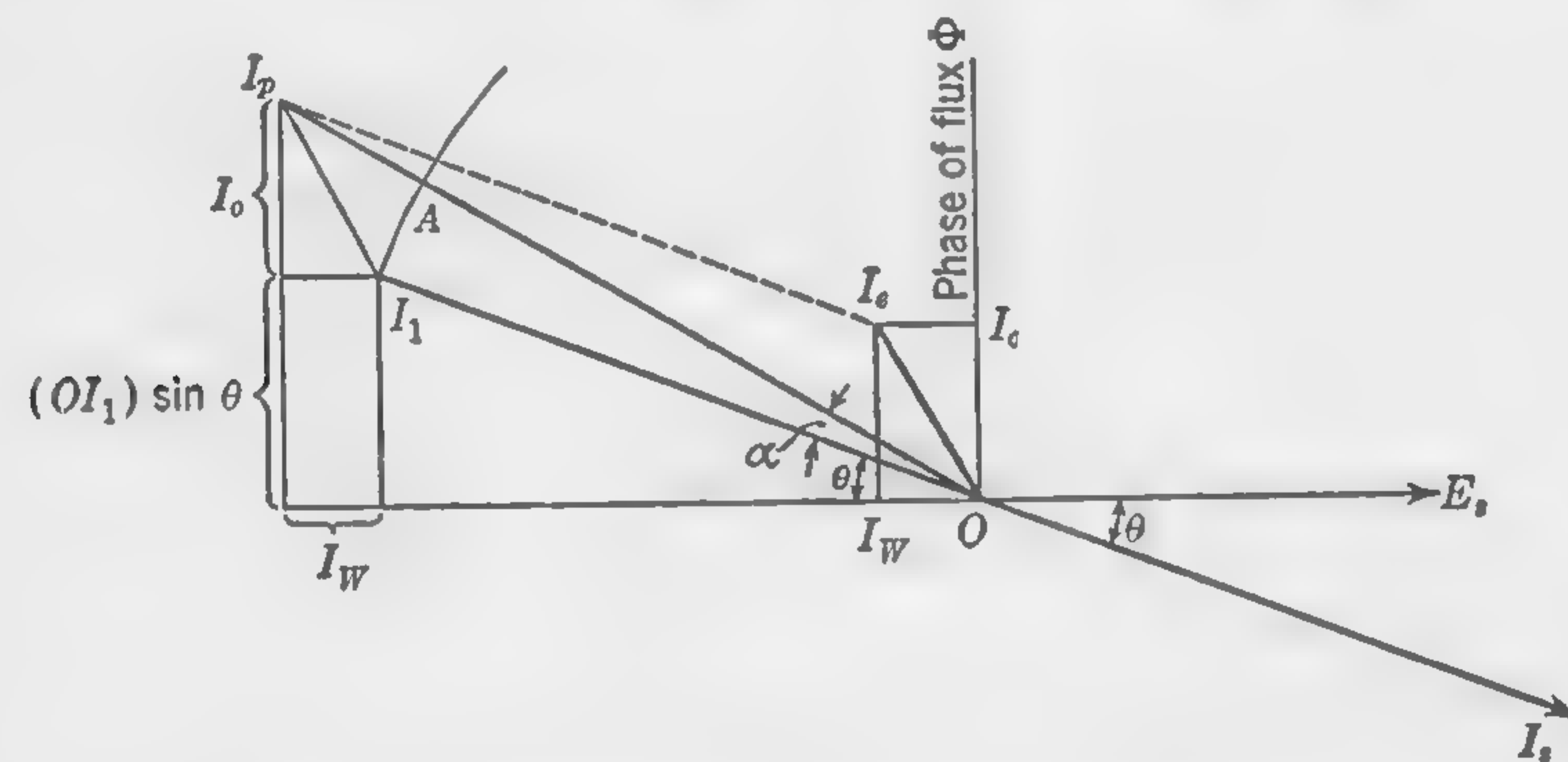


FIG. 177. Vector diagram for current transformer.

$E_s I_s$  volt-amp, or  $E_s I_s \cos \theta$  watts. This burden must be thought of as including not only the instrument burden but also the resistance (and reactance, if any) of the secondary transformer winding and the connections between transformers and instrument. The phase of the flux in the transformer core will therefore be drawn exactly  $90^\circ$  in advance of the vector  $OE_s$ . The vector  $OI_1$  is the current component in the primary circuit which exactly balances the current  $I_s$  magnetically; that is to say, it is exactly opposite in direction to  $OI_s$  and equal in length to  $I_s(T_s/T_p)$ , where  $T_s$  and  $T_p$  are the secondary and primary turns, respectively. The vector  $OI_e$ , representing the total exciting current component, is calculated as explained in connection with Fig. 160, and the current in the primary is  $I_p$ , resulting from the (vectorial) addition of  $I_1$  and  $I_e$ .

*Calculation of Phase Angle.* In order to calculate the phase angle  $\alpha$  between the vectors  $OI_1$  and  $OI_p$ , we may write

$$\tan (\theta + \alpha) = \frac{I_1 \sin \theta + I_o}{I_1 \cos \theta + I_w} \quad (u)$$

also,

$$\tan (\theta + \alpha) = \frac{\tan \theta + \tan \alpha}{1 - \tan \theta \tan \alpha} \quad (b)$$

Equate formulas (a) and (b) and multiply out. This leads to the expression

$$\tan \alpha = \frac{I_o \cos \theta - I_w \sin \theta}{I_1 + (I_o \sin \theta + I_w \cos \theta)} \quad (c)$$

The length of the vector  $I_1$  is  $I_s(T_s/T_p)$ , which is always very large in comparison with the quantity  $(I_o \sin \theta + I_w \cos \theta)$ , which may therefore be omitted from the denominator of Eq. (c); whence the approximate value of the tangent of the phase angle is

$$\tan \alpha = \frac{I_o \cos \theta - I_w \sin \theta}{\left(\frac{T_s}{T_v}\right) I_s} \quad (151)$$

*Calculation of Current Ratio.* Since the angle  $\alpha$  (Fig. 177) is always very small, rarely exceeding  $1^\circ$  and frequently limited to 30 or even 15 min., it follows that the arc of circle of radius  $OI_1$  approximates very closely a perpendicular erected on  $OI_1$  at the point  $I_1$ . In other words, the difference in length between the vectors  $OI_p$  and  $OI_1$  is equal to the projection of  $I_1I_p$  (or  $OI_e$ ) on  $OI_1$ , and this may be written  $I_w \cos \theta + I_o \sin \theta$ ; whence

$$I_p = \left( \frac{T_s}{T_p} \right) I_s + I_w \cos \theta + I_o \sin \theta$$

and the true transformation ratio for any particular secondary burden is

$$\left(\frac{I_p}{I_s}\right) = \left(\frac{T_s}{T_p}\right) + \frac{I_w \cos \theta + I_o \sin \theta}{I_s} \quad (152)$$

The magnetizing component  $I_o$  of the total exciting current component is calculated by the formula

$$I_o = \frac{\text{ampere-turns required for the core}}{\sqrt{2} T_n} \quad (153)$$

The "energy" component of the exciting current is

$$I_w = \left( \frac{T_o}{T_w} \right) \frac{\text{total power loss in core in watts}}{P_o} \quad (154)$$

where  $E_2$  = induced secondary voltage,



It is only by keeping the current components  $I_o$  and  $I_w$  very small in comparison with the total primary current that the ratio and phase angle errors can be kept within the required limits. This involves the use of the best quality of transformer iron and flux densities very much lower than those ordinarily used in power and distributing transformers. Figure 178 may be used for calculating the ampere-turns required for flux densities up to 17,000 lines per sq. in., and approximate values of the watts loss per pound of iron at 60 cycles may be read from Fig. 179.

Iron-nickel alloys, known as nickel-steel, vary considerably in respect to their magnetic properties. Properly annealed *hipernik* (Westinghouse

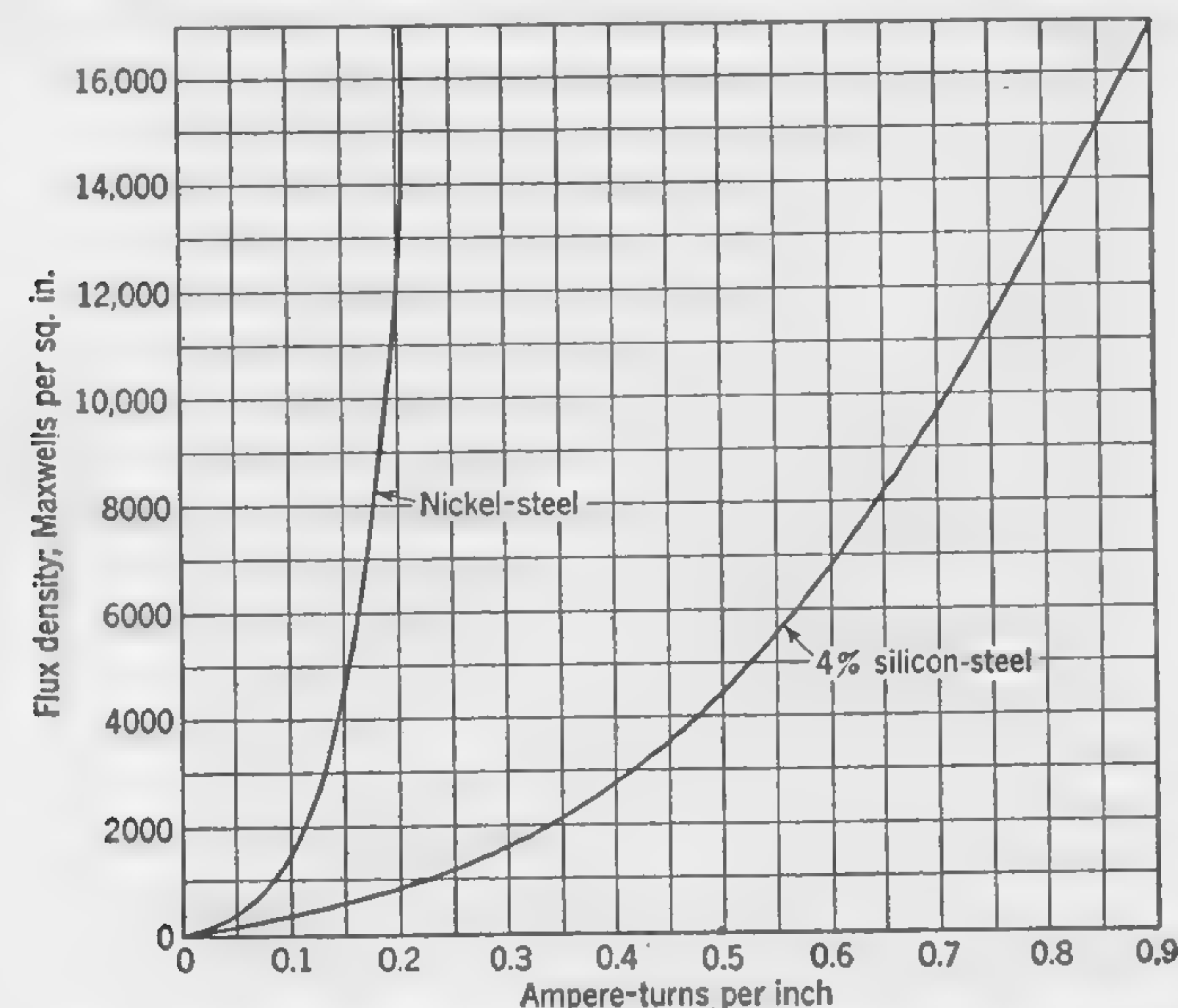


FIG. 178. Magnetization curves for low values of flux density.

Electric and Manufacturing Co.) takes only about half the exciting ampere-turns required for the sample of nickel-steel from which Fig. 178 has been plotted. Nickel-steel is much more costly than silicon-steel, but economy of weight and size may frequently justify its use for instrument transformers.

The burden imposed on a current transformer by a single instrument (ammeter or wattmeter) may vary between about 0.6 volt-amp with 0.9 power factor and 60 volt-amp with 0.5 power factor. The full-load secondary current is usually 5 amp.

**151. Illustrative Example. Design of Current Transformer for Watthour Meter.** The specification for this transformer is given at the top of the design sheet shown on page 398. It is not possible to calculate the various items in the order in which they are recorded on the

design sheet, but so far as possible this order will be followed in working out the numerical values.

*Items 1 to 5.* Within certain limits, a large number of turns in the windings will tend to reduce the errors because the exciting current component in the primary will be a small percentage of the total current. We shall assume the total secondary ampere-turns to be 1,400.

Since  $I_p = 200$  and  $I_s = 5$ , the number of turns are  $T_p = 7$  and  $T_s = 280$ , but a very slight change in the secondary turns may be made later to compensate for ratio error.

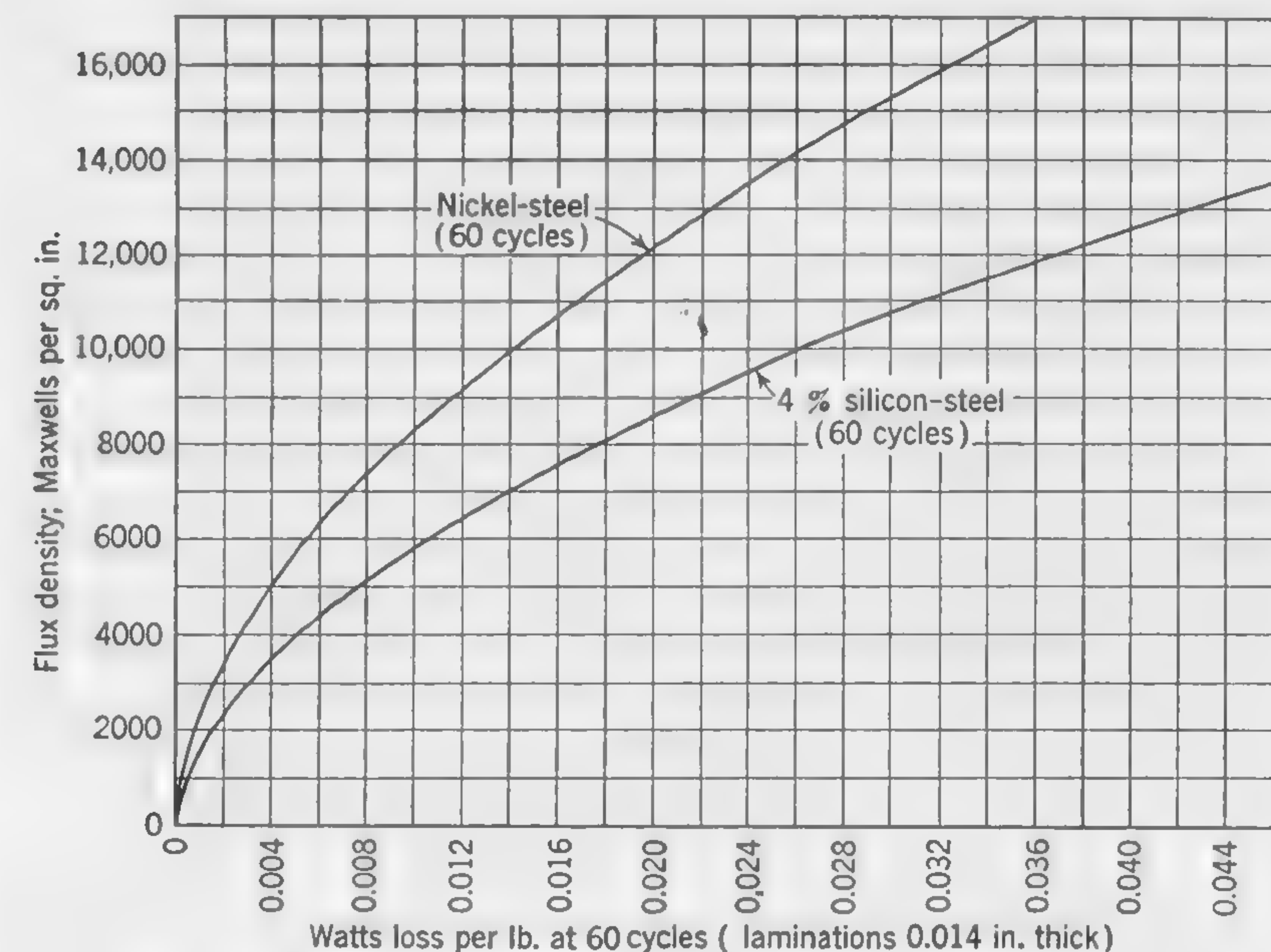


FIG. 179. Losses in transformer iron for low values of flux density.

Assuming a core-type transformer as shown in section (Fig. 180), there is no serious objection to winding both primary and secondary on both limbs as in a distributing or power transformer. We shall, however, assume the winding to consist of a single coil containing both primary and secondary turns.

*Items 6 to 8.* A high current density in the secondary should be avoided as it tends to increase the  $IR$  drop in the winding. This is apart from heating effects, which are not likely to give trouble on normal loads but may be very serious on momentary overloads such as occur in the case of short circuits on the primary system.

Assuming current densities of 1,100 and 1,400 amp per sq. in. in secondary and primary, respectively, we have  $5/1,100 = 0.00454$  as the



DESIGN SHEET FOR INSTRUMENT CURRENT TRANSFORMER

Specifications: ratio, 200/5; voltage of primary circuit, 6,600; 60 cycles

External burden { Volt-amperes = 3.5  
Power factor = 0.85

Permissible limits of error over range from 10 to 100 per cent of rated

current. . . . . { Phase angle: 20 min  
Ratio: 0.5 per cent

Item No.	Windings	Primary	Secondary
1	Secondary amp-turns.....		1,400
2	Full-load current, amp.....	200	5
3	Total number of turns.....	7	279
4	Number of coils.....	1	1
5	Turns per coil.....	7	279
6	Current density, amp per sq in.....	1,420	1,075
7	Cross section of conductor, sq in.....	0.141	0.00465
8	Dimensions of conductor.....	0.44 × 0.32	No. 13 square
9	Number of turns per layer of winding.....	7	43
10	Number of layers per coil.....	1	7
11	Insulation between layers, in.....	None	0.005
12	Mean length per turn, ft.....	0.95	0.76
13	Total length of wire, ft.....	6.7	213
14	Weight of copper, lb.....	3.6	4.23
15	Resistance of secondary at 75°C, ohms.....		0.413
16	IR drop in secondary, volts.....		2.06
17	Total secondary burden, volt-amp.....		14.1
18	Power factor of total burdern (cos θ).....		0.991

The Magnetic Circuit

19	Dimensions of window, in.....	4¼ by 1½
20	Total flux (maxwells) at 100 per cent rating.....	3,780
21	Flux density in iron of core, lines per sq in.....	1,890
22	Cross section of iron in core, sq in.....	2
23	Width of stampings in core, in.....	1½
24	Gross thickness of core, in.....	1½
25	Mean length of flux path, in.....	17¾
26	Weight of iron in core, lb.....	10
27	Sketch showing cross section through window.....	Fig. 180

Calculated Performance		Full Burden	1/10th Burden
28	Amp-turns per in. (from Fig. 178).....	0.35	0.05
29	Watts per lb (from Fig. 179).....	0.0015	0.000037
30	Component $I_o$ of exciting current.....	0.628	0.09
31	Component $I_w$ of exciting current.....	0.213	0.0525
32	Phase angle by formula (151).....	+10'	+14'
33	Per cent ratio error, by formula (152).....	0.21	0.037

cross section of the secondary wire. From the wire table on page 432, we select No. 13 square wire with a cross section of 0.00465 sq in. The current density in the secondary is, therefore,  $\Delta = 5/0.00465 = 1,075$  amp per sq in.

Before deciding upon the actual dimensions of the primary winding, which will probably consist of a fairly heavy conductor of rectangular section, it will be advisable to settle upon the approximate dimensions for the window or opening to accommodate the windings.

Items 19 to 24. By formula (134) we have  $sf = 10/(30 + 6.6) = 0.273$ , but this should be reduced at least 10 per cent because of the small size of the transformer. We shall try  $sf = 0.24$ ; whence, for an average current density of about 1,200, we have for the area of the opening in the core,  $H \times D = (2 \times 1,400)/(1,200 \times 0.24) = 9.7$  sq in. If the length  $H$  of the window is made equal to about twice the width  $D$ , we may try the dimensions  $H = 4\frac{1}{4}$  in. and  $D = 2\frac{1}{4}$  in. The width  $D$  may be altered later if necessary to accommodate the coils.

A rough estimate must now be made of the core cross section in order that the lengths of wire in the windings may be calculated. The total flux in the core will depend upon the *total* voltage to be generated in the secondary and not only on the amount of the external burden. We shall assume the total burden (including secondary winding and connecting leads) to be 15 volt-amp which, with a secondary current of 5 amp, means that the flux in the core must develop 3 volts in the 280 turns of secondary winding. Thus,

$$\Phi = \frac{3 \times 10^8}{4.44 \times 60 \times 280} = 4,000 \text{ maxwells}$$

Very low flux densities must be used in order to avoid exceeding the limits of error as specified. If we use a good quality of silicon-steel, which is a cheaper material than nickel-steel, we may select a flux density as low as  $B'' = 2,000$  lines per sq in. This leads to a core section about  $1\frac{1}{2}$  by  $1\frac{1}{2}$  in. which, with a stacking factor 0.89, makes the cross section of iron equal to  $1.5 \times 1.5 \times 0.89 = 2$  sq in.

Items 8 to 14. For the primary winding we need a copper cross section of about  $200/1,400 = 0.143$  sq in. and, since we have to insulate for 6,600 volts, we shall assume a winding layer  $3\frac{1}{4}$  in. long, leaving  $\frac{1}{2}$  in. at each end between high-tension winding and core. Two strips in parallel, each 0.44 by 0.16 in., wound one on top of the other to make one layer of seven turns will probably be satisfactory. The current density in primary is therefore  $200/[2(0.44 \times 0.16)] = 1,420$  amp per sq in. For the secondary, the length of layer may be  $3\frac{3}{4}$  in. There will be 7 layers of No. 13 square dec wire with 0.005-in. paper between layers.



As a check on width of window opening, and in order to calculate length of wire, we have the total thickness of coil built up as follows:

Insulation on core, and clearance	$t = 0.125$
Secondary coil consisting of 7 layers of wire with 0.005-in. paper between layers, and a small allowance for "bulging"	$s = 0.75$
Insulation between primary and secondary, built up of press-board, varnished cambric, or flexible mica, and cotton tape (no oil ducts)	$g = 0.15$
Primary coil, two layers of dec copper strip 0.16 in. thick, with allowance for bulging	$p = 0.45$
Insulation, primary to core (same as $g$ )	0.15
Total	$= 1.625$ in.

With a window opening  $D = 1\frac{5}{8}$  in., there should be plenty of room to accommodate the windings. The reason why this dimension is appreciably less than the estimated  $2\frac{1}{4}$  in. is that the windings are all on one limb instead of on both limbs as in power transformers, and also that solid insulation has been used and there are no ducts for oil circulation.

The mean length per turn of primary is 0.95 ft, and of the secondary, 0.76 ft. The weight of primary is 3.6 lb, and of secondary, 4.23 lb.

Items 15 to 18. From the wire table on page 431, the resistance per 1,000 ft of square No. 13 wire is found to be 1.846 ohms at 60°C. Whence the secondary resistance at 75°C is  $1.846 \times 0.213 \times [(235 + 75)/(235 + 60)] = 0.413$  ohm, and the  $IR$  drop is  $0.413 \times 5 = 2.065$  volts. Including connections between transformer and instrument, this drop might be 2.2 volts. In order to calculate the total burden (internal plus external), we have for the instrument burden,  $IZ = 3.5/5 = 0.7$  volt;  $IR = 0.7 \times 0.85 = 0.595$  volt, and  $IX = 0.7 \times 0.527 = 0.369$  volt. If we assume the reactance of the secondary winding and leads to be negligible, the total  $IR$  is 2.795 and the total  $IX$  is 0.369.

$\tan \theta = 369/2,795 = 0.132$ ; whence (from trigonometric tables)  $\cos \theta = 0.991$  and  $\sin \theta = 0.131$ . The total emf to be developed in the secondary winding is  $2.795/0.991 = 2.82$  volts, and the total secondary burden is  $2.82 \times 5 = 14.1$  volt-amp.

Items 19 to 27. The corrected window dimensions are  $4\frac{1}{4}$  by  $1\frac{5}{8}$  in. The total flux is  $\Phi = (2.82 \times 10^8)/(4.44 \times 60 \times 280) = 3,780$  maxwells; whence  $B'' = 3,780/2 = 1,890$  lines per sq in. when the secondary current has its full rated value of 5 amp.

The mean length of flux path in the core is  $2(4\frac{1}{4} + 1\frac{5}{8} + 3) = 17\frac{3}{4}$  in. The weight of iron is  $17.75 \times 2 \times 0.28 = 10$  lb.

Figure 180 shows a section through core and windings of the transformer as designed.

Items 28 to 31. From Fig. 178 we read the ampere-turns per inch for the iron (silicon-steel), about 0.35 for  $B'' = 1,890$ , and 0.05 for  $B'' = 189$ .

From Fig. 179 we read watts per pound = 0.0015 for  $B'' = 1,890$ . It is practically impossible to read the losses at one-tenth rated burden from this curve, but by assuming the iron loss to vary as  $B^{1.6}$ , we have, for  $B'' = 189$ , watts per pound =  $0.0015 \times (1/10)^{1.6} = 0.000037$ .

In calculating the magnetizing current component we shall make no allowance for joints in the magnetic circuit because the reluctance of the

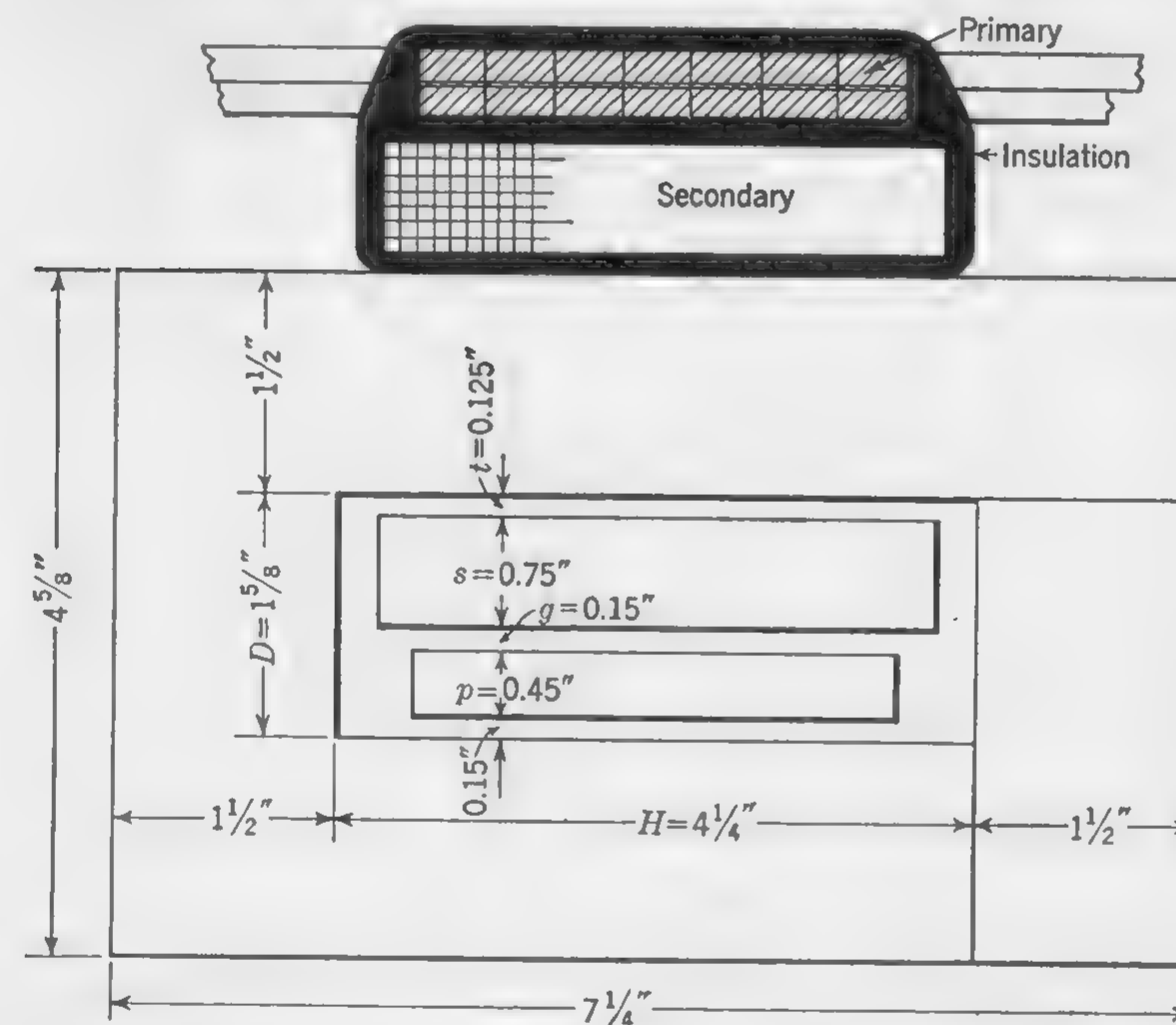


FIG. 180. Cross section through current transformer of Illustrative Example of Art. 151.

joints is negligible at very low flux densities. Then, by formula (153), at full load,

$$I_o = \frac{17.75 \times 0.35}{\sqrt{2} \times 7} = 0.628 \text{ amp}$$

and at one-tenth load,  $I_o = 0.09$  amp.

By formula (154), at full load,

$$I_w = 40 \times \frac{10 \times 0.0015}{2.82} = 0.213 \text{ amp}$$

and at one-tenth load,

$$I_w = 40 \times \frac{10 \times 0.000037}{0.282} = 0.0525 \text{ amp}$$



Item 32. By formula (151), the tangent of the phase angle with 100 per cent rated current is

$$\tan \alpha = \frac{0.628 \times 0.991 - 0.213 \times 0.131}{40 \times 5} = 0.00298$$

whence  $\alpha = +10'$ .

Similarly, with one-tenth rated current, we have  $\tan \alpha = 0.0041$  and  $\alpha = +14'$ .

These results are well within the specified limit of 20 min.

Item 33. If we leave the secondary winding unchanged with 280 turns, the ratio with full-rated current, by formula (152), is

$$\frac{I_p}{I_s} = 40 + \frac{0.213 \times 0.991 + 0.628 \times 0.131}{5} = 40 + 0.059$$

and with one-tenth rated current,

$$\frac{I_p}{I_s} = 40 + \frac{0.0525 \times 0.991 + 0.09 \times 0.131}{0.5} = 40 + 0.128$$

the maximum *percentage* ratio error being  $100 \times (0.128/40) = 0.32$  which is well within the specified limit of 0.5 per cent. If desired, this error can be reduced by altering the number of secondary turns. Thus, if we remove one turn of the secondary, the compensation for ratio error is  $279/40 = -0.143$ , which makes the actual ratio at full load equal to 39.916 and at one-tenth load, 39.985, the *percentage* errors being 0.21 and 0.037 respectively.

Since the calculated performance of this transformer is somewhat better than that called for in the specification, it is possible that some saving of material might be effected (1) by reducing the number of primary turns from 7 to 6 without decreasing the core section, or (2) by leaving the number of turns unchanged and slightly decreasing the core section. The greatest saving in *weight* would be obtained by using nickel-steel instead of silicon-steel for the transformer core.

*Effect of Overload on Temperature of Windings.* A short circuit may cause the current through the primary windings of current transformers to be from fifty to one hundred times the rated full-load value, and, unless the circuit breakers interrupt this current in a very short interval of time, the instrument transformer may burn up. This is apart from possible mechanical injury which will be considered in the following chapter.

In order to calculate the maximum length of time during which such a condition may exist without damage from overheating, it is usual to neglect the very small amount of heat which will be dissipated by surface radiation and consider merely the thermal capacity of the coils.

Assuming that a temperature above  $180^\circ\text{C}$  would be injurious to the insulation, and that the copper temperature is  $75^\circ\text{C}$  under normal oper-

ating conditions with 200 amp in primary, the permissible rise of temperature is  $180 - 75 = 105^\circ\text{C}$ .

The primary copper loss when the current is 200 amp at a density of 1,420 amp per sq in. may be calculated by formula (131) in Art. 130. Thus, at  $75^\circ\text{C}$ , the loss in the primary coils is  $3.6 \times [2.57(1,420)^2/10^6] = 18.6$  watts. The permissible watt-seconds per pound of copper are calculated as explained in Art. 64, and, since 177 watts will raise the temperature of 1 lb of copper  $1^\circ\text{C}$  in 1 sec, the permissible amount of heat which can be stored in the primary coil before the temperature becomes excessive is  $177 \times 3.6 \times 105 = 66,800$  watt-sec.

Suppose that, under short-circuit conditions, the current through transformer primary may be fifty times normal, or  $200 \times 50 = 10,000$  amp. The rate at which energy in the form of heat is being stored in the copper will be  $18.6 \times (50)^2 = 46,500$  watts, and since  $66,800/46,500 = 1.435$  sec, this is the maximum time during which the short-circuit current may pass through the coil without damage to the transformer.

### TEST PROBLEMS

1. Given a single-phase transformer: number of primary turns = 1,400; frequency = 60; flux in core = 600,000 maxwells. Calculate the full-load current in the secondary (low-pressure) winding when the output is 7.5 kva, the ratio of transformation being 10 to 1.

Ans. 33.5 amp.

2. Calculate the total magnetic flux in a 60-cycle transformer in which the induced emf is 2 volts per turn of winding.

Ans. 750,000 maxwells.

3. A single-phase transformer connected to a 2,300-volt 60-cycle circuit has 1,100 turns in the primary winding. The cross section of the iron core measures 3 by 4.5 in. Calculate the maximum flux density on the assumption of a stacking factor of 0.86.

Ans. 67,500 lines per sq in.

4. Calculate the amount of flux in the core (under the windings) of a 25-kva single-phase transformer, given the following particulars: full-load secondary current = 111 amp; frequency = 60; transformation ratio = 10 to 1; number of primary turns (high-tension side) = 750.

Ans. 1,125,000 maxwells.

5. The current densities in the primary (high-tension) and secondary (low-tension) windings of a transformer are 1,200 and 1,500 amp per sq in., respectively. The ratio of transformation is 10 to 1, and the mean length per turn of the primary is 10 per cent greater than that of the secondary. Calculate the resistance of the secondary winding, given that the primary resistance is 8 ohms.

Ans. 0.091 ohm.

6. In a transformer having a 10 to 1 ratio, the copper losses in the primary are 15 per cent less than in the secondary. The resistance per turn of the primary is 0.00394 ohm, and there are 1,485 more turns in the primary than in the secondary. Calculate the resistance of the secondary winding.

Ans. 0.0765 ohm.

7. Given a transformer connected to a constant pressure system at a frequency of 60 cycles, would the losses in the iron be greater or smaller if the frequency were changed to 25 cycles? Give reasons.

Ans. Greater, because the reduction in the number of flux reversals does not compensate for the increase of loss per pound per cycle due to the greater flux in the core.



8. Given a single-phase transformer connected to an 11,000-volt circuit; total iron loss = 400 watts; ampere-turns to produce maximum core density = 350; number of primary turns = 1,700. Calculate the current in the primary windings when the secondary is open-circuited. *Ans.* 0.15 amp.

9. Given that the exciting current of a 20-kva single-phase transformer on a 2,200-volt circuit is 5 per cent of the full-load current, and that the core loss is 0.9 per cent of the rated kilovolt-ampere output. Calculate the "wattless" or magnetizing component of the exciting current. *Ans.* 0.4475 amp.

10. The primary winding of a transformer connected to a 2,200-volt circuit consists of two coils which may be connected in series or in parallel. When they are in series, with secondary circuit open, the primary current is 0.32 amp and the power input is 150 watts. Calculate the no-load current and power factor when the primary coils are connected in parallel on a 1,000-volt circuit of the same frequency.

*Ans.* Current = 0.64, power factor = 0.213.

11. The net cross section of iron in the core of a single-phase transformer is 9 sq in., and the mean length of the magnetic circuit is 36 in. The flux density is 61,600 lines per sq in. and the permeability  $\mu = 2,400$ . The core loss is 0.8 watt per lb, and the transformer is connected to a 2,300-volt 60-cycle circuit. Calculate (a) the magnetizing component, (b) the "in-phase" component of the no-load primary current. Neglect the effect of joints in the magnetic circuit, and take the weight of a cubic inch of iron as 0.28 lb. *Ans.* (a) 0.131 amp, (b) 0.0316 amp.

12. Given a 10-kva transformer with full-load losses amounting to 70 watts in the iron and 140 watts in the copper. Calculate the efficiency at half load (unity power factor). *Ans.* 0.979.

13. Given a 3-kva transformer with an efficiency of 95.5 per cent at half load (unity power factor), and a copper loss of 90 watts at full load. Calculate the iron loss in watts. *Ans.* 47.5.

14. Given that the full-load copper losses are exactly twice the iron losses in a 50-kva transformer, and that the quarter-load efficiency is 96.5 per cent. Calculate the full-load efficiency at unity power factor. *Ans.* 0.977.

15. Given the following particulars in connection with a single-phase transformer: full-load output = 2,000 kva; primary volts = 66,000; secondary volts = 2,200; resistance of primary windings = 8.6 ohms; resistance of secondary windings = 0.0095 ohm; core loss = 14,000 watts. Calculate the efficiency at one-quarter load with unity power factor. Neglect effect of exciting current. *Ans.* 0.971.

16. Calculate the efficiency of a 25-kva transformer when operating at one-half maximum current output on a load of 0.7 power factor, given that the iron loss is 0.8 per cent of the rated output on unity power factor, and the full-load copper loss is 360 watts. *Ans.* 0.968.

17. Given a 30-kva transformer with core loss = 160 watts, and copper loss at half load = 85 watts. Calculate the all-day efficiency on a 4-hr basis (*i.e.*, 4-hr full load and 20-hr no load). *Ans.* 0.958.

18. Calculate the all-day efficiency of a 100-kva transformer operating under the following conditions: 6 hr on a load of 50 kw at 0.73 power factor; 3 hr on a load of 90 kw at 0.82 power factor; 15 hr with no load on secondary. The iron loss is 1,000 watts, and the full-load copper loss is 1,060 watts. *Ans.* 0.95 (nearly).

19. On the basis of a 4-hr full load and a 20-hr no load, the all-day efficiency of a 10-kva transformer is 0.947. The full-load copper losses (at unity power factor) are 140 watts. Calculate the core loss in watts. *Ans.* 70.

20. Calculate the percentage regulation on a load of unity power factor of a transformer having 2.5 per cent resistance drop and 11 per cent reactive drop.

*Ans.* 3 per cent (approx).

21. Given a 100-kva transformer with a 5 to 1 transformation ratio, and secondary (low-pressure) terminal voltage of 6,600 at full load. The "equivalent" primary resistance is 330 ohms, and the total leakage reactance is 1,000 ohms. Calculate the percentage regulation on unity power factor. *Ans.* 3.5 per cent (nearly).

22. Calculate the total *equivalent resistance*, in terms of the primary winding, of a 10 to 1 ratio transformer in which the primary copper loss is 20 per cent greater than the secondary copper loss, given that the resistance of the secondary (low-tension) winding is 1.5 ohms. *Ans.* 330 ohms.

23. With 100 amp taken from the terminals of a certain transformer connected to a 25-cycle primary supply circuit, the resulting total reactive drop is 5 per cent. Calculate the percentage reactive drop if the same transformer is rewound with 15 per cent more turns in both windings and connected to a 60-cycle circuit with a load drawing 110 amp from the secondary winding. Assume the terminal voltage and the dimensions of all leakage paths to remain unaltered. *Ans.* 17.5 per cent.

24. A 750-kva 60-cycle transformer, with primary wound for 66,000 volts, gives the following readings on short-circuit test (secondary winding short-circuited): volts at primary terminals = 2,200; primary current = 9 amp; watts = 4,500. Calculate (a) the reactive pressure drop in volts under working conditions with full-load current drawn from secondary, (b) the per cent regulation under the load condition which makes this a maximum, (c) the power factor of the load which produces this condition. Neglect the core loss and exciting current component in using the test data.

*Ans.* (a) 2,700 volts, (b) 4.22 per cent, (c) 0.227.

25. A certain transformer is found to have a current of 16 amp in the primary circuit when the secondary is short-circuited and 1,300 volts at normal frequency are applied across the primary terminals. The power input under this condition is 4,500 watts. Calculate the reactive pressure drop in volts with full-load current under normal working conditions, given that the total full-load copper losses are 9,000 watts. *Ans.* 1,795 volts.

26. Given that  $\frac{1}{4}$  gal of water per minute passing through cooling pipes in a transformer tank is required for every kilowatt of heat loss, and that 1 sq in. of pipe surface must be provided for every watt passing through the cooling coil from the heated oil to the water. Calculate (a) the length of 1-in. copper tube required to construct a cooling coil to dissipate  $3\frac{1}{2}$  kw, (b) the velocity of the water in the pipe. ( $7\frac{1}{2}$  gal = 1 cu ft)

*Ans.* (a) 93 ft, (b) 214 fpm.



## CHAPTER 13

### MECHANICAL DESIGN OF ELECTRICAL MACHINERY

#### 152. Relation between Mechanical and Electrical Machine Design.

In a book dealing with the elements of electrical machine design, a detailed study of the mechanical design of electrical machinery would be out of place. Many details of design, especially of machines for large outputs and high speeds, should preferably be left to competent mechanical engineers; but the electrical engineer should know enough about the strength and stiffness of materials, and the manner in which the various parts of a machine are proportioned to avoid overstressing and overstraining these materials, so that the machine for which he had made the electrical calculations shall be mechanically and economically satisfactory. The authors are of the opinion that the designer cannot be quite certain that his design is practical and suitable for its purpose unless he is able to produce a sketch or drawing covering the essential features of the design. It is particularly important that he should be able to make neat dimensioned sketches of machine parts, because, in addition to the practical value of this accomplishment, it is an indication that he has a clear conception of the actual or imagined thing and can make his ideas intelligible to others.

This chapter is not intended to provide the elementary training in mechanical engineering which is necessary to every electrical engineer, and for this reason the derivation of all rules and formulas has not been given.

The first two of the following articles deal with the forces exerted by a magnetic field on current-carrying conductors, and the unbalanced pull in dynamos, both of which illustrate the close connection between the mechanical and electrical problems which have to be considered in designing electrical machinery.

**153. Mechanical Forces on Current-carrying Conductors in a Magnetic Field.** In electrical machines and apparatus, whether dynamos or transformers, which generate or convert large amounts of power, the mechanical forces, due to the greatly increased leakage flux which occurs under conditions of heavy overload or short circuit, may be sufficient to

displace or bend conductors and coils unless these are suitably braced and secured in position.

The absolute unit of current may be defined as the current in a wire which causes 1-cm length of the wire, placed at right angles to a magnetic field, to be pushed sidewise with a force of 1 dyne when the density of the magnetic field is 1 gauss.

Since the ampere is one-tenth of the absolute unit of current, we may write

$$F = \frac{BIl}{10}$$

where  $F$  = force in dynes

$B$  = density of the magnetic field in gauss

$I$  = current in the wire, amperes

$l$  = length of the wire, centimeters in a direction perpendicular to the magnetic field

It follows that the force tending to push a coil of wire of  $T$  turns bodily in a direction at right angles to a uniform magnetic field of  $B$  gauss (see Fig. 181) is

$$F = \frac{BITl}{10} \quad \text{dynes}$$

If both current and magnetic field are assumed to vary periodically according to the sine law, passing through corresponding stages of their cycles at the same instant of time, we have the condition which is approximately reproduced in the practical transformer where the leakage flux passing through the windings is due to the currents in these windings. Since the instantaneous values of the current and flux density will be  $I_{\max} \sin \theta$  and  $B_{\max} \sin \theta$ , respectively, the average mechanical force acting upon the coil may be written

$$\text{Force} = \frac{Tl}{10} I_{\max} B_{\max} \frac{1}{\pi} \int_0^\pi \sin^2 \theta d\theta = \frac{TI_{\max} B_{\max}}{10 \times 2} \quad \text{dynes}$$

If the flux density is not uniform throughout the section of coil considered, the average value of  $B_{\max}$  should be taken. Let this average value of the maximum density throughout the cross section of the coil be

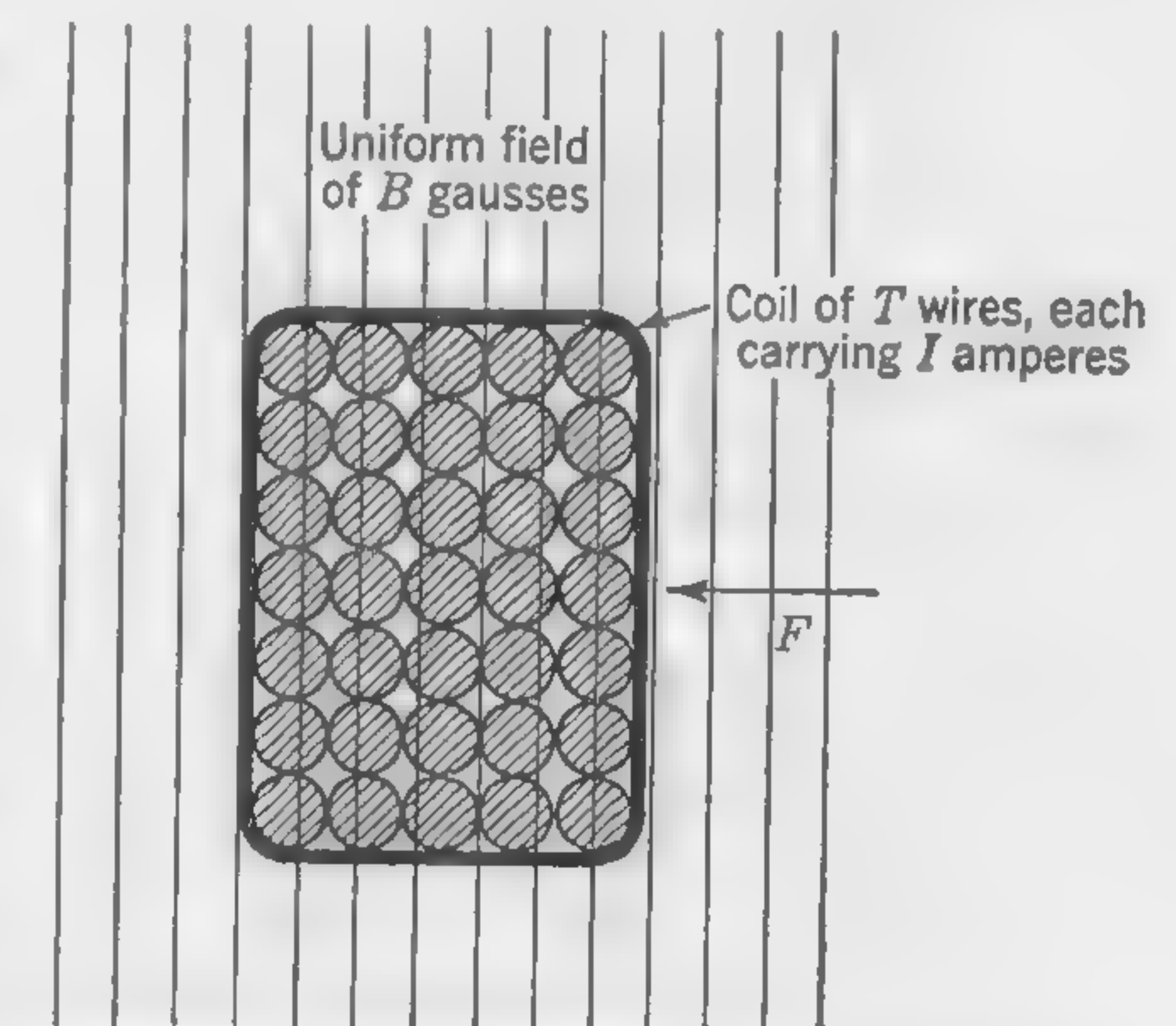


FIG. 181. Force acting on coil in magnetic field.



denoted by the symbol  $B_{am}$ . Then, since  $1 \text{ lb} = 444,800 \text{ dynes}$ , the expression for the average force tending to displace the coil is

$$\text{Force} = \frac{TI_{\max}B_{am}}{8,896,000} \quad \text{lb} \quad (155)$$

Except in a few special cases, the calculation of the leakage flux is not an easy matter, and the value of  $B_{am}$  in formula (155) cannot always be predetermined exactly, but it can usually be estimated with sufficient

accuracy for the purpose of the designer who requires merely to know approximately the magnitude of the mechanical forces which have to be resisted by proper bracing of the coils.

For the special case of transformer windings, a more convenient formula than (155) can be developed. Thus, in Fig. 182 the upper sketch shows a section through a group of primary and secondary windings which may be considered as a high-low group with  $(TI)$  amp-turns in each winding, whether primary or secondary. The lower figure represents approximately the manner in which the leakage flux density is distributed through the coils. The maximum value is easily calculated by assuming

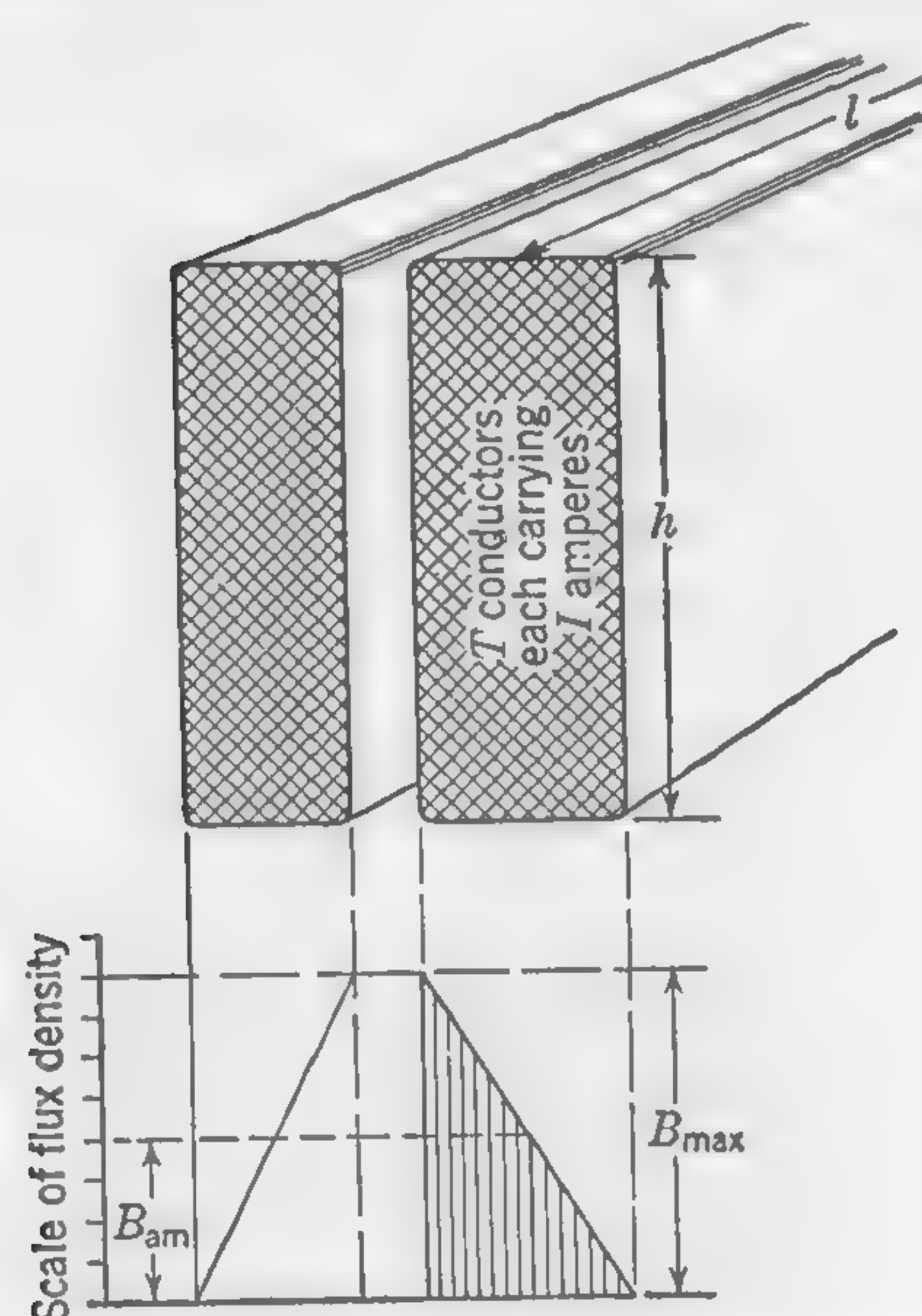


FIG. 182. One high-low section of transformer winding.

that the mmf acts upon an air path of length  $h$  centimeters and of cross section  $1 \text{ sq cm}$  in the gap between the coils; whence,

$$B_{\max} = 0.4\pi T(\sqrt{2} I) \frac{1}{h} \quad \text{gauss}$$

The density referred to as  $B_{am}$  in formula (155) will be  $\frac{1}{2} B_{\max}$  (see Fig. 182), and when this substitution is made in formula (155) we obtain for the average force acting on a portion of coil of depth  $h$  and length  $l$ :

$$\text{Force} = \frac{1.41 I^2 T^2 l}{10^7 h} \quad \text{lb} \quad (156)$$

where  $l$  and  $h$  must be expressed in the same units. It is important to bear in mind that, in this formula,  $T$  is the number of turns in either the primary or secondary winding of a single high-low group. Thus, if  $T_p$

and  $T_s$  stand for the total number of turns in primary and secondary, respectively, and  $n$  is the number of high-low groups,  $T = T_p/n$  when  $I$  is the current in the primary, and  $T = T_s/n$  when  $I$  is the current in the secondary.

*Example.* Using data from the design of current transformer of Illustrative Example of Art. 151, we shall calculate the pressure which tends to force apart the primary and secondary coils. Consider a portion of the winding 1 in. long, as indicated in Fig. 183. The width of the primary coil (measured perpendicularly to the cross section of Fig. 183) is  $3\frac{1}{4}$  in., and the number of turns is 7. Under normal full-load conditions, the current is 200 amp, and we shall suppose that, at the instant of short circuit, this current may be fifty times normal, or 10,000 amp.

The force acting on the section of coil of length  $l = 1$  in. and width  $h = 3\frac{3}{4}$  in., tending to push it away from the core, is, by formula (156),

$$\text{Force} = \frac{1.41(10,000)^2 \times 7^2 \times 1}{10^7 \times 3.75} = 184 \text{ lb}$$

In this calculation, the reluctance of the flux paths in the air outside the section of width  $h = 3\frac{3}{4}$  in. has been considered negligible; but, although it is not possible to calculate exactly the mechanical forces tending to deform or displace the windings, it is evident that these may be very great and that proper bracing of the coils is often necessary to prevent mechanical injury when abnormal overloads occur in the primary circuit of current transformers.

**154. Unbalanced Magnetic Pull.** When the rotating portion of an electric generator or motor is exactly in the center of the stationary ring of poles or stator stampings, as the case may be, the radial pull of all the poles on one side of a diameter is exactly balanced by the pull of the poles on the opposite side. If from any cause, such as improper assembly of parts or wear of bearings, the rotor is out of center with the stator, there will be an unbalanced magnetic pull tending to draw the rotor over toward the side where the air clearance between pole and armature is smallest.

Knowing the total flux per pole and the area under the pole face, it is an easy matter to calculate the approximate pull per pole with normal (or average) air gap. Then, with the same ampere-turns on the pole, the pull when this air gap is slightly increased or decreased may be calcu-

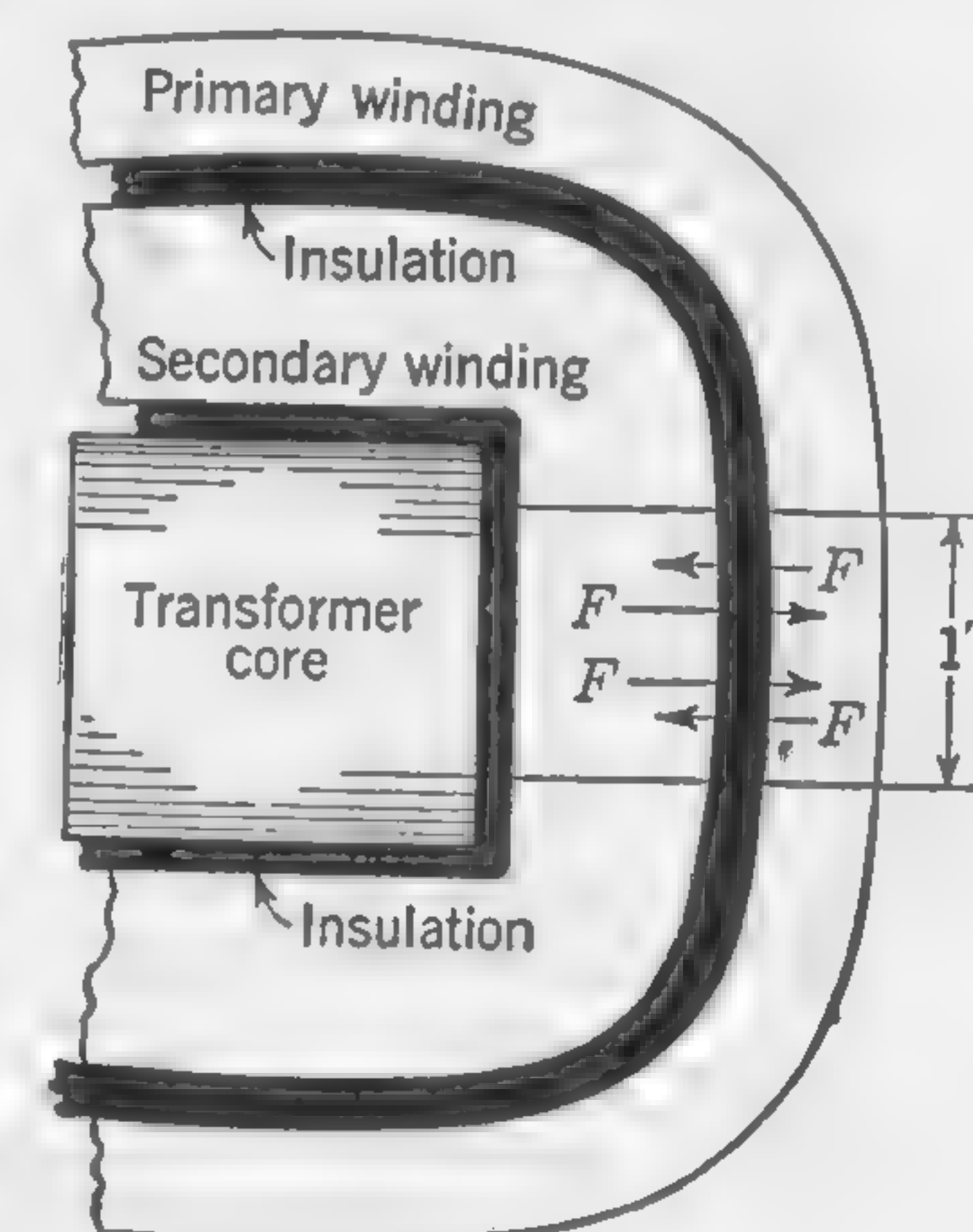


FIG. 183. Illustrating mechanical forces acting on transformer coils.



lated by neglecting the effect of changing permeability of the iron, and assuming that the flux density in the air gap varies inversely as the length of the gap. Let  $P$  = pull in pounds per pole when the air gap is of normal, or average length  $\delta$ , and let  $g$  = length of air gap as modified by displacement of rotor center; then *pull per pole* =  $P(\delta/g)^2$  lb. This is the pull exerted radially (*i.e.*, in the direction of the axis of the pole). If the displacement of the rotor is vertically downward, as indicated in Fig. 184, the vertical component of the pull will be  $P(\delta/g)^2 \sin \theta$ , where  $\theta$  is the angular position of the pole with reference to the horizontal diameter.

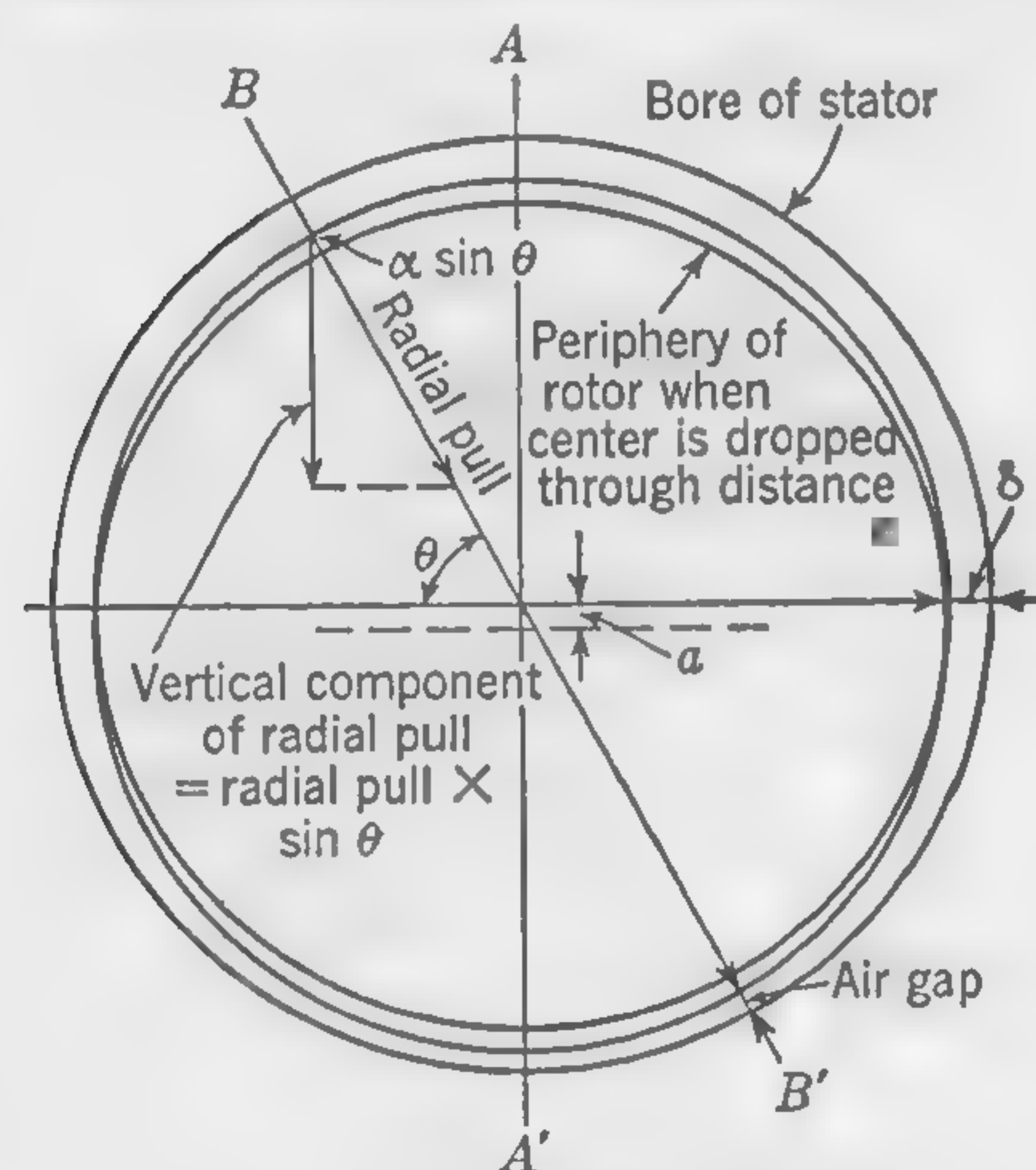


FIG. 184.

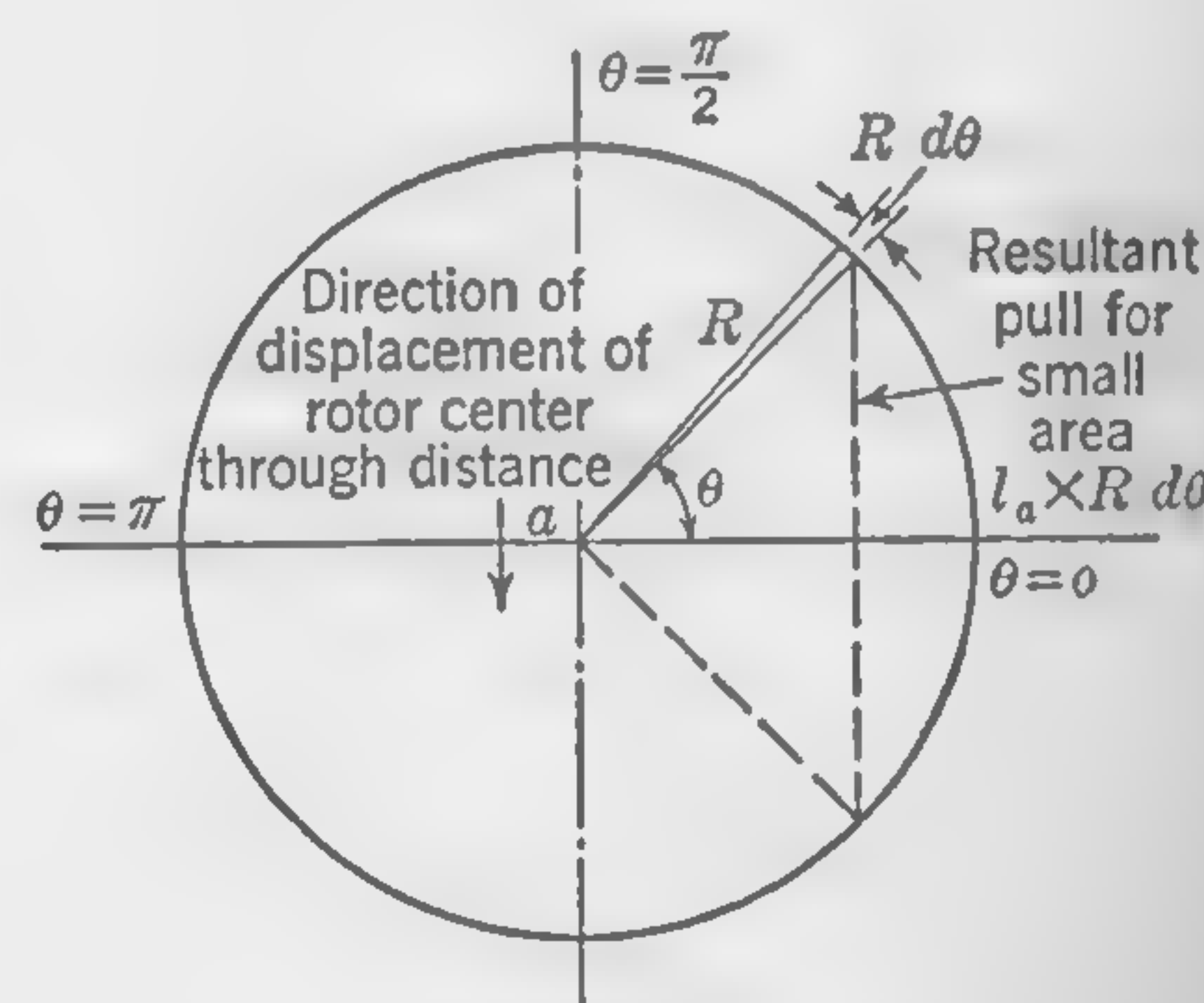


FIG. 185.

FIGS. 184 and 185. Diagrams illustrating unbalanced magnetic pull on rotor.

Let  $a$  = vertical displacement of rotor center, then the length of gap at the top is  $g = \delta + a$ , and at the bottom,  $g = \delta - a$ . When the angle between the center line of the pole and the horizontal diameter is  $\theta$ , the length of air gap is  $g = \delta \pm a \sin \theta$ . The resultant downward pull of any pair of poles situated at equal distances above and below the horizontal diameter is, therefore,

$$\left. \begin{array}{l} \text{Difference of pull between two} \\ \text{equidistant poles above and} \\ \text{below the axis of reference} \end{array} \right\} = P \sin \theta \left[ \left( \frac{\delta}{\delta - a \sin \theta} \right)^2 - \left( \frac{\delta}{\delta + a \sin \theta} \right)^2 \right] \quad \text{lb} \quad (157)$$

A close approximation to the quantity in brackets when  $a$  is small relatively to  $\delta$  is  $(4a \sin \theta)/\delta$ , so that the simplified expression becomes:

$$\left. \begin{array}{l} \text{Resultant pull per pair of poles} \\ \text{occupying similar positions on} \\ \text{opposite sides of reference axis} \end{array} \right\} = P \times 4 \sin^2 \theta \left( \frac{a}{\delta} \right) \quad \text{lb} \quad (158)$$

*Example—Unbalanced Magnetic Pull.* The following data are given in connection with a 75-kw 4-pole generator:

Poles centered along axes  $45^\circ$  with the vertical

Normal air gap ("equivalent") = 0.222 in.

Area under one pole face = 106 sq in.

Flux density under center of pole = 48,800 lines per sq in. (approx)

It is desired to calculate the unbalanced magnetic pull on the armature under open-circuit conditions, assuming the center line of the shaft to be displaced  $\frac{1}{32}$  in. from the center of the pole faces, (1) when this displacement is vertically downward, and (2) when the displacement is at an angle of  $45^\circ$  with the vertical (*i.e.*, along the diameter which passes through the axis of two opposite poles).

On account of the falling off of the flux density near the pole tips (see Fig. 60) we shall use a slightly smaller value of air-gap density in these calculations, (say) 47,500 lines per sq in.\*

Since the magnetic pull in an air gap is  $P = B^2 A / 72 \times 10^6$ , where  $B$ , is the flux density in lines per square inch, and  $A$  is the area of the pole face,

$$P = \frac{(47,500)^2 \times 106}{72 \times 10^6} = 3,320 \text{ lb}$$

With  $\theta = 45^\circ$ ,  $\sin \theta = 0.707$ ; whence, by formula (158), the resultant pull per pair of poles is

$$3,320 \times 4(0.707)^2 \times \frac{1}{32 \times 0.222} = 935 \text{ lb}$$

and, since there are two pairs of similarly placed poles, the total resultant unbalanced pull is  $935 \times 2 = 1,870$  lb.

Using the same formula for one pair of opposite poles with  $\theta = 90^\circ$  and  $\sin \theta = 1$ , we obtain the same result as for case (1), namely 1,870 lb.

It is customary to make frames and shafts of sufficient stiffness to permit of an unbalanced pull approximately equal to the weight of the complete rotating part.

Formulas (157) and (158) take no account of magnetic saturation in the iron portions of the circuit, but, when the air gap is decreased, this will result in the available mmf across the air gap being less than with

\* If the values of flux density vary considerably over the armature surface under the pole face, as, for instance, in a-c generators under all conditions of loading, and d-c machines under heavy load when the flux distribution is distorted by the armature mmf (see curve C, Fig. 60), it would be necessary to calculate the pull for several small areas over which the flux density is approximately constant and then add these together to obtain the total pull per pole. As an alternative it may sometimes be possible to obtain mathematically an expression for the square root of the mean square of the flux density under the pole face for use in the pull formulas.



the normal gap, so that the flux density will not be exactly inversely proportional to the gap length. The effect of iron saturation may be taken into account, but, with a small displacement of the rotor, it is customary to neglect it, merely bearing in mind that the method outlined above gives a value for the unbalanced pull somewhat greater than it is likely to be in practice.

There are other causes which tend to reduce the amount of the unbalanced pull. Thus, if the armature winding is provided with local closed paths of low resistance, as in multiple-wound d-c dynamos with equalizer rings, the larger currents in the conductors where the gap is smallest will have a demagnetizing effect upon the poles and so to some extent will counteract the flux variations and reduce the amount of the unbalanced pull.

The formulas developed for calculating the difference of pull per pair of symmetrically placed poles may be easily modified to render them applicable to machines without salient poles, such as induction motors, or to machines having a large number of salient poles. The simplest of the two formulas [*i.e.*, formula (158)] is sufficiently accurate for most practical purposes, and, if we use the symbol  $P_s$  to represent the average pull per unit area of air-gap surface between stator and rotor with normal length of air gap, we have

$$P_s = \frac{pP}{2\pi R l_a}$$

where  $P$  = pull per pole, as already defined

$p$  = number of poles

$R$  = radius of circle through polar surface

$l_a$  = axial length of polar surface (or armature)

The difference of pull between two small elements of pole surface of width  $Rd\theta$  and length  $l_a$ , situated at an angle  $\theta$  respectively above and below the diameter normal to the displacement  $a$  (see Fig. 185), is  $P_s R d\theta l_a \times 4 \sin^2 \theta (a/\delta)$ , and the summation of all such component forces for values of  $\theta$  between  $\theta = 0$  and  $\theta = \pi$  will be the total resultant pull. Thus,

$$\begin{aligned} \text{Total unbalanced pull} &= 4P_s R l_a \left(\frac{a}{\delta}\right) \int_0^\pi \sin^2 \theta d\theta \\ &= 2\pi R l_a P_s \times \frac{a}{\delta} \\ &= pP \left(\frac{a}{\delta}\right) \end{aligned} \quad (159)$$

**155. Design of Stator Frames.** The possibility of unbalanced magnetic pull which has been discussed in the preceding article suggests that

ample strength and stiffness are required in the yoke rings or housings which support the poles of d-c dynamos and the stator stampings of alternators and a-c motors.

The yoke ring of a d-c dynamo must be of sufficient cross section to carry the flux, and sketch *a* (Fig. 186) shows a cross section which will generally be satisfactory for a small machine. The width  $w$  is usually made wider than the pole cores so as to cover and afford protection to the field coils. The radial depth  $h$  is then calculated to give the cross section required for the magnetic circuit. In larger machines, the thickness  $h$  might be so small relatively to the diameter  $D_f$  that the frame

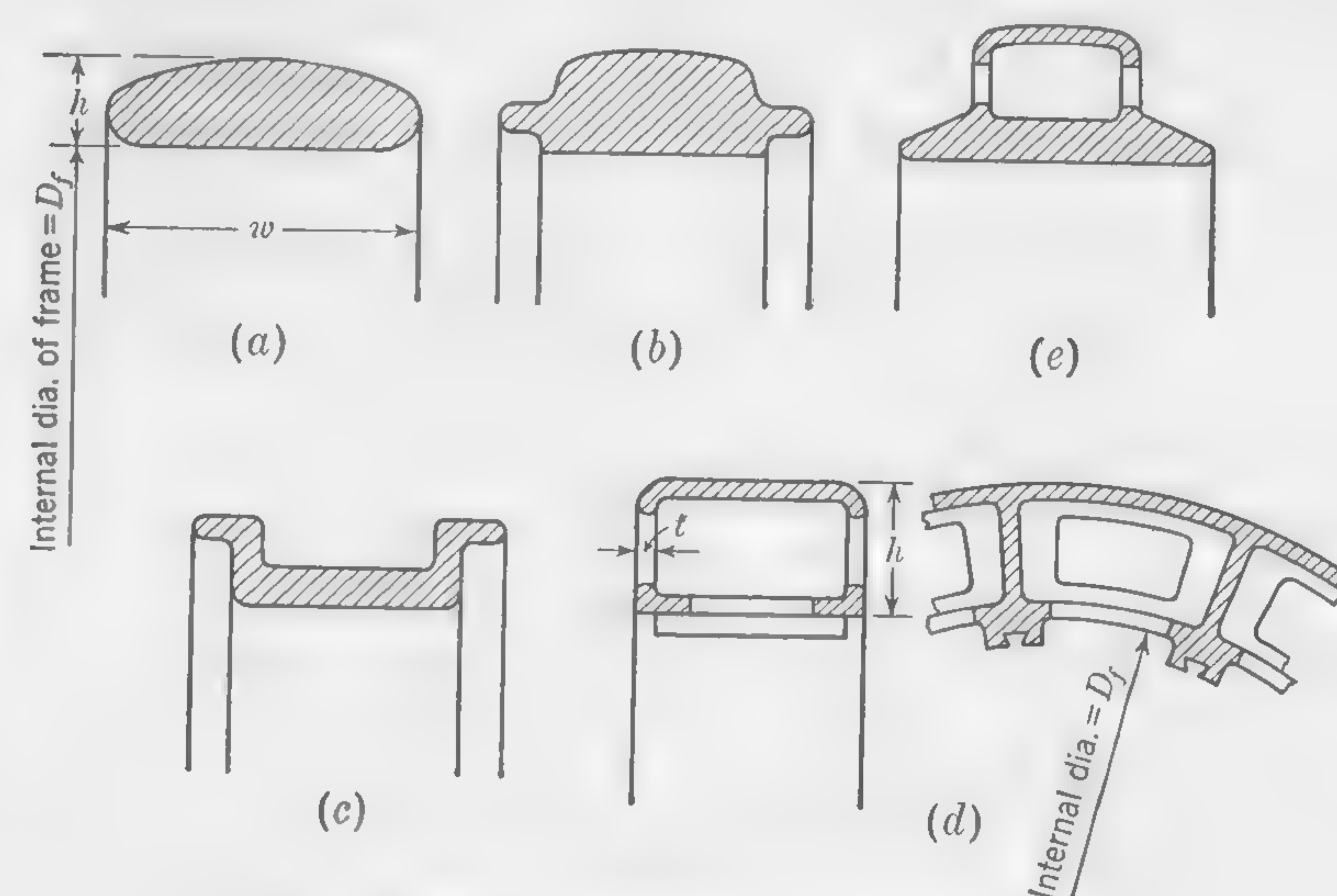


FIG. 186. Cross sections of yoke rings and stator frames.

would not be sufficiently rigid; but, by putting the required amount of metal into a cross section of the form shown at *b* or *c*, the stiffness of the yoke ring is increased. The section *d* shows a box-section frame for alternator or a-c motor which combines stiffness with lightness (*i.e.*, the material is so disposed in the cross section that a rigid frame is obtained with comparatively thin walls of metal). It is important that the dimension  $h$  should not be too small, and it should increase as the diameter  $D_f$  increases. The depth  $h$  is usually from one-fourteenth to one-tenth of the internal diameter  $D_f$ . A convenient rule for the purpose of approximating over-all dimensions is

$$h = 1.5 + \frac{D_f}{12} \quad \text{in.}$$

where  $D_f$  is the internal diameter in inches.



For the thickness of metal in cast frames, we may use the formula

$$t = 0.25 + 0.01 D_f \quad \text{in.}$$

for frames up to 100 in. in diameter. For larger diameters add 0.15 in. to the thickness of metal for every 20-in. increase in diameter over 100 in.

The sketch *c* (Fig. 186) shows how the necessary stiffness may be obtained in large dynamos by combining the box section of *d* with the wide but thin section which would be satisfactory magnetically but not mechanically.

During recent years, great advances have been made in replacing castings by electrically welded steel plates and structural sections. Not only the supporting frames of the type illustrated by sketch *d* (Fig. 186), but also bed plates, rotor spiders, and even the bearing pedestals are now

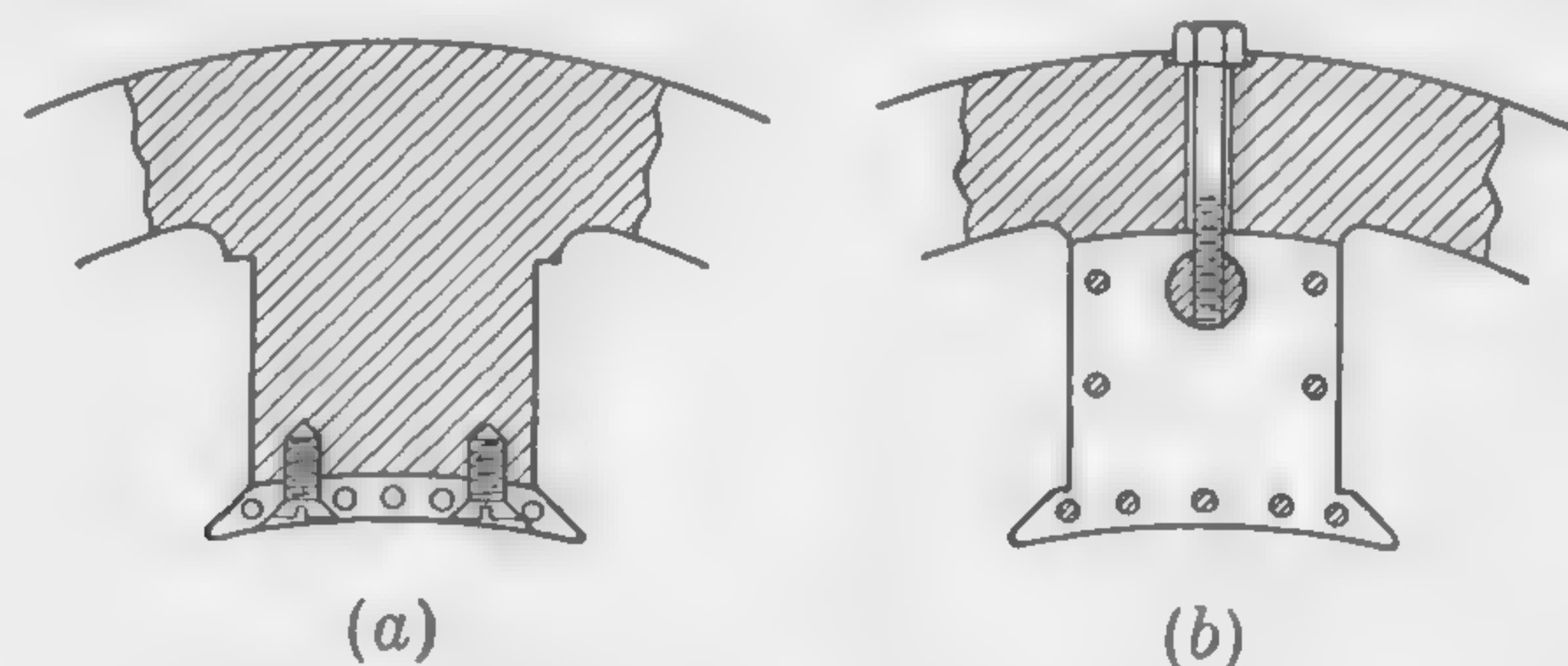


FIG. 187. Poles and pole shoes of d-c dynamo.

frequently constructed of welded steel parts. The design of such parts should be undertaken only by experienced mechanical engineers, because the problems to be solved involve questions of adequate *stiffness* in addition to *strength*, and an arc-welded generator or motor is not merely a machine of the older type in which the cast-iron parts have been replaced by built-up steel parts of the same shape. The designer must not be influenced by previous practice with cast-iron parts.

Among the advantages resulting from the replacement of castings by welded steel structures are (1) saving the cost of patterns, (2) saving space and expense of storing patterns, (3) more reliable construction, since there is always a possibility of failure from internal strains, blow holes, or other hidden defects in castings, (4) considerable reduction in weight and saving in shipping costs.

**156. Pole Cores and Pole Shoes.** In small dynamos the poles are sometimes cast solid with the yoke. The cross section of the pole core is then usually circular or elliptical in shape, and the pole shoes—preferably built up of sheet-iron punchings—are secured to the machined surface of the pole core generally as indicated at *a* (Fig. 187). When the complete pole is built up of sheet-iron punchings, it may be secured to the yoke

ring as indicated at *b*. There are many other ways of securing pole shoes and pole cores to the frame, the aim being, in all cases, to obtain good magnetic joints and provide for the easy removal and replacement of field coils.

Figure 188*a* shows solid poles dovetailed into the rotor casting. The dovetails are made a good fit and the poles are pressed into the rotor body. Keys may be provided in slow-speed machines, and they facilitate the removal and replacement of the poles, but they tend to increase the stresses and are rarely used in high-speed machines. The castings between the coils are provided in large, high-speed machines to support the coils and prevent deformation under the action of centrifugal force.

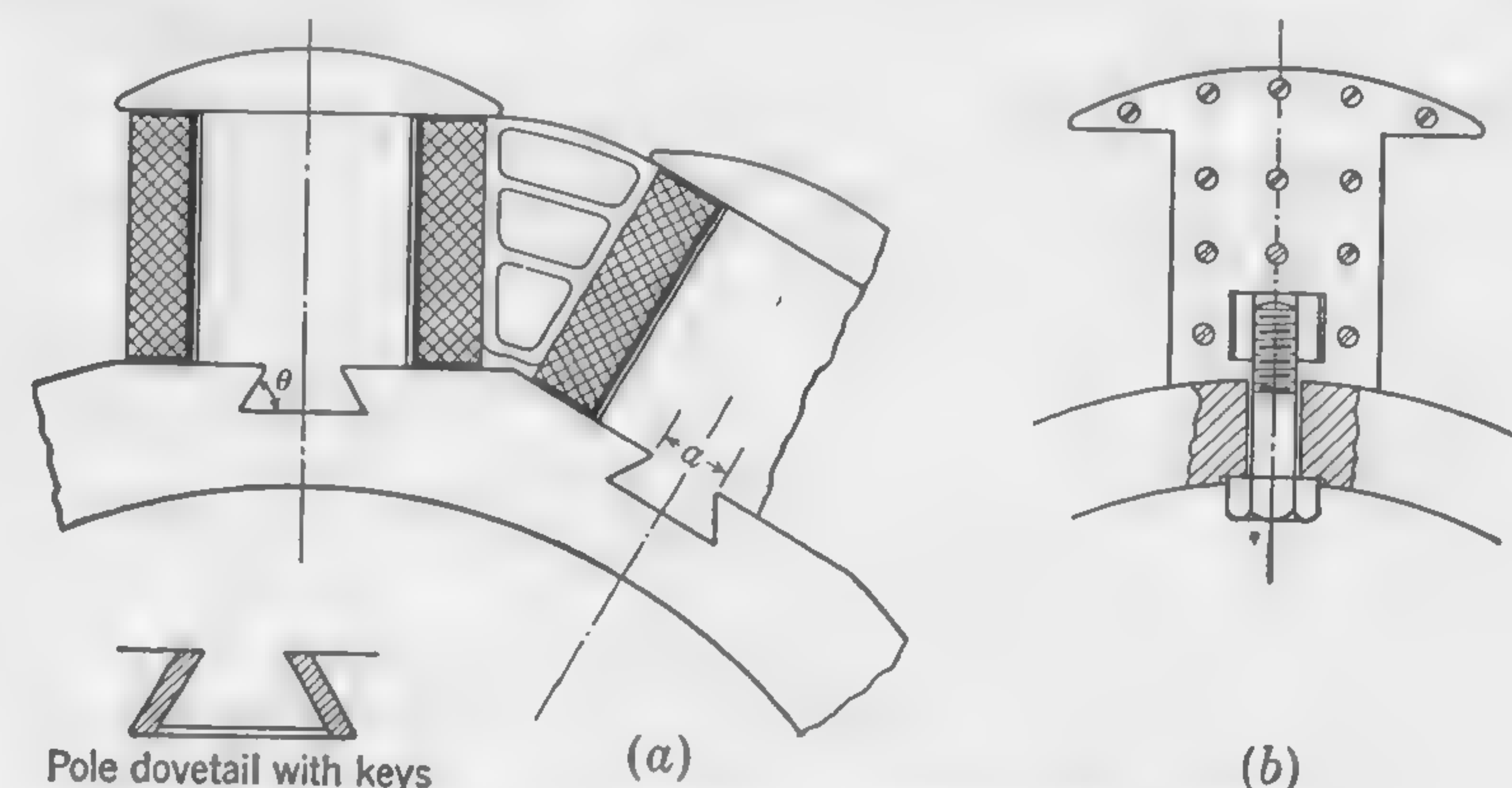


FIG. 188. Methods of securing poles to rotor casting.

They do not extend over the whole area of the coil side but are placed with suitable intervals, leaving unsupported portions of the windings between them.

Figure 188*b* shows one form of construction for securing laminated poles to the machined surface of the rotor body.

**157. Shafts and Bearings.** The diameter of a shaft for an electric generator or motor is determined by considerations of stiffness (*i.e.*, ability to resist deflection due to the weight of rotor or unbalanced magnetic pull) rather than strength to transmit power by torsion. If the diameter of the shaft were no larger than necessary to transmit the torque, it would be too small to withstand the forces tending to deflect it; in other words, it would bend to such an extent that unsatisfactory running conditions would result. It is, therefore, mainly as a beam of circular cross section that the shaft should be considered, and, since the deflection of such a beam varies directly as the cube of the span and inversely as the cube of the diameter, it follows that the shaft diameter should bear a definite relation to the distance between bearings.



Since the weight of rotor and the corresponding span or distance between bearings will not vary much in different designs of machines for the same *output* and *speed*, it is possible to determine approximately the size of shaft required without exact information regarding weight of rotating parts and distance between bearings. A convenient formula for the diameter of horizontal solid steel shafts for electric generators is

$$\text{Diameter} = 0.84 \sqrt[3]{\frac{\text{output in watts}}{\text{rpm}}} \quad \text{in.} \quad (160)$$

An approximate dimension for the maximum shaft diameter is thus obtained. It should be checked with formulas to be found in the handbooks for mechanical engineers after the distance between bearings and the amount and distribution of the loads are known.

**Journal Diameters—Length of Bearings.** The diameter of the shaft in the bearings is something less than the maximum diameter near the center where it passes through the rotor hub or armature core. When the maximum diameter is 6 in. and upward, a good rule is to make the journal diameter 2 in. smaller than the maximum diameter. In the case of small shafts, the journal diameter should be about two-thirds of the diameter at center. The length of bearing in dynamos and alternators is about  $2\frac{3}{4}$  times the diameter.

**158. High-speed Rotors—Centrifugal Force.** When a body of weight  $W$  lb revolves at the rate of  $N$  rpm at a distance  $R$  ft from the axis of rotation, the centrifugal force is

$$F = 0.000341WRN^2 \quad \text{lb} \quad (161)$$

The radius  $R$  is the distance between the axis of rotation and the center of gravity of the body. This formula has a direct application in the calculation of bolt diameters when the salient poles of an a-c generator are secured to the rotor body in the manner illustrated by Fig. 188*b*. It is assumed that there is no force tending to bend the bolts, but that they have merely to withstand the outward pull in the direction of the radius passing through the center of gravity of the pole. The cross section of the bolt or bolts should be such that the stress at the normal working speed does not exceed 15,000 lb per sq in. for mild-steel bolts.

**Effect of Dovetails.** When the pole is dovetailed into the rotor body in the manner illustrated by Fig. 188*a*, the direct radial pull over the cross section of width  $a$  is calculated by means of formula (161). If the pole is built up of steel laminations, the stress should not exceed 10,000 lb per sq in.

The calculation of the stress over the cross section  $S$  (Fig. 189) is not so easily made. It is desired to calculate the force  $OF$  due to the cen-

trifugal pull of the poles on each side of the cross section  $S$ . Each pole pulls with a force  $AP$  in the direction of the radius through the center of gravity of the pole, and the magnitude of this force is easily calculated by means of formula (161). This force exerts a pressure  $AF$  normal to the surface of the dovetail, the angle of which is  $\theta^\circ$ . The amount of this force is, therefore,  $AF = \frac{1}{2}AP/\cos \theta$ . If there are  $p$  poles on the rotor, the angle  $PO'F$  is equal to  $(180/p)^\circ$ . It follows from the vector construction of Fig. 189 that the angle  $AFB$  is equal to  $\theta - (180/p)$ ; whence

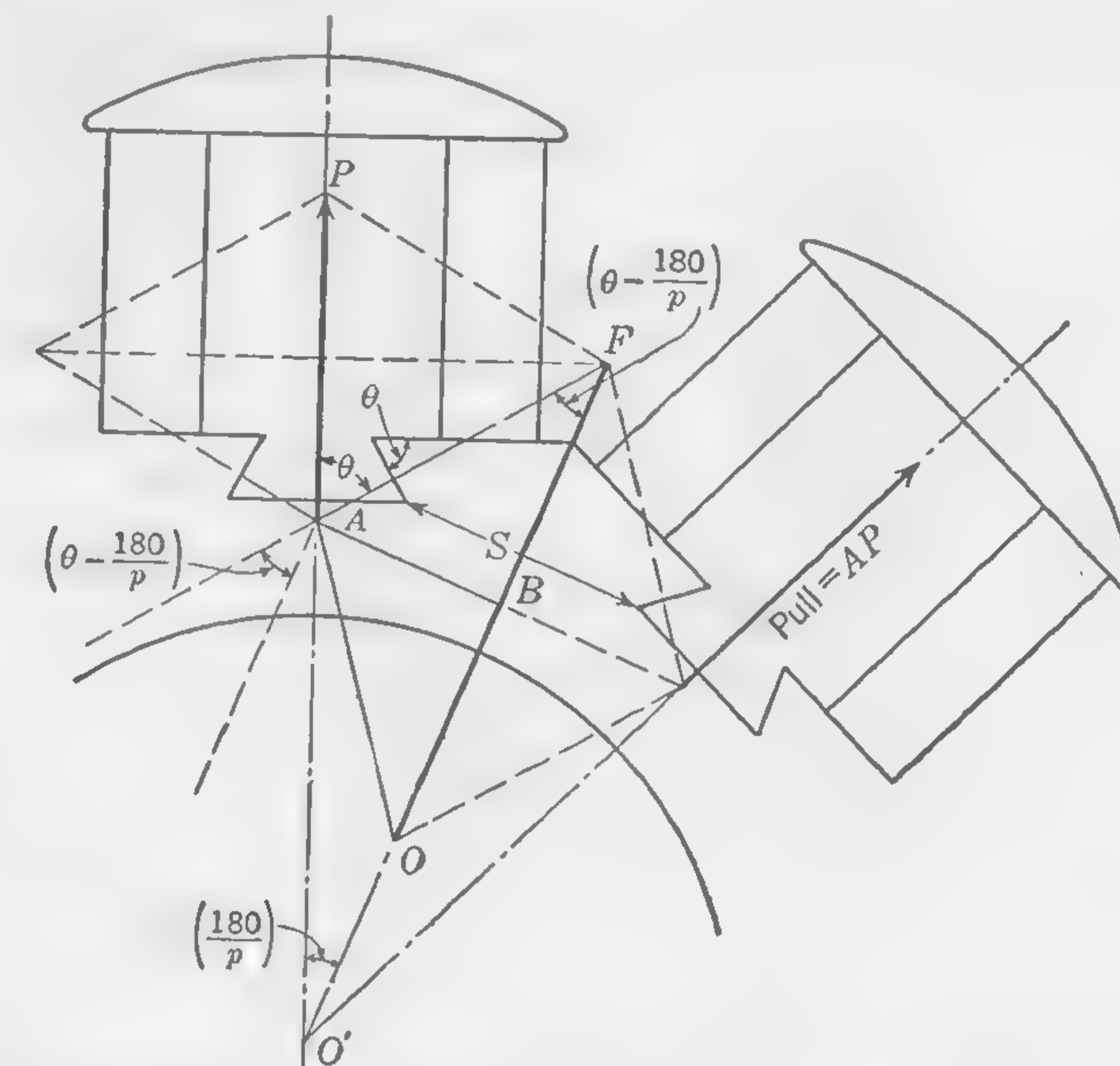


FIG. 189. Diagram illustrating stresses when poles are dovetailed into rotor body.

the total force acting normally to the cross section  $S$ , due to the pressure exerted by the poles on each side of the section considered, is

$$OF = 2BF = 2AF \cos \left( \theta - \frac{180}{p} \right)$$

and, since  $AF = \frac{1}{2}AP/\cos \theta$ , we have finally

$$OF = \text{total radial pull per pole} \times \frac{\cos [\theta - 180/p]}{\cos \theta} \quad (162)$$

In addition to this pull, the centrifugal force due to the small portion of the rotor body above the cross section considered should be taken into account.

The formula (162) may be used for calculating the stresses in the teeth of cylindrical rotors, such as the field magnets of turbo-alternators.



## NUMERICAL EXAMPLE

*Mechanical Stress at Root of Rotor Teeth.* Using data obtained from the turbo-alternator design of Illustrative Example of Art. 91, we shall calculate the stress at the root of the rotor teeth when the machine is running at the normal speed of 1,800 rpm.

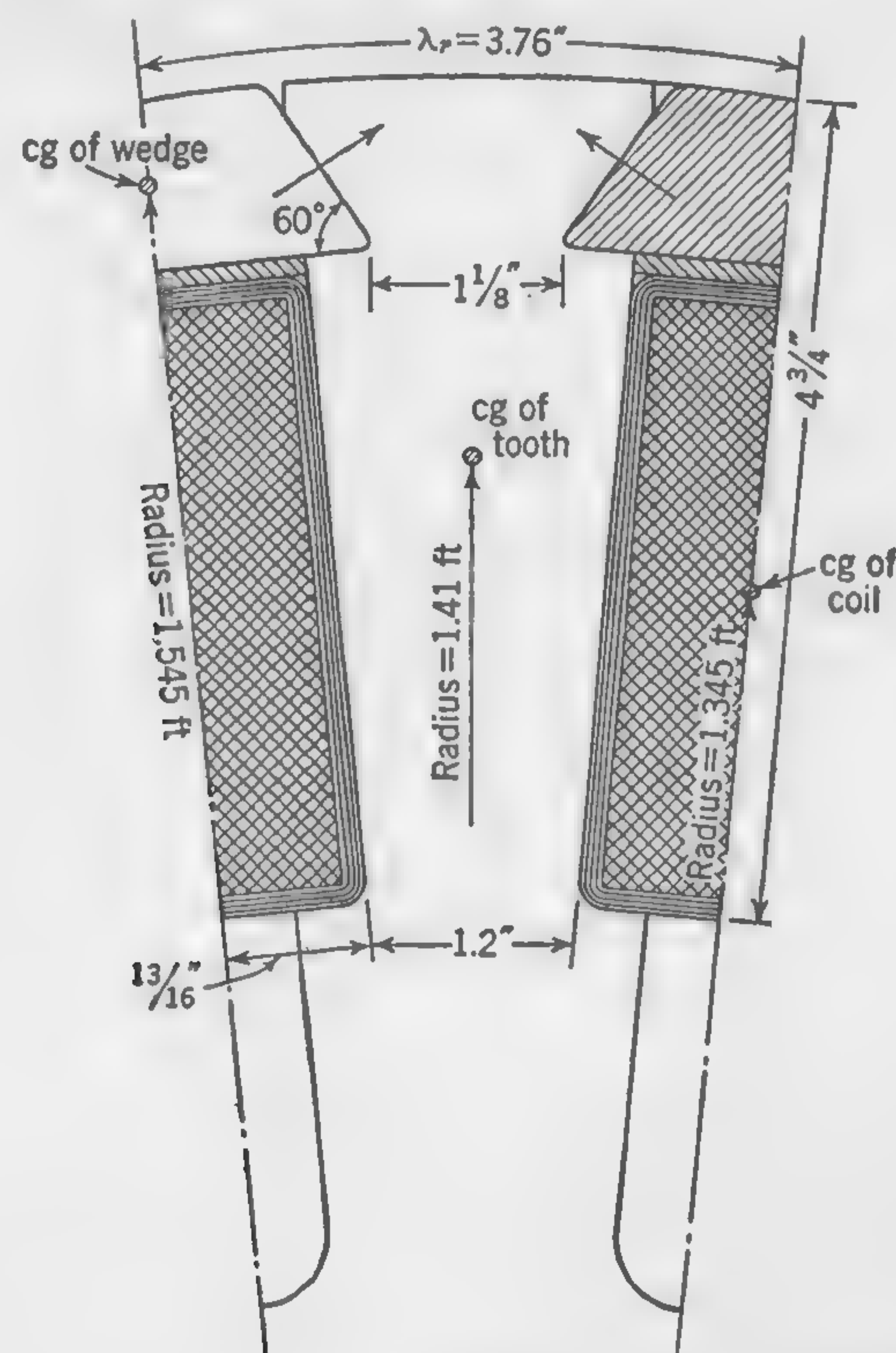


FIG. 190. Rotor tooth of turbo-alternator designed in Illustrative Example of Art. 91.

Figure 190 gives the dimensions of the rotor tooth and slot, the angle of the wedge being taken as  $60^\circ$ , which is usual. Other required data are:

Speed = 1,800 rpm

Number of rotor teeth = 32

Weight of wedge per inch length = 0.7 lb

Radius of center of gravity of wedge = 1.545 ft

Approximate weight of windings in one slot, per inch length of slot = 1.5 lb

Radius of center of gravity of windings = 1.345 ft

Weight of one tooth per inch length of rotor =  $2\frac{1}{4}$  lb

Radius of center of gravity of tooth = 1.41 ft

The direct radial pull per inch length of rotor, as calculated by formula (161), is

For the tooth,  $0.000341 \times 2.25 \times 1.41 \times (1,800)^2 = 3,500$  lb

For the wedge, 1,200 lb (approx)

For the contents of one slot, 2,230 lb

The centrifugal pull of the wedge and contents of slot exerts a pressure at the top of the tooth in a direction perpendicular to the side of the wedge. The resultant pull in the direction of the radius passing through the center of the tooth is obtained by combining the forces in the manner explained in connection with Fig. 189, so that we may use formula (162) with the angle  $\theta = 60^\circ$ , and the angle  $(180/p) = (180/32) = 5^\circ, 37'$ . The resultant force due to the wedge and slot winding is, therefore,

$$(1,200 + 2,230) \times \frac{\cos(60^\circ - 5^\circ 37')}{\cos 60^\circ} = 4,000 \text{ lb}$$

The width of tooth at the root is 1.2 in. and the stress in the metal is, therefore,  $(4,000 + 3,500)/1.2 = 6,250$  lb per sq in. This value is less than half the permissible maximum stress at normal speed, which indicates that there is an ample factor of safety.

The width of the rotor tooth at the top where it is undercut to accommodate the wedge is about  $1\frac{1}{8}$  in., from which it is obvious that the stress at this point will not be excessive not only because the cross section here is nearly as large as at the root of the tooth, but also because the total pull is less by the amount of the centrifugal force acting on the portion of the tooth below the cross section considered.

*Bursting of Rotor Rims—Binding Wire on Armatures.* When formula (161) is applied to every part of the rim of a flywheel, and all the component forces are resolved in a single direction perpendicular to a diameter, a new formula is obtained which gives the tension in the rim. This is simply the total centrifugal force as expressed by formula (161) divided by  $2\pi$ ; whence

$$\text{Total tension in flywheel rim} = 0.00005427WRN^2 \quad \text{lb} \quad (163)$$

where  $W$  = total weight of rim in pounds

$R$  = mean radius in feet

$N$  = number of revolutions per minute

The maximum stress will be in the metal near the outer surface of the rim where the velocity is highest. If  $D$  is the outside diameter of the wheel in feet, the stress per square inch of section of a steel flywheel is:

$$\begin{aligned} \text{Stress in pounds per square inch} &= 0.00029D^2N^2 \\ &= 0.0000291v^2 \end{aligned} \quad (164)$$

where  $v$  is the peripheral velocity in feet per minute.



*Binding Wire on Armatures.* Bands consisting of a single layer, about half an inch wide, of phosphor bronze or piano steel wire are sometimes used instead of wedges to secure the armature windings in the slots, and also to hold the overhanging portions of armature or rotor windings in position. The tension in these bands due to their own weight is calculated by formula (163) or (164), but to this must be added the tension due to the centrifugal force acting on the windings which it is the purpose of these bands to keep in position.

Let  $W_b$  = weight of wire bands in pounds

$R_b$  = radius of band in feet

$W_w$  = weight of winding on armature or rotor in pounds

$R_w$  = radius to center of gravity of small section of winding in feet

then the total tension in the bands due to centrifugal force is

$$\text{Tension} = 0.00005427N^2(W_bR_b + W_wR_w) \quad \text{lb}$$

This quantity, divided by the cross section of the wire in the bands, is the tensile stress, which should not exceed 15,000 lb per sq in. for phosphor bronze and 25,000 lb per sq in. for piano steel wire.

*Bursting of Rotors with Salient Poles.* When the rotor consists of a number of projecting poles either bolted to, or dovetailed into, the rotor casting, as illustrated in Fig. 188, the stress tending to burst the rotor rim is due not merely to the tension in the casting considered as a flywheel, but also to the radial pull of the poles. The radial pull per pole is the centrifugal force per pole and coil as calculated by formula (163) *plus* the magnetic pull. If  $P$  stands for this total radial pull per pole, and we assume the total number  $p$  of poles to be very large, the tension in the rotor rim will be

$$\left. \begin{array}{l} \text{Tension in rim of flywheel} \\ \text{carrying } p \text{ salient poles} \end{array} \right\} = \left\{ \begin{array}{l} \text{tension due to} \\ \text{weight of rim,} \\ \text{calculated by} \\ \text{formula (163)} \end{array} \right\} + \frac{pP}{2\pi} \quad \text{lb} \quad (165)$$

This formula is only approximate, because it assumes the pull of the poles to be uniformly distributed over the rotor periphery. It gives results that are too small when the angular distance between poles is large. Also, when the poles are dovetailed into the rim, there is a wedging action which tends to increase the stress in the cross section immediately below the dovetail. Unless the application of formula (165) indicates that there is a large factor of safety, the stress at any given section should be calculated by resolving the several forces into components normal to the section considered.

*Critical Speeds of Shafts.* In the design of high-speed machines such as turbo-alternators, with horizontal shafts, what is known as the critical speed or whirling speed must be taken into account when determining the shaft diameter. When the machine is at rest, the shaft is deflected downward, so that the center of mass is slightly below the axis of rotation. This same condition continues at the lower speeds, but, as the speed increases, it will ultimately reach a particular value at which the centrifugal force will exactly counteract the force tending to bend the shaft, and at this particular critical speed the shaft retains its bent form while rotating; whence the term "whirling speed." This is the first critical speed. There are other higher values of critical speed with smaller amplitude of vibration, at which the frequency of the bending due to the weight of the rotating parts will correspond exactly with the frequency of vibration of the shaft considered as a deflected spring.

The maximum deflection of the rotor due to its own weight together with the unbalanced magnetic pull (if any) can be calculated within a fair degree of accuracy when the position of the bearings and the cross section of the shaft are known. Suppose this deflection to be  $\delta$  in. Then, since the whirling speed is the number of revolutions per minute  $N$  which will cause the centrifugal force  $F$  to be the same as the weight  $W$  which causes the bending of the shaft, we may substitute  $W$  for  $F$  and  $\delta/12$  for  $R$  in formula (161) and write  $12 = 0.000341\delta N^2$ . This leads to the formula

$$\text{Whirling speed of shaft} = \frac{188}{\sqrt{\text{deflection in inches}}} \quad (166)$$

In turbo-alternators the whirling speed is generally higher than the running speed, but this is not a necessary condition of design; and in d-c steam-turbine-driven dynamos, where the provision of a commutator calls for the smallest possible diameter of shaft, the whirling speed is commonly lower than the normal running speed. In such cases it is necessary to pass through the critical speed, causing vibration of the rotor, every time the machine is started or stopped; but this is not a serious objection.

Formulas for calculating the critical speeds of shafts are given in the handbooks for mechanical engineers. A good rule in the design of high-speed electrical machinery is to arrange for the whirling speed to be at least 25 per cent above, or 25 per cent below, the running speed.

**159. Mechanical Design of Commutators.** The mechanical design of small commutators for slow-speed dynamos, such as the one illustrated in Fig. 191, is a very simple matter and, generally speaking, it is unnecessary to calculate the stresses and deflections due to centrifugal force acting on the commutator bars of slow-speed dynamos; but when the speed of the commutator surface exceeds 4,000 fpm and the distance between



clamping rings is considerable, it is advisable to calculate the load due to centrifugal action with a view to providing a sufficient depth of bar to give the required strength and stiffness.

The proper mechanical design of commutators for high-speed machines such as continuous-current turbo-generators is a matter of very great importance. The type of commutator is then generally as illustrated by

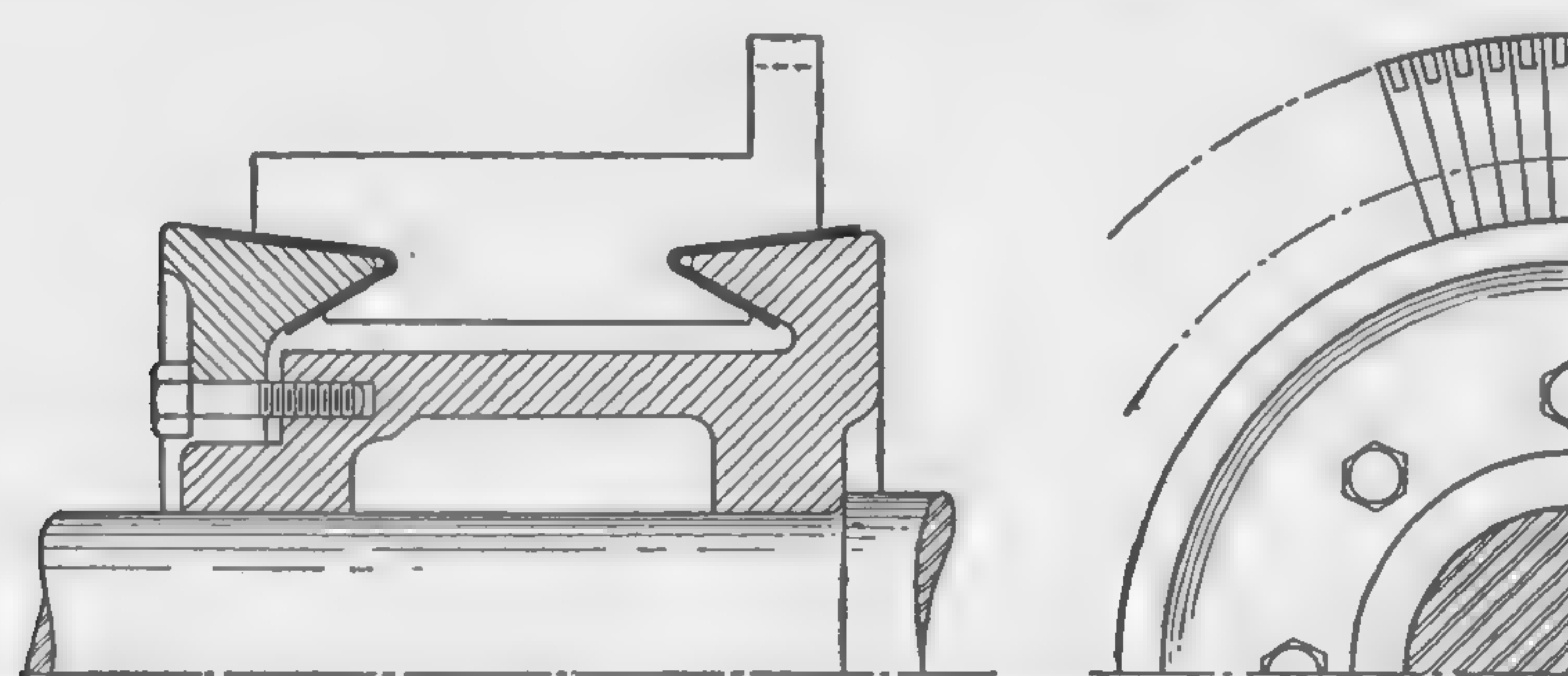


FIG. 191. Small commutator.

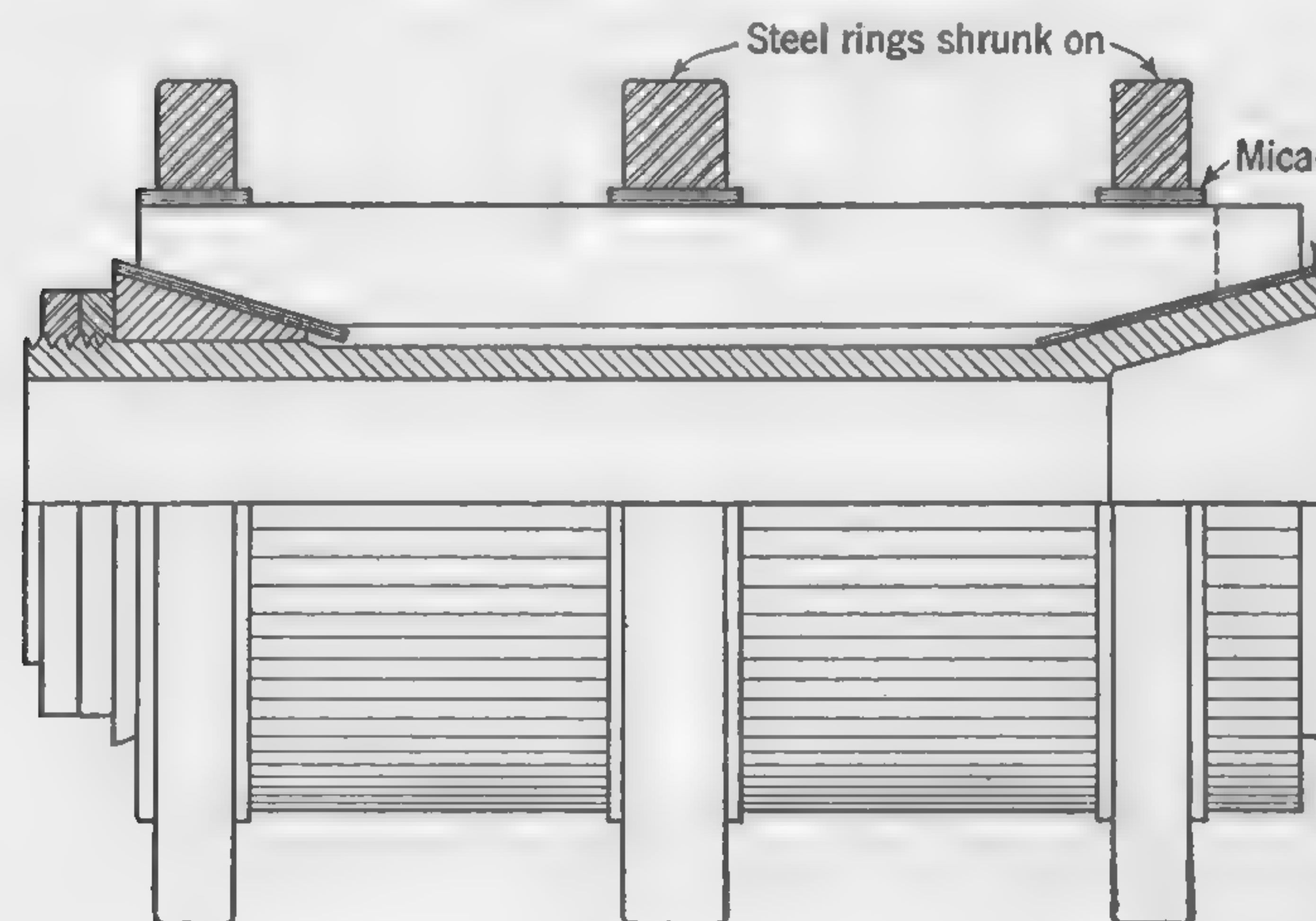


FIG. 192. High-speed commutator of large size.

Fig. 192, which shows a number of nickel-steel rings shrunk onto the commutator over insulating bands of mica.

The mechanical design of large commutators involves many problems other than the calculation of the bending action due to the centrifugal force. These include the calculation of stresses set up by the pressure of the coned clamping rings on the bars, and the possible abnormal stresses caused by temperature expansion of long copper bars. In this connection, the design shown in Fig. 20 has some advantage over that of Fig. 191, because the elastic extension of the long bolts will generally prevent

excessive stresses due to this cause. In this article it is proposed merely to indicate how the pressure and deflection due to centrifugal force may be calculated.

*Calculation of Strength and Stiffness of Commutator Bars.* The centrifugal force due to the weight of one commutator bar may be considered as a load uniformly distributed over the length  $l$  of the bar (see Fig. 193). Let  $P$  be the total amount of this load, as calculated by for-

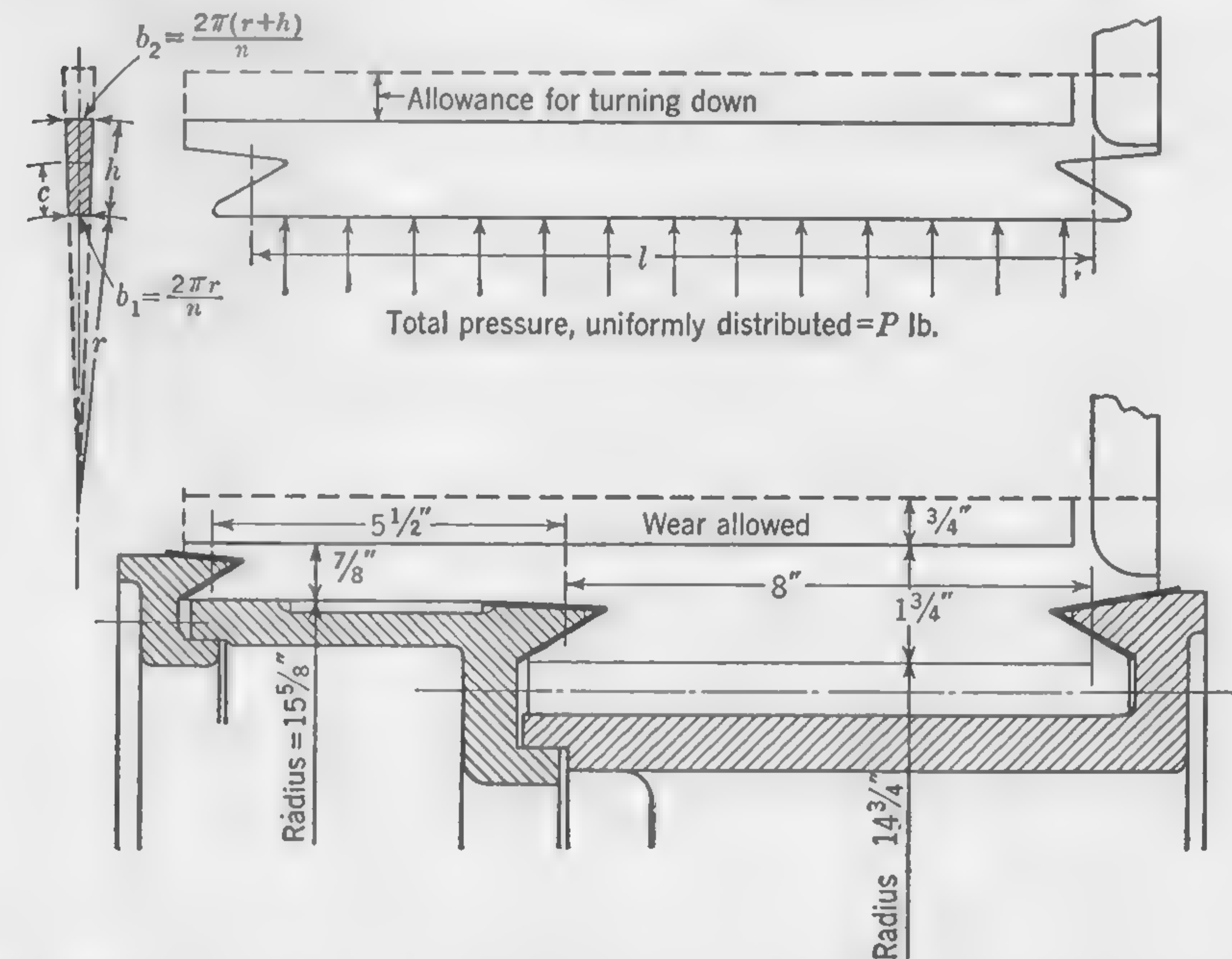


FIG. 193. Illustrating calculations for strength and stiffness of long commutator bars.

mula (161), then the maximum external moment—which will occur at the center of the bar—is

$$M = \frac{Pl}{8} \quad (167)$$

The weight of one copper segment of length  $l$  in., expressed in terms of the dimensions of Fig. 193, and assuming the mica thickness to be negligible, is

$$W = 0.32lh \frac{\pi(2r + h)}{n} \quad \text{lb}$$

where  $n$  stands for the total number of segments in the commutator. Putting this value of  $W$  in the formula (161), and taking the mean diameter  $(2r + h)$  as being a close enough approximation to the diameter



through the center of gravity of the copper section, the total centrifugal force acting on one bar is

$$P = \frac{14.3}{10^6} \times \frac{h(2r + h)^2 N^2}{n}$$

Substituting in formula (167) we get

$$M = \frac{1.8}{10^8} \times \frac{l^2 h(2r + h)^2 N^2}{n} \quad \text{in.-lb} \quad (168)$$

The maximum unit stress in the bar is expressed by the formula

$$S = \frac{M}{(I/c)} \quad (169)$$

where the quantity  $I/c$  is the section modulus, being the moment of inertia  $I$  of the cross section divided by the distance  $c$  of the edge of the bar from the neutral axis. For hard-drawn copper bars, the maximum working limit for  $S$  is about 8,000 lb per sq in.

The deflection of a beam uniformly loaded will be greatest at the center, its value being

$$\text{Maximum deflection} = \frac{5Pl^3}{384EI} \quad (170)$$

where  $I$  is the moment of inertia of the cross section and  $E$  is the modulus of elasticity, or ratio of stress to strain. The numerical value of  $E$  for copper is about 16,000,000 lb per sq in. The maximum deflection as calculated by this formula should not exceed a few mils.

In order to simplify the calculations, we shall assume—as when obtaining an expression for  $M$ —that the thickness of the mica is negligible, so that, with  $n$  segments in the commutator, each segment may be considered as having the shape of a wedge of depth  $h$  in. and thickness  $b_1 = 2\pi r/n$  at the thin edge, and  $b_2 = 2\pi(r + h)/n$  at the thick edge (see Fig. 193). The expression for the moment of inertia of the section is then

$$I = \frac{\pi h^3(6r^2 + h^2 + 6rh)}{18n(2r + h)} \quad (171)$$

and for the section modulus

$$\frac{I}{c} = \frac{\pi h^2(6r^2 + h^2 + 6rh)}{6n(3r + 2h)} \quad (172)$$

The quantity  $h$  in these formulas is the depth of the bar, and this should be the estimated maximum depth after a reasonable deduction for wear and truing of commutator surface has been made. The usual allowance

for turning down is from  $\frac{1}{2}$  in. on small commutators to 1 in. on large commutators.

The ratio of the quantity given by formula (168) to the quantity given by formula (172) is the maximum fiber stress. A considerable simplification is effected by omitting the relatively negligible quantity  $h^2$  from the expression  $(6r^2 + h^2 + 6rh)$  of formula (172) and making a similar omission from the square of the quantity  $(2r + h)$  in formula (168). The final expression for the maximum fiber stress is

$$S = \frac{2.27}{10^6} \times \frac{l^2(3r + 2h)N^2}{h} \quad \text{lb per sq in.} \quad (173)$$

*Example—Stress in Commutator Bars Due to Centrifugal Force.* Consider a commutator  $34\frac{1}{2}$  in. in outside diameter, running at 600 rpm. The bars are  $2\frac{1}{4}$  in. deep and 13 in. long. We shall calculate the maximum stress in the copper due to centrifugal force, after the commutator has been turned down so that the depth of the bar is reduced to  $1\frac{1}{2}$  in. The quantities for use in formula (173) are:

$$\begin{aligned} r &= 15 \\ h &= 1.5 \\ l &= 13 \\ N &= 600 \end{aligned}$$

Then,

$$S = \frac{2.27 \times (13)^2[(3 \times 15) + (2 \times 1.5)](600)^2}{10^6 \times 1.5} = 4,420 \text{ lb per sq in.}$$

which is a safe figure.

Although the application of formula (173) may indicate that the copper bars in a commutator are *strong* enough to resist the action of centrifugal force, it does not follow that the design is satisfactory, because the elastic deformation or deflection may be excessive, owing to lack of *stiffness*. If the distance between supports is large, as in the case of the above numerical example, the maximum deflection should be calculated. This deflection, as given by formula (170), can be put into a more convenient form in terms of the dimensions on the upper sketch in Fig. 193. The approximate formula for the total pressure on the bar is

$$P = \frac{5.72lh(r^2 + rh)N^2}{10^5n} \quad \text{lb}$$

and for the moment of inertia of the cross section

$$I = \frac{\pi h^3(r^2 + rh)}{3n(2r + h)}$$



Putting  $E = 16 \times 10^6$  and substituting these values in formula (170), we obtain

$$\text{Maximum deflection} = \frac{4.44l^4(2r + h)N^2}{10^{10}h^2} \quad \text{mils} \quad (174)$$

wherein all the dimensions are in inches, and  $N$  is the number of revolutions per minute.

*Example—Stiffness of Commutator Bars.* Using the same numerical data as for the preceding example illustrating stress calculations, we have

$$\text{Maximum deflection} = \frac{4.44(13)^4 \times 31.5(600)^2}{10^{10}(1.5)^2} = 64 \text{ mils}$$

which is considerably more than would be permissible in practice. This shows that, in long commutators, the deflection may be excessive even

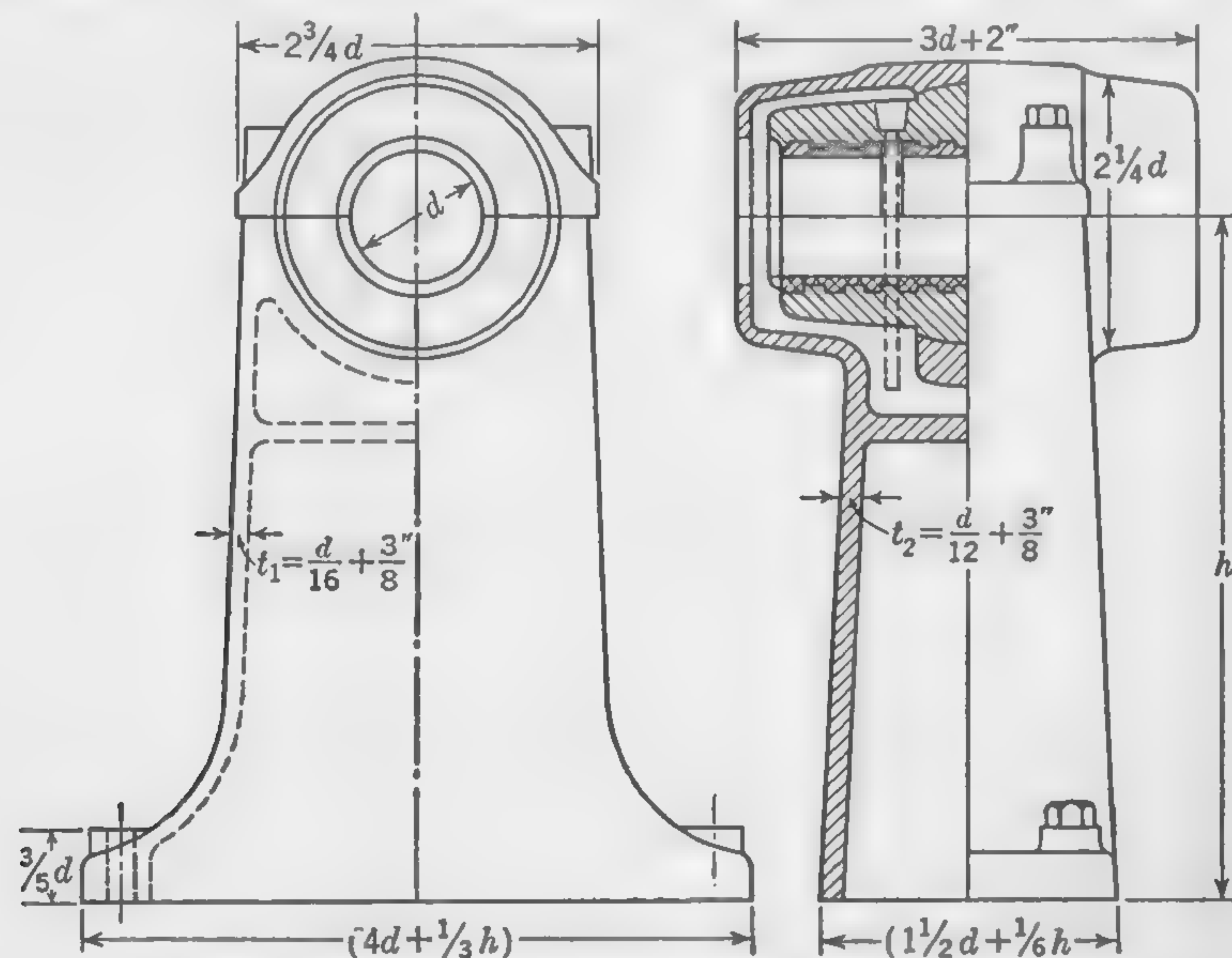


FIG. 194. Usual proportions of pedestal bearing for dynamo.

when the bars are of ample strength. In order to remedy this defect, the commutator might be designed as shown in the lower sketch of Fig. 193. This shows the bar held down at three points with comparatively short spaces between. The other alternative would be to make the depth  $h$  sufficient to provide the required stiffness with the original distance of 13 in. between clamping rings, but from an examination of formula (174) it is obvious that, since the deflection is proportional to the fourth power of  $l$ , a comparatively small reduction of this dimension will be more economical than a considerable increase of  $h$ .

Both sketches in Fig. 193 are drawn to the same scale and, therefore, serve to show the difference between the two designs of bar, the upper one being strong enough, but lacking in stiffness.

Applying formula (174)\* to the two sections of the modified design, we have, for the right-hand section of length  $l = 8$  in. and depth  $h = 1 3/4$  in.,

$$\text{Maximum deflection} = \frac{4.44(8)^4 \times 31.25(600)^2}{10^{10} \times (1.75)^2} = 6.7 \text{ mils}$$

and for the left-hand section with  $l = 5.5$  in. and  $h = 7/8$  in.,

$$\text{Maximum deflection} = \frac{4.44(5.5)^4 \times 32.125(600)^2}{10^{10} \times (0.875)^2} = 6.1 \text{ mils}$$

**160. Sundry Details of Mechanical Design.** There are many phases of the mechanical design of electrical machinery and many details of

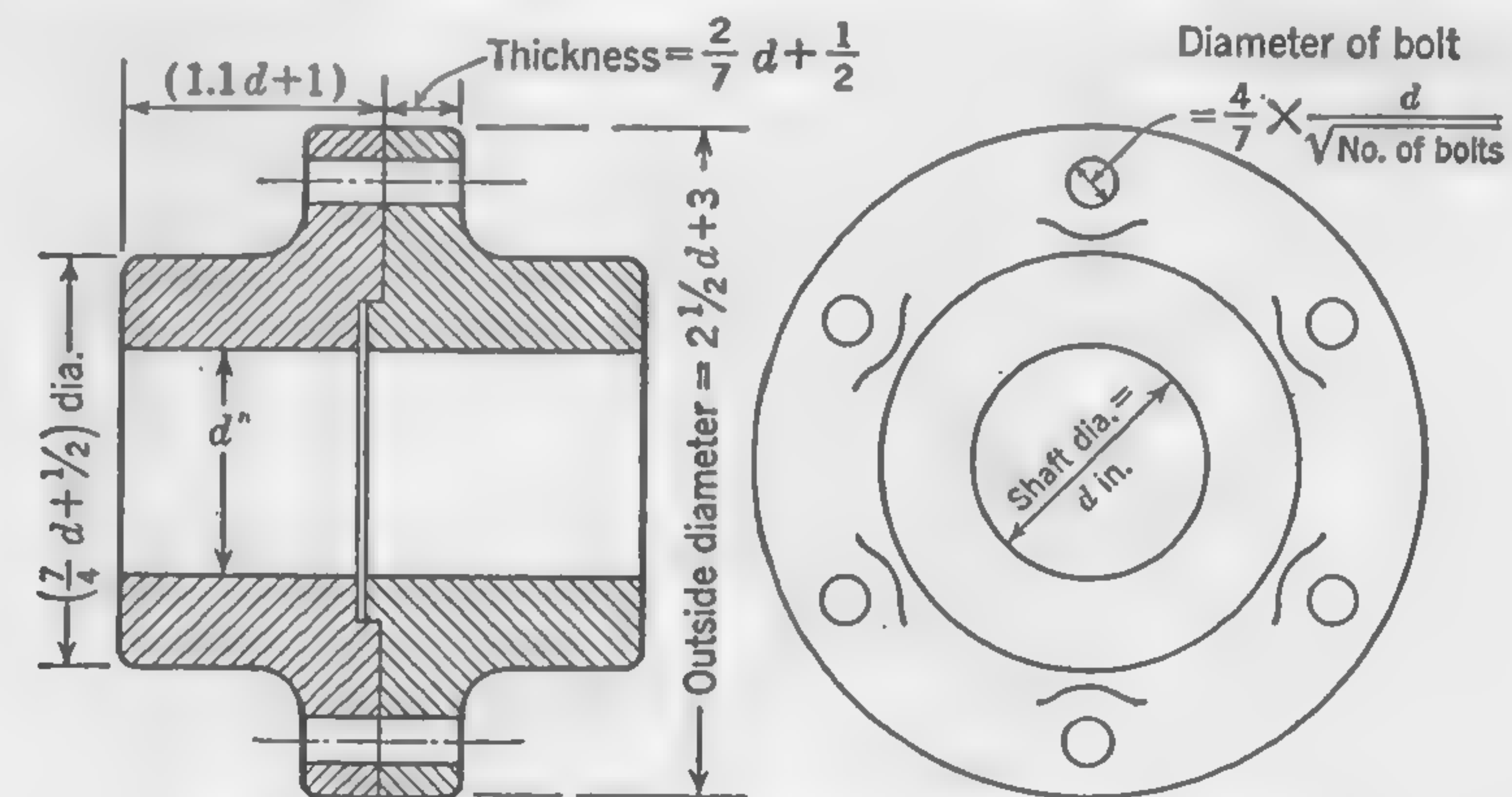


FIG. 195. Usual proportions of cast-iron shaft coupling.

construction which are beyond the scope of this book and will not be described in this chapter. Among these may be mentioned

Foundations and bedplates

Details of bearings—thrust bearings and pivot bearings for vertical shafts; systems of lubrication; ball bearings and roller bearings

Keys and keyways

Details of brush holders and brush gear

A few additional items are referred to in this article with a view to providing sufficient particulars to permit of a dimensioned sketch or assembly drawing being made of a generator or motor for which electrical design data are available.

\* This formula refers to a beam uniformly loaded and supported (not built in) at the two ends; it therefore gives results which are somewhat larger than would actually be obtained in a design of the type here considered.



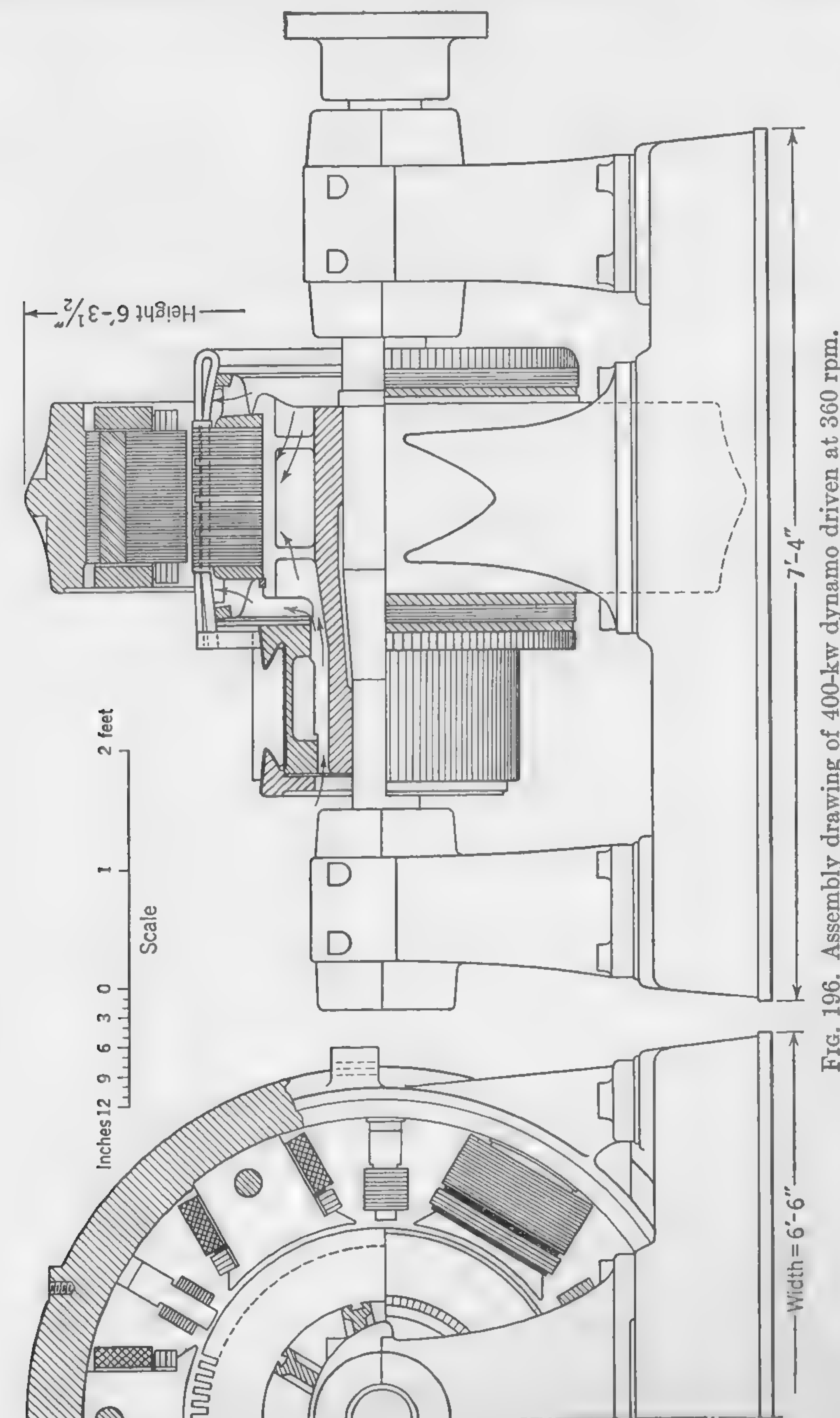


FIG. 196. Assembly drawing of 400-kw dynamo driven at 360 rpm.

*Outboard or Pedestal Bearing.* Figure 194 gives the usual proportions of a pedestal bearing expressed in terms of the height  $h$  and the journal diameter  $d$ . (Formulas for calculating the approximate shaft and bearing diameters were given in Art. 157.)

*Shaft Couplings.* Figure 195 gives usual proportions for cast-iron shaft couplings. The number of bolts in flange couplings is usually as follows:

For shaft diameters between 2 and 3 in., use 4 bolts

For shaft diameters between 3 and 8 in., use 6 bolts

For shaft diameters above 8 in., use 8 bolts

The bolt diameter may be calculated by the following formula, the standard size nearest to the calculated figure being selected:

$$\text{Bolt diameter} = \frac{4}{7} \times \frac{d}{\sqrt{\text{number of bolts}}}$$

where  $d$  is the diameter of the shaft in inches.

*General Assembly Drawing of Dynamo.* Approximate over-all dimensions of a 400-kw 600-volt dynamo arranged for direct-coupling to an engine running at 360 rpm are given in Fig. 196. This drawing is not intended to show all the details of mechanical design, being merely an assembly drawing such as the designer of electrical machinery should be able to produce in order to determine approximately the space occupied by the machine and to satisfy himself that the assembly of the several parts results in a design of which the appearance and proportions are satisfactory. The diameter of shaft and the coupling dimensions, also the over-all dimensions of the pedestal bearings, are in accordance with the particulars given in this chapter; but such details as brush gear, coil connections, terminals, lubrication, bolts, keys, and the method of securing the base to the foundation, have purposely been omitted from the drawing.



# APPENDIX 1

TABLE I. WIRE TABLE, BROWN AND SHARPE GAGE, ROUND COPPER WIRES

Gage No., B & S	Diameter, in. (bare)	Area of cross section		Weight, lb per 1,000 ft (bare)	Approx diameter dec (mils)	Approx number of turns per in. dec	Resistance, ohms per 1,000 ft		Gage No., B & S
		Sq in.	Cir mils				15°C (59°F)	60°C (140°F)	
0	0.32490	0.0829100	105,560.0	319.500	338	2.95	0.0964	0.1142	0
1	0.28930	0.0657300	83,690.0	253.300	302	3.30	0.1217	0.1440	1
2	0.25760	0.0521200	66,370.0	200.900	270	3.69	0.1534	0.1816	2
3	0.22940	0.0413300	52,630.0	159.300	242	4.12	0.1934	0.2290	3
4	0.20430	0.0327800	41,740.0	126.400	216	4.60	0.2439	0.2888	4
5	0.18190	0.0260000	33,090.0	101.200	194	5.13	0.3076	0.3642	5
6	0.16200	0.0206100	26,250.0	79.500	174	5.70	0.3880	0.4590	6
7	0.14430	0.0163500	20,820.0	63.000	156	6.36	0.4890	0.5790	7
8	0.12850	0.0129700	16,510.0	50.000	140	7.10	0.6170	0.7300	8
9	0.11440	0.0102800	13,090.0	39.600	126	7.88	0.7780	0.9210	9
10	0.10190	0.0081500	10,380.0	31.400	114	8.70	0.9810	1.1610	10
11	0.09070	0.0064600	8,230.0	24.900	103	9.60	1.2370	1.4640	11
12	0.08080	0.0051300	6,530.0	19.800	93	10.65	1.5590	1.8460	12
13	0.07200	0.0040700	5,178.0	15.700	84	11.80	1.9660	2.3280	13
14	0.06410	0.0032300	4,107.0	12.430	76	13.00	2.4800	2.9360	14
15	0.05710	0.0025600	3,260.0	9.860	68	14.50	3.1270	3.7020	15
16	0.05080	0.0020300	2,583.0	7.820	62	15.90	3.9420	4.6670	16
17	0.04530	0.0016100	2,048.0	6.200	56	17.50	4.9730	5.8870	17
18	0.04030	0.0012760	1,624.0	4.920	51	19.20	6.2700	7.4200	18
19	0.03590	0.0010120	1,288.0	3.900	46	21.30	7.9000	9.3600	19
20	0.03200	0.0008020	1,022.0	3.090	42	23.30	9.9700	11.8000	20
21	0.02850	0.0006360	810.0	2.450	38	25.60	12.5700	14.8800	21
22	0.02530	0.0005030	642.0	1.945	35	27.80	15.8600	18.7000	22
23	0.02260	0.0004010	510.0	1.542	32	30.30	20.0000	23.6600	23
24	0.02010	0.0003170	404.0	1.223	30	32.30	25.2000	29.8400	24
25	0.01790	0.0002520	320.0	0.970	27	35.70	31.8000	37.6000	25
26	0.01590	0.0001985	254.0	0.769	24	40.00	40.2000	47.5000	26
27	0.01420	0.0001584	202.0	0.610	22	43.50	50.6000	60.0000	27
28	0.01260	0.0001255	159.0	0.484	21	45.50	63.8000	75.4000	28
29	0.01126	0.0000995	126.0	0.384	19	50.00	80.3000	95.0000	29
30	0.01003	0.0000789	100.5	0.304	17	55.00	101.0000	119.5000	30
31	0.00893	0.0000626	79.7	0.241	16	59.00	127.5000	151.0000	31
32	0.00795	0.0000496	63.2	0.191	15	62.00	160.5000	190.0000	32
33	0.00708	0.0000394	50.1	0.152	14	67.00	203.0000	240.0000	33
34	0.00630	0.0000312	39.7	0.120	13	72.00	256.0000	303.0000	34



TABLE II. WIRE TABLE, SQUARE DOUBLE-COTTON-COVERED  
COPPER WIRES

Gage No. B & S	Area of cross-section		Ft per lb	Turns per sq in.	Resistance			
	Sq in.	Cir mils			1,000 ft		Lb	
					25°C	75°C	25°C	75°C
1	0.0801	102,216	3.20	10.2	0.103	0.123	0.00033	0.00040
2	0.0632	80,164	4.07	12.6	0.130	0.156	0.00053	0.00064
3	0.0490	62,670	5.21	15.9	0.169	0.203	0.00088	0.00105
4	0.0397	50,729	6.42	19.8	0.207	0.248	0.00133	0.00160
5	0.0312	39,729	8.19	24.6	0.266	0.319	0.00218	0.00262
6	0.0254	32,371	10.05	30.8	0.327	0.393	0.00328	0.00393
7	0.0200	25,475	12.76	38.2	0.415	0.498	0.0053	0.00635
8	0.0158	19,970	16.23	47.8	0.530	0.636	0.0086	0.01032
9	0.0122	15,616	20.67	61.7	0.680	0.815	0.0140	0.0168
10	0.0100	12,532	25.7	77.0	0.840	1.01	0.0216	0.0260
11	0.00775	9,800	32.8	98.0	1.08	1.30	0.0354	0.0425
12	0.00603	7,630	42.2	119	1.38	1.65	0.0583	0.0700
13	0.00465	5,909	54.3	148	1.79	2.15	0.0970	0.1163
14	0.00355	4,545	70.2	182	2.32	2.78	0.1630	0.1635

TABLE III. WIRE TABLE, BARE AND DCC COPPER RIBBON

Bare		Insulated (dcc)		Area of cross section		Resistance (1,000 ft)	
Thickness	Width	Thickness	Width	Sq. in.	Cir mils	25°C	75°C
0.025	0.258	0.043	0.270	0.00632	8,040	1.32	1.57
	0.365	0.045	0.377	0.00899	11,400	0.924	1.10
0.032	0.102	0.047	0.112	0.00304	3,880	2.73	3.25
	0.129	0.048	0.139	0.00391	5,190	2.13	2.54
	0.182	0.049	0.193	0.00560	7,140	1.48	1.77
	0.258	0.050	0.270	0.00804	10,200	1.03	1.23
	0.365	0.052	0.377	0.00115	14,600	0.725	0.864
0.040	0.102	0.055	0.112	0.00374	4,760	2.22	2.65
	0.129	0.056	0.139	0.00482	6,130	1.73	2.06
	0.162	0.056	0.173	0.00614	7,810	1.35	1.61
	0.204	0.057	0.215	0.00782	9,950	1.06	1.27
	0.258	0.058	0.270	0.00998	12,700	0.833	0.993
	0.325	0.059	0.337	0.0127	16,100	0.656	0.783
	0.365	0.060	0.377	0.0143	18,200	0.583	0.695
0.045	0.091	0.057	0.101	0.00366	4,660	2.27	2.71
	0.144	0.060	0.155	0.00605	7,700	1.37	1.64
	0.190	0.060	0.201	0.00805	10,250	1.03	1.23
0.051	0.072	0.062	0.083	0.00314	3,990	2.65	3.16
	0.081	0.062	0.092	0.00360	4,580	2.31	2.76
	0.102	0.064	0.113	0.00467	5,940	1.78	2.12
	0.114	0.064	0.125	0.00528	6,720	1.57	1.58
	0.129	0.065	0.140	0.00604	7,690	1.37	1.64
	0.162	0.065	0.173	0.00773	9,840	1.08	1.28
	0.182	0.066	0.194	0.00875	11,100	0.950	1.13
	0.204	0.066	0.216	0.00987	12,600	0.842	1.00
	0.258	0.067	0.271	0.0126	16,100	0.658	0.785
	0.325	0.067	0.338	0.0160	20,400	0.518	0.618
	0.365	0.068	0.378	0.0181	23,000	0.459	0.548
0.057	0.081	0.068	0.092	0.00408	5,200	2.04	2.43
	0.091	0.068	0.102	0.00465	5,920	1.79	2.13
	0.129	0.071	0.140	0.00682	8,680	1.22	1.45
	0.144	0.071	0.155	0.00767	9,770	1.08	1.29
	0.204	0.072	0.216	0.0111	14,100	0.749	0.593
0.061	0.081	0.075	0.092	0.00472	6,020	1.76	2.10
	0.091	0.075	0.102	0.00529	6,730	1.57	1.87
	0.102	0.077	0.113	0.00599	7,630	1.39	1.65
	0.114	0.077	0.125	0.00676	8,610	1.23	1.47



TABLE III. WIRE TABLE, BARE AND DCC COPPER RIBBON.—(Continued)

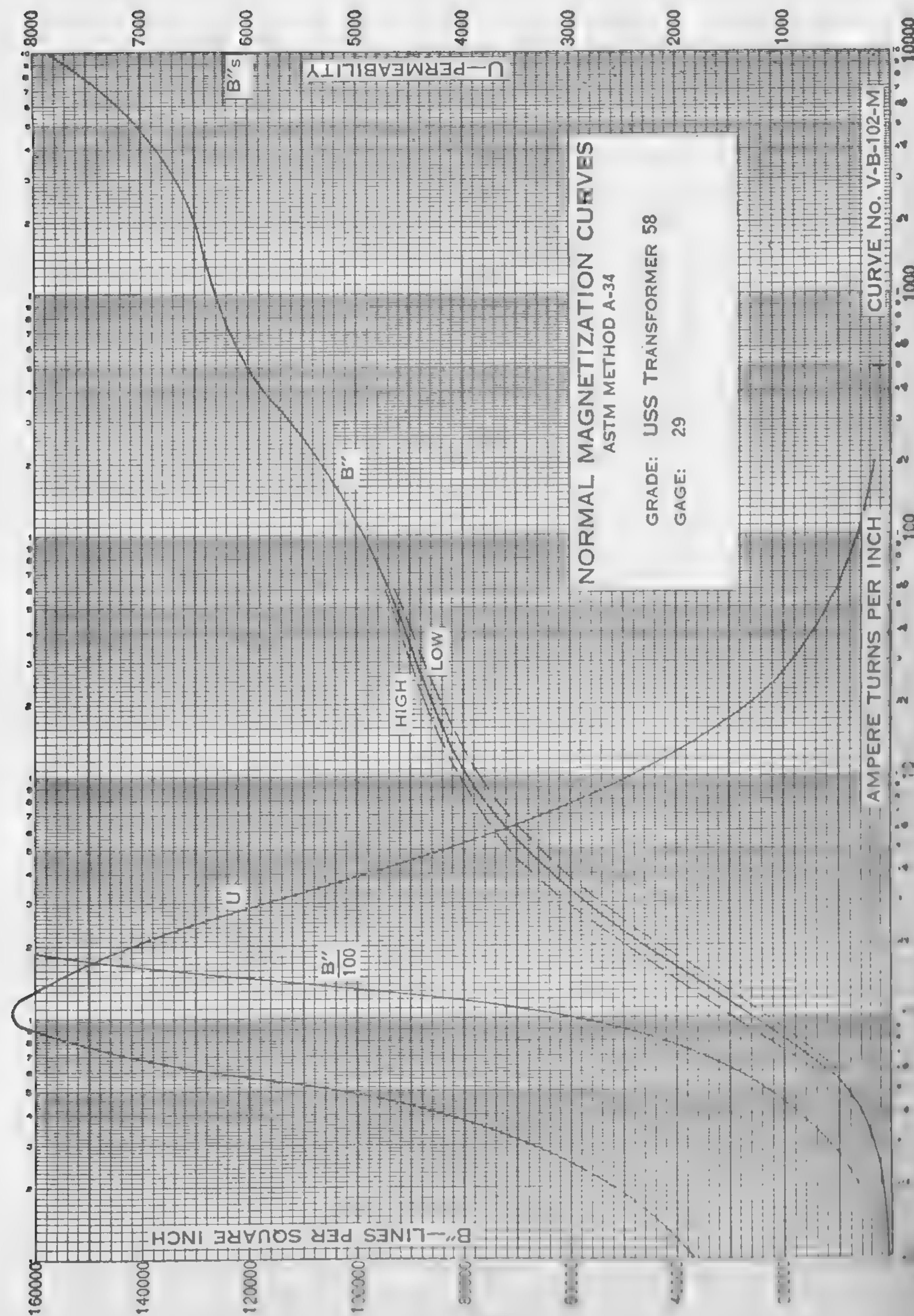
Bare		Insulated (dcc)		Area of cross section		Resistance (1,000 ft)	
Thickness	Width	Thickness	Width	Sq in.	Cir mils	25°C	75°C
0.064	0.129	0.078	0.140	0.00772	9,830	1.08	1.28
	0.144	0.078	0.155	0.00868	11,100	0.957	1.14
	0.162	0.078	0.173	0.00983	12,500	0.845	1.01
	0.182	0.079	0.194	0.0111	14,100	0.747	0.892
	0.204	0.079	0.216	0.0125	15,900	0.663	0.791
	0.258	0.080	0.271	0.0160	20,300	0.520	0.620
	0.325	0.081	0.338	0.0203	25,100	0.410	0.489
	0.365	0.081	0.378	0.0228	29,100	0.364	0.434
0.072	0.129	0.086	0.140	0.00875	11,100	0.949	1.13
	0.144	0.086	0.155	0.00983	12,500	0.845	1.01
	0.182	0.087	0.194	0.0126	16,000	0.661	0.788
	0.204	0.087	0.216	0.0142	18,000	0.587	0.700
	0.258	0.087	0.271	0.0180	23,000	0.460	0.549
	0.325	0.088	0.338	0.0229	29,100	0.353	0.433
0.081	0.102	0.094	0.114	0.00773	9,840	1.08	1.28
	0.114	0.094	0.126	0.00870	11,100	0.955	1.14
	0.129	0.095	0.141	0.00991	12,600	0.838	1.00
	0.144	0.095	0.156	0.0111	14,200	0.746	0.890
	0.162	0.095	0.175	0.0126	16,000	0.660	0.787
	0.182	0.096	0.195	0.0142	18,100	0.585	0.697
	0.204	0.096	0.217	0.0160	20,400	0.520	0.620
	0.258	0.097	0.272	0.0204	25,900	0.408	0.487
	0.325	0.098	0.339	0.0258	32,800	0.322	0.384
	0.365	0.099	0.379	0.0290	37,000	0.290	0.286
0.091	0.129	0.105	0.141	0.0112	14,300	0.741	0.884
	0.144	0.105	0.156	0.0126	16,000	0.661	0.788
	0.162	0.105	0.175	0.0142	18,100	0.585	0.697
	0.204	0.106	0.217	0.0180	23,000	0.461	0.550
	0.258	0.107	0.272	0.0229	29,200	0.362	0.432
	0.325	0.108	0.339	0.0290	37,000	0.286	0.341
	0.410	0.109	0.424	0.0368	46,900	0.226	0.260
0.102	0.129	0.116	0.142	0.0126	16,100	0.658	0.785
	0.162	0.117	0.176	0.0160	20,400	0.520	0.620
	0.182	0.118	0.196	0.0180	23,000	0.461	0.550
	0.204	0.118	0.218	0.0203	25,800	0.410	0.489
	0.258	0.119	0.273	0.0258	32,800	0.322	0.384
	0.325	0.120	0.340	0.0326	41,500	0.255	0.301

TABLE III. WIRE TABLE, BARE AND DCC COPPER RIBBON.—(Continued)

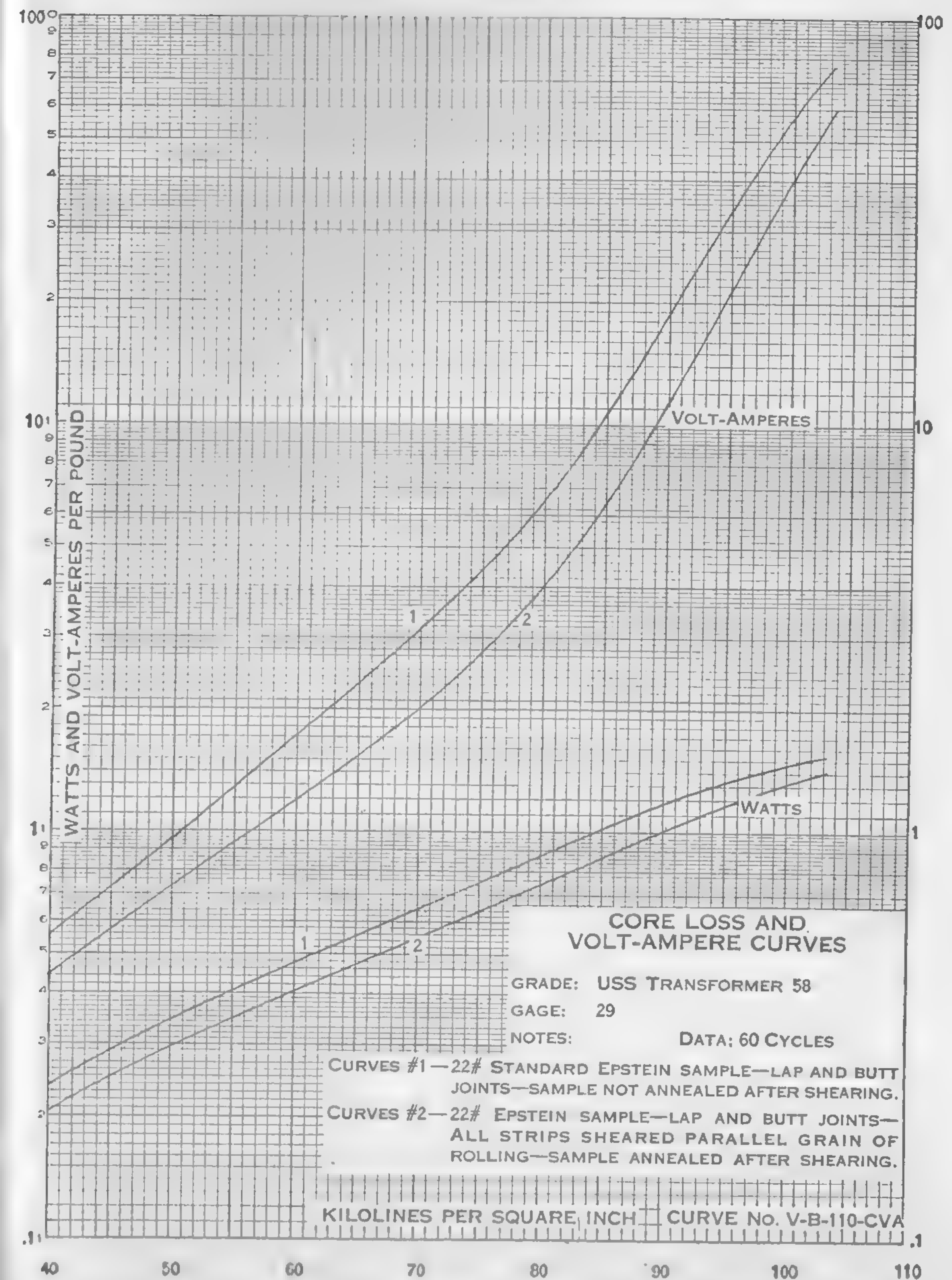
Bare		Insulated (dcc)		Area of cross section		Resistance (1,000 ft)	
Thickness	Width	Thickness	Width	Sq in.	Cir mils	25°C	75°C
0.114	0.144	0.130	0.159	0.0156	19,900	0.533	0.635
	0.162	0.131	0.178	0.0176	22,500	0.471	0.562
	0.182	0.132	0.198	0.0199	25,400	0.417	0.497
	0.204	0.132	0.220	0.0224	28,600	0.370	0.442
	0.258	0.133	0.275	0.0286	36,400	0.291	0.347
	0.325	0.134	0.342	0.0362	46,100	0.229	0.274
	0.410	0.135	0.427	0.0459	58,500	0.181	0.216
0.129	0.162	0.147	0.179	0.0201	25,600	0.414	0.494
	0.204	0.148	0.221	0.0255	32,500	0.326	0.389
	0.258	0.149	0.276	0.0325	41,300	0.256	0.305
	0.325	0.150	0.343	0.0411	52,300	0.202	0.241
	0.410	0.151	0.428	0.0521	66,300	0.160	0.190
0.144	0.182	0.163	0.200	0.0254	32,300	0.327	0.390
	0.204	0.163	0.222	0.0286	36,400	0.291	0.347
	0.258	0.165	0.276	0.0363	46,300	0.229	0.273
	0.289	0.165	0.307	0.0408	51,900	0.204	0.243
	0.325	0.166	0.344	0.0460	58,500	0.181	0.216
0.162	0.204	0.182	0.223	0.0322	41,000	0.258	0.307
	0.258	0.184	0.278	0.0410	52,200	0.203	0.242
	0.325	0.185	0.345	0.0518	66,000	0.160	0.191
0.182	0.229	0.202	0.249	0.0398	50,700	0.209	0.249
	0.289	0.204	0.310	0.0507	64,600	0.164	0.195
	0.365	0.206	0.386	0.0645	82,200	0.129	0.154
0.204	0.235	0.227	0.260	0.0460	58,600	0.181	0.215
	0.258	0.227	0.280	0.0507	64,600	0.164	0.195
	0.325	0.228	0.347	0.0644	82,000	0.129	0.154



# APPENDIX 2



# APPENDIX 2



APPENDIX FIG. 2. Core loss and volt-ampere curves for U.S.S. Transformer Steel No. 58-29 gage.



## INDEX

- Action, transformer, 265
- Air gap, 239, 274
  - ampere-turns for, 97, 102, 118
  - density in, 11, 94, 97, 100, 102, 115, 118, 238
  - apparent, 11
  - equivalent, 92, 126, 236, 309
  - induction motor, 309
  - leakage flux in, 313
  - length of, 16, 178, 204, 266
  - formula for, 17
  - permeance of, 91, 113
- All-day efficiency, 363, 379, 391
- Alloys, iron-nickel, 396
- A-c generators (*see* Generators)
- A-c machinery, 168
- Alternator, efficiency of, 258, 262
  - regulation of, 179, 259
  - salient poles for, 210, 255
  - single-phase, 218
  - turbo-, 196, 231, 418
- Amortisseur winding, 218
- Ampere-conductors per pole, 14, 217
- Ampere-turns, air gap and teeth, 97, 102, 118
  - armature, 14, 217, 220
  - commutating pole, 76
  - demagnetizing, 101, 104
  - field, 130
  - magnetizing, 310
  - series-field, 118
  - shunt-field, 118
- Apparent gap density, 11
- Arc, pole, 12
- Armature, ampere-turns on, 14, 217, 220
  - binding wire for, 420
  - density of, 197
  - temperature rise of, 146, 148, 151, 165
- Armature coils, 20
  - full-pitch, 61, 71, 278
- Armature core, 40
  - length of, 37
- Armature design, example of, 41
- Armature flux, 63, 74
- Armature mmf, 214, 218, 220
- Armature reactance, 249
- Armature reaction, 62, 101, 249
- Armature resistance, 37
  - equivalent, 380
- Armature teeth, 40
- Armature windings, 20, 181
  - chorded, 22
  - concentric chain, 182
  - distributed, 171
  - double-layer, 20, 191, 294, 301
  - frog-leg, 20, 29
  - full-pitch, 61, 71, 278
  - lap, 20, 184, 201, 291, 294
  - length of, 187
  - multiplex, 20
  - paths in, 20
  - polyphase, 181
  - reactive voltage drop in, 189
  - reentrancy of, 23
  - resistance of, 37, 187
  - short-pitch, 21, 71, 278, 301
  - simplex-lap, 24
  - simplex-wave, 25
  - single-layer, 191
  - spread of, 186
  - three-phase, 301, 310
  - types of, 20
  - wave, 20, 183, 304
- Bearings, 415, 427
  - length of, 416
  - pedestal, 429
- Bedplates, 427
- Binding wire, 420
- Bolts, 429
- Brush-contact drop, 52
- Brush-contact resistance, 81
- Brush friction, 52
- Brush holders, 88, 427
- Brush pitch, 103
- Brush pressure, 87
- Brush shift, 80, 103
- Brushes, 51, 58
  - losses in, 144
- Bushings, transformer, 367



- Chorded windings, 22
- Circle diagram, 306
  - characteristics from, 322
  - construction of, 318, 326
  - limitations of, 329
  - torque calculations from, 320
  - use of, 320
- Circle ratio, 325
- Circuit, equivalent, 329
  - magnetic, 130, 209
- Circular-mil area, 132
  - formula for, 120
- Coefficient, of cooling, 123, 150, 195
  - leakage, 245
- Cogging, 280, 291
- Coil pitch, 21
- Coils, armature, 20, 61, 78, 278
  - multielement, 26
  - transformer, 351
- Combinations, rotor-slot, 280
- Commutating poles, 63, 72
  - ampere-turns on, 76
  - design of, 75
- Commutation, straight-line, 82
  - theory of, 59
  - zone of, 63, 68
    - flux in, 70
- Commutator, 24, 423
  - deflection of, 424
  - design of, mechanical, 421
  - high-speed, 422
  - length of, 52
  - losses in, 142, 143
  - stiffness of, 423
  - stress in, 425
  - temperature rise in, 144
  - undercut, 88
- Commutator pitch, 21
- Commutator segments, number of, 35
- Compensating windings, 85, 115
- Compounding, flat, 105
- Concentrated windings, 171
- Conductivity, thermal, 160, 164
- Cooling, 195
  - coefficient of, 123, 150, 195
  - transformer, 345, 375, 400
- Cooling ducts, 247
- Cooling surfaces, 122, 149
- Copper losses, 374, 377, 384
- Core length, 37
- Core losses, 190, 276, 381, 384
  - calculation of, 141
  - table of, 140
- Core-surface reactance, 255
- Cores, armature, 40
  - cruciform, 349, 370
  - pole, 414
- Cores, ribbon, 381
  - transformer, 348, 375, 400
    - joints in, 355
- Corrugations, transformer, 366
- Couplings, 427
- Creepage distance, 347
- Critical speed, 421
- Cruciform cores, 349, 370
- Current, end-ring, 281, 292
  - exciting, 391, 401
  - magnetizing, 309, 380
  - short-circuit, 253, 259, 321
  - starting, 321
- Current density, 36, 82, 187, 202, 270, 278, 397
  - rotor-bar, 281
- Current ratio, 394
- Current transformers, 393
  - design of, 396
  - phase-angle error in, 394, 402
  - ratio error in, 402
- Curve, saturation, 125, 130, 133
- Curves, magnetization, 98, 354, 396
  - specific-loading, 272
- Cusps, synchronous, 291
- Deflection, commutator, 424
- Delta connection, 173, 304
- Demagnetizing ampere-turns, 101, 104
- Density, air-gap, 11, 94, 97, 100, 102, 116, 118, 238
  - apparent, 11
  - current, 36, 82, 187, 202, 276, 278, 301, 397
  - tooth, 94, 100, 238
    - apparent, 288
- Design, armature, 41
  - commutating pole, 75
  - commutator, 421
  - d-c motors, 154
  - field magnet, 117, 123, 126, 231
  - generator, 41
  - mechanical, 406
  - pole shoe, 16
  - transformer, 370, 382, 392
- Diagram, circle, 306
- D-c motors, design of, 154
- Distributed windings, 171, 210
- Distribution factor, 172, 296
- Double-layer windings, 20, 191, 204, 301
- Dovetails, 416
- Drop, brush-contact, 52
- Ducts, 192
  - axial, 147
  - cooling, 247
  - radial, 148

- Ducts, ventilating, 39, 275, 290
- Dynamo, 7
  - efficiency of, 152
- Eddy-current losses, 117, 149
- Efficiency, all-day, 363, 379, 391
  - alternator, 258, 262
  - dynamo, 152
  - generator, 154
  - induction motor, 267, 294
  - transformer, 362, 364, 370, 390
    - maximum, 379, 391
- End-connection reactance, 192
- End flux, 63
- Equivalent air gap, 92, 126, 236, 309
- Equivalent circuit, 329
- Equivalent permeance, 227
- Equivalent reactance, 326
- Equivalent resistance, 380
  - of induction motors, 318
- Equivalent slot flux, 226
- Exciting current, transformer, 352, 391
- Factor, distribution, 172, 296
  - form, 171
  - leakage, 78, 80, 116, 127, 131, 245
  - pitch, 172, 192, 296
  - power, of induction motors, 268, 294, 307, 327, 328
  - space, 348, 399
  - stacking, 383, 385
  - winding, 192, 286, 296, 326
- Field, magnetic, 7, 406
- Field ampere-turns, 130
- Field magnet, 209
  - design of, 117, 123, 126, 231
- Field windings, distributed, 210
- Flat compounding, 105
- Flux, armature, 63, 74
  - distribution of, 212
  - end, 63
  - leakage (*see* Leakage flux)
  - slot (*see* Slot flux)
  - slot-leakage, 220
  - zone of commutation, 70
- Flux density, air-gap, 94, 118, 178, 238
  - apparent tooth, 40
  - armature core, 40
  - distribution of, 112, 114, 116
  - induction-motor, 267, 271
  - transformer, 344
  - yoke, 127
- Flux map, 106, 107, 109
- Force, centrifugal, 410, 419
- Force, magnetic, 407
  - magnetizing, 99
  - magnetomotive (*see* Magnetomotive force)
  - mechanical, 406
  - transformer, 408
- Form factor, 171
- Formula, output, 8, 273, 286
- Foundations, 427
- Fractional-pitch windings, 21, 71, 278, 301
- Fractional-slot winding, 304
- Frames, stator, 412
- Frequency, 52
- Friction, brush, 52
- Friction losses, 143, 153
  - commutator, 142
- Frog-leg windings, 20, 29
- Full-pitch armature coils, 61, 71, 278
- Full-pitch windings, 22, 71, 278
- Gap, air (*see* Air gap)
- Generators, a-c, power output of, 175
  - voltage of, 188
  - voltage equation for, 170
  - cost of, 55
  - design of, 41
  - durability of, 56
  - efficiency of, 154
  - losses in, 55, 138, 151, 193, 258, 263
  - overcompounding of, 105
  - synchronous, 168, 169, 248
- Heat, 365
  - specific, 157
- Heating, intermittent, 155
- High-low section, 351, 357
- High-tension winding, 373
- Holders, brush, 88, 427
- Hottest-spot temperature, 161, 369
- Hysteresis, 149
- Induction motors, 265, 306
  - air gap for, 309
  - characteristics of, 331
  - design of, 266, 284, 297
  - efficiency of, 267, 294
  - equivalent circuit of, 329
  - equivalent resistance of, 318
  - flux density in, 267, 271
  - heating of, 336
  - horsepower of, 322
  - leakage flux in, 312
  - magnetizing current of, 309
  - noise in, 291



- Induction motors, no-load current in, 311
  - output equation for, 273
  - power of, 283
  - power factor of, 268, 294, 307, 327, 328
  - reactive drop in, 317
  - windings for, 276
- Inherent regulation, 259
- Instrument transformers, 393
- Insulation, kinds of, 32
  - thermal conductivity of, 164
  - transformer, 346, 376, 400
- Intermittent heating, 155
- Internal temperature, 160
- Iron, losses in, 301
- Iron-nickel alloys, 396
- Joints, transformer core, 355
- Keys and keyways, 427
- Laminations, 117, 147, 300
- Lap windings, 20, 184, 201, 291, 294
- Leakage, magnetic, 353, 355
  - slot, 225, 313
  - transformer, 353
  - zig-zag, 256
- Leakage coefficient, 245
- Leakage factor, 78, 80, 116, 127
  - average, 131
- Leakage flux, 79, 105, 312, 360
  - air-gap, 313
  - calculations of, 108, 313
  - equivalent, 314
  - in induction motors, 312
  - transformer, 353, 360
- Leakage permeance, 79, 107, 112, 325
  - formula for, 79
- Leakage reactance, 325
- Length, air-gap, 16, 17, 178, 204, 266
  - axial, 274
  - bearings, 416
  - commutator, 52
  - core, 37
- Loading, specific (*see* Specific loading)
- Losses, brush, 144
  - commutator, 142, 143
  - copper, 374, 377, 384
  - core, 140, 141, 190, 276, 381, 384
  - eddy-current, 117, 149
  - friction, 143, 153
  - generator, 55, 138, 151, 193, 258, 263
  - heat, 365
  - hysteresis, 149
  - iron, 301
- Losses, teeth, 149, 276
  - transformer, 364, 375, 381, 397
  - windage, 153
- Low-tension winding, 375
- Machinery, a-c, 168
- Magnet, field (*see* Field magnet)
- Magnetic circuit, 130, 209
- Magnetic field, 7, 406
- Magnetic forces, 407
- Magnetic leakage, 353, 355
- Magnetic pull, unbalanced, 409, 411
- Magnetization curves, 98, 354, 396
- Magnetizing ampere-turns, 310
- Magnetizing current, 309, 380
- Magnetizing force, 99
- Magnetomotive force (mmf), 212
  - armature, 214, 218, 229
  - distribution of, 103
- Map, flux, 106, 107, 109
- Mechanical design, 406
- Mechanical stresses, 418
- Mesh connection, 173, 304
- Motors, characteristics of, 327, 333
  - d-c, design of, 154
  - equivalent circuit of, 329
  - induction (*see* Induction motors)
  - slip-ring, 279, 294
  - temperature rise of, 337
  - wound-rotor, 279, 294
- Multielement, 26
- Multiplex windings, 20
- Noise, induction-motor, 291
- Oil-immersed transformer, 346, 364, 368
- Output formula, 8, 273, 286
- Overcompounding, 105
- Pedestal bearing, 429
- Pedestals, 426
- Peripheral velocity, 12, 275, 296
- Permeability, 96
- Permeance, air-gap, 91, 113
  - equivalent, 227
  - leakage, 79, 107, 112, 125
- Phase angle, transformer, 394, 402
- Phases, number of, 169
- Pitch, brush, 103
  - coil, 21
  - commutator, 21
  - fractional, 21
  - full, 22, 71, 278

- Pitch, pole, 12, 13
  - slot, 287
- Pitch factor, 172, 192, 296
- Pole arc, 12
- Pole cores, 414
- Pole face, shape of, 210
- Pole-face windings, 85, 115
- Pole pitch, 12, 13
- Pole shoes, 117, 414
  - construction of, 179
  - design of, 16
- Pole-speed combinations, 16
- Poles, commutating, 63, 72, 75, 76
  - dimensions of, 117
  - number of, 13, 15
  - properties of, 176
  - salient, 210, 255, 420
- Power, induction-motor, 283
- Power factor, induction-motor, 268, 294, 307, 327, 328
- Pressure, brush, 87
- Pull, magnetic, 409, 411
- Ratio, current, 394
- Ratio error, 402
- Reactance, armature, 249
  - core-surface, 255
  - end-connection, 192
  - equivalent, 326
  - leakage, 325
  - synchronous, 251
- Reactance voltage, 24
- Reaction, armature, 62, 101, 249
- Reactive voltage, 189, 355, 359
- Reentrancy of windings, 23
- Regulation, 352
  - alternator, 179, 259
  - inherent, 259
  - transformer, 353, 361, 364, 380, 391
  - voltage (*see* Voltage regulation)
  - zero-power-factor, 250
- Reluctance, tooth, 91
- Resistance, armature, 37
  - brush-contact, 81
  - equivalent, 380
  - induction-motor, equivalent, 318
  - rotor, 282
  - of series-field winding, 134
  - of shunt-field winding, 133
  - transformer, 380, 390
  - of windings, 37, 187
- Resistance drop, internal, 105
- Ribbon cores, 381
- Rims, rotor, 419
- Rotor bars, current density in, 281
  - skew of, 281, 292
- Rotor rims, 419
- Rotor-slot combinations, 280
- Rotor windings, 278, 303
- Rotors, bursting of, 420
  - high-speed, 416
  - resistance of, 282
  - rims of, 419
  - squirrel-cage, 281, 291
  - double, 279
  - wound, 294
- Rule, Simpson's, 97, 241
- Salient poles, 210, 255, 420
- Saturation, tooth, 226, 236
- Saturation curve, 125, 130, 133
- Section, high-low, 351, 357
- Segments, commutator, 35
- Series field, 118
- Series-field winding, resistance of, 134
- Shafts, 415
- Shift, brush, 80, 103
- Shoes, pole, 117, 414
- Short-circuit current, 253, 259, 321
- Short-circuit emf, example of, 71
- Short-pitch windings, 21, 71, 278, 301
- Shunt-field winding, 117, 118, 132
  - current density in, 121
  - exciting current in, 121
  - resistance of, 133
- Silicon steel, 381
- Simpson's rule, 97, 241
- Single-layer windings, 191
- Skew, rotor-bar, 281, 292
- Slip, 282
- Slip-ring motor, 279, 294
- Slot flux, 67, 73, 226
  - equivalent, 226
  - formulas for, 69
- Slot leakage, 225, 313
- Slot-leakage flux, 220
- Slot pitch, 287
- Slot-tooth proportions, 187
- Slots, 239
  - number of, 31
- Space factors, 348, 399
- Specific heat, 157
- Specific loading, 176, 200, 267
  - curves of, 272
  - definition of, 10
  - values of, 12
- Speed, 283
  - critical, 421
  - synchronous, 265
  - whirling, 421
- Speed-pole combinations, 16



- Squirrel cage, 279, 281, 291
  - double, 279
- Stacking factor, 383, 385
- Star connection, 173, 198
- Stator-rotor combinations, 280
- Stator windings, 276, 291, 294, 310
- Stator yoke, 300, 413
- Stators, 412
- Steel, silicon, 381
- Stiffness, commutator, 423
- Stress, commutator, 425
- Stresses, mechanical, 418
- Synchronous cusps, 291
- Synchronous generators, 168
  - regulation of, 248
  - speeds of, 169
- Synchronous reactance, 251
- Synchronous speed, 265
  
- Tanks, transformer, 366, 387
- Teeth, 239
  - ampere-turns for, 97, 102, 118
  - armature, 40
  - losses in, 149, 276
  - taper of, 96
- Temperature, hottest-spot, 161, 369
  - internal, 160
- Temperature rise, 121, 134, 137, 150, 159, 195, 337
  - armature, 146, 148, 151, 165
  - commutator, 144
  - of motors, 337
  - transformer, 364, 392, 402
- Thermal capacity, 155
- Thermal conductivity, 160, 164
- Three-phase windings, 301, 310
- Tooth density, calculation of, 94, 100, 238
- Tooth reluctance, 91
- Tooth saturation, 226, 236
- Tooth-slot proportions, 187
- Torque, 268, 283
  - maximum, 328, 332
  - slip for, 332
  - starting, 308, 321, 328
- Torque calculations from circle diagram, 320
- Transformer action, 265
- Transformer equation, 340
- Transformers, 339
  - all-day efficiency of, 363, 379, 391
  - bushings for, 367
  - coils in, 351
  - cooling of, 345, 365, 368
    - water, 368
  - copper losses in, 375
  - core-type, 341, 397

- Transformers, cores of, 348, 355, 375, 400
  - corrugations in, 366
  - cruciform core, 349, 370
  - current (*see* Current transformers)
  - current density in, 344
  - design of, 370, 382, 392
  - distribution, 341, 370
  - efficiency of, 362, 364, 379, 390, 391
  - exciting current in, 352, 391
  - flux density in, 344
  - forces in, 408
  - high-low sections in, 351, 357
  - instrument, 393
  - insulation for, 346, 376, 400
  - leakage flux in, 360
  - losses in, 364, 375, 381, 397
  - magnetic leakage in, 353, 360
  - oil-immersed, 346, 364, 368
  - output equation for, 343
  - phase angle, 394, 402
  - power, 341, 392
  - regulation of, 353, 380, 391
  - resistance of, 390
    - equivalent, 380
  - ribbon-core, 381
  - self-cooling, 365
  - shell-type, 341, 356
  - stacking factor for, 383, 385
  - tanks for, 366, 387
  - temperature rise in, 364, 392, 402
  - theory of, 339
  - types of, 341
  - vector diagram for, 360, 394
  - voltage regulation of, 353, 361, 364
  - windings for, 375, 387, 408
- Turbo-alternators, 196, 231, 418

Undercut commutator, 88

- Vector diagram, transformer, 360, 394
- Velocity, peripheral, 12, 275, 296
- Ventilating ducts, 39, 275, 299
- Ventilation, 137
  - forced, 147, 196
- Voltage, a-c generator, 188
  - apparent developed, 224
  - reactance, 24
  - reactive, 189, 355, 359
- Voltage equation, a-c generator, 170
- Voltage regulation, 248, 353
  - formulas for, 361
  - transformer, 353, 364, 380, 391

Watt-hour meter, current transformer for, 396

- Windings, resistance of, 37, 187
  - rotor, 278, 303
  - series-field, 134
  - short-pitch, 21, 71, 278, 301
  - shunt-field (*see* Shunt-field winding)
  - single-layer, 191
  - spread of, 186
  - stator, 276, 291, 294, 310
  - three-phase, 301, 310
  - transformer, 375, 387, 408
  - wave, 20, 183, 304
- Wire, binding, 420
- Wire size, series-field, 118
  - shunt-field, 118, 120
- Wound-rotor motor, 279, 294
  
- Yoke, density in, 127
  - dimensions of, 117
  - stator, 300, 413
  
- Zero-power-factor regulation, 250
- Zig-zag leakage, 256
- Zone of commutation, 63, 68, 70